VIBRATORY HAMMER COMPACTION OF GRANULAR MATERIALS

By

Nathan Ntanda Chilukwa

(Beit Scholar)

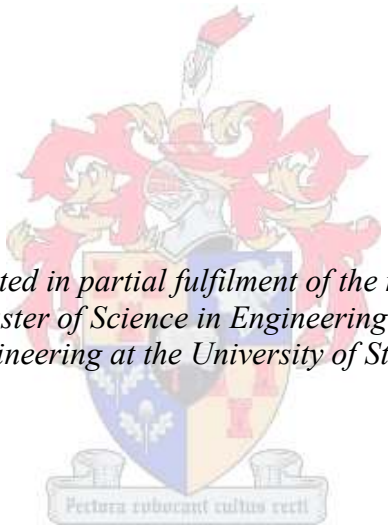

Thesis presented in partial fulfilment of the requirements for the degree Master of Science in Engineering in the Faculty of Engineering at the University of Stellenbosch

Promoter:

Prof. Kim Jenkins PhD

SANRAL Chair in Pavement Engineering

Faculty of Engineering

Department of Civil Engineering

Co-promoter:

Mrs Chantal Rudman

Lecturer in Pavement Engineering

Faculty of Engineering

Department of Civil Engineering

March 2013

DEDICATED TO MAX CHILUKWA

DECLARATION

By submitting this thesis electronically, I declare that the entirety of the work contained therein is my own, original work, that I am the sole author thereof (save to the extent explicitly otherwise stated), that reproduction and publication thereof by Stellenbosch University will not infringe any third party rights and that I have not previously in its entirety or in part submitted it for obtaining any qualification.

Signed: . Date : February 11, 2013

EXECUTIVE SUMMARY

Compaction is one of the key processes in the construction of road pavement layers. Not only is it significant in ensuring the structural integrity of the material in the road layers, but it also has an influence on the engineering properties and performance of the soil material. A poorly compacted material is characterised by low density, high porosity and below standard shear strength. This, as a result causes rutting, moisture susceptibility, potholing, corrugations and passability problems on the road. Therefore, it is vitally important that field compaction is done correctly. For this reason, laboratory compaction methods have been developed to simulate the field compaction process in the laboratory.

The Mod AASHTO test has long been used as the laboratory compaction method of choice by virtue of its simplicity and the lack of bulky equipment required. However, previous studies have established that the Modified AASHTO method does not adequately simulate field compaction criteria especially for cohesionless materials. Two reasons have been advanced;

- The Mod AASHTO compaction method does not adequately simulate the compaction done in the field when the granular mix is laid;
- The compaction method may cause disintegration of the material.

Alternative tests have been considered and much research has focused upon the use of a modified demolition hammer (vibratory hammer) for laboratory compaction of granular materials.

This study undertook to evaluate the influence of test factors pertinent to the vibratory hammer compaction method. The influence of these test factors on compaction time and obtainable material density was assessed with the objective of developing a compaction method for granular materials. Vibratory hammer compaction tests were conducted on G3 hornfels, G4 hornfels and G7 sandstone material types and to a lesser extent, reclaimed asphalt (RA). Densities obtained were referenced to Mod AASHTO compaction density.

Findings of the study showed that, the mass of the tamping foot has a significant influence on the obtainable compaction density. Other factors such as, moisture content, frequency and frame rigidity were also found to affect compaction with the vibratory hammer. In addition, it is shown that the surcharge load does not significantly influence the obtainable compaction

density but does contribute to the confinement of the material and restricts the upward bounce of the hammer.

On the basis of the results and findings, a compaction method was proposed, incorporating test parameters and factors that would provide ideal results for a set compaction time. Repeatability tests showed that, the developed vibratory hammer compaction method was effective in compacting graded crushed stone material types (i.e. G3 and G4) and probably RA. The test was not as effective on the G7 material. Further studies on this material (G7) are required.

In addition to the previous testing regime, a comparative assessment of the developed vibratory hammer compaction method in relation to the vibratory table method was done. The results show that the vibratory hammer is capable of producing specimens of densities comparable to those of the vibratory table.

A sieve analysis undertaken before and after compaction showed that compaction with the developed vibratory hammer compaction method does not result in any significant material disintegration.

Based on the results of this study, a specification for the determination of maximum dry density and optimum moisture content of granular material using the vibratory hammer is recommended.

OPSOMMING

Kompaksie is een van die belangrikste prosesse in die konstruksie van die padplaveisel. Dit is nie net waardevol vir die versekering van strukturele integriteit van die materiaal, maar dit het ook 'n invloed op die ingenieurseienskappe en vermoë van die grond materiaal. 'n Swak gekompakteerde materiaal word gekenmerk deur 'n laë digtheid, hoë porositeit, on onvoldoende skuifweerstand. Die kenmerke maak die material vatbaar vir vogen. Lei tot spoorvorming, slaggate, golwe en deurgangs probleme op die pad. Dit is dus uiters noodsaaklik dat veld kompaksie korrek gedoen word. Om hierdie rede, is kompaksie metodes in die laboratorium ontwikkel om sodaend veldkompaksie te simuleer.

Die “Mod AASHTO” laboratorium kompaksie toets is die gekose laboratorium kompaksie metode op grond van sy eenvoudigheid en gebruik van minimale toerusting. Vorige studies het egter bevestig dat die “Mod AASHTO”-metode nie veldkompaksie akkuraat kan simuleer nie, veral vir kohesielose materiaal. As gevolg van twee hoofredes;

- Die Mod AASHTO kompaksiemetode is nie ‘n realistiese en vergelykende simmulering van kompaksie soos dit in die veld gedoen word nie;
- Die kompaksie metode mag verbrokkeling van die materiaal veroorsaak.

Alternatiewe toetse was oorweeg en baie navorsing het gefokus op die gebruik van 'n aangepaste vibrerende hamer.

Hierdie studie het onderneem om verskeie relevante toetsfaktore van die vibrerende hamer en hul invloed op die kompaksie en verkrygbare digtheid te bestudeer. Die invloed van hierdie toetsfaktore op kompaksietyd en verkrygbare materiaal digtheid was geassesseer met die doel om 'n kompaksiemetode vir granulêre materiaal te ontwikkel.

Vibrerende hammer kompaksietoetse was uitgevoer op G3 hornfels, G4 hornfels en G7 sandsteen materiaal en tot 'n mindere mate herwinde asfalt. Digthede verkry was verwys na die Mod AASHTO kompaksie digtheid. Resultate van die studie het getoon dat die gewig van die stamp voet ‘n merkwaardige invloed het op die verkrygbare kompaksie digtheid. Ander faktore soos voginhoud, frekwensie en raam styfheid het ook getoon om kompaksiedigtheid te beïnvloed met die vibrerende hammer. Benewens was ook getoon dat die toeslaglading geen beduidende invloed het op die verkrygbare kompaksie digtheid nie, maar wel bydrae tot die inperking van die materiaal en verhoed die vertikale terugslag van die hammer.

Gebaseer op die resultate en bevindinge was ‘n kompaksiemetode voorgestel wat toets parameters integreer met toetsfaktore en tot volg ideale resultate vir ‘n gegewe kompaksietyd voorsien. Herhaalde kalibrasie toetse het getoon dat die ontwikkelde kompaksiemetode effektief is in die kompaktering van gegradeerde gebreekte klip materiaaltipes (G3 en G4) en moontlik herwanne asfalt. Die toets was nie so doeltreffend op die G7 materiaal nie. Verdere studies op hierdie materiaal (G7) is dus nodig.

Addisioneel tot die vorige toets, is bevind dat ‘n vergelykende assesering van die ontwikkelde vibrerende hammer kompaksiemetode in verhouding tot die vibrerende tafel. Die resultate wys dat die vibrerende hammer die vermoë het om toetsmonsters met digthede vergelykbaar met die vibrerende tafel te produseer.

Sifanalise voor en na kompaksie het getoon dat verdigting met die ontwikkelde vibrerende hamer kompaksie metode nie lei tot die disintegrasie van die materiaal nie. Gebasseer op die resultate van dié studie was ‘n spesifikasie vir die bepaling van maksimum droé digtheid en optimale voginhoud van granulêre material aangeraai.

ACKNOWLEDGEMENTS

Dave Thomas, an American businessman once said “Many people believe that support is something that you give to someone you feel sorry for or that it means propping up someone who would fail unless you were there to give him a boost. But that's not the way I see it. Support is the boost you can give someone who can help himself but who needs a partner to open a window or push aside a roadblock”. I agree with Dave Thomas and would therefore like to express my sincere gratitude and appreciation to the Beit Trust Organisation for pushing aside the roadblock and providing the financial and material support for my studies.

My studies at Stellenbosch University have not been without challenges; thankfully I have had wonderful support from a whole lot of people. I would therefore, like to thank the under listed, who have helped me in more ways than one, through out my time at Stellenbosch University:

- My study leader, Prof. Kim Jonathan Jenkins for guidance, counsel and mentorship.
- Ms Chantal Rudman, my co-study leader, for guidance, kind assistance and support.
- Dion Viljoen and Johan Muller of the technical/mechanical support at Stellenbosch University for building the new frame.
- BSM Laboratories (Pty) Ltd for providing the scarifying tool
- Laboratory technicians Gaven Williams and Colin Isaacs, for helping with material acquisition and general assistance in the lab.
- Dr Anton Du Plessis of the Central Analytical Facilities for aiding with the CT scans.
- Bevans Burns for information on the operability of the vibratory hammer
- Janine Myburgh, Alett Slabbert and Amanda de Wet for kind and tireless assistance.
- My family for the encouragement and support.
- Course mates, friends and colleagues too numerous to mention, I thank you all for the wonderful interactions.

Lastly and most importantly, I would like to express my sincere gratitude and appreciation to God the Almighty for being with me throughout my life and guiding me in all my endeavours.

TABLE OF CONTENTS

LIST OF TABLES

LIST OF FIGURES

LIST OF PLATES

ABBREVIATIONS AND ACRONYMS

ASTM	American Standard Test Method
BS	British Standard
BSM	Bitumen Stabilised Materials
CAF	Central Analytical Facilities
CCC	Continuous Compaction Control
CSIR	Council for Scientific and Industrial Research
FD	Fraction Density
GM	Grading Modulus
GPS	Global Positioning System
IC	Intelligent Compaction
ICMV	Intelligent Compaction Measurement Value
MDD	Maximum Dry Density
Mod AASHTO	Modified American Association of State Highways and Transport Officials
MV	Measurement Values
NZS	New Zealand Standard
OMC	Optimum Moisture Content
OMC_M	OMC obtained from Mod AASHTO Compaction
QA	Quality Assurance
QC	Quality Control
RA	Reclaimed Asphalt
RFR	Rigid Frame
RTK	Real Time Kinematic
SA	South Africa
SAPDM	South African Pavement Design Model
SBD	Shakedown Bulk Density
SD	Space occupied by Solid Particles
SFR	Soft Frame
SU	Stellenbosch University
TMH	Technical Methods for Highways
WFD	Weighted Fraction Density
ZAV	Zero Air Voids

CHAPTER 1: INTRODUCTION

1.1 BACKGROUND

Compaction is one of the key processes in the construction of road pavement layers. Not only is it significant in ensuring the structural integrity of the material in the road layers, but it also has an influence on the engineering properties and performance of the soil material. A poorly compacted material is characterised by low density, high porosity, below standard shear strength and is susceptible to moisture. This as a result causes rutting, potholing, corrugations and passability problems on the road. Therefore, it is vitally important that field compaction is done correctly. For this reason, laboratory compaction methods have been developed to simulate the field compaction process in laboratory.

Laboratory compaction tests not only allow for the determination of material engineering properties and performance through tests such as the tri-axial test, but also provide the basis for determining the degree of compaction and moisture requirements to achieve the required engineering properties of the soil in the field. There are various methods by which a material can be compacted. These methods are based on the way the load is applied and include; static, impact, vibratory, gyratory and kneading. These methods are explained in detail in Section 2.3.4.

Laboratory compaction tests are meaningless unless they are able to simulate the field compaction process they are intended to represent. The greatest care should be taken that the field behaviour is reproduced in the laboratory; otherwise the laboratory results will have little significance in the field process which is supposedly being studied. This could lead to serious consequences regarding the practical conclusions and would mislead engineers who rely principally on the results of the laboratory tests for making decisions concerning the field compaction process (Rodriguez, Castillo and Sowers, 1988).

Some of the laboratory compaction methods in use presently include (among others); The Modified American Association of State Highway and Traffic Officials (Mod AASHTO Test), Marshall Hammer, Gyratory compaction, Vibratory Table and Vibratory Hammer. Both the Mod AASHTO and Marshall Hammer are impact compaction methods whereas the Vibratory Hammer and Vibratory Table are based on vibration.

1.2 RATIONALE

The Mod AASHTO test has long been used as the laboratory compaction method of choice by virtue of its simplicity and the lack of bulky equipment required. Speedy inspection tests can be done using portable tools which can also be taken to site, thus the test is used for field compaction control. However, studies have shown that the Mod AASHTO method is not the best method of simulating field compaction especially for cohesionless materials. Passeto and Baldo (2004) highlighted two reasons in this regard;

- The compaction method characteristic of the Mod AASHTO does not adequately simulate the compaction done in the field when the granular mix is laid;
- The compaction method may cause disintegration of the material.

Apart from the Mod AASHTO test, the vibratory table test is another method detailed in Technical Methods for Highways 1 (TMH1) for compaction of granular material. However, the use of vibratory tables is limited. This is probably because vibratory tables are not portable and their operation is tasking. In fact, in many instances the vibratory table test method is disregarded and Proctor (AASHTO) tests are performed in its place due to ease and familiarity (Melton and Morgan, 2010). Alternatives tests for compaction of granular material have been considered and much research has focused upon the use of a modified demolition hammer (vibratory hammer) for laboratory compaction. This study builds upon recent research conducted at Stellenbosch University on compaction of granular material using the vibratory hammer.

1.3 PROBLEM STATEMENT

Research previously conducted at Stellenbosch University (SU) led to the development of a protocol for the compaction of both Bitumen Stabilised Material (BSM) and granular materials using the vibratory hammer (Kelfkens, 2008). Variability in results were, however, noted when the compaction method was used at a commercial laboratory (BSM Laboratories (Pty) Ltd). While compaction to 99% of Mod AASHTO density could be achieved with the vibratory hammer at SU, only 95% of Mod AASHTO density could be achieved at the BSM Laboratories (Pty) Ltd. In addition, a significant amount of variability in the test results for different types of material were noted. The disparity in these results necessitated further investigation into the variables that might influence compaction with the vibratory hammer.

1.4 RESEARCH OBJECTIVE

A reliable laboratory test method must produce results that are both repeatable and reproducible. Repeatability is defined as the capability of producing almost identical results by several rounds of measurement done by the same technician, using the same test method, the same equipment and in the same laboratory. Reproducibility on the other hand is defined as the capability of producing almost identical results using the same test method but with different technicians in different laboratories using different equipment (Livneh, 1994 and Shahin 2010).

Results obtained with the vibratory hammer at SU could not be reproduced at the BSM Laboratories (Pty) Ltd.

The objective of this research is to explore the viability of using the vibratory hammer compaction method with granular materials to manufacture laboratory specimens. Investigations focus on the quality of specimens achieved (primarily the density) and the cause of variability observed in the various test results. A number of factors influence the quality of specimens manufactured with a vibratory hammer. The first is the natural variability in the properties and mineral constituents of the material, where samples taken from the same source and tested under the same conditions yield different results. The second is the test conditions of the experiment (i.e. surcharge, mould size, experience of technician etc) (Shahin, 2010). The latter can be further subdivided into random and systematic errors. Random errors may be caused by unknown and unpredictable changes in the experiment. These (random errors) often have a normal distribution and statistical methods may be used to analyze the results. Systematic errors may result from problems with the measuring instrument or data processing or human errors in the use of the instruments. This research focuses on a number of aspects related to both factors.

To achieve the research objectives, the following was done;

- Investigate the vibratory hammer compaction for a variety of granular material containing plastic and non-plastic fines as well as reclaimed asphalt (RA).
- Investigate the influence of various factors including moisture, frequency, surcharge, frame rigidity and mass of tamping foot on obtainable density.
- Investigate interlayer bond resulting from different scarifying methods.

- Propose a compaction method for the compaction of granular material using the vibratory hammer.

Tests with three different methods; Mod AASHTO, vibratory hammer, and vibratory table, were conducted in order to establish a broad base for comparison of the various compaction methods. 150mm diameter x 300mm high triaxial specimen were manufactured using the vibratory hammer and vibratory table. The densities were referenced to the Mod AASHTO density.

1.5 LAYOUT OF THE REPORT

The layout of the thesis is as follows:

Chapter 1 gives the background to the research. The rationale for carrying out this research, the problem statement and objectives of the research are stated.

Chapter 2, Literature Study: details the theory and principles of compaction. An account is given of the fundamentals of laboratory and field compaction relevant to the study. Recent research on the vibratory hammer as well as literature on the British, New Zealand and American standards for vibratory hammer compaction is reviewed. An introduction of the latest advancements in field compaction equipment is also accounted for.

Chapter 3 describes the experimental design. An account is given of the material characteristics, test setup and procedures followed in the preparation and testing of materials. Chapter 4 presents the exposition of the results and findings of the tests. The study is concluded in Chapter 5 and recommendations made in Chapter 6.

REFERENCES

KELFKENS R.W.C, 2008. **Vibratory Hammer Compaction of Bitumen Stabilised Material.** Dissertation for Master of Science in Engineering, University of Stellenbosch.

LIVNEH M. 1994. **Repeatability and Reproducibility of Manual Pavement Distress Survey Methods.** 3rd International Conference on Managing Pavements

MELTON J.S. and MORGAN T., 1996. **Evaluation of Tests for Recycled Material Aggregates for Use in Unbound Application**, Final Report for RMRC Project No. 6, Recycled Materials Resource Center, Durham, N.H.

PASETTO M, and BALDO N, 2004. **Comparative analysis of compaction procedures of unbound traditional and non-conventional materials**, Taylor & Francis Group, London, ISBN 90 5809 699 8. –Pavement Unbound

RODRIGUEZ A.R., del CASTILLO H and SOWERS G.F., 1988. **Soil Mechanics in highway Engineering**. Trans Tech Publications, Republic of Germany.

SHAHIN W. A, 2010. **Investigation of the variability in the results of the NZ vibrating hammer compaction test**. Dissertation for Master of Science in Engineering, University of Auckland, New Zealand.

CHAPTER 2: LITERATURE STUDY

2.1 INTRODUCTION

This Section of the report details the general theory and principles of compaction. Included is a discussion of the vibratory hammer laboratory compaction method (which is the subject of this research), the MOD AASHTO compaction (against which the densities were referenced) and the vibratory table method (used for comparison purposes). Field compaction is also discussed in Section 2.3.7 along with compaction control.

2.2 PAVEMENT STRUCTURE

Roads are constructed from layers of compacted materials which generally increase in quality through the pavement layers to the road surface (Figure 2-1) (Hill, Dawson and Mundy, 2001). Road pavements comprise three basic components (Wirtgen, 2010);

- Surfacing: The riding surface which is usually the part of a road that is visible
- Structural Layers: The load spreading layers, consisting of different materials, often extending to depths in excess of one metre.
- Subgrade: The existing "earth" upon which the road is built.

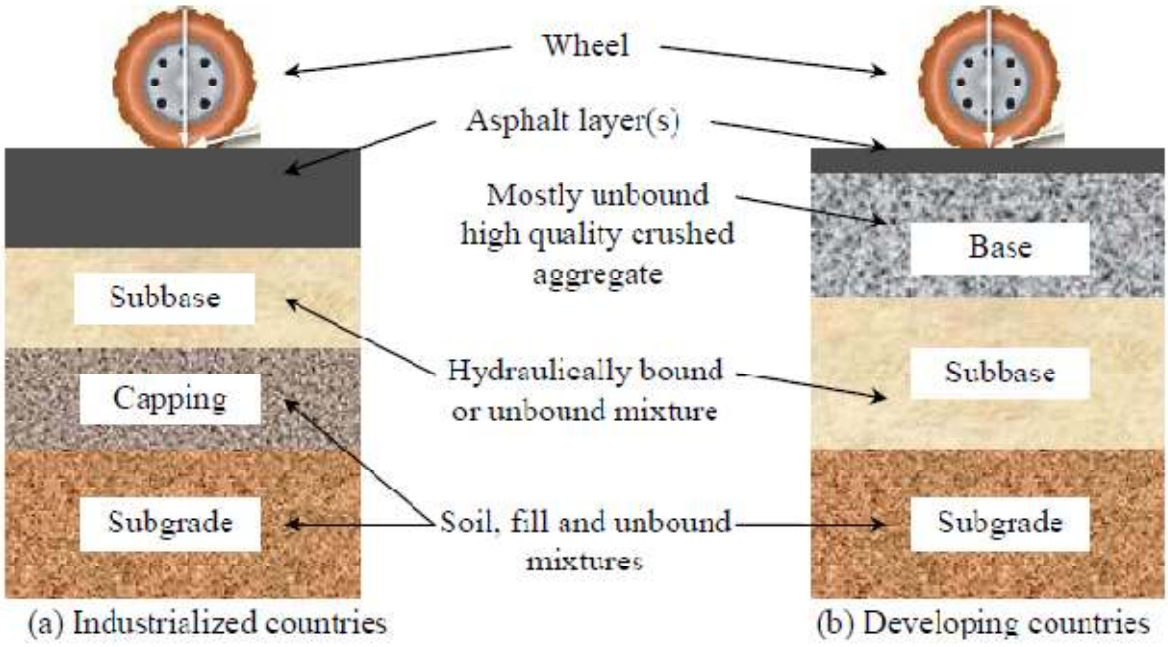

Figure 2-1: Schematic pavement structure, typical sections and material options (Araya, 2011)

The surfacing is the pavement's interface with the traffic and the environment. In most developing countries, for economic reasons, the surfacing layer is very thin with a limited structural function. It mainly provides protection against water ingress and traffic abrasion (Araya, 2011). A road's rideability (evenness), colour, skid resistance and water resistance are the main characteristics of a surfacing layer/wearing course. The structural layers help transfer the load from the surface to the subgrade. Each layer is designed to support the weight of the layers placed on it plus part of the loading applied. Therefore each layer must be constructed of the right material and be of proper thickness and density. If one layer is not strong enough, the road fails. The structural make up of the road is such that upper layers are stiffer than lower layers leading down to the subgrade which is the weakest of them all. Therefore, the stresses applied by a wheel at the surface (Figure 2-2) are effectively reduced within the pavement structure by spreading them over a wide area of the subgrade (Wirtgen 2010).

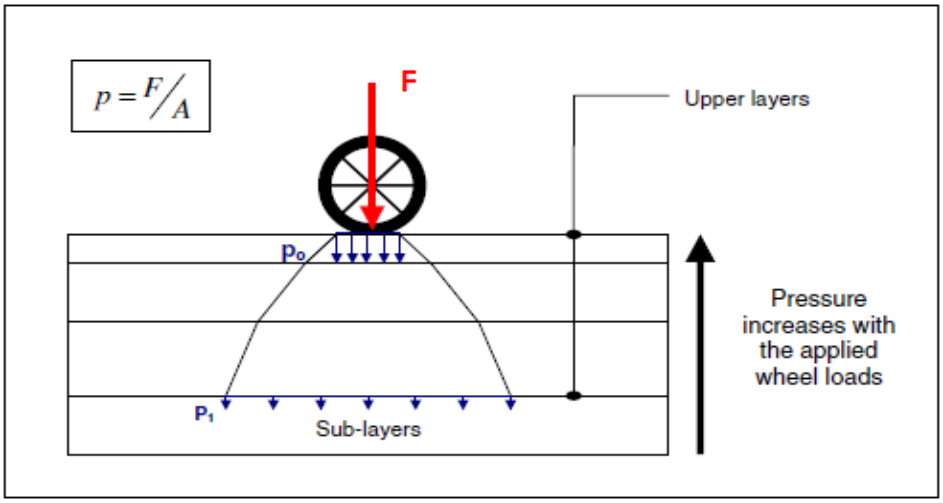

Figure 2-2: Load transfer through pavement layers (Wirtgen, 2002)

2.3 COMPACTION

Pavement layer compaction during construction has a major effect on the structural bearing capacity of a pavement. A well compacted material will have high strength (i.e. bearing capacity) and hence increased load spreading ability and resistance to permanent deformation. In addition, potential ingress of water into the pavement layer is also restricted as a result of the close packing (densification) of the material. Effective compaction is therefore one of the most economical methods to improve the structural capacity of pavements (TRH 4, 1996).

2.3.1 Definition of Compaction

Compaction is defined as the mechanical densification to improve the strength, reduce the compressibility and enhance the rigidity of soils. It usually entails a fairly rapid reduction in the void volume and a corresponding reduction in the volume of the soil. These changes are usually equal to the loss in volume of air, as water is seldom driven out of the voids during the process (Rodriguez, Castillo and Sowers, 1988).

The degree of compaction is measured by the dry unit weight of the compacted material. A denser and more compacted material is able to support heavier loads without deforming (bending, cracking, moving). This is because compaction brings about a closer arrangement of soil particles (Figure 2-3). The subgrade material which supports a heavy structure must be very dense or it will compact even more under load, causing the structure to settle (SPECIALTY SALES LLC, 2011).

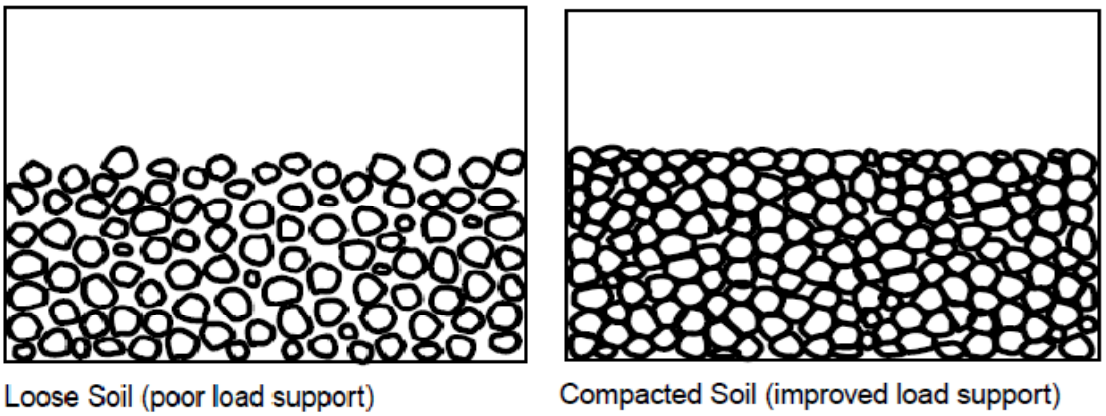

Figure 2-3: Loose Soil Structure and Compacted Soil Structure (Carson, 2004)

2.3.2 History of Compaction

'The effects of soil compaction have been recorded since the 1800s when Benjamin Lincoln of New England wrote about the consequences of letting livestock wander and graze throughout wooded areas. Benjamin noticed that the weight of livestock contributed greatly to the compaction of soil particles, hardening soil to the point where little or no oxygen could be contained, and resulting in the death of plant life in the surrounding areas. Livestock was, for better or worse, used for compacting soil in agricultural communities until the arrival of compaction equipment. Even the use of horses and mules to pull carts and wagons affected the soil to the point of compaction' (Ritchiewiki, 2011).

'The effect of new technology through the introduction of machinery made compaction equipment beneficial to many construction applications. Compaction equipment, such as rollers and compactors, can be traced as far back as the 1700s when French pioneer Nicholas Cugnot invented a self-propelling steam traction engine. The first steam roller appeared in France in 1860 and made its way to America, thanks to Aveling & Porter. Motor rollers dominated the 1900s and compactors appeared shortly thereafter' (Ritchiewiki, 2011).

2.3.3 Objectives of Compaction

Carson (2004) and Shahin (2010) discuss the fundamental objectives for compacting soil;

- Increase strength and hence load bearing capacity of the soil.
- Prevent frost damage of the material.
- Reduce compressibility i.e. reducing the potential of long term settlement of fills and soils (provide stability).
- Reduce permeability i.e. restraining flow of water through the soil layer. Hence avoiding swelling and contraction of the soil.
- Reduce void ratio; helps prevent water from being withheld by the material thus maintaining strength and stiffness properties.

2.3.4 Types of Compaction

Compaction processes can be classified under the following categories;

Impact compaction

Impact compaction involves dropping a hammer of a known weight through a set height onto the soil (Shahin, 2010). This is typical of impact rollers in the field. Impact rollers (Plate 2-1) can impart as much as 25kJ of energy to the ground per blow with depth of influence exceeding 5m in certain material (Jumo and Geldenhuys, 2004). The Marshal hammer is a typical laboratory impact compaction test.

Plate 2-1: Impact Roller (Jumo and Geldenhuys, 2004)

Static compaction

Static compaction involves compressing a pre-weighed specimen in a cylindrical mould by placing it in a compression testing machine and applying compression forces until maximum density is reached (Shahin, 2010). Static smooth-wheeled rollers and static sheepsfoot (or pad-foot) rollers incorporate this principle.

Kneading compaction

Kneading compaction rearranges particles into a more dense mass by squeezing particles together. The process is especially effective at the surface of the lift material. The longitudinal and transverse kneading action is essential when compacting heavily stratified soils such as clay type soils. It is also the desired process for the compaction of the final wearing surface of an asphalt pavement. The kneading action helps to close the small, hairline cracks through which moisture could penetrate and cause premature pavement failure. Sheepsfoot rollers and staggered wheel, rubber tyred rollers are specifically designed to deliver such type of compactive force.

Gyratory compaction is a type of laboratory compaction that simulates the kneading process. It was developed by the Department of Transport (formerly Texas Highway Department) and later improved by the U.S Army corps of Engineers. The kneading action of the gyratory

compactor is coupled with a long loading time and lower stiffness response, which encourages compaction of visco-elastic materials. It is hardly used for compaction of granular material. The Gyratory compactor has been used for compaction of visco-elastic material since the early 1930s. Compaction is achieved by the application of a vertical stress via end platens to a known mass of material within a 100 or 150mm internal diameter mould. The longitudinal axis of the mould is rotated (gyrated) at a fixed angle to the vertical whilst the platens are kept parallel and horizontal. The original gyratory compactor has since been modified into the Superpave gyratory compactor by lowering its angle and speed of gyration and adding real-time specimen-height recording capabilities (Yildirim et al, 2000).

Vibratory compaction

Vibratory compaction incorporates an engine-driven mechanism to create a downward force in addition to the machine's own weight. Vibratory compaction, through the vibrations, sets particles in motion, moving them closer together resulting in a denser packing of the material. The vibrations affect both the top layers as well as deeper layers (Carson, 2004). The vibratory hammer and vibratory table both work on the principle of vibratory compaction.

2.3.5 Factors that Affect Compaction

Compaction forces are applied to overcome frictional forces between particles in a soil. These (forces) otherwise tend to resist this compactive effort. The magnitude of the frictional forces will vary depending on soil type, moisture conditions, particle shape, plasticity and gradation. Sections 2.3.5.1 to 2.3.5.8 discuss some of the factors that affect compaction.

2.3.5.1 Moisture

Moisture acts as a lubricant during compaction allowing material particles to slide past each other to achieve the desired density. Too little moisture impacts negatively on this lubrication effect resulting in inadequate compaction. Conversely, too much moisture leaves water filled voids in the material after compaction. This reduces the load bearing capacity of the material (Kelfkens, 2008). For a given soil and using a particular compaction method, there is an optimum moisture content which produces the maximum dry unit weight obtainable with that procedure.

By compacting the soil material at varied moisture contents and measuring the dry densities at these moisture contents, a relationship between the dry density and moisture content can be

established (Figure 2-4). The optimum degree of compaction for a specific compactive effort is the highest density (Maximum Dry Density (MDD)) obtainable when the compaction is carried out on the material at varied moisture contents. The moisture content at which the highest density is obtained is called the Optimum Moisture Content (OMC) (TMH1, 1986).

Rodriguez, Castillo and Sowers (1988) explain the concept of Optimum Moisture Content; it is suggested that optimum moisture can be illustrated by the effect of moisture on the soil grains. In fine grained soils at low water contents, the water occurs in capillary form, producing tension between the particles and lumps that cannot be easily broken. This makes compaction difficult. An increase in water content reduces the capillary tension, softens the lumps and makes the soil easy to compact. If however, the water content is so great that there is free water, so that the voids in the soil are nearly filled, the soil cannot be compacted because water cannot be instantaneously squeezed out. The optimum moisture is a compromise between additional moisture enhancing soil grain mobility and added moisture interfering with void reduction.

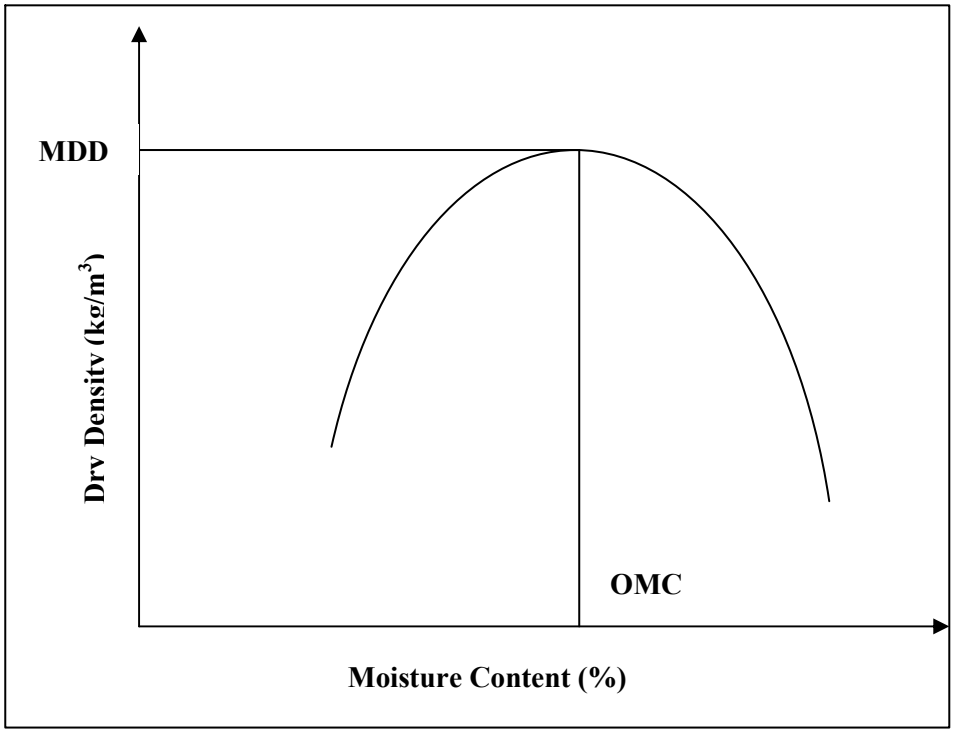

Figure 2-4: Typical Density- Moisture Relationship (Craig, 2004)

2.3.5.2 Soil Type

Different soil types behave differently with respect to maximum density and optimum moisture. Therefore, each soil type has its own unique requirements and controls both in the field and for testing purposes (Carson, 2004). Three basic soil groups can be identified in this regard;

- Cohesive
- Organic
- Cohesionless (Granular)

Cohesive soils have a particle size ranging from 0.001 to 0.06mm and include Clay and Silt. These soils are dense and tightly bound together by molecular attraction. Impact compaction methods are better suited for such type of soil (Drnevich Evans and Prochaska, 2007). Proper water content, evenly distributed, is critical for compaction (Carson, 2004). The typical relationship illustrated in Figure 2-4 is observed after compaction of cohesive soils. The MDD is that at the peak of the curve and the corresponding moisture content, the OMC. These values obtained in the laboratory are subsequently used as target values for field compaction.

Organic soils are not suitable for compaction and are therefore not discussed further.

Cohesionless soils (also called Granular soils) have size ranging from 0.06 to 60mm and include Sand and Gravel. They are typically known for their water draining properties thus pore water pressures do not build up during the compaction process (Rodriguez, Castillo and Sowers, 1988). Because of the cohesionless nature of these materials, Impact compaction is not an appropriate compaction mechanism for their compaction. Particles simply displace under each hammer drop when impact compaction tests are performed. Sand particles rearrange with each successive impact, but not much densification may occur. Granular material need confinement in order to be compacted effectively and vibration is the most efficient way to provide for reorientation of sand grains into a denser packing (Drnevich, Evans and Prochaska, 2007).

D'Appolonia et al (1969 cited in Drnevich, Evans and Prochaska, 2007) explain the mechanism through which compaction of granular soils occurs by vibration. It is suggested

that two different compaction mechanisms are at work; when sufficient acceleration is present, grains with less confinement are subjected to a free-fall and then an impact with each cycle of vibration that efficiently reorients the grains into a denser packing. Particles with greater confinement never experience free-fall and are densified less efficiently through cycles of dynamic stresses. For particles with no confinement though, vibrations cause chaotic motion and the soil is actually loosened.

2.3.5.3 Particle Size Distribution

The stability of an unbound granular layer is derived mainly from particle interlock and surface friction. The particle size distribution is therefore an important characteristic for strength determination (Siswosoebrotho, Widodo and Augusta, 2005). The particle size distribution of the material (i.e. coarse, fine, well-graded or poorly-graded) has a direct influence on all the engineering properties (i.e. MDD and OMC) (Semmelink, 1995). Therefore, well-graded material will have higher MDD compared to uniform material as shown in Figure 2-5.

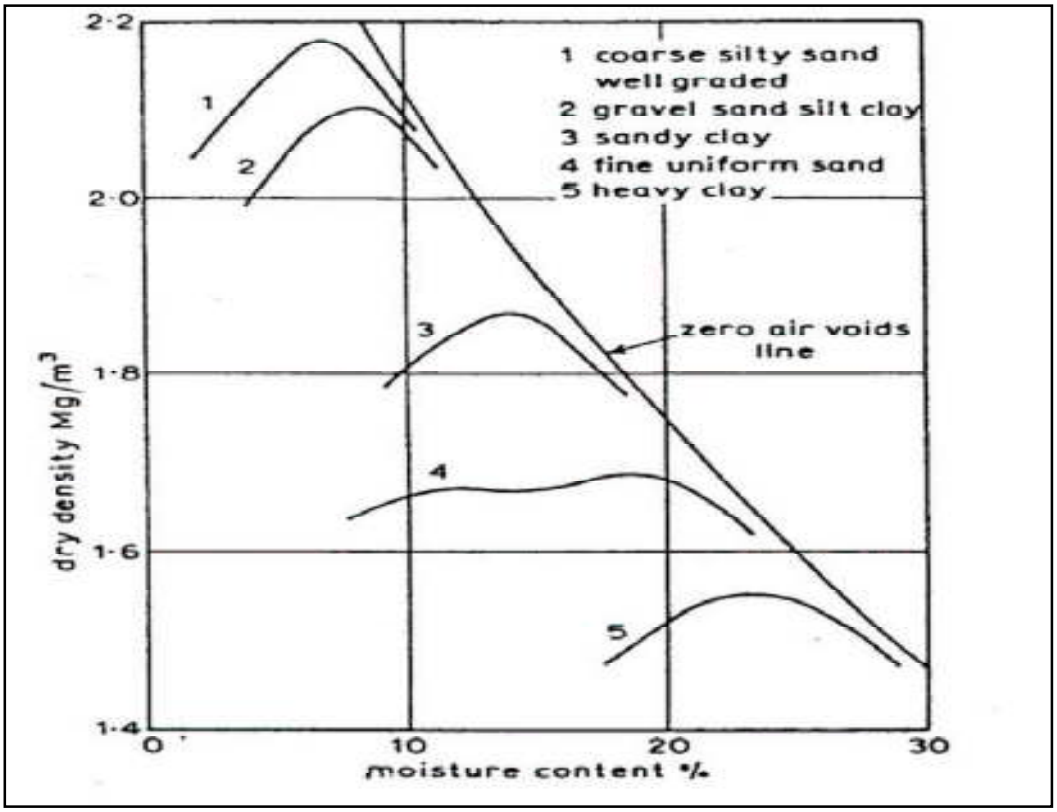

Figure 2-5: Compaction curves for some typical soils (Huang, 2003)

Research by Nijboer (1948 as cited by Vavrik, 2000) showed that the ideal grading for maximum packing of aggregate occurred with the Fuller equation raised to the power of 0.45. The Fuller equation is;

$$P = 100 \text{ x } \left(\frac{d}{D}\right)^{n}$$

Where;

P = Percentage passing a sieve with opening d (mm)

D = Maximum aggregate size (mm)

n = constant (= 0.45)

In the field, material in its natural state is never found to this ideal grading. But using material with a wider range of particle sizes (well graded) will always produce a denser mix than material of uniform grading (Semmelink and Visser, 1994). This is because the amount of voids in the uniformly-graded material is much greater than that in a well graded material. In a well graded material, the fine particles fill up the voids between the coarse particles and this leads to a much denser arrangement of particles and thus higher dry densities (Semmelink, 1995).

The Zero Air Voids (ZAV) line indicated in Figure 2-5 is a unique line for a given specific gravity of soil solids. The ZAV dry unit weight at a particular moisture content is the theoretical maximum value of dry unit weight, which means that all the voids spaces of the compacted material are filled with water. No portion of the dry density-moisture curve can lie to the right of the ZAV (Craig, 2004).

2.3.5.4 Particle Shape and Texture

Research has shown that particles with higher angularity will result in better interlock upon compaction. Similarly, Semmelink and Visser (1994) point out that particle interlock at points of interparticle contact is much greater for particles with a harsh surface texture than with a smooth one. However, the shape and texture factors that resist shearing also resist compaction. Higher compactive efforts are therefore required to compact angular aggregates with a harsh surface texture to the same density as a rounded aggregate with a smooth surface texture.

Semmelink (1995) explains the two simple yet effective parameters to quantify the effect of particle shape and texture, namely the weighted fraction density (WFD) and the shakedown bulk density (SBD). 'For the WFD each sieved fraction of a particular material is separately shake tamped in a plastic measuring cylinder until the volume reaches a minimum (i.e. there is no discernable change in volume or the volume starts to increase again). Depending on the particle size, different sizes of cylinders are used (diameter = approximately 4 times the particle size or larger). The aim is to get the tightest packing (smallest volume) without applying a force on top of the sample and the amount of tamping energy is therefore not fixed. The fractional density (FD) of each fraction is then determined by dividing the mass of the fraction by its minimum volume and expressing this as a percentage of space occupied by the solids (i.e. % SD). The WFD is then determined for the total grading by multiplying the FD value of each fraction by its fractional contribution by mass to the total grading' (Semmelink, 1995).

'The SBD of the total sample is determined by pouring the total sample into a large plastic measuring beaker (5 litre) and shake tamping it until the volume is a minimum. In the case of materials containing +4.75mm material, the sample is first divided into two fractions, namely the +4.75mm material and -4.75mm material. The +4.75mm material is placed in the bottom of the beaker and levelled, where after the -4.75mm material is placed on top and the sample shake tamped. This is done to get a smooth surface on top; the fines work their way down into the voids during the shake-tamping of the sample. The SBD is the density of the shake tamped sample (i.e. mass divided by volume) expressed as a percentage of the space occupied by solids (i.e. SD)' (Semmelink, 1995).

2.3.5.5 Fines Content and Plasticity Index

'The density and hence stability of an aggregate material is affected by the amount of fines contained in it. An aggregate with little or no fines gains stability from grain-to-grain contact (Figure 2-6a). It is characterised by a relatively low density but is pervious and not frost susceptible. This material is however difficult to handle during construction because of its non-cohesive nature. An aggregate that contains sufficient fines to fill all voids between the aggregate grains will still gain its strength from grain-to-grain contact but has increased shear resistance (Figure 2-6b). Its density is high and its permeability is low. This material is moderately difficult to compact but is ideal from the standpoint of stability. As shown in Figure 2-6c, material that contains a great amount of fines has no grain-to-grain contact and

the aggregate merely 'float' in the soil. Its density is low; it is practically impervious and it is frost susceptible. In addition, the stability of this type of material is greatly affected by adverse water conditions. Paradoxically, the material at times is quite easy to handle during construction and compacts quite readily' (Yoder and Witczak, 1975 cited in Siswosoebrotho, Widodo and Augusta, 2005).

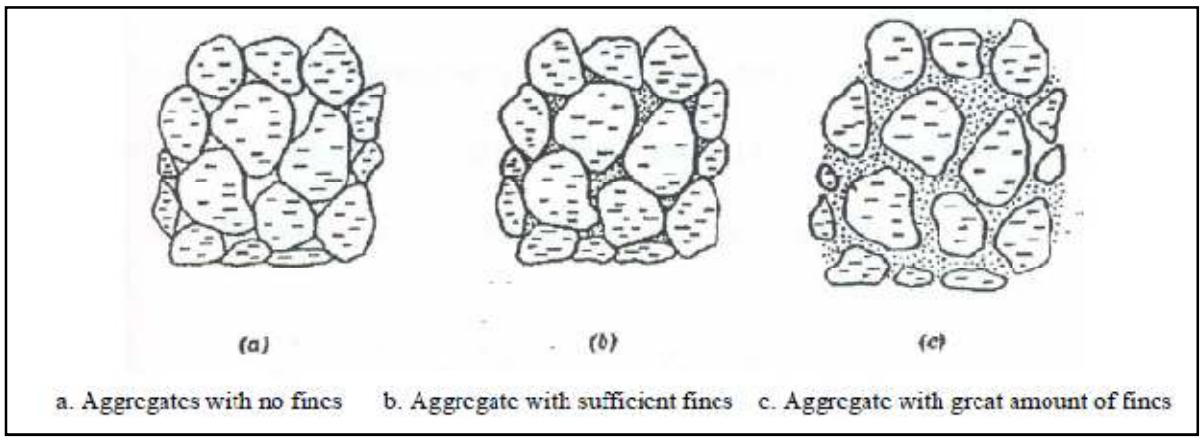

Figure 2-6: Physical states of Soil Aggregates Mixture (Yoder and Witczak, 1975 cited in Siswosoebrotho, Widodo and Augusta, 2005)

The effect of the plasticity of the fines on the density of the material shows that when the amount of fines is very low, plasticity has very little influence on density. However, as the amount of fines increases, plasticity has an increased effect. A study by Siswosoebrotho, Widodo and Augusta, (2005) showed that maximum density is obtainable at a fines content of 4% and the density reduces as the percentage of plastic fines increases.

2.3.5.6 Coarse Fraction

'The dry density increases with an increase in the percentage of coarse particles to a certain limit, beyond which it then drops. If the percentage of coarse particles is constant, but there is a change in the grain size distribution of the coarse fraction, then the maximum dry density increases as grading improves' (Rodriguez, Castillo and Sowers, 1988).

2.3.5.7 Soundness and Crushing Strength

Semmelink and Visser (1994), point out that the crushing strength is generally not a very serious problem in road building materials. The particles are generally fairly small and the contact pressure will normally be much lower than the crushing strength of the material. However, TRH9 cautions that soft materials which pulverize under the compaction

equipment should be handled with care. If possible such material should be artificially reduced by rolling to a condition near to its final state before use.

2.3.5.8 Compaction Energy

Compaction is not merely a densification process in which particles are brought closer together with an overall high dry density, but is an energy consuming process in which forces act to produce a definite result (Grobler, 1990). The higher the energy of compaction, the higher is the maximum dry density and the lower is the optimum moisture content (Figure 2-7) (Das, 2004).

Different compaction methods impart different compactive energies resulting in different dry densities and moisture content. For this reason, the MDD and OMC specifications for field compaction control must be made with a reference to the type of test method used for the laboratory compaction process (Drnevich, Evans and Prochaska, 2007).

For field compaction, if the soil in the field is drier than the optimum moisture content, an increase in compactive energy will increase the obtainable dry unit weight. If soil in the field is much wetter than the optimum moisture content, heaving of the soil rather than an increase in compaction will occur as the compactive energy is increased (USACE, 1995).

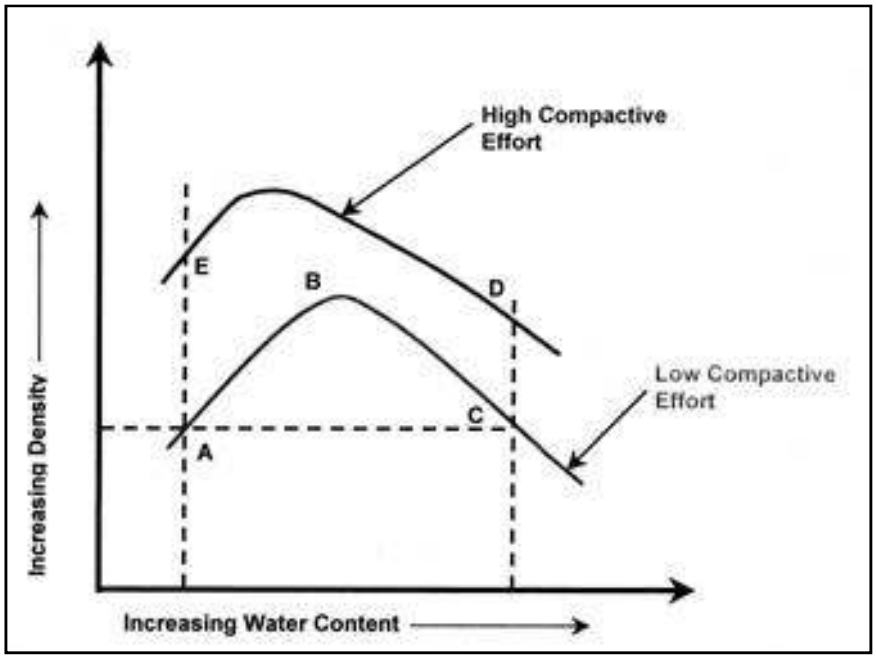

Figure 2-7: Typical Density-Moisture relationship showing varying compactive effort

2.3.6 Laboratory Compaction

Rodriguez, Castillo and Sowers (1988) explain that laboratory standard compaction tests have two main uses. First, soils are compacted to obtain data for earth structure projects; the compacted soils are tested for such properties as strength, deformability, permeability and tendency to crack. The representativity of the test is essential, in that soil specimens produced in the laboratory should represent the same mechanical properties of materials compacted in the field. The second use of the compaction test is for field quality control and this is discussed in Section 2.3.7.2. Sections 2.3.6.1 to 2.3.6.3 discuss some characteristics of the laboratory compaction methods that were studied, with emphasis placed on the vibratory hammer compaction which is the subject of this research.

2.3.6.1 Modified AASHTO

The modified AASHTO test, an improvement of the standard AASHTO test, was developed in 1958 as an ASTM standard test to take account of the advancements in field compaction equipment. The modified AASHTO test entails compacting soil at known moisture content in a 2.3cm^3 cylindrical mould of standard dimensions using a 4.5kg rammer, with a foot approximately 50mm in diameter, falling freely through a 457mm height. The soil is compacted in five (5) approximately equal layers, each layer receiving 55 blows distributed over the whole layer in 5 cycles of 11 blows each (Craig, 2004). Table 2-1 lists the differences between the standard AASHTO test and the modified AASHTO test.

Table 2-1: Differences between Standard and modified AASHTO Test (Das, 2004)

	Standard AASHTO	**Modified AASHTO**
Hammer Weight (kg)	2.5	4.5
Drop Distance (mm)	304	457
Energy (kJ/m^3)	241.4	2394.8
Number of Layers	3	5
Number of Blows/Layer	25	55
Mould Diameter (mm)	152.4	152.4
Mould Height (mm)	127	127
Mould Volume (cm^3)	2.3	2.3

Testing procedures for the standard and modified AASHTO are the AASHTO T99 and T180 respectively. The corresponding American Society for Testing and Materials (ASTM) testing procedures are D 698 and D 1557 respectively (Connelly, Jensen and Harmon, 2008). The tests are also detailed in the South African Technical Methods for Highways (TMH1) and the British Standard, BS 1377.

Engineers have realised since the late fifties that the standard and Mod AASHTO tests are not suitable for determining the dry density of all material types, particularly coarse granular material (Araya, 2011). In spite of this, the method continues to be widely used for laboratory test specimen compaction and field compaction control in Southern Africa and most parts of the world. This is due to a lack of an alternative compaction method that provides the ease and portability that comes with the AASHTO compaction methods.

2.3.6.2 Vibratory Table

Vibratory compaction is considered the most suitable method for compacting granular soils as it provides the required confinement needed for effective compaction of these soils. Full depth compaction of the specimen is achieved with this method (vibration) (Shahin, 2010). The vibratory table is an instrument currently used for vibratory compaction of granular material. In this test, a soil filled mould is fastened to a vertically-vibrating table with a sinusoid-like time vertical displacement relationship. A surcharge is applied to the surface of the soil. The mould is vibrated for a given amount of time, which varies depending on the frequency of the vibrations (Drnevich, Evans and Prochaska, 2007).

The table consists of three sections; a base, spring system and vibrating table top. The table top consists of a metal plate mounted on a steel frame with an electric motor supplying the vibratory force mounted on the bottom side of the top frame. The setup of the vibratory table at Stellenbosch University is shown in Plate 2-2. The method of compaction with the vibratory table is detailed in TMH1 Method A11T (1986).

TMH1 specifies a compaction time of two minutes on a standard vibrating table with a frequency of 47 ± 3 Hz and an amplitude of 1 ± 0.5mm. Table 2-2 gives the specifications of the vibratory table available at Stellenbosch University. The vibratory table at Stellenbosch University has a lower amplitude compared to that specified in TMH1.

Aside from the soil type, variables that influence the effectiveness of compaction using vibratory table are water content, time of compaction, amplitude of vibration, surcharge,

mould size and frequency. Tests conducted on a variety of granular material in either oven-dry or saturated condition to determine the influence of these variables on the maximum dry unit weights achieved during a vibrating table test showed that dry unit weights increased as the amplitude of vibrations increased. Also higher dry unit weights were consistently obtained in smaller mould sizes for a given soil (Drnevich, Evans and Prochaska, 2007).

Plate 2-2: Stellenbosch University Vibratory Table Setup

Table 2-2: Stellenbosch University Vibratory Table specifications

Power input (W)	1200
Impact rate (/min)	3000
Surcharge (kg)	50
Soil layers (No.)	5
Vibration frequency (Hz)	50
Vibration amplitude (mm)	0.1 - 0.4
Time of vibration (minutes)	2
Compactive Energy (kJ/m^3)	1110.3

Frequent problems that plague the vibrating table are failure to maintain calibration, wearing out of parts and sensitivity to electrical fluctuations. They are rather expensive and non-portable and tests are time consuming (Drnevich, Evans and Prochaska, 2007). Alternatives have been considered for compaction of granular material and recent research has focused upon the use of a modified demolition hammer (vibratory hammer) for laboratory compaction.

2.3.6.3 Vibratory Hammer

Originally designed for heavy duty demolition work, vibratory hammers (see Plate 2-3) are now utilised for soil compaction. Compaction with vibratory hammer is done using an electric vibratory hammer operating at a specified frequency and power rating. Soil is compacted in a cylindrical mould of standard dimensions. The vibration from the hammer is transferred into the soil through a steel rod with a circular foot (tamping foot) of nearly the same circumference as the mould. The soil is compacted in layers by the hammer action and a steady force (surcharge) applied to the vibratory hammer to prevent it from bouncing up and down on the surface of the soil. The final compacted height is measured using a steel ruler. The mass of the soil and mould is then weighed, and the weight of the empty mould subtracted from it. From these measurements of height and net weight the density can be calculated (Montgomery, 1999).

Plate 2-3: Vibratory Hammer setup at Stellenbosch University

The use of the vibratory hammer was first investigated in 1964 by Parsons A. W. According to Shahin (2010), Parsons' investigation focused on five different aspects of the test;

- type of hammer and tamper size
- magnitude of static load (surcharge) applied
- period of operation of hammer
- size and shape of the mould
- voltage supplied to the hammer

Since then, various studies on the subject have resulted in the publication or drafting of several standard test specifications in Europe, New Zealand and in the United States.

In 1967, based on Parsons work, the vibratory hammer compaction test was introduced in that year's revision of the British standard method of tests for soils of civil engineering purposes (BS 1377) (Clayton et al. 2011). The British have since adopted two test methods to accommodate a wider range of material types. BS 5835 Part 1: *"Recommendations for testing of aggregates Part 1 – Compactability of graded aggregates*" was developed due to the fact that the BS 1377 was deemed unreliable when applied to aggregates that are commonly used for road sub-base and base materials. BS EN 13286-4:2003 Part 4: *"Test methods for laboratory reference density and water content – vibratory hammer"* which was originally a European Standard was later adopted as a British Standard (Shahin, 2010). In the USA, research work by Drnevich, Evans and Prochaska (2007) led to the development of the American Society for Testing Materials' (ASTM) standard test method for the vibratory hammer (ASTM D7328-07, 2007). In New Zealand (NZ), the vibratory hammer compaction test (New Zealand Standard (NZS) 4402: 1986) has since replaced the Mod AASHTO for field compaction control (Kelfkens, 2008).

2.3.6.3.1 Vibratory Hammer Properties

A number of properties are important with regard to the vibratory hammer. These properties include the power rating, energy, amplitude and frequency. Table 2-3 gives the specifications of the vibratory hammer at Stellenbosch University.

Table 2-3: Specifications of Vibratory Hammer at Stellenbosch University

Specification	Criteria
Power Rating	1500W
Frequency	900 to 1890 beats/min (15-31.5Hz)
Point Energy	25 J

Below is a discussion of some of the properties of the vibratory hammer and their influence on compaction;

Power

'The degree of compaction, among other things is dependent on the compactive effort applied. Thus the hammer input power rating has a significant influence on the variation of the vibrating hammer compaction test results. This is due to the fact that hammers with high input power ratings apply a greater compactive effort on the specimen during compaction than a hammer with a relatively lower input power rating' (Shahin, 2010). A study conducted in New Zealand on the effect of the hammer input power found that there was a noticeable increase in dry density for hammers with higher input power ratings (Figure 2-8).

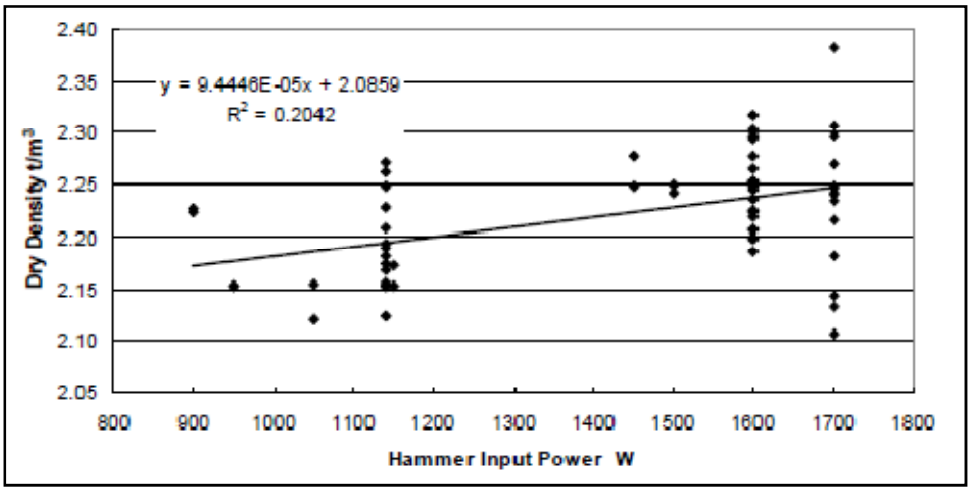

Figure 2-8: Variation of Dry Density with Hammer power rating (Opus International Consultants Ltd, 2008 cited in Shahin, 2010)

Shahin (2010) also compared the compaction resulting from two vibratory hammers; the Kango hammer with a power rating of 1700 Watts, 550 Watts more than the Metabo hammer. Significantly different results were produced from the two hammers. The more powerful

Kango hammer produced higher dry density values than the Metabo hammer. This was despite both hammers passing the calibration test specified in the New Zealand standard.

In a correlation experiment of the compaction of two vibratory hammers; a Kango hammer with a Power rating of 750 watts and a Bosch hammer with a power rating of 1500 watts, Kelfkens (2008) deduces that the more powerful Bosch hammer takes significantly less time to compact the same material to 100% of Mod AASHTO density as compared to the Kango hammer. Even though the reasons for the difference in compaction time is discussed it is highly possible that it (power rating) had a major role to play in the difference.

Compaction Energy

An appreciation of the compaction energy of the vibratory hammer is essential in understanding its compaction effects. Literature provides a number of methods for computing the compactive energy of the vibratory hammer. The first considers the the frequency of the vibratory hammer, the static weight, the amplitude, the number of layers and the compaction time. This is shown in Equation 2-1 (Weston, 2001 and Kelfkens, 2008).

$$E = \frac{Wh \times Freq \times Amp \times CompTime \times No.Layers}{1000 \times Vol.mould} \qquad \text{Equation 2-1}$$

Where;

E = Energy (kJ/m^3)

Wh = Static weight of the vibratory hammer (including tamper) (N)

Freq = frequency (Hz)

Amp = amplitude (m)

CompTime = Compaction Time (Sec)

No. Layers = Number of layers compacted

Vol. mould = Volume of the mould (m^3)

The second method for computing the compactive energy considers the point energy of the vibratory hammer. This (point energy) is the energy delivered per impact of the tamper. Point energy is machine specific and is indicated by the manufacturer. Less compaction effort is needed to obtain an equivalent level of compaction using a vibratory hammer with higher point energy compared to one with lower point energy [Twagira, 2010]. Also less compaction

time is required to compact to the same level of compaction with the vibratory hammer with higher point energy than one with lower point energy. Computation of the compactive energy using this method is illustrated in Equation 2-3 (Lange, 2005).

$$E = \frac{\text{Point Energy (J)x Freq x compTime x No.Layers}}{\text{1000 x Vol.mould}} \qquad \text{Equation 2-2}$$

Where;

E = Energy (kJ/m^3)

Vol. mould = Volume of the mould (m^3)

The first method does not consider the point energy of the vibratory hammer which clearly plays a pivotal role in determining the compactive effort required for compaction. The second method considers the point energy, however, the environment under which the hammer is able to deliver this (point) energy is not clearly defined. This is especially so considering that the hammer is meant for hand operation and is only modified for use as a compactor. The second method also does not take into account the amplitude. However, it is possible that the amplitude may have been taken into account in defining the point energy.

Frequency and Amplitude

The compaction effect of a vibration based compaction machine depends on the amplitude and frequency in addition to the static load. With regard to the vibratory hammer, frequency is the number of vibrations or the number of times the tamping foot hits the surface of the sample per unit time and amplitude is the distance that the tamping foot of the vibratory hammer moves into the sample during compaction. With high amplitude, compaction to a greater depth of material can be achieved. Conversely, low amplitude limits the depth effect, but the risk of aggregate crushing is reduced (See illustration in Figure 2-9) (Compaction Concepts, 2012).

While the amplitude of the vibratory hammer cannot be changed, most hammers provide for a number of frequency setting options. Prochaska, Drnevich, Kim and Sommer (2005) investigated the effect of frequency on the compaction with vibratory hammer. Tests were performed at 28Hz and 56Hz. It was found that the higher frequency setting produced consistently higher dry unit weights than the lower frequency setting.

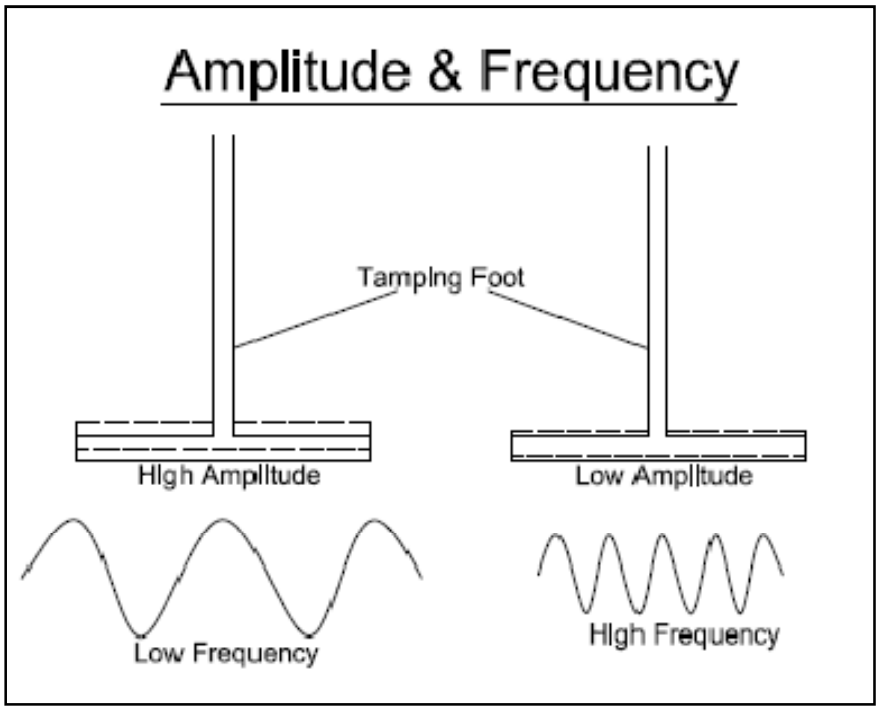

Figure 2-9: Illustration of Amplitude and Frequency

2.3.6.3.2 Vibratory Hammer Operability and Lift

Information regarding the functional mechanism of the vibratory hammer is based on a personal conversation with Mr Bevan Burns of the BSC workshop in Cape Town, South Africa. Reference is made to the schematic of the vibratory hammer parts attached in Appendix A. Shown in brackets are the part numbers.

The Bosch vibratory hammer at Stellenbosch University works on the principle of pneumatics. It has openings on the hammer pipe (35) through which air is able to penetrate. The hammer also has a control bushing (55), connected to a compression spring (29), which closes the openings and traps air in the hammer pipe when force is applied from the top. An eccentric cog wheel (72) drives a connecting rod (70) up and down the hammer pipe, compressing and decompressing the trapped air in a pneumatic action.

The air compressed by the connecting rod on its forward stroke, pushes against a striker (57) that pounds down on the attached tamping foot. On the backstroke of the connecting rod, the air is decompressed, before another stroke from the connecting rod comes in to repeat the cycle. The striker smashes down on the tamping foot over 30 times each second, so the tamping foot pounds up and down in the material around 1890 times per minute (the frequency of the hammer).

On the backstroke of the connecting rod, the tamping foot is relaxed. It is probably for this reason that vibratory hammers do not come with a set amplitude. However, an amplitude effect is created in the operation of the vibratory hammer as explained by Carson (2004). Just as most vibration based methods, compaction with the vibratory hammer takes place from top to bottom and bottom to top. As the tamper hits the soil, the impact travels to the hard surface below and then returns upward. This sets all particles in motion and compaction takes place. As the soil becomes compacted, the impact has a shorter distance to travel. More force returns to the machine, making it lift off the material higher. This lift is responsible for the amplitude effect. The magnitude of the lift is dependent on the static load of the hammer. Burns points out that the more weight (surcharge) applied on the hammer, the less efficiently it operates.

2.3.6.3.3 Vibratory Hammer Frame

Opposed to operating the hammer by hand, the frame of the vibratory hammer is important in ensuring that the hammer is guided and kept in a vertical position during compaction. This reduces the amount of physical labour required during compaction and eliminates human errors (Kelfkens, 2008).

The overriding factor in the design of the frame varies. It would appear, from the images (Figure 2-10) of the BS, ASTM and DELFT frames, that portability of the frame plays an influential role in the design. Drnevich, Evans and Prochaska (2007) point out that the (ASTM) frame can be easily disassembled and the individual parts loaded into a vehicle even by a single person. Also the 25mm thick base plate offers adequate strength, eliminating the need for a rigid foundation. Therefore, compaction tests can be performed on jobsites. However, the repeated assembling and disassembling of the frame present points of weakness in the structure of the frame. Kelfkens (2008) observed ‘shaking’ of a similar type of frame during compaction. This reduces the efficiency of compaction with the hammer as energy is lost to the shaking of the frame. This motivated the construction of a semi rigid frame (attached to rigid structure) for the hammer at Stellenbosch University (Plate 2-3). Therefore, even with portability as the overriding factor, the frame should be designed with adequate rigidity to minimise loss of energy.

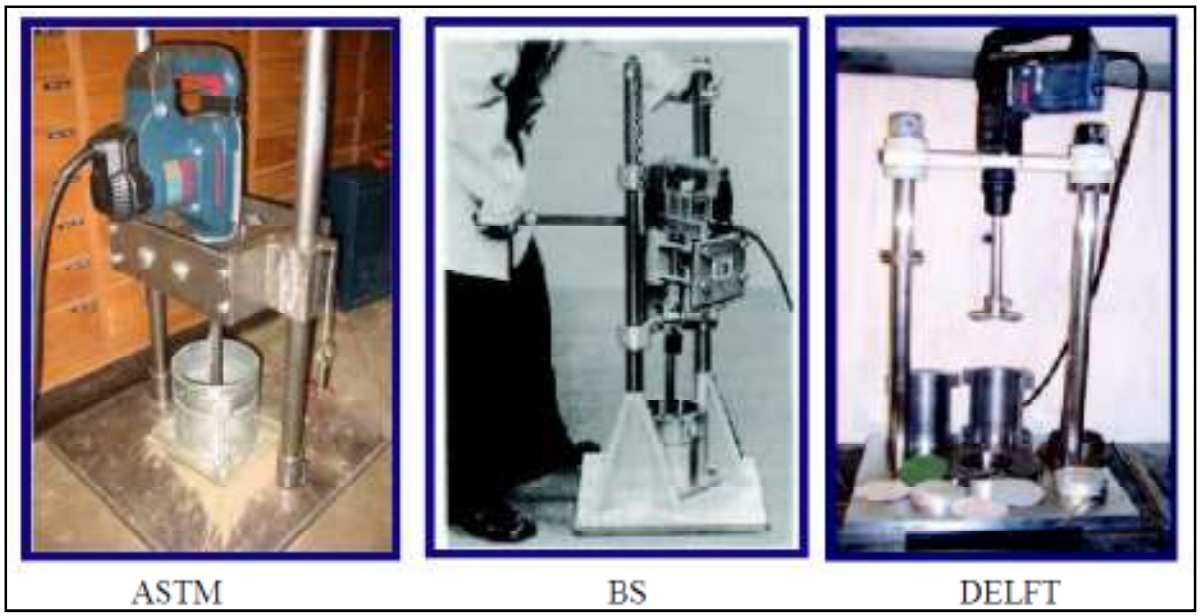

Figure 2-10: Vibratory hammer Frames for the ASTM, BS and DELFT

2.3.6.3.4 Calibration

Among other factors, the type of vibratory hammer can be a cause of variability in vibratory hammer compaction test results. Different vibratory hammers (with different specifications) are likely to produce different results. This is evident in both Kelfkens' (2008) and Shahin's (2010) research work where comparative tests with two different hammers produced different results. To ensure reproducibility of results, it is imperative that the environment under which the test is performed is consistent regardless of the location where the test is conducted. One way of eliminating the type of hammer as a cause of variability in results is to specify in the standard, the type of hammer to be used for the compaction test, as in Kelfkens, 2008. However, doing this will not only disadvantage competing manufacturers of the hammers but one has to take into consideration the fact that it is not only the type of hammer that matters but its age as well. 'The vibratory hammer degrades and loses its full power as it gets older' (Shahin, 2010). This is due to wear and tear of the mechanical parts, particularly the cog wheel. For this reason, a calibration procedure is considered a better solution to the problem. The calibration test is carried out to determine whether the vibratory hammer is in satisfactory working order, and able to comply with the test requirements (BS 1377).

BS Calibration Test

The BS 1377 calibration test for the vibratory hammer uses a 5kg sample of clean, dry, Leighton Buzzard silica sand that has not been previously used. The sand, with 100% passing the 600µm test sieve and 100% retained on the 63µm test sieve, is mixed with water to raise its moisture content to 2.5 ± 0.5%. At least three (3) compaction tests are carried out on the sample to produce three specimens. The mean dry density of these specimens is then determined. The vibratory hammer is considered suitable if the mean dry density obtained exceeds 1.74 Mg/m^3.

NZ Calibration Test

Like the British calibration, a 10kg sample of Leighton Buzzard silica sand is obtained, of which at least 75% passes the 600µm test sieve. The coarse fraction is discarded. Sufficient water is mixed with the sand to raise the moisture content to 2.5 ± 5%. The material is compacted according to the procedure specified in the standard. Three specimens are produced. The mean dry density is determined and if it exceeds 1.74t/m^3 the hammer is considered suitable for the compaction procedure (Kelfkens, 2008).

ASTM Calibration Test

For the ASTM calibration test, standard sand conforming to the requirements of 20-30 sand specifications found in the ASTM specifications C778, is tested. Before the test is performed the material should be stored in such a way that freezing and/or contamination does not occur; if the material was previously used it should not be re-used. A dry specimen mass of 7 kg is required and must have a moist mass of atleast 9kg. A representative sample meeting this specification is selected using a riffler or splitter or any such method, quartering included. The vibratory hammer and mould (152mm diameter) are then prepared. The sand is then compacted according to method A described in the ASTM standard. After compaction the dry density is calculated; should the specimen meet or exceed a dry density of 1.76t/m^3 (17.29kN/m^3) then the vibratory hammer may be accepted as having sufficient energy (ASTM D7328-07).

2.3.6.3.5 Particle Packing and Degradation

Normally compaction results in a reorientation of the particles and a subsequent reduction in voids as the particles are packed closer together. Particle packing characteristics resulting

from compaction has an influence on engineering properties of the material. Grobler (1990) suggests that some compaction methods simply squeeze the particles together with little or no relocation or reorientation, while with others there is a considerable amount of relative movement of particles. This leads to large differences in the engineering characteristics. Rodriguez, Castillo and Sowers (1988) point out that the differences in the properties obtained by soil are largely due to variation in structure, which reflect differences in the angular deformations caused by different compaction methods. Grobler (1990) further suggests that vibratory compaction has the ability to achieve excellent particle orientation while impact compaction results in very little particle orientation and hence compaction.

Semmelink (1995) suggests that particle size distribution (grading) after compaction has an influence on the dry density-moisture relationship of the material. It is further suggested that because the amount of voids after compaction in a fine material (such as sand or clay) is much greater than that in a well-graded crushed stone, it has a much higher OMC than that of the well graded crushed stone. Excessive breakdown to smaller size particles leads to an increase in the void content which in turn lowers the MDD and bearing capacity that can be achieved and increases the moisture requirement for optimal compaction.

Computer Tomography scanning (CT-scanning) can be used to evaluate the density and void profile of a compacted specimen. CT-scanning (also called X-ray computed tomography) is a medical imaging method employing tomography created by computer processing to generate a three-dimensional image of the inside of an object from a large series of two-dimensional X-ray images taken around a single axis of rotation (Figure 2-11). It does this by detecting differences in densities and atomic numbers of the scanned sample. CT scanning has the advantage of been a non-destructive testing method.

Kelfkens (2008), using CT-scan, found no evidence of crushing or particle degradation after compaction with the vibratory hammer. However, a higher void content at the layer interface was observed. It was suggested that this could be due to excessive scarification of the surface of the layer. Therefore, to minimise the void content at the intersection of two layers, 100% of Mod AASHTO compaction should be sought for each individual layer. Also scarifying of the layers by more than 10mm in depth should be avoided (Kelfkens, 2008 and Twagira, 2010).

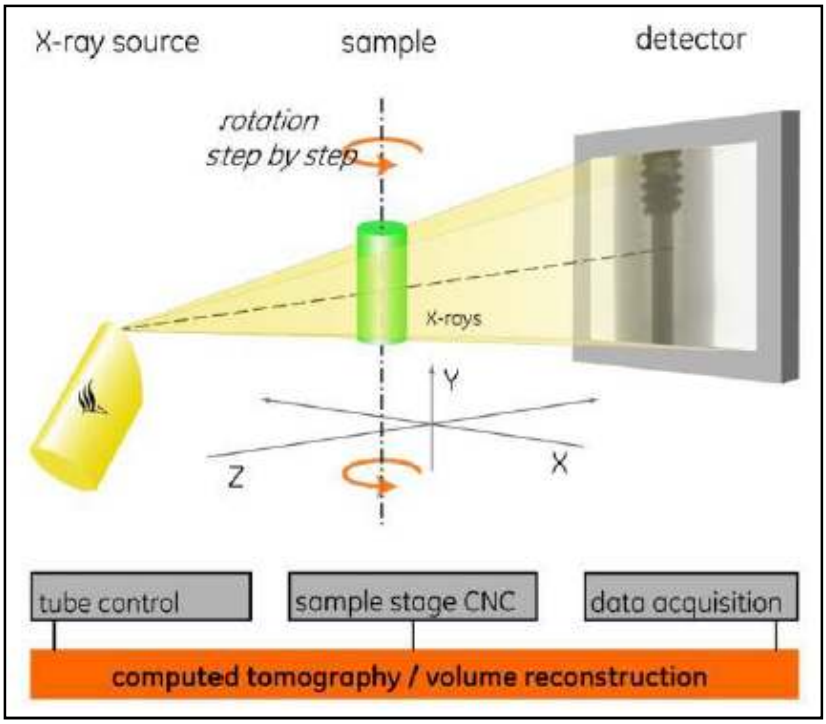

Figure 2-11: The CT-scan technique (CAF, SU 2012)

Prochaska and Drnevich (2005) (through sieve analysis of the material before and after compaction in accordance with the standard ASTM test, C 136) also showed that negligible degradation of the material occurs after compaction with the vibratory hammer. Shahin (2010) however, cautions that significantly more powerful hammers may cause degradation of the material.

2.3.6.3.6 Recent Research on the Vibratory Hammer

In 2004, Hoff, BaklØkk and Aurstad undertook a study to assess the effect of compaction on the resilient modulus and permanent deformation characteristics. The study considered granitic gneiss material and four compaction methods i.e. Gyratory compaction, Mod. AASHTO, Vibratory Hammer (Kango) and Vibratory Table. Differences in the resistance against permanent deformation of the material compacted to the same density with different methods were observed, whereas there was no definitive difference in the resilient modulus. It was concluded that the vibratory methods (hammer and table) produced specimen with higher resistance to incremental failure compared to other methods.

In the United States, Drnevich, Evans and Prochaska in 2007 undertook a study on the effect of vibratory hammer compaction on oven dried granular soils. The primary objective of the study was to investigate the feasibility of a vibratory hammer test for compaction control of

granular soils. The study considered sands and mixtures of sand and fines. The following observations were made:

- dry density results of the vibratory hammer were comparable to those obtained from vibratory table tests and modified AASHTO but significantly greater than the ones obtained from standard AASHTO tests
- no significant degradation of the material occurred for the vibratory hammer test.
- the test is applicable to a broad range of soils compared to vibratory table compaction tests (up to 35% non-plastic fines and up to 15% plastic fines).

Drnevich, Evans and Prochaska (2007) also showed (through a pilot implementation project) that the vibratory hammer method of compaction is applicable to the placement of well-graded aggregate bases; as the performance of the compaction equipment in the field is sufficient to achieve specified maximum dry unit weights. It was concluded that the vibratory hammer appeared to be a better alternative to the AASHTO and vibratory table tests for compaction of granular soils.

The American Society for Testing and Materials' (ASTM) standard test method for the Vibratory Hammer (ASTM D7328-07, 2007) was developed based on the results of the study by Drnevich, Evans and Prochaska in 2007. The standard is divided into two methods (Method A and Method B) depending on the percentage of maximum particle size present in the aggregate.

- Method A – Applies to material passing a 19.0mm sieve and containing up to 35% of the total dry mass passing a 75 μm sieve.
- Method B – Applies to material passing a 50mm sieve and containing up to 35% of the total dry mass passing a 75 μm sieve

In New Zealand, a study by Opus International Consultants Limited in 2008 found that repeatability and reproducibility values of the NZ vibratory hammer compaction test are higher than the ones stated in standards both in America and the United Kingdom. Shahin in 2010 undertook a study with the objective of developing a sound and scientific understanding of the variability in the results of the NZ vibratory hammer compaction test. Repeated tests with the vibratory hammer were conducted. X-ray diffraction tests on the aggregate used for testing were also undertaken. It was observed that repeatability values of the NZ vibratory

hammer test were higher than values stated in the USA and UK standards by more than 70% in some cases. This was attributed to natural sources in the test method itself as well as the natural variability in the properties of aggregate.

Table 2-4 compares the technical specifications for the vibratory hammer test in three (3) countries; Britain, New Zealand and United States.

Table 2-4: Comparison of the Technical Specifications of the Vibratory Hammer test

	Britain	**New Zealand**	**United States**	
	BS 1377-4, 1990	**NZ4402, 1986**	**ASTM D7328-07, 2007**	
			Method A	**Method B**
Mould Diameter, (mm)	152 ± 0.5	152 ± 0.5	152.4 ± 0.7	279.4 ± 1
Mould Height, (mm)	127	127	116.4 ± 0.5	231 ± 0.5
Mould Volume, (cm^3)	2305	2305	2124	14163
Hammer Input Power, (W)	600-750	60-1200	9.5-12	9.5-12
Hammer Frequency, (Hz)	25-45	4.2-10	64-70	64-70
Tamper Mass (Max. kg)	3	3	-	-
Layer (No.)	3	2	3	3
Compaction time per layer, (S)	60	180	60	52 ± 5
Surcharge, (N)	300-400	300 ± 50	350 ± 13	350 ± 13
Foot piece Diameter (mm)	145 ±2	145	-	-
Impact Energy (J)	-	-	10- 12	10- 12

The range covered by the input power of the NZ vibratory hammer is particularly large and so is the difference between the input power of the ASTM vibratory hammer and those of the NZ and BS. It was indicated in Section 2.3.6.3.1 that hammers with high input power ratings apply greater compactive effort. Therefore, it is expected that varied results are obtainable at these input power ratings.

Table 2-4 also highlights significant differences in specified operating frequencies for the BS, NZS and the ASTM. The difference between the frequency of the NZ vibratory hammer and the ASTM vibratory hammer is particularly large. Section 2.3.6.3.1, under frequency and amplitude, indicates that higher compactive densities are obtainable at high frequencies.

2.3.6.3.7 South African Research on Vibratory Hammer

Weston in 2001, conducted research with the objective of determining the influence of the compaction method on the volumetric and mechanical properties of foamed bitumen mixes. Four laboratory compaction methods were considered;

- Marshall,
- Hugo,
- Gyratory and
- Kango Vibratory Hammer

A hydrostatic double-drum vibrating roller was used to simulate field compaction. Weston (2001) showed that the compaction method had a significant influence on the Indirect Tensile Strength (ITS) test and Indirect Tensile Test (ITT) results. It was also observed that the vibratory hammer and the Gyratory compaction methods were the most efficient methods of compaction based on compaction energy requirements.

In 2005, Lange conducted research on the suitability of the vibratory hammer compaction method for compaction of various types of cohesive soils (with plasticity index ranging from 3 to 27%) and compared its effectiveness against the Mod AASHTO compaction method. He also sought to verify the energy of compaction imparted with the vibratory hammer by modelling its functionality. Tests were conducted on various untreated low quality material types suitable for use in construction of subgrade layers or as embankment fill material. The method of compaction used for the vibratory hammer was BSS 1377: 1975 Test 14.

Results of the study showed that the vibratory hammer compaction method was effective for soil material with low plasticity index of up to 4% and less effective for material with higher plasticity. Through a detailed study that involved stripping down of the hammer and studying its mechanism, a theoretical model describing the mechanical method by which the system generated energy was developed. Lange was able to verify the manufacturer's rated point energy of the Kango vibratory hammer used.

A comprehensive study on the vibratory hammer compaction of BSMs was undertaken by Kelfkens in 2008. The objective of the study was to develop an experimental procedure for the compaction of BSM-foam and BSM-emulsion using the vibratory hammer. Tests were conducted on G2[1] quality graded crushed stone material stabilised with foamed bitumen (80/100 bitumen) and bitumen emulsion (60/40 Anionic Stable Grade), and recycled material. Repeatability tests were performed on G5 material. The level of density of the vibratory hammer was expressed as a percentage of the Mod AASHTO compaction. Comparative tests

[1] G2 is the South African classification system for crushed or natural gravel material (TRH14)

were done with the vibratory table. Kelfkens (2008) made the following observations from the study:

- Compaction time to 100% of Mod AASHTO decreased with increase in moisture content.
- Moisture content and surcharge weight have an influence on the achieved refusal density. The higher the moisture content, the higher the bracket of refusal density; and the higher the surcharge load in combination with the moisture content, the higher the bracket in which the refusal density falls.
- The vibratory hammer produces specimen with very low voids content.
- The extent to which the surface of the layers is scarified has an influence on the level of voids content at the intersection of the two layers.
- The vibratory hammer takes less time to compact to 100% of Mod AASHTO compared to the vibratory table. The vibratory hammer also gives more control and accuracy over the target density and the final level of the specimen.

Kelfkens (2008) developed three compaction protocols for the compaction of BSMs using the vibratory hammer; *Protocol 1 for Moisture-density relationship, Protocol 2 for analysis of refusal density for specification purposes and Protocol 3 for laboratory specimen procurement*.

Kelfkens (2008) recommends further testing of aggregates types; G1, G3, G4, G5, G6, G7 etc to further develop and improve on the compaction protocols.

Twagira (2010) highlights that the compaction method of laboratory prepared BSM specimens is a primary factor in producing mix designs which simulate durability behaviour in field conditions. It is concluded that the vibratory hammer sufficiently compacts BSMs in a fashion similar to field conditions. It is also highlighted that the vibratory hammer is relatively cheap and easy to use and has higher point energy. Therefore less compaction effort is required to obtain an equivalent level of compaction compared to other methods.

2.3.6.4 Vibratory Hammer versus Vibratory Table

The current method of compaction of granular material is the vibratory table test which is detailed in TMH1. However, as stated in Section 1.2, the vibratory table has its own shortcomings. Hence the researches into the development of the vibratory hammer

compaction test. Unfortunately it is not possible to compare the two methods of compaction at the same compactive energy because this energy cannot always be accurately quantified. Moreover, it is affected by certain imponderable factors that influence process efficiency. Therefore, the dry densities achieved and the procedures that bring a soil to this density are compared instead. With both methods based on vibration, it is believed that the skeletal structure of a specimen from vibratory table compaction will be similar to the skeletal structure of one produced using the vibratory hammer.

Table 2-5 gives specifications of the vibratory table and vibratory hammer at Stellenbosch University. The CSIR vibratory table is also included for comparison purposes. The SU vibratory table has a relatively higher frequency compared to the vibratory hammer. The amplitude and frequency of the hammer are more comparable with the CSIR vibratory table. The amplitude of the vibratory table at SU (0.4mm) is less than that specified in TMH1 (1+0.5mm) but comparable to that specified in ASTM standard for vibratory table test (ASTM D4253-00).

Table 2-5: Specifications of Vibratory Table and Vibratory Hammer

	Vibratory Table (SU)	**Vibratory Table (CSIR)**	**Vibratory Hammer**
Power Input [W]	1200	1100	1500
Impact Energy [J]	-	-	6-25
Impact Rate [/min]	3000	1800	900 - 1890
Frequency [Hz]	50	12 – 60 (30)	15 - 31.5
Amplitude [mm]	0.1 - 0.4	0.5 - 4	5[1]
Layers [No.]	5	3	5
Surcharge [Kg]	50	50	35

[1]Assumed

Kelfkens (2008) compared the two methods of compaction (vibratory hammer and vibratory table). It is observed that compaction to 100% of Mod AASHTO with the vibratory hammer takes less time than with the vibratory table. It is also observed that densities obtained from vibratory hammer compaction are comparable with those obtained using the standard vibratory table compaction method. Prochaska and Drnevich (2005) also observed comparable dry densities after compaction of various types of oven-dried granular soils using the vibratory hammer and vibratory table.

2.3.7 Field Compaction Methods

Field compaction of soils is done using various types of rollers. A minimum number of passes must be made with the chosen compaction equipment to produce the required degree of compaction. This number, which depends on the type and mass of the equipment and on the thickness of the soil layer, is usually within the range of 3 to 12. Above a certain number of passes no significant increase in dry density is obtained (Craig, 2004).

The most commonly used types of compaction rollers are (Das, 2004);

- Sheepsfoot roller
- Smooth-wheeled roller (or smooth drum roller)
- Pneumatic roller

The energy that is required to compact soils in the field can be applied by means of any of the four methods; Kneading compaction, Static compaction, Dynamic or Impact compaction and Vibratory compaction. Each of the methods is differentiated by the nature of the forces applied and the duration of the forces (Rodriguez, Castillo and Sowers, 1988). For this reason, each roller serves a different purpose and is suitable for compaction of a particular soil type such as for cohesive soils; sheepsfoot rollers or pneumatic rollers provide the kneading action. Silty soils can be effectively compacted by sheepsfoot roller/pneumatic roller or smooth wheel roller. For compacting sandy and gravelly soil, vibratory rollers are most effective. If granular soils have some fines, both smooth wheel and pneumatic rollers can be used (Ministry of Railways, 2005).

Sheepsfoot Roller

Sheepsfoot rollers (Plate 2-4) comprise of a drum of widths ranging from 120 to 180cm and diameters ranging from 90 to 180cm. Projections, differently shaped, like sheepsfoot are fixed on the drums. The lengths of these projections range from 17.5 to 23cm. The contact area of the foot ranges from 35 to 56 cm^2 or more. The loaded weight per drum ranges from about 30kN for the smaller sizes to 130kN for the larger sizes (Murthy, 2003). These rollers are effective in compacting cohesive soils (Das, 2004).

Plate 2-4: Sheepsfoot Roller (Shahin, 2010)

'When sheepsfoot rollers are used, the feet must penetrate into the loose lift. If they ride on top, the machine is too light and the ballast must be increased. With succeeding passes, the feet should "walk out" of the layer. The number of passes required for the feet to walk out of the layer will be used to control compaction of subsequent layers. If the feet do not walk out, the machine is too heavy and is shearing the soil or the soil is too wet' (Virginia department of transport, 2013).

A concentrated pressure that changes in both angle and magnitude is applied at the points where the feet penetrate the soil. The pressure exerted by the sheepsfoot roller as it moves over the soil with its feet is not constant time wise; the feet penetrate the soil, exerting ever increasing pressures which reach a maximum at the moment the foot is vertical and thus at its maximum penetration. From then on, the pressure reduces until the foot is withdrawn.

Research on compaction with the sheepsfoot roller indicates that the contact pressure under the feet of the roller has no effect on the compaction of the soils. However, an increase in contact area results in an increase in compaction (Table 2-6). This allows for reduction in number of passes of the roller. If the number of feet per drum is increased, the percentage of coverage increases correspondingly but the contact pressure is reduced (Rodriguez, Castillo and Sowers, 1988).

Figure 2-12 shows the effect of number of passes of the sheepsfoot roller on degree of compaction. It is shown that after 10 to 12 passes of the roller, the density achieved begins to taper off indicating reduced increases in compaction. Therefore it would be prudent to stop compaction at such a point. This however, should be decided after field trials (Ministry of

Railways, 2005). The variable compaction force of the sheepsfoot roller is referred to as kneading (Rodriguez, Castillo and Sowers, 1988)

Table 2-6: Effect of Contact Pressure and Contact Area on Compaction (Ministry of Railways, 2005)

Type of Soil	Contact Pressure (kg/cm^2)	Contact Area (cm2)	Number of Passes	Compaction (%)
Clayey sand	17.5	43.75	9	99
	31.5	43.75	9	99
Silty Clay -I	17.5	43.75	8	102
	35	43.75	8	101
	52.5	43.75	8	101
Heavy Clay	8	75.25	64	108
	17.5	31.5	64	108
Silty Clay II	8	113.68	64	112
	17.5	248.67	64	111
Sandy Clay	8	75.25	64	104
	17.5	31.5	64	104
Mixture of gravel, sand and clay	8	75.25	64	100
	17.5	31.5	64	99

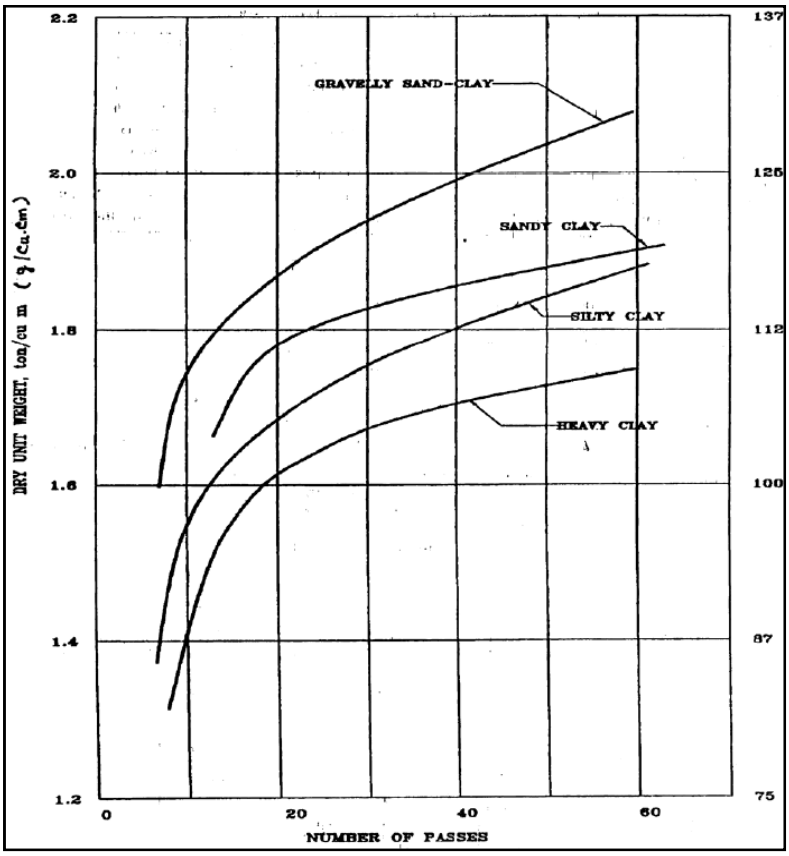

Figure 2-12: Effect of Number of Passes on the Degree of Compaction with the Sheepsfoot Roller (Ministry of Railways, 2005)

Smooth wheel Roller

Plate 2-5: Smooth Wheel Roller (Shahin, 2010)

Smooth wheel rollers (Plate 2-5) are compaction devices that use steel drums to compress the underlying layers. They are characterised by diameter, width and weight. They can have one, two or even three drums. Tandem (2 drum) rollers are most often used for asphalt compaction while single drum rollers are used for granular material. The drums can be either static or vibratory.

Static smooth wheel rollers vary in mass/meter width from 2100kg to over 54000kg. They rely on the dead weight to effect compaction and are suitable for compaction of most soils except uniform and silty sands (Smith and Smith, 1998). These rollers compact from the top down and are effective at speeds of 3–6 km/h. Figure 2-13 shows that the relationship among roller speed, number of passes and output volume of compacted material for smooth wheel rollers is linear. The output of the roller is maximum for the first pass at minimum speed. Subsequent passes even with higher speeds of the roller does not result in increased output (Ministry of Railways, 2005).

Smooth wheel vibratory rollers form the backbone of most pavement layer compaction because the cohesion properties of these layers are normally limited (Semmelink, 1995). The mass/meter width of vibratory rollers range from 270kg to over 5000kg. The compactive effort of vibratory rollers is influenced by drum loading, amplitude and frequency and the speed. They have frequencies ranging from 12 to 80Hz and amplitudes from 0.3 to 2.5mm. The vibration is achieved by employing eccentric, rotating or reciprocating masses within the drum of the roller (Plate 2-6). The rotating eccentric mass provides fast up-and-down movement of the roller drum (vibration). In some systems, two eccentric masses rotate in

opposite directions (counter vibration) or in sync (oscillation). This produces rapidly changing forward/reverse, rocking movement of the roller drum (Wirtgen Group, 2011).

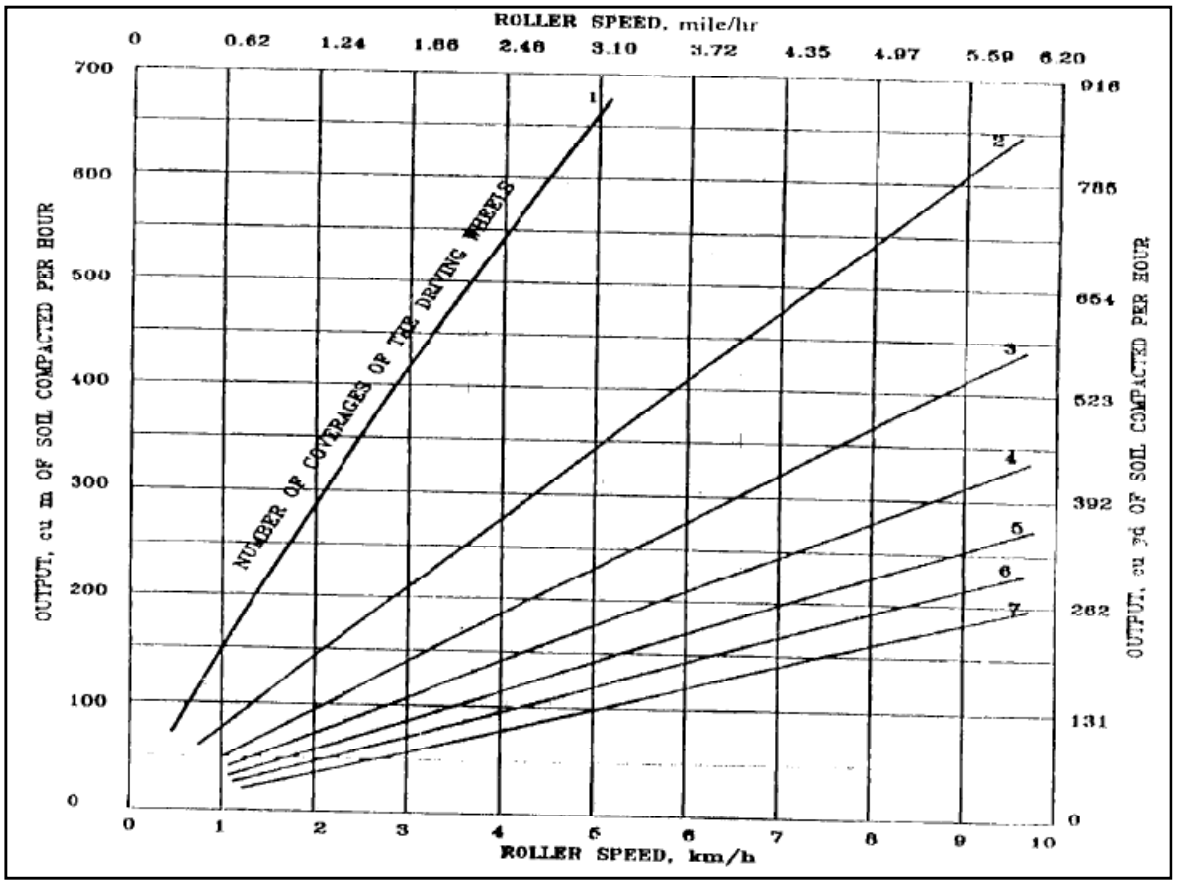

Figure 2-13: Relation between roller speed, number of passes and output (Ministry of Railways, 2005)

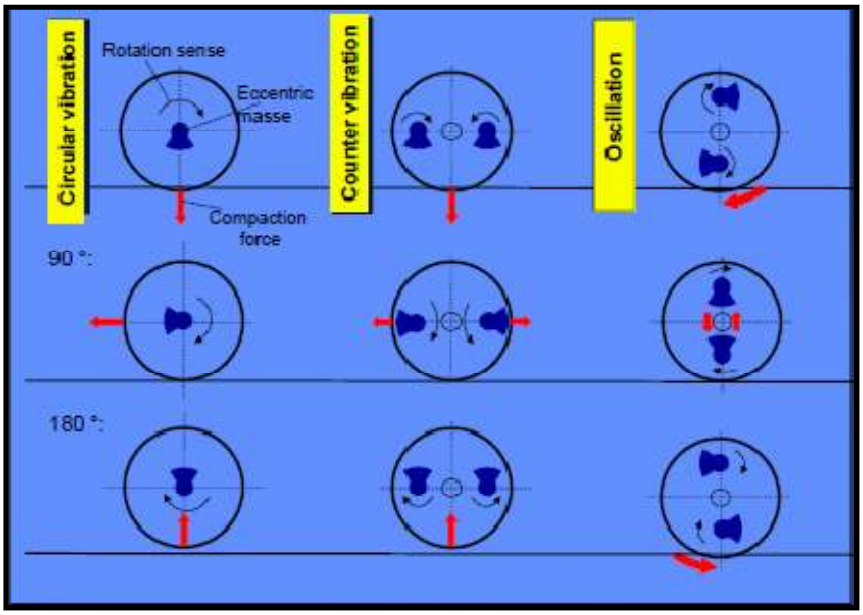

Plate 2-6: Eccentric Masses of vibratory roller

'Vibratory rollers are very powerful and versatile and require considerably less passes than static rollers. The vibration reduces friction in the material so that the interaction between the deadweight and dynamic load increases the density' (Bomag, 2009). When using vibrating rollers, it is extremely important to ensure that the rollers function properly and that rolling is always done in the direction of the eccentric moment. On dual amplitude rollers, this direction normally reverses when the amplitude is changed. A high amplitude/low frequency combination should be used initially for deep compaction. A change should be made to low amplitude/high frequency when the change in measured density is small between successive roller coverage. A full roller pass is defined as two roller coverage applied in opposite directions on the same track with the same roller force (Semmelink, 1995).

High frequencies do not allow high rolling speeds. Otherwise a bow wave may be created that may lead to cracking. Best results on both clays and granular soils are obtained when the frequency of vibration is in the range 2200 – 2400 cycles per minute (Smith and Smith, 1998). High amplitudes may also lead to aggregate crushing.

Pneumatic Roller

Plate 2-7: Pneumatic-tyred Roller

Heavy pneumatic-tired rollers (PTRs) (Plate 2-7) are designed so that the weight can be varied to apply the desired compactive effort. They are designed with a steering/oscillating axle at the front and a rigid drive at the rear (Bomag, 2009). Rollers with capacities up to 50 tons usually have two rows of wheels, each with four wheels and tyres designed for 621 kPa inflation. PTRs can be obtained with tyres designed for inflation pressures up to 1034 kPa. The effectiveness of PTRs is affected by the load per wheel, tire pressure, width of roller, percentage coverage per pass, overlapping of passes and speed of the roller. As a rule, the

higher the tire pressure the greater the contact pressures and, consequently, the greater the compactive effort obtained. Thus, at higher pressure, the number of passes required to achieve a particular dry density can be reduced. However, if the tyre pressure is too high a bearing capacity failure will occur and the soil layer may be rutted without compaction. Also it is not advisable to increase the tire pressure unless the load per wheel is increased in the same proportion, because this reduces the contact area and horizontal confinement, and tends to reduce compaction with increasing depth (Rodriguez, Castillo and Sowers, 1988).

The effect of number of passes and the tyre pressure on dry density of three types of soils viz. plastic clay, sandy clay and gravel-sand-clay is shown in Figure 2-14. It is shown that with the increase in tyre pressure, dry density also increases. It is also shown that passes beyond 16 does not have any more effect on compaction.

PTRs should be used to finish off the compaction of pavement layers. Because of their high tyre pressures, they are very useful for compacting the top 50mm layer (particularly asphalt layers), which vibrates slightly loose when a vibratory roller is used for initial compaction. The kneading and flexing effect of their (PTRs) wheels leads to a homogenous distribution of the mix and closes the pores on the surface of asphalt layers. PTRs should be properly ballasted and the tyre pressure corrected before use. (Bomag, 2009 and Semmelink, 1995).

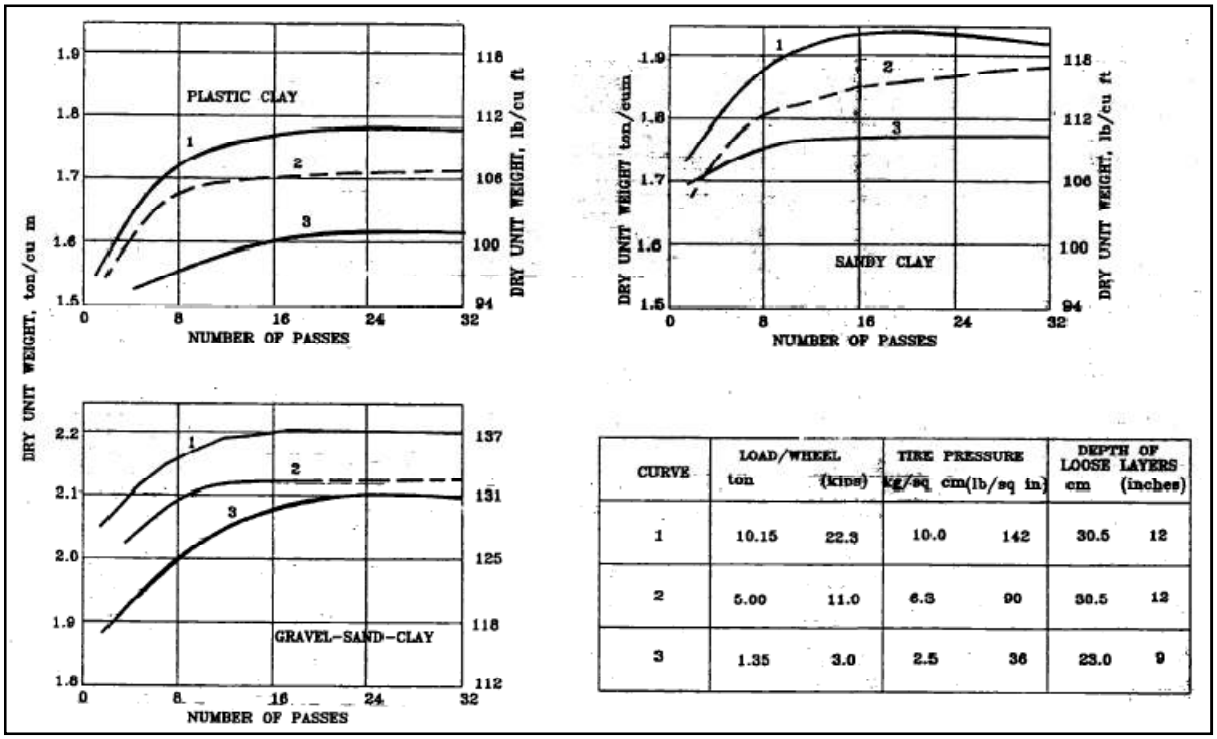

CURVE	LOAD/WHEEL ton	(kips)	TIRE PRESSURE kg/sq cm	(lb/sq in)	DEPTH OF LOOSE LAYERS cm	(inches)
1	10.15	22.3	10.0	142	30.5	12
2	5.00	11.0	6.3	90	30.5	12
3	1.35	3.0	2.5	36	23.0	9

Figure 2-14: Effect of No. of Passes and Tyre Pressure of PTR on the Dry Density of Various Soils

2.3.7.1 Selection of Compaction Equipment

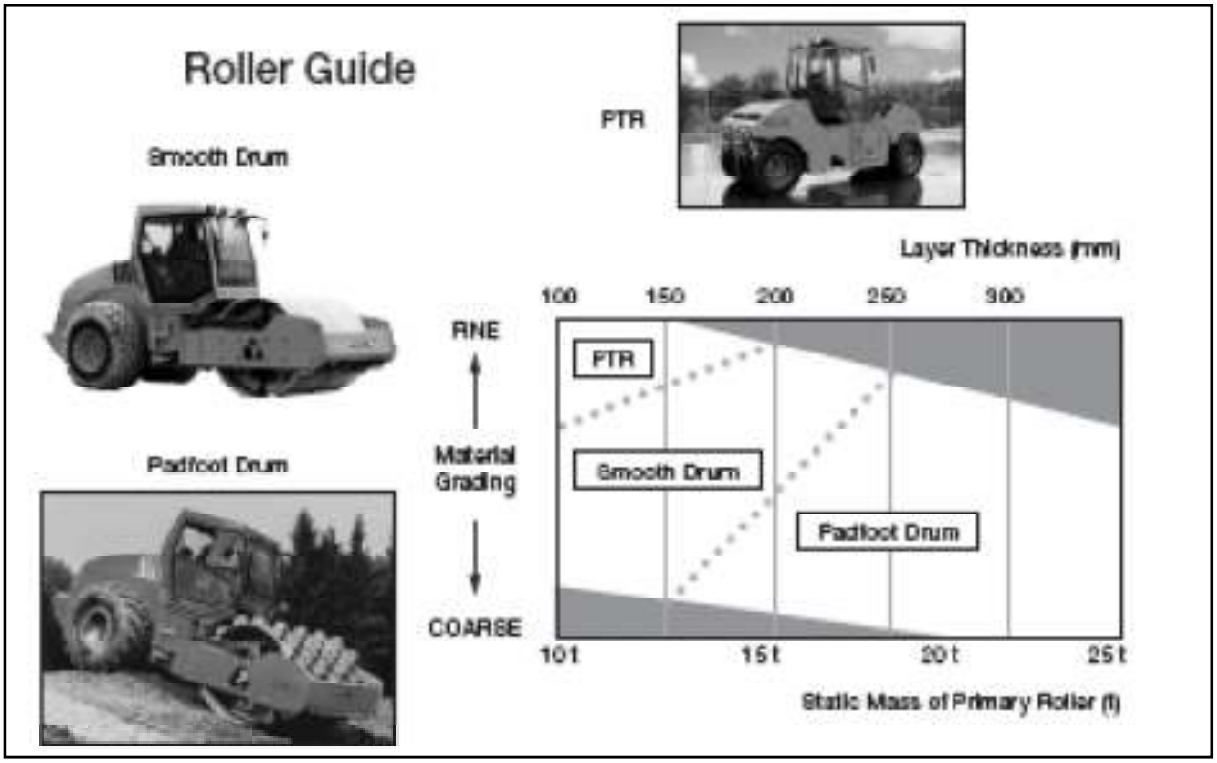

Figure 2-15: Guide to Roller Selection (Wirtgen, 2004)

The selection of the most suitable compaction process depends on a variety of factors: soil conditions, required degree of compaction, maximum depths of compaction, site-specific considerations such as sensitivity of adjacent structures or installations, available time for completion of the project, access to equipment and material and, last but not least, the competence of the contractor. To ensure effective compaction in the shortest possible time, it is imperative that appropriate equipment is used whenever possible and a high degree of quality control and site supervision is maintained (Massarsch and Fellenius, 2005). By rule of thumb, the thicker the soil layer to be compacted, the heavier the equipment required to-produce an adequate degree of compaction (Craig, 2004). Figure 2-15 provides a guide on roller selection based on material layer thickness and grading.

2.3.7.2 Over-Compaction

When a compactor makes too many passes over a layer, the soil may be over-compacted. Over-compaction occurs when the material is compacted in excess of the specified density range. Depending on material type, over-compaction will manifest itself as cracks, remoulding of the surface of the compacted soil or severe permanent deformation upon

passage of the compactor. This is the result of a reduction in air-voids to a low level with the generation of excess pore water pressures. Over-compaction reduces soil density, wastes time, and causes unnecessary wear to the compaction machine. (Highways Agency, 1994).

2.3.7.3 Field Compaction Control

The results of laboratory compaction tests are not directly applicable to field compaction because the compactive effort in the laboratory tests are different, and are applied in a different way, from those produced by field equipment. Further, the laboratory tests are carried out on material smaller than 20 or 37.5mm. However, the MDD obtained in the laboratory cover the range of dry density normally produced by field compaction equipment (Craig, 2004).

There are two approaches to achieving a satisfactory standard of compaction in the field. These are *method* and *end-product* compaction (Craig, 2004). In *method* compaction the type and mass of compaction equipment, the layer depth and the number of passes are specified. The problem with this method is that the material properties, moisture conditions and subgrade support may vary resulting in some road sections being over compacted while others are inadequately compacted (Jumo and Geldenhuys, 2004).

In the more preferred *end-product* compaction the required dry density is specified. The dry density of the compacted fill must be equal to or greater than a stated percentage of the maximum dry density obtained in one of the standard laboratory compaction tests. Table 2-7 gives the nominal field compaction densities detailed in TRH 4.

Semmelink (1995) argues against specifying densities, emphasizing that if material is not compacted optimally at construction phase, the layer will further densify under traffic loading. The densification is dependent on the traffic loading and the in-situ moisture content. Most of the rutting presently found on South African roads is attributed to this. Therefore, rather than compacting a layer to 90%, 93%, 95%, 97% or 100% modified AASHTO, compaction of all road building material should only be terminated when refusal density is reached (i.e. the dry density at which further application of compactive effort does not improve the dry density level when compacted at OMC).

‘Once the MDD and OMC of a soil has been determined in a laboratory test, a field unit weight determination must be performed after the fill has been compacted. Field unit weight determinations verify whether the required relative compaction or relative density was

achieved, and if the water content in the field is appropriate for the specified purpose of the fill. Several field unit weight determination methods are available. Older methods include the Sand Cone and Rubber Balloon methods. However, a quicker and more modern field unit weight determination method is the nuclear method' (Drnevich V.P., Evans A.C and Prochaska A.B, 2007).

Table 2-7: Nominal Field compaction requirements for construction of pavement layers (TRH4)

Pavement Layer	Material or Layer	Target Density (Relative Compaction)
Base	Crushed Stone	
	G1	86-88% Apparent Relative Density
	G2	100-102% mod AASHTO
	G3	98-100% mod AASHTO
	Gravel G4	98-100% mod AASHTO
	Cemented	
	C3/C4	97-98% mod AASHTO
Subbase	Gravel (G4/G5)	
	Upper	95-97% mod AASHTO
	Lower	95% mod AASHTO
	Cemented (C3/C4)	
	Upper	96% mod AASHTO
	Lower	95% mod AASHTO
Selected Layers	Upper	93-95% mod AASHTO
	Lower	90-93% mod AASHTO

Sand Cone Method

'In this method, a small hole is dug in the compacted material to be tested. The soil is removed and weighed, then dried and weighed again to determine its moisture content. The specific volume of the hole is determined by filling it with calibrated dry sand from a jar and cone device (Figure 2-16). The dry weight of the soil removed is divided by the volume of sand needed to fill the hole. This gives the density of the compacted soil. This density is

compared to the maximum mod AASHTO density obtained earlier, which gives the relative density of the soil that was just compacted' (Carson, 2004).

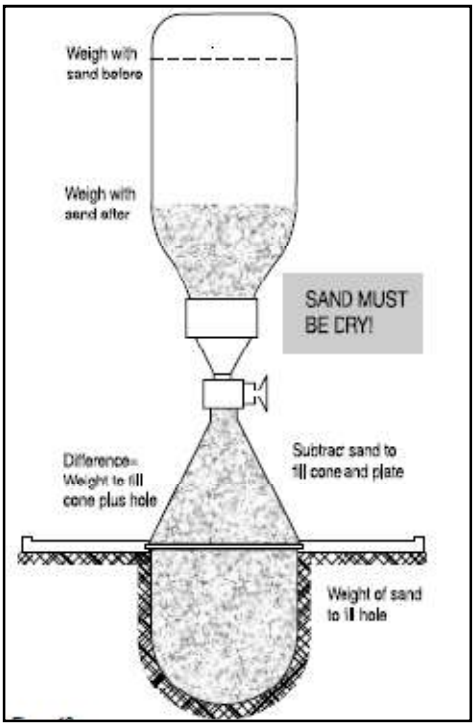

Figure 2-16: Sand Cone Test (Carson, 2004)

Rubber Balloon Method

'The volume of an excavated hole in a given soil is determined using a liquid filled calibrated cylinder used to fill a thin rubber membrane. This membrane is displaced to fill the hole. The in-place unit weight is determined by dividing the wet mass of the soil removed by the volume of the hole. The moisture content and the in place unit weight are used to calculate the in-place dry unit weight. The volume is read directly on the graduated cylinder' (Murthy, 2003).

Nuclear Method

Through a Nuclear Density meter, radiation is sent through the soil from a source to a receiver (Figure 2-17). The device uses transmitted radiation to determine both moisture content and density.

The major advantage of this method- which enables relatively precise, reliable and repeatable results – (provided it is properly calibrated) is its extremely short measuring time. Contrary to

the older core extraction and material replacement methods for which an overall time requirement – including the laboratory analysis – of approximately 24 hours is necessary, a nuclear density measurement can be carried out in approximately 5 minutes. It also offers the advantage of being a non-destructive measurement method (Wirtgen, 2002).

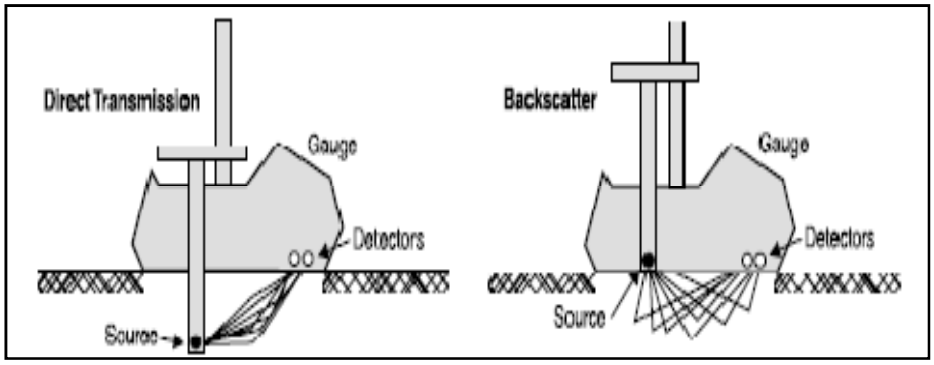

Figure 2-17: Nuclear Density Test (Carson, 2004)

2.3.7.4 Intelligent Compaction

Compaction machinery and technology for construction sites have continuously improved to improve their compaction effort. Recent developments in field compaction methods have led to advanced compaction technology termed Intelligent Compaction (IC) (Plate 2-8) also known as Continuous Compaction Control (CCC).

'Achieving uniformity in field compaction is key for performance of pavement layers. Generally in-situ spot tests (with nuclear or non-nuclear gauge density devices) or cores tests are required for the quality control (QC) and/or quality assurance (QA). However, there are many issues associated with this conventional density control method, including but not limited to; 1) In-situ spot tests or cores are limited and often conducted at random locations and thus the tests are not representative of the entire pavement area; 2) There may be weak or unqualified compaction areas unidentified by the limited spot tests; 3) The density of top bound layer is limited to indicate the structural capacity of the entire pavement layers. As a result, non-uniform and unsatisfactory compaction may be outcomes, leading to premature failure and worse long-term performance. Therefore intelligent compaction has been developed to address these issues' (FHWA, 2011).

Intelligent compaction is a compaction method that uses sensing equipment (on the roller) that reads subgrade strength, density, stiffness, or modulus based on compaction equipment behaviour. The rollers are equipped with real time kinematic (RTK) Global Positioning

System (GPS), roller integrated measurement system, feedback controls and onboard real-time display of all IC measurements. IC rollers maintain a continuous record of measurements that include the number of roller passes, roller integrated measurement value (ICMV), GPS locations of the roller, roller vibration amplitudes/frequencies and HMA surface temperatures, etc. Based on the real time onboard colour-coded display of the above measurements, roller operators can either manually or allow the IC roller to automatically adjust the machine settings for optimum compaction (FHWA, 2011).

This type of technology started in the late seventies in Europe with the work of BOMAG in Germany, AMMANN in Switzerland and Geodynamik in Sweden, the three leading companies in this type of technology (Briaud and Seo, 2003). The technology has since spread to Japan and the United States.

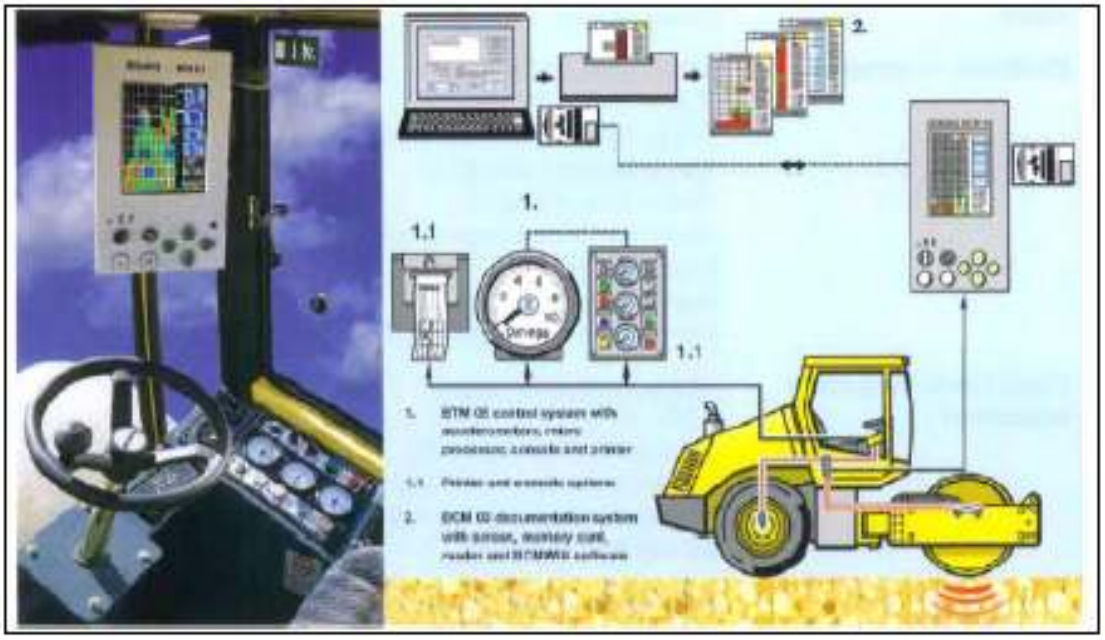

Plate 2-8: BOMAG Intelligent Compaction System (Briaud and Seo, 2003)

Although each manufacturer's system has its own specific methods of execution, all IC systems generally function in the same way by measuring and reacting to the response from the material being compacted. The compaction system uses compaction meters or accelerometers mounted in or about the drum to monitor both the horizontal and vertical reaction of the drum to the material it is compacting. The methodology to calculate material response to compaction is often proprietary, resulting in various types of ICMV. These (ICMV) are then calibrated to correlate to a material modulus or density measured by other test device (FHWA, 2011).

Briaud and Seo, (2003), identified the following benefits and drawbacks of IC technology (Table 2-8);

Table 2-8: Advantages and Disadvantages of IC Technology (Briaud and Seo, 2003)

Advantages	Disadvantages
Higher efficiency and maximized productivity by automatic control of amplitude, frequency and speed	Requires sophisticated equipment in a rugged environment
Minimized number of passes	Requires operator training
Higher adaptability (thin/thick layer, soft/stiff subbase)	More expensive than conventional compaction
Wider application range	
Optimal compaction results, better quality	
More uniform compaction	
Less aggregate crushing	
Better flatness	
Complete coverage of compaction surface evaluation	
Dynamic measurement of soil stiffness	
No danger of over compaction	
Compaction control on the job	
Easy to operate	
Extended life of the roller by minimizing the double jump situation	

The potential for IC technology has since been recognised in South Africa. Problem areas of the technology have been identified that, if addressed, could pave way for the introduction of the technology in the SAPDM (Paige-Green, 2011). These areas are:

- Correlation between Measurement Values (MVs) of different IC systems
- Correlation between MVs of rollers and traditional acceptance tests
- Correlation between roller MVs and possible future field Quality Control/Quality Assurance (QC/QA) test procedures
- Statistical evaluation of compaction control and uniformity
- Development of IC specifications and QC procedures

Intelligent compaction systems may potentially provide substantial benefits to the South African road construction industry. A study in the US showed that the cost of IC model

compactors runs 20 to 30 percent higher than conventional compactors, however, Briaud and Seo (2003) suggest that the initial cost of the equipment is negated when benefits of its use are compared to the conventional approach.

2.4 SUMMARY

Laboratory compaction methods are meant to be simple and economical simulations of field compaction processes. Through laboratory studies, a better understanding of field compaction would be gained and informed decisions regarding compaction in the field would be made. The shortfalls of the current laboratory methods for compaction of granular materials have been highlighted in Section 2.3.6. A major gap still exists between field compaction and laboratory compaction. While material in the laboratory is compacted in controlled confinement conditions i.e. in moulds and on solid foundations, field compaction is done on variable support conditions and edge effects. In addition, the compaction method characteristic of the Mod AASHTO with amplitude of 457mm is different and does not simulate well the amplitudes and compaction characteristic of most field compaction methods. Studies have indicated that the vibratory table better simulates field compaction in the laboratory. However, its use is limited for reasons highlighted in Section 2.3.6.2.

Table 2-9 compares the two compaction methods i.e. vibratory table and Mod AASHTO. It is shown that the Mod AASHTO compaction method imparts higher compactive energy per unit volume compared to the vibratory table. The Mod AASHTO also has a significantly high amplitude compared to the vibratory table.

Table 2-9: Vibratory table and Mod AASHTO compaction Specifications

	Vibratory Table (SU)	**Mod AASHTO**
Mould Diameter,(mm)	150	152.4
Mould Height, (mm)	300	127
Mould Volume, (cm^3)	5301.4	2316.7
Power Input (W)	1200	-
Impact Energy (J)	-	-
Impact Rate (/min)	3000	-
Frequency (Hz)	50	-
No. Blows/layer	-	55
Amplitude (mm)	0.1 - 0.4	457.2
Layers (No.)	5	5
Surcharge (Kg)	50	-
Energy (kJ/m^3)	1110.3	2394.8

There is a need for an alternative laboratory compaction method in this regard. The vibratory hammer has the potential to fulfil this requirement. Standard compaction tests with the vibratory hammer have been developed in America, Britain and New Zealand. In South Africa, the protocol developed in 2008 for vibratory hammer compaction has produced different results in different laboratories. In its continued development therefore, various factors that may influence compaction with the vibratory hammer require further investigation.

The literature also highlights how the amplitude effect is created in the operation of the vibratory hammer. This is critical because the amplitude effect will be affected by the mass of the surcharge as well as the tamping foot, two of the primary test factors in this study. It is notable that the BS and NZ standards specify a tamping foot of not more than 3 kg in mass and 145mm in diameter while the ASTM specifies a tamping foot of 3.4 kg and 146mm in diameter. However, the interaction of different masses of tamping foot and surcharge load on the obtainable density with the vibratory hammer has not been fully investigated.

The literature highlights significant differences in specified operating frequencies for the BS, NZS and the ASTM. The BS specifies an operating frequency range of 25 to 45Hz, the NZ standard; 4.2 to 10Hz and the ASTM; 64 to 70Hz. The SU vibratory hammer operating at a frequency of 31.5Hz is more comparable with the BS specification. It is noted that the suitability of frequency depends on the thickness of the layer of material been compacted. High frequencies (and low amplitudes) are suited for compacting material of lesser thickness while low frequencies (and high amplitudes) are better for greater depths of material.

The overriding factor in design of, particularly the ASTM, vibratory hammer frame is portability. As highlighted in the literature, the frame can be assembled and disassembled easily. However, repeated assembling and disassembling of the vibratory hammer frame presents points of weakness in the structure of the frame. It is postulated that a weak frame would result in inefficiencies in compaction with the vibratory hammer.

The next chapter outlines the experimental design and methodology adopted for the investigation.

REFERENCES

ARAYA A.A. 2011**. Characterisation of Unbound Granular Materials for Pavements**. Dissertation for Doctor of Philosophy, Delft University of Technology.

ASTM D4253-00. 2006. **Standard Test Methods for Maximum Index Density and Unit Weight of Soils using a Vibratory Table**. Annual Book of ASTM Standards, Vol 04.08. West Conshohocken, ASTM International.

ASTM D7382-07. 2008. **Standard Test Methods for Determination of Maximum Dry Unit Weight and Water Content Range for Effective Compaction of Granular Soils Using a Vibrating Hammer**. Annual Book of ASTM Standards, Vol 04.09. West Conshohocken, ASTM International

BOMAG GmbH, 2009. **Basic Principles of Asphalt Compaction.** BOMAG GmbH, Hellerwald, D-56154 Boppard

BRIAUD J-L AND SEO J, 2003. **Intelligent Compaction: Overview and Research Needs.** Texas A&M University

BS 1377: Part 4, 1990. **British Standard methods of test for Soils of Civil Engineering Purposes. Part 4. Compaction – related tests: Method for Determination of Dry Density/Moisture Content using Vibrating Hammer.** British Standards Institution

BURNS B., 2012. **Discusion on operational mechanism of Vibratory Hammer (Phonecall)** (Personal communication, 13th August, 2012)

CARSON, 2004, **Soil Compaction Handbook**, Multiquip Inc, Carlifornia, USA.

CENTRAL ANALYTICAL FACILITY (CAF), 2012. **CT Scanner.** Available at: http://academic.sun.ac.za/saf/services/downloads/services8/Stellenbosch%20CT%20Scanner%20info%20brochure.pdf. Department of Forestry. Stellenbosch University (Accessed: August 31, 2012)

CLAYTON C.R.I. MATHEWS M.C. and SIMONS N.E., 2011. **Site Investigation**. Available at: www.geotechnique.info. (Accessed on 14/11/2011)

COMPACTION CONCEPTS, 2012. **Asphalt, HF-Roller and Concept Comparison**. Available at: www.podshop.se/Content/21/opensearchresult.aspx?file...L.pdf (Accessed: May 2, 2012)

CONNELLY J, JENSEN W and HARMON P. 2008. **Proctor Compaction Testing.** The Nebraska Department of Roads.

COOPER Technology 2012. Available at: http://www.cooper.co.uk/info/index.asp?page=crt_gyr_en_gyratory_compactor_33 (Accessed: July 15, 2012)

CRAIG R.F. 2004, **Craig's Soil Mechanics**, 7th Edition, TJ International Ltd.

DAS B. M., 2004. **Foundation Engineering**, 5th Edition, Thomson Learning.

DRNEVICH V.P., EVANS A.C. and PROCHASKA A.B., 2007. **A Study of Effective Soil Compaction Control of Granular soils**. Publication FHWA/IN/JTRP-2007/12. Joint Transport Research Program, Indiana Department of Transportation and Purdue University, West Lafayette, Indiana, doi: 10.5703/1288284313357

FHWA, 2011. **Accelarated Implementation of Intelligent Compaction Technology for Embankment Subgrade Soils, Aggregate Base and Asphalt Pavement Materials** – Final Report. Federal Highway Administration, Washington DC, Report No. FHWA-IF-12-002

GROBLER J.E. 1990. **Development of Procedures for Large Stone Mix Design.** Dissertation for Master of Science in Engineering, University of Stellenbosch.

HIGHWAYS AGENCY, 1994. Design Manual for Roads and Bridges: Construction of Highway Earthworks. Available at: http://www.dft.gov.uk/ha/standards/dmrb/vol4/section1/ha7094.pdf (Accessed: February 6, 2013)

HILL A.R., DAWSON A.R. and MUNDY M., 2001. **Utilisation of Aggregate Materials in Road construction and Bulk Fill**. Available: http://www.sciencedirect.com/science/article/pii/S0921344901000672 (Accessed: March 8, 2012)

HOFF I. BAKLØKK L.J. and AURSTAD J., 2004. **Influence of Laboratory Compaction method on Unbound Granular Materials,** 6th International symposium on pavements unbound. Norway.

HUANG Y.H. 2003. **Pavement Analysis and Design**. 2nd Edition. Prentice Hall

HUHTALA M., DAWSON A.R., and MUNDY M.J., 1999. **Unbound Granular Materials for Road Pavements**. COST-337 and COURAGE

JUMO I and GELDENHUYS J. 2004. **Impact Compaction of Subgrades - Experience on the Trans-Kalahari Highway including Continuous Impact Response (CIR) as a method of quality control.** Document Transformation Technologies cc. Proceedings of the 8th Conference on Asphalt Pavements for Southern Africa (CAPSA'04) ISBN Number: 1-920-01718-6

KELFKENS R.W.C, 2008. **Vibratory Hammer Compaction of Bitumen Stabilised Material.** Dissertation for Master of Science in Engineering, University of Stellenbosch.

LANGE P.D. 2005. **Validation of the Vibrating Hammer for Soil Compaction Control.** Dissertation for Master of Technology in Civil Engineering, University of Johannesburg.

MASSARSCH, K.R. and FELLENIUS, B.H., 2005. **Deep Vibratory Compaction of Granular soils.** Chapter 19 in Ground Improvement-Case Histories, Elsevier publishers, B. Indranatna and C. Jian, Editors, pp. 633 – 658.

MELTON J.S. and MORGAN T., 1996. **Evaluation of Tests for Recycled Material Aggregates for Use in Unbound Application**, Final Report for RMRC Project No. 6, Recycled Materials Resource Center, Durham, N.H.

MINISTRY OF RAILWAYS, 2005. **Study Report on Compaction Equipments and Construction Machinery.** Report No. GE – R – 76. Government of India

MONTGOMERY D. E. 1999. **Initial Critique of Existing Papers on Dynamic Compaction of Stabilised Soil samples.** Development Technology Unit, School of Engineering, University of Warwick

MURTHY V.N.S. 2003. **Geotechnical Engineering Vol. 10: Principles and Practices of Soil Mechanics and Foundation Engineering.** Marcel Dekker Incorporated.

PAIGE-GREEN P., 1996. **Recommendations on the use of Marginal Base Course materials in Low Volume Roads in South Africa**. Report PR 91/201, Research and Development Advisory Committee, Department of Transport, Pretoria.

PAIGE-GREEN P. AND KANNEMEYER L. 2011. **Revision of the South African Pavement Design Method: Intelligent Compaction**. Available at: http://www.csir.co.za/Built_environment/Infrastructure_engineering/21RPF/22%20Paige-Green%202.pdf (Accessed: June 06, 2012)

PROCHASKA A.B and DRNEVICH V.P. 2005. **Example Paper: One Point Vibrating Hammer Compaction Tests for Granular Soils.** Available at: https://engineering.purdue.edu/TDR/SampleManuscript.pdf (Accessed: February 15, 2012)

PROCHASKA A.B., DRNEVICH V.P., KIM D., and SOMMER P.E. 2005. **A Vibrating Compaction Test for Granular Soils and Dense Graded Aggregates**. TRB 84th Annual Meeting, Washington D.C.

RITCHIEWIKI (2011), Available at: http://www.ritchiewiki.com/wiki/index.php/soil_compaction (Accessed: September 27, 2011)

RODRIGUEZ A.R., del CASTILLO H and SOWERS G.F., 1988. **Soil Mechanics in Highway Engineering**. Trans Tech Publications, Republic of Germany.

SEMMELINK C.J, 1995. **Optimal Compaction of Untreated Road Building Materials in South Africa.** Division of Road and Transport Technology, CSIR, Pretoria, South Africa.

SEMMELINK C.J and VISSER A.T., 1994. **Effect of Material Properties on Compactability and Bearing Capacity.** Journal of Transportation Engineering

SHAHIN W. A, 2010. **Investigation of the Variability in the Results of the NZ Vibrating Hammer Compaction Test**. Dissertation for Master of Science in Engineering, University of Auckland, New Zealand.

SISWOSOEBROTHO B.I., WIDODO P. and AUGUSTA E., 2005. **The influence of Fines and Plasticity on the Strength and Permeability of Aggregate for Base Course Material.** Proceedings of the Eastern Asia Society for Transportation Studies.

SMITH G.N and SMITH I.G.N. 1998. **Elements of Soil Mechanics.** 7th Ed. Blackwell Science Ltd. United Kingdom.

SPECIALTY SALES LLC, 2011. Available at: http://www.specialtysalesllc.com/nutra-bond_compaction.htm (Accessed: December 28, 2011).

THEYSE H.L. 2002. **Stiffness, Strength and Performance of Unbound Aggregate Material: Application of South African HVS and Laboratory Results to California Flexible Pavements**. CSIR Transportek, Pretoria, South Africa.

TMH1. 1986. **Technical Methods for Highways: Standard Methods of Testing Road Construction Materials**. 2nd Ed. Committee of State Road Authorities, Pretoria, South Africa.

TRH 20, 1990. **The Structural Design, Construction and Maintenance of Unpaved Roads**. Pretoria: Committee on Land Transport Officials (COLTO). Technical Recommendations for Highways.

TRH 4, 1996. **Structural Design of Flexible Pavements for Interurban and Rural Roads**. Pretoria: Committee on Land Transport Officials (COLTO). Technical Recommendations for Highways.

TRH 14, 1985. **Guidelines for Road Construction Materials**. Pretoria: Committee on Land Transport Officials (COLTO). Technical Recommendations for Highways.

TRH 9, 1982. **Construction of Road Embankments.** Pretoria: Committee on Land Transport Officials (COLTO). Technical Recommendations for Highways.

TWAGIRA E. M, 2010. **Influence of Durability properties on performance of Bitumen Stabilised Material.** Dissertation for Doctor of Philosophy (Engineering), University of Stellenbosch.

USACE, 1990. **US Army Corps of Engineers EM 1110-2-1911: Construction Control for Earth and Rock-Fill Dams**, September 30.

VAVRIK W.R. 2000. **Asphalt Mixture Design Concepts to Develop Aggregate Interlock**. Dissertation for Doctor of Philosophy in Civil Engineering, University of Illinois.

VIRGINIA DEPARTMENT OF TRANSPORT, 2013. **Appendix E: Compaction Characteristics and Equipment.** Available at: http://www.virginiadot.org/business/resources/Materials/MCS_Study_Guides/bu-mat-AppendixESoils.pdf. (Accessed: February 5, 2013).

WESTON C.T., 2001, **A Study into the Mechanical Properties of Foamed Bituminous Stabilised Materials**, Dissertation for Master of Science in Engineering, Cape Peninsular University of Technology

WIRTGEN GROUP, 2002. **Wirtgen Road Construction Manual: Internal Service Brochure for Sales Managers and Service Engineers.** 3rd Edition. Wirtgen GmbH. Germany

WIRTGEN GROUP, 2004. **Wirtgen Cold Recycling Manual.** 2nd Edition. Wirtgen GmbH. Germany

WIRTGEN GROUP, 2011. **Vibration – Oscillation.** Available at: http://www.hamm.eu/media/pdf/serienprospekte_1/Hamm_Oszi_Flyer_Englisch_08-11-web.pdf (Accessed: November 23, 2012)

WILSON B. 2004. **Never Guess Again: Intelligent compaction making precision commonplace at the jobsite**. Available at: http://www.roadsbridges.com:80/rb/index.cfm/powergrid/rfah=|cfap=/CFID/3211407/CFTOKEN/89068603/fuseaction/showArticle/articleID/5396. (Accessed: June 6, 2012).

YILDIRIM Y., SOLAIMANIAN M and KENNEDY T.W., 2000. **Mixing and Compaction Temperatures for Hot Mix Asphalt Concrete.** Centre for Transportation Research. The University of Texas at Austin

CHAPTER 3: RESEARCH DESIGN AND METHODOLOGY

3.1 INTRODUCTION

This Chapter discusses the research design and methodology adopted to conduct the research. Included are; the materials selected for testing, equipment used, test factors and protocols for conducting the tests.

3.2 MATERIALS

Four material types were selected for testing. Table 3-1 gives the materials types and the motivation for selecting these materials;

Table 3-1: Materials tested

	Material Type			
	G3 Graded Crushed Stone	G4 Natural Gravel	G7 Gravel-Soil	Reclaimed Asphalt (RA)
Motivation	G3 is a high quality granular material obtained by crushing rock, boulder or coarse gravel. It is used in the base course of pavement structures (TRH 14).	Naturally occuring gravel material with all particles passing the 63mm sieve. Typically used in the subbase course of pavement structures (TRH14).	Typically used as a selected layer above the subgrade. It is also naturally occuring sand based material with lesser quality compared to G4.	Material reclaimed from an existing road that has reached the end of its useful life, through milling and/or full depth removal of the upper layers.
Source	Lafarge-Eeste Rivier Quarry	Lafarge-Tygerberg Quarry	Afrimat-Hamlet	Lafarge- Much Asphalt
Parent Rock	Hornfels	Hornfels	Sandstone	

3.2.1 Material Characteristics

Grading

The material obtained from the quarry contained aggregates with particle size greater than 19mm. This particle size is considered too large for 150mm diameter laboratory specimen. Therefore, all aggregates retained on the 19mm sieve were removed and replaced with aggregates <19mm. The material was graded in accordance to recommendations contained in

TRH14 (1985). Figures 3-1, 3-2, 3-3 and 3-4 show the material grading for the G3, G4, RA and G7 materials respectively.

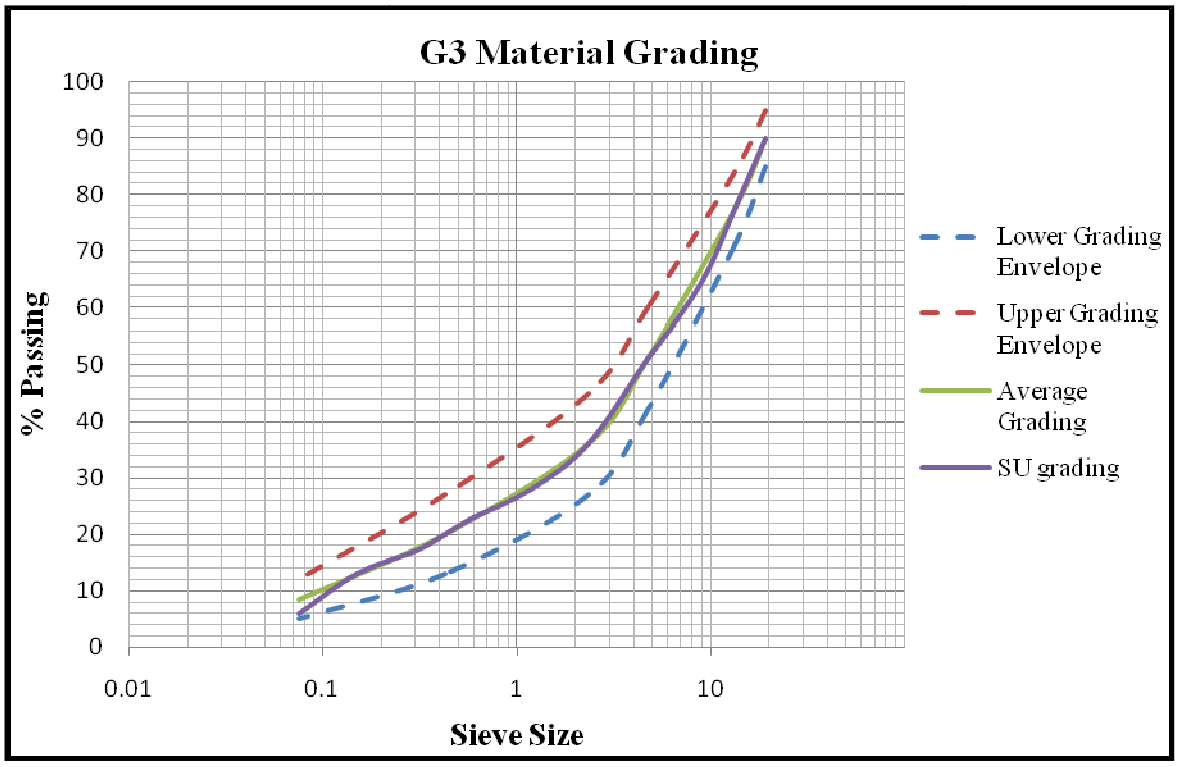

Figure 3-1: G3 Material Grading

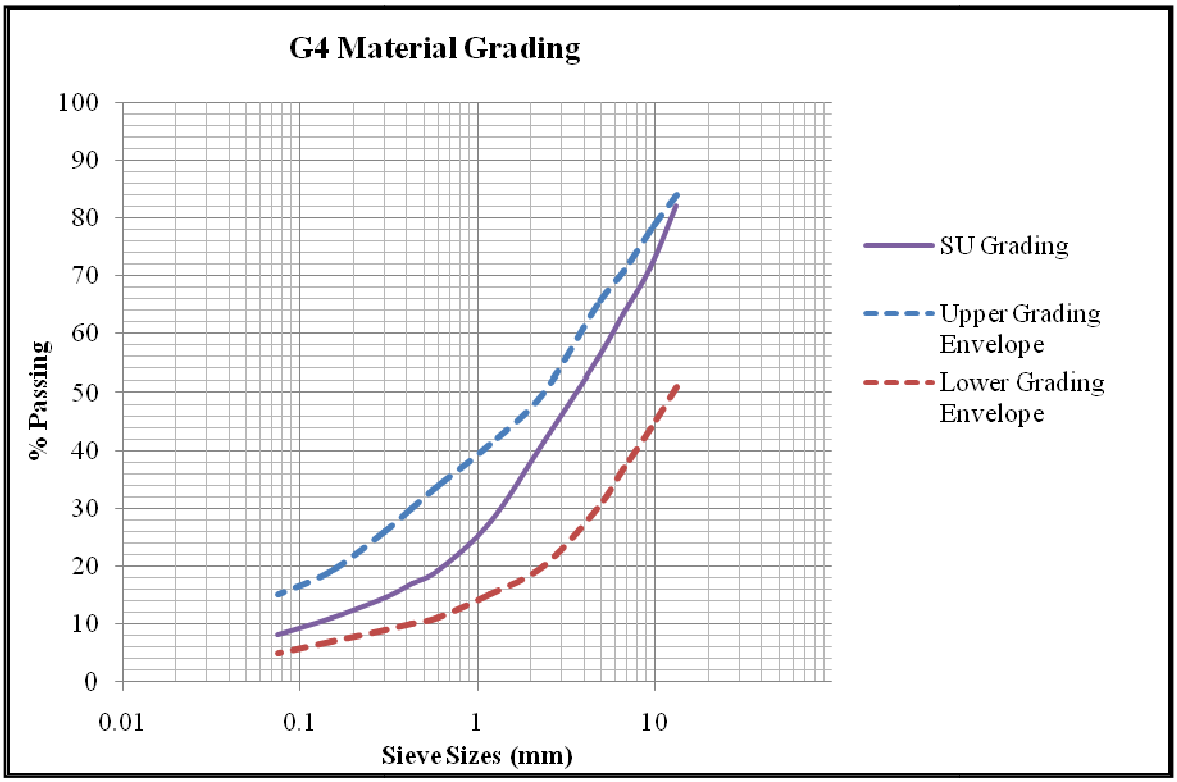

Figure 3-2: G4 Material Grading

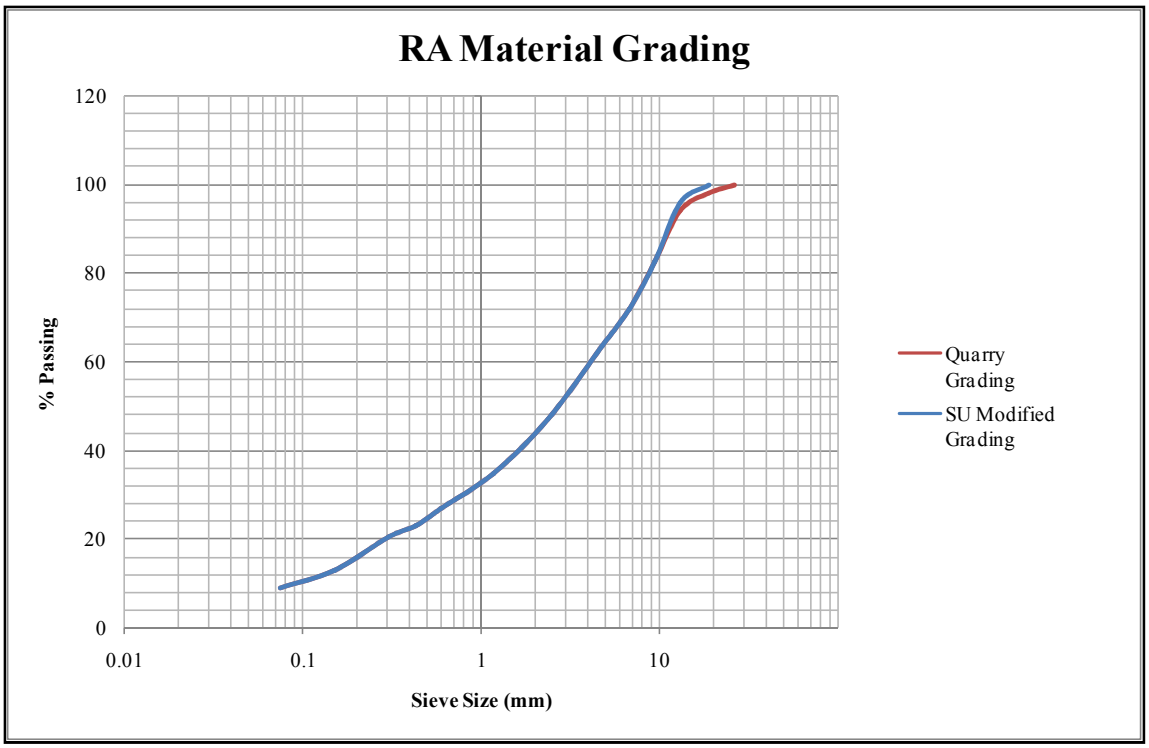

Figure 3-3: RA Material Grading

G7 material has no grading requirements. TRH14, however, recommends a minimum Grading Modulus (GM) of 0.75. Also, Jooste, Long and Hefer (2007) suggest a filler content (material passing the 0.075mm sieve) for G7 materials of between 25 and 30%. Therefore, modifications were made to the grading of the G7 material obtained from the quarry so as to increase the filler content to 25%. Also all material retained on the 19mm sieve was removed and replaced with material passing the 19mm sieve. Figure 3-4 shows the grading of the material and Table 3-2 indicates the grading modulus.

Atterberg Limits and GM

Table 3-2 presents the material characteristics of the selected material as determined at SU.

Table 3-2: Atterberg Limits, OMC, MDD and GM

Description	G3	G4	G7	RA
Liquid Limit (%)	NP	NP	26.2	NP
Plastic Limit (%)	NP	NP	21.3	NP
Plasticity Index (%)	NP	NP	4.9	NP
Linear Shrinkage (%)	NP	NP	5	NP
Grading Modulus (Allowable Min.)	1.57 -	1.61 -	1.85 (0.75)	

NP - Non-Plastic

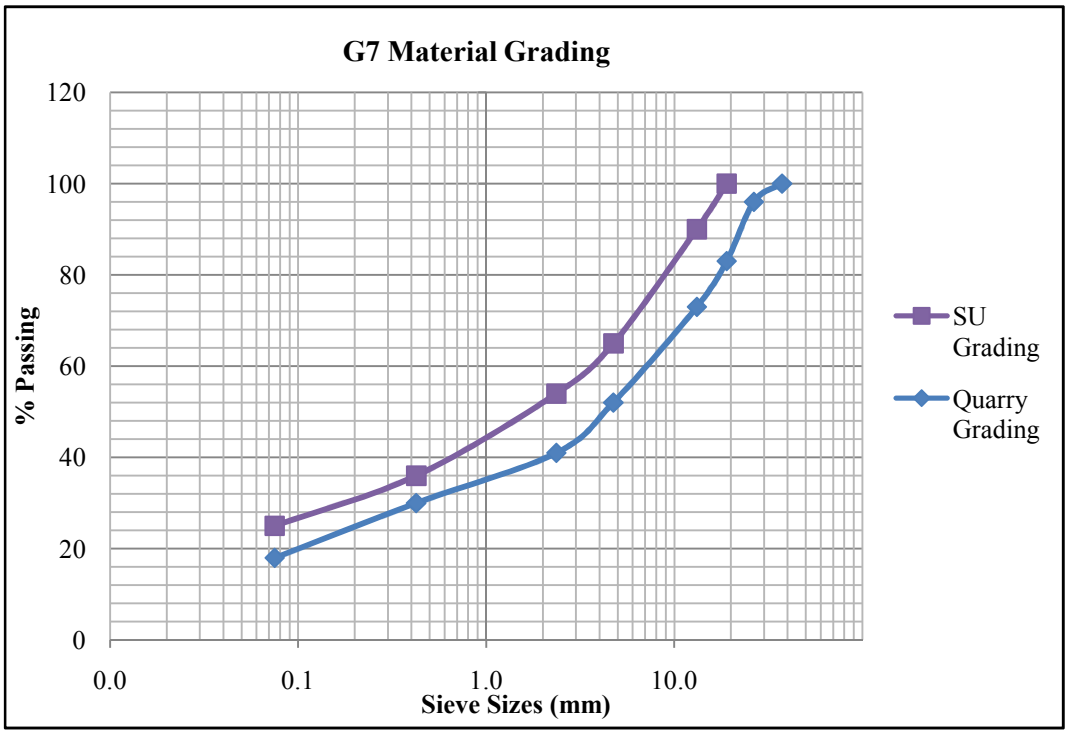

Figure 3-4: G7 Material Grading

3.3 TESTS AND EQUIPMENT

This section describes the tests conducted and the apparatus used to conduct the tests:

3.3.1 Mod AASHTO Compaction

The Mod AASHTO compaction test was done according to TMH1 Method A7 (1986) to obtain the moisture-density relationship and hence the MDD and OMC (denoted OMC_M for ease of reference) of the material (See Section 4.2). The material was compacted in a 152mm diameter by 152mm high mould (with an effective depth of 127mm) in five approximately equal layers with each layer receiving 55 blows of a 4.536kg hammer dropping through a height of 457.2mm.

3.3.2 Vibratory Hammer Compaction

The technical specifications of the vibratory hammer available at Stellenbosch University are presented in Table 3-3. The initial setup of the hammer is shown in Plate 2-3.

Table 3-3: Specifications of Vibratory Hammer

Specification	Criteria
Power Rating	1500W
Frequency	900 to 1890 beats/min (15-31.5Hz)
Point Energy	25 J

Frame Modification

After the first phase of testing, shaking of the support frame was observed as layer compaction densities neared refusal density levels. It was postulated that this led to energy losses resulting in inefficiencies in operation of the hammer. Further inadequacies were noted with the frame including;

- Misalignment of the hammer with the mould
- Bending of metal plate supporting the surcharge load
- Misalignment of the mounting frame
- Degrading of the wooden platform
- Misalignment of the support sections
- Friction on the sleeves of the sliding frame
- Lateral movement of the mould during compaction
- Lateral movement of the hammer due to lack of a bottom support.

Therefore, a decision was made to modify the frame (by making it more rigid) so as to minimise the energy lost to shaking of the frame and inefficiencies resulting from the aforementioned inadequacies. Generally stiffer material sections were considered in making the modifications. Plate 3-1 shows the setup of the upgraded vibratory hammer.

While it is not easy to quantify the rigidity, the new frame was designed so as not to have any discernable shaking or vibrations of the frame supports during compaction. Details of the original (old) frame are contained in Kelfkens (2008). The following modifications were made to the frame;

- The 20mm cylindrical hollow section supports were replaced with 25mm diameter solid sections. It was envisaged that these would provide a more rigid support structure for the hammer.

Plate 3-1: Stellenbosch University Setup of Upgraded Vibratory Hammer

- The mounting frame of the hammer did not support the hammer through its centre of gravity. This caused alignment problems and lateral movements of the hammer. This may have also caused moment effect due to eccentricity of the support. A new mounting frame was built that would support the hammer through its centre of gravity. The hammer is supported from the bottom as well and aligned with the position of the mould to avoid lateral movement during compaction (see Plate 3-2 and Plate 3-3). This is to ensure that the only movement of the tamping foot on the sample is in the vertical direction thus making it more efficient.

- The metal to metal contact of the cylindrical sleeves on the sliding frame resulted in frictional forces. To reduce this, the cylindrical sleeves were replaced with Super Ball Bushing at the top support and Hi-Lube Vesconite Bushing impregnated with lubricating oil at the bottom support (see Plate 3-2 and Plate 3-4) to ensure that friction between the supports and sliding frame was eliminated.

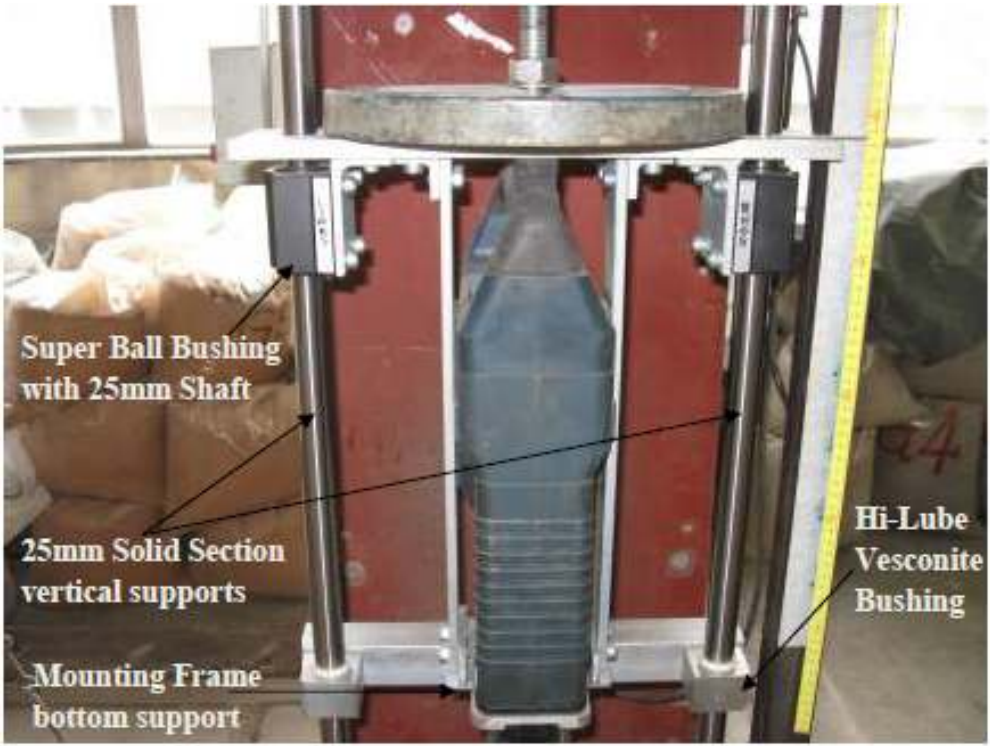

Plate 3-2: Vibratory Hammer Mounting Frame

Plate 3-3: Rear view of Vibratory Hammer Mounting Frame

Plate 3-4: Super Ball Bushing and Hi-Lube Vesconite Bushing

- The wooden platform made out of plywood (Density 508.9kg/m^3) had degraded due to the long period of usage. The central section of the wood piece, supporting the metal plate had subsided. A higher density Supawood board (Density 704kg/m^3) was considered for replacement. In addition to the higher density, the supawood board was chosen due to its structural make up. Unlike the plywood board that may contain honeycomb void spaces within it, the supawood board is homogenous in its structural make up ensuring that the density is uniform all over the board.

Plate 3-5: Bottom Wood Piece and Base Plate for holding mould in position

- Guide rods were fixed on the base plate to sit the mould in position during compaction and a locking mechanism to hold down the mould. This would ensure that no lateral movement of the mould occurs during compaction (Plate 3-5).

Technical drawings of the modified frame are appended in Appendix B.

Tests were performed to compare the effect of the modified 'rigid' frame (denoted RFR) against the original 'soft' frame (denoted SFR) (see Figure 3-5).

The following aspects with regard to compaction with the vibratory hammer were investigated;

Moisture content

A previous study that investigated the effect of moisture content on compaction with the vibratory hammer, established that high densities are obtainable at high moisture contents. In this study, the effect of moisture was investigated at moisture contents; 80 and 90% of OMC_M. These moisture contents were selected by considering that the vibratory hammer would probably impart more compactive effort compared to the mod AASHTO compaction method.

Surcharge Load

In addition to the static load which includes the self weight of the hammer and the sliding frame with all its components, a surcharge load/weight is applied to the vibratory hammer to keep it from bouncing up during compaction. The static load of the SU vibratory hammer is 16.5kg excluding tamper (before upgrade). The effect on compaction of applying 10kg and 20kg surcharge loads was investigated. Application of these surcharge loads brings the total weight applied (excluding tamper) to 26.5 and 36.5kg respectively.

After the modifications, the static load increased by about 5kg from 16.5kg to 22.1kg. To maintain the same overall weights applied on the sample (26.5 and 36.5kg) for the second phase of testing with the 'rigid frame', one of the 10kg surcharge loads was replaced with a 5kg surcharge load. Therefore, the effect of the surcharge load was observed by applying 5kg and 15kg weights.

Frequency

The SU Bosch vibratory hammer used for testing has six frequency settings ranging from 15Hz to a maximum of 31.5Hz. All tests were performed at the highest frequency (31.5Hz) setting. Comparative tests on two material types (G3 and G7) were performed at frequencies; 25.67 and 19.67Hz to determine the influence of frequency on the compaction.

Tamping foot

Two tampers of weights 3kg and 4.6kg (Plate 3-6) were used for compaction to determine the effect of the weight of the tamping foot on compaction.

Plate 3-6: Tampers

3.3.3 Comparative Tests with Vibratory Table

Tests with the vibratory table were conducted to evaluate how vibratory hammer compacted specimen compare with those compacted using the vibratory table. Table 2-2 gives the specifications of the vibratory table and Plate 2-2 shows the setup of the vibratory table at Stellenbosch University. The procedure for conducting tests with the vibratory table is detailed in TMH1 Method A11T (1986). The procedure in TMH1 provides for a compaction time of 2 minutes per layer for each of the three layers to achieve a specimen height of 127mm. However, for the purpose of this study, 300mm high specimens were manufactured in five approximately equal layers. In order to reference the density to mod AASHTO density, the time to compact each layer to 100% of mod AASHTO (i.e. layer thickness of 60mm) and the density achieved after 2 minutes (i.e. if the time to 100% of mod AASHTO density is less than 2 minutes) of compaction were observed.

3.3.4 Integrity of Interlayer Bond

Previous studies have indicated an increased amount of void spaces at the layer interfaces. This is attributed to the scarification done after compaction of each layer. In this study, scarification of the vibratory hammer compacted specimen was done by two means; a scarifying tool (Plate 3-7) and using a drill. This was done to compare the effect of each of these scarification methods on the void profile at the layer interface. CT-scan was employed to visualize the void profile resulting from the two means of scarification, at the layer interface.

Plate 3-7: Scarifying tool

3.3.5 Sieving Analysis

Sieve analysis before and after compaction with the vibratory hammer was performed to evaluate occurrence of particle degradation.

3.4 EXPERIMENTAL PLAN

Figure 3-5 shows the flow chart of the experiment design covering all of the above tests. VT represents vibratory table while RFR and SFR represent ‘rigid frame’ and ‘soft frame’ of the vibratory hammer, respectively.

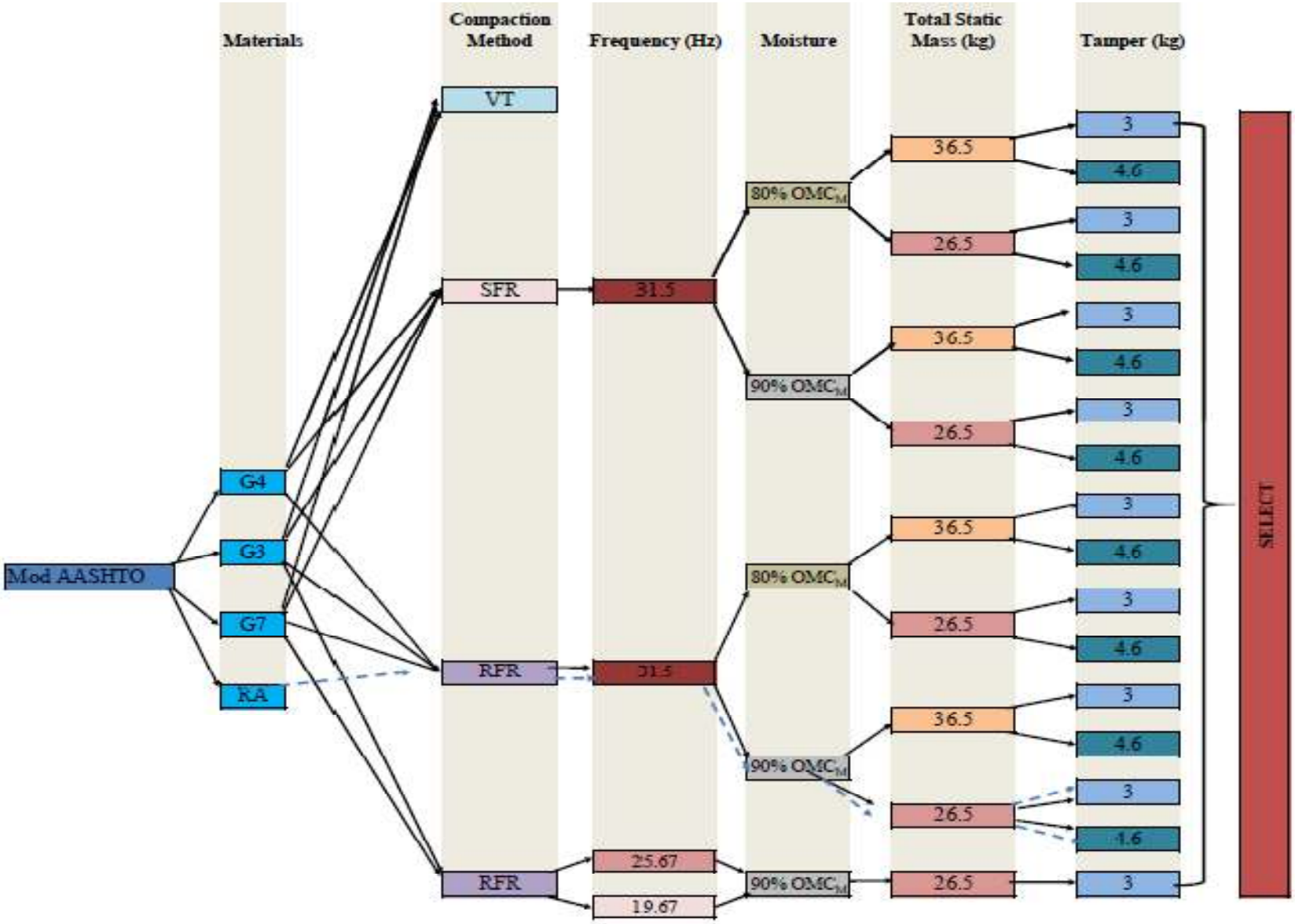

Figure 3-5: Flow Chart for manufacturing Specimen

Due to time constraints only a limited study of the RA material was performed. Testing was done for the two tampers at a single moisture content and surcharge as shown in Figure 3-5.

3.5 COMPACTION PROCEDURES

3.5.1 Vibratory Hammer

Two specimens for each test were manufactured using the following procedure;

Step A1: Determine the moisture density relationship of the materials following the TMH1 procedure for Mod AASHTO (TMH1: Method A7).

Step A2: The density determined in Step A1 will be used as the target dry density and the moisture content calculated as a percentage (80% and 90%) of the OMC determined in step A1.

Step A3: From the target dry density in Step A1 and the moisture content in step A2, the mass of the compacted specimen is calculated from Equation 3-1. The 2kg of material is added for moisture determination.

$$SP_m = SC_m + 2kg = \frac{\rho \times V}{1 + MC_t} + 2 \qquad \text{Equation 3-1}$$

Where;

SP_m = *Dry Sample mass (kg)*

SC_m = *Dry Specimen mass (kg)*

ρ = *Target dry density (kg/m^3)*

V = *Volume of mould (m^3)*

MC_t = *Target moisture content*

Step A4: The specimen mass calculated in Step A3 is divided into five (5) equal portions to determine the mass of material to be compacted per layer. The extra two (2) kg is used to determine the moisture content by means of the standard oven drying method detailed in TMH1.

Step A5: The mounted vibratory hammer is lowered into the empty mould until the foot piece rests on the base of the mould. The position of the base of the sleeve is marked out as the 'zero line' as shown in Figure 3-6.

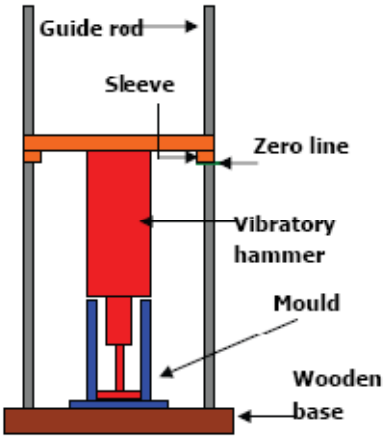

Figure 3-6: Marking off of Zero Line

Step A6: The vibratory hammer is then raised a distance of 60mm measured from the marked 'zero line' (using a 150mm steel rule). This position (denoting the target dry density) is marked out clearly as shown in Figure 3-7.

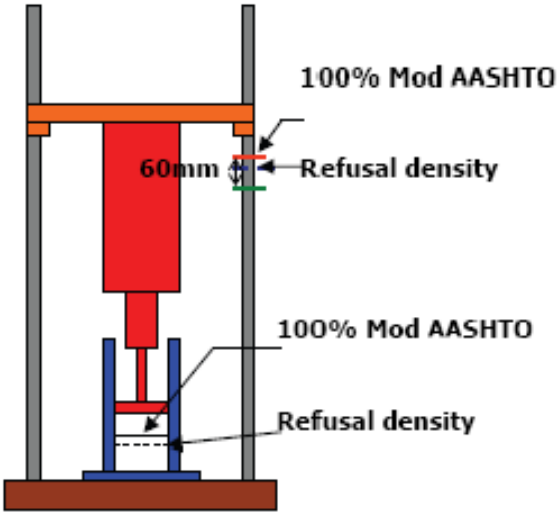

Figure 3-7: Target Dry Density Line and Refusal Density

Step A7: One of the portions in Step A4 is poured into the mould and the vibratory hammer lowered until the tamping foot rests on the surface of the material.

Step A8: The vibratory hammer is switched on and simultaneously a stop watch is started. The material is compacted until the base of the sleeve reaches the marked point of

Step A6. The vibratory hammer is switched off and simultaneously, the stop watch stopped. The time is recorded.

Step A9: The mounted vibratory hammer is switched on again and simultaneously the stop watch started. The material is compacted further, stopping the vibratory hammer at regular intervals and recording the thickness of the layer and the time intervals. The thickness is equivalent to the distance from the 'zero line' to the base of the sleeve. This is done until the same height is recorded three (3) times. This height is then the refusal density and is clearly marked.

Step A10: The mounted vibratory hammer is raised.

Step A11:60mm is measured from the marked refusal density height of the previously compacted layer (Figure 3-8).

Step A12: The surface of the compacted layer is scarified to ensure interlocking of layers. This is done using the drill or the scarifying tool (Plate 3-7). The scarifying tool works by lowering the circular end of the tool in the material so that the projections penetrate the surface of the material. The tool is then rotated back and forth in the material so as to disturb the surface of the layer of material.

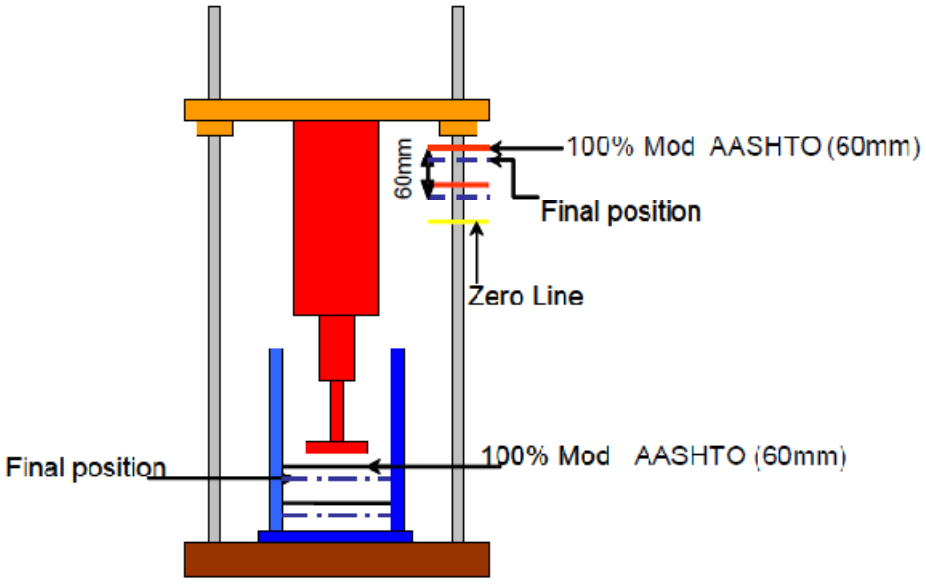

Figure 3-8: Target Dry density and Refusal Density of Second layer

Step A13: A second portion of the material from Step A4 is poured into the mould.

Step A14: Steps A8 to A13 are repeated until all the portions in Step A4 have been compacted with the refusal height of each layer becoming the 'zero line' of the next layer.

Step A15: The compacted specimen is measured and weighed.

3.5.2 Vibratory Table

Two specimens for each test were manufactured using the following procedure;

Step B1: The layer mass is determined as in Steps A1 to A4 in Section 3.5.1.

Step B2: A steel split mould is clamped to the vibratory table as shown in Plate 2-2.

Step B3: The frequency was set to 50Hz as per TMH1 Method A11T specifications. The amplitude was set at the highest setting (0.4mm).

Step B4: One portion of the material is taken and poured into the mould.

Step B5: The 50kg surcharge is placed in the mould at the surface of the material

Step B6: The vibratory table is switched on and the time to compact the material to the target dry density (Figure 3-9) is recorded.

Step B7: The material is further compacted until a cumulative compaction time of 2 minutes is achieved.

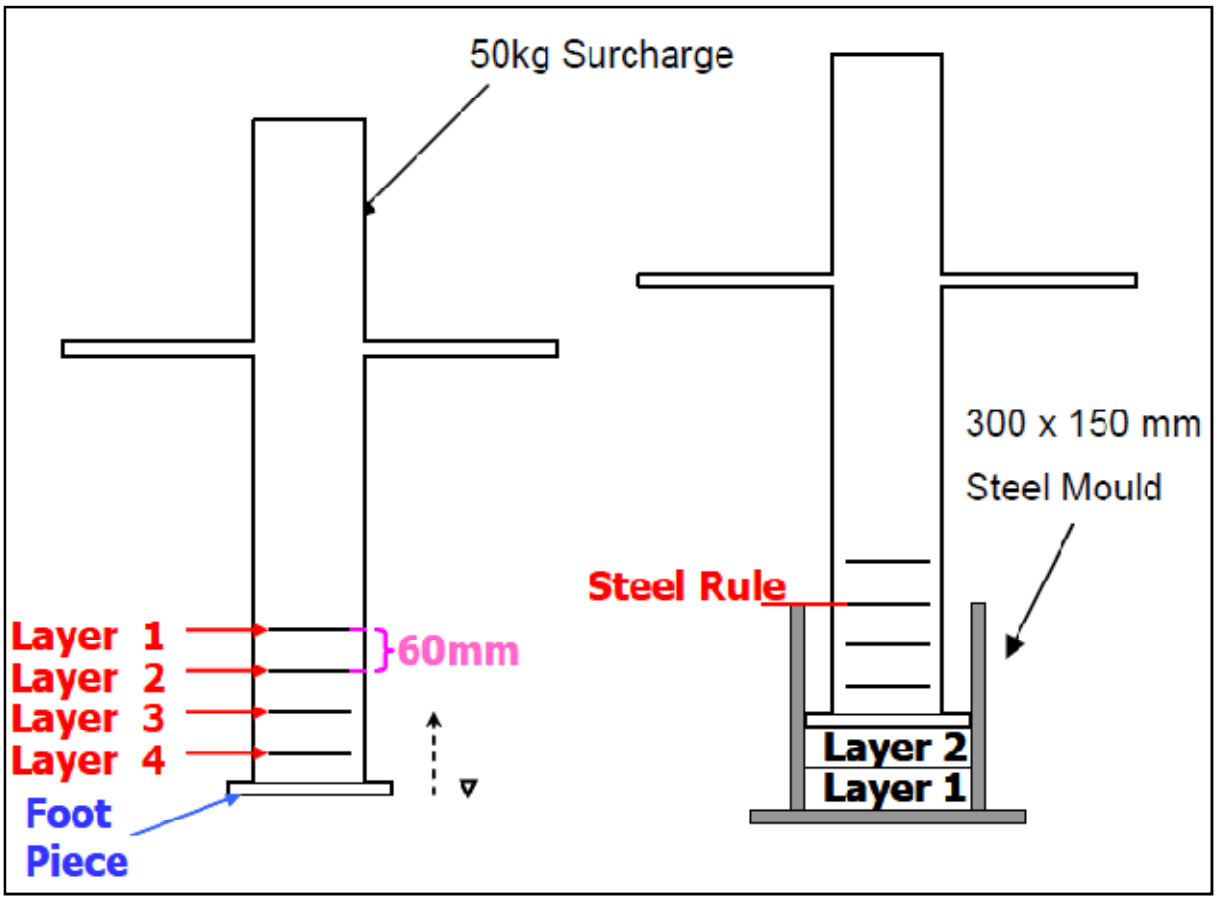

Figure 3-9: Target Dry Density – Vibratory Table

Step B8: The final height of the material is marked out on the 50kg surcharge. This height is used as the zero height for the next layer of material.

Step B9: The 50kg surcharge is removed and the surface of the compacted material is scarified.

Step B8: The next portion of material is poured into the mould.

Step B9: Steps B5 to B8 are repeated until all the material is compacted.

Step B10: The compacted specimen is removed, weighed and measured.

REFERENCES

JOOSTE F., LONG F. AND HEFER A. 2007. **Technical Memorandum: A Method for Consistent Classification of Materials for Pavement Rehabilitation Design.** Gauteng Department of Public Transport, Roads and Works and SABITA

TMH1. 1986. **Technical Methods for Highways: Standard Methods of Testing Road Construction Materials**. 2nd Ed. Committee of State Road Authorities, Pretoria, South Africa.

TRH 14, 1985. **Guidelines for Road Construction Materials**. Pretoria: Committee on Land Transport Officials (COLTO). Technical Recommendations for Highways.

CHAPTER 4: RESULTS PRESENTATION AND DISCUSSION

4.1 INTRODUCTION

This chapter of the report presents the results of the experiments and the interpretations thereof.

4.2 MOISTURE – DENSITY RELATIONSHIP

Figure 4-1 presents the moisture-density relationships of the G3, G4 and G7 materials. The MDD and OMC (OMC_M) obtained from the Mod AASHTO compaction method was used as reference density for the vibratory hammer compaction. The MDD and OMC_M are presented in Table 4-1. The MDD and OMC_M for the RA material were obtained from Matteo Dal Ben, a PhD student at Stellenbosch University.

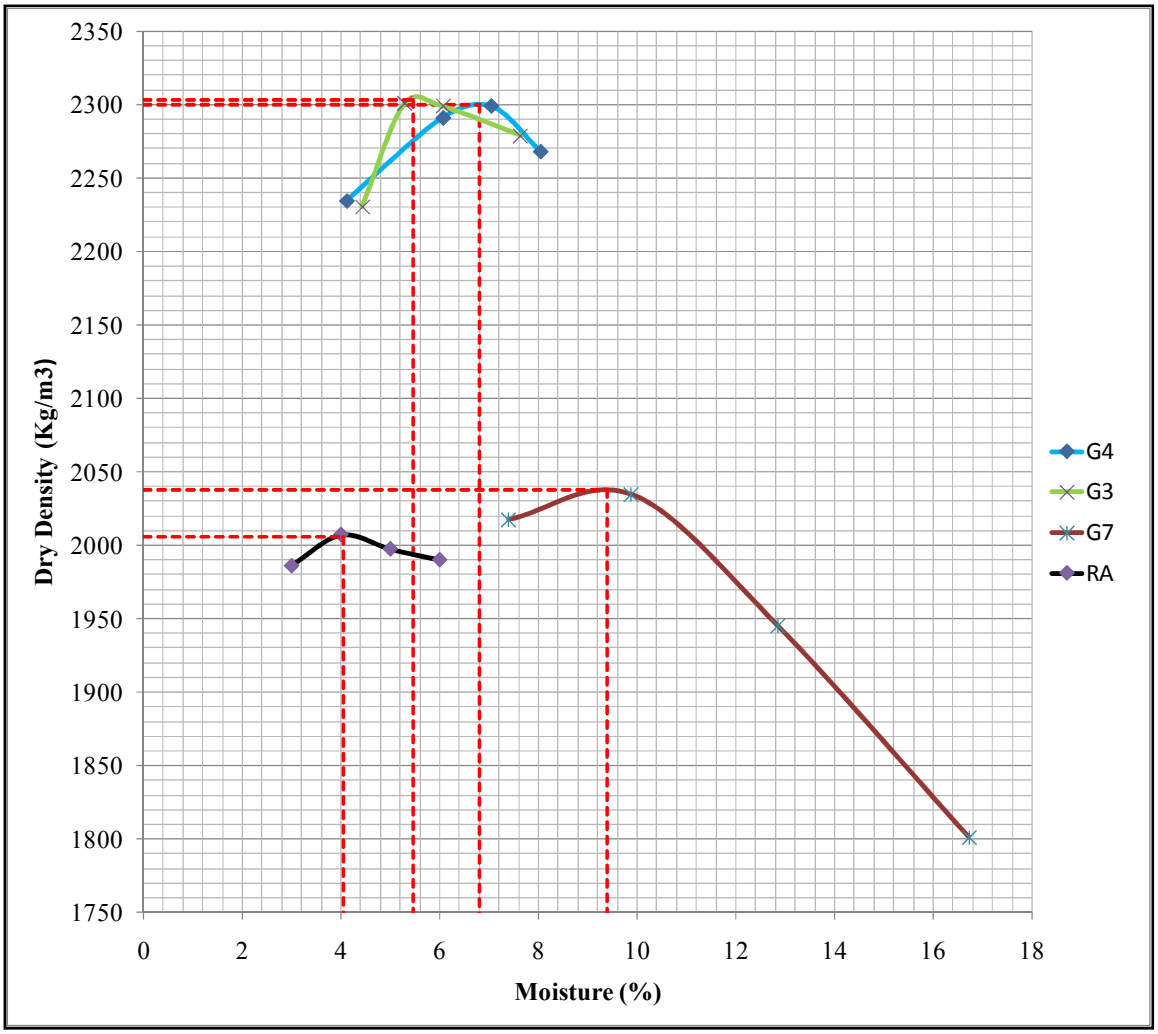

Figure 4-1: Moisture-Density Relationships

Table 4-1: OMC and MDD of the Material

Description	G3	G4	G7	RA
OMC (%)	5.46	6.8	9.4	4.05
MDD (kg/m^3)	2303	2300	2038	2006

4.3 VIBRATORY HAMMER COMPACTION

Two variables were observed for the vibratory hammer tests; the time to compact each layer to 100% of Mod AASHTO density and the overall specimen density obtained. As stated in Section 3.5.1, the mass of material (specimen mass) obtained from Equation 3-1, if compacted in five equal layers each to a height of 60mm (100% of Mod AASHTO density), the specimen obtained should in theory have a density of 100% of Mod AASHTO density. Therefore, the time to compact each layer to 100% of Mod AASHTO was observed. However, to ascertain layer densities over time, compaction of each layer was continued until refusal density (i.e. no more increase in density is observed).

4.3.1 Results from vibratory hammer/'soft frame'

Results of all the individual tests are appended in Appendices C, E and G for G3, G4 and G7 materials respectively. Consolidated results of the compaction time are presented for discussion in Figure 4-2, Figure 4-3 and Figure 4-4 for G3, G4 and G7 materials respectively. Figure 4-5, Figure 4-6 and Figure 4-7 show the trend of the compaction density over time for the G3, G4 and G7 materials respectively. Discussions of the Figures follow in Sections 4.3.1.1 to 4.3.1.3. The codes used for notation of the Figures e.g. G3SFR means G3 material for Soft frame.

4.3.1.1 Influence of Tamping Foot

At the same moisture content and same surcharge load, the influence of the 3kg and 4.6kg tampers on compaction time and densities obtained was observed.

The results show that less time is required to compact to the same level of density (100% of Mod AASHTO density) with the 3kg tamping foot compared to the 4.6kg tamping foot. This is evident for all three material types and combinations of moisture content and surcharge load. This difference is more pronounced with the G3 and G7 materials. For instance, Figure 4-2 shows that at 80% of OMC_M and 20kg surcharge, it took 32 seconds to compact layer 4 to 100% of Mod AASHTO density with the 4.6kg tamper, 26 seconds more than the 3kg tamper.

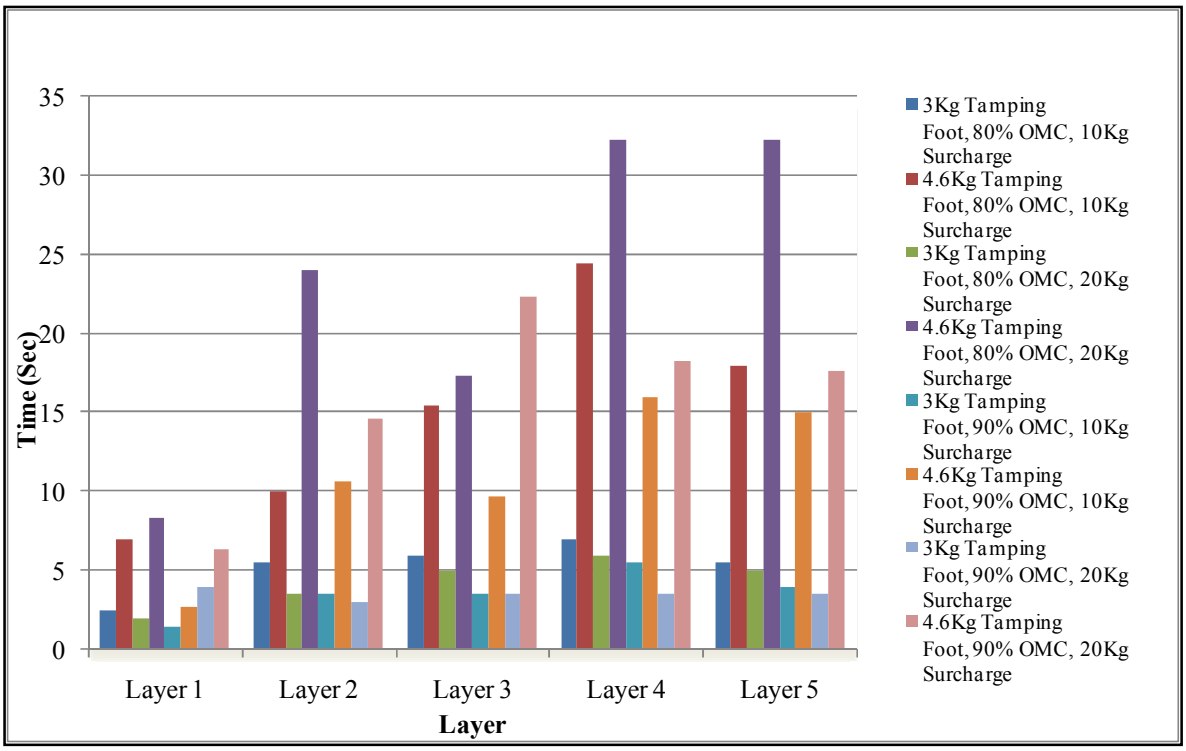

Figure 4-2: Compaction Time to 100% of Mod AASHTO per layer – G3SFR

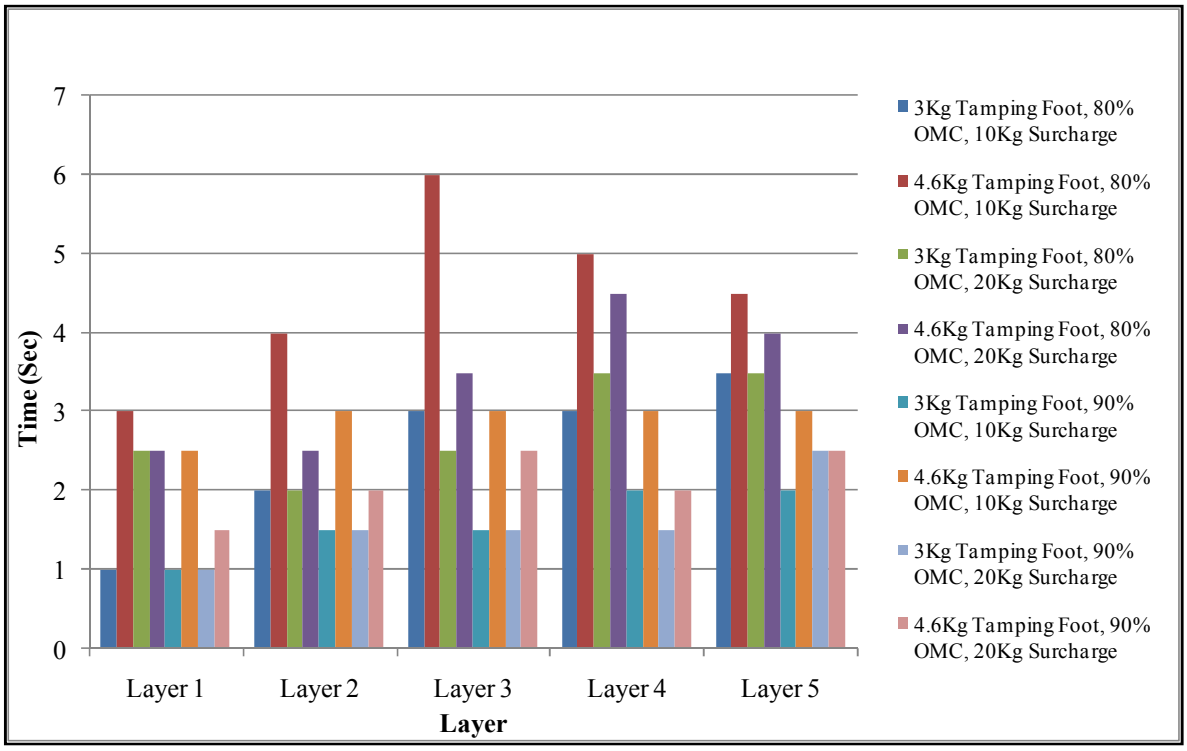

Figure 4-3: Compaction Time to 100% of Mod AASHTO per layer – G4SFR

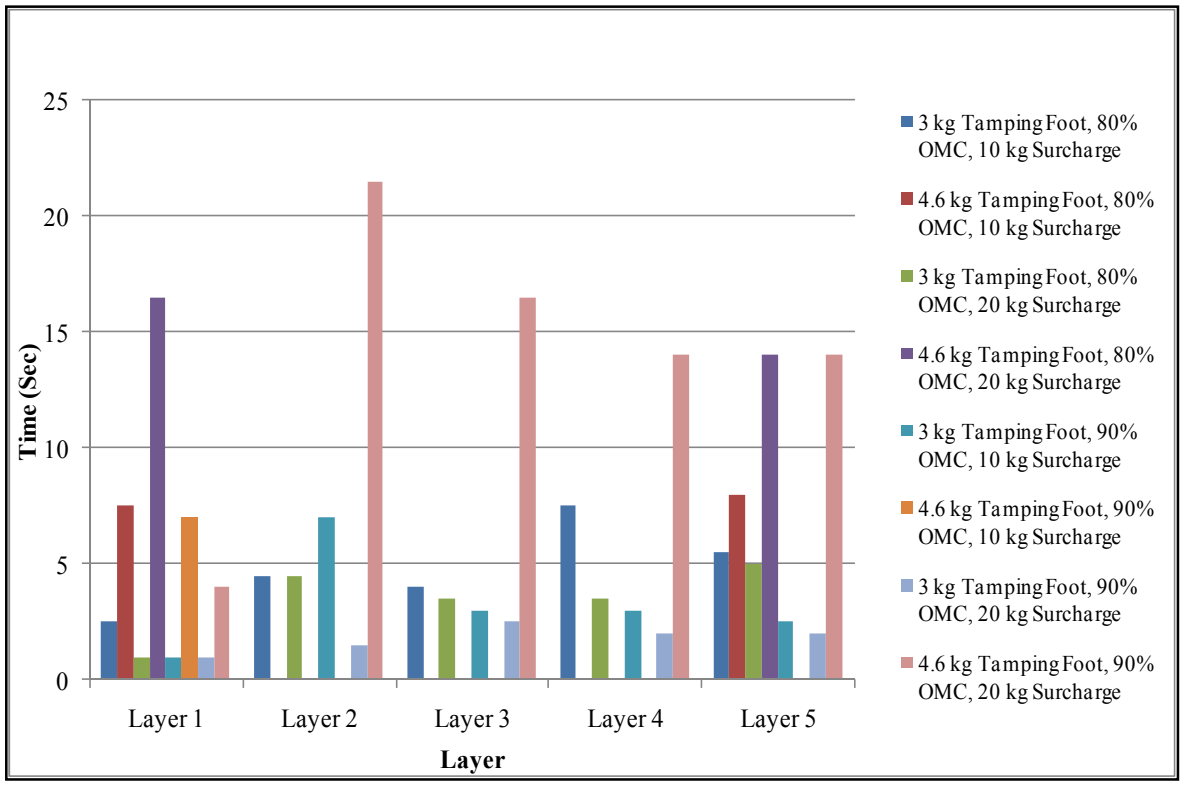

Figure 4-4: Compaction Time to 100% of Mod AASHTO per layer – G7SFR

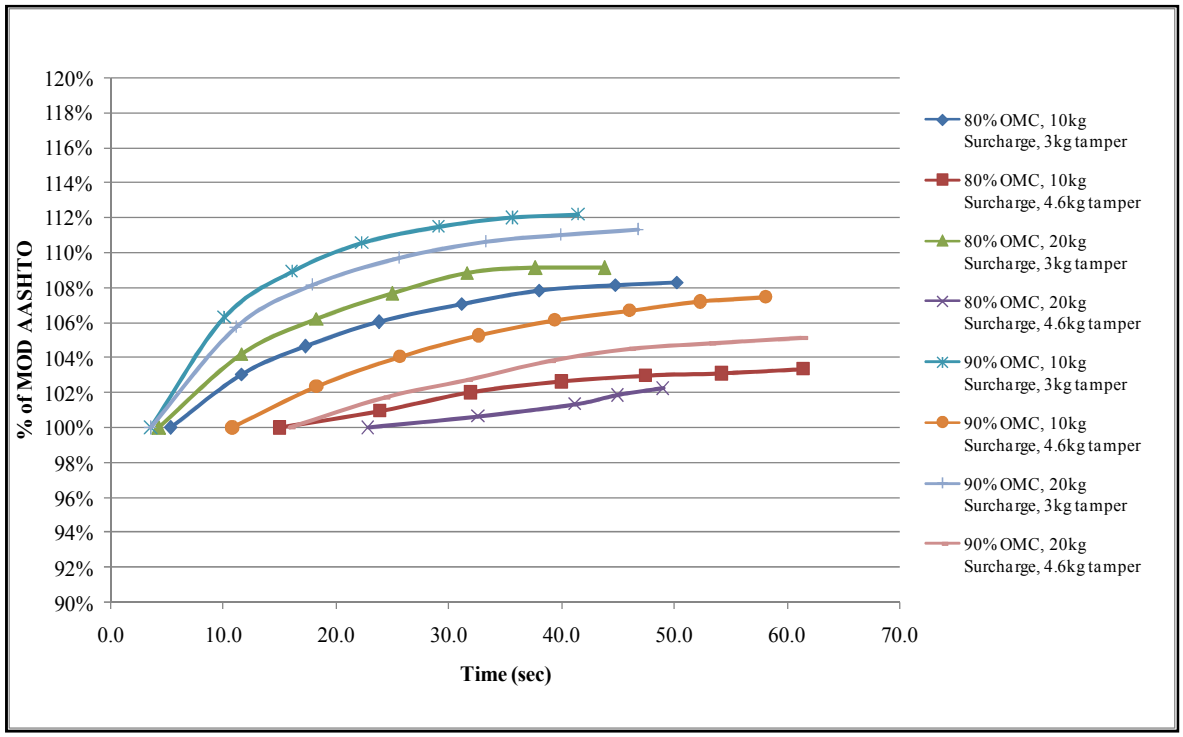

Figure 4-5: Compaction Profile to refusal density– G3SFR

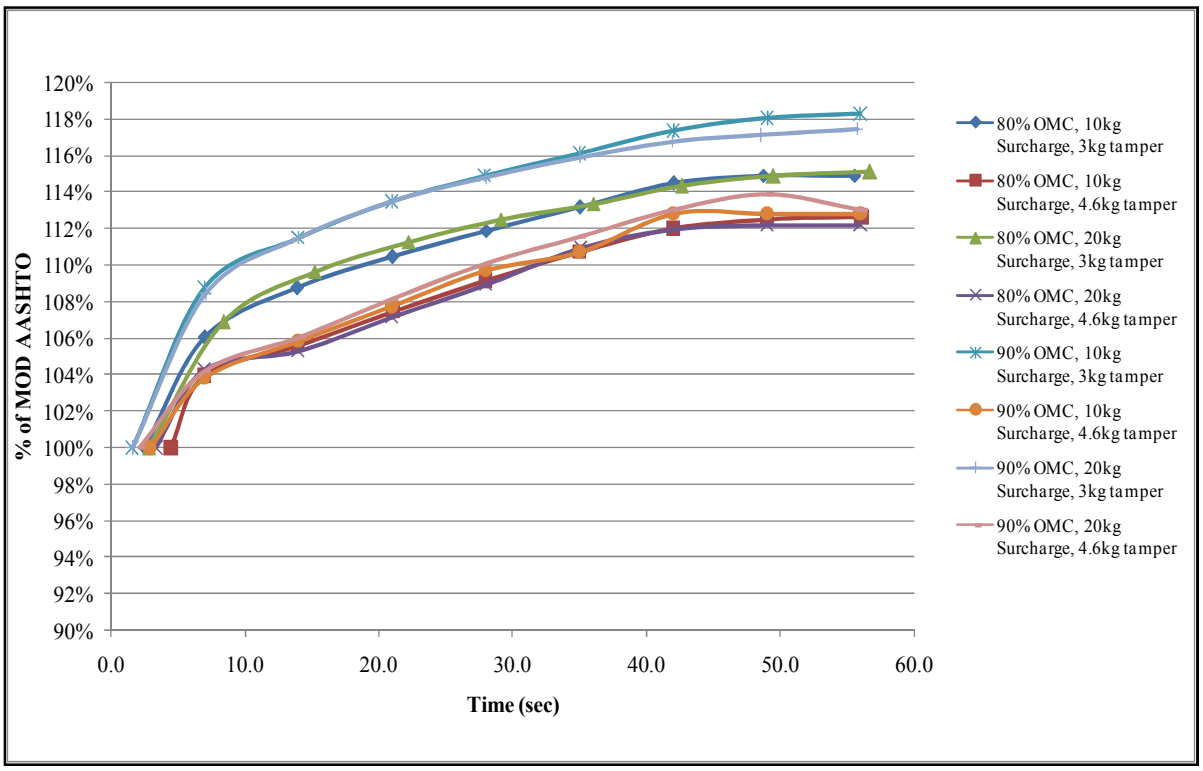

Figure 4-6: Compaction Profile to refusal density– G4SFR

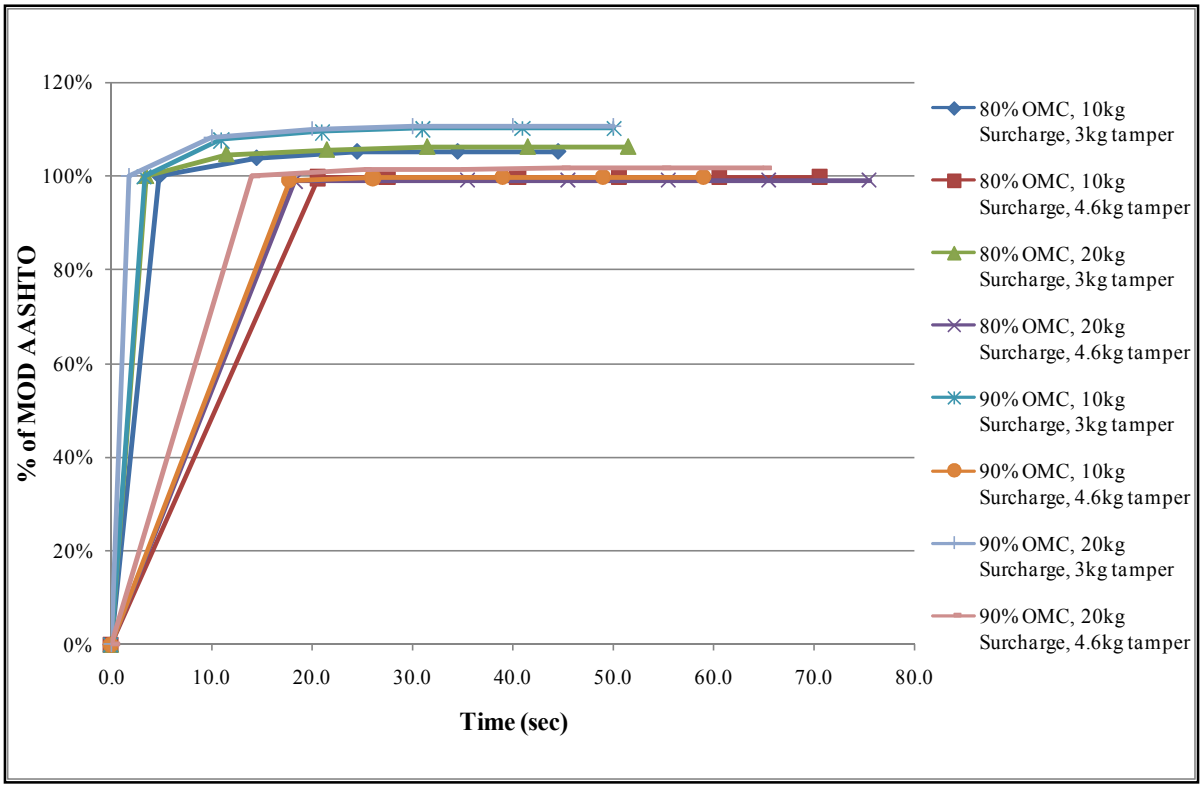

Figure 4-7: Compaction Profile to refusal density– G7SFR

Similarly for the G7 material, layer compaction to 100% of Mod AASHTO density could not be attained in some cases even after long periods of compaction with the 4.6kg tamper, hence the gaps in the data in Figure 4-4. The consistency with all three material types indicates a strong probability that the behaviour is due to the tampers and not the materials but may be more pronounced depending on nature of material. The results also show a general upward trend in compaction time to 100% of Mod AASHTO with each consecutive layer. The least time is required to compact the first layer. This is probably due to the support layer and its energy dissipation capability. The first layer is compacted on a metallic base plate (support) that provides more confinement and less energy loss. However, as layers are added, the lower layers act as supports and energy is dissipated to these support layers.

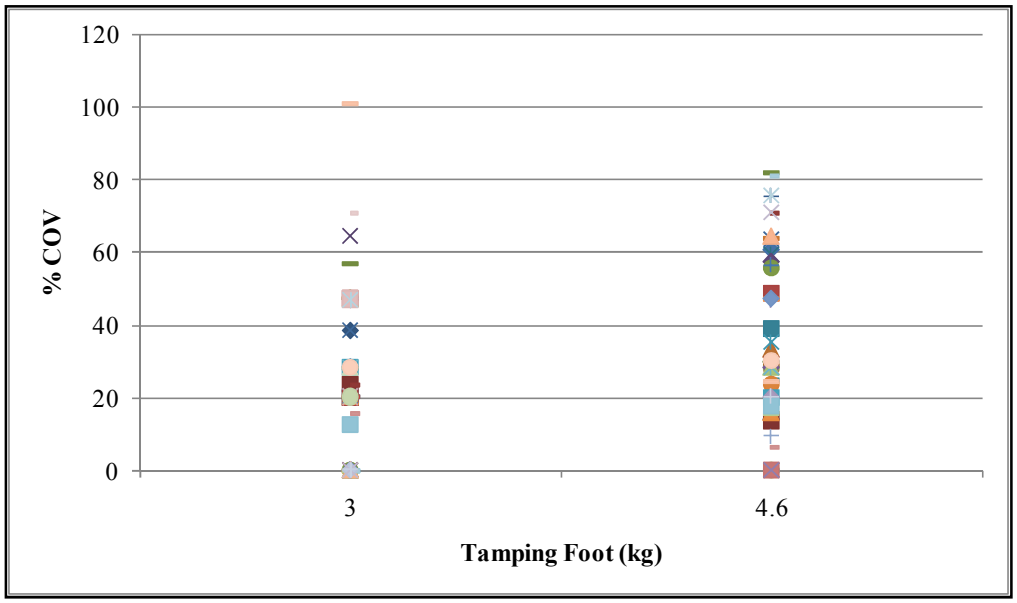

Figure 4-8: % COV of Compaction time to 100% of Mod AASHTO density for G3, G4 and G7 materials

Figure 4-8 is a plot of the percentage coefficients of variation (% COV) of the time to compact each layer to 100% of Mod AASHTO for the three materials i.e. G3, G4 and G7. It is shown that the 3kg tamping foot gives more consistent compaction time results compared to the 4.6kg tamping foot.

Figure 4-5, Figure 4-6 and Figure 4-7 show a sharp increase in density (shown by steeper slopes) after attainment of 100% of Mod AASHTO density, after which the graphs tend to flatten out indicating attainment of refusal densities (i.e. no significant increase in density over time). Steeper slopes are obtained for the combination of factors with the 3kg tamping foot compared to the 4.6kg tamping foot. Also higher layer refusal compaction densities are

obtainable for the combination of factors with the 3kg tamping foot. Figure 4-5 shows that for the G3 material, the highest layer refusal densities were obtained for the 3kg tamping foot in combination with 10kg surcharge at 90% of OMC_M moisture. For the G7 material 100% of Mod AASHTO density could not be obtained for some layers. This is shown in Figure 4-7 where the graphs flatten out at around 98-99% of Mod AASHTO density.

The higher layer densities culminated into high specimen densities for the 3kg tamper as shown in Figure 4-9, Figure 4-10 and Figure 4-11 for the G3, G4 and G7 materials respectively. However, the specimen densities were less than the average layer refusal densities. Reasons for this could be errors in measurements of material quantities and moisture contents or/and material sticking to sides of the mould.

Differences ranging from 3.3% to 6.8% in specimen compaction densities were observed between the two tampers for the G3 material (Figure 4-9). For the G4 material, the range was from 3% to 4.6% (Figure 4-10) and for the G7 material, the difference was even higher, ranging from 4.7% to 8.7%.

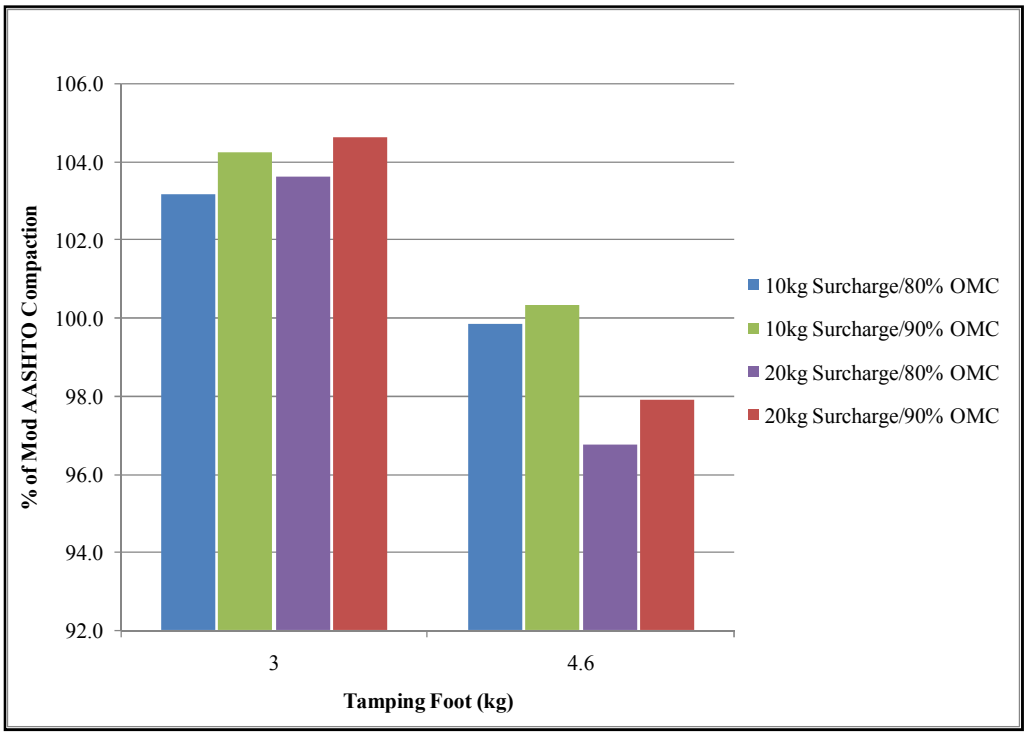

Figure 4-9: Effect of Tamping Foot on Refusal Density – G3SFR

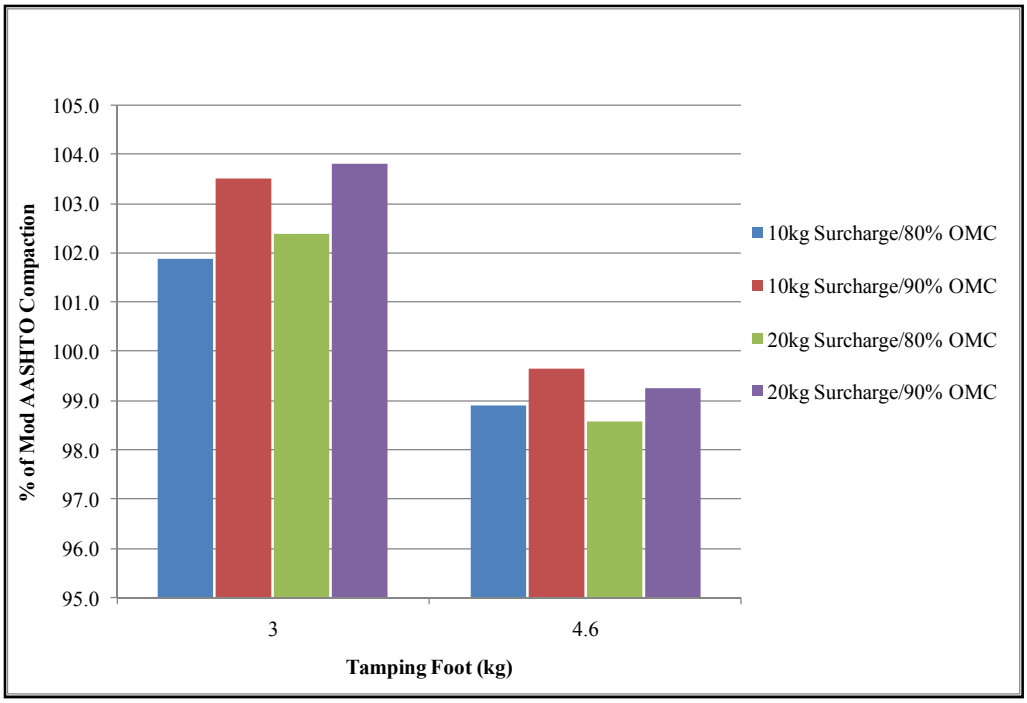

Figure 4-10: Effect of Tamping Foot on Refusal Density – G4SFR

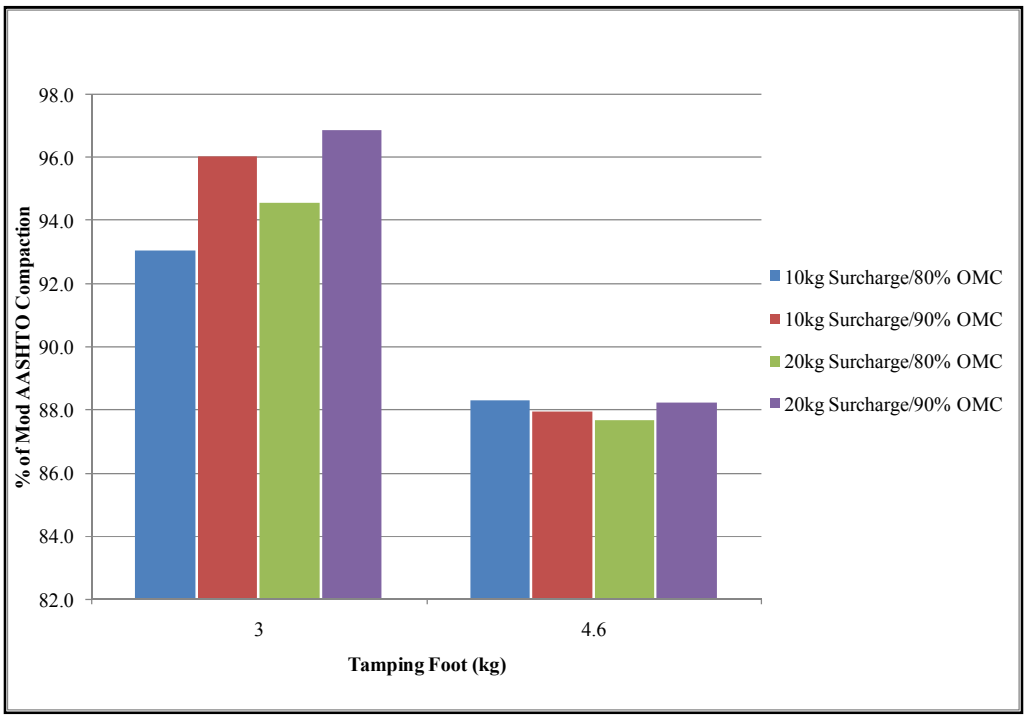

Figure 4-11: Effect of Tamping Foot on Refusal Density – G7SFR

4.3.1.2 Influence of Moisture

By keeping the surcharge and tamping foot constant, the influence of moisture on compaction time and on densities attained was observed. The tests were conducted at moisture contents of 80% and 90% of OMC_M.

The effect of moisture on compaction time can be seen in Figure 4-2, Figure 4-3 and Figure 4-4 for the G3, G4 and G7 materials respectively. The results show that shorter compaction times are required to get to the same level of density at 90% of OMC_M moisture compared to 80% of OMC_M. This behaviour is consistent for all three material types and combinations of surcharge and tamping foot. Figure 4-2 shows, in layer 4 of the G3 material, a 14 seconds difference between the 80% and 90% of OMC_M moisture for the combination of the 20kg surcharge and 4.6kg tamper.

Compaction density is also favoured by high moisture contents. This is observed in the compaction trends in Figure 4-5, Figure 4-6 and Figure 4-7. The results show that high layer densities are obtained at the 90% of OMC_M compared to 80% of OMC_M. The difference in obtainable compaction densities at the two moisture contents can also be seen in Figure 4-9, Figure 4-10 and Figure 4-11 for the G3, G4 and G7 materials respectively. The results show that the difference is more pronounced for the 3kg tamping foot with the G4 and G7 materials and less pronounced for 4.6kg tamping foot. The G3 material showed differences of between 0.5% and 1.1% while the G4 material showed differences ranging from 0.7% to 1.6% at the two moisture contents. A 3% difference in density was observed for the G7 material at the two moisture contents for the combination of the 10kg surcharge and 3kg tamping foot (Figure 4-11).

4.3.1.3 Influence of Surcharge

To determine the influence of the surcharge load on compaction, experiments were performed using two surcharge loads i.e. 10kg and 20kg. The effect of the surcharge loads on compaction time and on densities attained was observed.

The time to compact each layer to 100% of Mod AASHTO density was recorded for the two surcharge loads in alternate combinations with 3 and 4.6kg tampers at moisture contents of 80% and 90% of OMC_M (see Section 3.3.2). The effect of the surcharge load on compaction

time can be observed at constant moisture and surcharge in Figure 4-2, Figure 4-3 and Figure 4-4 for G3, G4 and G7 materials respectively.

The results show no significant difference in compaction time to 100% of Mod AASHTO density for the two surcharge loads in combination with the 3kg tamper for the G3 and G4 materials. The 10kg surcharge load in combination with the 4.6kg tamper showed less compaction time for the G3 material but the converse was observed for the G4 material. Compaction times were slightly lower with the 20kg surcharge load in combination with the 3kg tamper compared to the 10kg surcharge for the G7 material. However, in most cases the differences in compaction time were too small, particularly in the G4 material (ranging from 0.5 to 3 seconds), and therefore may not necessarily indicate surcharge load preference.

The layer compaction trends in Figure 4-5, Figure 4-6 and Figure 4-7 for the G3, G4 and G7 materials show that the surcharge load has a marked influence on the obtainable layer densities for the G3 materials but does not fully influence the obtainable density for the G4 and G7 materials.

At constant moisture and tamping foot, the influence of surcharge load on the obtainable specimen density for the G3, G4 and G7 materials can also be observed in Figure 4-9, Figure 4-10 and Figure 4-11 respectively. The results show that the surcharge load has a marginal influence on the obtainable density particularly in combination with the 3kg tamping foot. A significant difference in density was however, observed with the G3 material for the 4.6kg tamping foot. The 10kg surcharge in combination with the 4.6kg tamping foot produced specimens of density 2.4% (at 90% of OMC_M) and 3.1% (at 80% of OMC_M) higher than the 20kg surcharge as shown in Figure 4-10.

4.3.2 Results from vibratory hammer/'rigid frame'

The primary purpose of modifying the frame was to make it more efficient by reducing on the energy lost to the shaking of the frame and friction on the sleeves. The tests above were repeated to observe the influence that a more 'rigid frame' would have on the compaction time and obtainable compaction densities. Results of the tests are appended in Appendices D, F and H. The consolidated results for the layer compaction time to 100% of Mod AASHTO are shown for the G3, G4 and G7 materials in Figure 4-12, Figure 4-13 and Figure 4-14 respectively. The layer density profiles are shown in Figure 4-15, Figure 4-16 and Figure 4-17 for the G3, G4 and G7 materials respectively. Discussions follow thereafter in Sections

4.3.2.1 to 4.3.2.3. The code used for notation of the Figures e.g. G3RFR means G3 material for rigid frame.

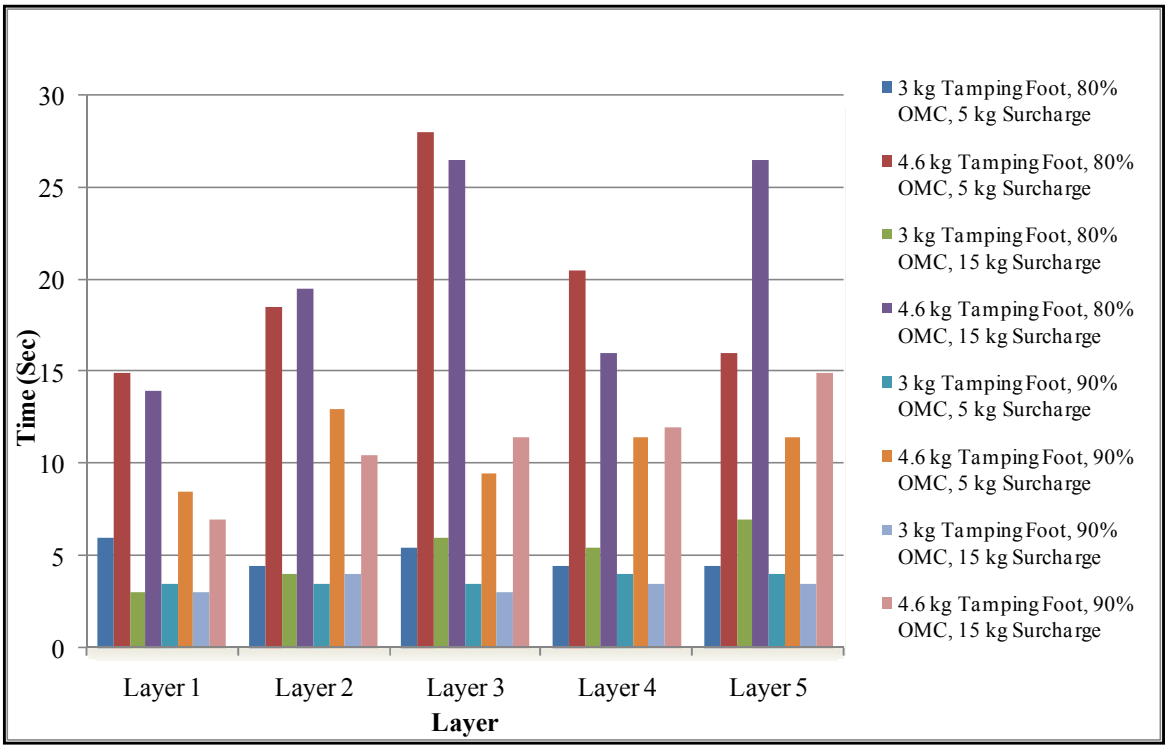

Figure 4-12: Compaction time to 100% of Mod AASHTO density per layer – G3RFR

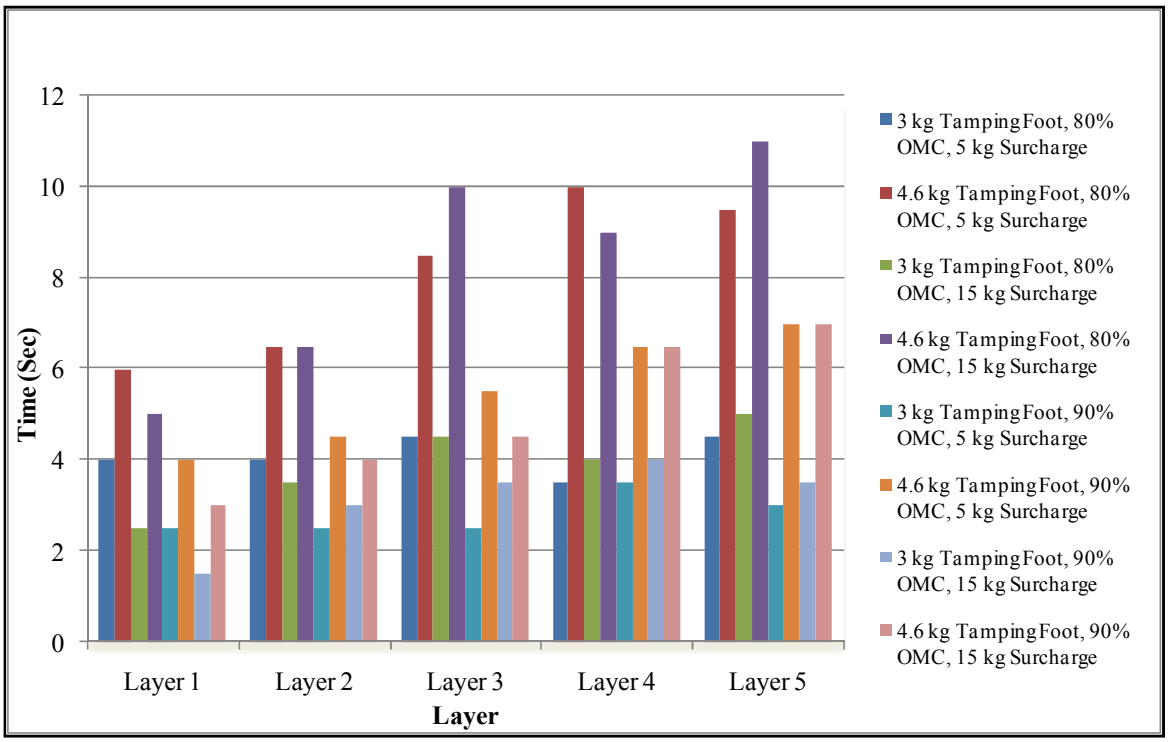

Figure 4-13: Compaction time to 100% of Mod AASHTO density per layer – G4RFR

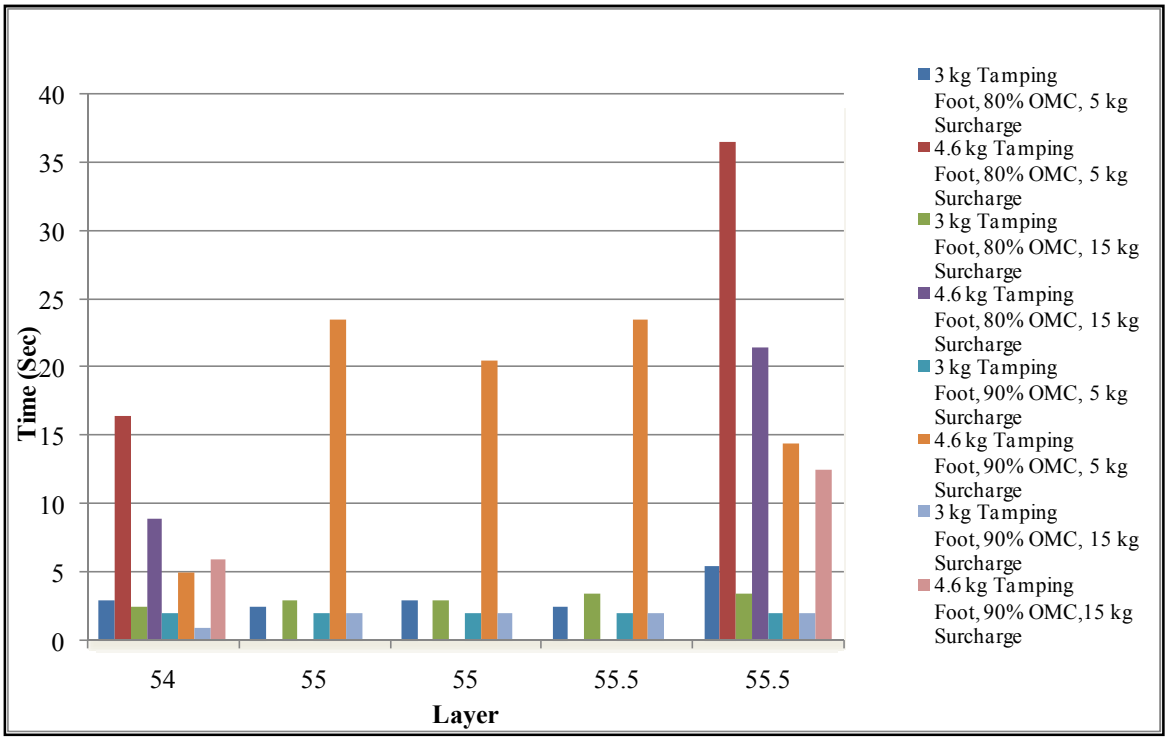

Figure 4-14: Compaction time to 100% of Mod AASHTO density per layer – G7RFR

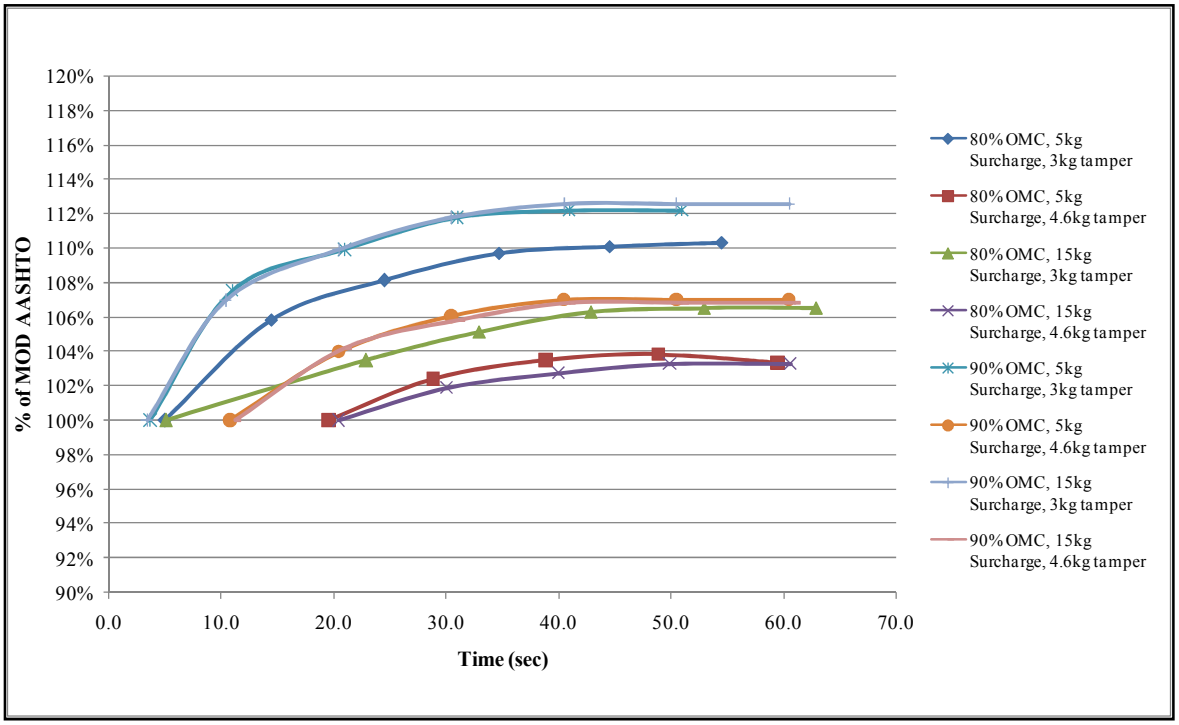

Figure 4-15: Compaction Profile to refusal density – G3RFR

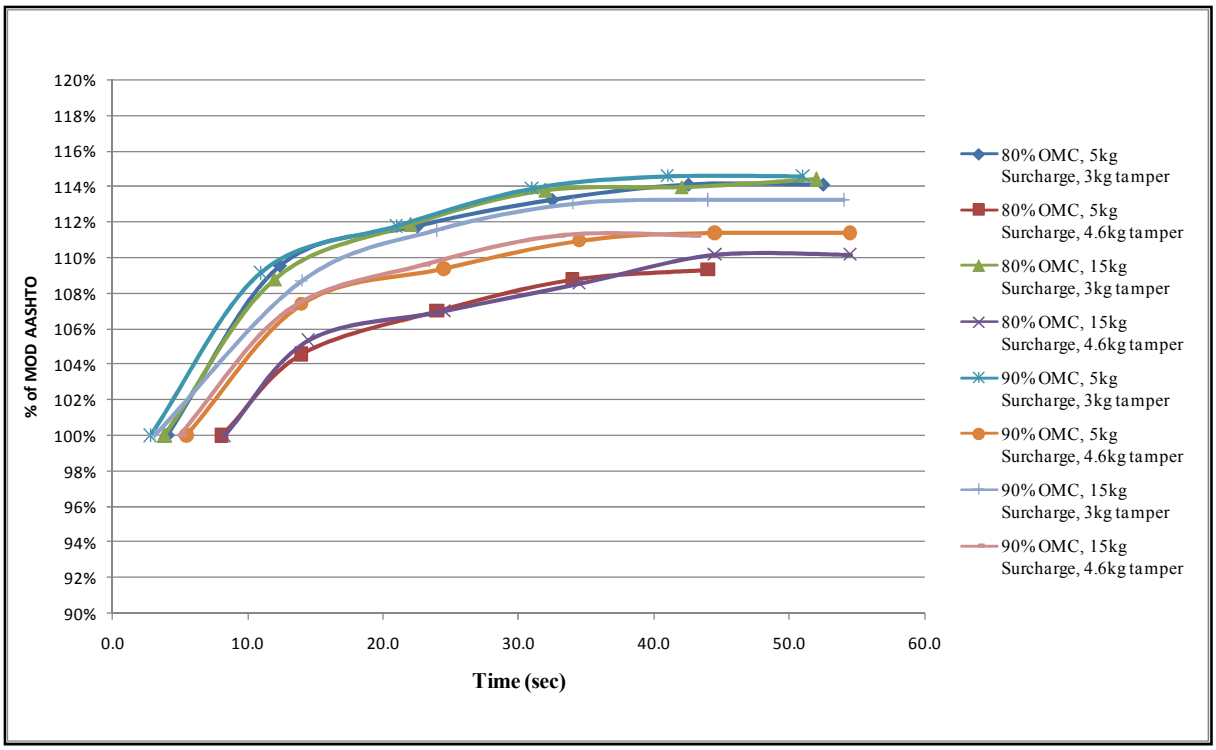

Figure 4-16: Compaction Profile to refusal density– G4RFR

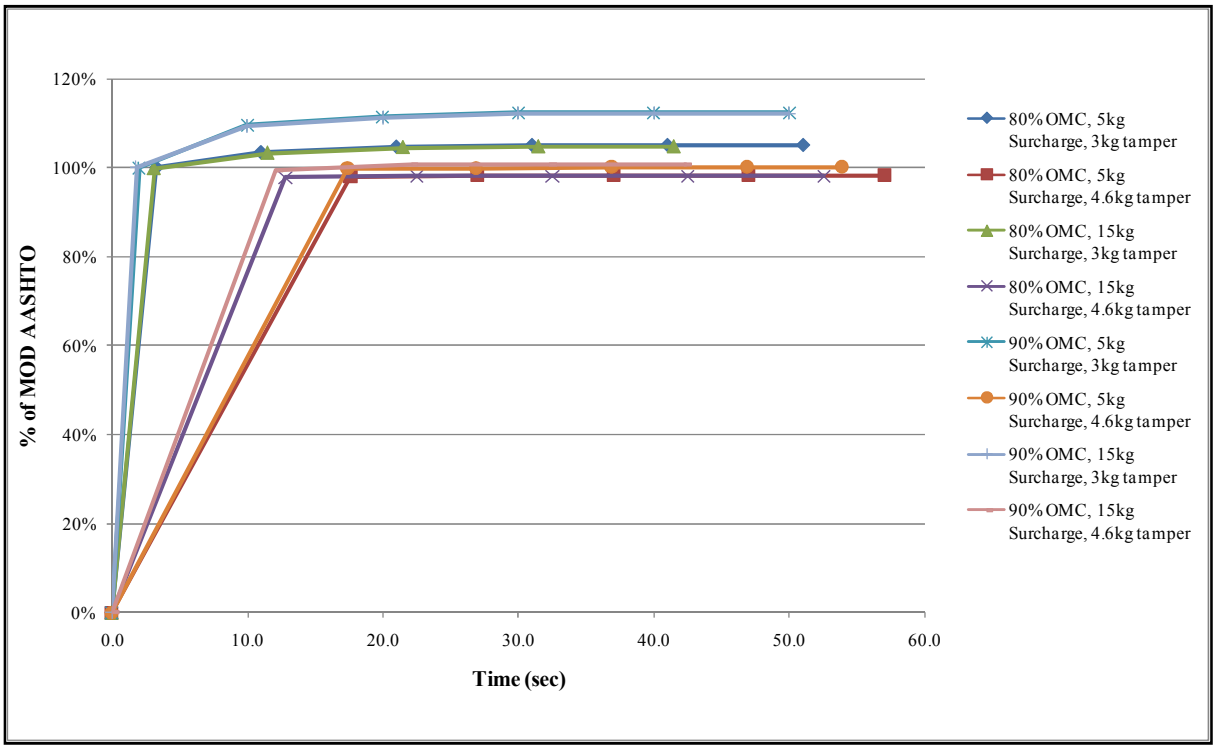

Figure 4-17: Compaction Profile to refusal density– G7RFR

4.3.2.1 Influence of Tamping Foot

Results from the rigid frame also show that less time is required to compact to the same level of density (100% of Mod AASHTO density) with the 3kg tamping foot compared to the 4.6kg tamping foot for all three material types and combinations of moisture content and surcharge load. Approximately 11 seconds average difference in compaction time was observed between the 3kg and 4.6kg tampers for the G3 material (Figure 4-12) while the G4 material showed approximately 3 seconds difference between the two tampers (Figure 4-13). 100% of mod AASHTO layer compaction could not be achieved in some cases for the G7 material especially for the 4.6kg tamping foot as shown in Figure 4-14.

Higher layer refusal densities were obtained with the 3kg tamper compared to the 4.6kg tamper. This is shown in the layer density profiles in Figure 4-15, Figure 4-16 and Figure 4-17 for the G3, G4 and G7 materials respectively. The high layer densities culminated into high refusal specimen densities as shown in Figure 4-18, Figure 4-19 and Figure 4-20 for G3, G4 and G7 materials respectively. Differences in densities between the 3kg and 4.6kg tampers ranged from 2.8% to 6% for the G3 material, 4.1% to 4.4% for G4 and 0.7% to 9.9% for the G7 material. As was observed with the soft frame, specimen densities obtained were less than average layer densities for probably the same reasons highlighted in Section 4.3.1.1.

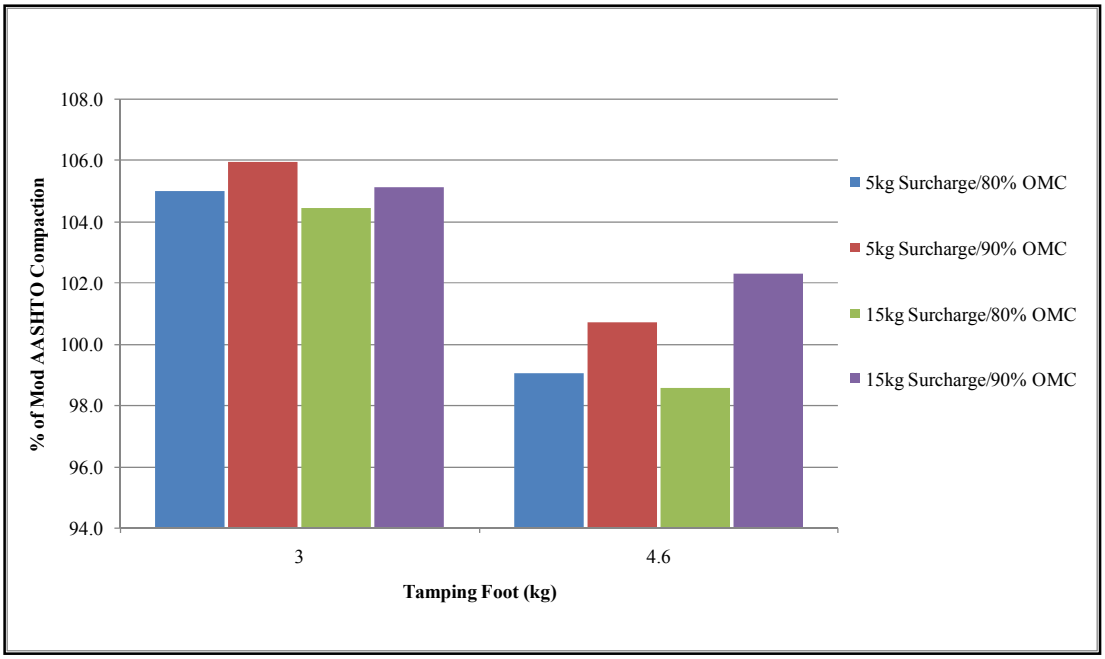

Figure 4-18: Effect of Tamping Foot on Refusal Density – G3RFR

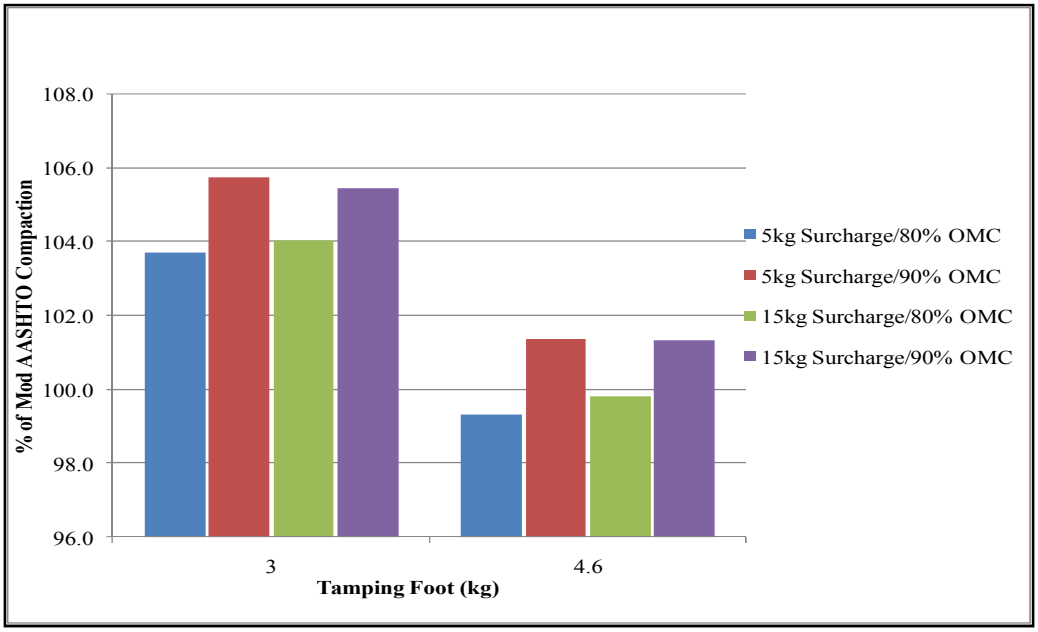

Figure 4-19: Effect of Tamping Foot on Refusal Density – G4RFR

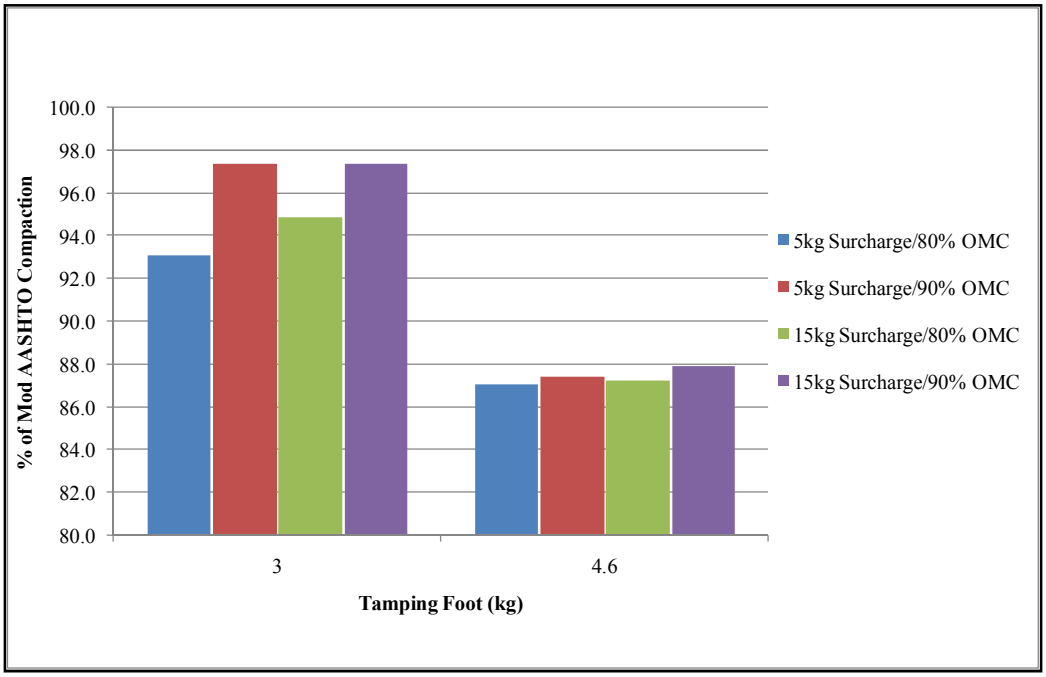

Figure 4-20: Effect of Tamping Foot on Refusal Density – G7RFR

4.3.2.2 Influence of Moisture

The effect of moisture on compaction time for the rigid frame is shown in Figure 4-12, Figure 4-13 and Figure 4-14 for G3, G4 and G7 materials respectively. Shorter compaction times are required to get to the same level of density at 90% of OMC_M compared to 80% of OMC_M. Differences between the two moisture contents averaged 5 seconds for the G3 material and 2

seconds for the G4 material across all layers. For the G7 material, 100% of mod AASHTO density could not be attained for some layers particularly at 80% of OMC_M.

Higher layer densities were obtained at 90% of OMC_M compared to 80% of OMC_M. This is shown in the compaction profiles in Figure 4-15, Figure 4-16 and Figure 4-17 for G3, G4 and G7 materials respectively. Higher specimen densities are also obtainable at the higher moisture content (90% of OMC_M) as shown for G3, G4 and G7 materials in Figure 4-18, Figure 4-19 and Figure 4-20 respectively. This is particularly evident with the 4.6kg tamper for the G3 material with the difference averaging 3%. For the G4 material, the difference in specimen density between 90% and 80% of OMC_M averaged 2% for the 3kg tamper and 1.5% for the 4.6kg tamper. The difference was marginal for the 4.6kg tamper but averaged 3% for the 3kg tamper of the G7 material.

4.3.2.3 Influence of Surcharge

After the frame modifications, the surcharge loads were changed from 10kg and 20kg to 5kg and 15kg as explained in Section 3.3.2. The effect of the surcharge loads in alternate combinations with 3 and 4.6kg tampers at moisture contents of 80% and 90% of OMC_M was observed for compaction time and obtainable densities.

The results show no significant difference in compaction time to 100% of Mod AASHTO density for the two surcharge loads as was the case with the soft frame.

The layer compaction trends in Figure 4-15, Figure 4-16 and Figure 4-17 for the G3, G4 and G7 materials follow the same profile for both 5kg and 15kg surcharge loads in most cases. Specimen densities also do not show much difference between the two surcharge loads. This is indicative of the marginal influence of the surcharge load on compaction with the vibratory hammer.

4.3.3 Comparison of the two different frames

The results of the ‘soft frame’ and the ‘rigid frame’ are compared below under compaction time and compaction density.

Compaction Time

A comparison of the layer compaction times of the ‘soft frame’ and the ‘rigid frame’ shows a slight increase in compaction time of the lower layers with the rigid frame, particularly the

first layer. Thus the compaction time across all five layers is more consistent with the 'rigid frame'. This is observed for all the three material types and therefore should be a result of the frame modifications. A possible reason could be that the supawood platform (on which the base plate is supported) provides a cushioning effect for the lower layers. This presents an opportunity for a single compaction time to be applied across all five layers. It is notable that single compaction times are applicable to all layers in the ASTM and BS and NZ standards for vibratory hammer compaction methods as well.

Density

More consistency in the compaction profiles were also observed with the rigid frame. Compaction profiles of the soft frame indicated that lower layers would achieve much higher densities than upper layers. This is shown in Figure 4-21. However, with the rigid frame, this variability in densities achieved was reduced and consistent densities were achievable across the five layers (Figure 4-22). The typical profiles shown in Figure 4-21 and Figure 4-22 show the layer density profiles for the 'soft frame' and the 'rigid frame' at the same moisture content (90% of OMC_M), same tamping foot (3kg) and static load. The consistency in layer densities of the 'rigid frame' shows the benefits of the frame modifications in reducing inconsistencies in densities.

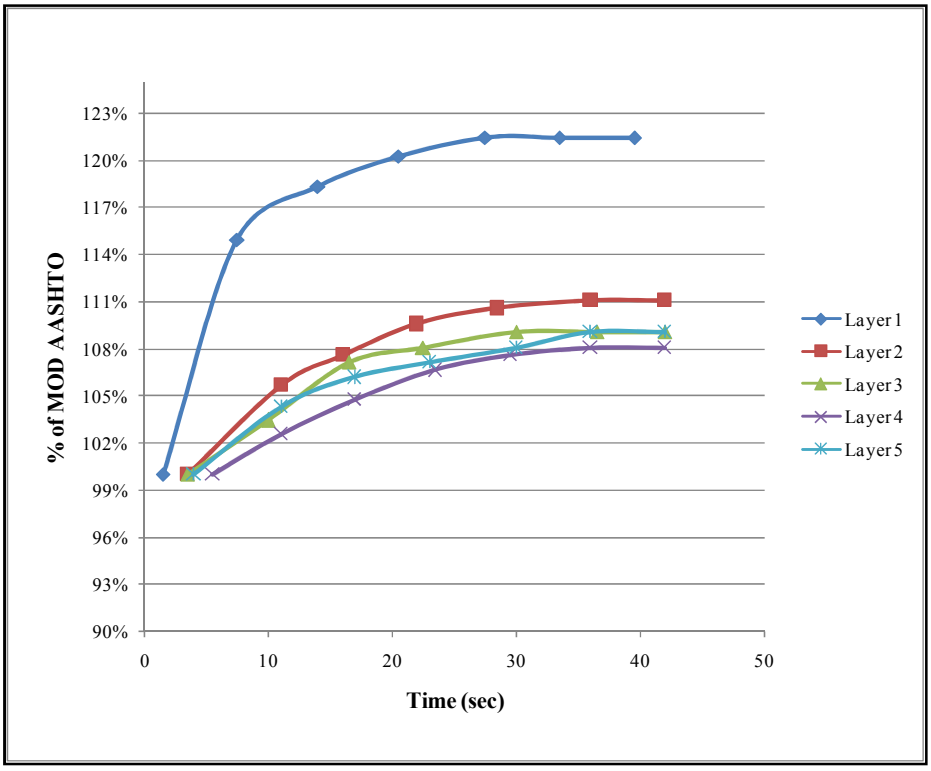

Figure 4-21: Typical layer density profile for 'soft frame'.

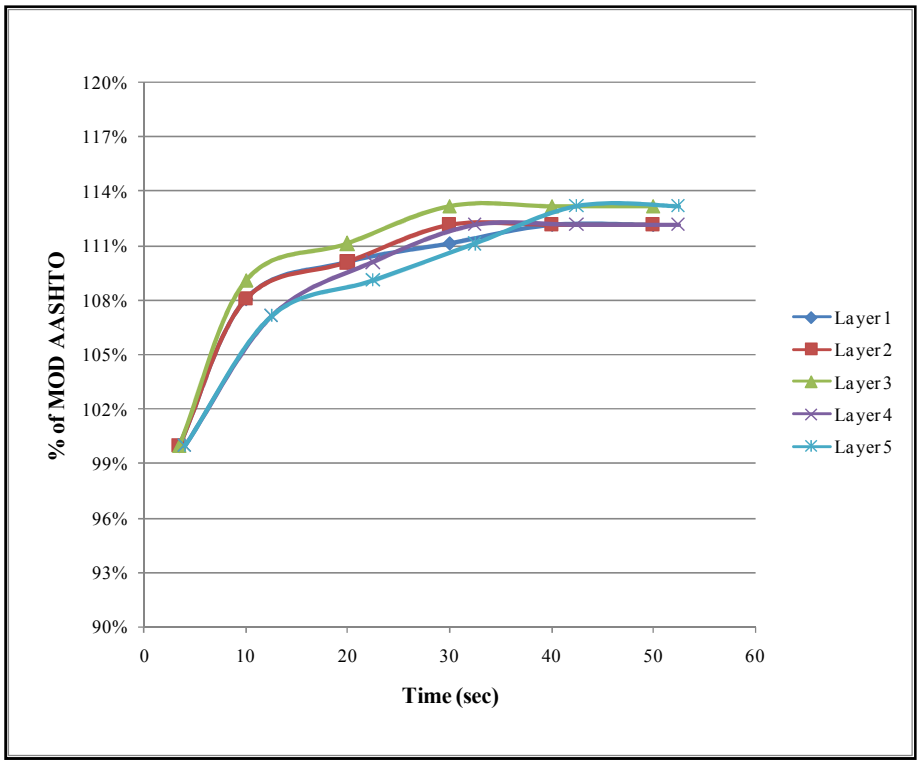

Figure 4-22: Typical layer density profile for 'rigid frame'

Figure 4-23, Figure 4-24 and Figure 4-25 show the effect of the frame modifications on the obtainable specimen densities for the 'soft frame' (SFR) and the 'rigid frame' (RFR) for G3, G4 and G7 materials respectively. As stated in Section 3.3.2, the surcharge loads had to be changed (after the frame modifications) to 5 and 15kg so as to maintain the same total static masses. In Figure 4-23 to Figure 4-25, the total static masses (instead of the surcharge loads) have been indicated for both the SFR and RFR for the sake of clarity in presentation.

The results indicate an increase in density after frame modification for the G4 material for all combinations of surcharge load, tamper and moisture content. More consistent increases were noted with the 3kg tamper. The highest percentage increase in density (2.2%) was observed for the 3kg tamper at 90% of OMC_M and 26.5kg total static mass whilst the lowest (0.4%) was observed for the 4.6kg tamper at 80% of OMC_M moisture and 26.5kg total static mass.

For the G3 material, increases in density ranged from 0.4% to 2.8% with the highest recorded for the 4.6kg tamper at 90% of OMC_M and 36.5kg total static mass. A reduction in density of 0.4% was however observed for the 4.6kg/26.5kg tamper/total static mass combination at 80% of OMC_M.

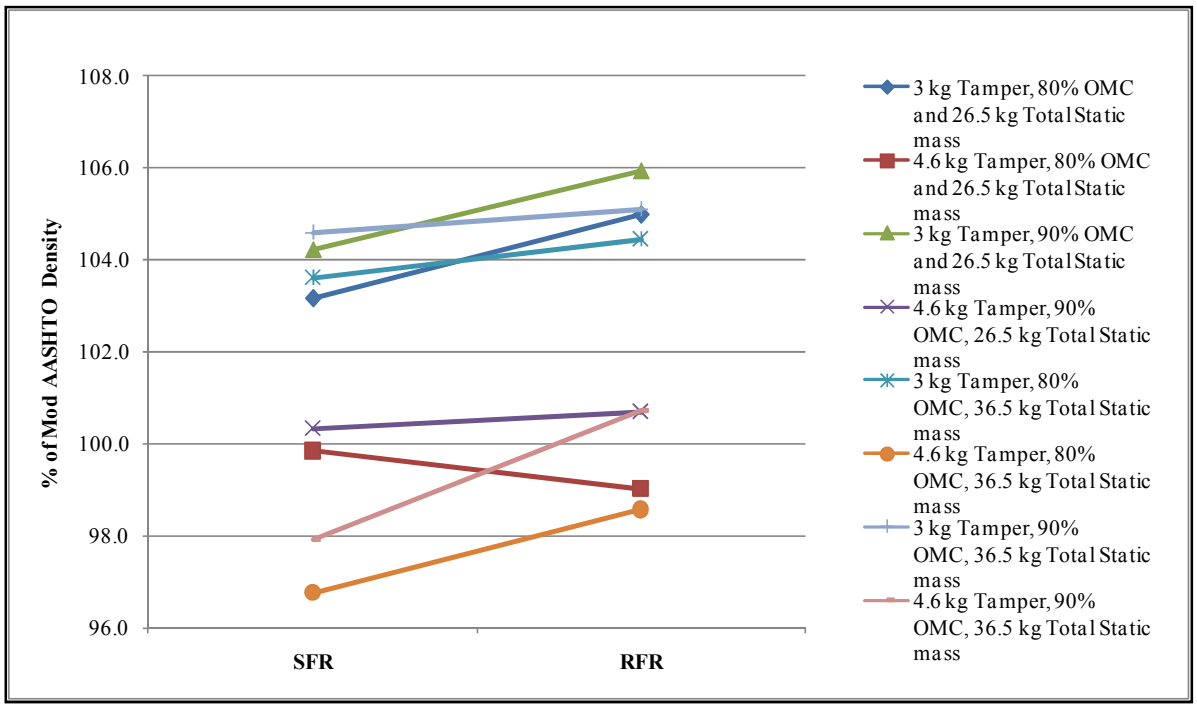

Figure 4-23: Effect of Frame Modifications on Compaction Densities – G3

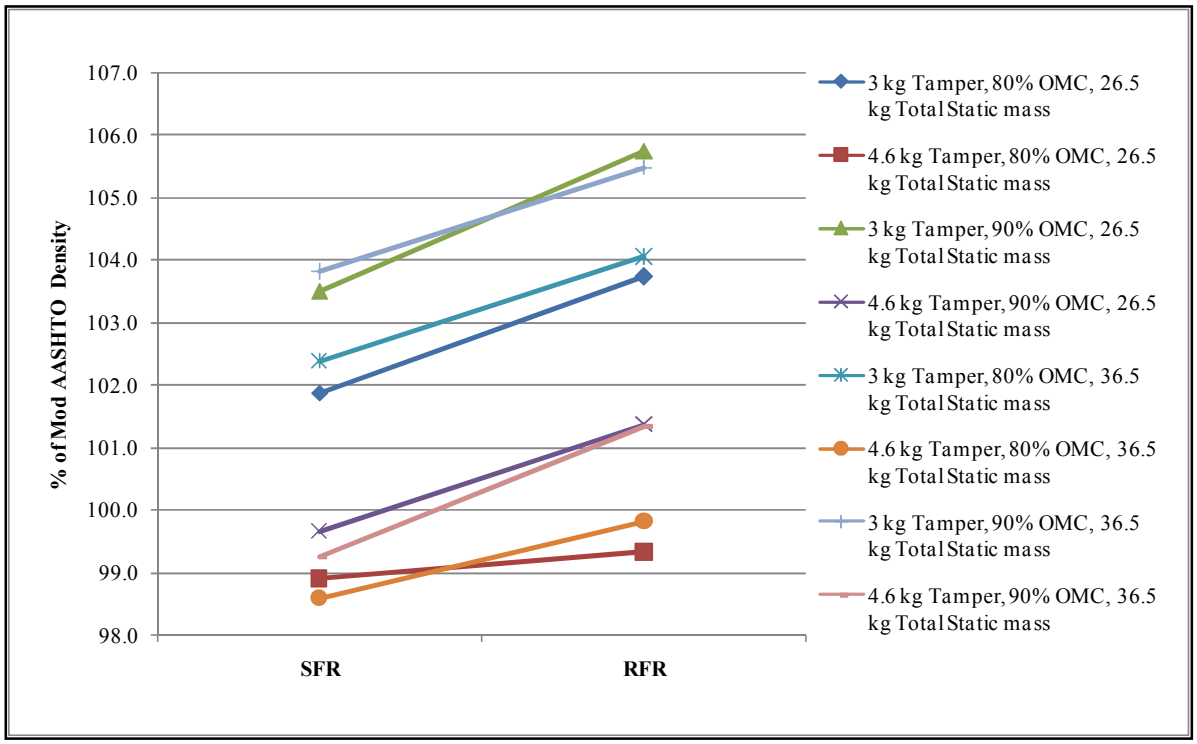

Figure 4-24: Effect of Frame Modifications on Compaction Densities – G4

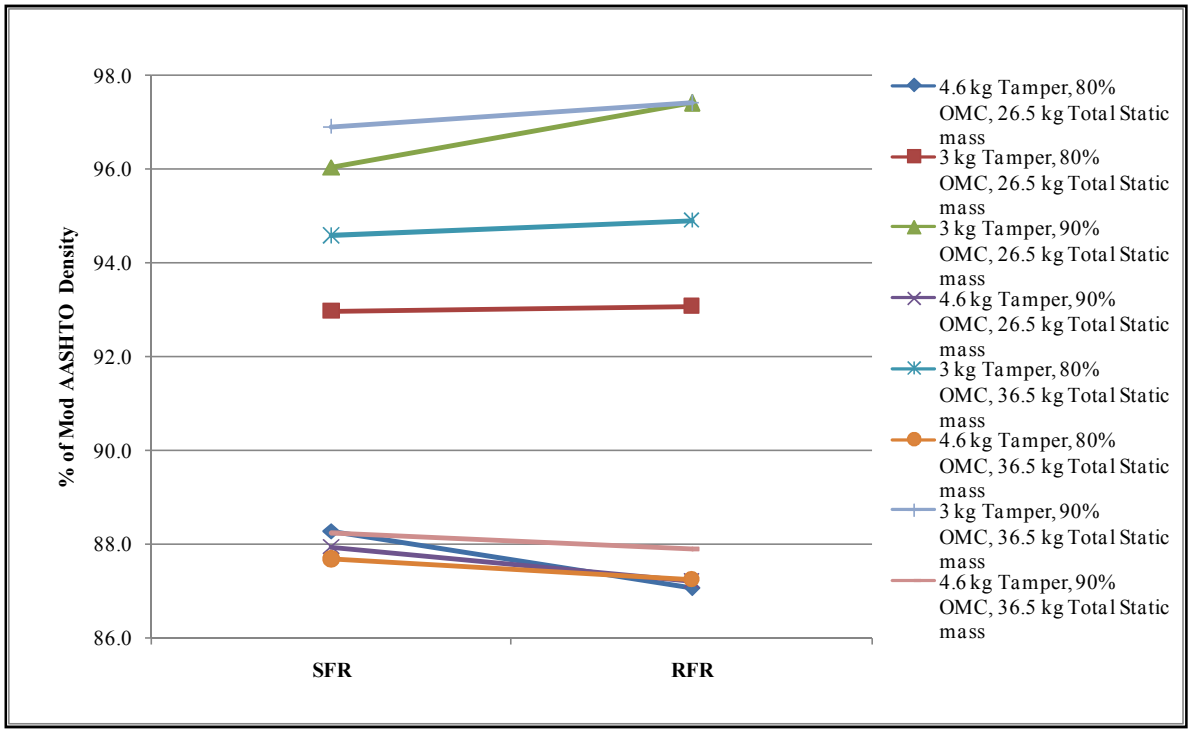

Figure 4-25: Effect of Frame Modifications on Compaction Densities – G7

An increase of 1.4%, the highest increase in density was observed for the 3kg/26.5kg tamper/total static mass combination at 90% of OMC_M for the G7 material. Marginal increases of (between 0.1% and 0.5%) were observed for all other combinations of the 3kg tamper. Marginal reductions in compaction density (between 0.3% and 1.2%) were observed for the 4.6kg tamper. However, this is probably due to material variability than the frame modifications.

4.3.4 Influence of Frequency

The frequency is an important factor for compaction. In addition to the amplitude, the frequency determines what type of compactive force a machine produces. At lowest frequency, the machine can be considered to operate by impact method and at higher frequency the machine can be considered to operate by means of vibration. However, this analogy is too simplistic and the distinction between impact and vibration depends on various other factors.

The vibratory hammer at Stellenbosch University is currently operated at the highest frequency setting (31.5Hz). This is the frequency at which all tests in this study were performed (see Figure 3-5). However, to assess the influence that frequency has on the

compaction with the vibratory hammer, comparative tests were performed on the G3 and G7 materials at frequencies of 25.67Hz and 19.67Hz.

The results of the tests are discussed below for compaction time to 100% of Mod AASHTO density and for densities attained.

Compaction time

The influence of frequency on compaction time to 100% of Mod AASHTO per layer was assessed and the results are presented in Figure 4-26 and Figure 4-27 for the G3 and G7 materials respectively.

The results show that at high frequency, less time is required to reach the same level of layer compaction. Also less variability in compaction time per layer is observed at the higher frequency.

At 25.67 and 19.67Hz, the G3 material showed an increase in compaction time per subsequent layer from the first. Layer compaction times to 100% of Mod AASHTO density increased by an average of 4 seconds for the decrease in frequency from 31.5Hz to 25.67Hz and by approximately 9 seconds for the decrease in frequency from 25.67Hz to 19.67Hz. The results also show a linear relationship of the layer compaction times for the G3 material. At 19.67Hz and 25.67Hz, the compaction time increases linearly from the first layer to the last, while at 31.5Hz the compaction time is constant across the five layers.

With the G7 material, the compaction time per layer varied at 25.67Hz and 19.67Hz. Higher compaction times (i.e. average 10 seconds) were observed for the second, third and fourth layers at the frequency of 25.67Hz. However, the first and last layers were compacted in less than 5 Seconds. At a frequency of 19.67Hz, 100% of Mod AASHTO density could not be achieved for some of the layers even after a prolonged period of compaction (See Figure 4-30). Therefore, the compaction times per layer indicated in Figure 4-27 are until refusal density i.e. no further reduction of the layer depth (but less than 100% of Mod AASHTO density). Longer compaction times were observed at 19.67Hz with the fourth layer requiring the longest time (28 Seconds) to reach refusal density.

These results would explain the longer compaction times specified in the NZ standard for vibratory hammer. The NZ standard specifies a frequency range of 4.2 to 10Hz and a compaction time per layer of 180 seconds.

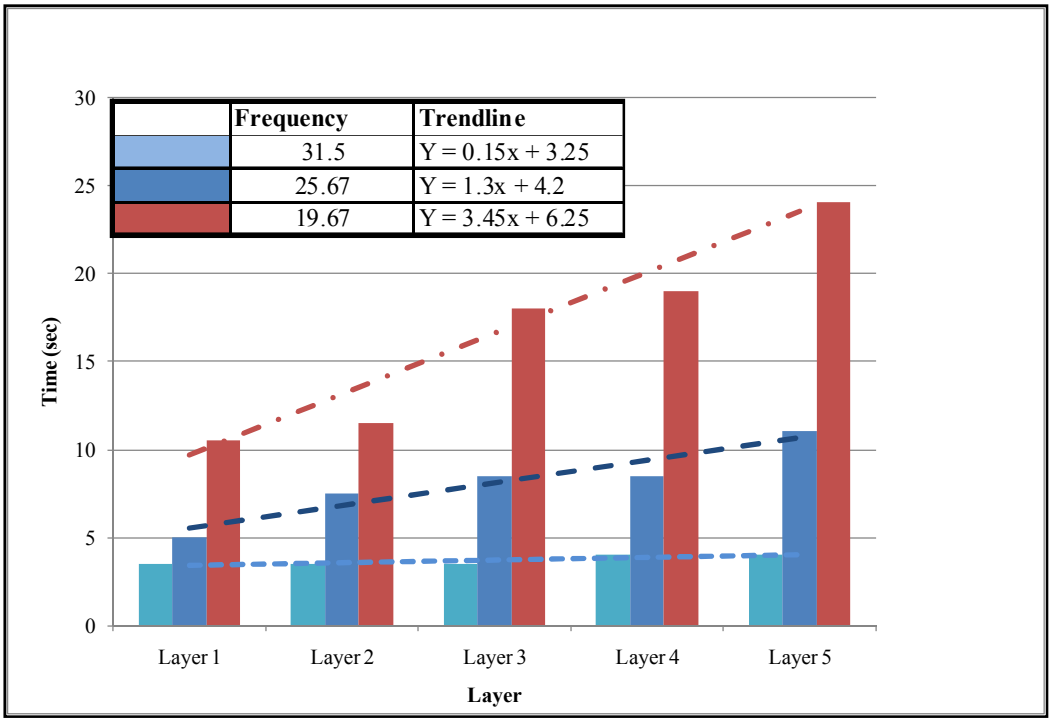

Figure 4-26: Influence of Frequency on Compaction time to achieve 100% of Mod AASHTO density – G3

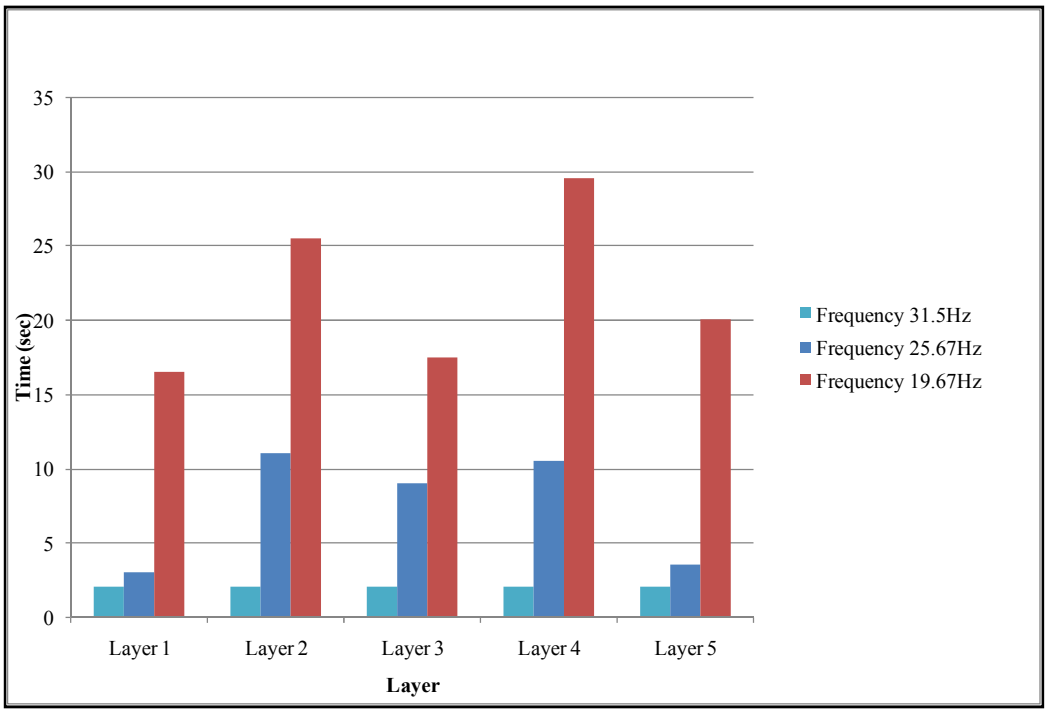

Figure 4-27: Influence of Frequency on Compaction time to achieve 100% of Mod AASHTO density – G7

Compaction Density

Figure 4-28 and Figure 4-30 show the compaction density profiles and Figure 4-29 and Figure 4-31 show the refusal densities obtained at each frequency for the G3 and G7 materials respectively at the three frequencies compared (i.e. 31.5Hz, 25.67Hz and 19.67Hz).

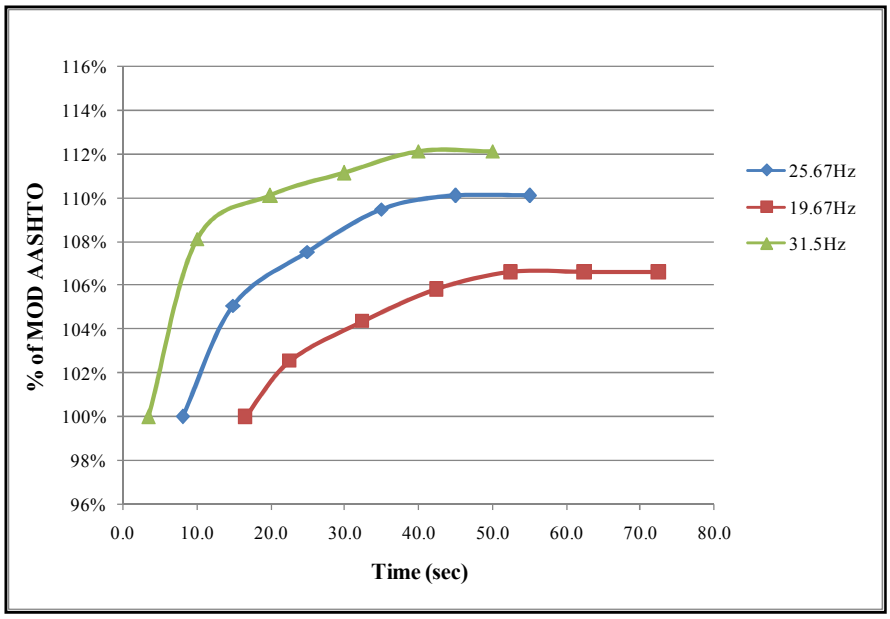

Figure 4-28: Compaction Density Profile at different frequencies – G3

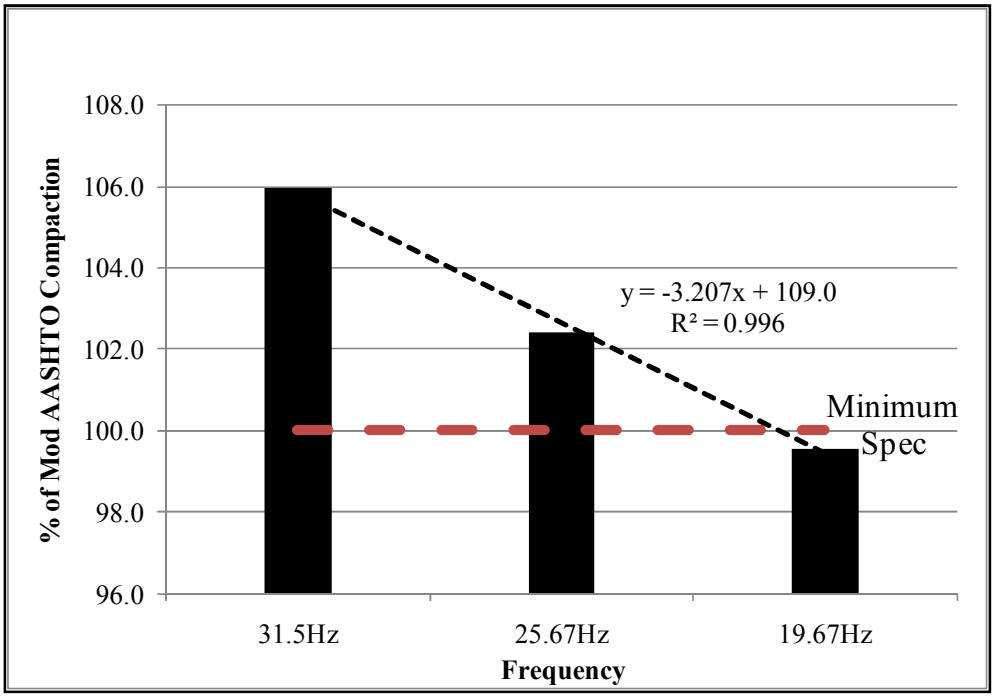

Figure 4-29: Refusal Densities – G3

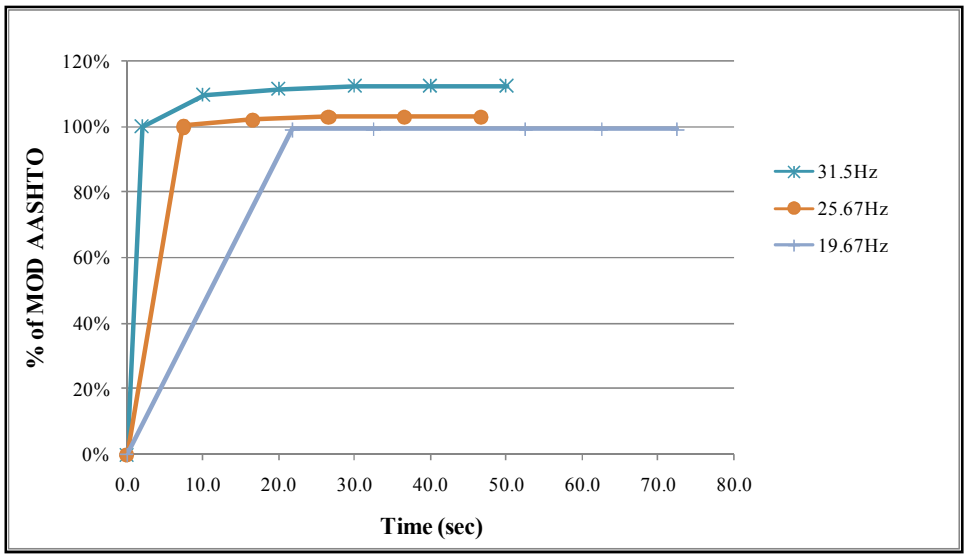

Figure 4-30: Compaction Density Profile at different Frequencies – G7

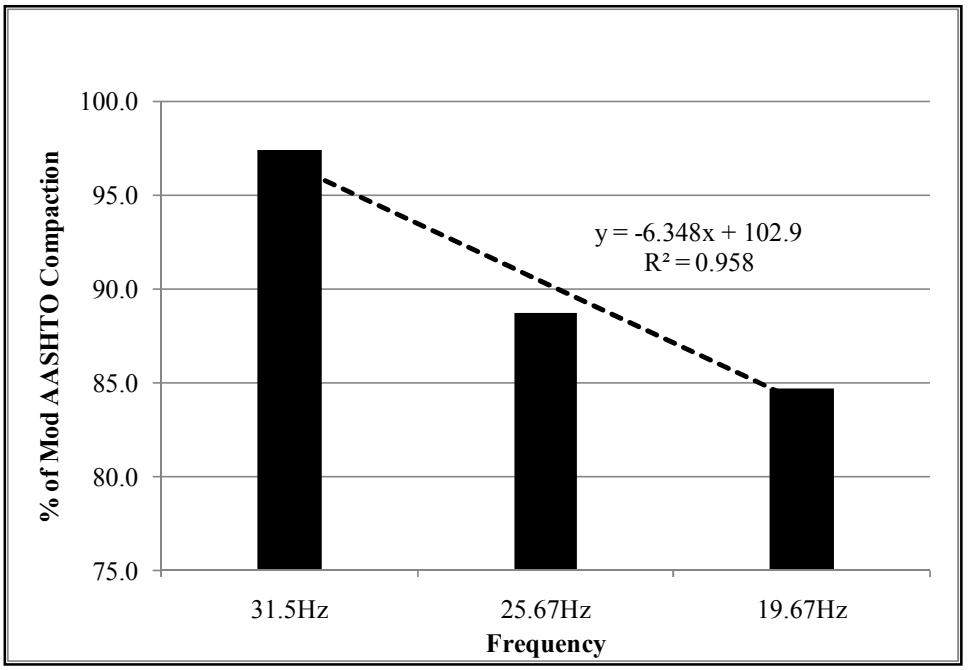

Figure 4-31: Refusal Densities – G7

The compaction profiles show a reduction in layer compaction densities from the 31.5Hz to 19.67 Hz for both the G3 and G7 materials. The results also show that high refusal densities are obtainable at high frequency. The G3 material showed a linear reduction in density of approximately 3% for the 6Hz reduction in frequency assessed (i.e. from 31.5Hz to 25.67Hz and from 25.67Hz to 19.67Hz). Figure 4-29 also indicates a cut off point for the attainment of 100% of Mod AASHTO to be 25.67Hz. The G7 material showed a significantly higher

difference in compaction moving from 31.5Hz to 25.67Hz (8% difference) and a lower difference moving from 25.67Hz to 19.67Hz (3%).

4.4 RECLAIMED ASPHALT

The term Reclaimed Asphalt (RA) is given to any 100% asphalt material that is recovered from an existing trafficked pavement. RA material is finding increasing use in pavement layers due mostly to its cost effectiveness and the need for sustainability. Wirtgen (2010) differentiates between two types of RA material based on the activeness or inactiveness of the bitumen contained within it. Inactive RA has properties similar to those of graded crushed stone, while active RA exhibits inherent cohesive properties. Such cohesion tends to resist compaction effort and limits the density achievable after compaction.

Due to time constraints, a limited study of RA material was conducted. 100% RA material was tested at 90% OMC_M moisture content using a single surcharge load of 5kg for the two tampers (see Figure 3-5). The time to compact each layer to 100% of Mod AASHTO density was assessed and the results are appended in Appendix K. Consolidated results are shown in Figure 4-32. Figure 4-33 shows the compaction profiles and Figure 4-34 shows the densities obtained.

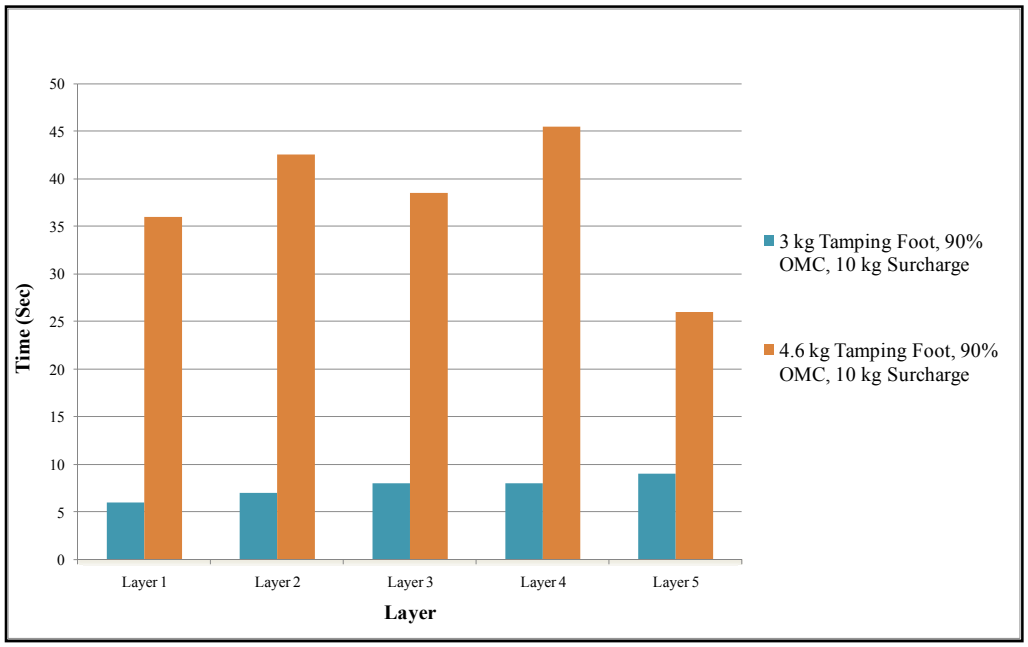

Figure 4-32: Compaction Time to 100% of Mod AASHTO density– RA

The results show a significant difference in compaction time between the 3kg tamping foot and the 4.6kg tamping foot. Using the 3kg tamping foot, 100% of Mod AASHTO density per

layer could be attained in less than 10 seconds. With the 4.6kg tamping foot, more than 25 seconds was required to reach the same level of compaction. Also the 3kg tamping foot showed more consistency in compaction time per layer compared to the 4.6kg tamping foot.

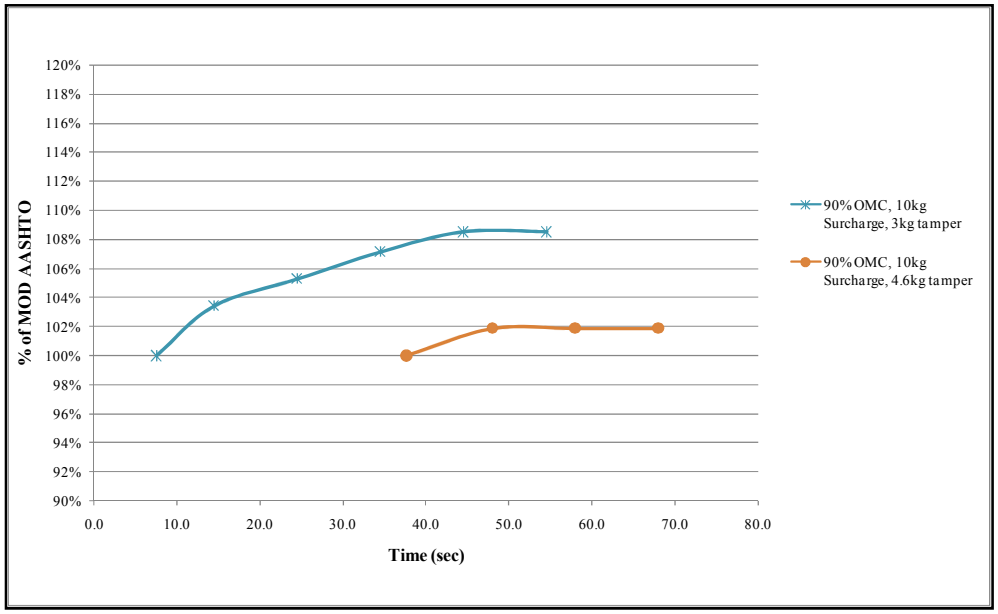

Figure 4-33: Compaction Profile to refusal density - RA

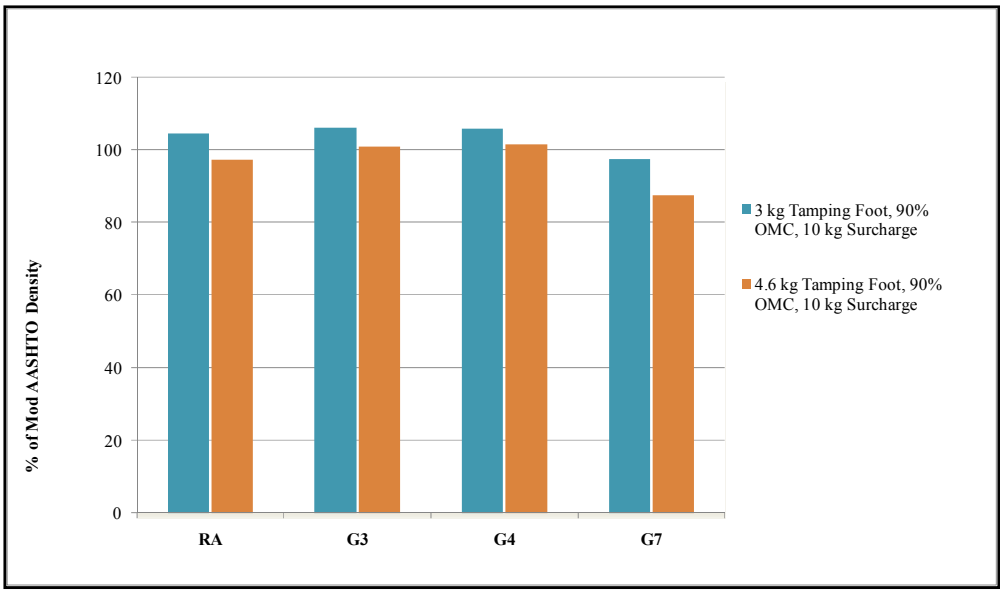

Figure 4-34: Refusal Densities

The results also show that higher layer compaction densities were attained using the 3kg tamping compared to the 4.6kg tamping foot (Figure 4-33). Consequently a higher specimen density was obtained when using the 3kg tamping foot; a difference of approximately 7% (Figure 4-34). Figure 4-34 also compares the densities attained for the RA material and the

G3, G4 and G7 materials at the same moisture level and surcharge. It is shown for the RA material that the obtainable densities are comparable with those of G3 and G4 materials.

4.5 STATISTICAL ANALYSIS

An Analysis of Variance (ANOVA) was performed to determine the significance of the influence of each of the primary test factors shown in Figure 3-5 i.e. tamping foot, moisture and surcharge load (also called sources of variation), on the obtainable compaction density (also called variable). ANOVA is a general technique used to test the hypothesis that the means among two or more groups are equal, under the assumption that the sampled populations are normally distributed (Montgomery and Runger, 2007). It works by examining the difference between the samples as well as the difference within a sample.

The ANOVA partitions the total variability in the sample data (also called the total sum of squares, SS_T) into two component parts; the sum of squares of differences between treatment means and the grand mean ($SS_{Treatments}$) and a sum of squares of differences of observations within a treatment from the treatment mean (SS_E).

$$SS_T = SS_{Treatments} + SS_E \qquad \text{Equation 4-1}$$

Each component corresponds to a different source of variability. Differences between observed treatment means and the grand mean measure the differences between treatments, while differences of observations within a treatment from the treatment mean can be due only to random error (Montgomery and Runger, 2007).

The variance (abbreviated as MS for Mean of Squares) defined as the average squared deviation from the mean is determined by dividing the variation by the degree of freedom (df). Mulusa (2009) defined degree of freedom as the number of values that are free to vary once certain parameters have been established. Usually degree of freedom is taken as one less than the sample size but in general it is the number of values minus the number of parameters being estimated.

The mean of squares of each of the two components of the total variability is determined by dividing the sum of squares of each component by its respective degree of freedom.

$$MS_{Treatments} = \frac{SS_{Treatments}}{df_{Treatments}} \qquad \text{Equation 4-2}$$

$$MS_E = \frac{SS_E}{df_E}$$ Equation 4-3

The test statistic, used in testing the equality of treatment means is the F statistic. The F statistic is the ratio of the two sample variances.

$$F = \frac{MS_{Treatments}}{MS_E}$$ Equation 4-4

The critical value of the F statistic is obtained from tables at the chosen α level and the degrees of freedom.

ANOVA calculations are best presented in table format (ANOVA table). Rows representing sources of variation and five columns for degrees of freedom (df), variation (SS), variance (MS), F statistic and the critical F value or the p value.

ANOVA for this study was performed using a spreadsheet developed by Dean Christolear (2010). The α level chosen for the test is 0.05. This means that test factors with p values less than 0.05 have a significant effect on the obtainable density. The ANOVA was performed on results of the upgraded 'rigid frame'. The results of the analysis are shown in Table 4-2, Table 4-3 and Table 4-4 for G3, G4 and G7 materials respectively.

Table 4-2: ANOVA Table – G3

ANOVA Table for G3 Material					
Factor	**df**	**Sum of Sq.**	**Mean Sq**	**F**	**p**
Tamper	1	115.025625	115.0256	338.9337	7.8E-08
Moisture	1	7.155625	7.155625	21.08471	0.001774
Surcharge	1	0.765625	0.765625	2.255985	0.171498
Tamper x Moisture	1	1.155625	1.155625	3.405157	0.10221
Tamper x Surcharge	1	0.275625	0.275625	0.812155	0.393805
Moisture x Surcharge	1	0.000625	0.000625	0.001842	0.966822
Tamper x Moisture x Surcharge	1	0.105625	0.105625	0.311234	0.592189
Error	8	2.715	0.339375		
Total	15	127.199375			

Table 4-3: ANOVA Table – G4

ANOVA Table for G4 Material					
Factor	**df**	**Sum of Sq.**	**Mean Sq**	**F**	**p**
Tamper	1	73.96	73.96	55.40075	7.31E-05
Moisture	1	12.6025	12.6025	9.440075	0.015291
Surcharge	1	0.0625	0.0625	0.046816	0.834114
Tamper x Moisture	1	0.01	0.01	0.007491	0.933157
Tamper x Surcharge	1	0.04	0.04	0.029963	0.866875
Moisture x Surcharge	1	0.3025	0.3025	0.226592	0.646791
Tamper x Moisture x Surcharge	1	3.2312E-27	3.23E-27	2.42E-27	1
Error	8	10.68	1.335		
Total	15	97.6575			

Table 4-4: ANOVA Table - G7

ANOVA Table for G7 Material					
Factor	df	Sum of Sq.	Mean Sq	F	p
Tamper	1	272.25	272.25	400.3676	4.06E-08
Moisture	1	15.21	15.21	22.36765	0.001484
Surcharge	1	1.5625	1.5625	2.297794	0.168027
Tamper x Moisture	1	8.1225	8.1225	11.94485	0.008617
Tamper x Surcharge	1	0.36	0.36	0.529412	0.4876
Moisture x Surcharge	1	0.49	0.49	0.720588	0.420625
Tamper x Moisture x Surcharge	1	1.1025	1.1025	1.621324	0.238658
Error	8	5.44	0.68		
Total	15	304.5375			

The results indicate for all three material types that the tamping foot has the most significant effect on the obtainable compaction density according to the hypothesis. The tamping foot for the G3 material has a p value of 0.000000078, G4 has 0.0000731 and the G7 has 0.0000000406. All three p values are way below the threshold level of 0.05. The results of the analysis also indicate that next to the tamping foot, the moisture content has the second largest effect on the obtainable density for all three materials. The interaction of the tamper and moisture is also shown to be significant in the G7 material with a p value of 0.008617 below 0.05. The analysis shows that the p value of the surcharge load for all three materials is above 0.05, the threshold value for the hypothesis. This shows that the influence of the surcharge load (on the obtainable compaction density) is not significant at the α level chosen.

Table 4-5 shows, for each material type, the ranking of the factors in terms of their influence on the obtainable compaction density.

Table 4-5: Test Factor Ranking

	Ranking		
Test Factor	**G3**	**G4**	**G7**
Tamper	1	1	1
Moisture	2	2	2
Surcharge	4	4	4
Tamper x Moisture	3	6	3
Tamper x Surcharge	5	5	7
Moisture x Surcharge	7	3	6
Tamper x Moisture x Surcharge	6	7	5

4.6 DEVELOPMENT OF COMPACTION METHOD

The primary objective of this study was to develop a compaction method for granular material using the vibratory hammer. To achieve this, a combination of the test factors studied have to be selected that will give the ideal results for a given compaction time. Results show that the 'rigid frame' gives relatively high compaction densities (particularly with the graded crushed stone material) compared to the 'soft frame'. Higher compaction densities were also obtained with the use of the 3kg tamper compared to the 4.6kg tamper. Results also show that high densities are obtainable at the high frequency (31.5Hz) and high moisture content (90% of OMC_M). The surcharge load applied on the hammer has marginal influence on the obtainable compaction density. Nonetheless, the surcharge load is needed to keep the hammer from bouncing up during compaction. Therefore, the test factors shown in Table 4-6 were proposed for the compaction method.

Table 4-6: Proposed Factors for Compaction Method

Tamping Foot (kg)	3
Frequency (Hz)	31.5
Surcharge (kg)	10
Total Static Load (kg)	35
Moisture (% of OMC_M)	90
Compaction Time per layer (Sec)	25

The surcharge load proposed is the average of the two considered in the second phase of the experiments (5kg and 15kg), thus resulting in a total static weight of 35kg. To arrive at a compaction time of 25 seconds the following was considered;

In order to reference the vibratory compaction to the Mod AASHTO, the quantity of material for vibratory hammer compaction is calculated as stated in Section 3.5.1. Using Equation 3-1, it is assumed that if the quantity of material obtained (SC_m) is compacted in five equal layers each to 100% of Mod AASHTO (60mm height), then the specimen would achieve 100% of Mod AASHTO density. Based on this premise, the vibratory hammer compaction time would be the average compaction time that achieves 100% of Mod AASHTO layer density. However, basing compaction time on this premise has, overtime, proven to be inadequate to achieve 100% of Mod AASHTO specimen density. The premise/theory leaves little room for error which might result from anything from inaccurate measurements to materials sticking to the sides of the mould. It was observed from the results of the tests for each of the more than 100 specimens tested that obtainable specimen densities were lower than the average layer densities achieved. This can be observed in Section 4.3 with the layer density profiles and refusal specimen densities attained. Furthermore, there is variability in layer compaction time, among the five layers as well as among different material types. It should be noted that the layer compaction times to 100% of Mod AASHTO density for all layers above the first may actually be more than what was found. This is because each layer was compacted up to refusal density thus providing a more-dense support for the subsequent layer.

The compaction profiles in Appendices C to H show that the compaction density tends to reach a plateau overtime, after which no significant increase in compaction density is observed. This is consistent to all materials tested. Therefore, the compaction time selected should be on the plateau. This would reduce the variability in layer densities obtained with vibratory hammer compaction. Based on the results of this study, a compaction time of 25 seconds was selected.

A comparison of the density profiles from compaction with the ‘soft frame’ against the ‘rigid frame’ shows that unlike was the case with the ‘soft frame’ where the lower layers would attain higher compaction densities compared to the subsequent layers, the ‘rigid frame’ shows consistency in compaction time and attained layer densities for all the five layers. Typical profiles are shown in Figure 4-21 and Figure 4-22. This means that a single compaction time can be applied to all the five layers.

4.7 REPEATABILITY TESTS FOR DEVELOPED COMPACTION METHOD

Repeatability tests were performed with the developed vibratory hammer compaction method to assess its effectiveness. Five repeat tests for each material type were performed. Results of the tests are shown in Table 4-7.

Table 4-7: Repeat Tests of the developed Vibratory Hammer test

	% of Mod AASHTO Density			
Test No.	**G3**	**G4**	**G7**	**RA**
1	101.8	103.0	95.9	101.4
2	102.3	103.3	96.8	101.4
3	101.4	102.8	96.2	100.7
4	102.3	103.0	96.7	100.9
5	101.4	103.2	95.9	101.3
Average	**101.8**	**103.1**	**96.3**	**101.1**
Std Dev	**0.475**	**0.216**	**0.423**	**0.328**
COV (%)	**0.467**	**0.210**	**0.439**	**0.325**

Average compaction densities of 101.8%, 103.1% and 101.1% of Mod AASHTO density were obtained for the G3, G4 and RA materials with coefficients of variations (COV) 0.467%, 0.210% and 0.325% respectively. This shows that the method is effective for compaction of graded crushed stone (G3 and G4) and probably RA material. The low variability in the results shows that the developed compaction method is capable of producing results with suitable consistency. Average 96.3% of Mod AASHTO density was obtained for the G7 material with a COV of 0.325%. This material (G7), presents difficulties in compaction (see Section 2.3.5.5). For this reason, TRH4 specifies field compaction requirements for G7 material between 90% and 95% of Mod AASHTO density (Table 2-7).

4.8 COMPARATIVE TESTS WITH VIBRATORY TABLE

The vibratory table compaction method is one of the standard vibration based compaction methods for graded crushed stone and cohesionless (granular) sand material. Theyse (2004 as cited in Kelfkens, 2008) points out that the vibratory table compaction method gives the best results in terms of producing the same material properties in the laboratory as those obtained on site. The developed vibratory hammer compaction method was compared to the vibratory table method. This was done to obtain an appreciation of the effectiveness of the developed vibratory hammer compaction method.

As was the case with the vibratory hammer, tests with the vibratory table were referenced to Mod AASHTO density. The results of the tests and comparison with the vibratory hammer compaction test are discussed below for compaction time and compaction densities obtained:

Compaction time

To appreciate the difference in compaction time between the vibratory table and the vibratory hammer, the time to compact each layer to 100% of Mod AASHTO density with vibratory table was observed. This was compared to the time to achieve the same level of density using the vibratory hammer for the 3kg/5kg tamper/surcharge combination at a moisture content of 90% of OMC_M. The results are given in Figure 4-35, Figure 4-36 and Figure 4-37 for G3, G4 and G7 materials respectively.

The results show that more compaction time is required to achieve an equivalent level of compaction using the vibratory table compared to the vibratory hammer. This difference is more pronounced with the G3 and G7 materials unlike the G4 material. Also the compaction times of the vibratory hammer show more consistency per layer with the G7 and less variability with the G3 and G4 materials compared to the vibratory table compaction time.

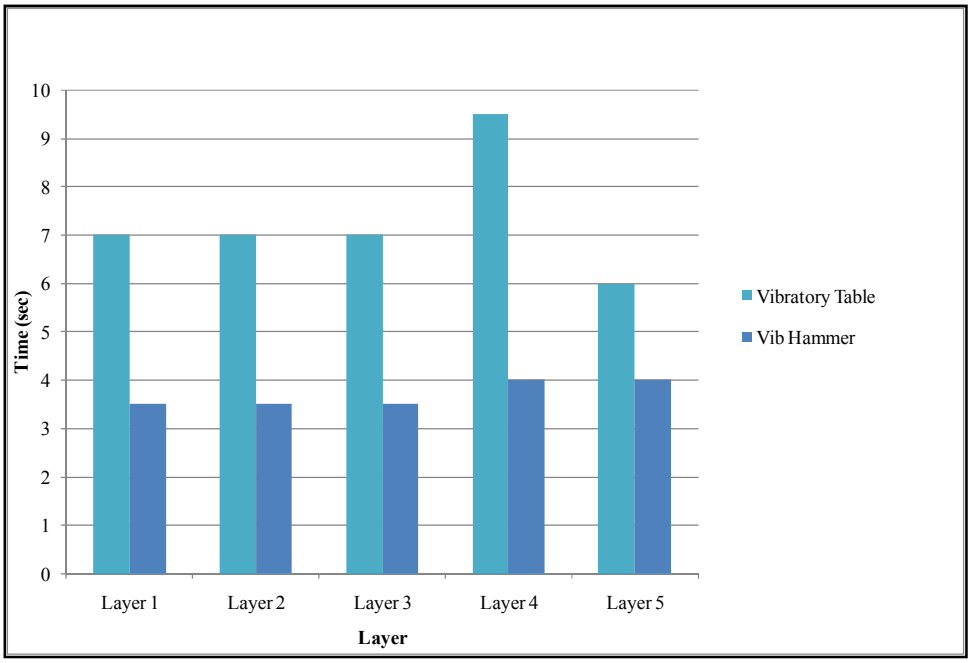

Figure 4-35: Vibratory Hammer versus Vibratory Table Compaction Time to achieve 100% of Mod AASHTO density – G3

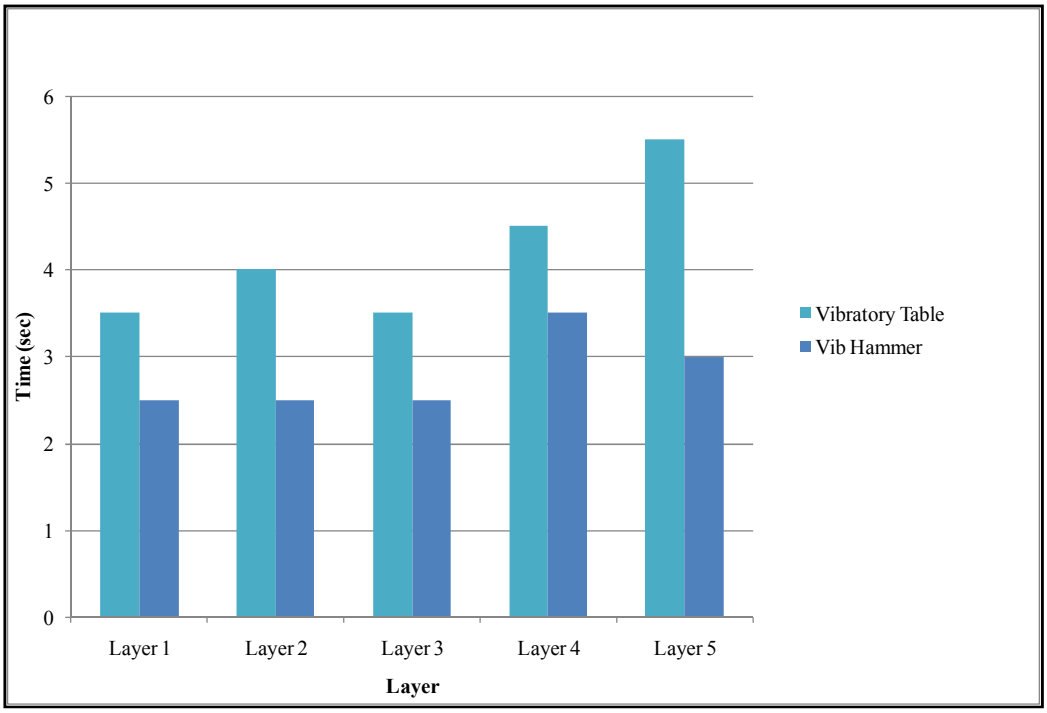

Figure 4-36: Vibratory Hammer versus Vibratory Table Compaction time to achieve 100% of Mod AASHTO density – G4

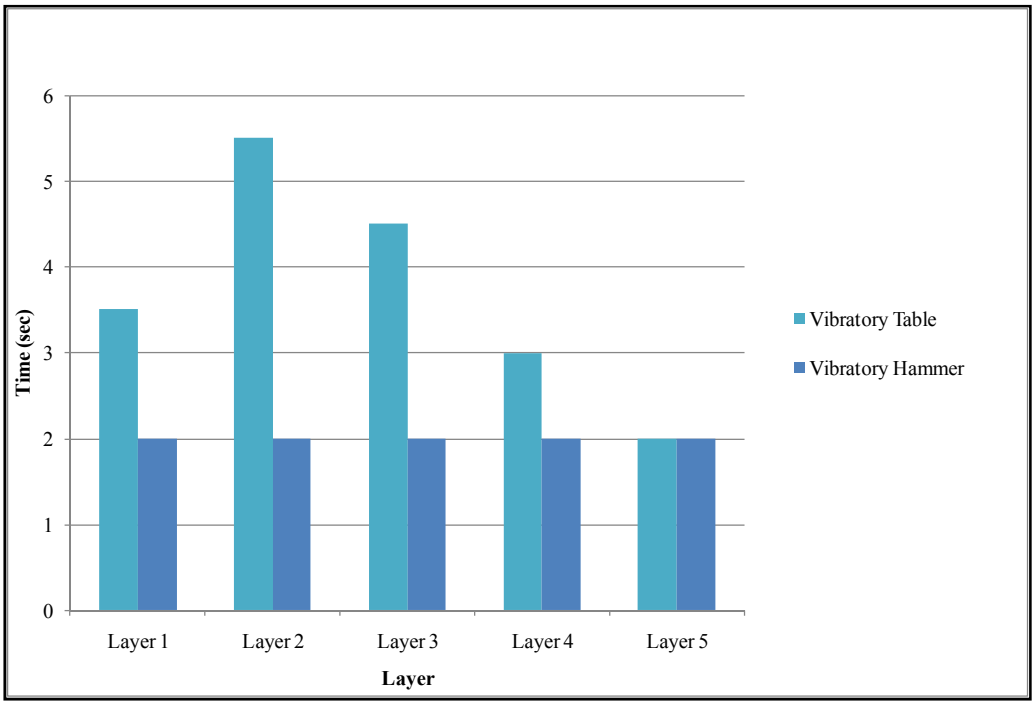

Figure 4-37: Vibratory Hammer versus Vibratory Table Compaction Time to achieve 100% of Mod AASHTO density – G7

Layer Densities

Figure 4-38, Figure 4-39 and Figure 4-40 present the layer densities attained with the G3, G4 and G7 materials respectively after 2 minutes (TMH1 specification) of compaction using the vibratory table and 25 seconds with the vibratory hammer.

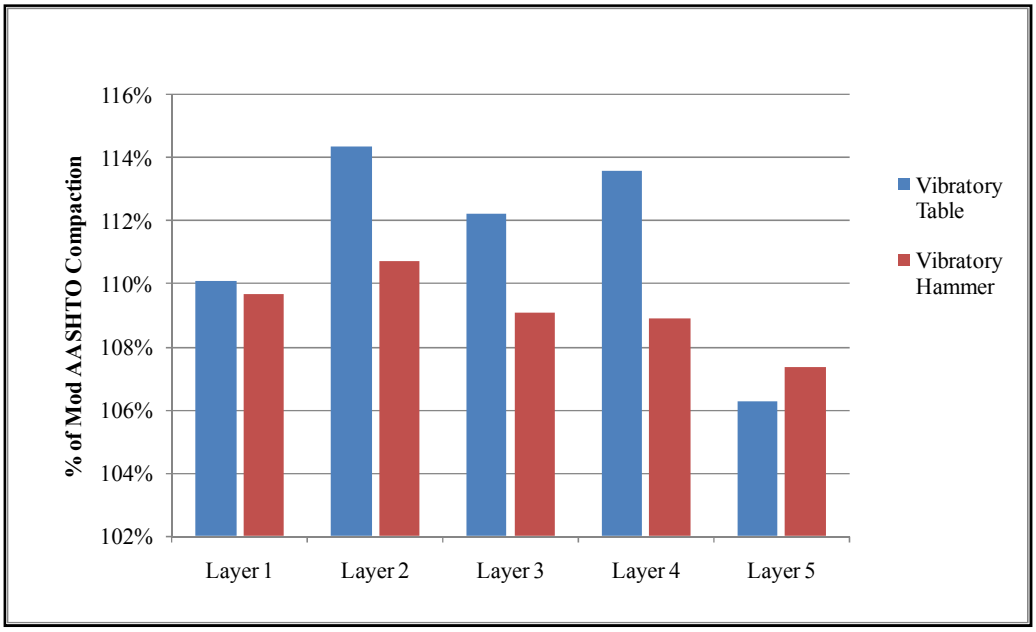

Figure 4-38: Layer compaction densities – G3

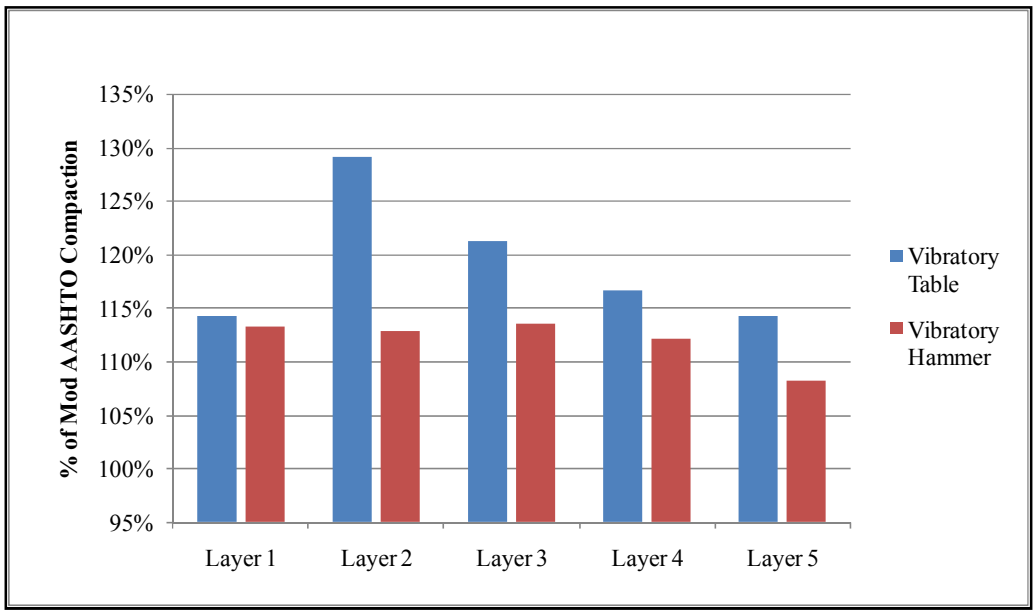

Figure 4-39: Layer compaction densities – G4

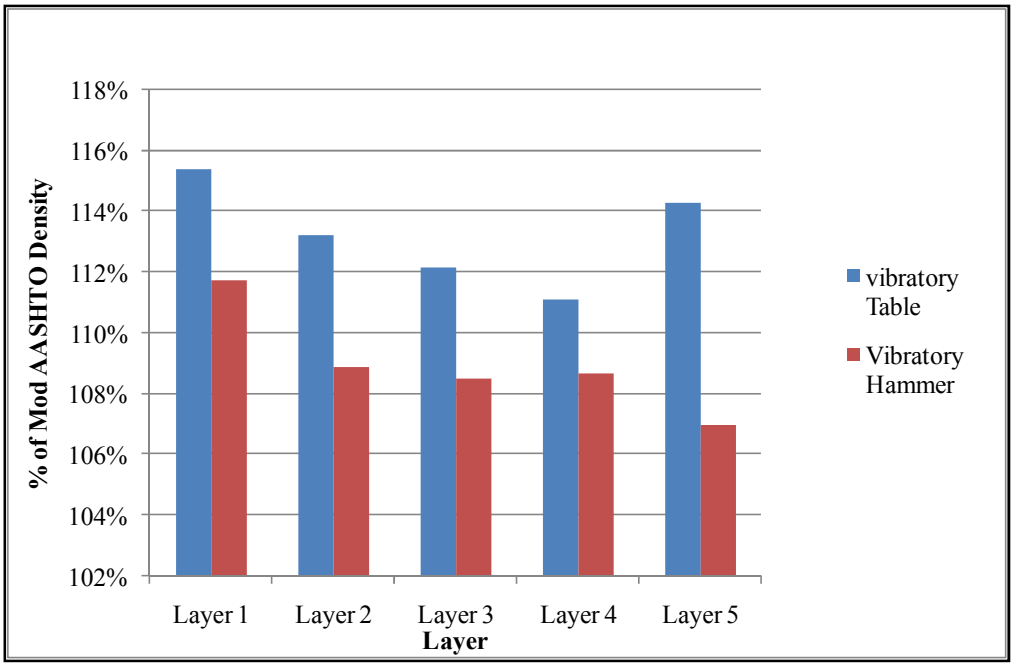

Figure 4-40: Layer compaction densities – G7

The results show that relatively higher layer densities are obtainable with the vibratory table compaction method compared to the vibratory hammer. An average difference of 3.7% in layer density between the vibratory table and vibratory hammer was obtained with the middle layers of the G3 material while the first and last layers showed an average difference of 1%. Similarly with the G4 material, high layer compaction densities were obtained with the middle layers. The highest difference of 16% was observed with the second layer. The G7 material exhibited high densities (of average difference; 3.8%) across all five layers with the vibratory table compaction method.

Specimen Density

The specimens compacted using the vibratory table showed higher densities compared to the developed vibratory hammer compacted specimens; this is shown in Figure 4-41 for the three material types. This shows that better compaction is obtained with the vibratory table. However, the vibratory table compacted specimens were also compared to specimens compacted to refusal densities using the vibratory hammer as shown in Figure 4-42. Results show that the vibratory hammer is capable of producing specimens of equivalent density as the vibratory table for graded crushed stone material (G3 and G4). With the G7 material, higher densities are obtained using the vibratory table compared to the vibratory hammer.

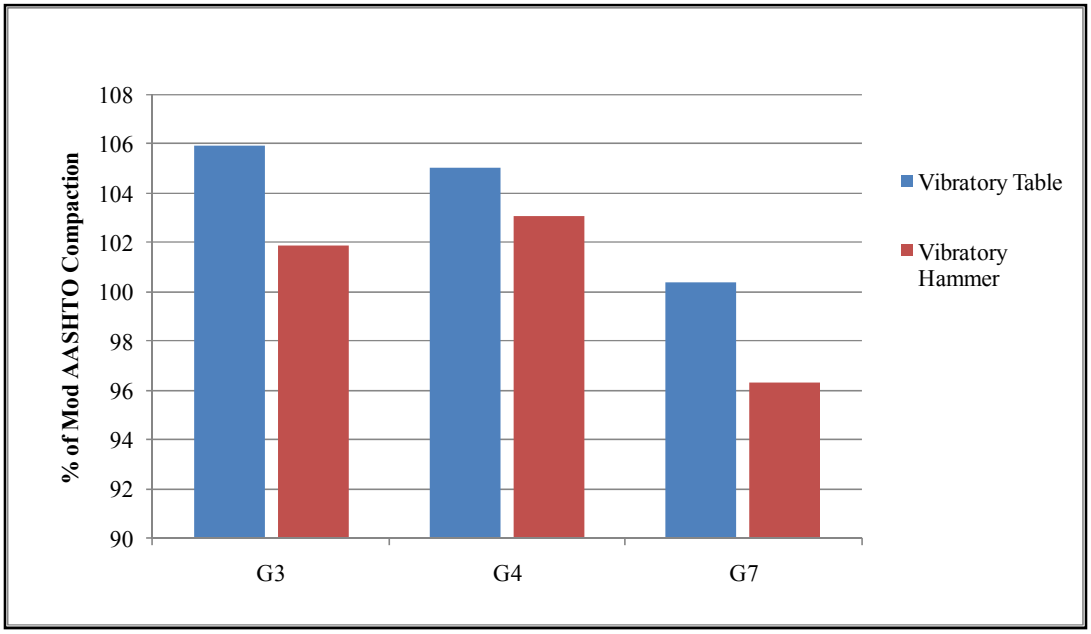

Figure 4-41: Specimen Compaction densities attained

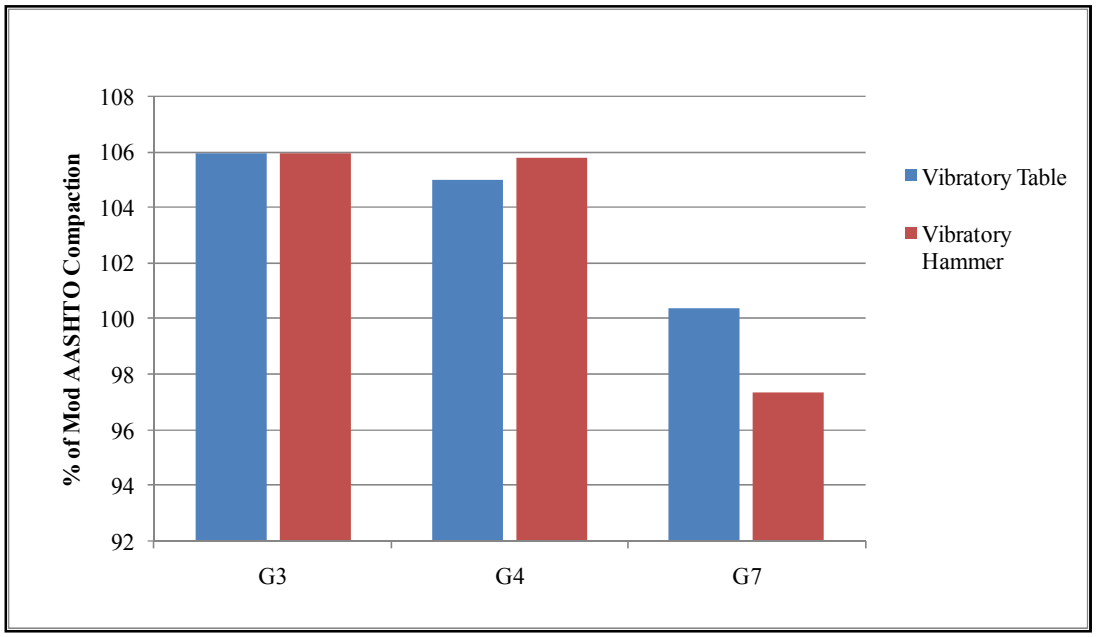

Figure 4-42: Refusal Densities

4.9 COMPACTIVE ENERGY

The compactive energies of the three compaction methods (vibratory hammer, vibratory table and Mod AASHTO) cannot be accurately compared as highlighted in Section 2.3.6.4. However, an indication of the difference in energies, based on the calculated compactive energies of the methods, can be obtained.

The material for the Mod AASHTO test is compacted in a mould of volume, different from the vibratory hammer and vibratory table methods. Therefore, energies can only be compared per unit volume of the compacted material. The compaction energy of the vibratory hammer and vibratory table can be calculated using Equation 2-1 in Section 2.3.6.3.1 reproduced here for easy reference.

$$E = \frac{\text{Wh x Freq x Amp x CompTime x No.Layers}}{\text{1000x Vol.mould}}$$

Where;

E = Energy (kJ/m^3)

Wh = Static weight of the vibratory hammer or table (N)

Vol. mould = Volume of mould (m^3)

Freq = frequency (Hz)

Amp = amplitude (m)

CompTime = Compaction Time

No. Layers = Number of layers compacted

Also the compaction energy of the Mod AASHTO compactor can be calculated using Equation 4-5.

$$\mathbf{E = \frac{Wmh \text{ x } No.blows \text{ x } dh \text{ x } No.layers}{1000 \text{ x } vol.mould}} \qquad \text{Equation 4-5}$$

Where;

E = Energy (kJ/m^3)

Wmh = Weight of the drop hammer (N)

No.blows = No. of blows per layer

Vol. mould = Volume of mould (m^3)

dh = Drop height of the hammer (m)

No.layers = No. of layers compacted

The amplitude of the hammer depends on the static mass of the hammer (which is about 35kg in this case) and the resistance of the material being compacted, as explained in the literature. The amplitude will generally increase as the soil gets more compacted. Taking all this into

consideration, 5mm was assumed for the amplitude of this vibratory hammer. Wh of the vibratory hammer was taken as the combined weight (static weight) of the hammer, sliding frame and surcharge while for the vibratory table, it was taken as the 50kg surcharge. Table 4-8 shows the results of the comparison.

Table 4-8: Comparison of compactive energies

Vibratory Hammer		**Mod AASHTO**		**Vibratory Table**	
Wh	344.3	Wmh	44.145	Wh	490.5
Freq (Hz)	31.5	No.Blows/layer	55	Freq (Hz)	50
Amp (m)	0.005	dh (m)	0.457	Amp (m)	0.0004
CmpTime (S)	25	No. layers (No.)	5	CmpTime (S)	120
No. Layers	5	Vol. Mould (m^3)	0.00231667	No Layers	5
Vol. Mould (m^3)	0.00530144			Vol. Mould (m^3)	0.00530144
Energy (kJ/m^3)	**1285.6**	**Energy (kJ/m^3)**	**2394.8**	**Energy (kJ/m^3)**	**1110.3**

The results of the comparison shows that a high compactive effort is imparted using the Mod AASHTO method. The developed compaction method with the vibratory hammer is second with 1285.6 kJ/m^3 (1109.2 kJ/m^3 lower than the Mod AASHTO energy). The vibratory table imparts a compactive energy of 1110.3 kJ/m^3, which is 175.3 kJ/m^3 lower than the vibratory hammer. However, results of the tests indicate quite the opposite. Higher densities were obtained with the vibratory table compared to the vibratory hammer and the Mod AASHTO. There are two possible explanations for this; one is that the Mod AASHTO test results in high pore pressures building up in the material. This is due to the high amplitude of the test method coupled with the fact that unlike the vibratory hammer and vibratory table, the Mod AASHTO rammer is only 50mm in diameter. Therefore, each blow of the rammer impacts only on some 10% of the surface of the layer being compacted. High pore pressures have a negative effect on compaction. Material particles are pushed away from each other at high pressure and the densest material arrangement is not achieved. On the other hand, vibration based compaction methods (with low amplitudes) do not result in high pore pressure build ups in the material. Therefore, a denser arrangement of material is obtained. This would suggest that the vibration based compaction methods are much more efficient and result in better packing of material. A second and perhaps a more likely explanation is that the methods provided in literature for calculating the compactive energies of the vibratory hammer and vibratory table are inadequate. In particular, Equation 2-1 suggests that the compactive energy of the vibratory hammer depends on, among other factors, the static

weight. This would suggest that high compactive energies can be imparted with a large amount of static weight. However, larger amounts of static weight not only limit the effectiveness of operation of the vibratory hammer (as pointed out in the literature) but results of this and other studies have also shown that the surcharge load applied has marginal influence on the obtainable density with the vibratory hammer.

The second method stated in Section 2.3.6.3.1 for computing the compactive energy of the vibratory hammer is to consider the manufacturer's rated point energy of the hammer. This is the amount of energy that is delivered per impact/blow of the tamper. The Bosch hammer used in this study has a rated point energy of 25J. This means that at an operating frequency of 31.5Hz, the hammer imparts 18 568 kJ of energy per unit volume of material compacted. This is shown in Table 4-9. The energy of the ASTM method is also included for comparison.

Table 4-9: Compactive Energy of vibratory hammer based on Point Energy

Vibratory Hammer		
	SU	**ASTM**
Point Energy (kJ)	0.025	0.012
Freq (Hz)	31.5	70
CmpTime (S)	25	60
No Layers	5	3
Vol. Mould (m^3)	0.00530	0.00212
Energy (kJ/m^3)	**18 568.08**	**71 320.75**

This method indicates that the vibratory hammer imparts significantly high energy compared to the Mod AASHTO (8 times higher). Density results, on the other hand, do not show too significant a difference between the vibratory hammer and Mod AASHTO. One flaw of this method of computing the energy (as stated in Section 2.3.6.3.1) is that the condition under which the vibratory hammer is able to impart a point energy of 25J (SU vibratory hammer) is not defined. It is important to remember that the vibratory hammer is not made for compaction but for demolition works. Instead of a frame and application of static load, the hammer is designed for hand operation. The effect of the framing and application of static load on point energy is not known.

4.10 ANALYSIS OF COMPACTED SPECIMEN

4.10.1 CT- Scan

To appreciate the particle packing characteristics a CT-scan of the vibratory hammer and vibratory table produced specimens was proposed. The scan was proposed to primarily assess the void profile resulting from the two compaction methods particularly at the layer interfaces. Three specimens each of the G3 and G7 material were proposed for scanning at the Central Analytical Facility (CAF) of the Department of Forestry at Stellenbosch University. The three specimens would include two compacted using the vibratory hammer but scarified using the two different methods explained in Section 3.3.2, and one compacted using the vibratory table. The material packing characteristics resulting from the developed vibratory hammer compaction method were also to be compared to that of the vibratory table compaction method.

The first attempt to scan the entire 150mm diameter specimens proved futile because the specimen were too large and too dense to obtain a clear resolution with the CT-scan available at CAF. The scan works by sending a spectrum of x-rays through the object and the absorbed radiation is measured on a sensor on the opposite end. However, depending on the thickness and density of the material been scanned, some of the spectrum is completely absorbed in the material and is not measured on the sensor screen resulting in a blank image. This happens mostly for the middle part of the specimen due to the longer distance through which the x-rays have to traverse.

Plate 4-1: Cut Specimens

Therefore an attempt was made to reduce the diameter of the specimen by cutting off a quarter size of the thickness using a saw cutter. The cutting was relatively successful for the G7 material but unsuccessful for the G3 material. The G3 material crumbled as the saw cutter cut through the larger aggregate (Plate 4-1).

A second attempt to scan the sliced G7 material produced distinct images of the internal structure of the specimen. A stack of such images were obtained over the height of the specimen. However, volume ratios of the voids and materials could not be calculated as the software used to analyse the images could only detect voids on the periphery of the specimen and not in the middle parts of the specimen. Therefore the void profile of the specimen could not be established. However, Figure 4-43 shows images of the slices at the intersection (interface) of two layers for both scarifying methods. It would appear from these images, that the scarifying tool gives a smoother transition at the layer interface.

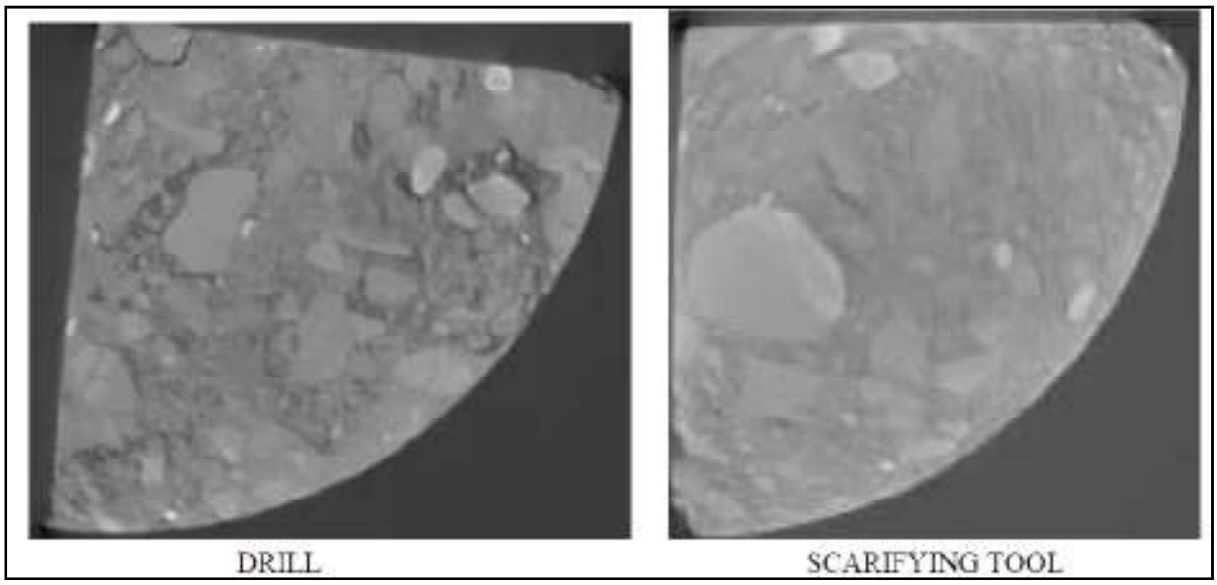

Figure 4-43: CT-Scan images

4.10.2 Sieve Analysis

Soil disintegration during compaction is a problem especially when more disintegration occurs during laboratory compaction than field compaction as is usually the case. When disintegration occurs, the maximum dry density increases so that the laboratory maximum value is not representative of field conditions. In such a case, the maximum dry density is difficult to achieve in the field (ASTM D7328-07).

To check for particle disintegration after compaction, a dry sieve analysis before and after compaction with the developed vibratory hammer compaction method, was performed. The results of the analysis are shown in Figure 4-44, Figure 4-45 and Figure 4-46 for G3, G4 and G7 materials respectively.

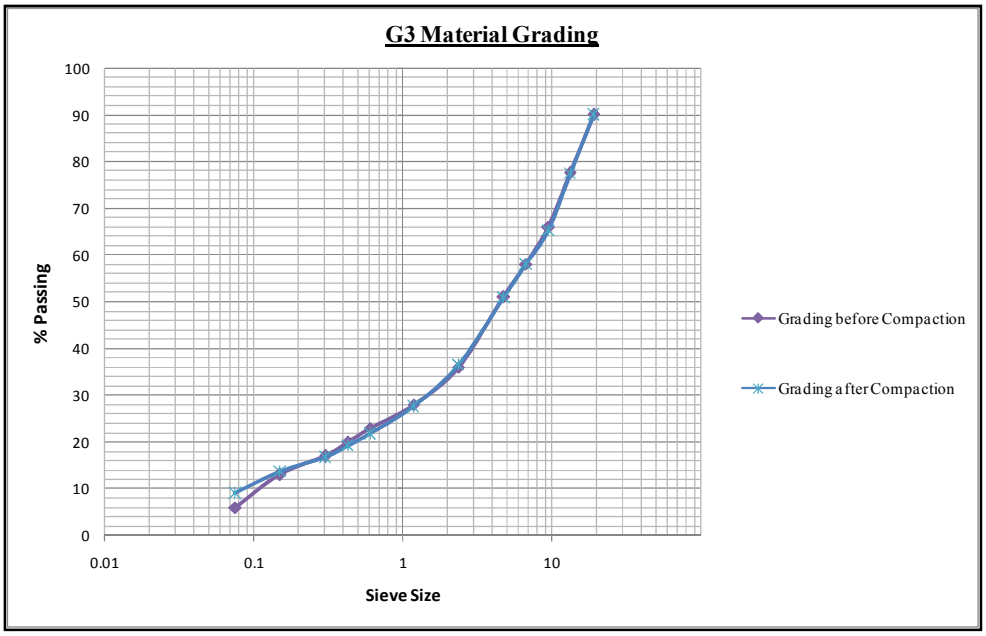

Figure 4-44: Grading Analysis after compaction – G3

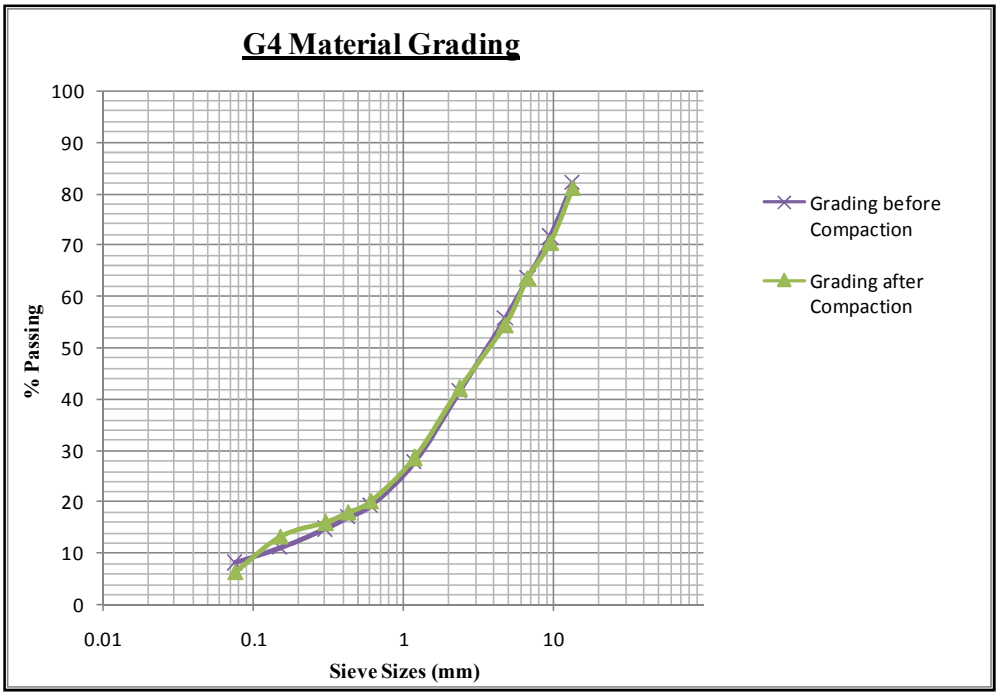

Figure 4-45: Grading Analysis after compaction – G4

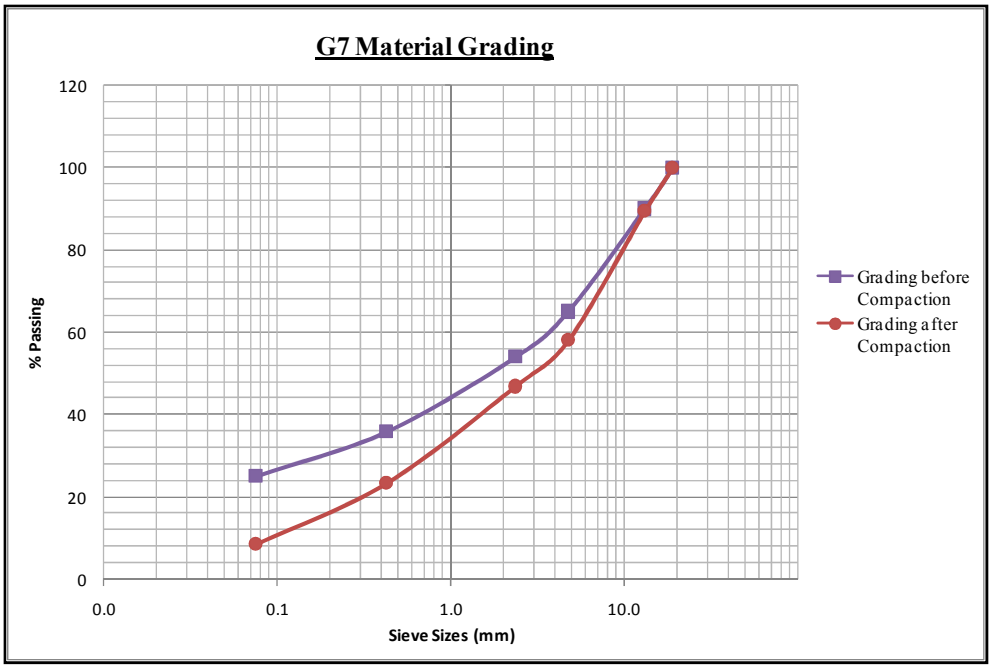

Figure 4-46: Grading Analysis after compaction – G7

The results illustrate that the developed compaction method does not result in any significant crushing or disintegration of material. Instead, a significant amount of cementation of the filler content was visually observed and is also evident in the sieve analysis of the G7 material (Figure 4-46). This is typical of clayey type material after wetting.

4.11 SUMMARY

In this section, the results of the experiments have been illustrated and analysed. From the results and analysis it can be deduced that the mass of the tamping foot plays a significant role towards material compaction with the vibratory hammer. Additionally, factors such as frequency, moisture content and frame rigidity have been investigated with regard to their influence on vibratory hammer compaction. Using factors that produced ideal results, a compaction method was proposed for compaction of granular material using the vibratory hammer. The method, through repeatability tests, proved to be effective for compaction of G3, G4 and RA material but less effective for G7 material.

The next chapter gives conclusions drawn from the results of the experiments presented here.

REFERENCES

ASTM D7382-07. 2008. **Standard Test Methods for Determination of Maximum Dry Unit Weight and Water Content Range for Effective Compaction of Granular Soils Using a Vibrating Hammer**. Annual Book of ASTM Standards, Vol 04.09. West Conshohocken, ASTM International

DEAN CHROSTOLEAR. 2010. **3 Factor Design of Experiments**. Available at: http://www.cpkinfo.com/DOE.html (Accessed: September 31, 2012)

WIRTGEN GROUP, 2010. **Wirtgen Cold Recycling Technology.** 3rd Edition. Wirtgen GmbH. Germany.

MONTGOMERY D.C. and RUNGER G.C. 2007. **Applied Statistics and Probability for Engineers.** 4th Edition. John Wiley & Sons, Inc.

MULUSA W.K. 2009. **Development of a simple Tri-axial test for characterising Bitumen Stabilised Materials.** Dissertation for Master of Science in Engineering, University of Stellenbosch.

CHAPTER 5: CONCLUSION

5.1 INTRODUCTION

In this study, a number of factors pertinent to compaction with the vibratory hammer were evaluated. Test factors and their influence on compaction with the vibratory hammer were identified and appreciated. This Chapter provides conclusions made after synthesis of the results of the tests and analysis in Chapter 4.

5.2 TAMPING FOOT

Results allied to the tamping foot illustrate that the mass of the tamping foot plays a significant role on the obtainable compaction density with the vibratory hammer. The 1.6kg difference in mass of the two tampers compared can result in differences of over 8% in compaction density as observed with the G7 material. Additionally the 3kg tamping foot provides more consistent results for both compaction time and density compared to the 4.6kg tamping foot. This can be attributed to the operation of the vibratory hammer and the creation of an amplitude effect as explained in Section 2.3.6.3.2 of the literature study. The 4.6kg tamper, due to its weight, tends to resist the lift that creates the amplitude effect. Thus the effects of vibration, which are a combination of frequency and amplitude, are lessened and the material is not compact adequately.

5.3 MOISTURE

The moisture content of the material has a significant influence on the compaction time and the obtainable density. This was shown in the ANOVA at the chosen α level of 0.05. This infers that high moisture contents enhance particle mobility resulting in faster packing of the particles. The high moisture content also results in a structure with a high degree of particle orientation and hence high density.

5.4 SURCHARGE LOAD

The surcharge load does not significantly influence the obtainable compaction density with the vibratory hammer. This was confirmed with the ANOVA in Section 4.5. The results are consistent with the findings of Prochaska, Drnevich , Kim and Sommer (2005).

5.5 FREQUENCY

Higher densities are obtainable at high frequency. The results show that a 6Hz difference in frequency can result in a difference of more than 3% in obtainable compaction density with the vibratory hammer. In addition, at high frequency, less compaction time is required to achieve the same level of compaction.

5.6 FRAME MODIFICATIONS

The frame modifications entailed making the frame more rigid and reducing friction effects from the sliding frame. The modifications resulted in an increase in obtainable compaction density with the vibratory hammer of between 0.4% and 2.8%. The modification of the frame also resulted in less variability of the layer compaction time and density. This illustrates that the efficiency of compaction with the vibratory hammer can be affected by the type of frame used for the hammer.

5.7 INTERLAYER BOND

One of the objectives of the CT – scan was to determine the difference in void profile as a result of scarifying using the scarifying tool (supplied by BSM Laboratories (Pty) Ltd) and the traditional drill. Unfortunately CT – scan of the specimens did not go as planned. However, a visual analysis of the photographic images suggests that specimens scarified with the scarifying tool appear to have a smoother transition at the interface. This is due to the short depth of influence of the scarifying tool. The short depth of influence of the tool might also be responsible for delamination of the layers which was observed with some specimens.

Table 5-1 gives a summary of the effects of the aforementioned test factors on obtainable density with the vibratory hammer.

Table 5-1: Summary of Effects of tests factors on obtainable densities

Test Factor	**Effect on Density**		
	G3/G4	G7	RA
Tamping Foot mass (↑)	↓	↓	↓
Moisture (↑)	↑	↑	-
Surcharge (↑)	*	*	-
Frequency (↑)	↑	↑	-
Frame Rigidity (↑)	↑	**	-

↑Increase -Not tested **Variable results
↓Decrease *No significant change

5.8 GENERAL CONCLUSIONS

A compaction method for granular material using the vibratory hammer was developed. Repeatability tests assert that, the method is effective for compaction of graded crushed stone (G3 and G4) and probably RA material. The consistency in densities obtained, infers that the method offers sound repeatability.

The comparative tests with the vibratory table showed that the developed vibratory hammer compaction method is capable of producing specimens with densities that are comparable to the vibratory table produced specimens however with much less effort. The vibratory hammer also has the potential of portability. A portable frame of the hammer can be manufactured allowing the hammer to be used on site provided there is a source of electricity.

Methods available in literature for computing the compactive energy of the vibratory hammer appear to be flawed and may not indicate actual energies imparted during the compaction process. The differences in computed energy using the two method is huge (1 285 viz 18 568kJ/m^3) as is the difference between the SU and ASTM energy (18 568 vs 71 321kJ/m^3). Further research is required on the actual energy imparted by the vibratory hammer particularly in relation to the rated point energy of the hammer.

The study on RA material was too limited. Nonetheless, results obtained illustrate a similar response and trend as the granular material (to the two tampers). However, the response of RA material to compaction could vary depending on the activeness (or lack thereof) of the bitumen content. Therefore, more studies on varieties on this material are necessary.

With the G7 material, 100% of Mod AASHTO specimen compaction could not be attained with the vibratory hammer. The highest density attained was 97%. This could be attributed to the material type. The G7 material comprised a high filler content and relatively high plasticity of the fines. The inherent cohesive properties of this type of material tend to resist particle movement required for vibratory compaction. Therefore, until further research that may suggest otherwise, vibratory hammer compaction is unsuitable for plastic cohesive material.

CHAPTER 6: RECOMMENDATIONS

6.1 INTRODUCTION

In this study, the compaction of 150mm diameter x 300mm high specimen was considered. Such large specimens have the advantage of reduced effects from the boundary condition (i.e. friction from the top and bottom plates). However, such large specimen might be considered too large for routine moisture-density tests and further research is recommended for vibratory hammer compaction of smaller size specimen. Nonetheless, based on the findings of this study the following compaction procedure is recommended when using the vibratory hammer for compaction of 150mm diameter x 300mm high specimen.

6.2 SCOPE

6.2.1. This test method covers the determination of maximum dry density and optimum water content range of granular material. The compaction of a 150mm diameter x 300mm high specimen of granular material will be performed using a vibratory hammer, e.g. the Bosch GSH 11E®, with a surcharge of 10kg mounted in a frame. Compaction of the material will take place with the aggregate at room temperature i.e. 25ºC.

6.2.2. The test method will only apply to material passing the 19mm sieve. All material retained on the 19mm sieve should be crushed to pass the 19mm sieve.

6.3 APPARATUS

6.3.1 A vibratory hammer with a rated power input of 1500W, a frequency in the range of 15 to 31Hz and a manufacturer's rated impact energy of 25J.

6.3.2 Chisel for tamping layers

6.3.3 Sieves: from 19mm down complying with SABS 197

6.3.4 Scarifying tool such as that shown in Plate 3-7 (Chilukwa, 2013) of diameter 148mm and with projections not exceeding 10mm.

6.3.5 A balance to weight up to 15kg, accurate to 5g.

6.3.6 A mixing basin approximately 500mm in diameter

6.3.7 A drying oven, thermostatically controlled and capable of maintaining a temperature of 105 to 110˚C

6.3.8 A steel split mould 152mm in diameter and 300mm in height with an extension piece and clasps to fix the mould to the base of the frame.

6.3.9 Circular mould papers with diameter of 150mm.

6.3.10 Non-stick spray e.g. non stick cooking spray purchased at any supermarket.

6.3.11 A tamping foot; 3kg mass and 148mm in diameter

6.3.12 Material Scoop (90mm Φ x 85mm h)

6.3.13 Adjustable spanner to fasten and loosen surcharge load to the vibratory hammer.

6.3.14 The vibratory Hammer should be mounted on a hammer frame that allows for free vertical movement of the hammer. The frame should be rigid enough to ensure that no discernable shaking of the frame occurs during compaction. A mounting frame should be designed to securely hold the vibratory hammer in a vertical position and aligned to the position of the mould underneath. The mounting frame should be fitted with a provision for a surcharge of 10kg to be mounted to the vibratory hammer. There should be a pulley system connecting the frame and mounting head. This allows for easy lifting and lowering of the vibratory hammer. The total mass of vibratory hammer, surcharge and mounting frame and tamper should be 35kg. At the base of the frame should be a metal plate atleast 8mm thick bolted down a wooden platform. The metal plate should have guide bolts to keep the mould in position (and restrict lateral movement) and clamps to hold down the mould. The wooden platform should be made out of supawood with density not less than 704kg/m3 (see Appendix B and Section 3.3.2 of Chilukwa, 2013).

6.3.15 Steel ruler of length >300mm

6.4 METHOD

6.4.1 Preparation of the material

An adequate quantity of the air-dried sample is sieved through a 19mm sieve. Material retained on the 19mm sieve is crushed to pass the 19mm sieve and added to the portion of material passing the sieve. The material should be mixed thoroughly and quartered so as obtain five basins of 14kg each of similar material.

6.4.2 Mixing

Weigh the material in each basin accurately to the nearest 5g and transfer to mixing basin. Add moisture to each of the five samples using a range of moisture contents, from 2% moisture to 12% moisture; in increments of 2%.

6.4.3 Preparation of the mould

Ensure that mould is clean and then spray the interior of the mould with the non-stick spray. Fix and align the mould to the base of the frame directly below the tamping foot of the vibratory hammer using the clamps. Place two of the circular paper sheets at the base of the mould to prevent material from sticking to the bottom (base plate).

6.4.4 Preparing the vibratory hammer

Fix the mounting frame to the vibratory hammer and fit hammer onto the guide rods. Place the 10kg surcharge load onto the mounting head and fasten tightly. Using the pulley system raise the vibratory hammer to the maximum height it can be raised or to an adequate height that will allow the operator to work beneath the vibratory hammer. Lower the vibratory hammer into the mould, checking that the vibratory hammer is perpendicular to the base of the mould i.e. the tamping foot is flat on the base with no point of the foot slightly raised. Allow the vibratory hammer to rest in the mould with no material present. Mark clearly the position (zero line) where the lower end of mounting frame rests on the guide rod using a suitable marker. Raise the vibratory hammer and measure up from the initial mark 300mm and mark this clearly.

6.4.5 Compaction

The material should be compacted in five approximately equal layers for 25 seconds each. The material is placed in the mould using a material scoop. Fill the scoop with the prepared material and level off the scoop and place it in the mould. Add three scoops of material to provide a starting layer thickness of 92mm. Using the chisel, work the material around in order to evenly distribute it in the mould; distribute the particles evenly as well i.e. not too much fine material on top or too much coarse material on top, but rather a fair distribution of each i.e. unsegregated. Lower the vibratory hammer till the foot piece comes to rest on the material.

Check that the vibratory hammer is set to a frequency of 31,67Hz. Switch on the hammer and allow for 25 seconds of compaction. Raise the vibratory hammer. Using the scarifying tool, scarify the entire surface area of the top of the compacted layer. After the surface of a respective layer has been scarified, add the material for the next layer and compact accordingly.

*After Layer four has been compacted and scarified, the extension piece (collar) must first be fitted to the mould before adding the material for layer five. After adding the material for layer five, place a mould paper on top of the material and then lower the vibratory hammer into position; the paper helps prevent material of the final layer from sticking to the tamping foot.

After Layer five has been compacted and prior to raising the vibratory hammer measure the distance from the zero line to the lower end of the mounting frame with a steel rule. This distance is taken as the final height of the specimen.

6.4.6 Removing and handling the compacted specimen

Raise the vibratory hammer and remove the extension piece (collar). Disassemble the mould entirely. Place a plastic bag over the specimen and remove it taking care to pick the specimen up from the bottom end. Weigh the specimen after compaction to check the final mass of the specimen.

6.4.7 Determination of moisture content

Take a small sample (750-950 g) of material either just prior to, during or after compaction. Weigh the sample to the nearest 0.1g and dry to constant mass in an oven at 105 to 110˚ C.

6.4.8 Moisture – density curve

From the moisture content determined, the final mass of the compacted specimen and the final height measured, the dry density of the specimen may be determined. This represents one point on the moisture - density curve. The procedure is repeated for each of the four remaining samples (at increasing moisture contents) to determine other points on the curve. The curve is developed by plotting the final dry density of each of the specimens against their respective final moisture contents. The peak (point at which the curve turns) is the OMC (on the horizontal axis) of the vibratory hammer and the Maximum Dry Density (on the vertical axis).

6.5 CALCULATIONS

6.5.1 Addition of water

$$\text{Water (g)} = \frac{\text{target moisture content (\%)}}{\text{100 x mass of sample (g)}} \qquad \text{Equation 6-1}$$

6.5.2 Dry Density

$$\text{Volume of specimen } (m^3) = \pi \times 0.005625 \times \text{specimen height (m)} \quad \text{Equation 6-2}$$

$$\text{Dry Density } (kg/m^3) = \left(\frac{\frac{Fm}{1+0.1MC}}{\text{Vol.Specimen}} \right) \quad \text{Equation 6-3}$$

Where; Fm = Final Mass of the specimen (kg)

MC = Moisture Content (%)

NOTES

Layers should not be scarified deeper than 10mm. Scarifying deeper than 10mm results in inadequate bonding and an increased amount of voids between the layers.

Should the vibratory hammer not meet the specifications provided and where no suitable alternative compaction hammers can be sourced, then a vibratory hammer with a point energy of 25 ± 2 Joule should be used.

After a specimen has been compacted and removed from the mould, the mould should be cleaned by wiping off excess material from the mould walls. This should be done prior to the compaction of the next specimen.

When the specimen prepared is to be used in the laboratory and the first four layers have been compacted, add sufficient material to layer five so that that the final height of the specimen is 300mm or slightly higher. This is checked by viewing the final position of the mounting frame relative to the 300mm marked off point on the guide rod, a tolerance of 2mm either side of 300mm is allowed. For each of the finishing positions a description of the procedure to be followed is given in a) and b).

a) If the lower end of the mounting frame is level with the 300mm mark after compacting layer 5, the specimen is removed as previously described.

b) If the lower end of the mounting frame is above the 300mm mark after compacting layer 5 a steel straight edge is used to cut off the piece of the specimen extending out of the mould. Material is then sieved through a 4.75mm sieve on top of the specimen. The vibratory hammer is the lowered and the sieved material is compacted till the lower end

of the mounting frame reaches the 300mm mark. The specimen is then removed as previously described.

BIBLIOGRAPHY

ASTM D7382-07. 2008. **Standard Test Methods for Determination of Maximum Dry Unit Weight and Water Content Range for Effective Compaction of Granular Soils Using a Vibrating Hammer**. Annual Book of ASTM Standards, Vol 04.09. West Conshohocken, ASTM International

BS 1377: Part 4, 1990. **British Standard methods of test for Soils of Civil Engineering Purposes. Part 4. Compaction – related tests: Method for Determination of Dry Density/Moisture Content using Vibrating Hammer.** British Standards Institution

KELFKENS R.W.C, 2008. **Vibratory Hammer Compaction of Bitumen Stabilised Material.** Dissertation for Master of Science in Engineering, University of Stellenbosch.

TMH1. 1986. **Technical Methods for Highways: Standard Methods of Testing Road Construction Materials**. 2nd Ed. Committee of State Road Authorities, Pretoria, South Africa.

APPENDIX A: Schematic of the Vibratory Hammer

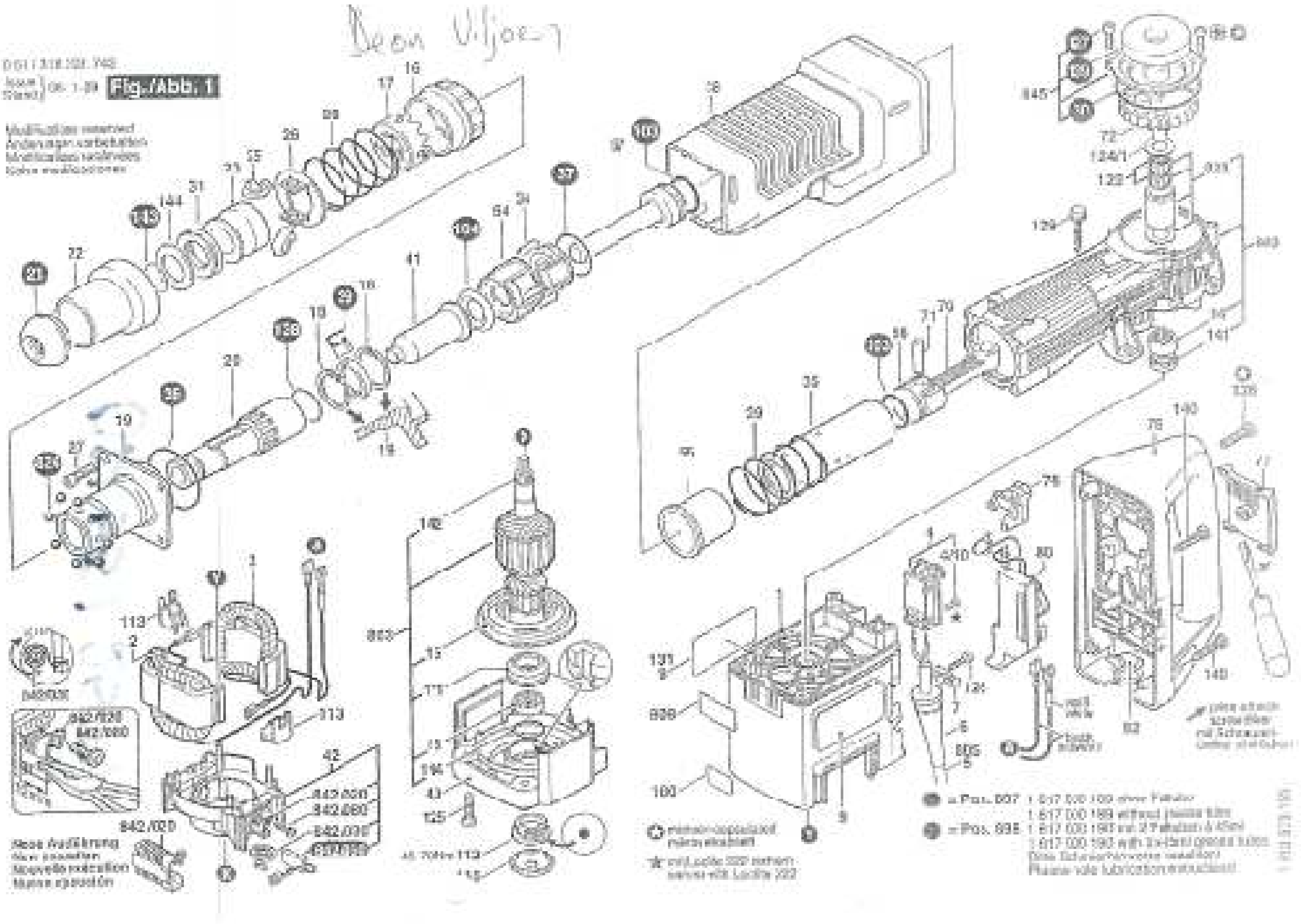
Fig./Abb. 1

APPENDIX B: Modified Frame

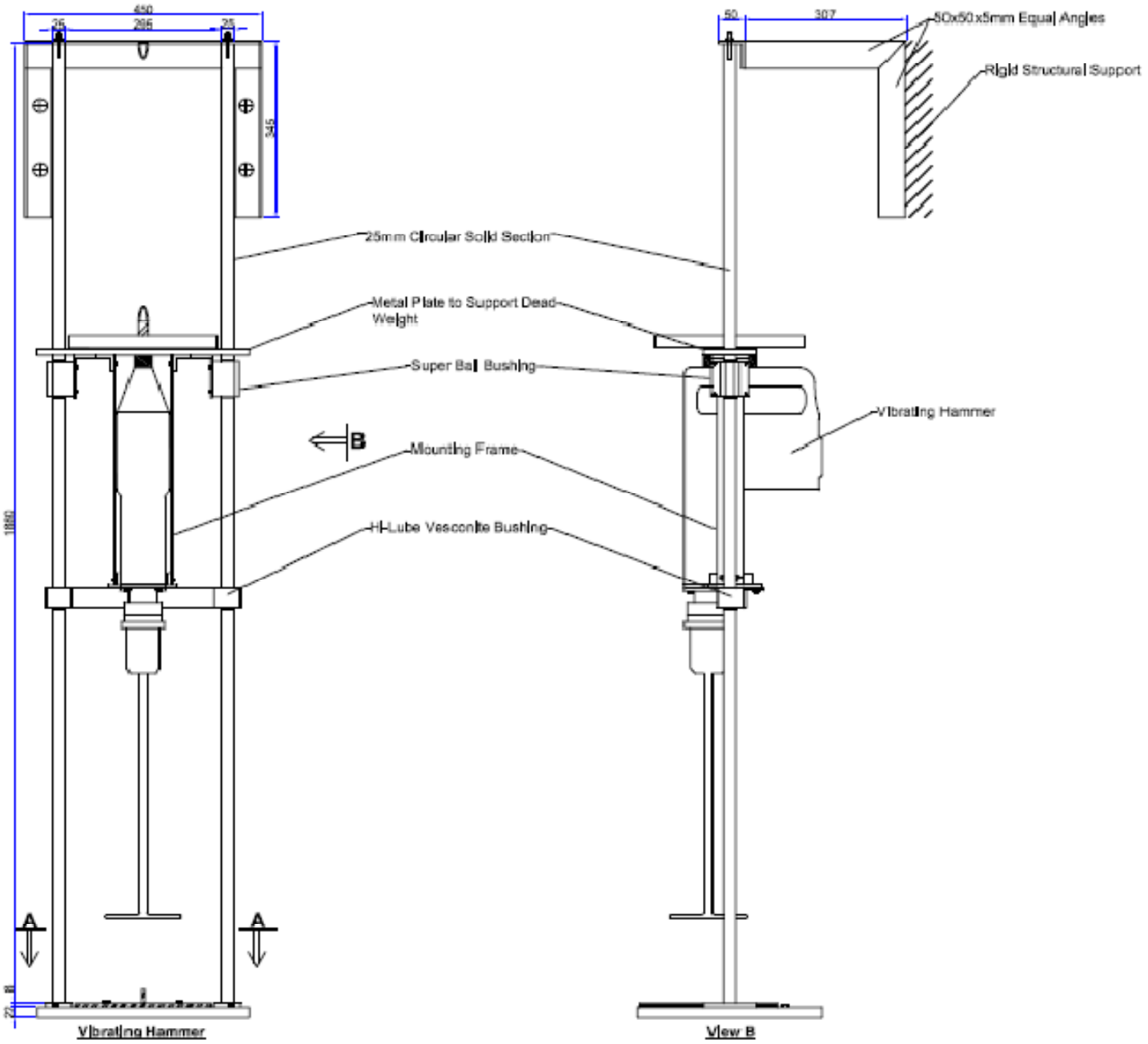
450
25
265
25
345
1860
22
A
A
B
25mm Circular Solid Section
Metal Plate to Support Dead Weight
Super Ball Bushing
Mounting Frame
Hi-Lube Vesconite Bushing
Vibrating Hammer
Vibrating Hammer
50
307
50x50x5mm Equal Angles
Rigid Structural Support
View B

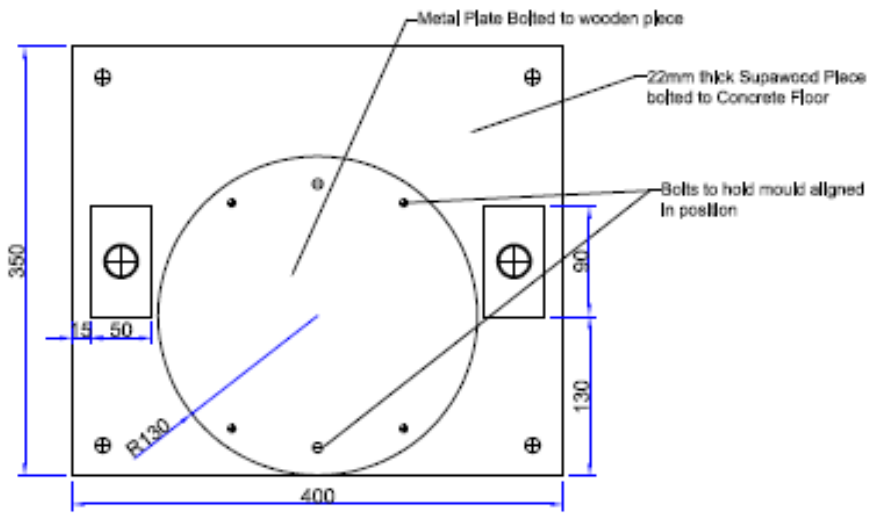

Section A-A

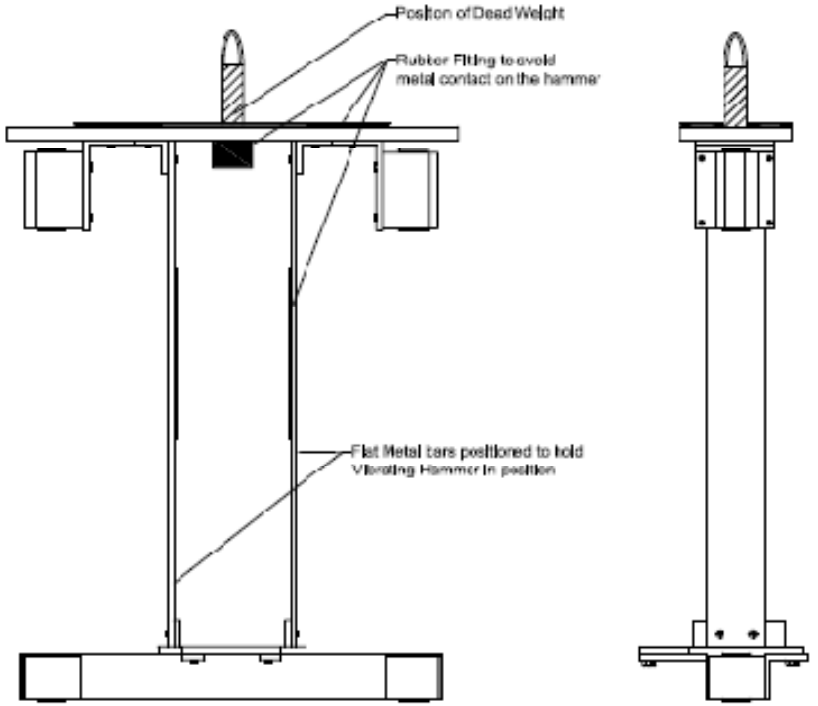

Mounting Frame

APPENDICES C, D, E, F, G, H, J AND K ROUTE MAP

APPENDIX C1: G3 material/Vibratory hammer/Soft frame				
a. TIME TO COMPACT EACH LAYER TO 100% MOD AASHTO				
b. TIME TO ACHIEVE REFUSAL DENSITY/DENSITY ACHIEVED				
Page number	Figure numbers	Variable		
		Tamping Foot (kg)	Surcharge/Total static mass (kg)	Moisture (% of OMC_M)
145	B-1 and B-2	3	10/26.5	80
146	B-3 and B-4	4.6	10/26.5	80
147	B-5 and B-6	3	20/36.5	80
148	B-7and B-8	4.6	20/36.5	80
149	B-9 and B-10	3	10/26.5	90
150	B-11 and B-12	4.6	10/26.5	90
151	B-13 and B-14	3	20/36.5	90
152	B-15 and B-16	4.6	20/36.6	90

APPENDIX C2: G3 material/Vibratory hammer/Soft frame				
EFFECT OF VARYING THE MOISTURE CONTENT				
TIME TO COMPACT EACH LAYER TO 100% MOD AASHTO DENSITY				
Page number	Figure numbers	Variable		
		Tamping Foot (kg)	Surcharge/Total static mass (kg)	Moisture (% of OMC_M)
153	B-17	3	10/26.5	80 and 90
153	B-18	3	20/36.5	80 and 90
154	B-19	4.6	10/26.5	80 and 90
154	B-20	4.6	20/36.5	80 and 90

APPENDIX C3: G3 material/Vibratory hammer/Soft frame				
EFFECT OF VARYING THE MASS OF THE TAMPING FOOT				
TIME TO COMPACT EACH LAYER TO 100% MOD AASHTO DENSITY				
Page number	Figure numbers	Variable		
		Tamping Foot (kg)	Surcharge/Total static mass (kg)	Moisture (% of OMC_M)
155	B-21	3 and 4.6	10/26.5	80
155	B-22	3 and 4.6	10/26.5	90
156	B-23	3 and 4.6	20/36.5	80
156	B-24	3 and 4.6	20/36.5	90

APPENDIX C4: G3 material/Vibratory hammer/Soft frame				
EFFECT OF VARYING THE SURCHARGE/TOTAL STATIC MASS				
TIME TO COMPACT EACH LAYER TO 100% MOD AASHTO DENSITY				
Page number	Figure numbers	Variable		
		Tamping Foot (kg)	Surcharge/Total static mass (kg)	Moisture (% of OMC_M)
157	B-25	3	10/26.5 and 20/36.5	80
157	B-26	3	10/26.5 and 20/36.5	90
158	B-27	4.6	10/26.5 and 20/36.5	80
158	B-28	4.6	10/26.5 and 20/36.5	90

APPENDIX D1: G3 material/Vibratory hammer/Rigid frame				
a. TIME TO COMPACT EACH LAYER TO 100% MOD AASHTO				
b. TIME TO ACHIEVE REFUSAL DENSITY/DENSITY ACHIEVED				
Page number	Figure numbers	Variable		
		Tamping Foot (kg)	Surcharge/Total static mass (kg)	Moisture (% of OMC_M)
159	B-29 and B-30	3	5/26.5	80
160	B-31 and B-32	4.6	5/26.5	80
161	B-33 and B-34	3	15/36.5	80
162	B-35 and B-36	4.6	15/36.5	80
163	B-37 and B-38	3	5/26.5	90
164	B-39 and B-40	4.6	5/26.5	90
165	B-41 and B-42	3	15/36.5	90
166	B-43 and B-44	4.6	15/36.5	90

APPENDIX D2: G3 material/Vibratory hammer/Rigid frame					
EFFECT OF VARYING THE FREQUENCY OF VIBRATION					
a. TIME TO COMPACT EACH LAYER TO 100% MOD AASHTO					
b. TIME TO ACHIEVE REFUSAL DENSITY/DENSITY ACHIEVED					
Page number	Figure numbers	Variable			
		Frequency (Hz)	Tamping Foot (kg)	Surcharge/Total static mass (kg)	Moisture (% of OMC_M)
167	B-45 and B-46	25.67	3	5/26.5	90
168	B-47 and B-48	19.67	3	5/26.5	90

APPENDIX D3: G3 material/Vibratory hammer/Rigid frame				
EFFECT OF VARYING THE MOISTURE CONTENT				
TIME TO COMPACT EACH LAYER TO 100% MOD AASHTO DENSITY				
Page number	Figure numbers	Variable		
		Tamping Foot (kg)	Surcharge/Total static mass (kg)	Moisture (% of OMC_M)
169	B-49	3	5/26.5	80 and 90
169	B-50	3	15/36.5	80 and 90
170	B-51	4.6	5/26.5	80 and 90
170	B-52	4.6	15/36.5	80 and 90

APPENDIX D4: G3 material/Vibratory hammer/Rigid frame				
EFFECT OF VARYING THE MASS OF THE TAMPING FOOT				
TIME TO COMPACT EACH LAYER TO 100% MOD AASHTO DENSITY				
Page number	Figure numbers	Variable		
		Tamping Foot (kg)	Surcharge/Total static mass (kg)	Moisture (% of OMC_M)
171	B-53	3 and 4.6	5/26.5	80
171	B-54	3 and 4.6	5/26.5	90
172	B-55	3 and 4.6	15/36.5	80
172	B-56	3 and 4.6	15/36.5	90

APPENDIX D5: G3 material/Vibratory hammer/Rigid frame				
EFFECT OF VARYING THE SURCHARGE/TOTAL STATIC MASS				
TIME TO COMPACT EACH LAYER TO 100% MOD AASHTO DENSITY				
Page number	Figure numbers	Variable		
		Tamping Foot (kg)	Surcharge/Total static mass (kg)	Moisture (% of OMC_M)
173	B-57	3	5/26.5 and 15/36.5	80
173	B-58	3	5/26.5 and 15/36.5	90
174	B-59	4.6	5/26.5 and 15/36.5	80
174	B-60	4.6	5/26.5 and 15/36.5	90

APPENDIX E1: G4 material/Vibratory hammer/Soft frame				
a. TIME TO COMPACT EACH LAYER TO 100% MOD AASHTO				
b. TIME TO ACHIEVE REFUSAL DENSITY/DENSITY ACHIEVED				
Page number	Figure numbers	Variable		
		Tamping Foot (kg)	Surcharge/Total static mass (kg)	Moisture (% of OMC_M)
175	B-61 and B-62	3	10/26.5	80
176	B-63 and B-64	4.6	10/26.5	80
177	B-65 and B-66	3	20/36.5	80
178	B-67and B-68	4.6	20/36.5	80
179	B-69 and B-70	3	10/26.5	90
180	B-71 and B-72	4.6	10/26.5	90
181	B-73 and B-74	3	20/36.5	90
182	B-75 and B-76	4.6	20/36.6	90

APPENDIX E2: G4 material/Vibratory hammer/Soft frame				
EFFECT OF VARYING THE MOISTURE CONTENT				
TIME TO COMPACT EACH LAYER TO 100% MOD AASHTO DENSITY				
Page number	Figure numbers	Variable		
		Tamping Foot (kg)	Surcharge/Total static mass (kg)	Moisture (% of OMC_M)
183	B-77	3	10/26.5	80 and 90
183	B-78	3	20/36.5	80 and 90
184	B-79	4.6	10/26.5	80 and 90
184	B-80	4.6	20/36.5	80 and 90

APPENDIX E3: G4 material/Vibratory hammer/Soft frame				
EFFECT OF VARYING THE MASS OF THE TAMPING FOOT				
TIME TO COMPACT EACH LAYER TO 100% MOD AASHTO DENSITY				
Page number	Figure numbers	Variable		
		Tamping Foot (kg)	Surcharge/Total static mass (kg)	Moisture (% of OMC_M)
185	B-81	3 and 4.6	10/26.5	80
185	B-82	3 and 4.6	10/26.5	90
186	B-83	3 and 4.6	20/36.5	80
186	B-84	3 and 4.6	20/36.5	90

APPENDIX E4: G4 material/Vibratory hammer/Soft frame				
EFFECT OF VARYING THE SURCHARGE/TOTAL STATIC MASS				
TIME TO COMPACT EACH LAYER TO 100% MOD AASHTO DENSITY				
Page number	Figure numbers	Variable		
		Tamping Foot (kg)	Surcharge/Total static mass (kg)	Moisture (% of OMC_M)
187	B-85	3	10/26.5 and 20/36.5	80
187	B-86	3	10/26.5 and 20/36.5	90
188	B-87	4.6	10/26.5 and 20/36.5	80
188	B-88	4.6	10/26.5 and 20/36.5	90

APPENDIX F1: G4 material/Vibratory hammer/Rigid frame				
a. TIME TO COMPACT EACH LAYER TO 100% MOD AASHTO				
b. TIME TO ACHIEVE REFUSAL DENSITY/DENSITY ACHIEVED				
Page number	Figure numbers	Variable		
		Tamping Foot (kg)	Surcharge/Total static mass (kg)	Moisture (% of OMC_M)
189	B-89 and B-90	3	5/26.5	80
190	B-91 and B-92	4.6	5/26.5	80
191	B-93 and B-94	3	15/36.5	80
192	B-95 and B-96	4.6	15/36.5	80
193	B-97 and B-98	3	5/26.5	90
194	B-99 and B-100	4.6	5/26.5	90
195	B-101 and B-102	3	15/36.5	90
196	B-103 and B-104	4.6	15/36.5	90

APPENDIX F2: G4 material/Vibratory hammer/Rigid frame				
EFFECT OF VARYING THE MOISTURE CONTENT				
TIME TO COMPACT EACH LAYER TO 100% MOD AASHTO DENSITY				
Page number	Figure numbers	Variable		
		Tamping Foot (kg)	Surcharge/Total static mass (kg)	Moisture (% of OMC_M)
197	B-105	3	5/26.5	80 and 90
197	B-106	3	15/36.5	80 and 90
198	B-107	4.6	5/26.5	80 and 90
198	B-108	4.6	15/36.5	80 and 90

APPENDIX F3: G4 material/Vibratory hammer/Rigid frame				
EFFECT OF VARYING THE MASS OF THE TAMPING FOOT				
TIME TO COMPACT EACH LAYER TO 100% MOD AASHTO DENSITY				
Page number	Figure numbers	Variable		
		Tamping Foot (kg)	Surcharge/Total static mass (kg)	Moisture (% of OMC_M)
199	B-109	3 and 4.6	5/26.5	80
199	B-110	3 and 4.6	5/26.5	90
200	B-111	3 and 4.6	15/36.5	80
200	B-112	3 and 4.6	15/36.5	90

APPENDIX F4: G4 material/Vibratory hammer/Rigid frame				
EFFECT OF VARYING THE SURCHARGE/TOTAL STATIC MASS				
TIME TO COMPACT EACH LAYER TO 100% MOD AASHTO DENSITY				
Page number	Figure numbers	Variable		
		Tamping Foot (kg)	Surcharge/Total static mass (kg)	Moisture (% of OMC_M)
201	B-113	3	5/26.5 and 15/36.5	80
201	B-114	3	5/26.5 and 15/36.5	90
202	B-115	4.6	5/26.5 and 15/36.5	80
202	B-116	4.6	5/26.5 and 15/36.5	90

APPENDIX G1: G7 material/Vibratory hammer/Soft frame				
a. TIME TO COMPACT EACH LAYER TO 100% MOD AASHTO				
b. TIME TO ACHIEVE REFUSAL DENSITY/DENSITY ACHIEVED				
Page number	Figure numbers	Variable		
		Tamping Foot (kg)	Surcharge/Total static mass (kg)	Moisture (% of OMC_M)
203	B-117 and B-118	3	10/26.5	80
204	B-119 and B-120	4.6	10/26.5	80
205	B-121 and B-122	3	20/36.5	80
206	B-123 and B-124	4.6	20/36.5	80
207	B-125 and B-126	3	10/26.5	90
208	B-127 and B-128	4.6	10/26.5	90
209	B-129 and B-130	3	20/36.5	90
210	B-131 and B-132	4.6	20/36.6	90

APPENDIX G2: G7 material/Vibratory hammer/Soft frame				
EFFECT OF VARYING THE MOISTURE CONTENT				
TIME TO COMPACT EACH LAYER TO 100% MOD AASHTO DENSITY				
Page number	Figure numbers	Variable		
		Tamping Foot (kg)	Surcharge/Total static mass (kg)	Moisture (% of OMC_M)
211	B-133	3	10/26.5	80 and 90
211	B-134	3	20/36.5	80 and 90
212	B-135	4.6	10/26.5	80 and 90
212	B-136	4.6	20/36.5	80 and 90

APPENDIX G3: G7 material/Vibratory hammer/Soft frame				
EFFECT OF VARYING THE MASS OF THE TAMPING FOOT				
TIME TO COMPACT EACH LAYER TO 100% MOD AASHTO DENSITY				
Page number	Figure numbers	Variable		
		Tamping Foot (kg)	Surcharge/Total static mass (kg)	Moisture (% of OMC_M)
213	B-137	3 and 4.6	10/26.5	80
213	138	3 and 4.6	10/26.5	90
214	139	3 and 4.6	20/36.5	80
214	140	3 and 4.6	20/36.5	90

APPENDIX G4: G7 material/Vibratory hammer/Soft frame				
EFFECT OF VARYING THE SURCHARGE/TOTAL STATIC MASS				
TIME TO COMPACT EACH LAYER TO 100% MOD AASHTO DENSITY				
Page number	Figure numbers	Variable		
		Tamping Foot (kg)	Surcharge/Total static mass (kg)	Moisture (% of OMC_M)
215	B-141	3	10/26.5 and 20/36.5	80
215	B-142	3	10/26.5 and 20/36.5	90
216	B-143	4.6	10/26.5 and 20/36.5	80
216	B-144	4.6	10/26.5 and 20/36.5	90

APPENDIX H1: G7 material/Vibratory hammer/Rigid frame				
a. TIME TO COMPACT EACH LAYER TO 100% MOD AASHTO				
b. TIME TO ACHIEVE REFUSAL DENSITY/DENSITY ACHIEVED				
Page number	Figure numbers	Variable		
		Tamping Foot (kg)	Surcharge/Total static mass (kg)	Moisture (% of OMC_M)
217	B-145 and B-146	3	5/26.5	80
218	B-147 and B-148	4.6	5/26.5	80
219	B-149 and B-150	3	15/36.5	80
220	B-151 and B-152	4.6	15/36.5	80
221	B-153 and B-154	3	5/26.5	90
222	B-155 and B-156	4.6	5/26.5	90
223	B-157 and B-158	3	15/36.5	90
224	B-159 and B-160	4.6	15/36.5	90

APPENDIX H2: G7 material/Vibratory hammer/Rigid frame					
EFFECT OF VARYING THE FREQUENCY OF VIBRATION					
a. TIME TO COMPACT EACH LAYER TO 100% MOD AASHTO					
b. TIME TO ACHIEVE REFUSAL DENSITY/DENSITY ACHIEVED					
Page number	Figure numbers	Variable			
		Frequency (Hz)	Tamping Foot (kg)	Surcharge/Total static mass (kg)	Moisture (% of OMC_M)
225	B-161 and B-162	25.67	3	5/26.5	90
226	B-163 and B-164	19.67	3	5/26.5	90

APPENDIX H3: G7 material/Vibratory hammer/Rigid frame				
EFFECT OF VARYING THE MOISTURE CONTENT				
TIME TO COMPACT EACH LAYER TO 100% MOD AASHTO DENSITY				
Page number	Figure numbers	Variable		
		Tamping Foot (kg)	Surcharge/Total static mass (kg)	Moisture (% of OMC_M)
227	B-165	3	5/26.5	80 and 90
227	B-166	3	15/36.5	80 and 90
228	B-167	4.6	5/26.5	80 and 90
228	B-168	4.6	15/36.5	80 and 90

APPENDIX H4: G7 material/Vibratory hammer/Rigid frame				
EFFECT OF VARYING THE MASS OF THE TAMPING FOOT				
TIME TO COMPACT EACH LAYER TO 100% MOD AASHTO DENSITY				
Page number	Figure numbers	Variable		
		Tamping Foot (kg)	Surcharge/Total static mass (kg)	Moisture (% of OMC_M)
229	B-169	3 and 4.6	5/26.5	80
229	B-170	3 and 4.6	5/26.5	90
230	B-171	3 and 4.6	15/36.5	80
230	B-172	3 and 4.6	15/36.5	90

APPENDIX H5: G7 material/Vibratory hammer/Rigid frame				
EFFECT OF VARYING THE SURCHARGE/TOTAL STATIC MASS				
TIME TO COMPACT EACH LAYER TO 100% MOD AASHTO DENSITY				
Page number	Figure numbers	Variable		
		Tamping Foot (kg)	Surcharge/Total static mass (kg)	Moisture (% of OMC_M)
231	B-173	3	5/26.5 and 15/36.5	80
231	B-174	3	5/26.5 and 15/36.5	90
232	B-175	4.6	5/26.5 and 15/36.5	80
232	B-176	4.6	5/26.5 and 15/36.5	90

APPENDIX J: Vibratory table compaction				
TIME TO COMPACT EACH LAYER TO 100% MOD AASHTO DENSITY				
Page number	Figure numbers	Variable		
		Material	Surcharge (kg)	Moisture (% of OMC_M)
233	B-177	G3	50	90
233	B-178	G4	50	90
234	B-179	G5	50	90

APPENDIX K: RA material/Vibratory hammer/Rigid frame				
a. TIME TO COMPACT EACH LAYER TO 100% MOD AASHTO				
b. TIME TO ACHIEVE REFUSAL DENSITY/DENSITY ACHIEVED				
Page number	Figure numbers	Variable		
		Tamping Foot (kg)	Surcharge/Total static mass (kg)	Moisture (% of OMC_M)
235	B-180 and B-181	3	5/26.5	90
236	B-182 and B-183	4.6	5/26.5	90

APPENDIX C: Test results for G3 material/ vibratory hammer compaction/soft frame

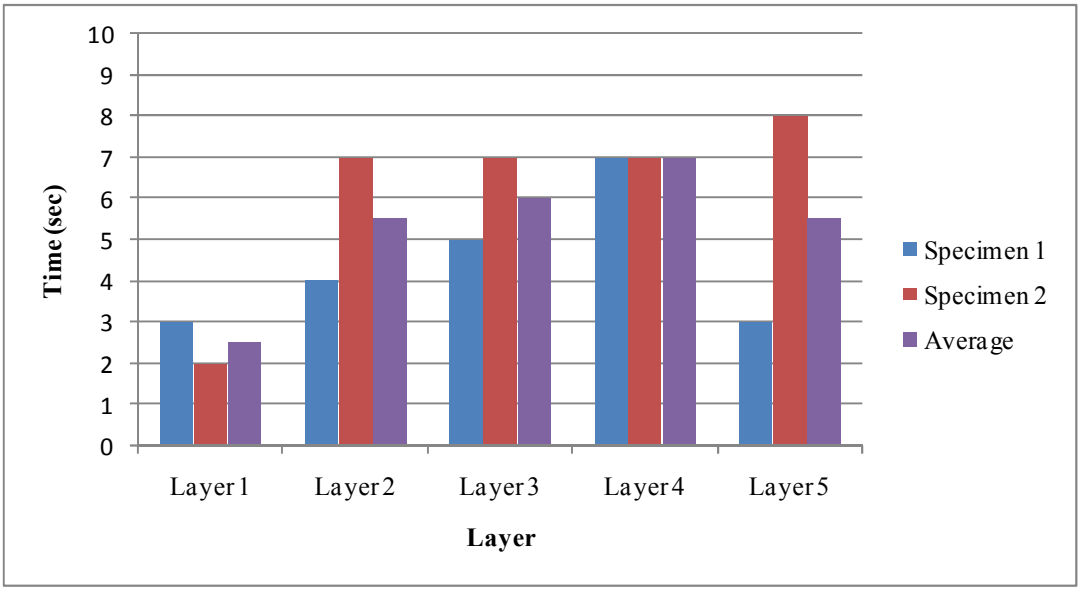

Figure B - 1: Compaction time for 3kg Tamper, 10kg Surcharge and 80% of OMC – G3SFR

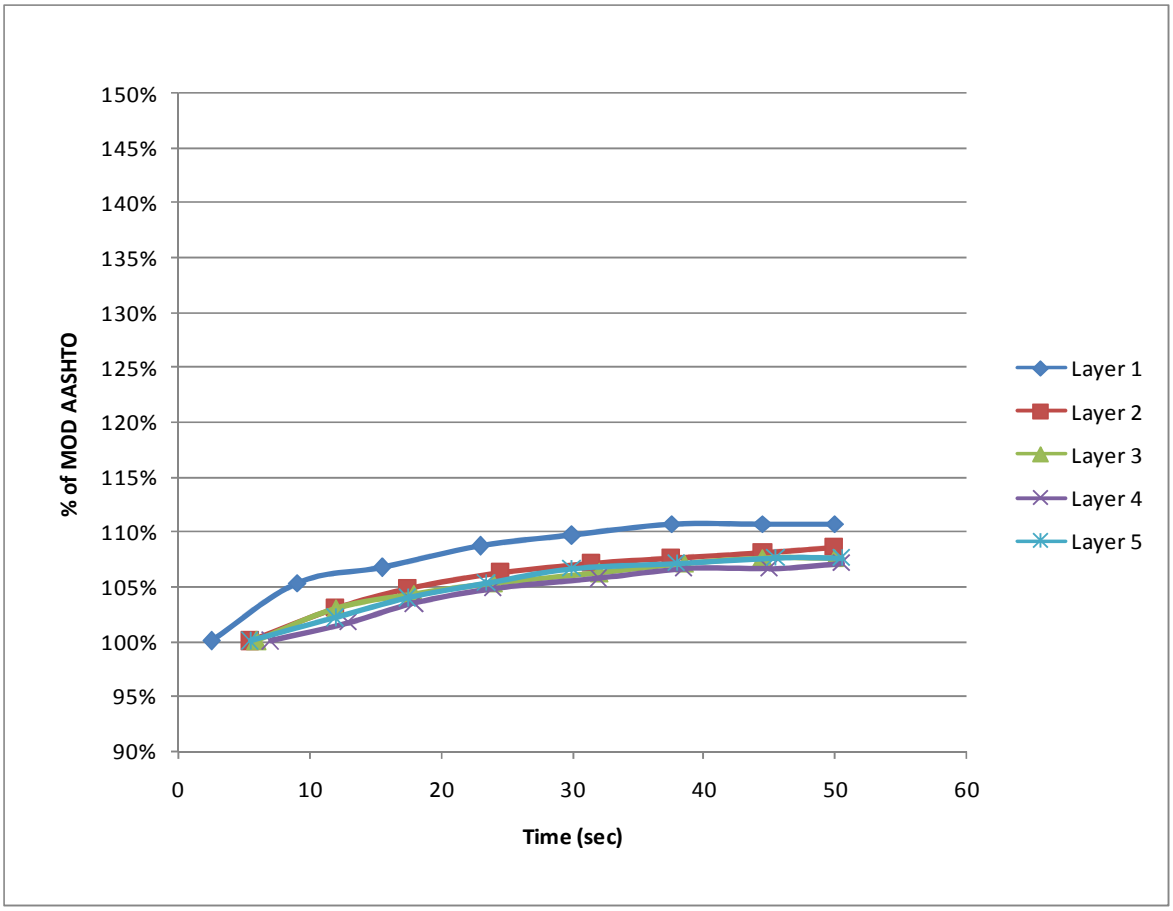

Figure B - 2: Compaction Profile for 3kg Tamper, 10kg Surcharge and 80% OMC – G3SFR

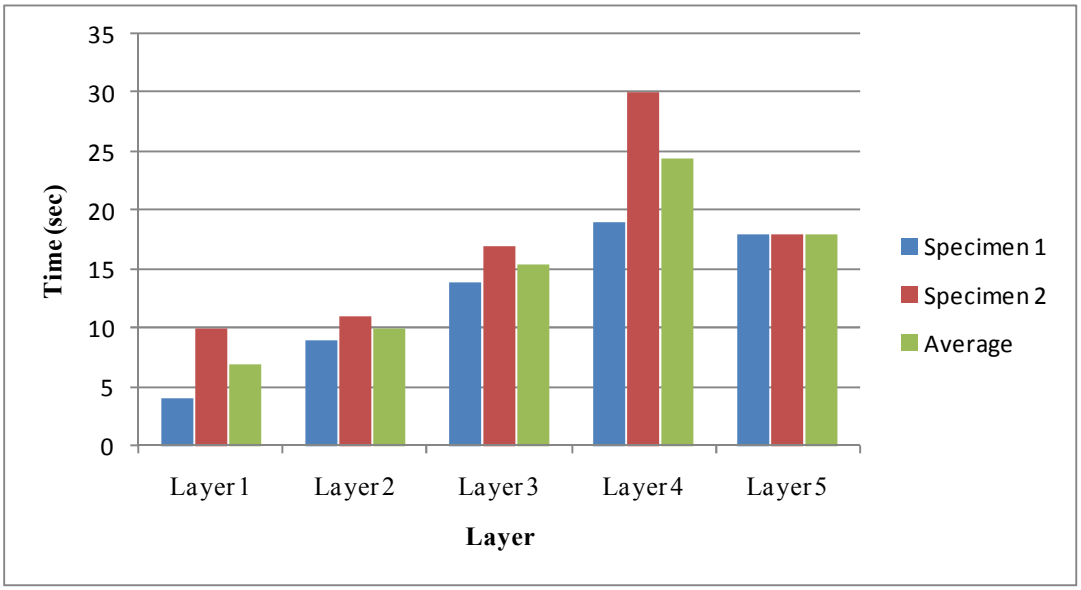

Figure B - 3: Compaction time for 4.6kg Tamper, 10kg Surcharge and 80% OMC – G3SFR

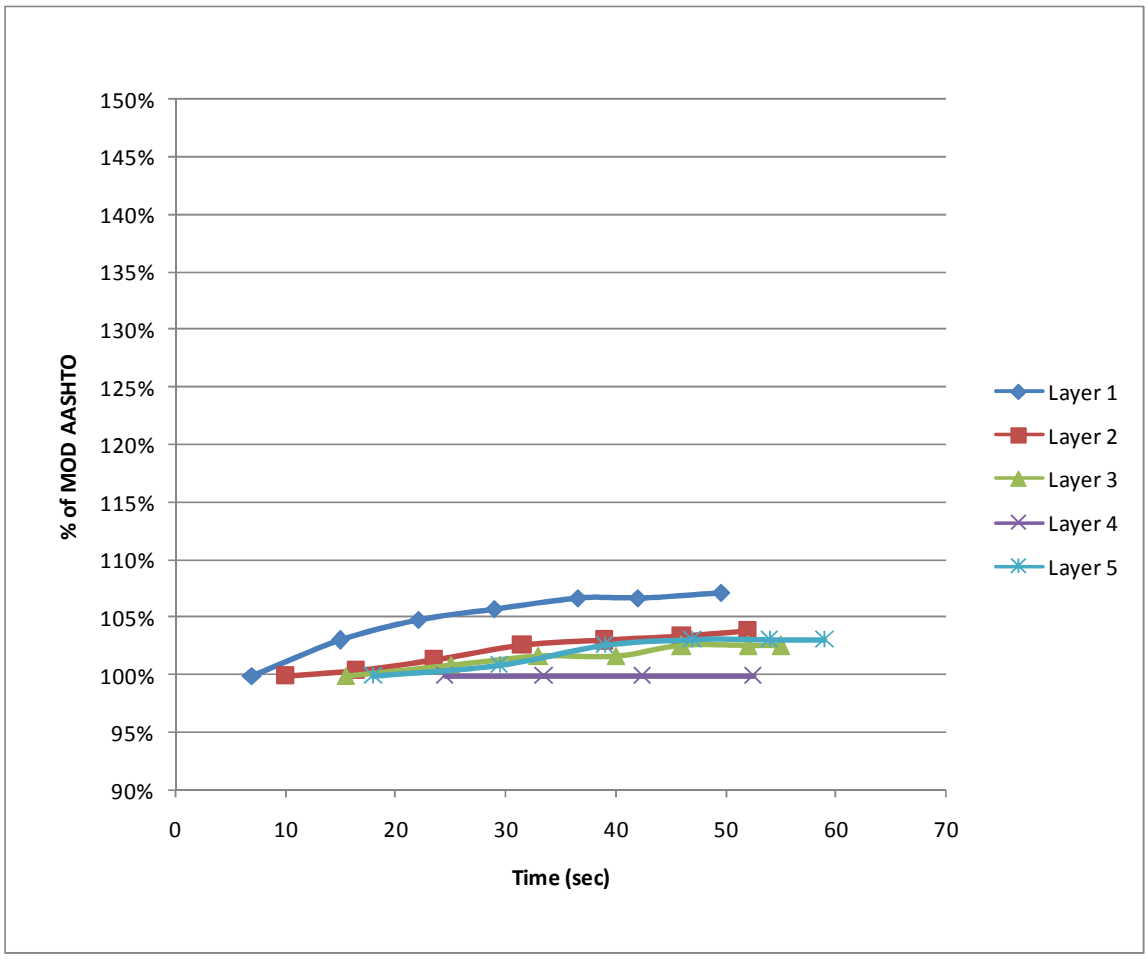

Figure B - 4: Compaction Profile for 4.6kg Tamper, 10kg Surcharge and 80% OMC – G3SFR

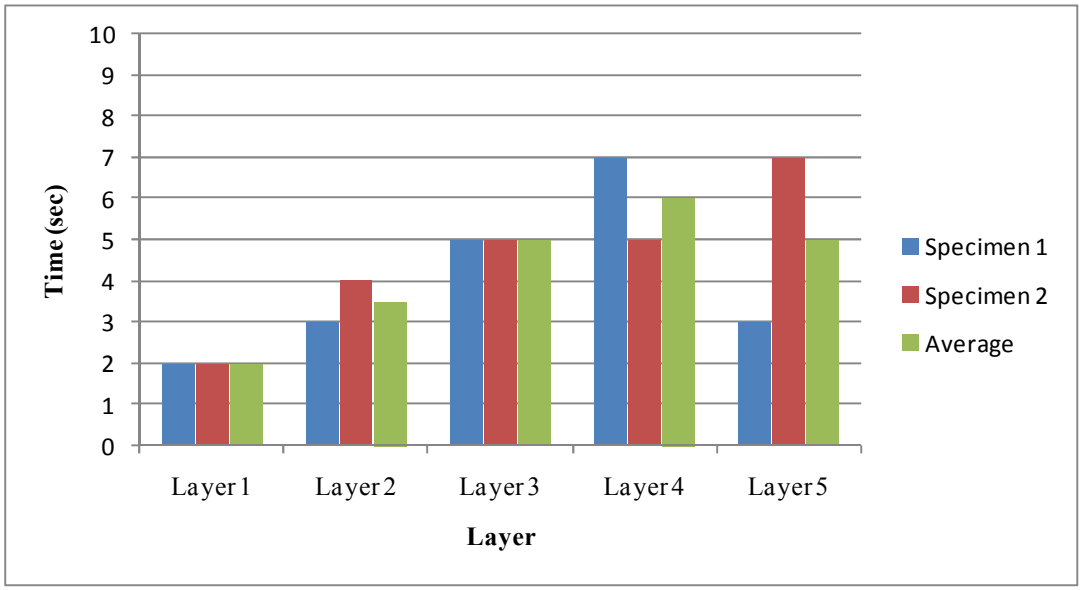

Figure B - 5: Compaction Time for 3kg Tamper, 20kg Surcharge and 80% Moisture – G3SFR

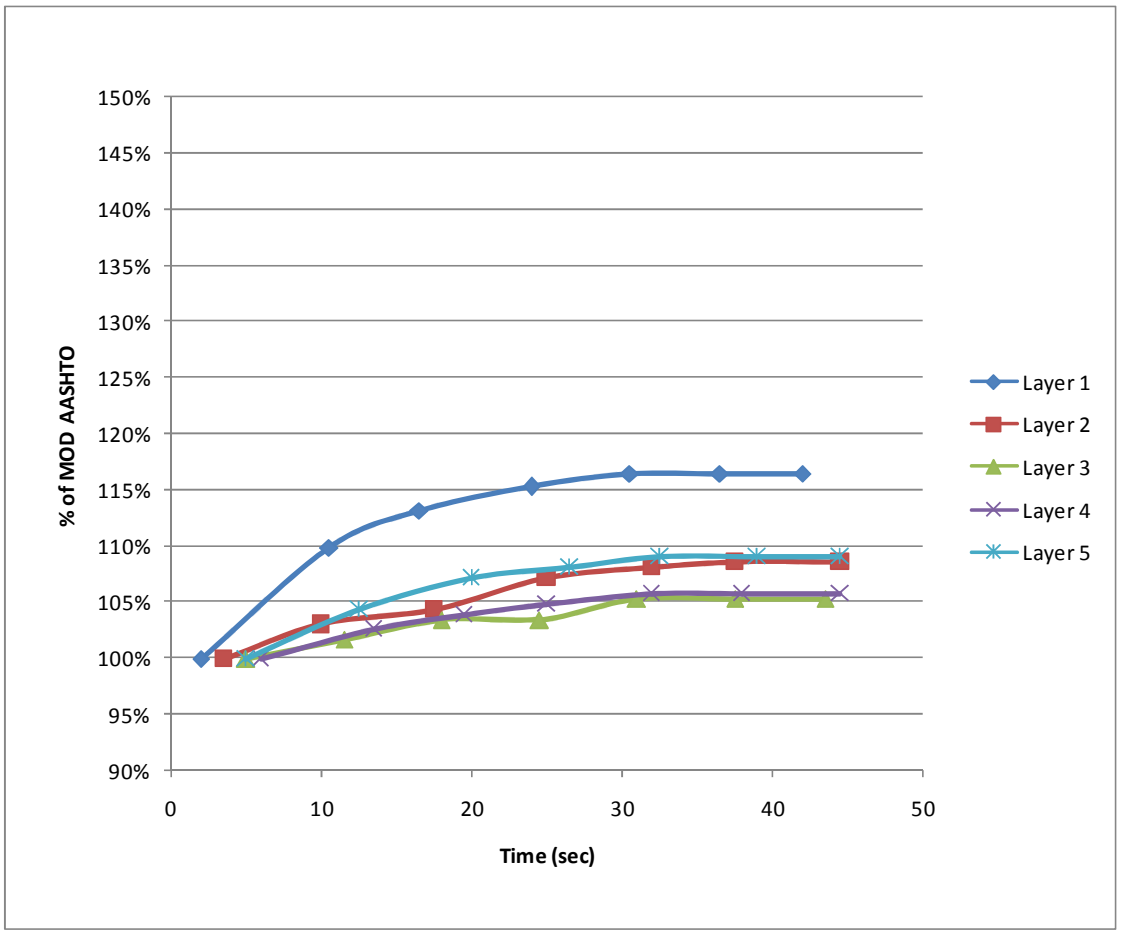

Figure B - 6: Compaction Profile for 3kg Tamper, 20kg Surcharge and 80% OMC – G3SFR

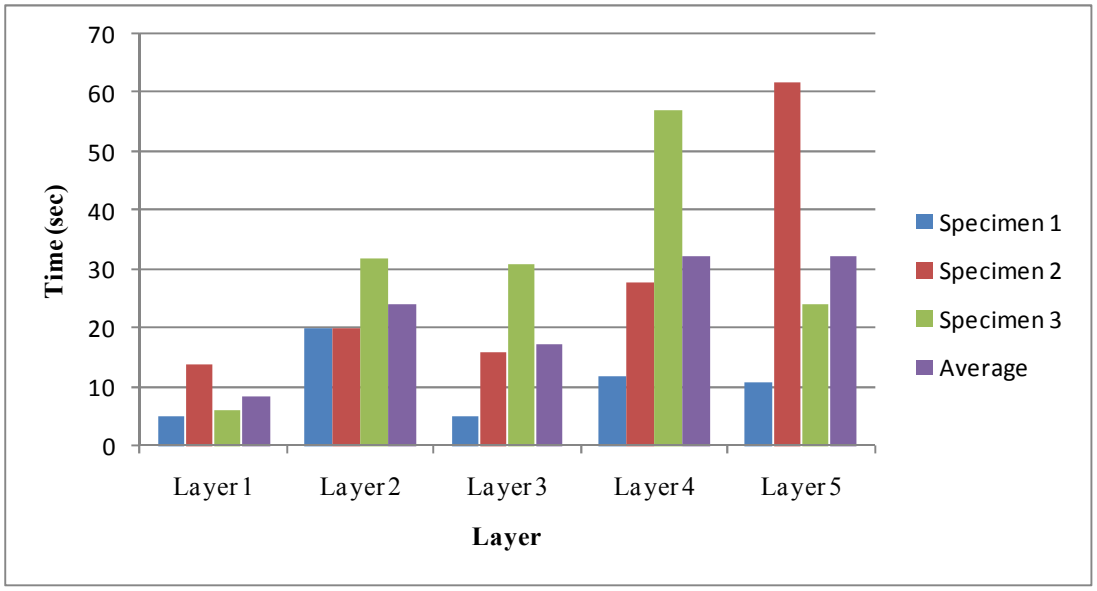

Figure B - 7: Compaction Time for 4.6kg Tamper, 20kg Surcharge and 80% OMC – G3SFR

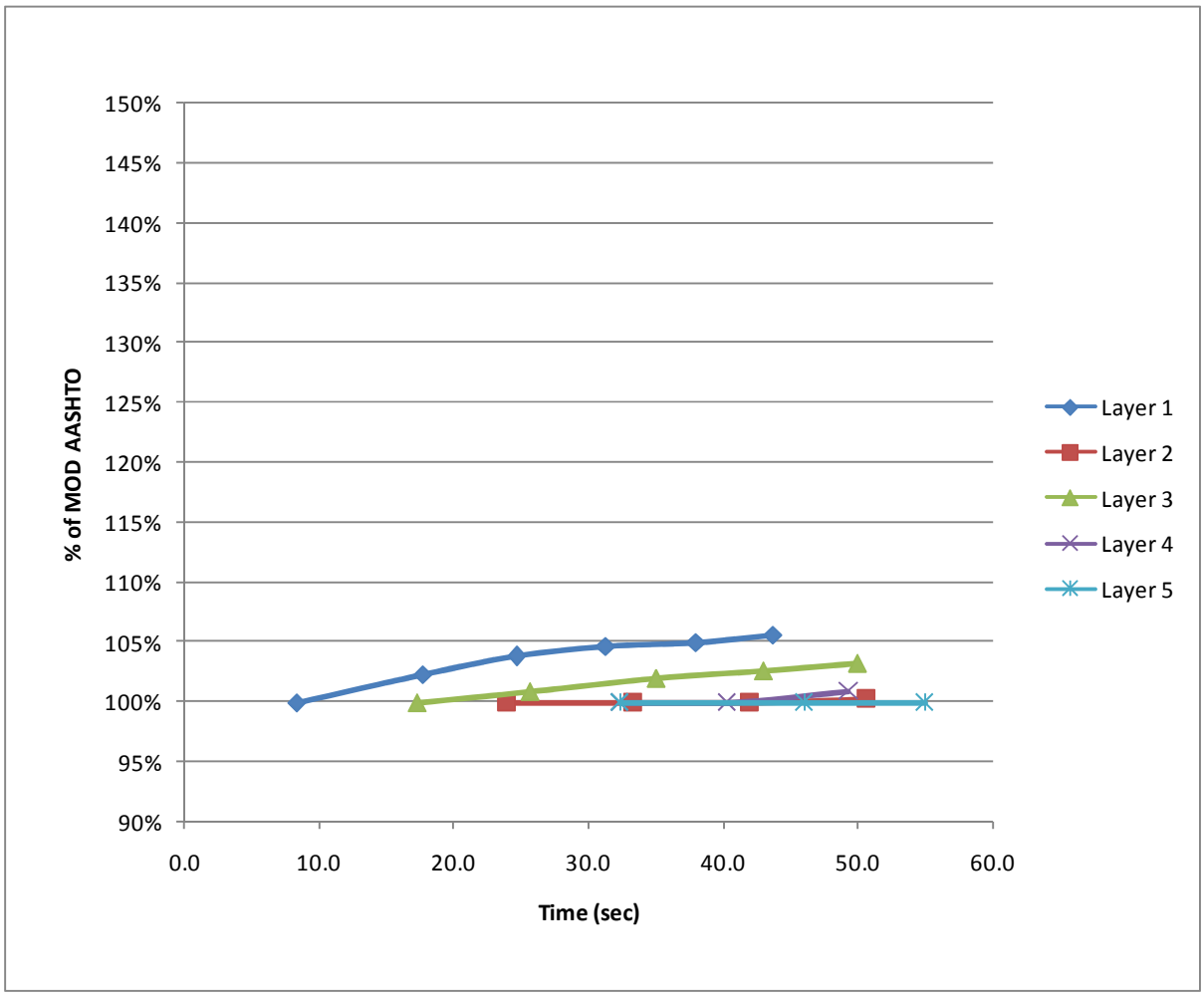

Figure B - 8: Compaction Profile for 4.6kg Tamper, 20kg Surcharge and 80% OMC – G3SFR

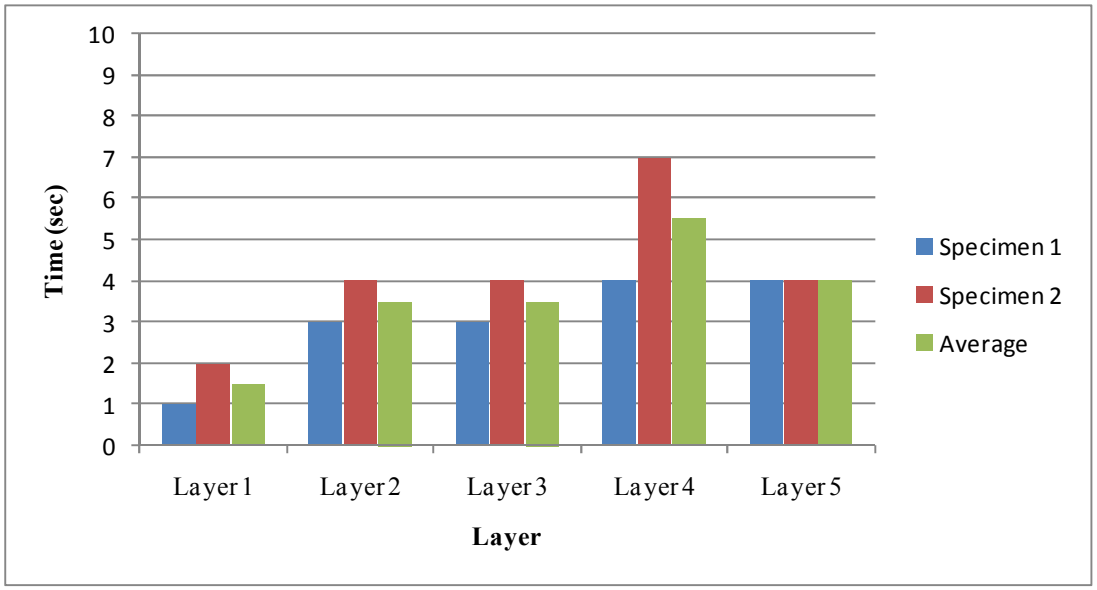

Figure B - 9: Compaction time for 3kg Tamper, 10kg Surcharge and 90% OMC – G3SFR

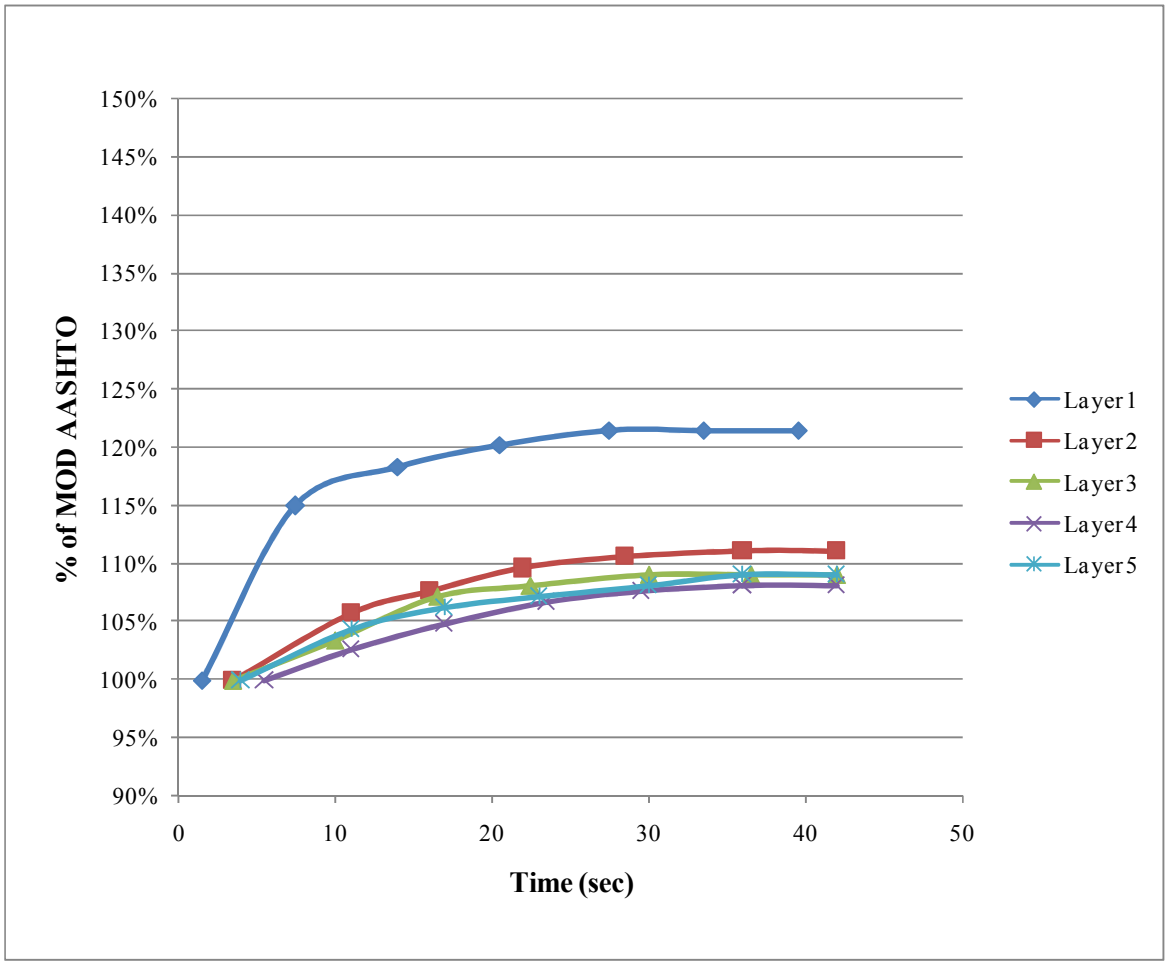

Figure B - 10: Compaction Profile for 3kg Tamper, 10kg Surcharge and 90% OMC – G3SFR

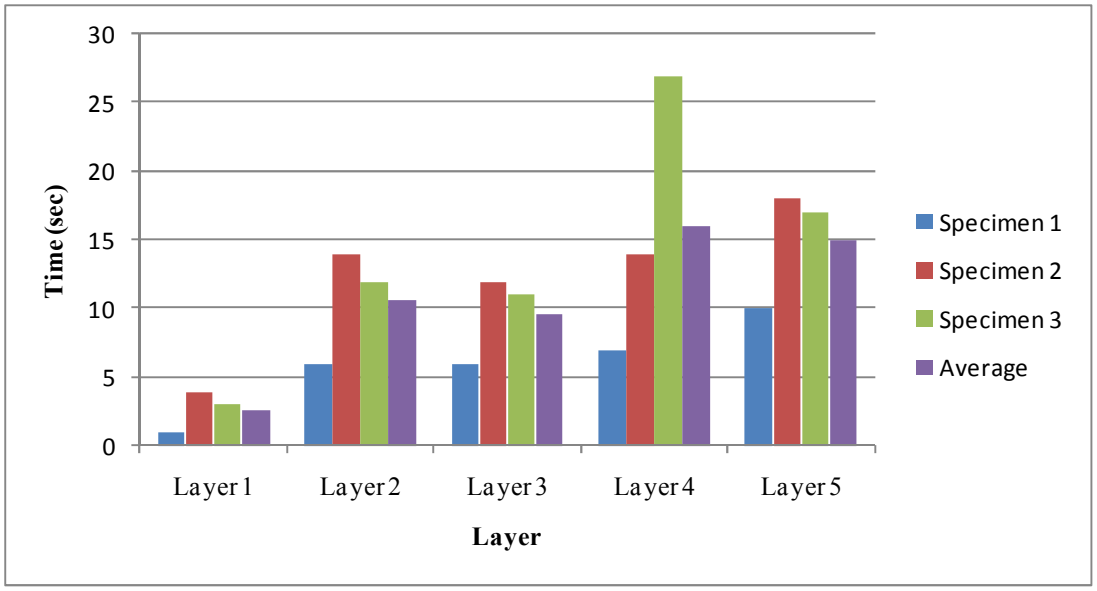

Figure B - 11: Compaction Time for 4.6kg Tamper, 10kg Surcharge and 90% OMC – G3SFR

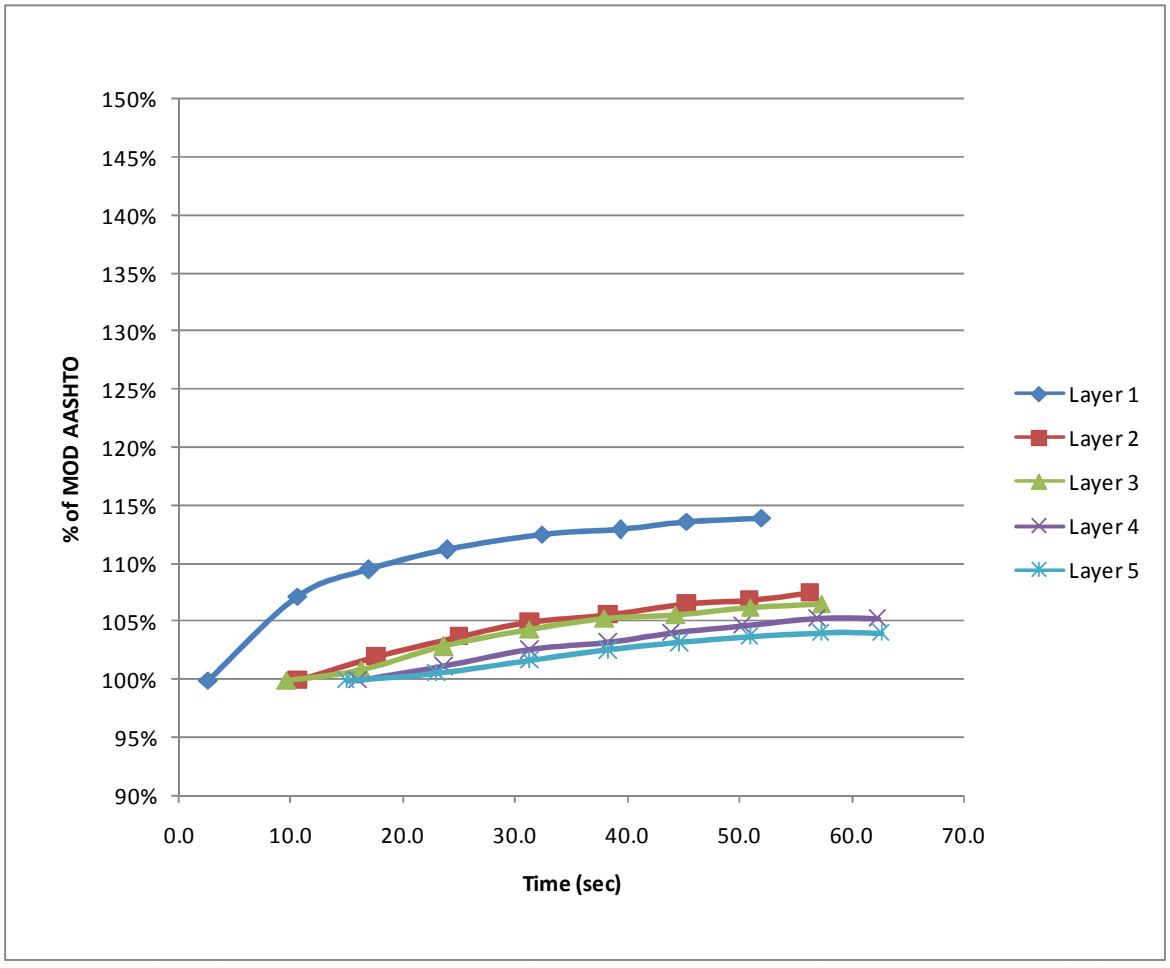

Figure B - 12: Compaction Profile for 4.6kg Tamper, 10kg Surcharge and 90% OMC – G3SFR

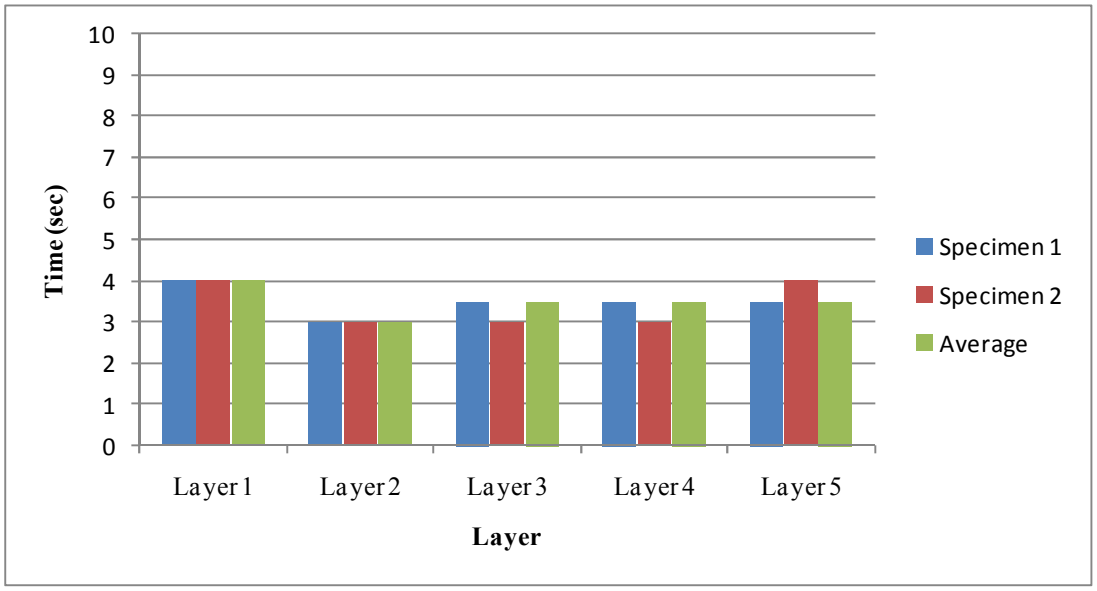

Figure B - 13: Compaction Time for 3kg Tamper, 20kg Surcharge and 90% OMC – G3SFR

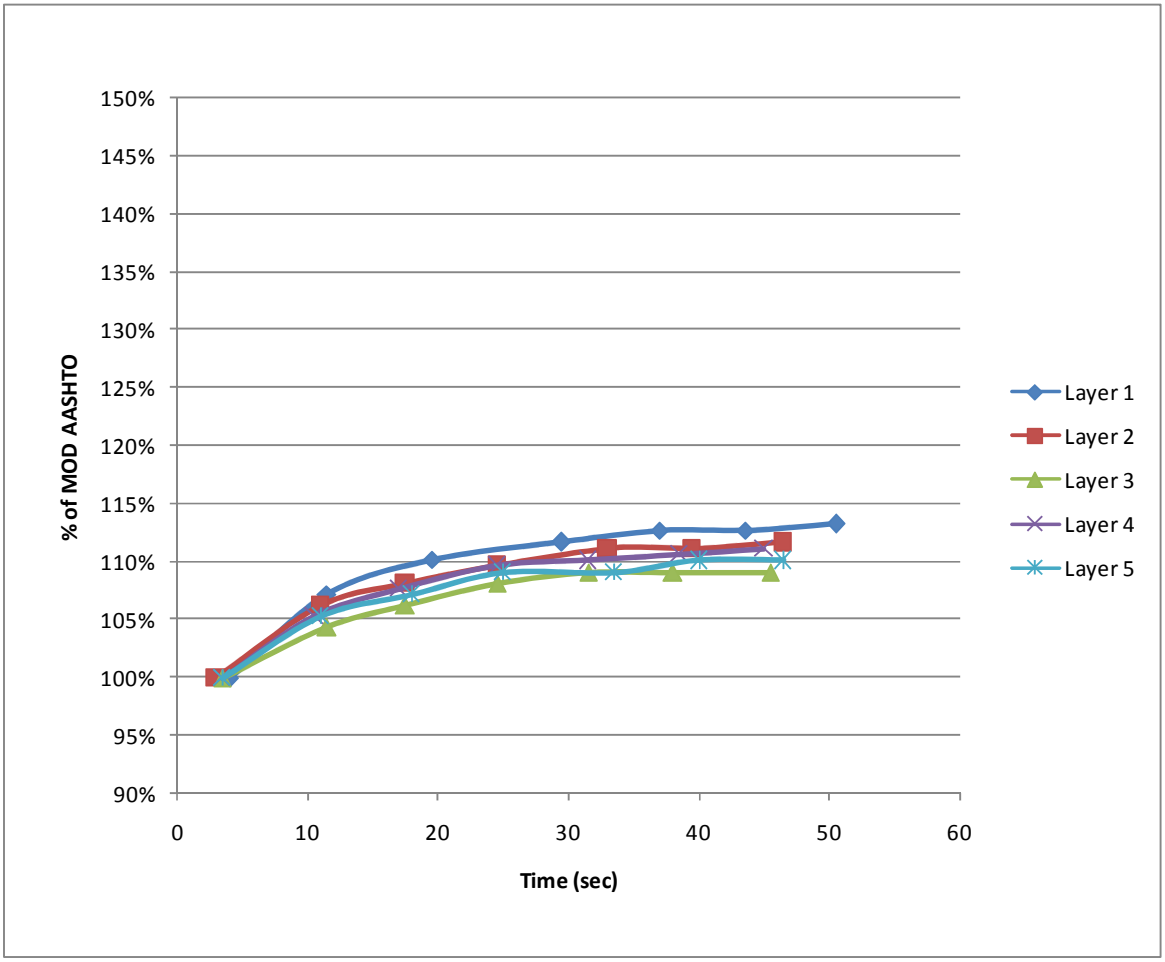

Figure B - 14: Compaction Profile for 3kg Tamper, 20kg Surcharge and 90% OMC – G3SFR

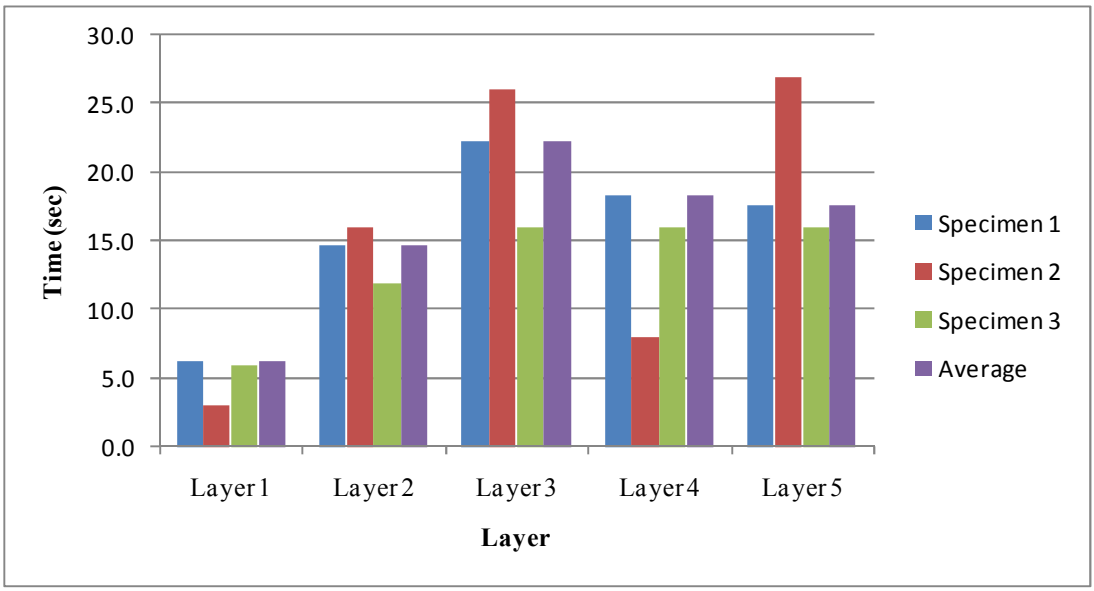

Figure B - 15: Compaction Time for 4.6kg Tamper, 20kg Surcharge and 90% OMC – G3SFR

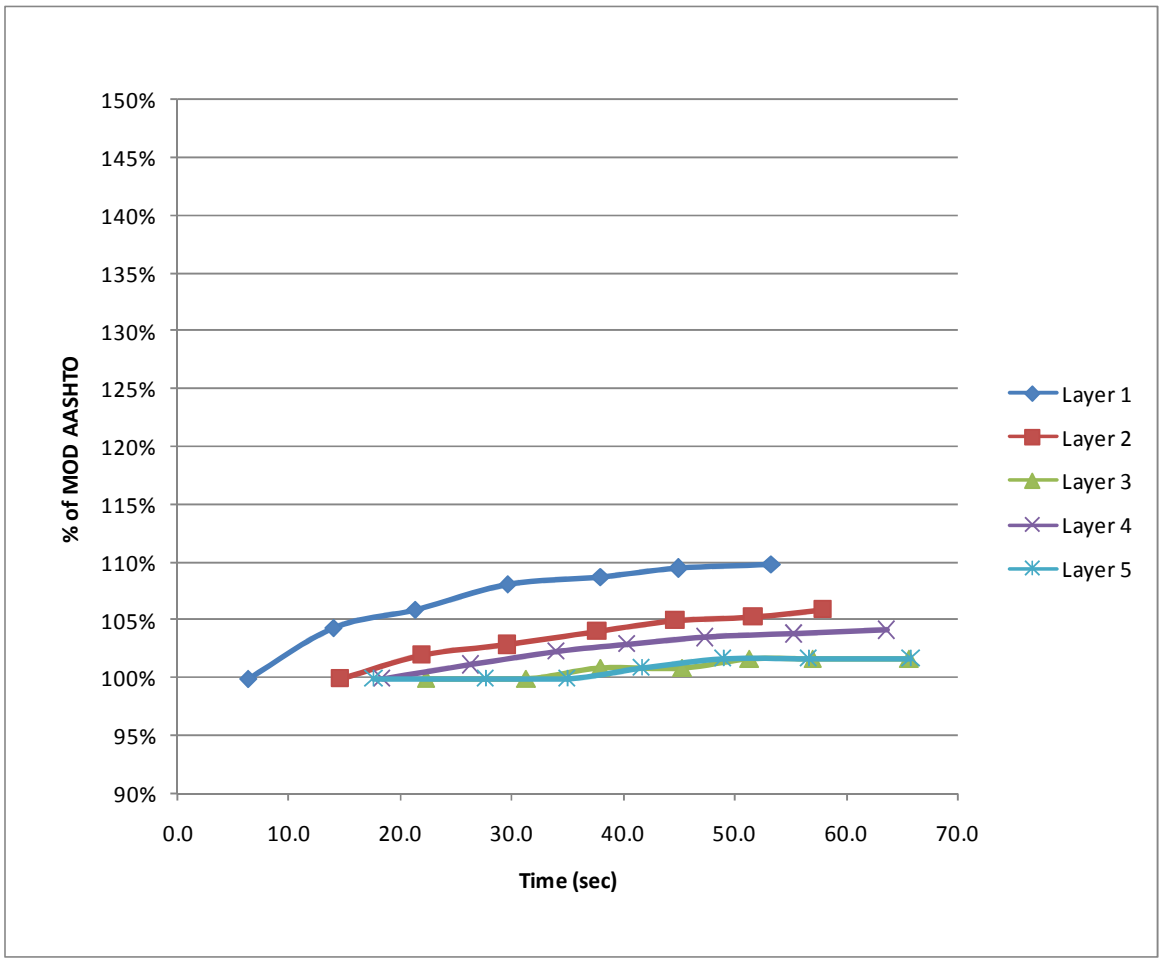

Figure B - 16: Compaction Profile for 4.6kg Tamper, 20kg Surcharge and 90% OMC – G3SFR

Effect of Moisture on Compaction Time - G3 Material (SFR)

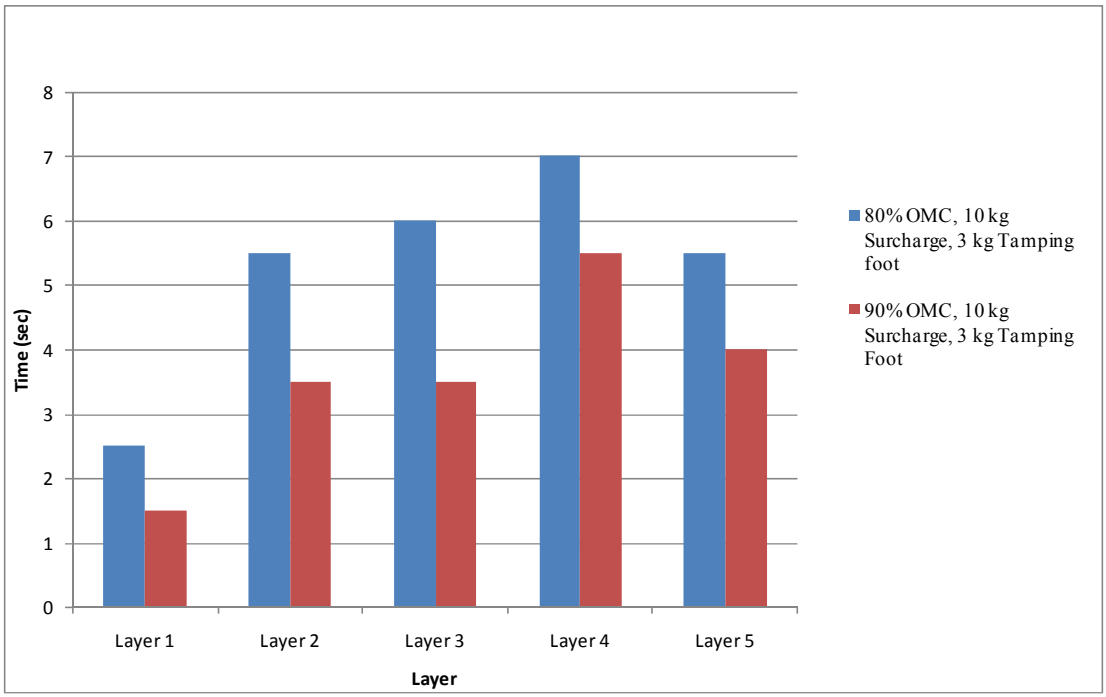

Figure B - 17: Effect of Moisture on Compaction Time at 10kg Surcharge and 3kg Tamper – G3SFR

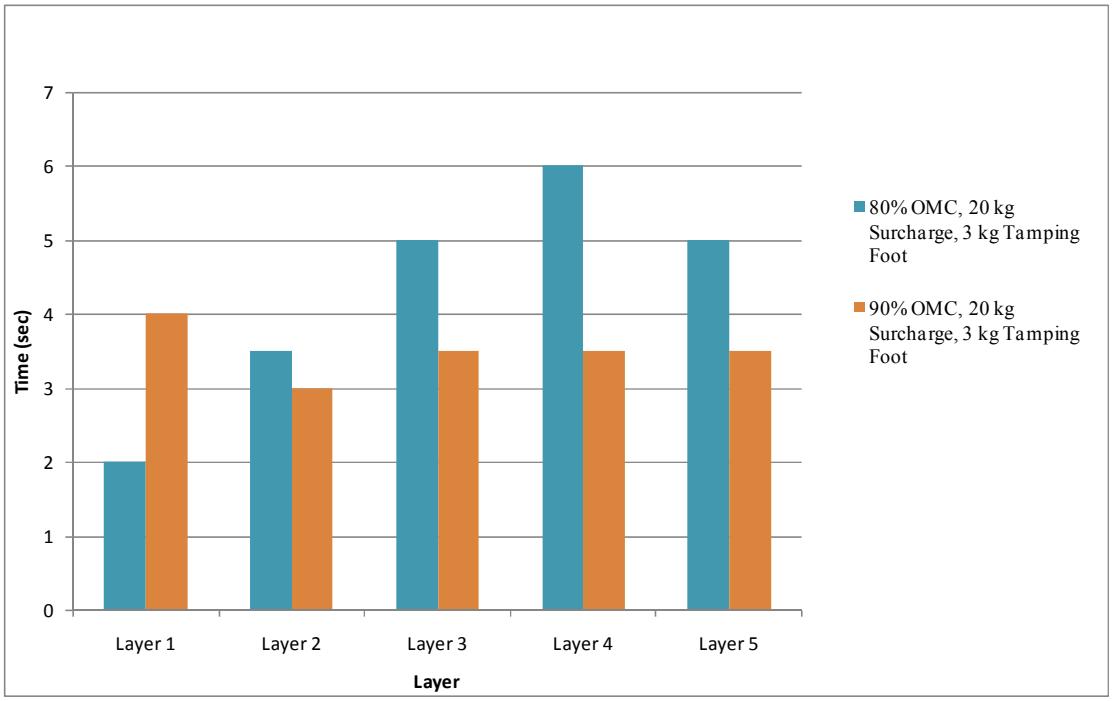

Figure B - 18: Effect of Moisture on Compaction time at 20kg Surcharge and 3kg Tamper – G3SFR

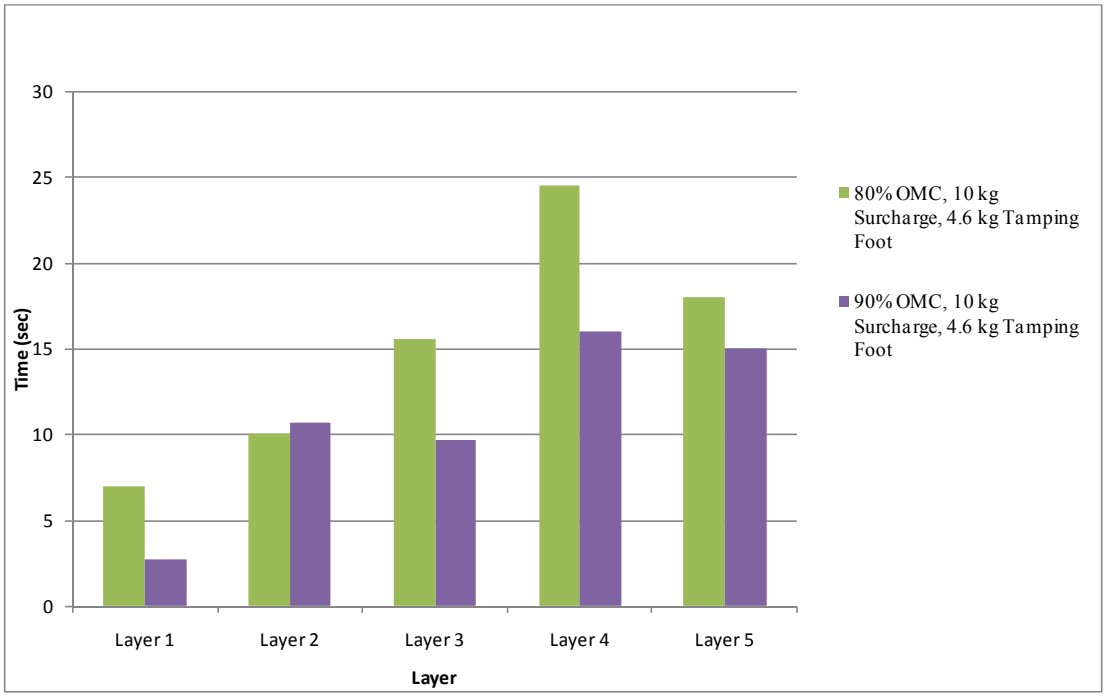

Figure B - 19: Effect of Moisture on Compaction Time at 10kg Surcharge and 4.6kg Tamper – G3SFR

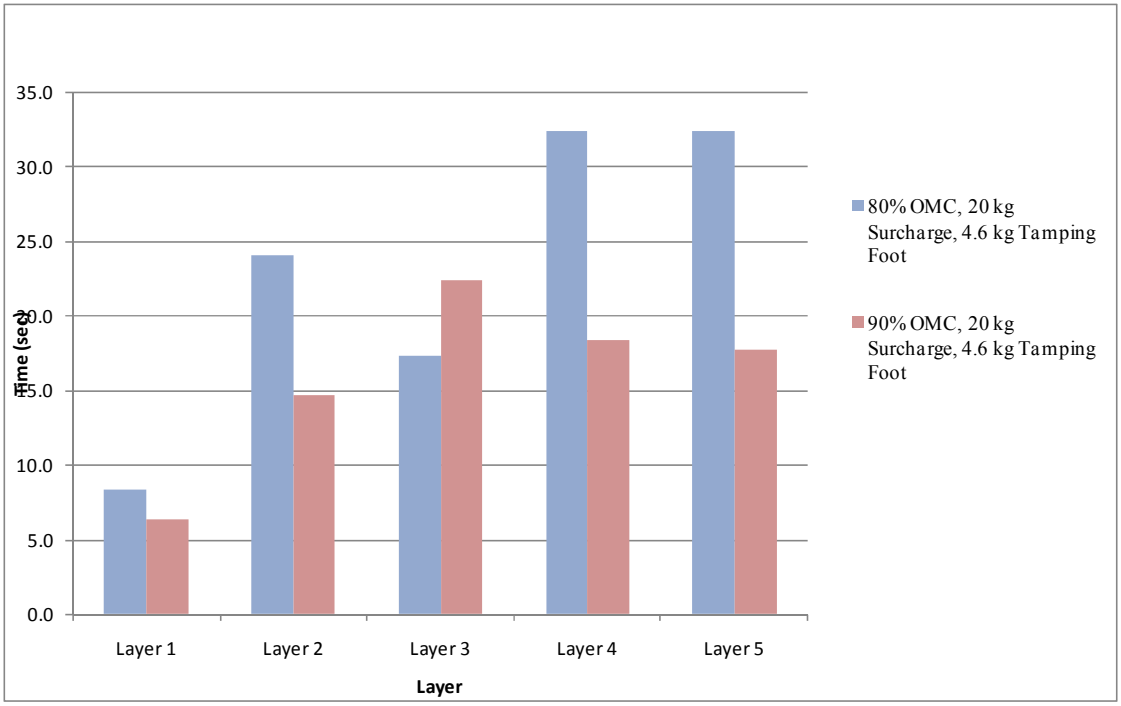

Figure B - 20: Effect of Moisture on Compaction Time at 20kg Surcharge and 4.6kg Tamper – G3SFR

Effect of Tamping Foot on Compaction Time – G3 Material (SFR)

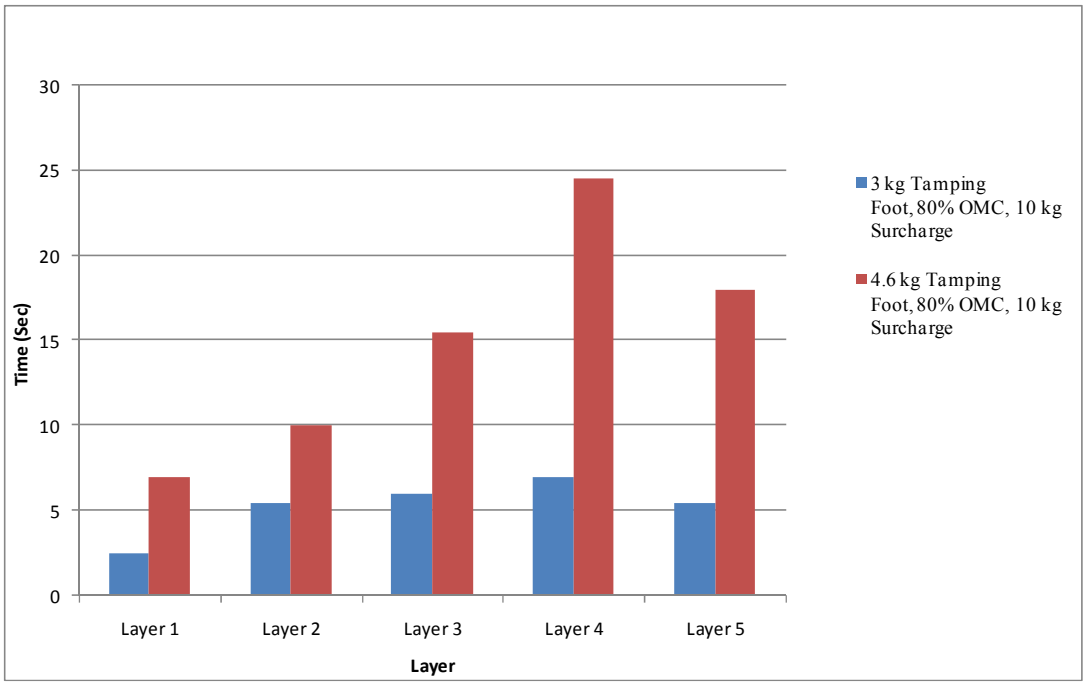

Figure B - 21: Effect of Tamper on Compaction Time at 80% OMC and 10kg Surcharge – G3SFR

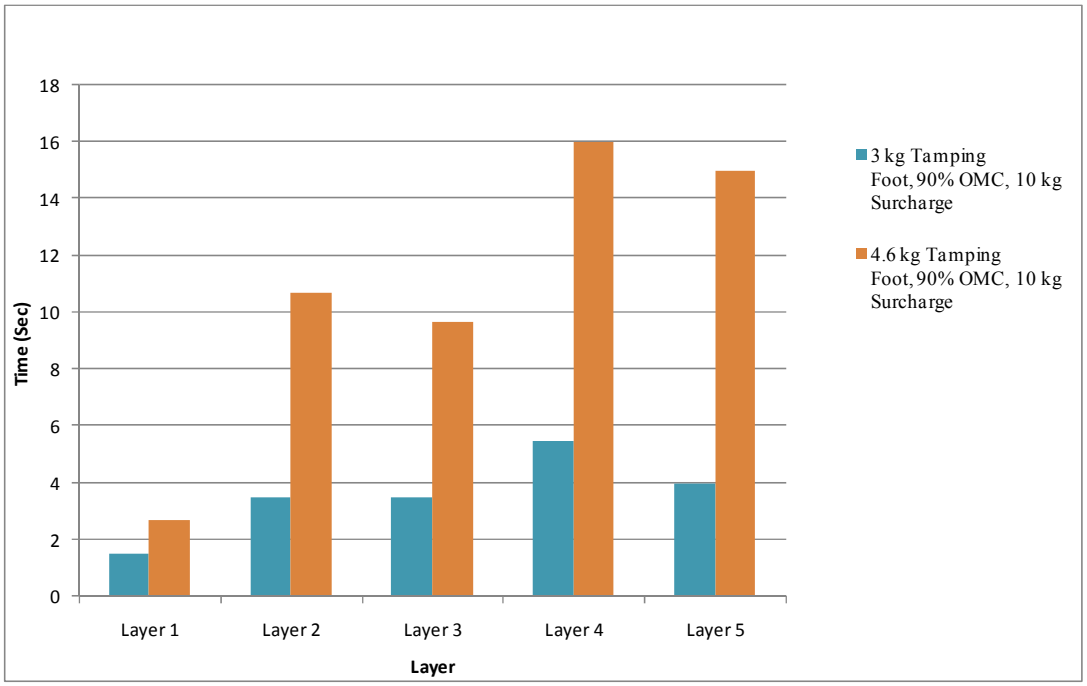

Figure B - 22: Effect of Tamper on Compaction Time at 90% OMC and 10kg Surcharge – G3SFR

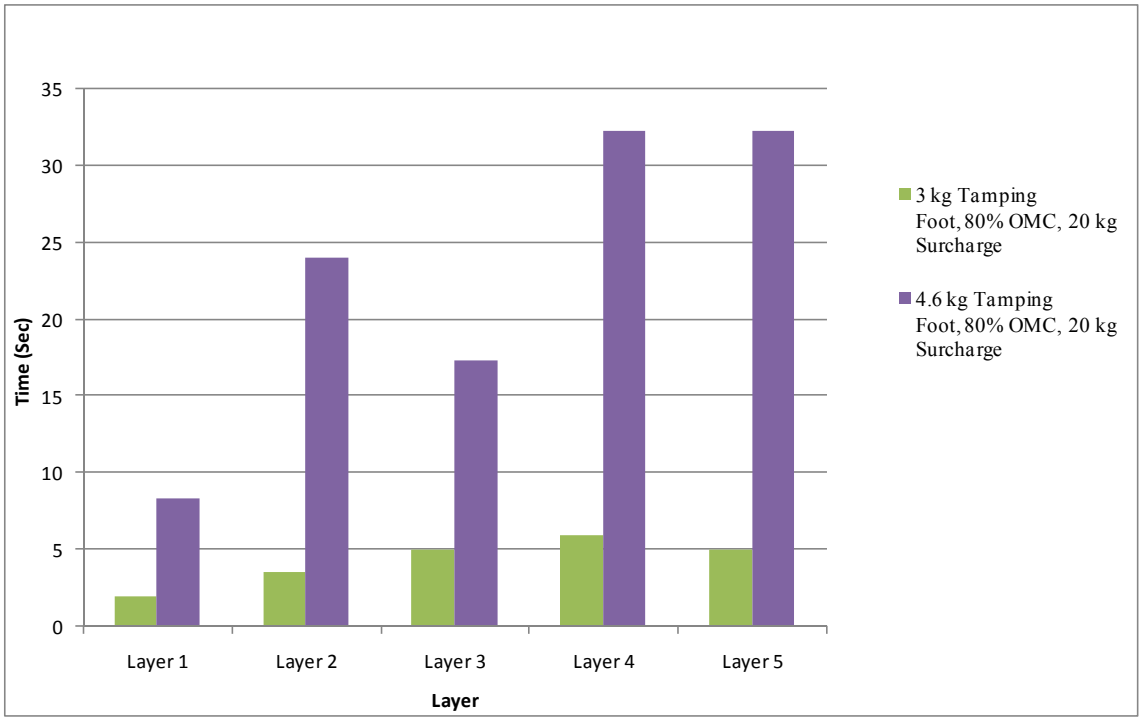

Figure B - 23: Effect of Tamper on Compaction Time at 80% OMC and 20kg Surcharge – G3SFR

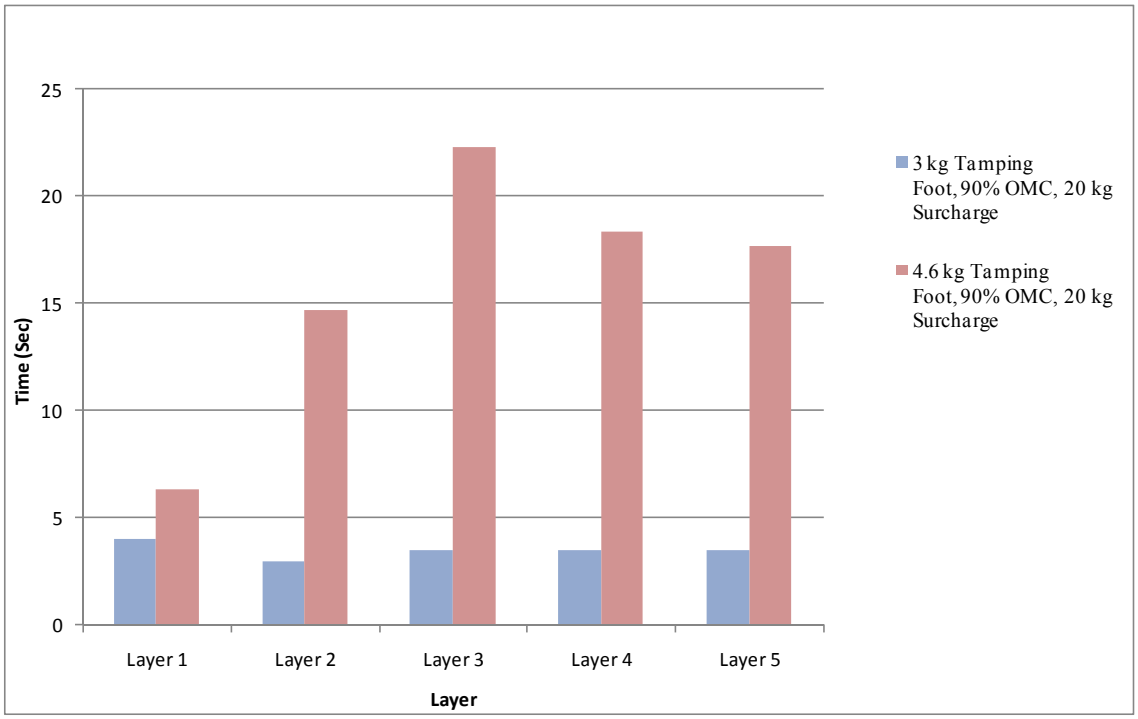

Figure B - 24: Effect of Tamper on Compaction Time at 90% OMC and 20kg Surcharge – G3SFR

Effect of Surcharge Load on Compaction Time – G3 Material (SFR)

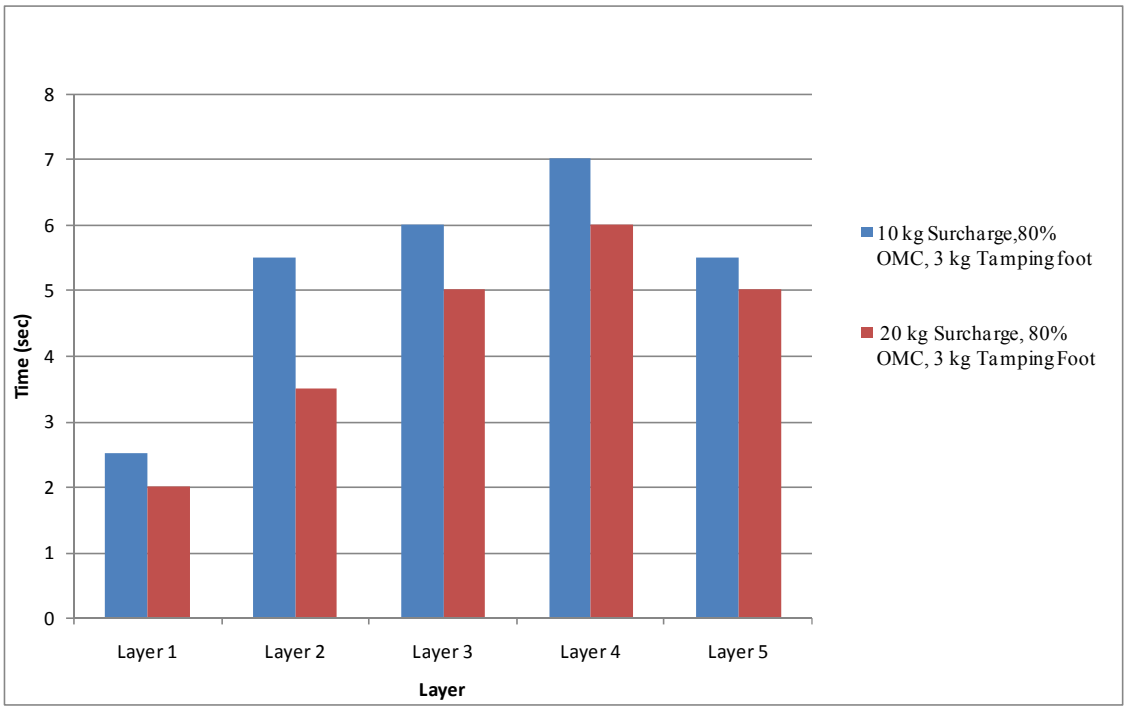

Figure B - 25: Effect of Surcharge on Compaction Time at 80% OMC and 3kg Tamper – G3SFR

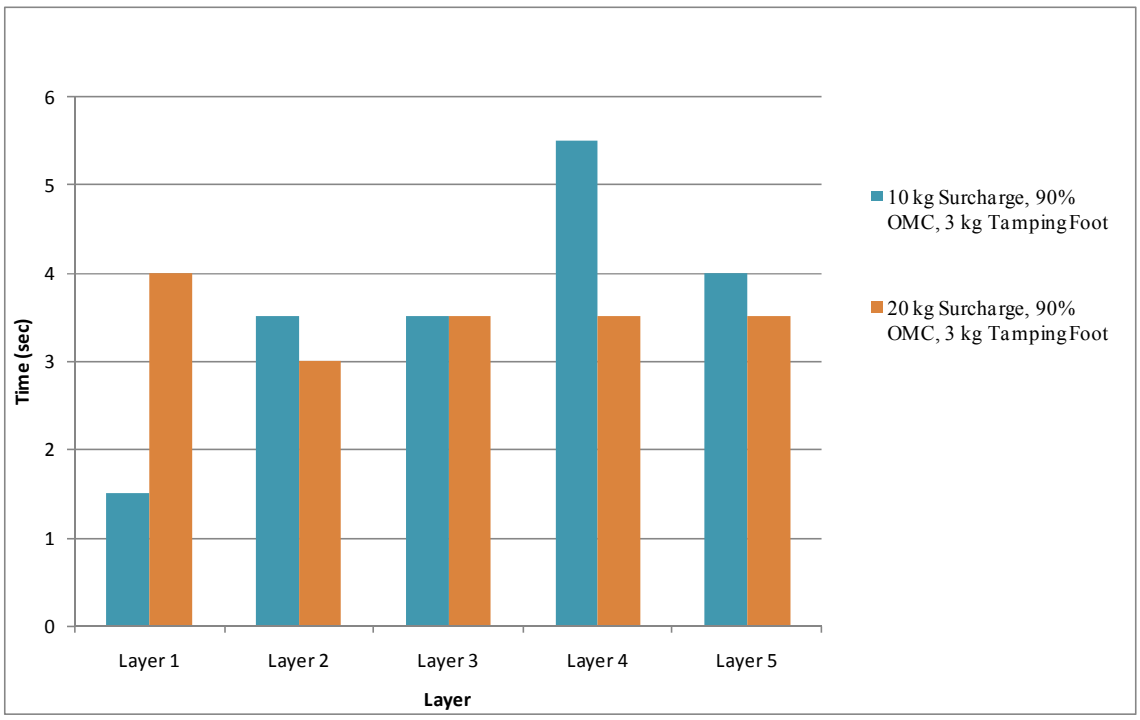

Figure B - 26: Effect of Surcharge on Compaction Time at 90% OMC and 3kg Tamper – G3SFR

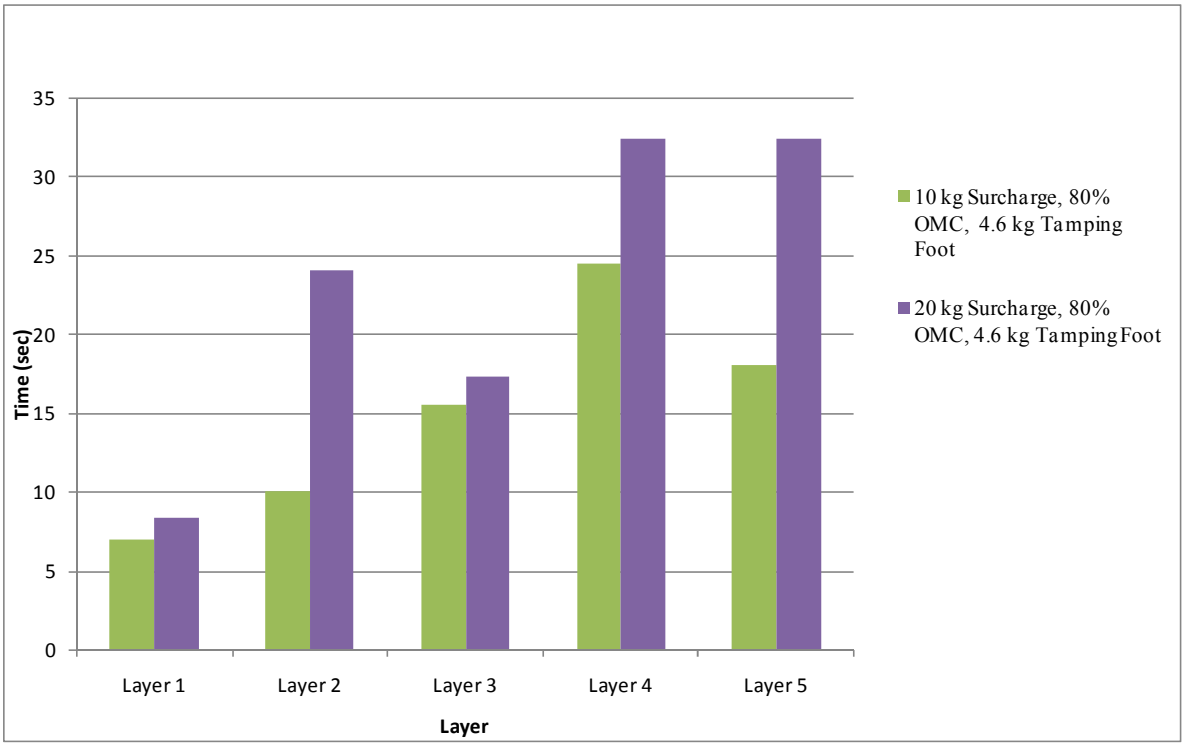

Figure B - 27: Effect of Surcharge on Compaction Time at 80% OMC and 4.6kg Tamper – G3SFR

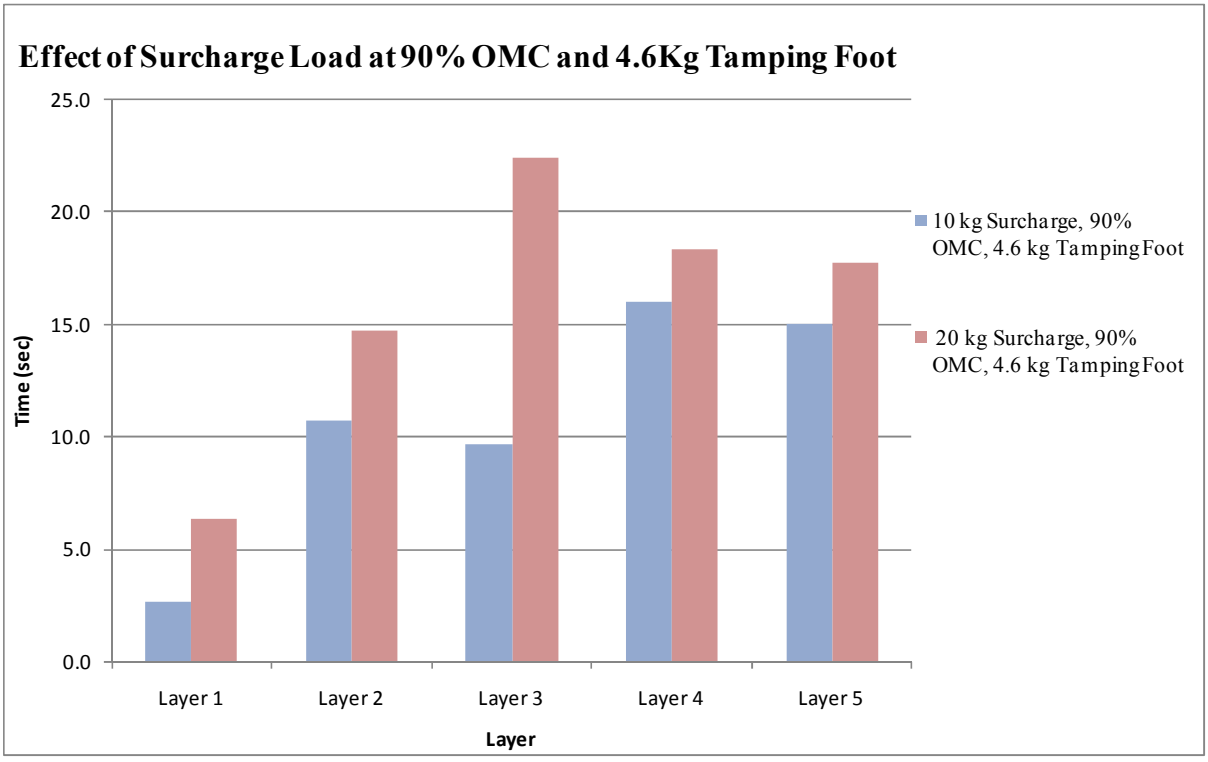

Figure B - 28: Effect of Surcharge on Compaction Time at 90% OMC and 4.6kg Tamper – G3SFR

APPENDIX D: Test results for G3 material/ vibratory hammer compaction/rigid frame

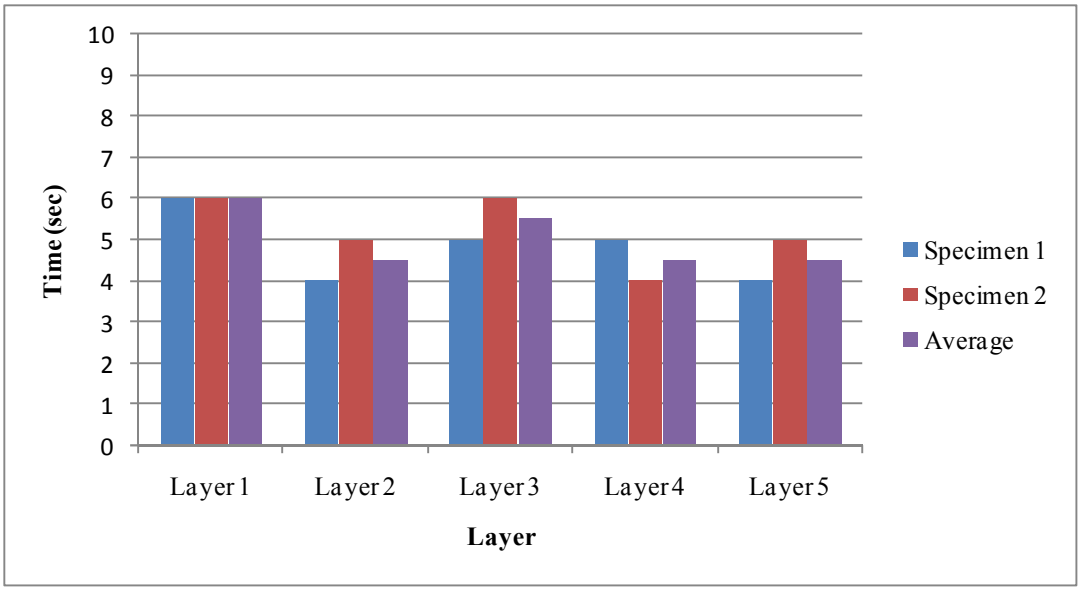

Figure B - 29: Compaction time for 3kg Tamper, 5kg Surcharge and 80% of OMC – G3RFR

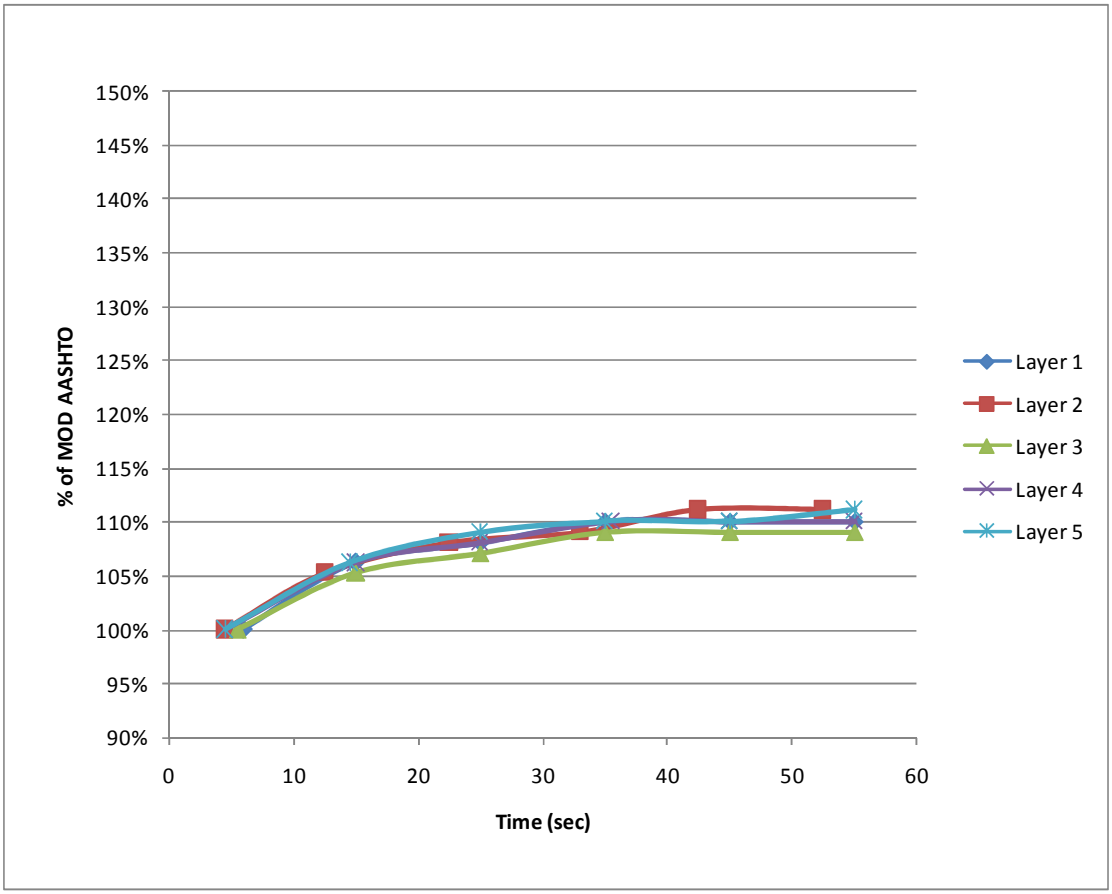

Figure B - 30: Compaction Profile for 3kg Tamper, 5kg Surcharge and 80% OMC – G3RFR

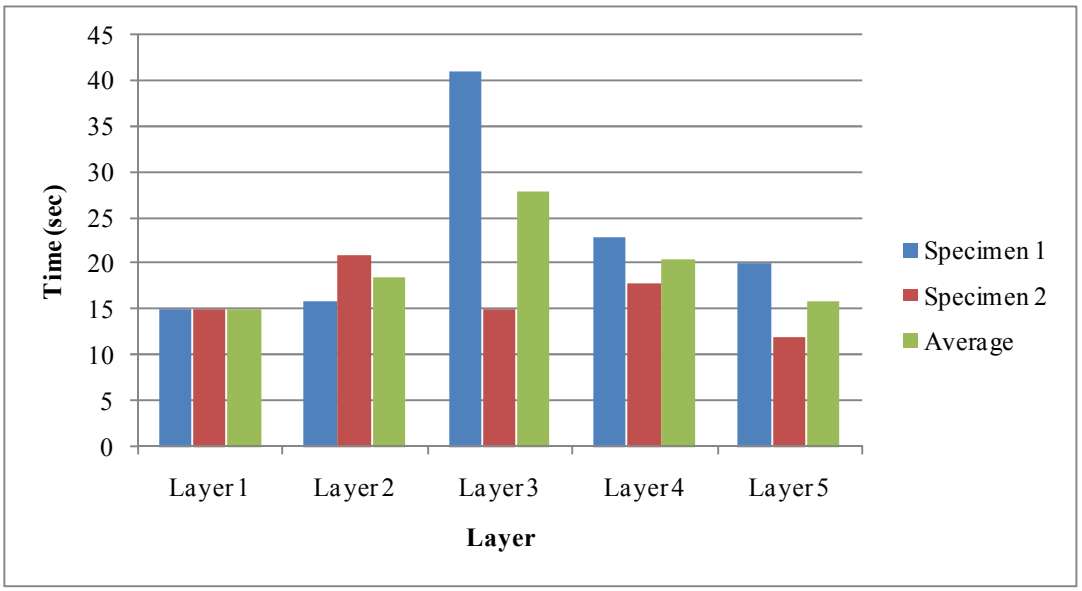

Figure B - 31: Compaction Time for 4.6kg Tamper, 5kg Surcharge and 80% OMC – G3RFR

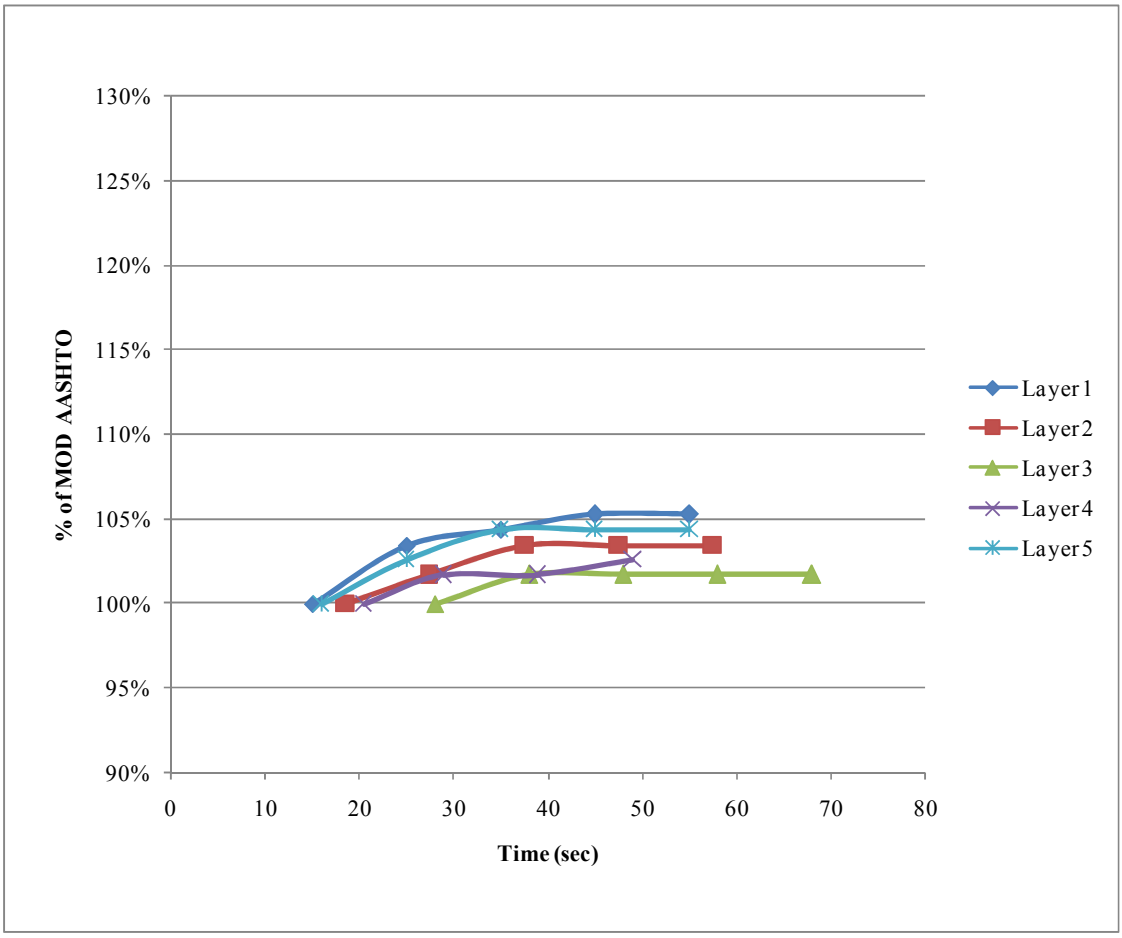

Figure B - 32: Compaction Profile for 4.6kg Tamper, 5kg Surcharge and 80% OMC – G3RFR

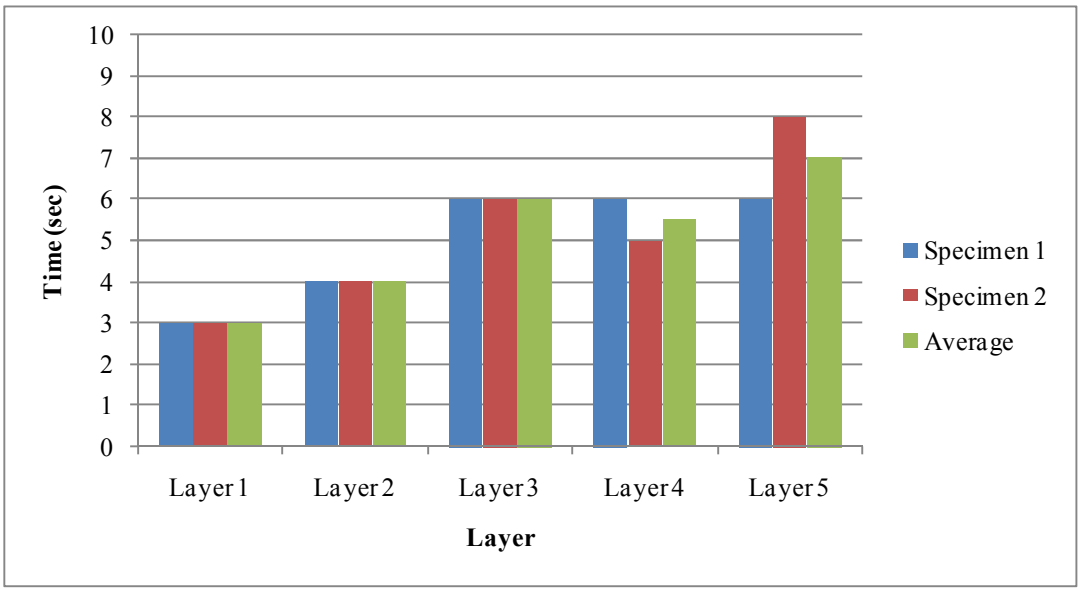

Figure B - 33: Compaction Time for 3kg Tamper, 15kg Surcharge and 80% OMC – G3RFR

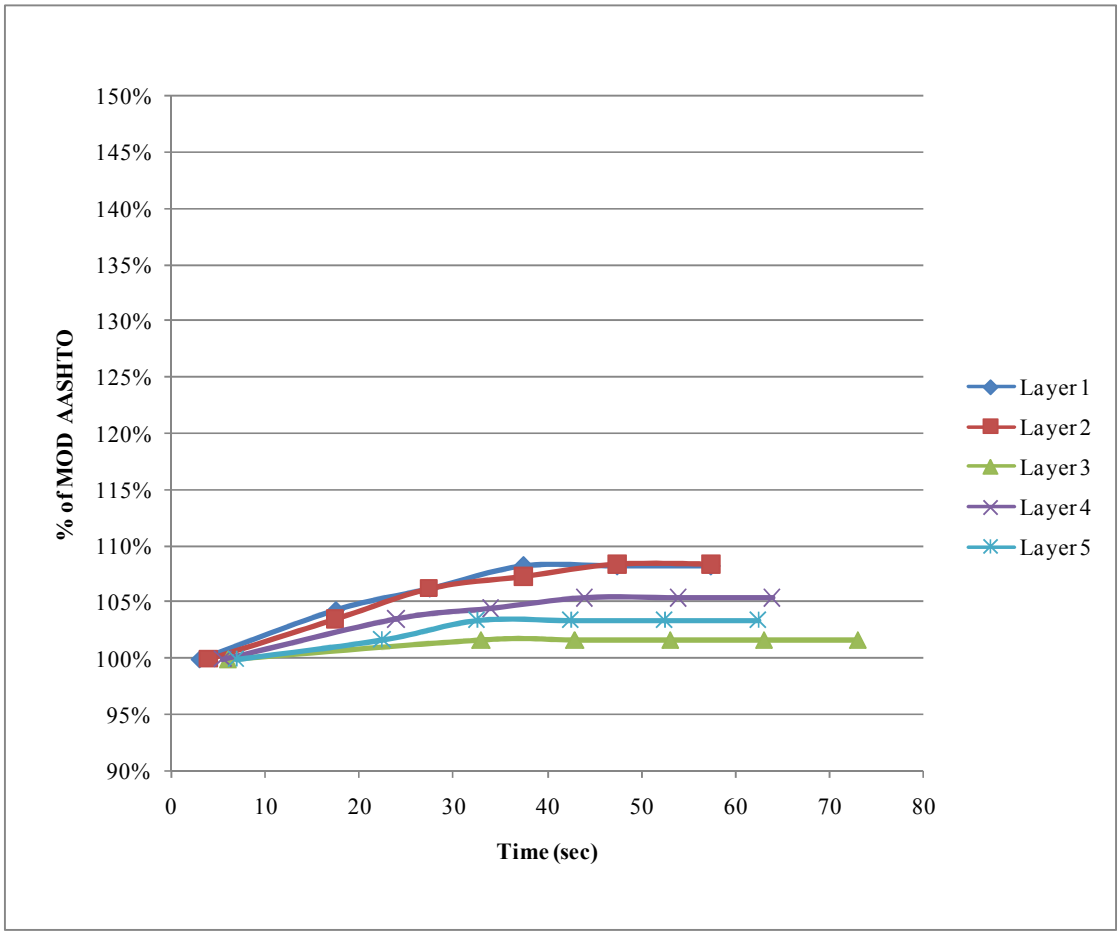

Figure B - 34: Compaction Profile for 3kg Tamper, 15kg Surcharge and 80% OMC – G3RFR

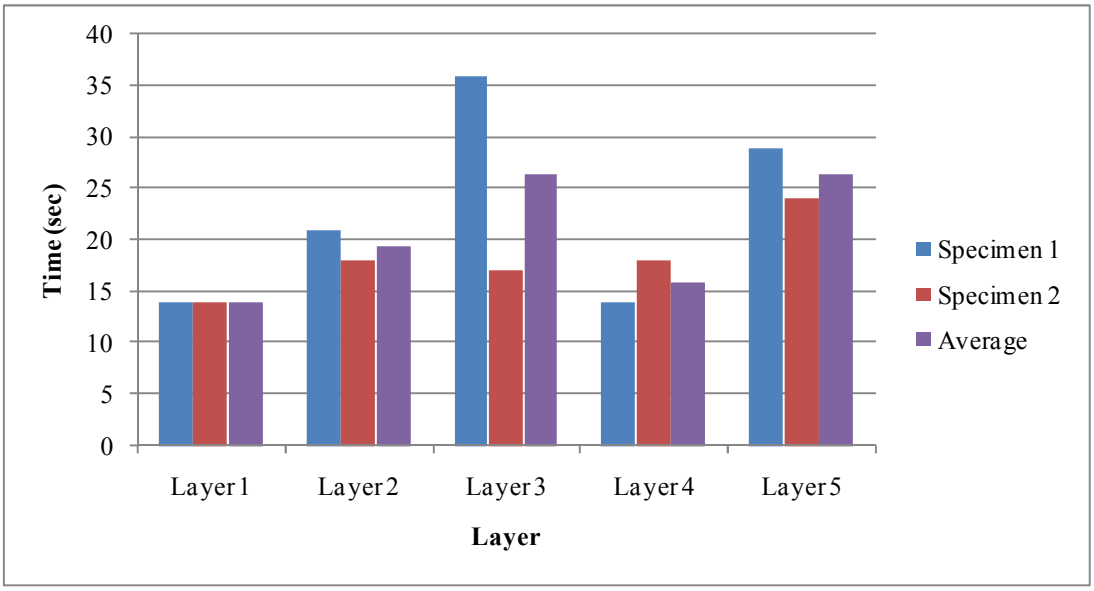

Figure B - 35: Compaction Time for 4.6kg Tamper, 15kg Surcharge and 80% OMC – G3RFR

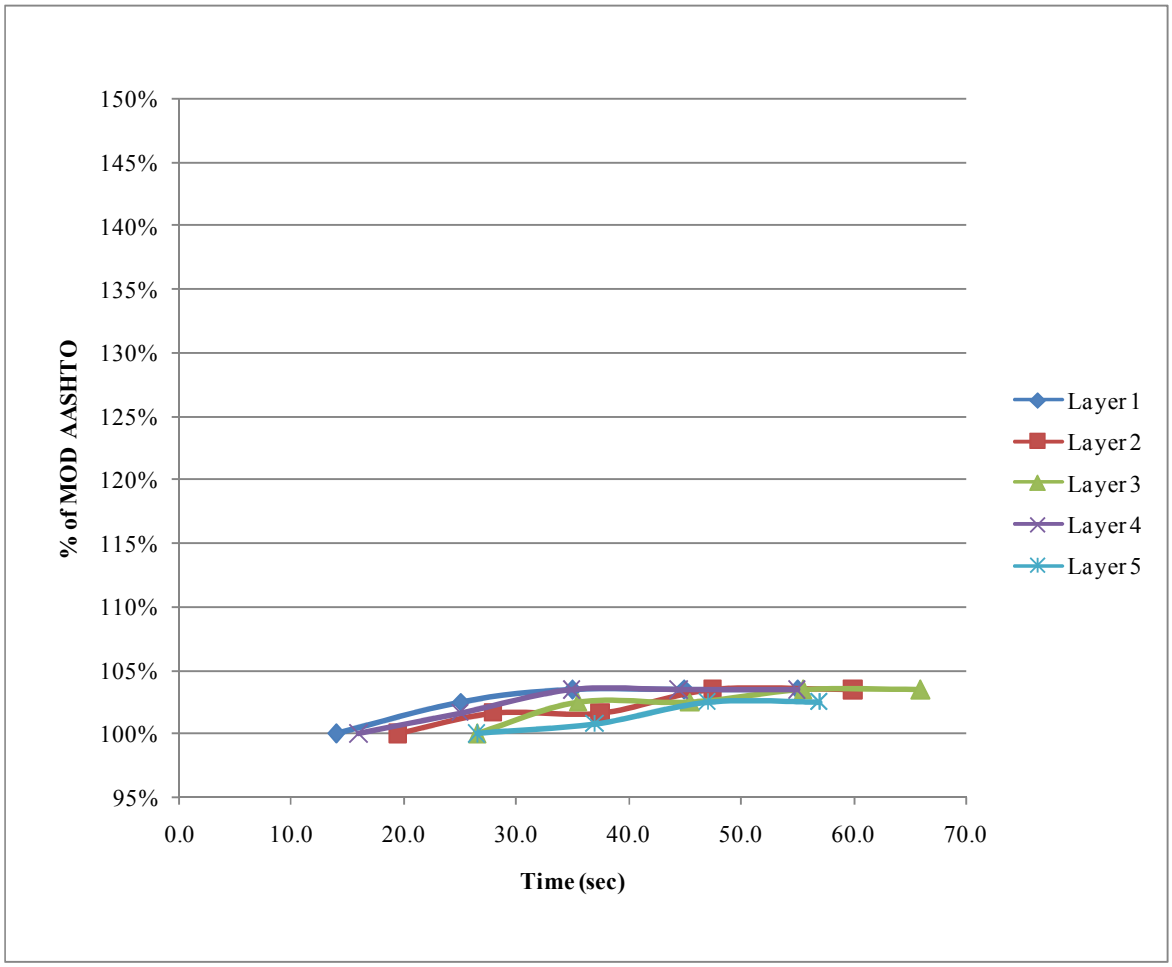

Figure B - 36: Compaction Profile for 4.6kg Tamper, 15kg Surcharge and 80% OMC – G3RFR

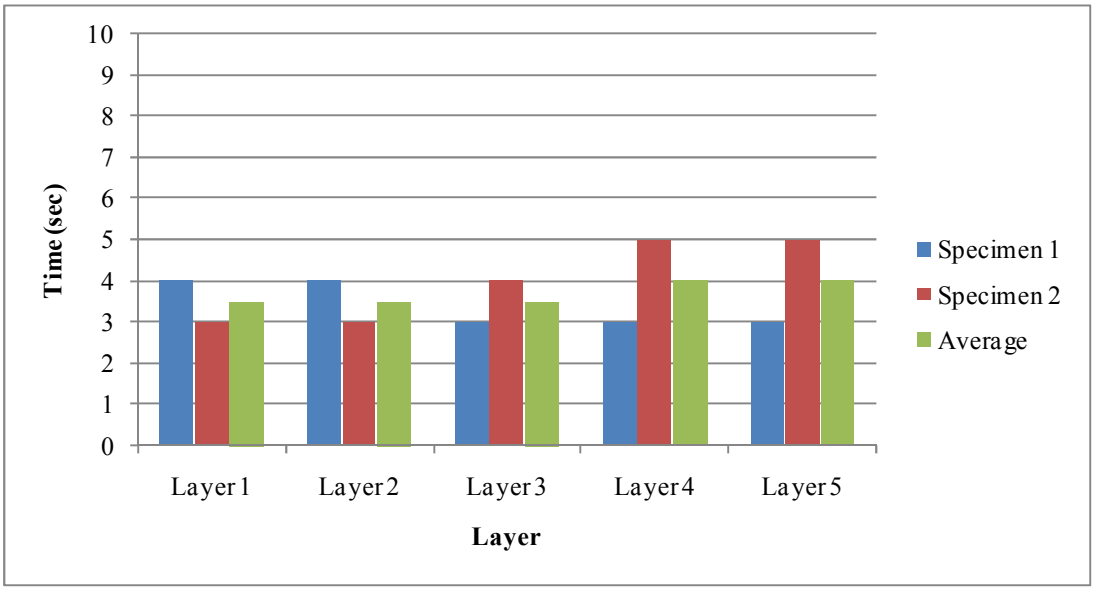

Figure B - 37: Compaction Time for 3kg Tamper, 5kg Surcharge and 90% OMC – G3RFR

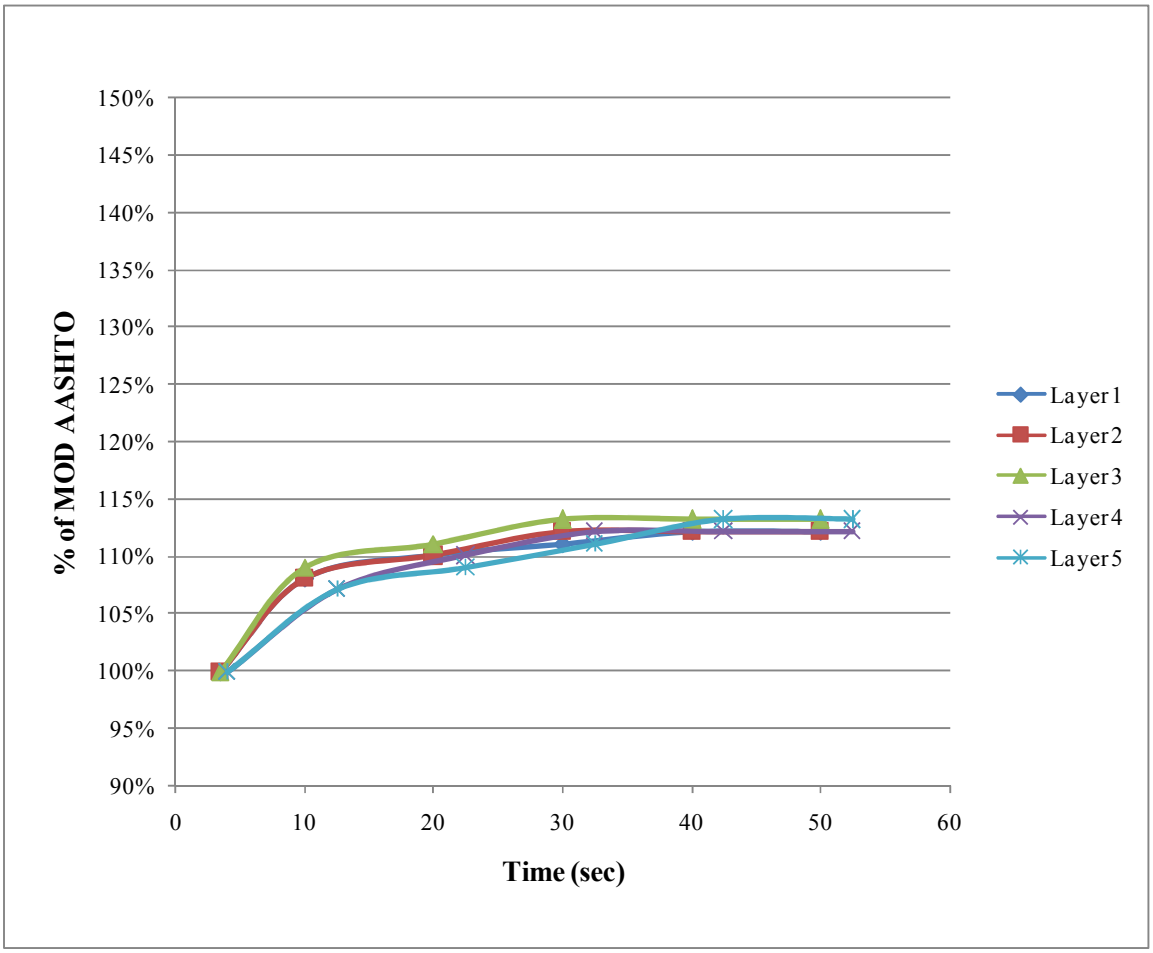

Figure B - 38: Compaction Profile for 3kg Tamper, 5kg Surcharge and 90% OMC – G3RFR

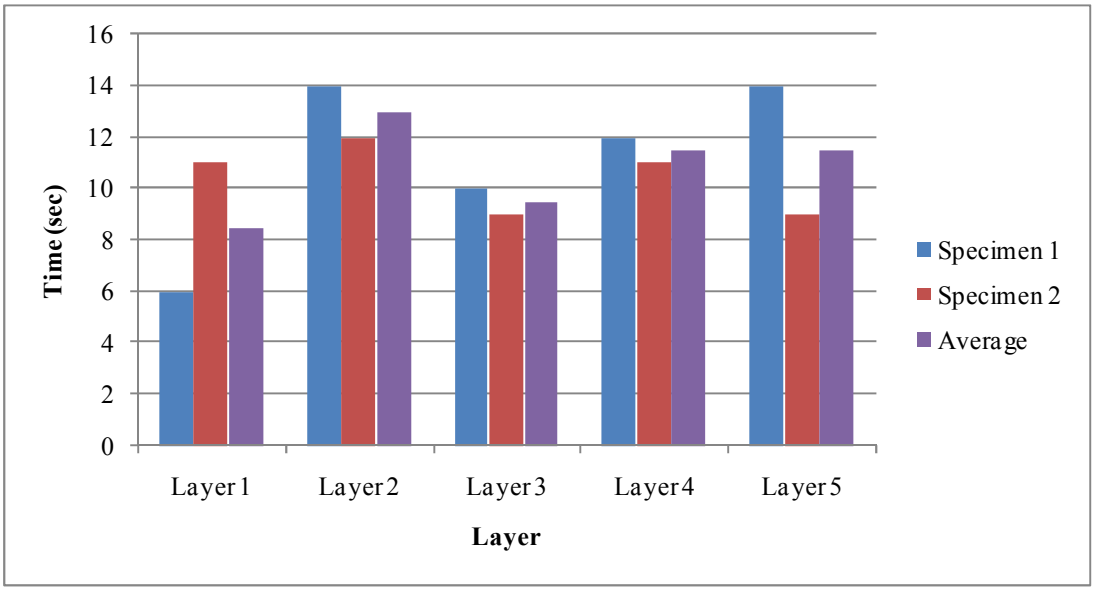

Figure B - 39: Compaction Time for 4.6kg Tamper, 5kg Surcharge and 90% OMC – G3RFR

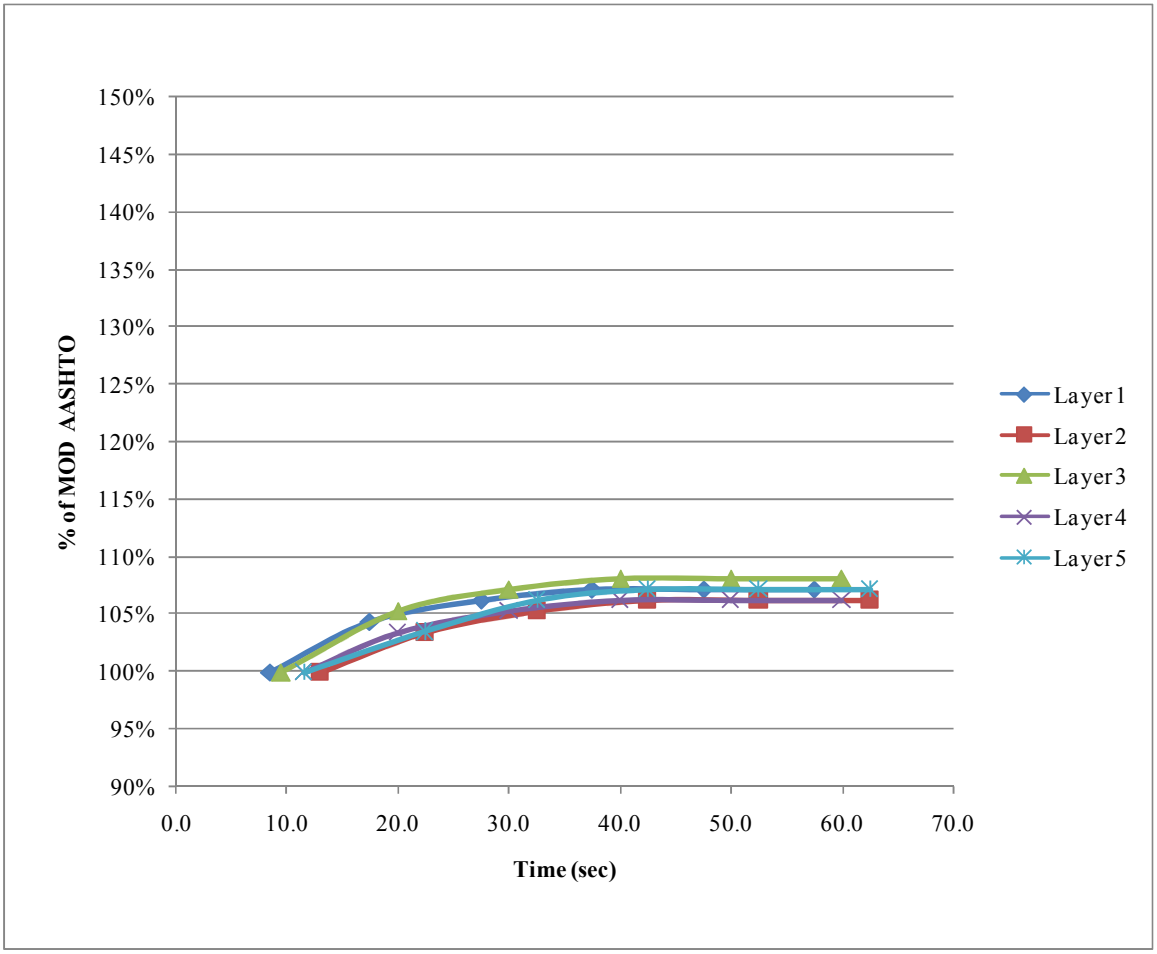

Figure B - 40: Compaction Profile for 4.6kg Tamper, 5kg Surcharge and 90% OMC – G3RFR

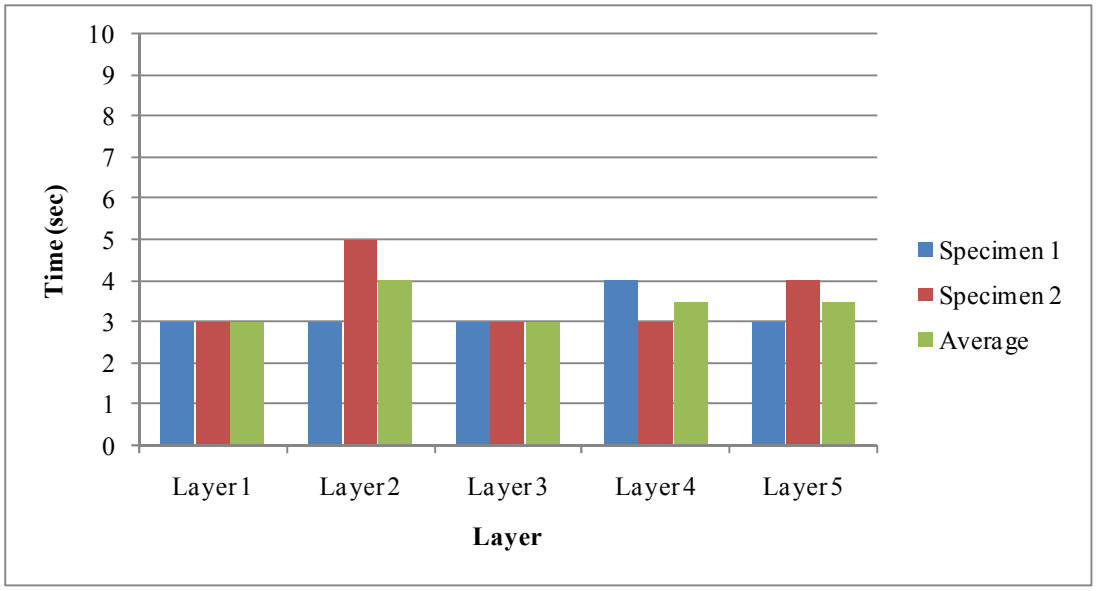

Figure B - 41: Compaction Time for 3kg Tamper, 15kg Surcharge and 90% OMC – G3RFR

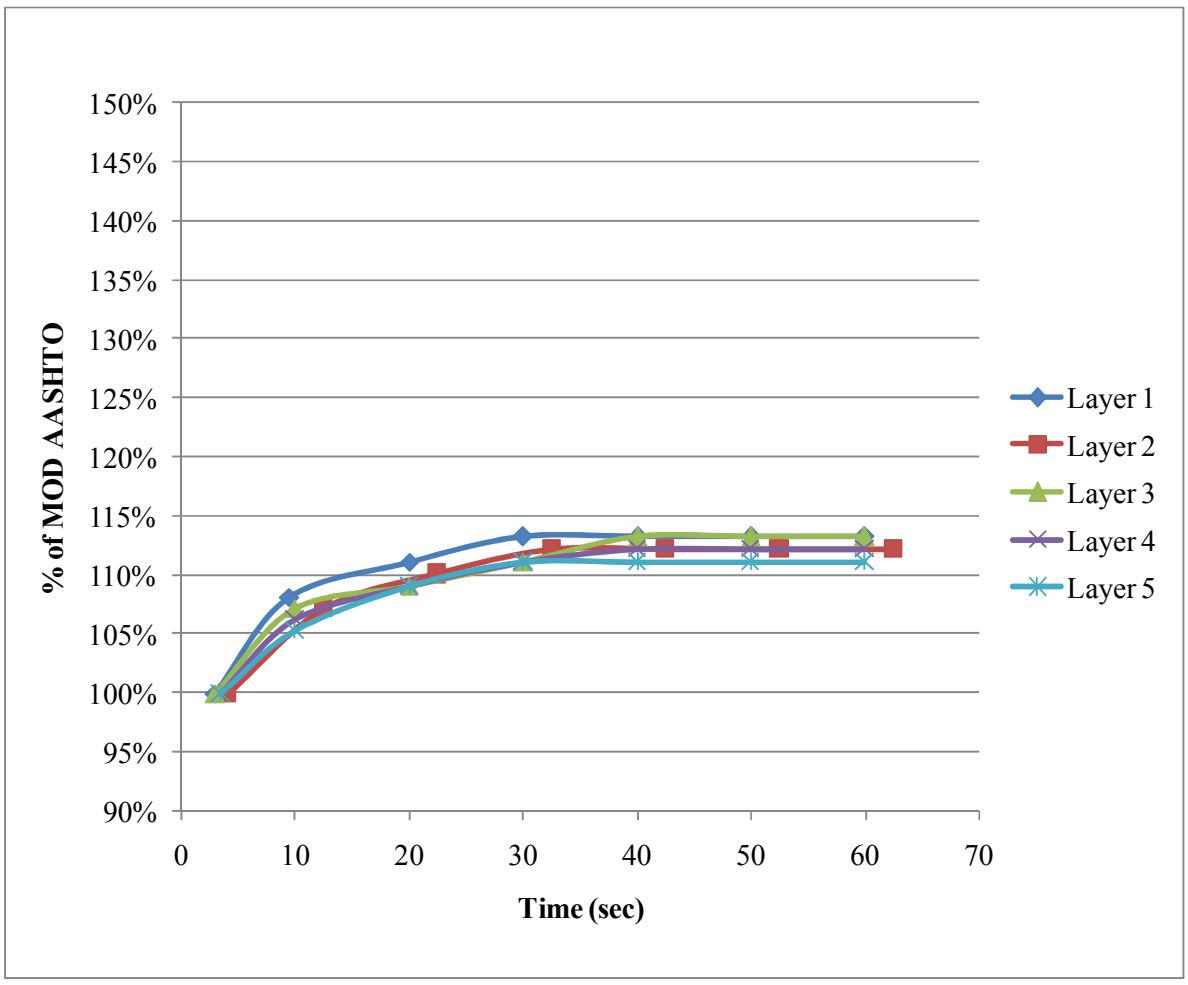

Figure B - 42: Compaction Profile for 3kg Tamper, 15kg Surcharge and 90% OMC – G3RFR

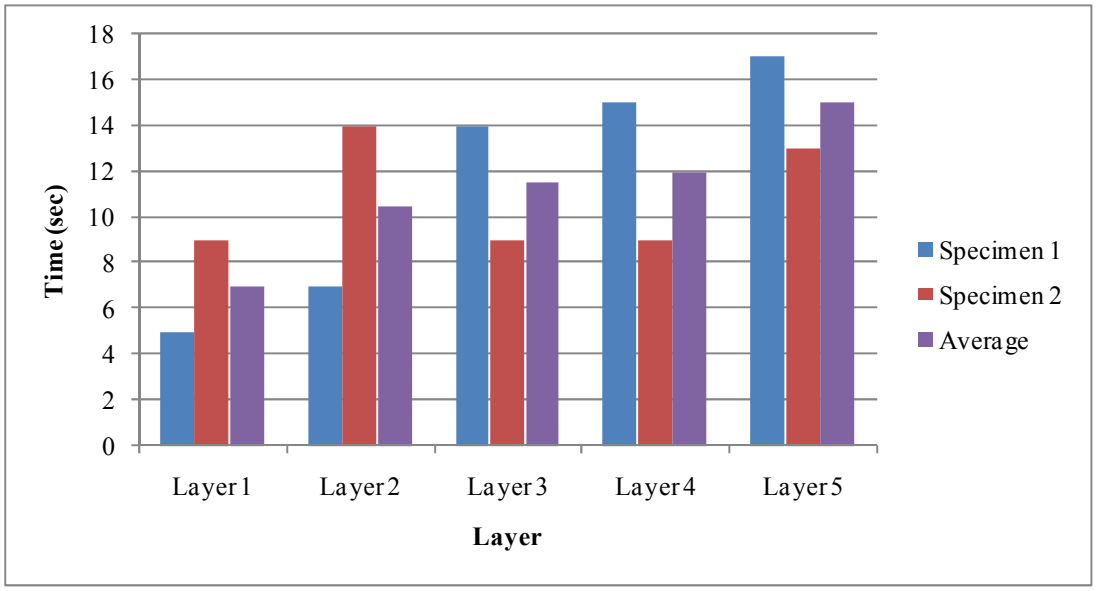

Figure B - 43: Compaction Time for 4.6kg Tamper, 15kg Surcharge and 90% OMC – G3RFR

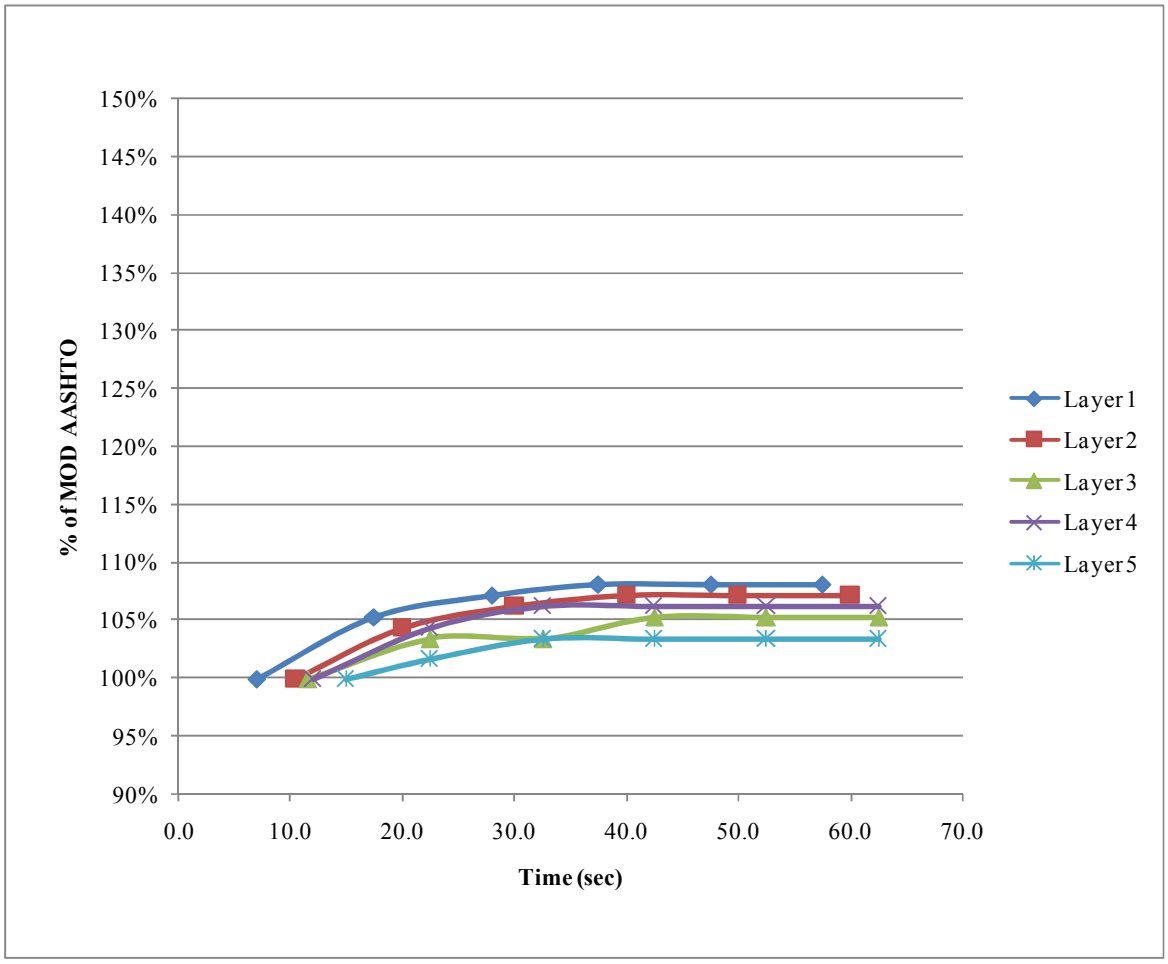

Figure B - 44: Compaction Profile for 4.6kg Tamper, 15kg Surcharge and 90% OMC – G3RFR

Frequency Tests – G3 (RFR)

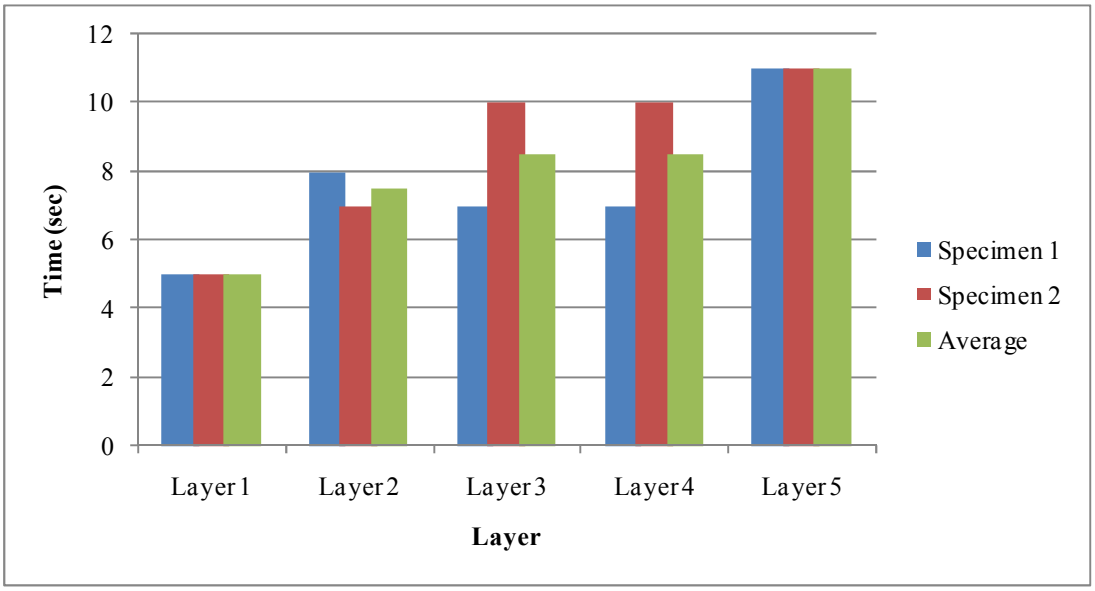

Figure B - 45: Frequency Test at 25.67Hz – Compaction Time (G3)

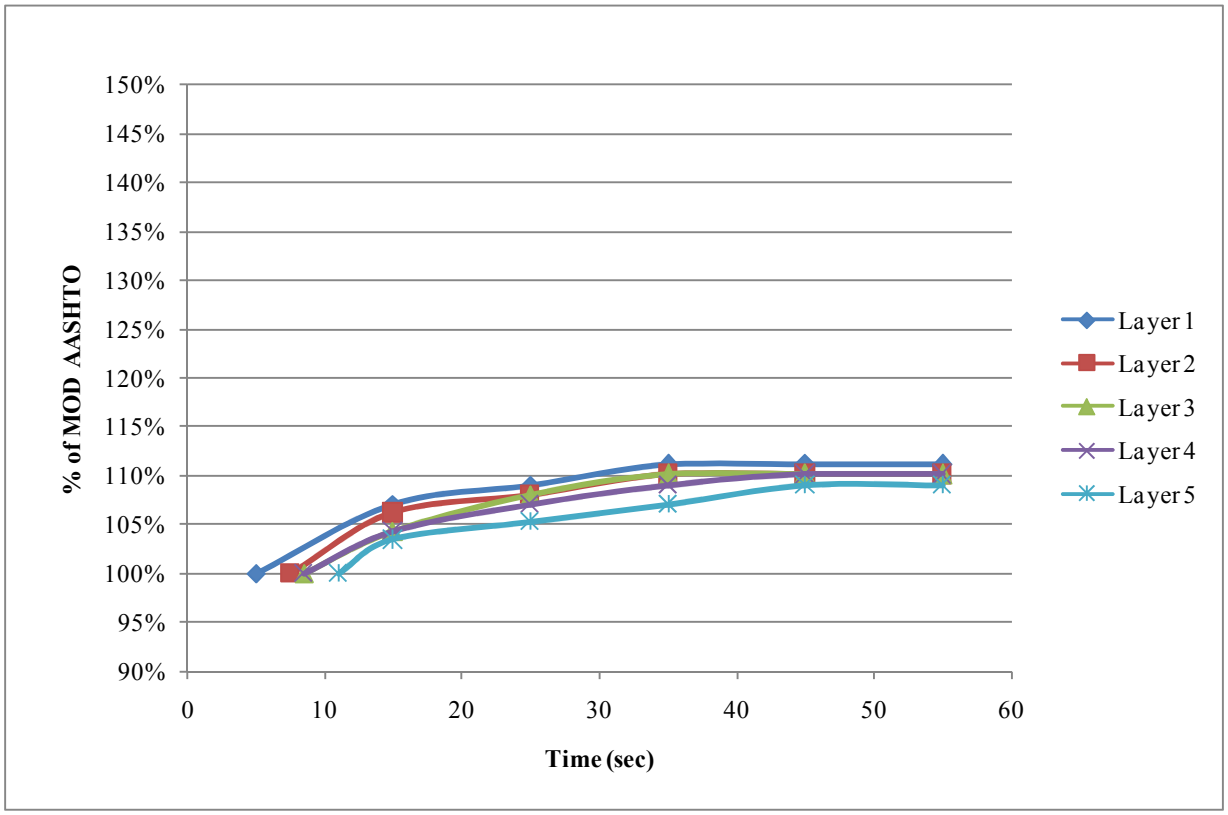

Figure B - 46: Frequency Test at 25.67Hz – Compaction Profile (G3)

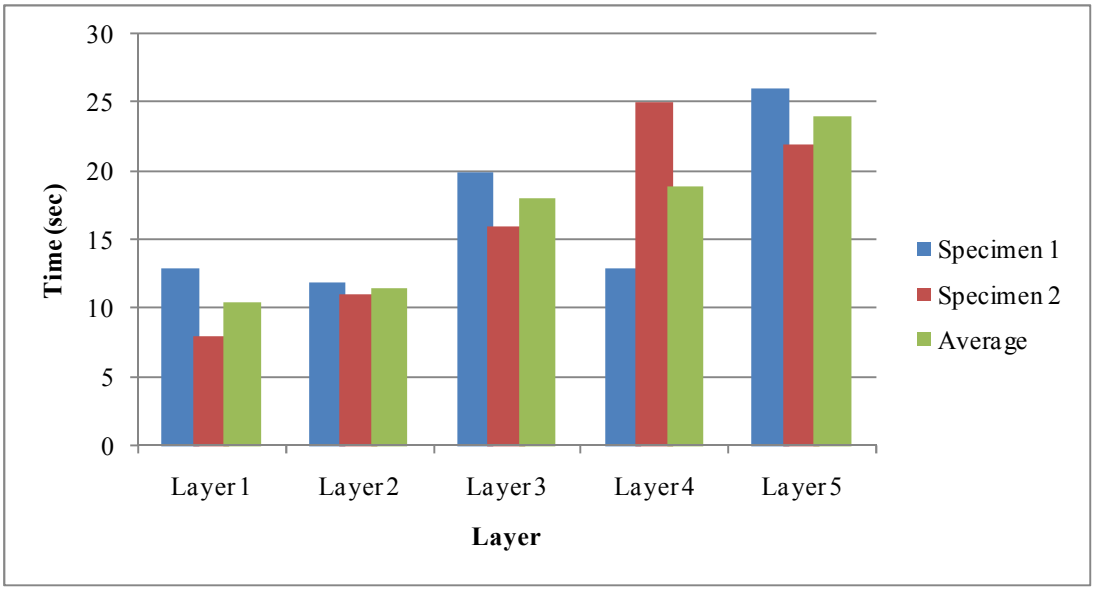

Figure B - 47: Frequency Test at 19.67Hz – Compaction Time (G3)

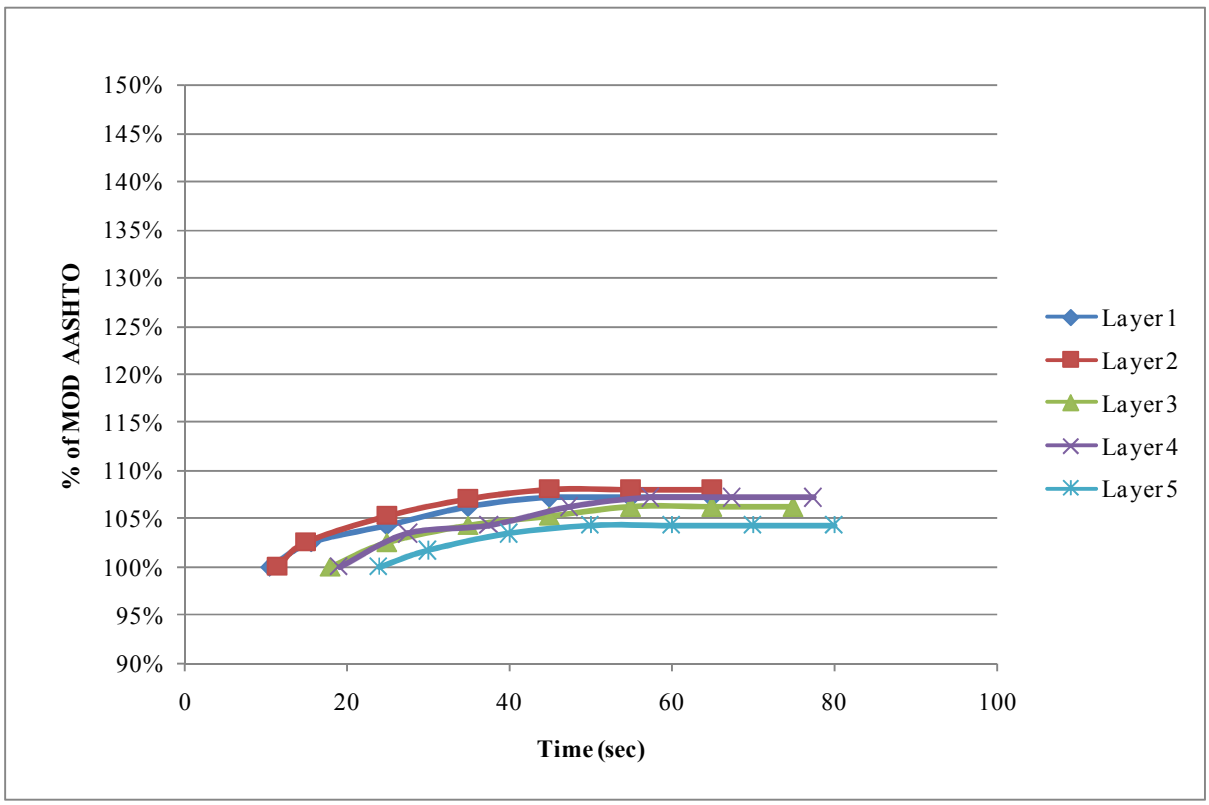

Figure B - 48: Frequency Test at 19.67Hz – Compaction Profile (G3)

Effect of Moisture on Compaction Time – G3 Material (RFR)

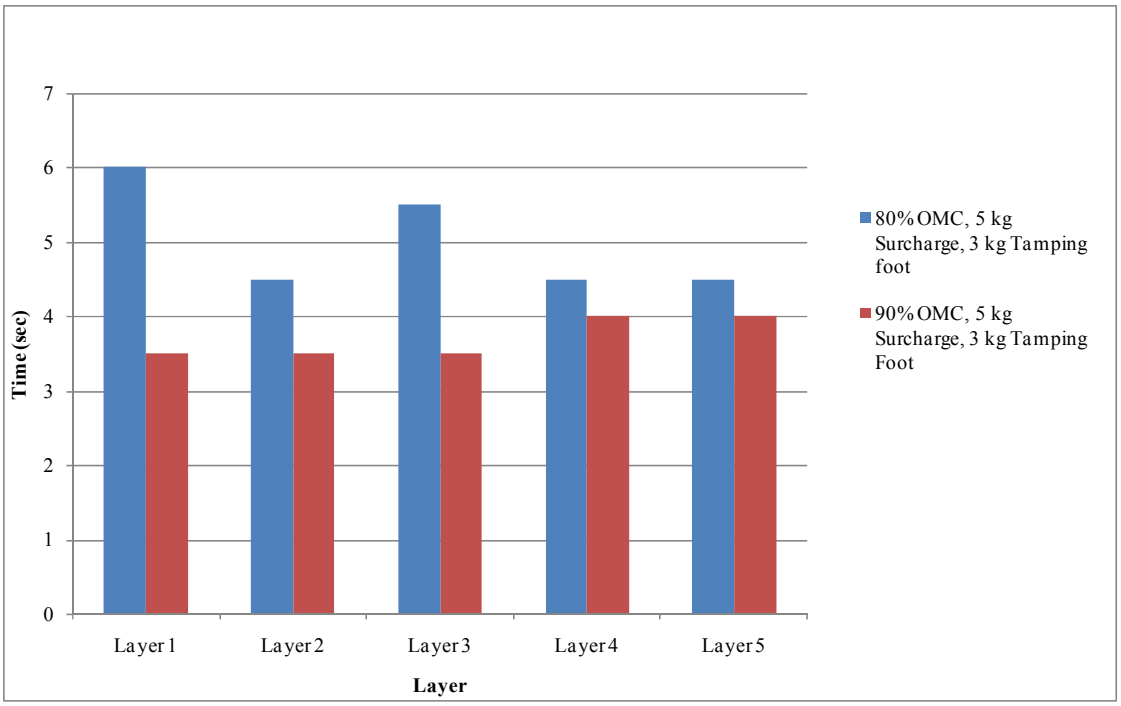

Figure B - 49: Effect of Moisture at 5kg Surcharge and 3kg Tamper – G3RFR

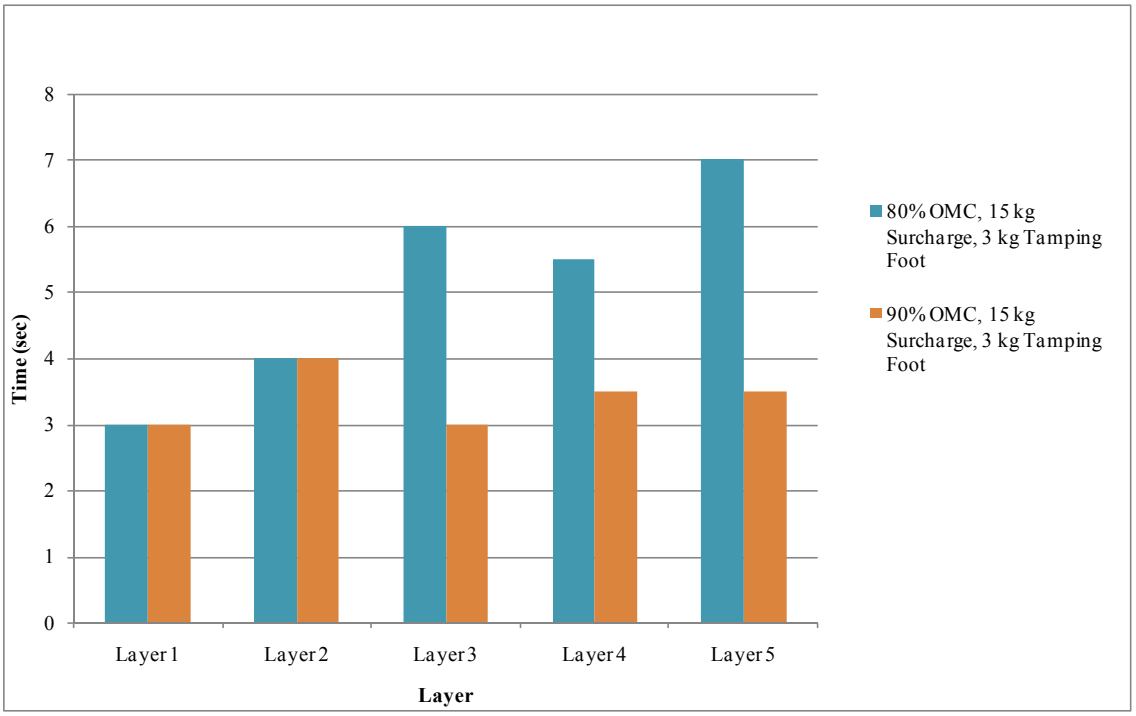

Figure B - 50: Effect of Moisture at 15kg Surcharge and 3kg Tamper – G3RFR

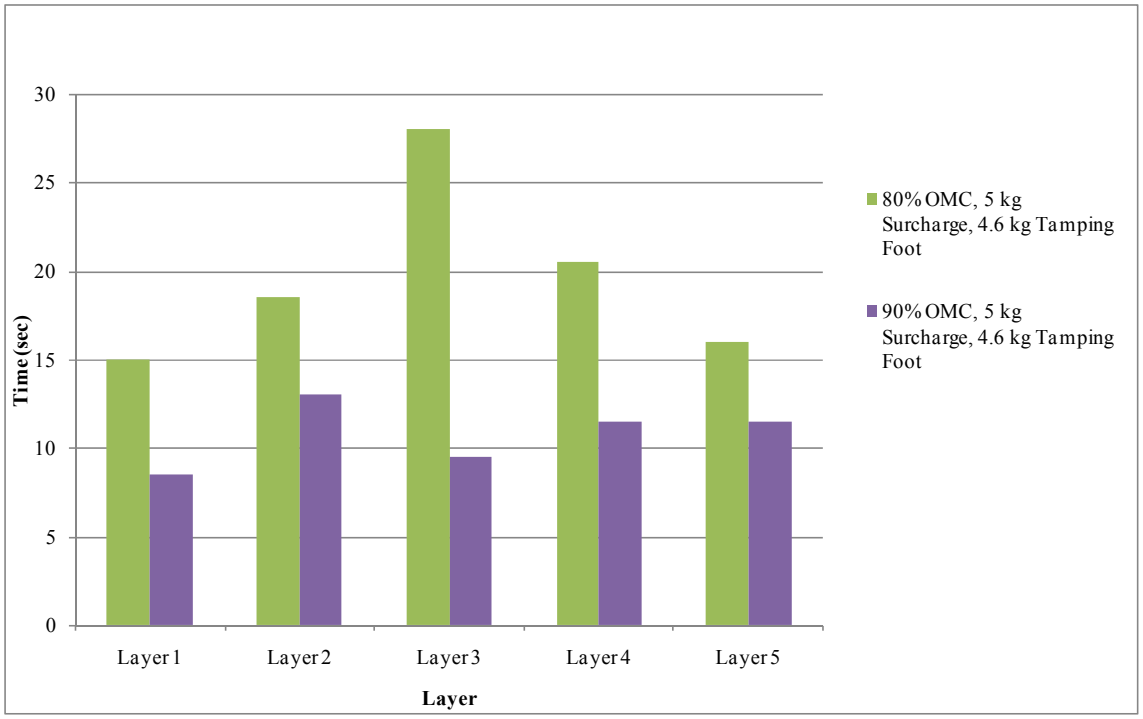

Figure B - 51: Effect of Moisture at 5kg Surcharge and 4.6kg Tamper – G3RFR

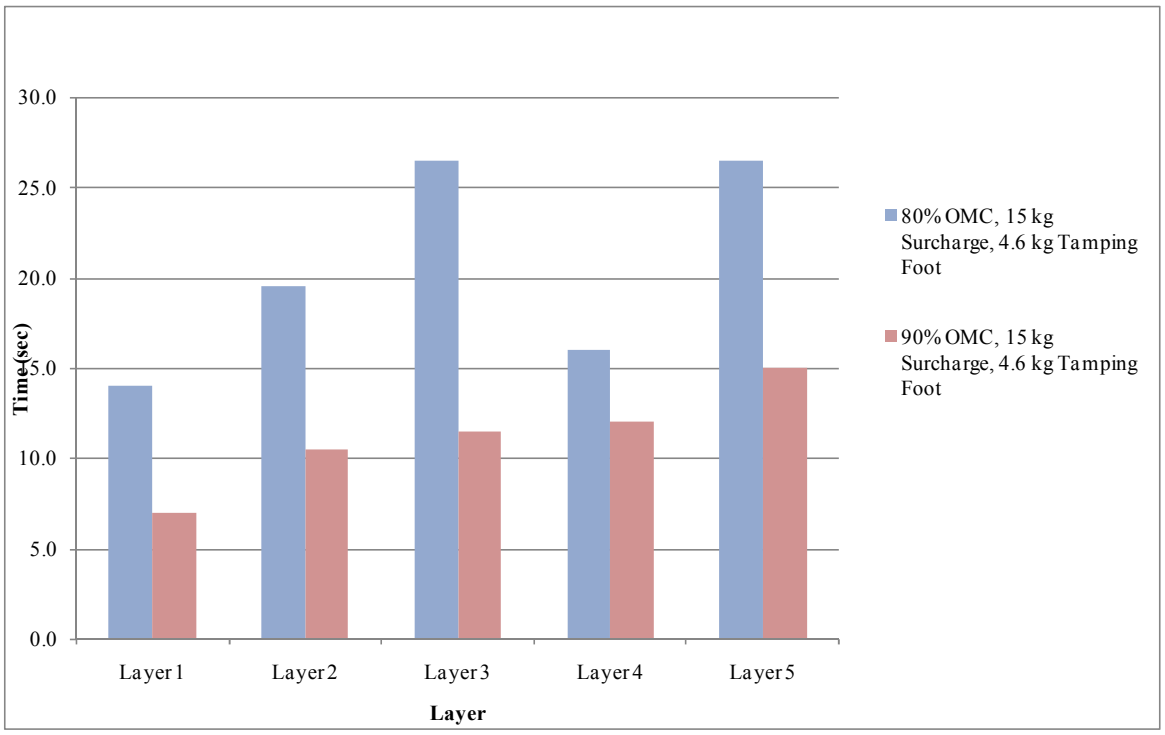

Figure B - 52: Effect of Moisture at 15kg Surcharge and 4.6kg Tamper – G3RFR

Effect of Tamping Foot on Compaction Time – G3 Material (RFR)

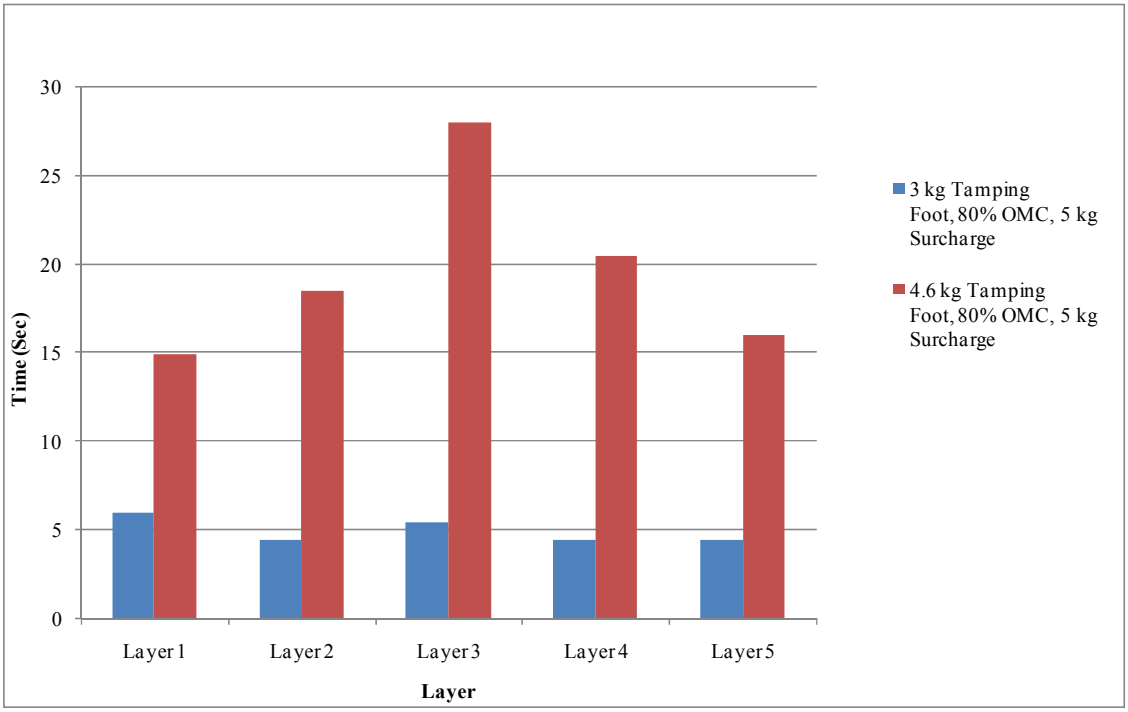

Figure B - 53: Effect of Tamping Foot at 80% OMC and 10kg Surcharge – G3 RFR

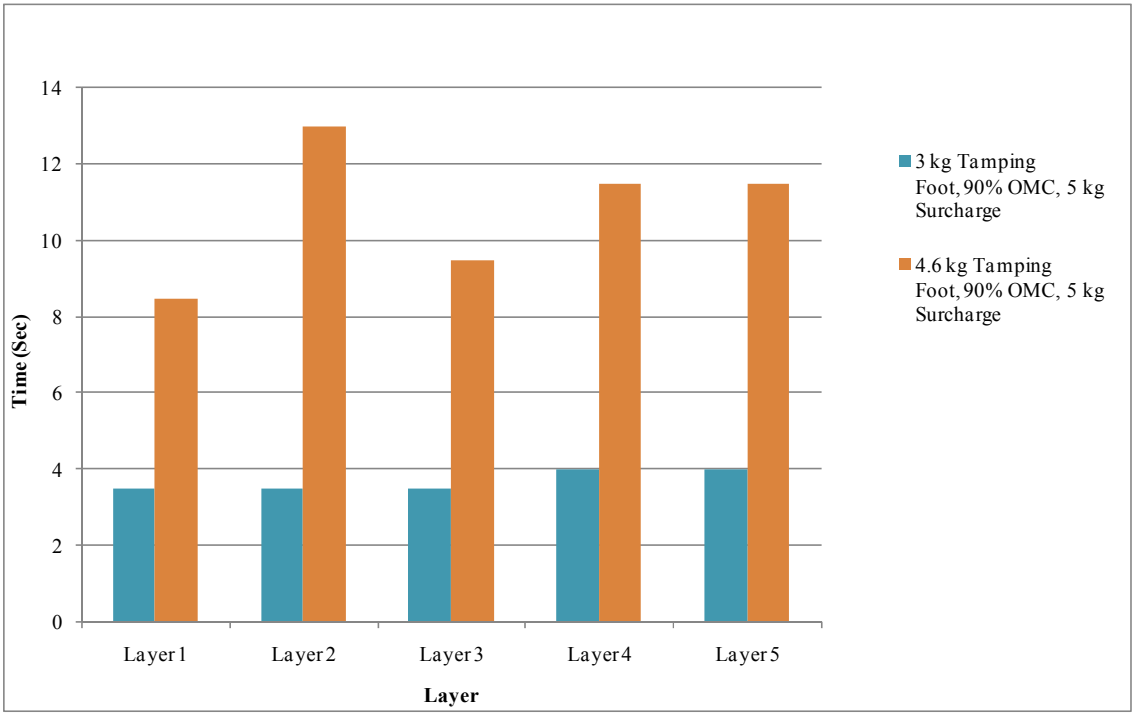

Figure B - 54: Effect of Tamping Foot at 90% OMC and 5kg Surcharge – G3RFR

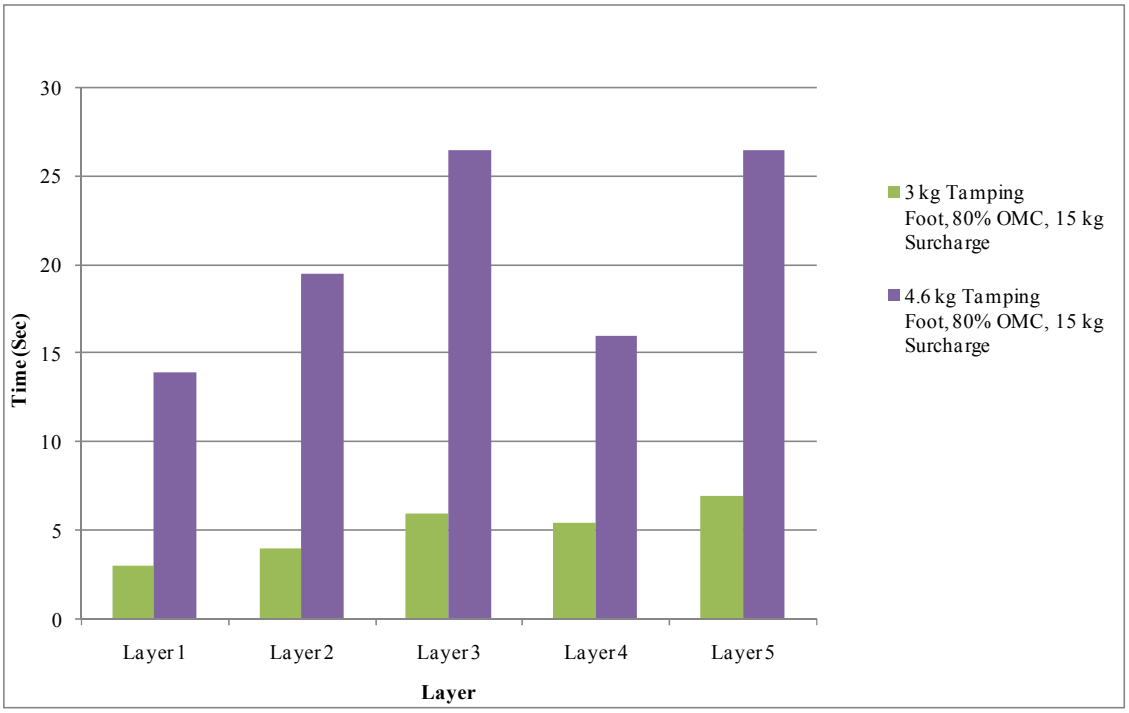

Figure B - 55: Effect of Tamping Foot at 80% OMC and 15kg Surcharge – G3RFR

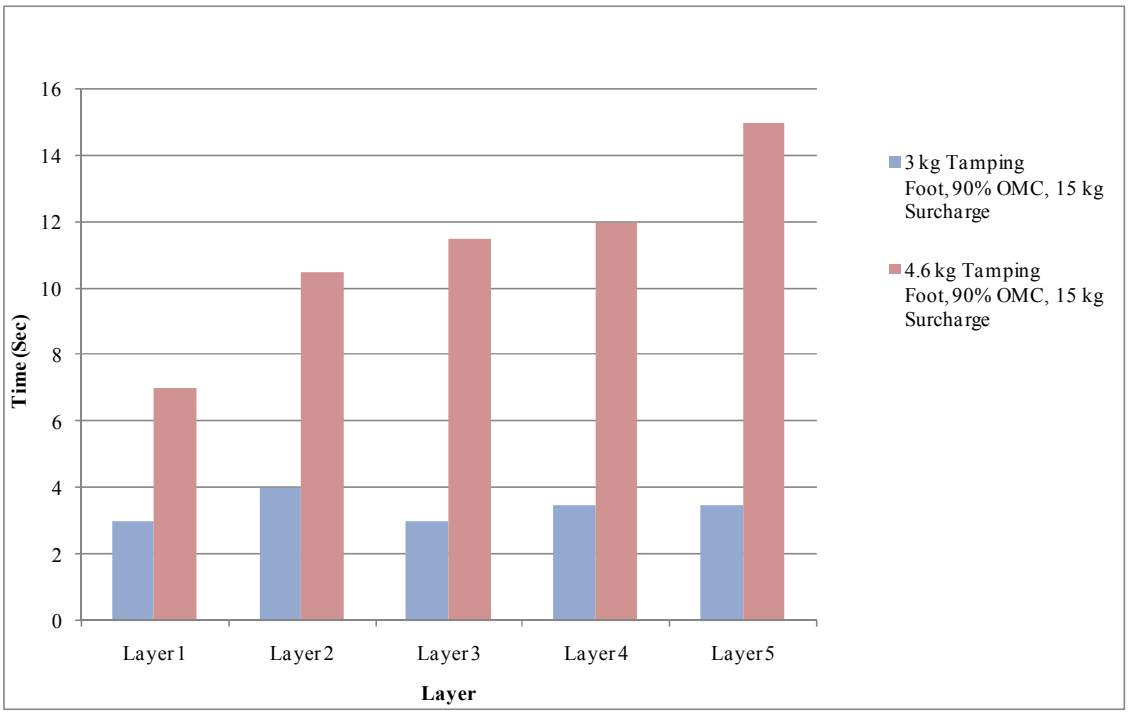

Figure B - 56: Effect of Tamping Foot at 90% OMC and 15kg Surcharge – G3RFR

Effect of Surcharge Load on Compaction Time – G3 Material (RFR)

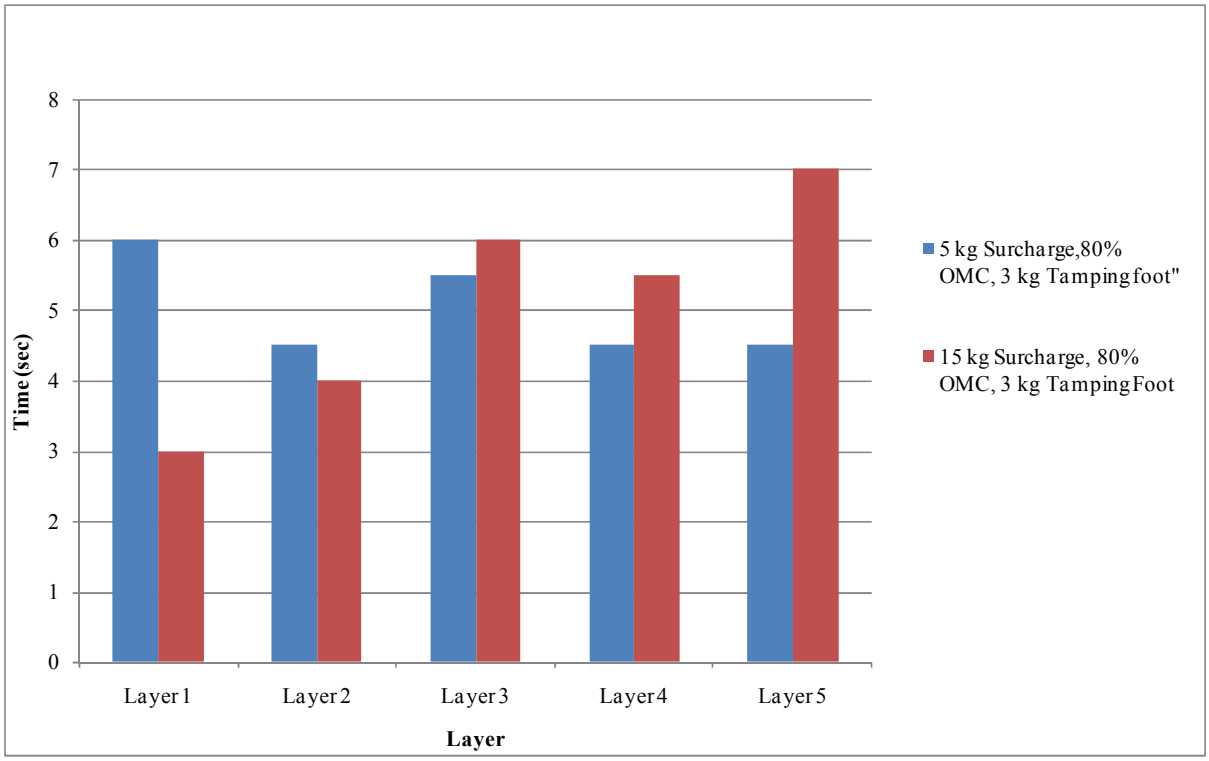

Figure B - 57: Effect of Surcharge Load at 80% OMC and 3kg Tamper – G3RFR

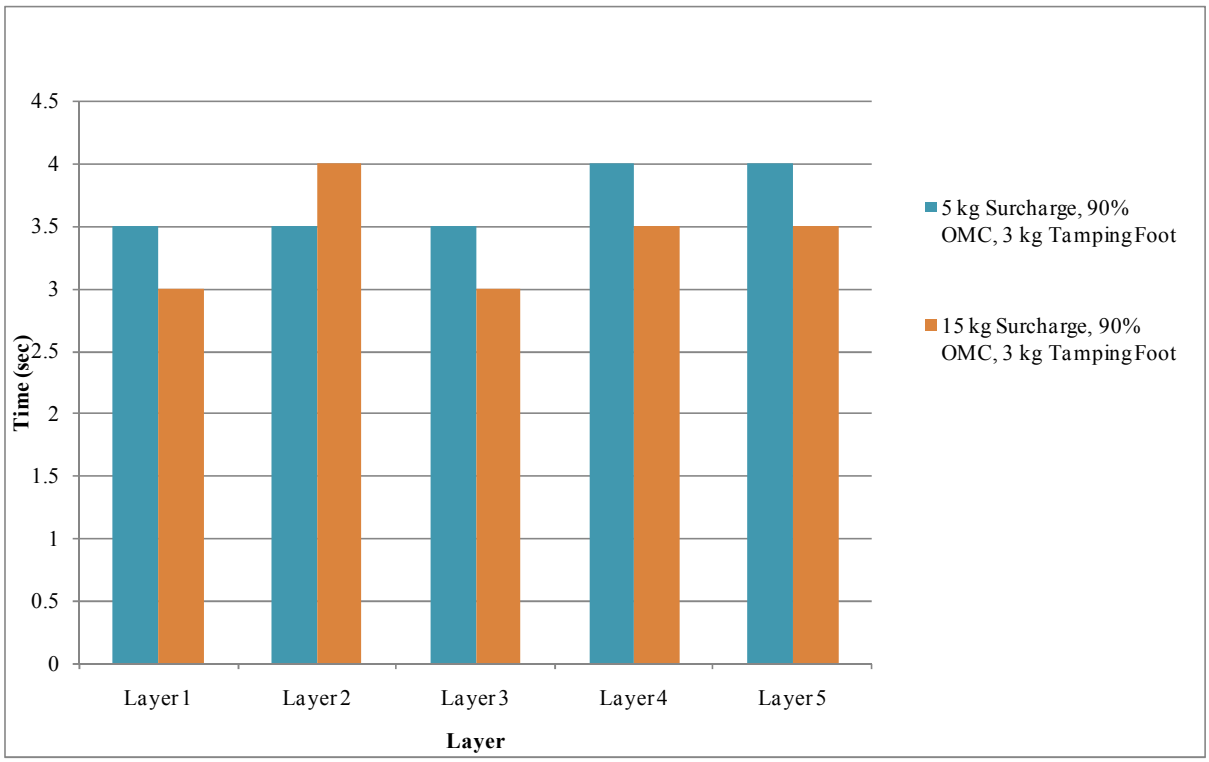

Figure B - 58: Effect of Surcharge Load at 90% OMC and 3kg Tamper – G3RFR

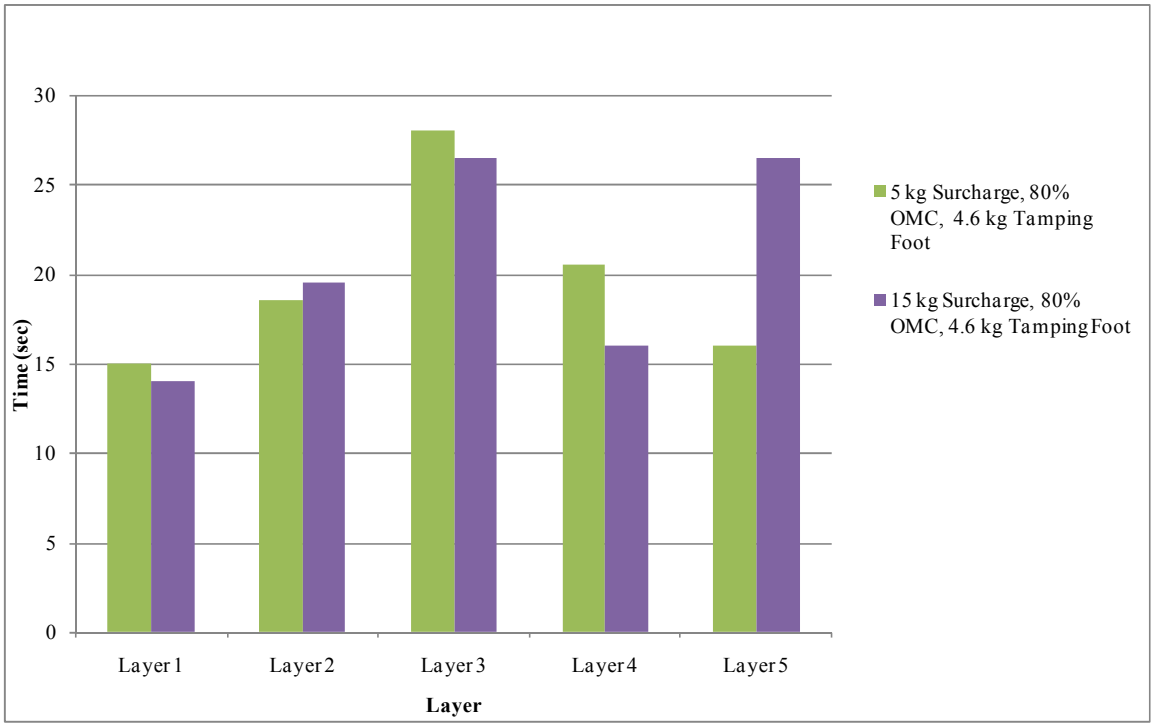

Figure B - 59: Effect of Surcharge at 80% OMC and 4.6kg Tamper – G3RFR

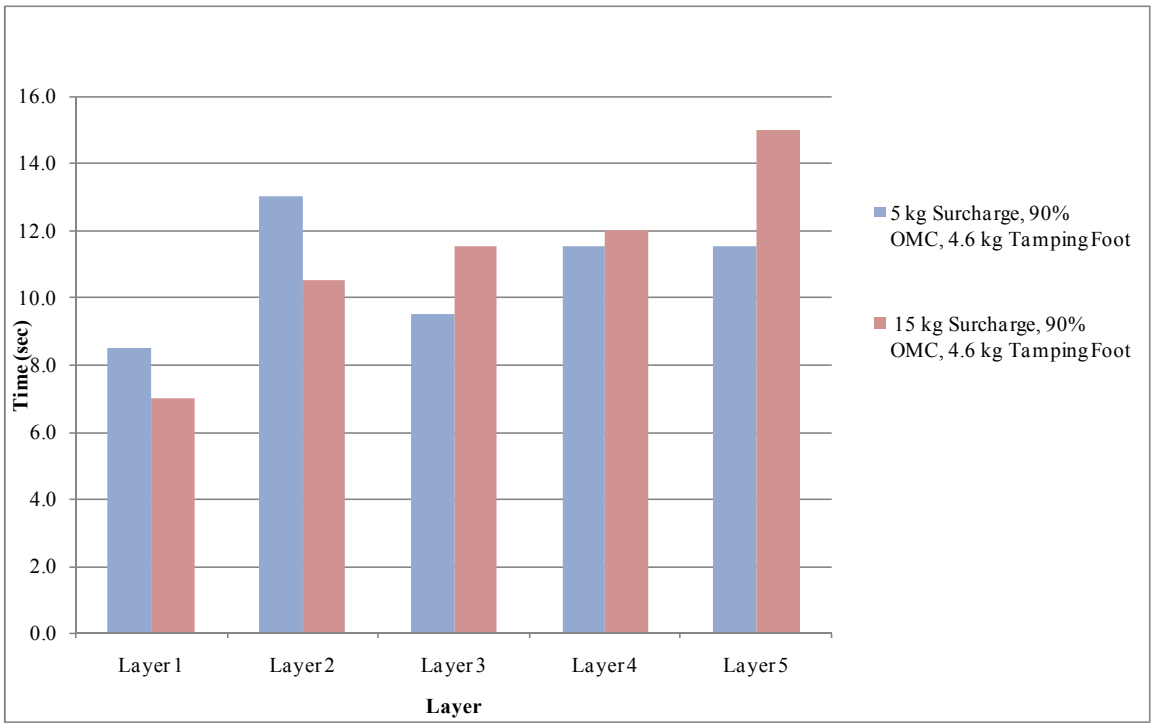

Figure B - 60: Effect of Surcharge Load at 90% OMC and 4.6kg Tamper – G3RFR

APPENDIX E: Test results for G4 material/ vibratory hammer compaction/soft frame

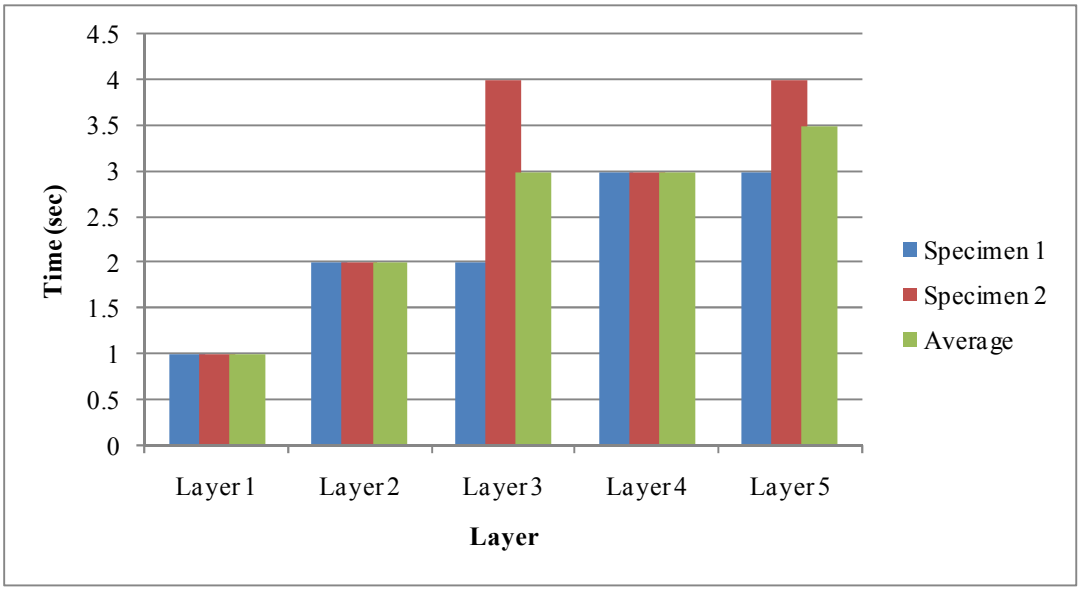

Figure B - 61: Compaction Time for 3kg Tamper, 10kg Surcharge and 80% OMC – G4SFR

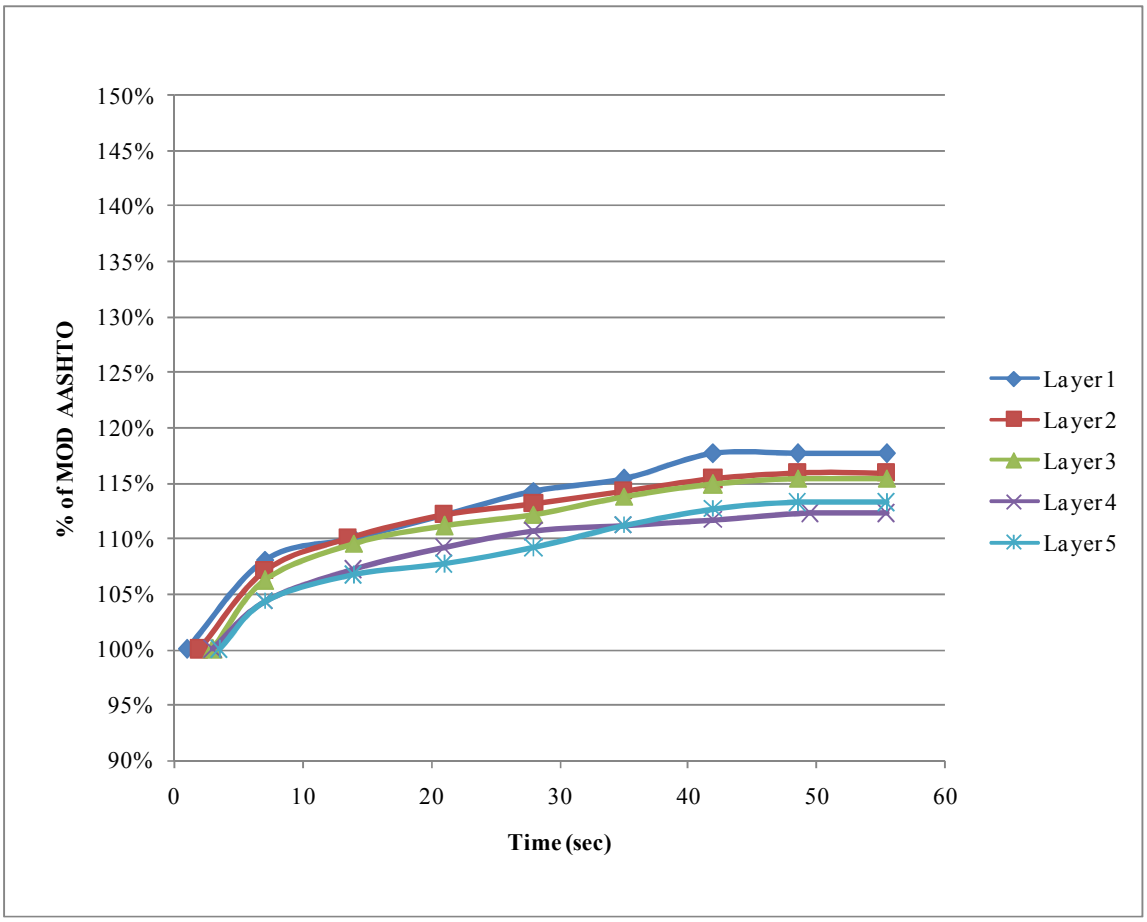

Figure B - 62: Compaction Profile for 3kg Tamper, 10kg Surcharge and 80% OMC – G4SFR

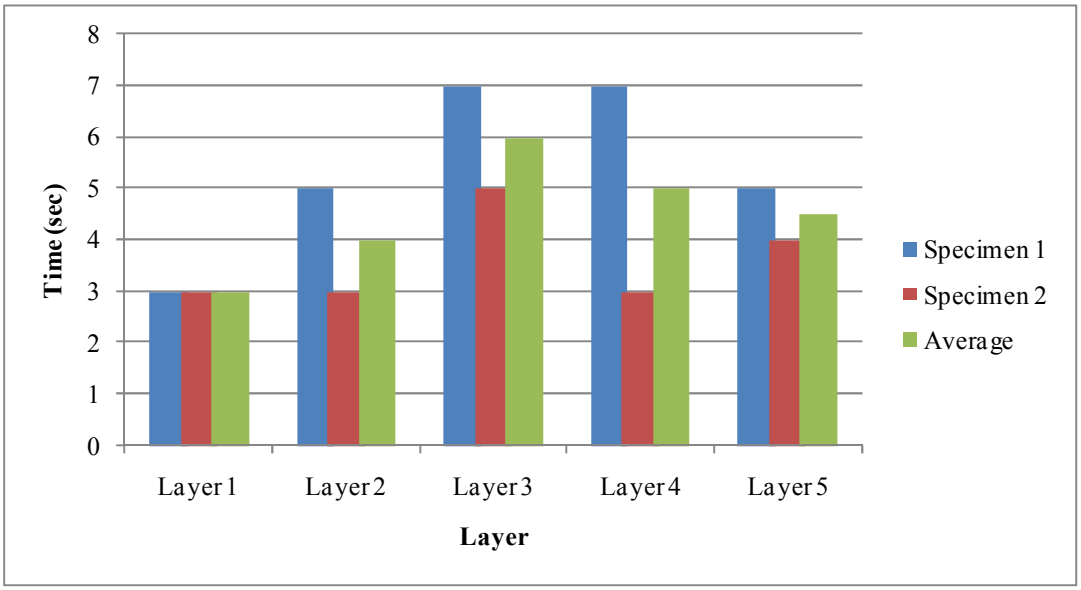

Figure B - 63: Compaction Time for 4.6kg Tamper, 10kg Surcharge and 80% OMC – G4SFR

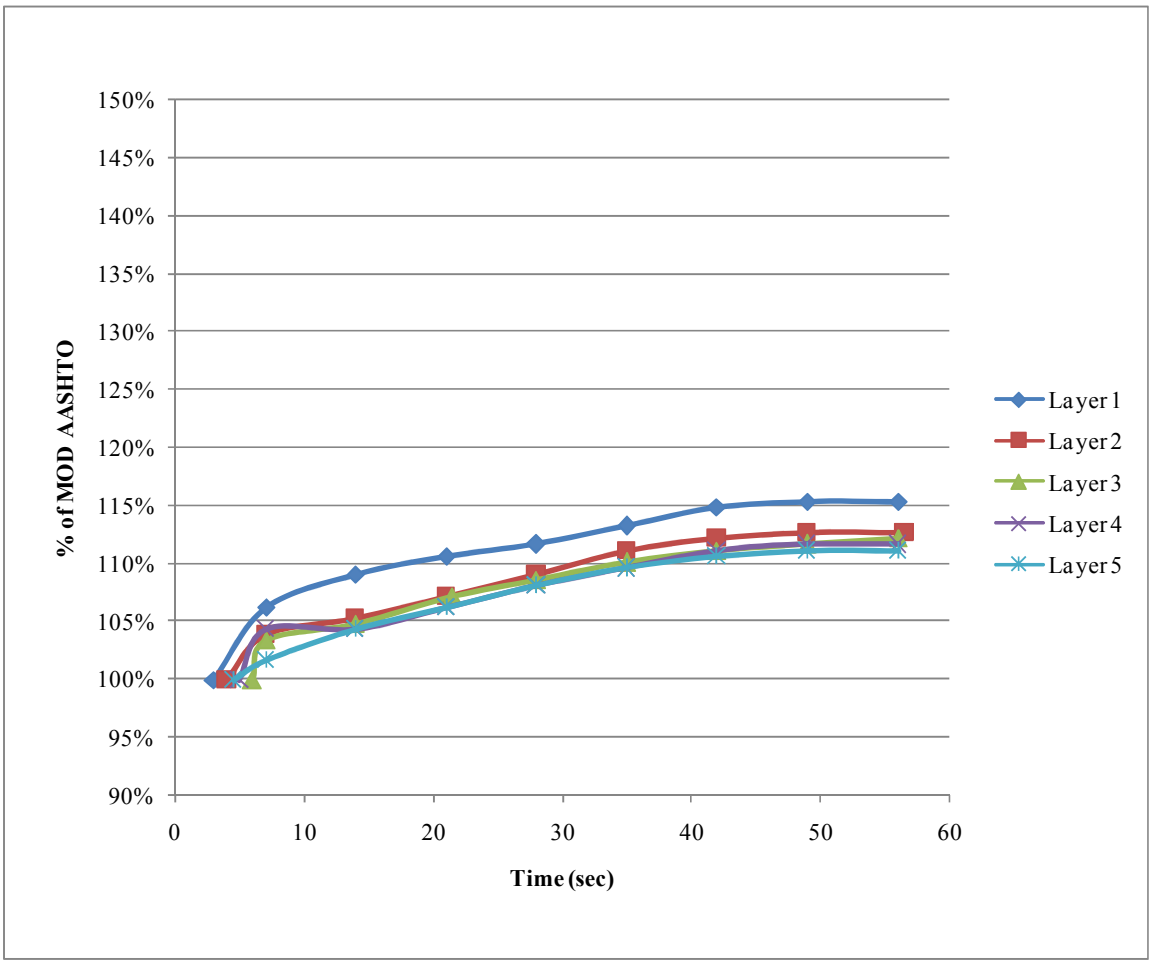

Figure B - 64: Compaction Profile for 4.6kg Tamper, 10kg Surcharge and 80% OMC – G4SFR

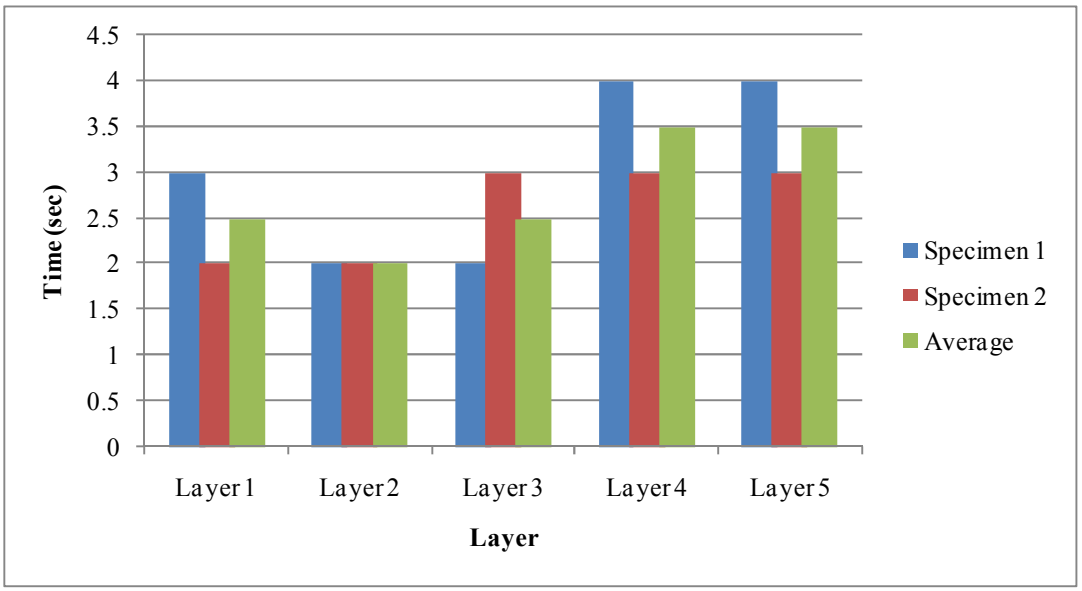

Figure B - 65: Compaction Time for 3kg Tamper, 20kg Surcharge and 80% OMC – G4SFR

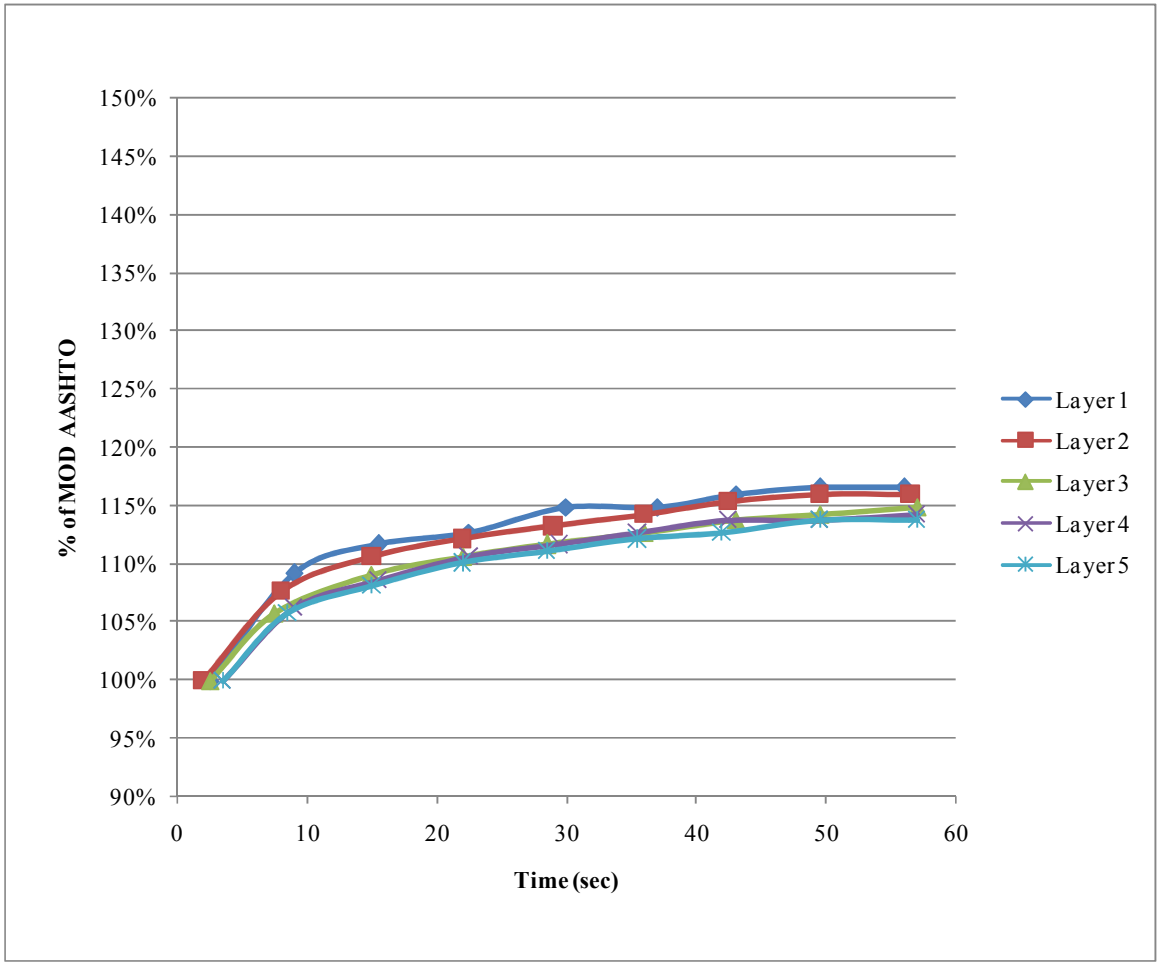

Figure B - 66: Compaction Profile for 3kg Tamper, 20kg Surcharge and 80% OMC – G4SFR

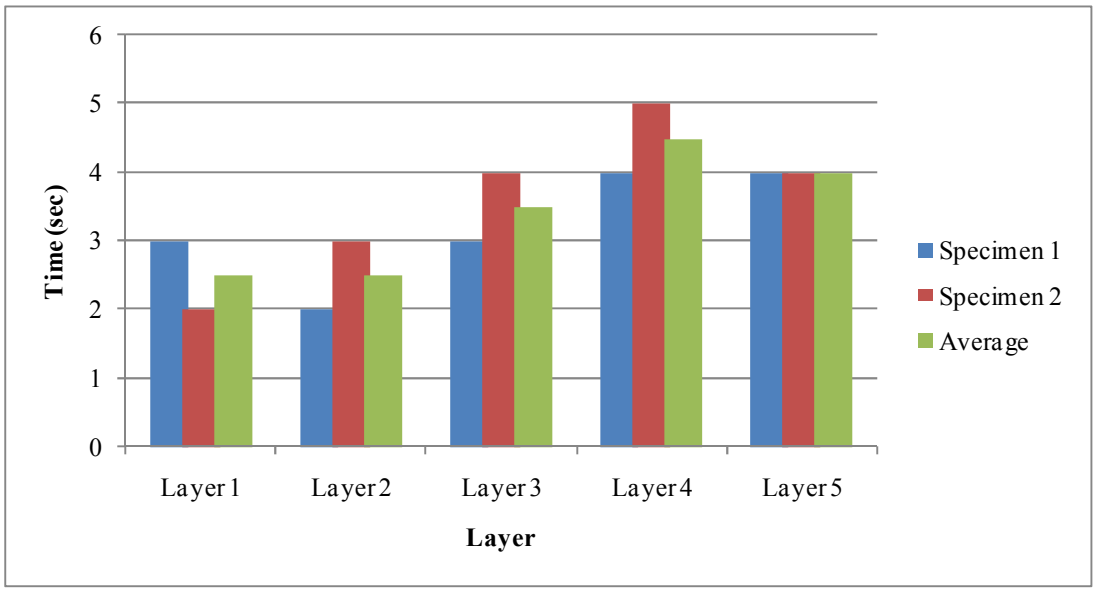

Figure B - 67: Compaction Time for 4.6kg Tamper, 20kg Surcharge and 80% OMC – G4SFR

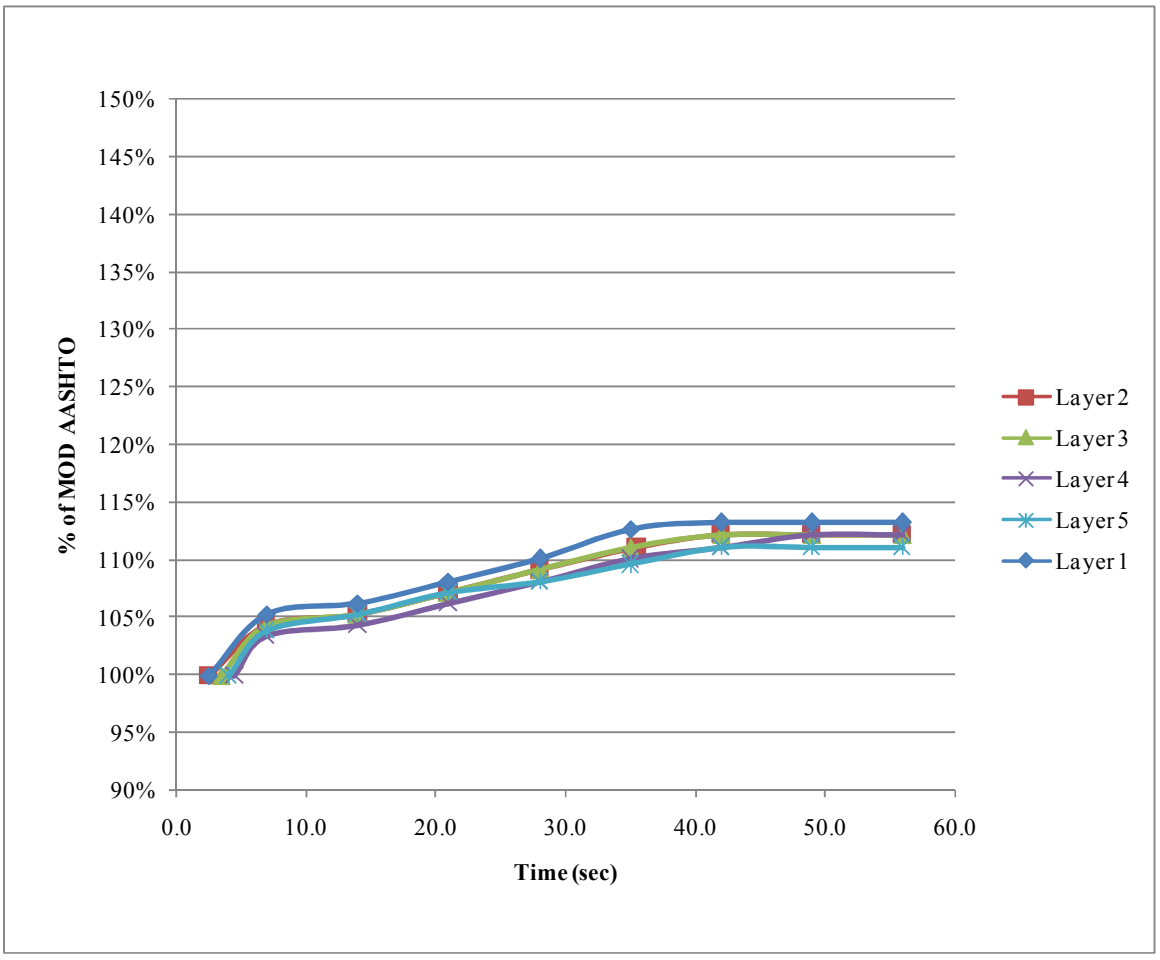

Figure B - 68: Compaction Profile for 4.6kg Tamper, 20kg Surcharge and 80% OMC – G4SFR

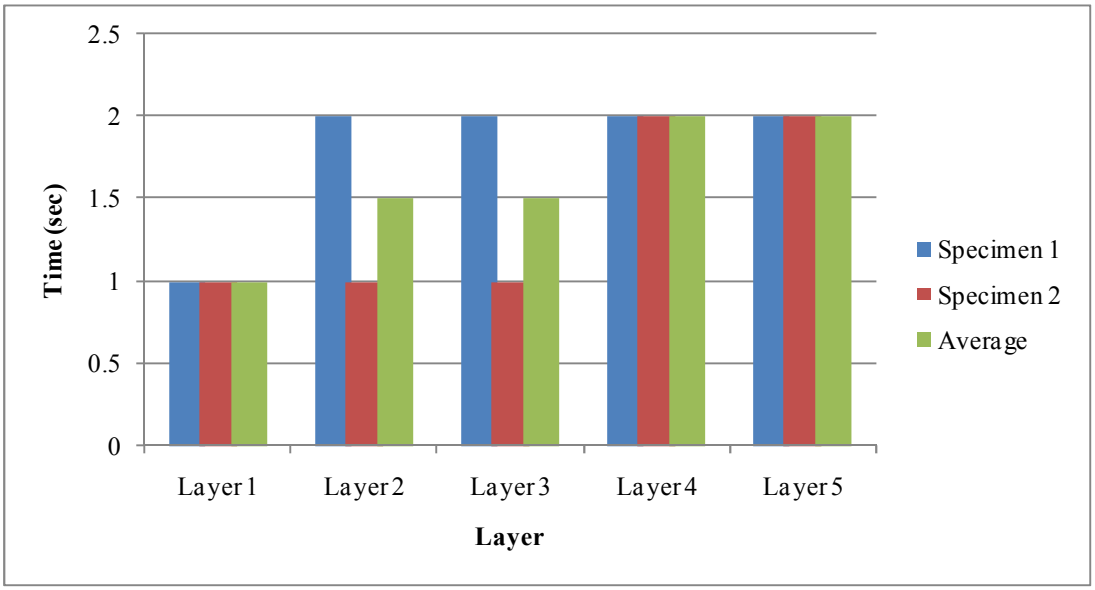

Figure B - 69: Compaction Time for 3kg Tamper, 10kg Surcharge and 90% OMC – G4SFR

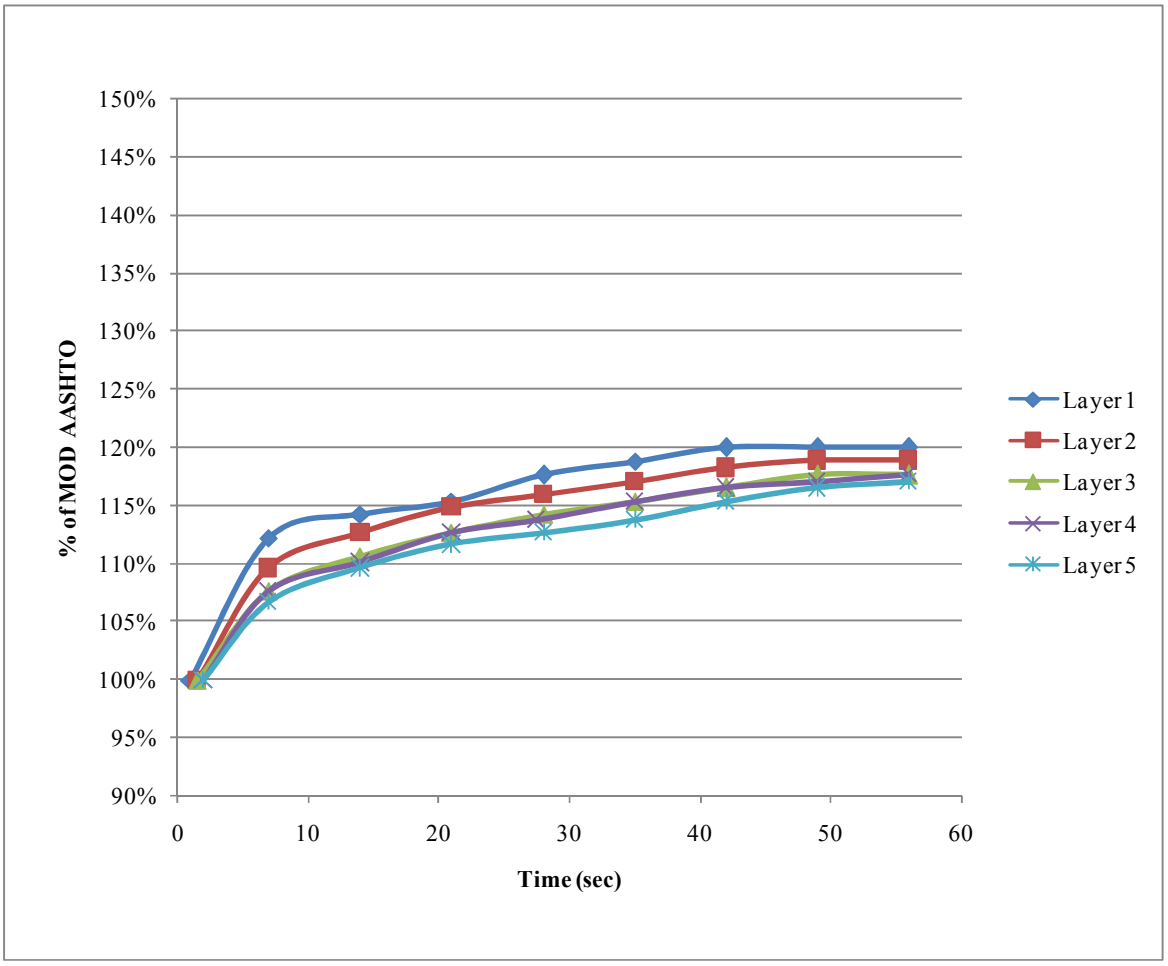

Figure B - 70: Compaction Profile for 3kg Tamper, 10kg Surcharge and 90% OMC – G4SFR

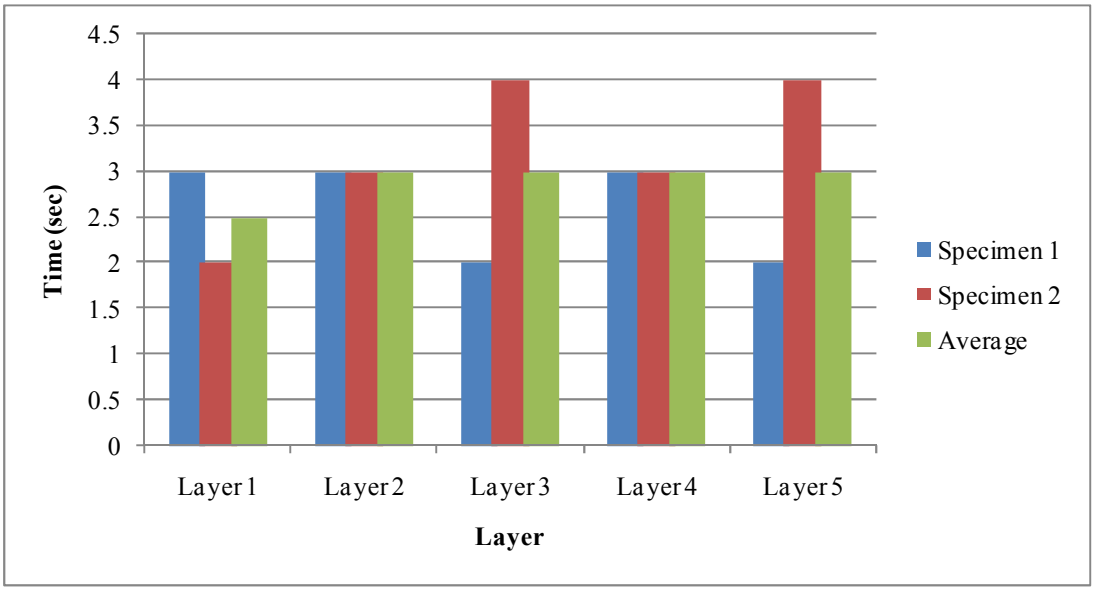

Figure B - 71: Compaction Time for 4.6kg Tamper, 10kg Surcharge and 90% OMC – G4SFR

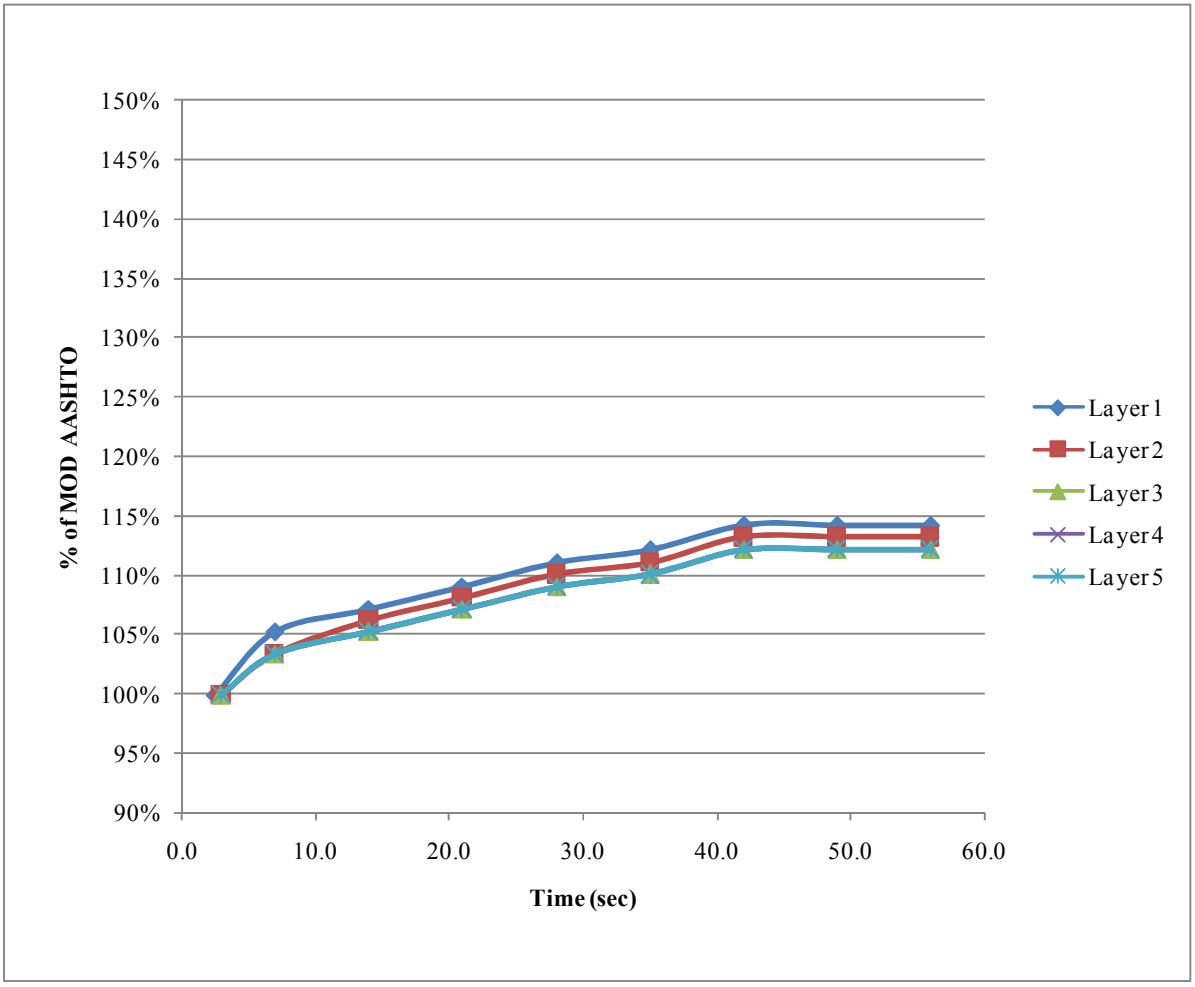

Figure B - 72: Compaction Profile for 4.6kg Tamper, 10kg Surcharge and 90% OMC – G4SFR

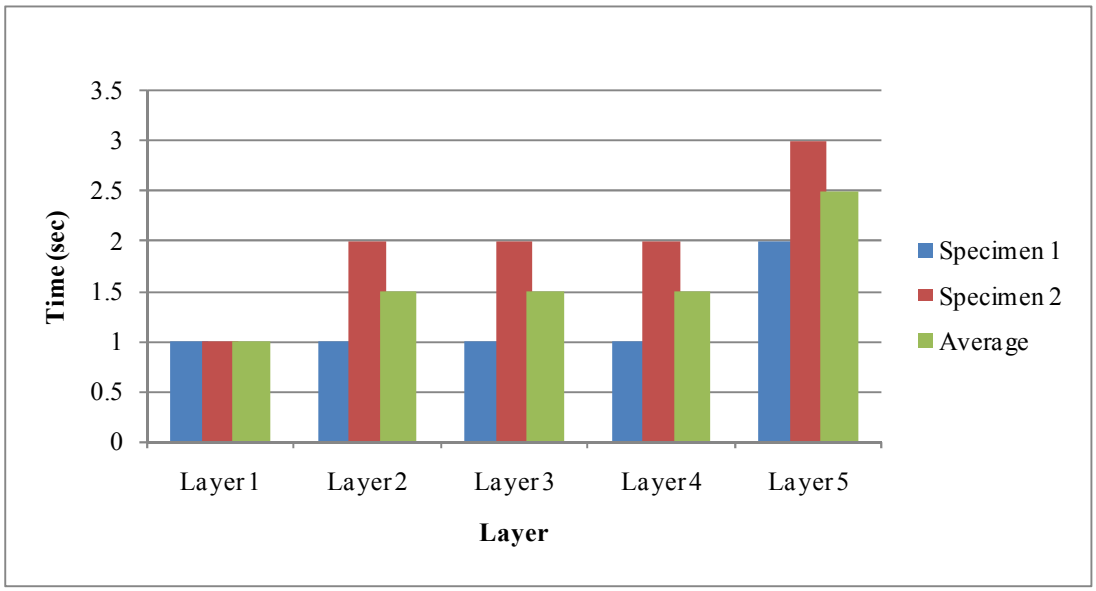

Figure B - 73: Compaction Time for 3kg Tamper, 20kg Surcharge and 90% OMC – G4SFR

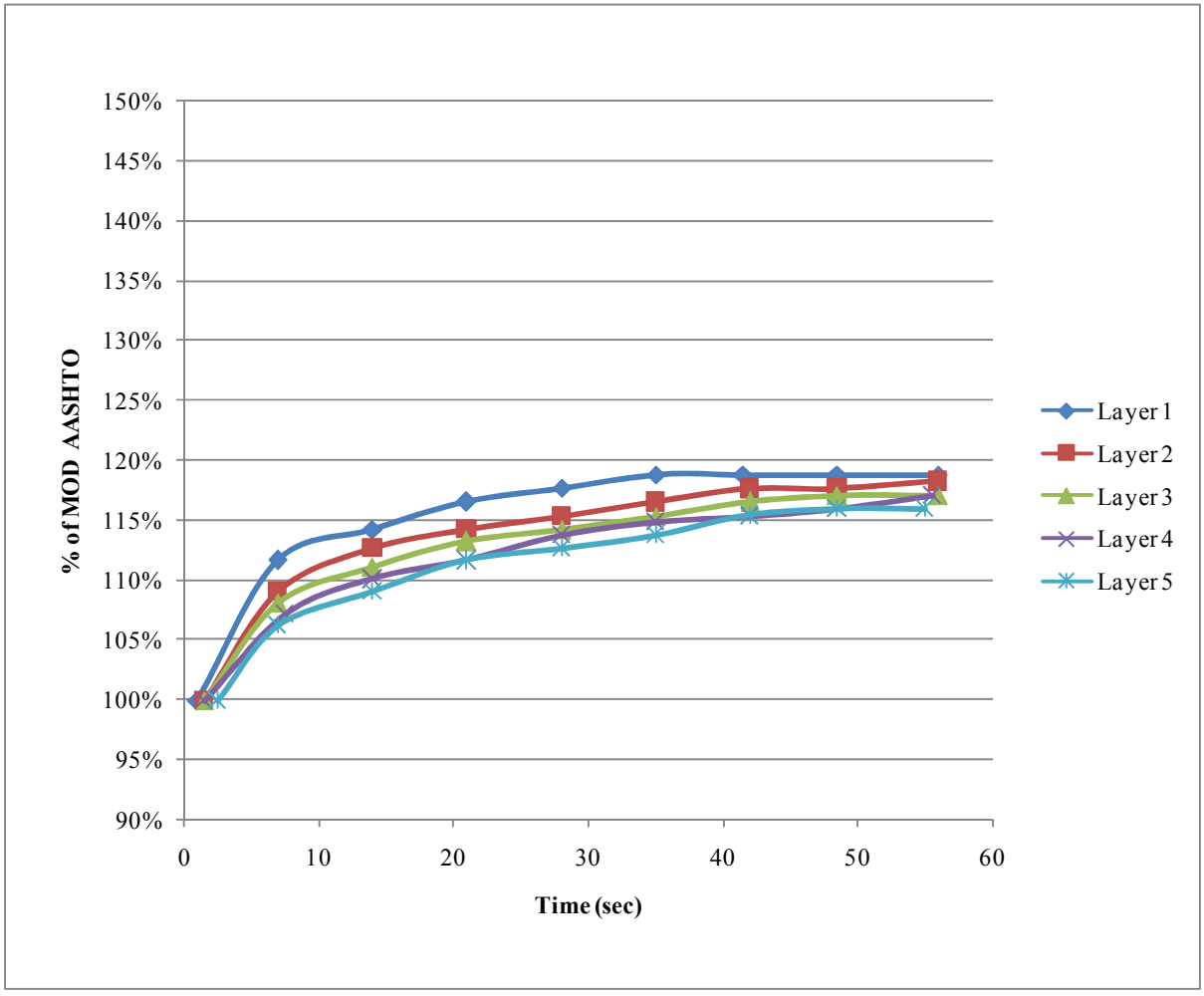

Figure B - 74: Compaction Profile for 3kg Tamper, 20kg Surcharge and 90% OMC – G4SFR

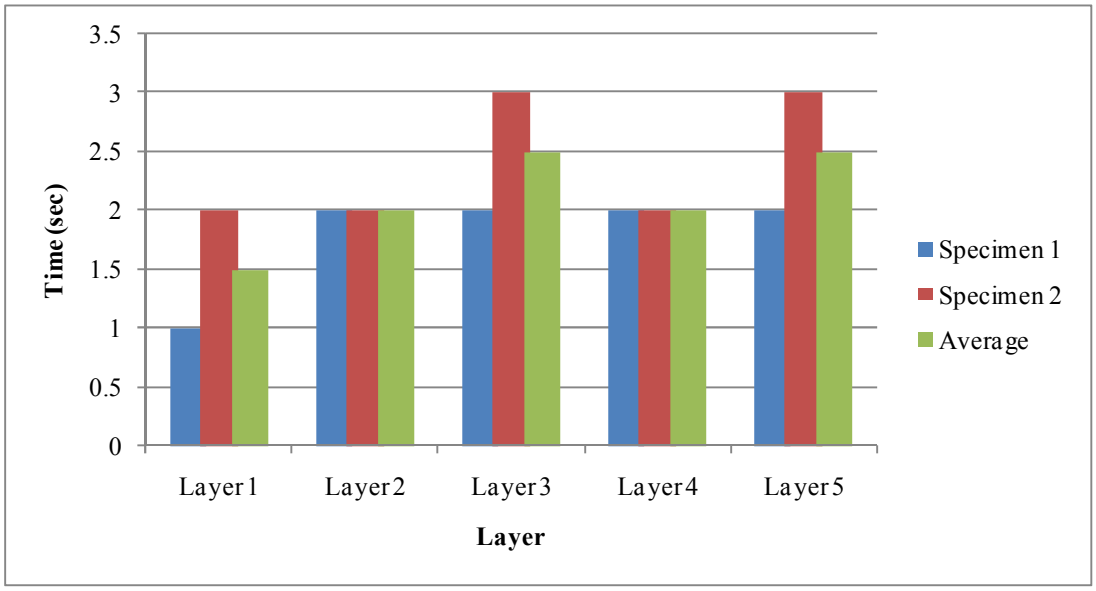

Figure B - 75: Compaction Time for 4.6kg Tamper, 20kg Surcharge and 90% OMC – G4SFR

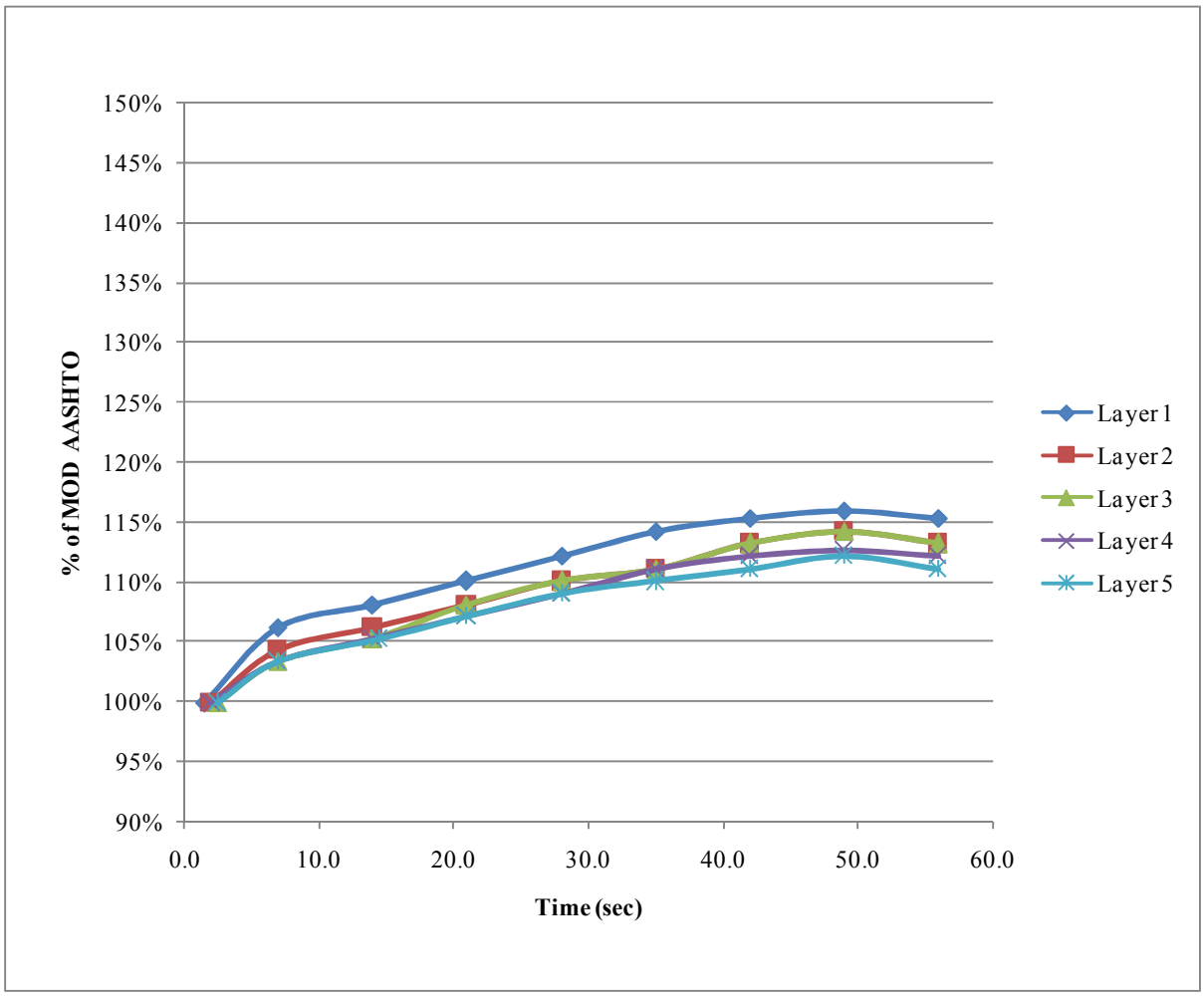

Figure B - 76: Compaction Profile for 4.6kg Tamper, 20kg Surcharge and 90% OMC – G4SFR

Effect of Moisture on Compaction Time – G4 (SFR)

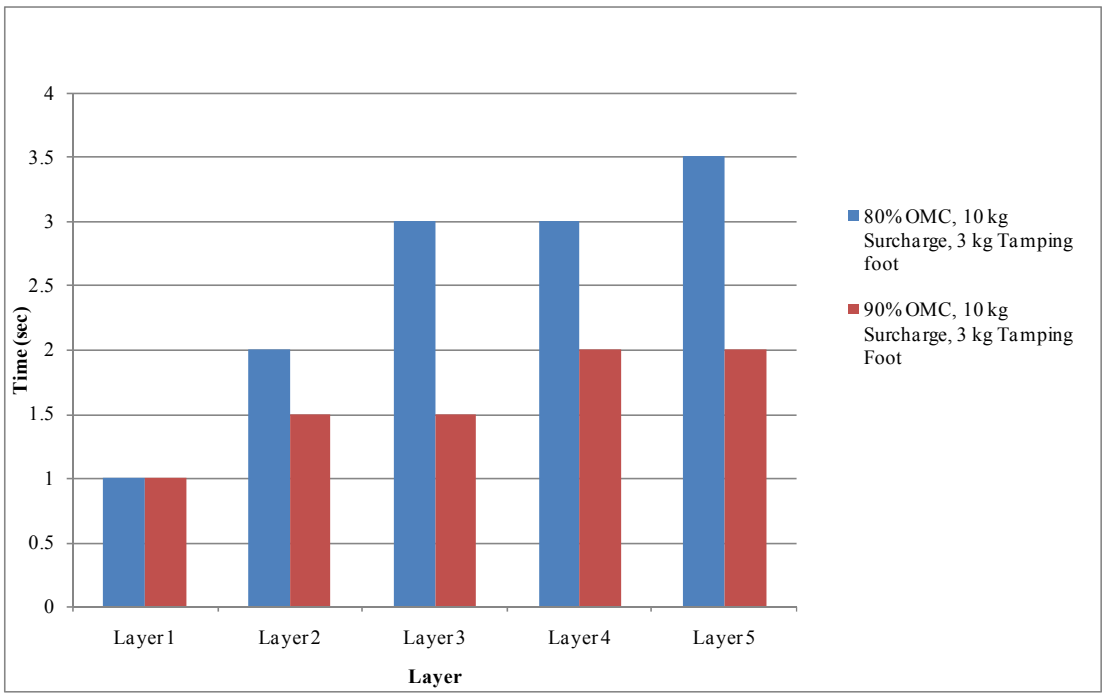

Figure B - 77: Effect of Moisture for 10kg Surcharge and 3kg Tamper – G4SFR

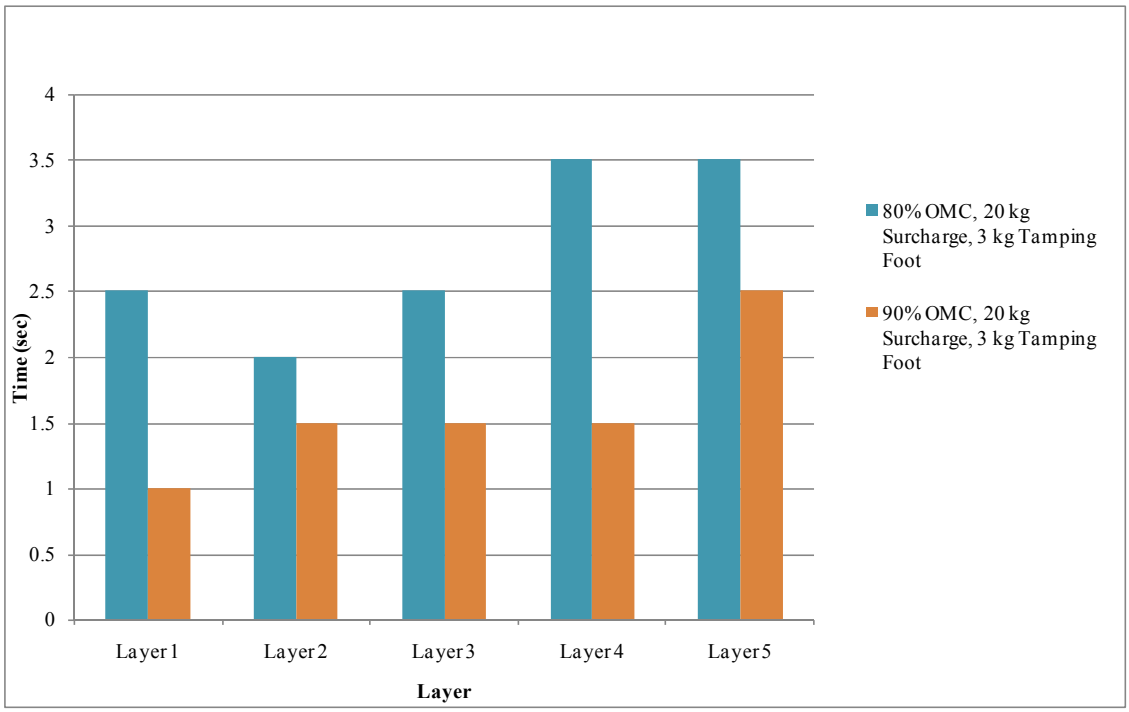

Figure B - 78: Effect of Moisture for 20kg Surcharge and 3kg Tamper – G4SFR

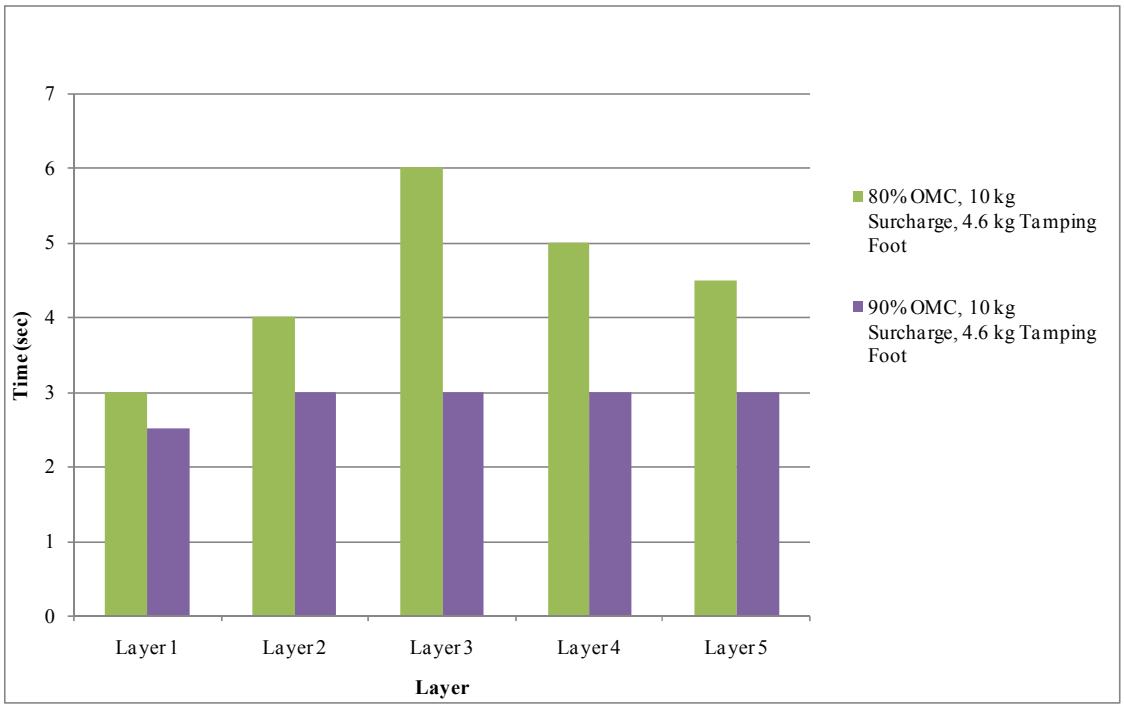

Figure B - 79: Effect of Moisture for 10kg Surcharge and 4.6kg Tamper – G4SFR

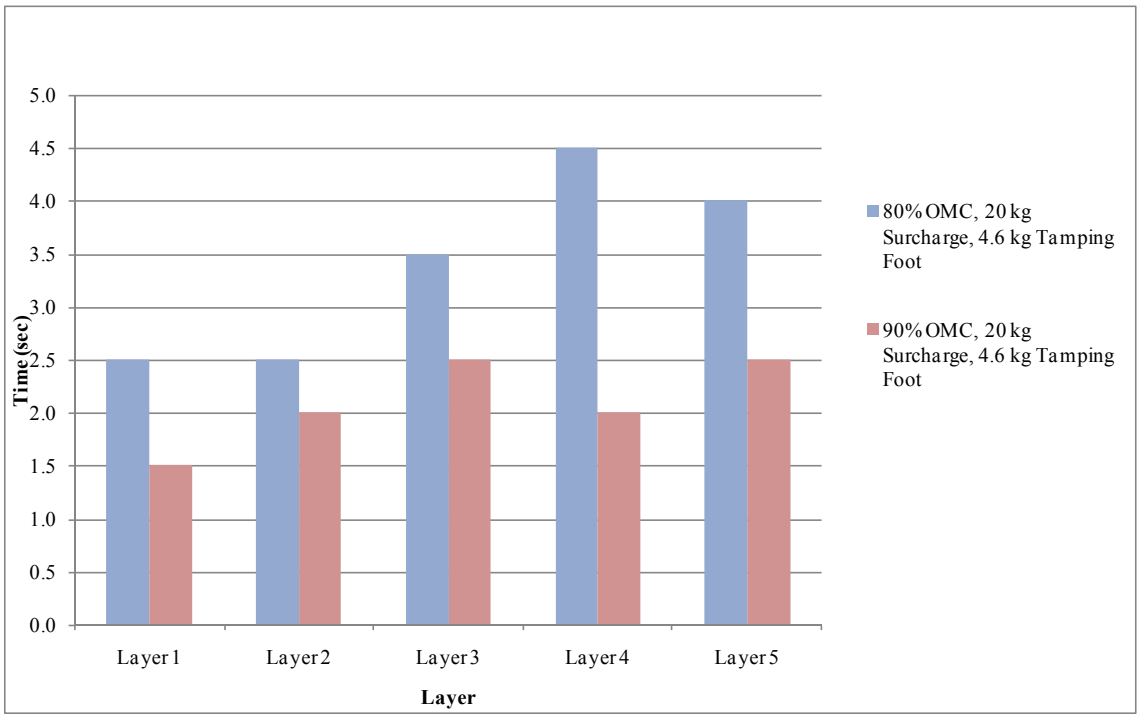

Figure B - 80: Effect of Moisture for 20kg Surcharge and 4.6kg Tamper – G4SFR

Effect of Tamping Foot on Compaction Time – G4 (SFR)

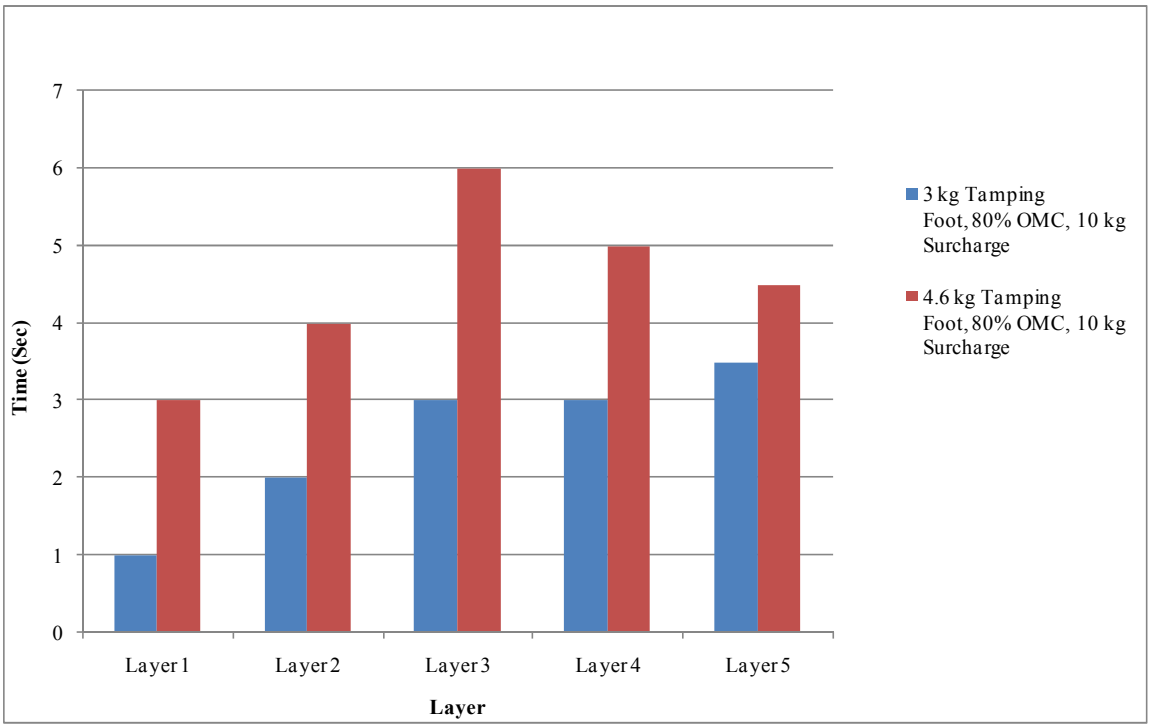

Figure B - 81: Effect of Tamper for 80% OMC and 10kg Surcharge – G4SFR

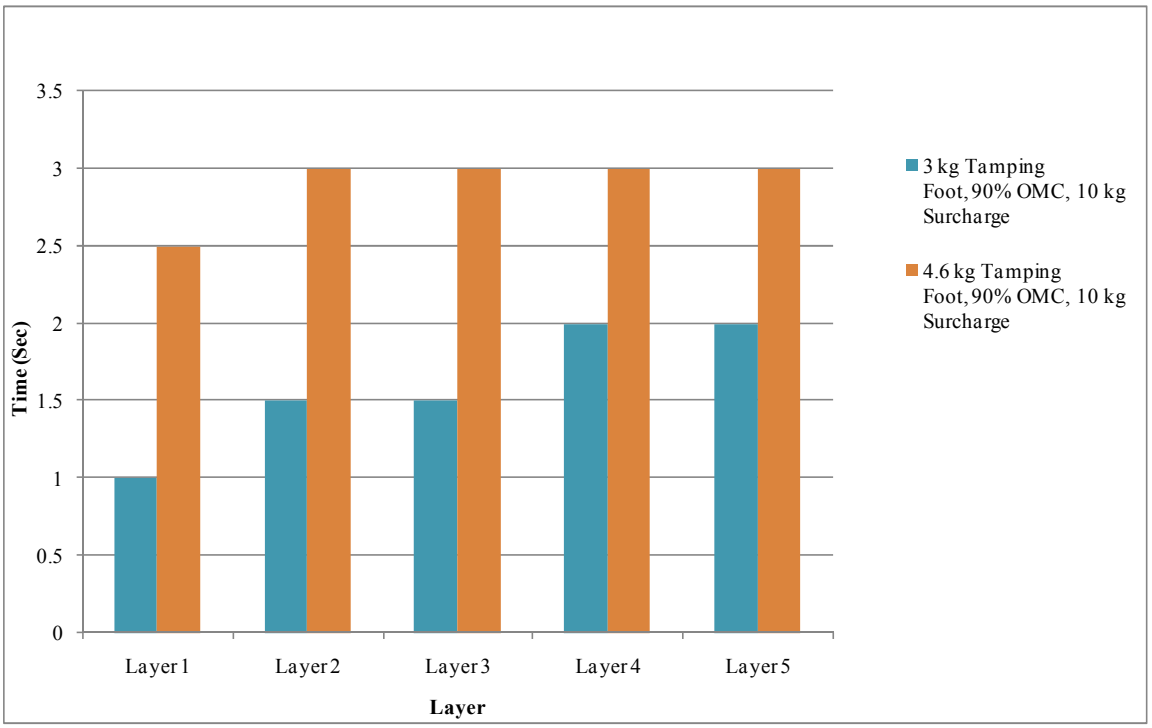

Figure B - 82: Effect of Tamper for 90% OMC and 10kg Surcharge – G4SFR

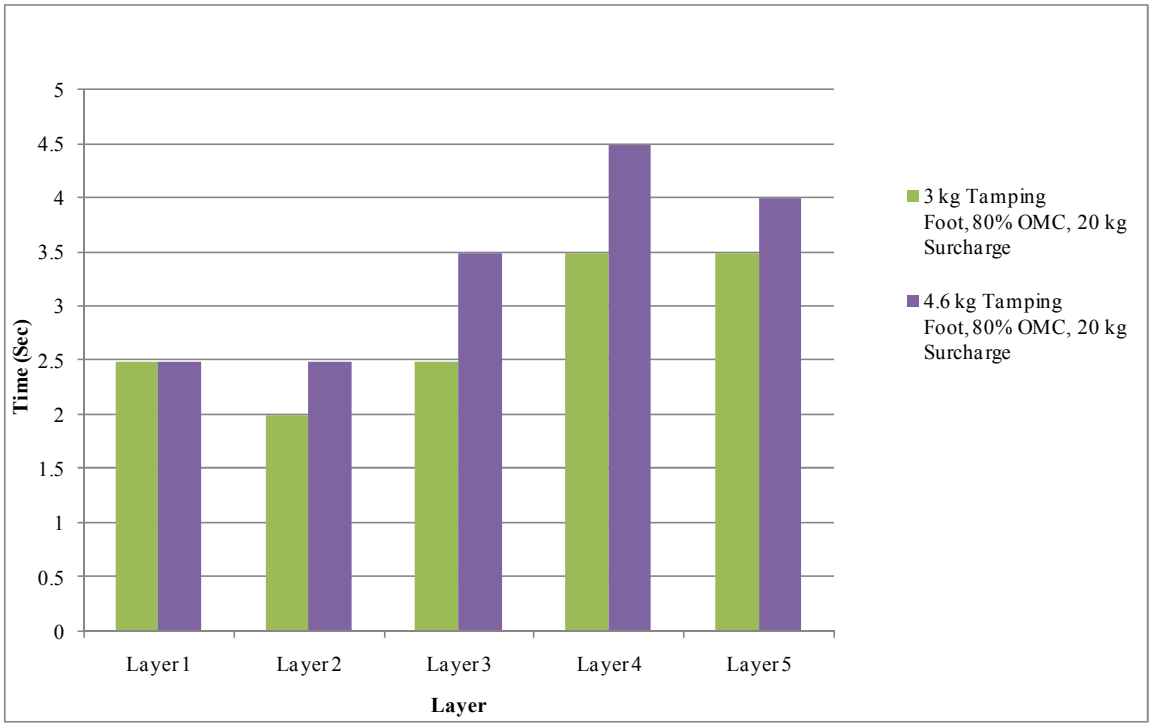

Figure B - 83: Effect of Tamper at 80% OMC and 20kg Surcharge – G4SFR

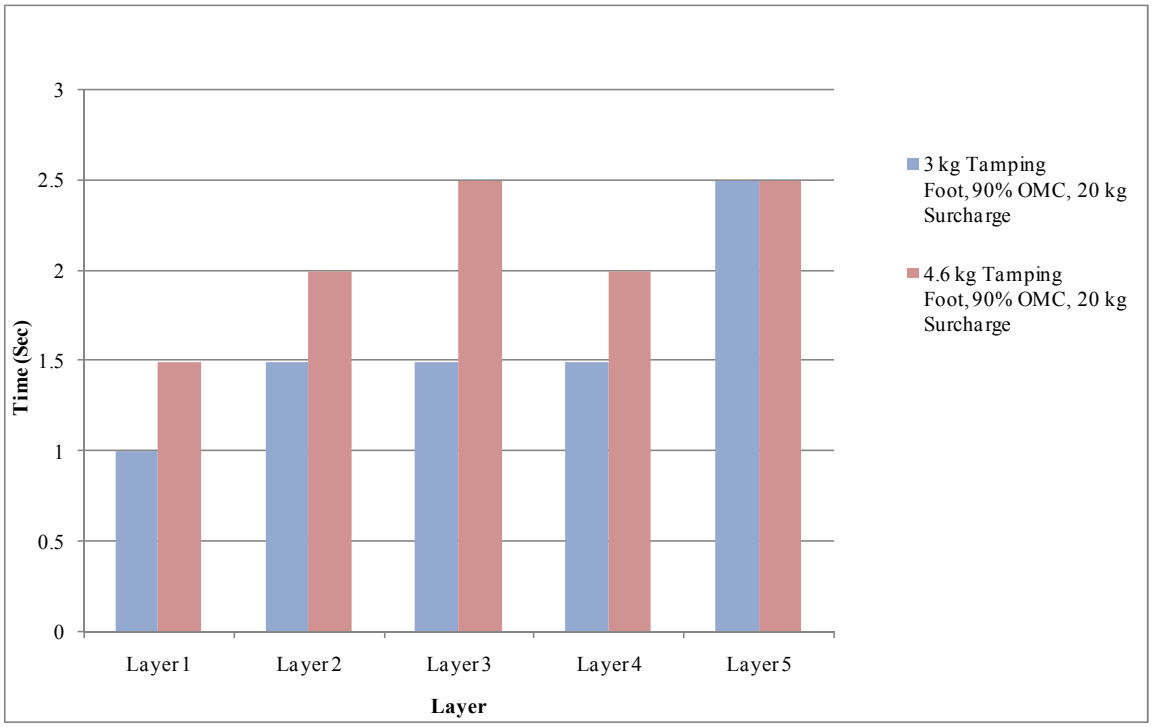

Figure B - 84: Effect of Tamper at 90% OMC and 20kg Surcharge – G4SFR

Effect of Surcharge Load on Compaction Time – G4 (SFR)

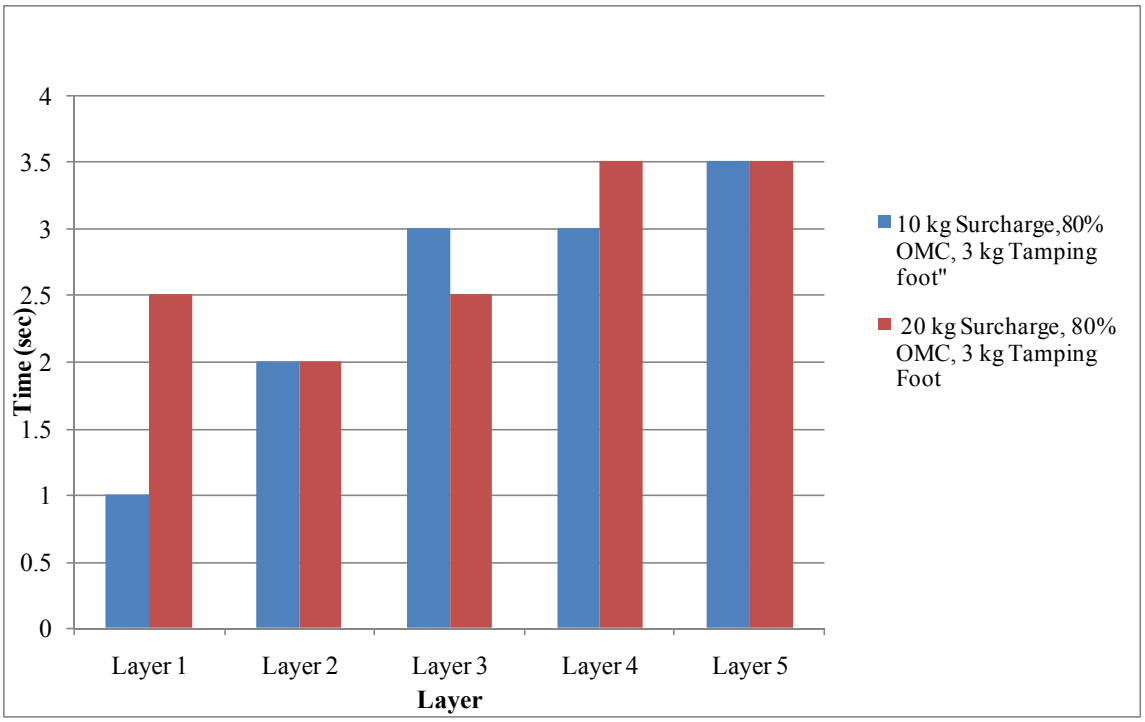

Figure B - 85: Effect of Surcharge Load at 80% OMC and 3kg Tamper – G4SFR

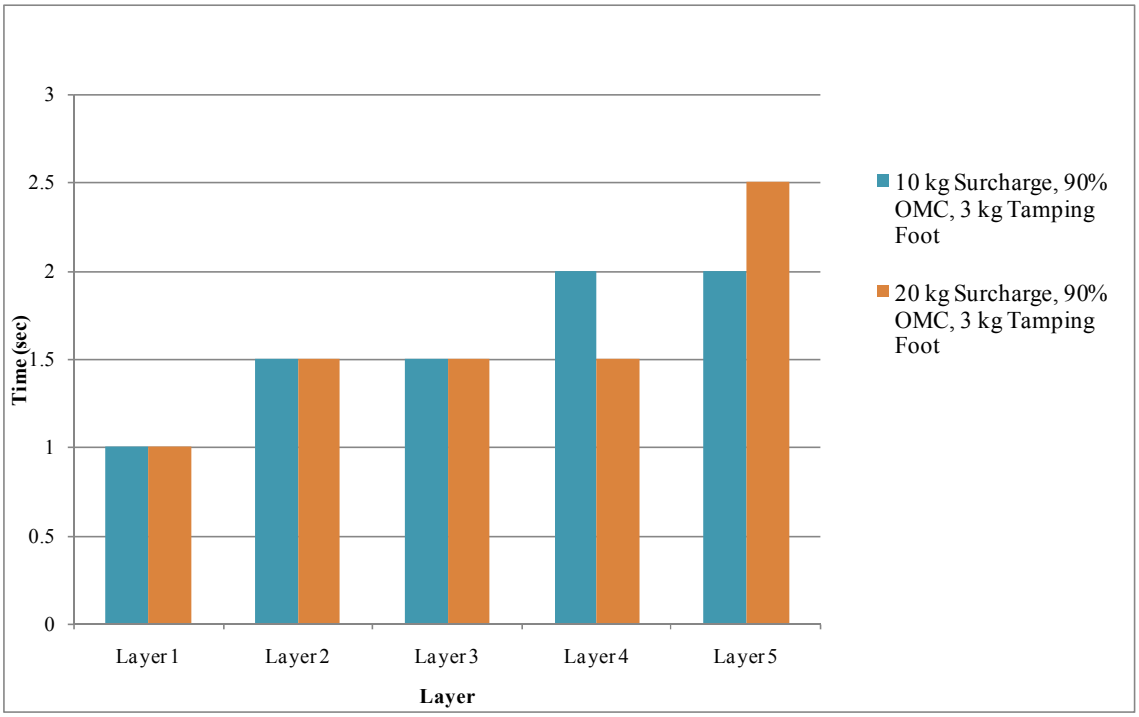

Figure B - 86: Effect of Surcharge Load at 90% OMC and 3kg Tamper – G4SFR

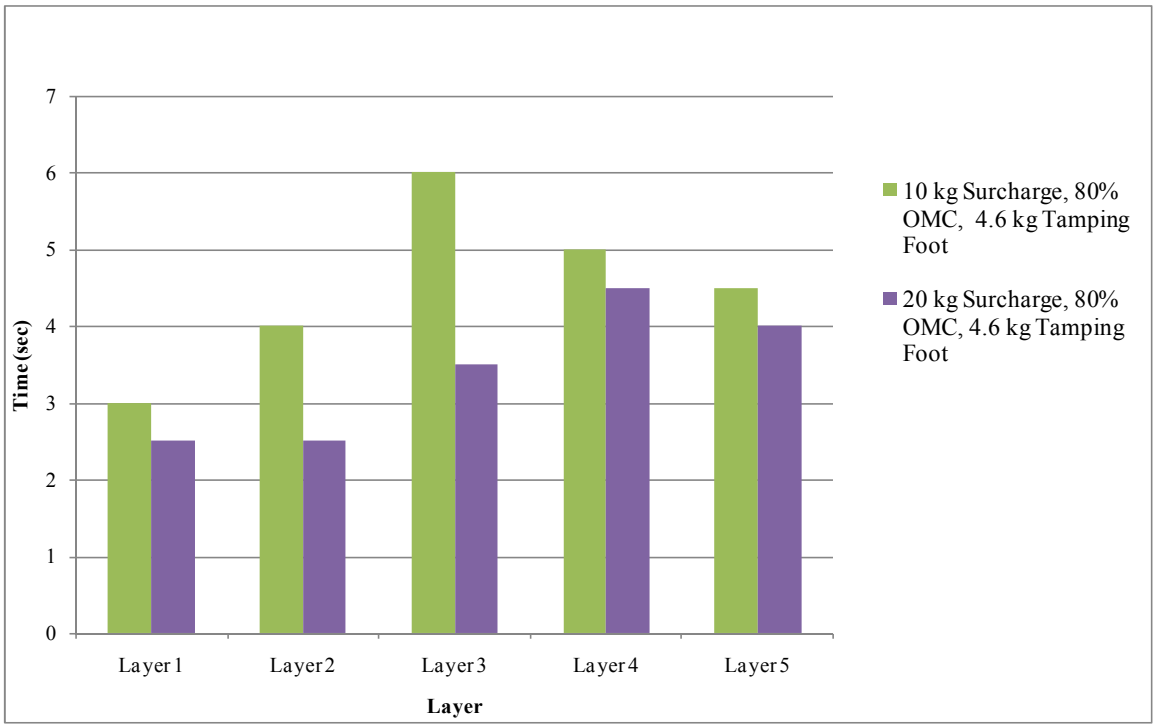

Figure B - 87: Effect of Surcharge Load at 80% OMC and 4.6kg Tamper – G4SFR

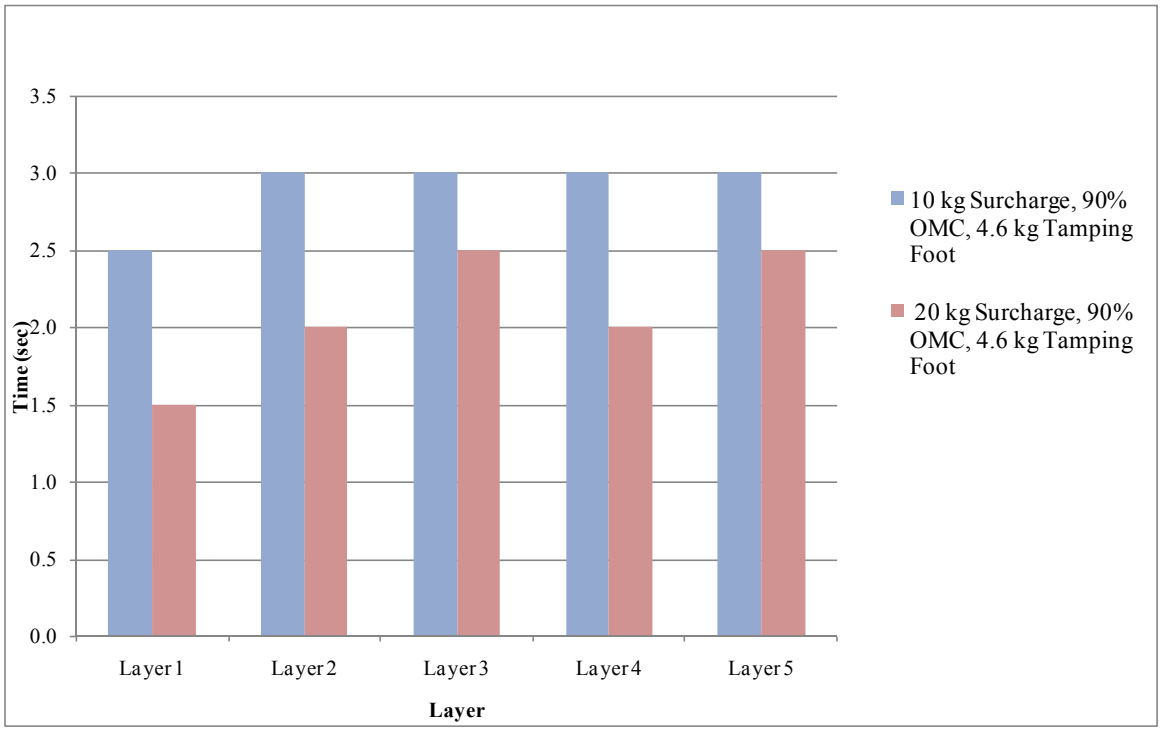

Figure B - 88: Effect of Surcharge Load at 90% OMC and 4.6kg Tamper – G4SFR

APPENDIX F: Test results for G4 material/vibratory hammer compaction/rigid frame

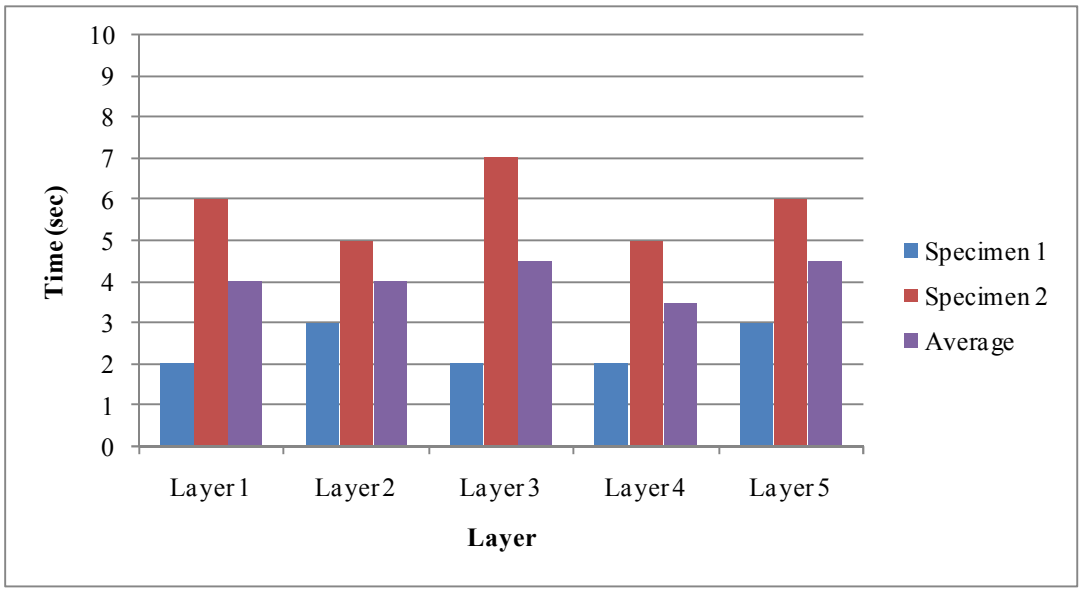

Figure B - 89: Compaction Time for 3kg Tamper, 5kg Surcharge and 80% OMC – G4RFR

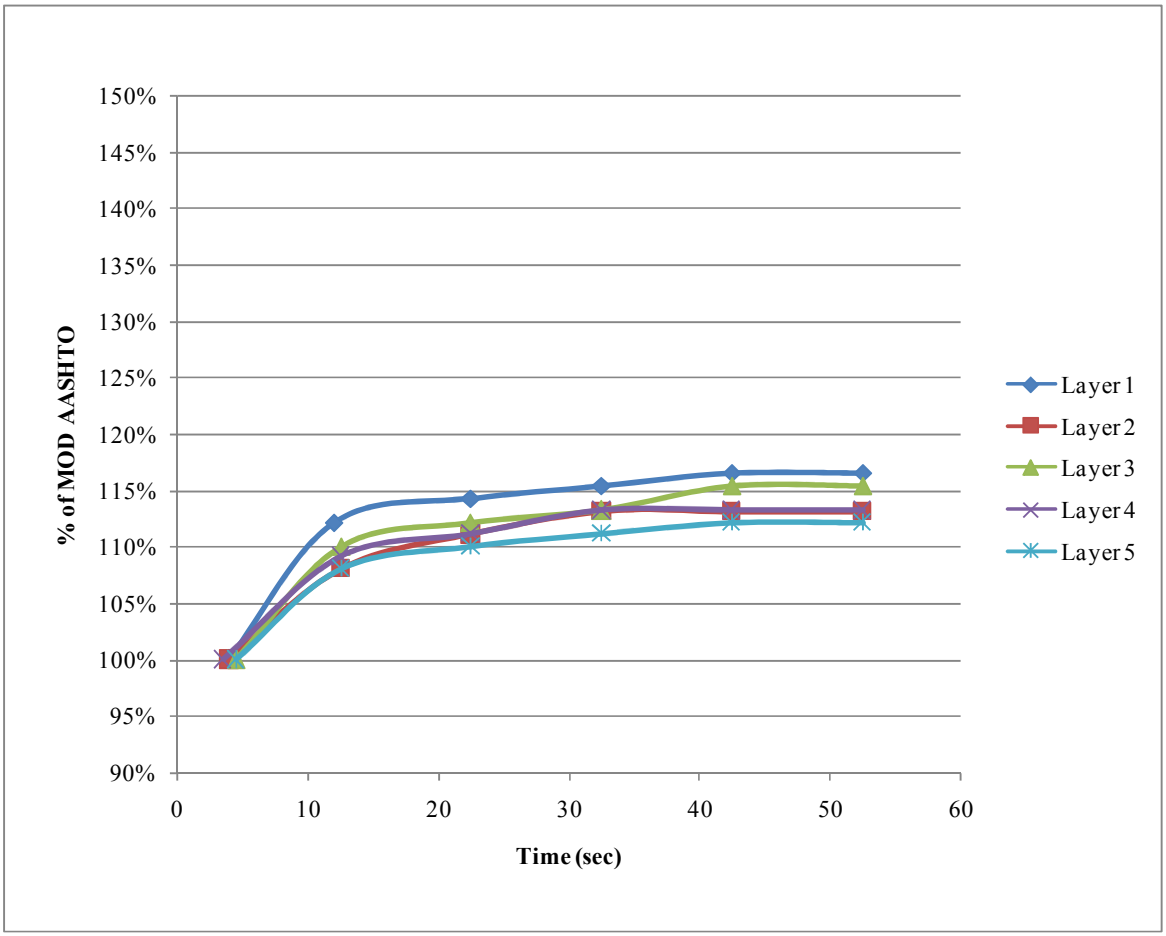

Figure B - 90: Compaction Profile for 3kg Tamper, 5kg Surcharge and 80% OMC – G4RFR

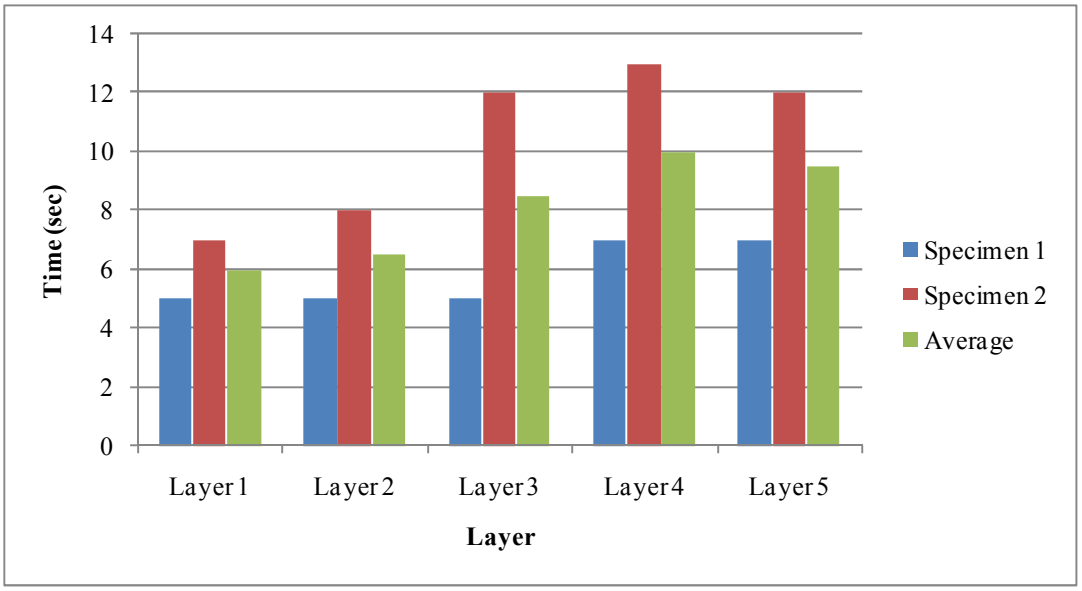

Figure B - 91: Compaction Time for 4.6kg Tamper, 5kg Surcharge and 80% OMC – G4RFR

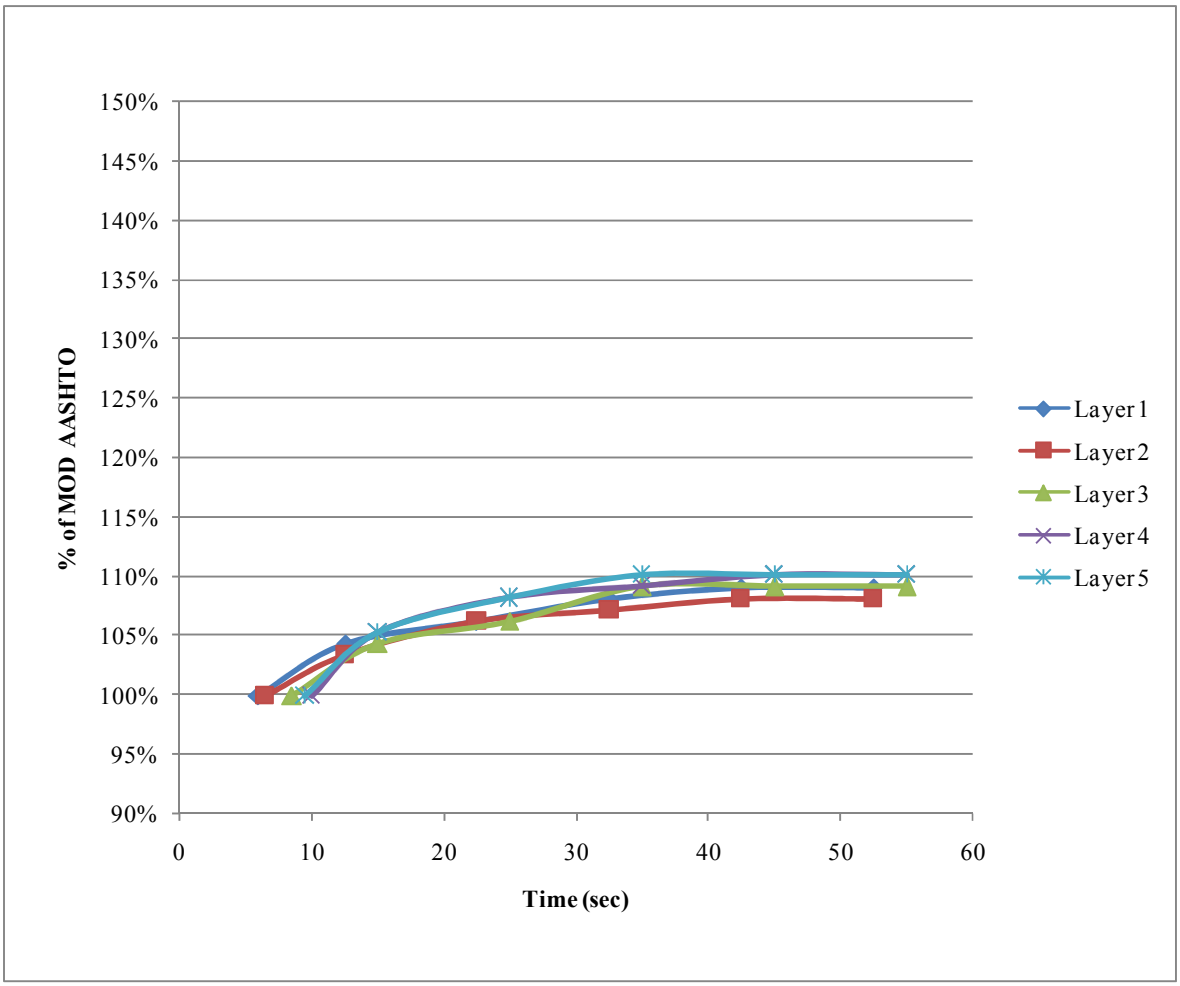

Figure B - 92: Compaction Profile for 4.6kg Tamper, 5kg Surcharge and 80% OMC – G4RFR

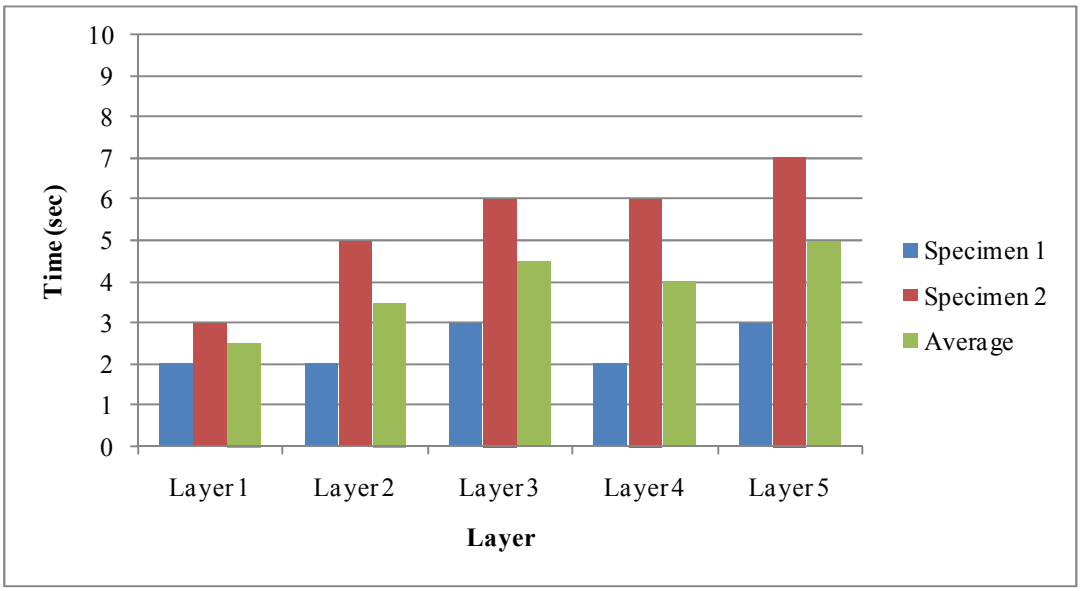

Figure B - 93: Compaction Time for 3kg Tamper, 15kg Surcharge and 80% OMC – G4RFR

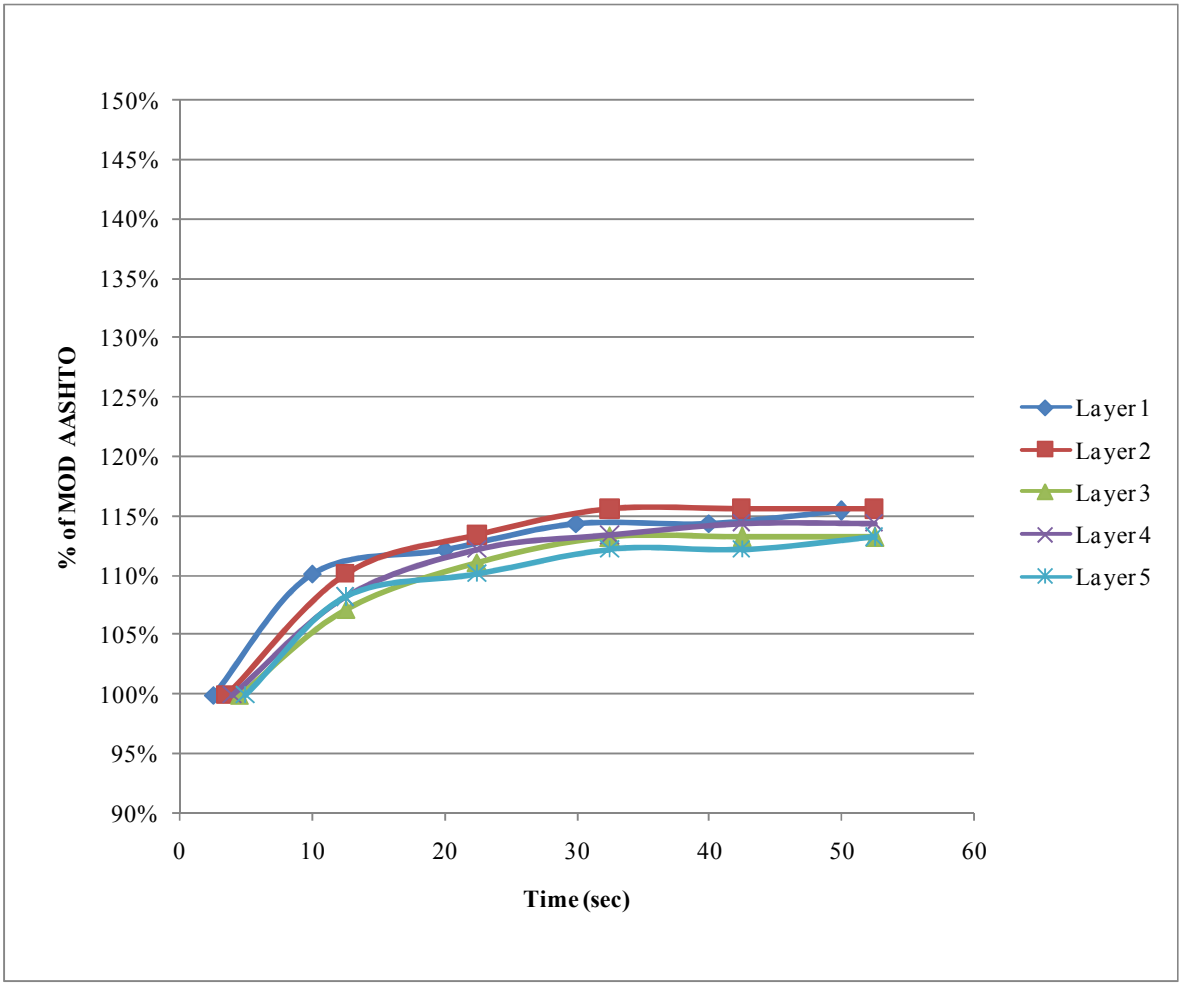

Figure B - 94: Compaction Profile for 3kg Tamper, 15kg Surcharge and 80% OMC – G4RFR

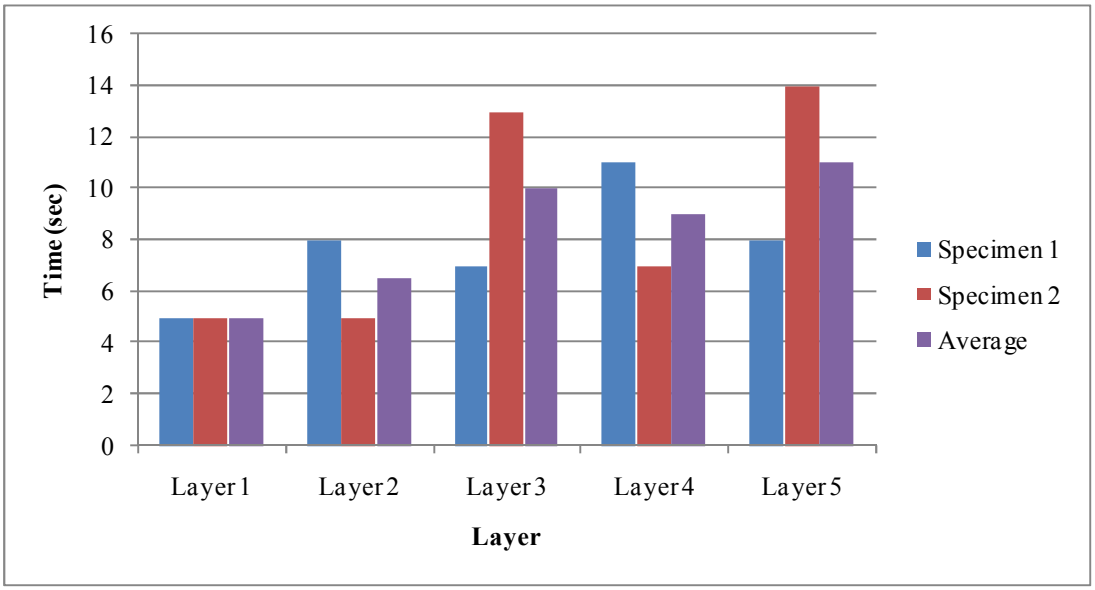

Figure B - 95: Compaction Time for 4.6kg Tamper, 15kg Surcharge and 80% OMC – G4RFR

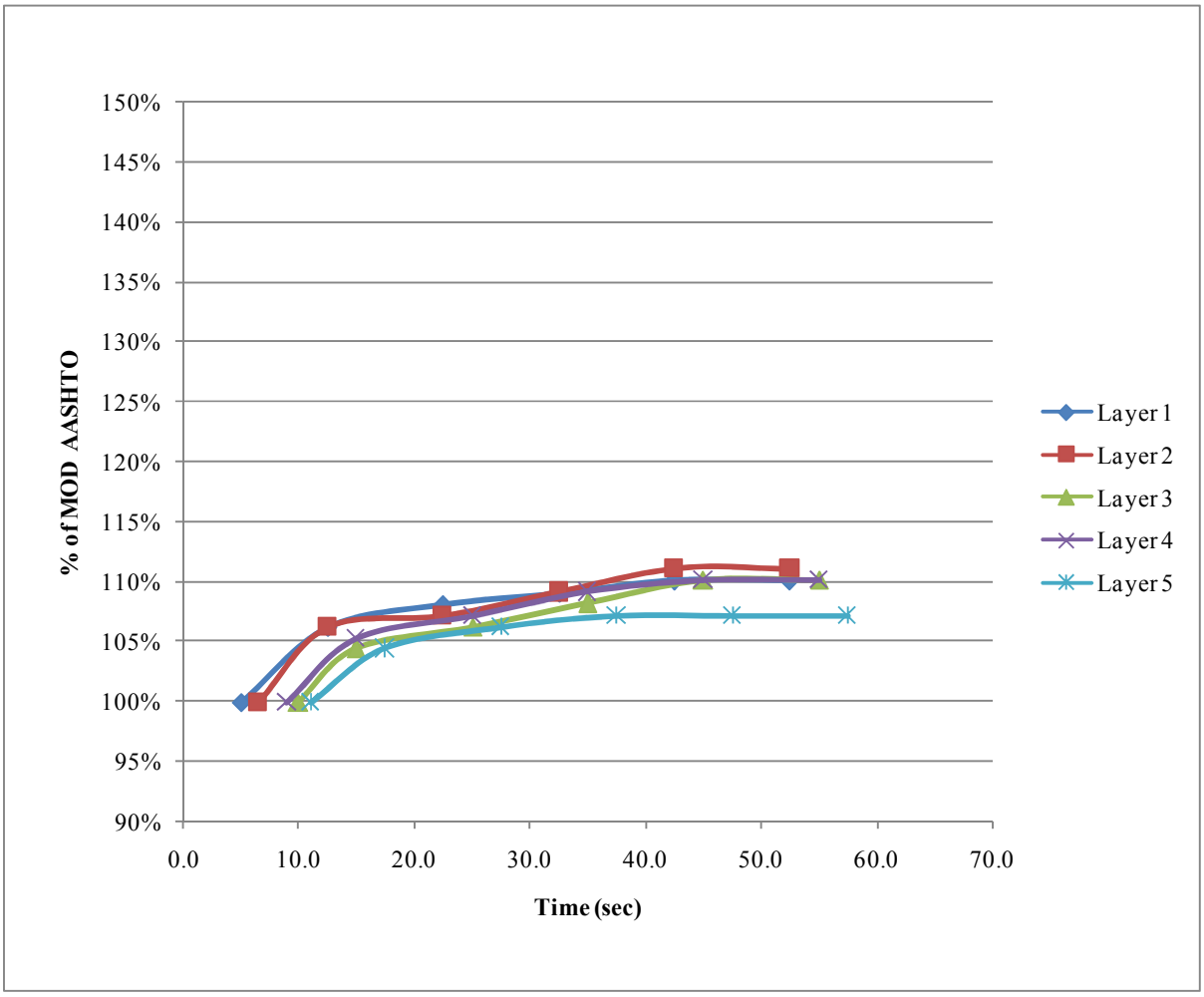

Figure B - 96: Compaction Profile for 4.6kg Tamper, 15kg Surcharge and 80% OMC – G4RFR

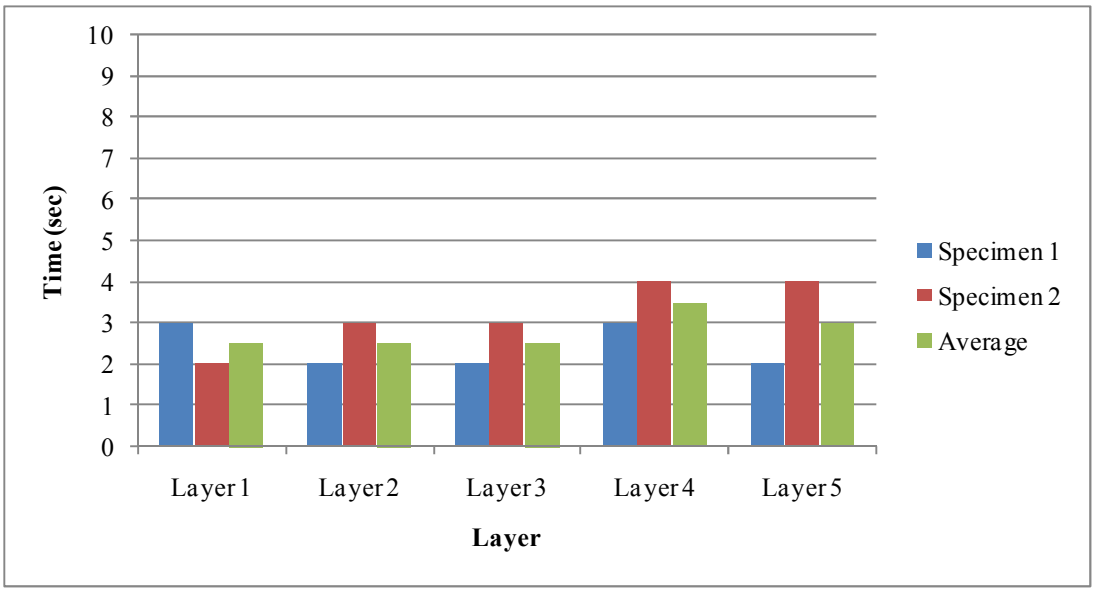

Figure B - 97: Compaction Time for 3kg Tamper, 5kg Surcharge and 90% OMC – G4RFR

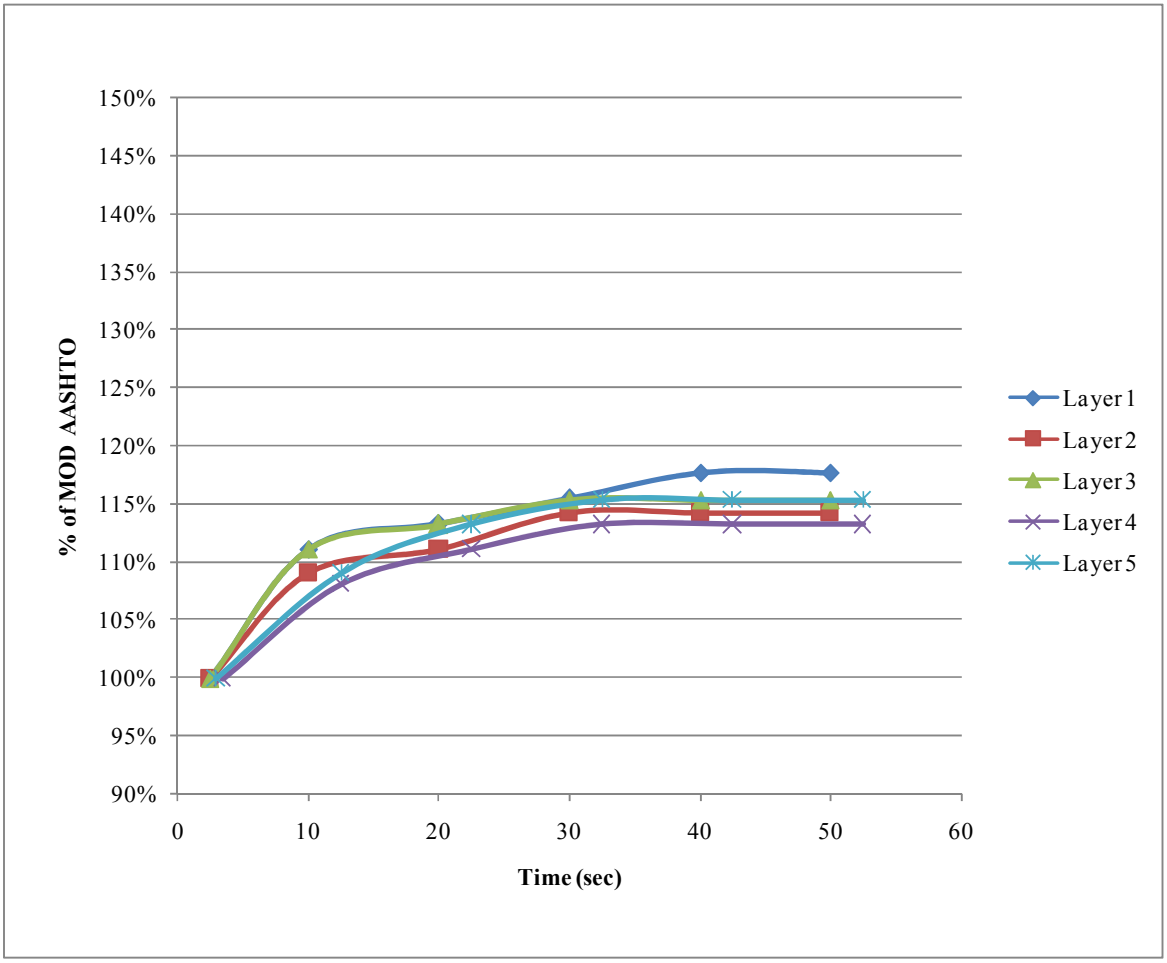

Figure B - 98: Compaction Profile for 3kg Tamper, 5kg Surcharge and 90% OMC – G4RFR

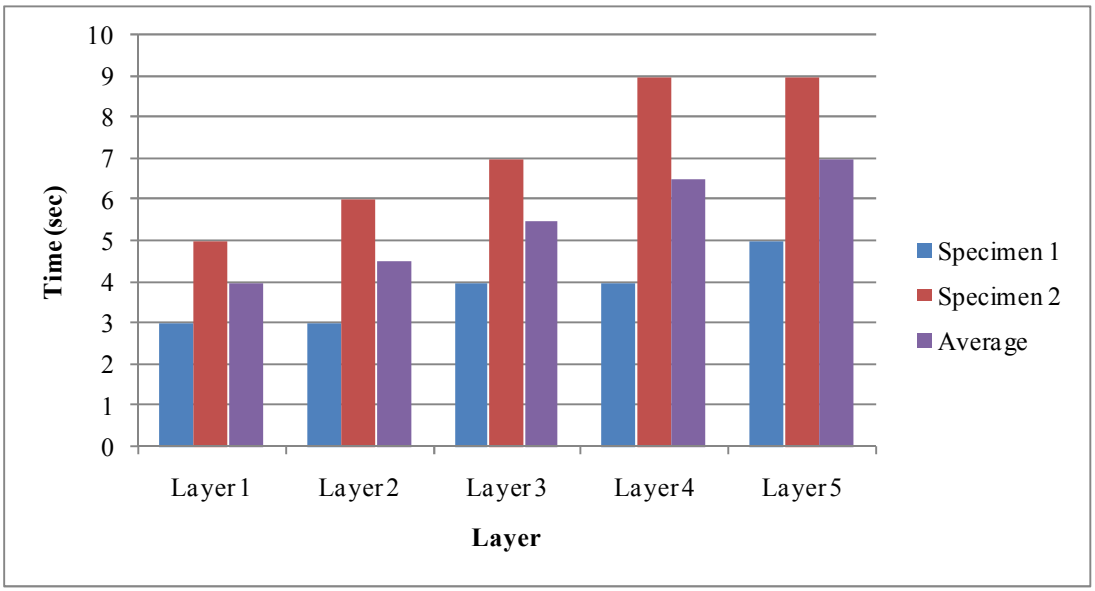

Figure B - 99: Compaction Time for 4.6kg Tamper, 5kg Surcharge and 90% Moisture – G4RFR

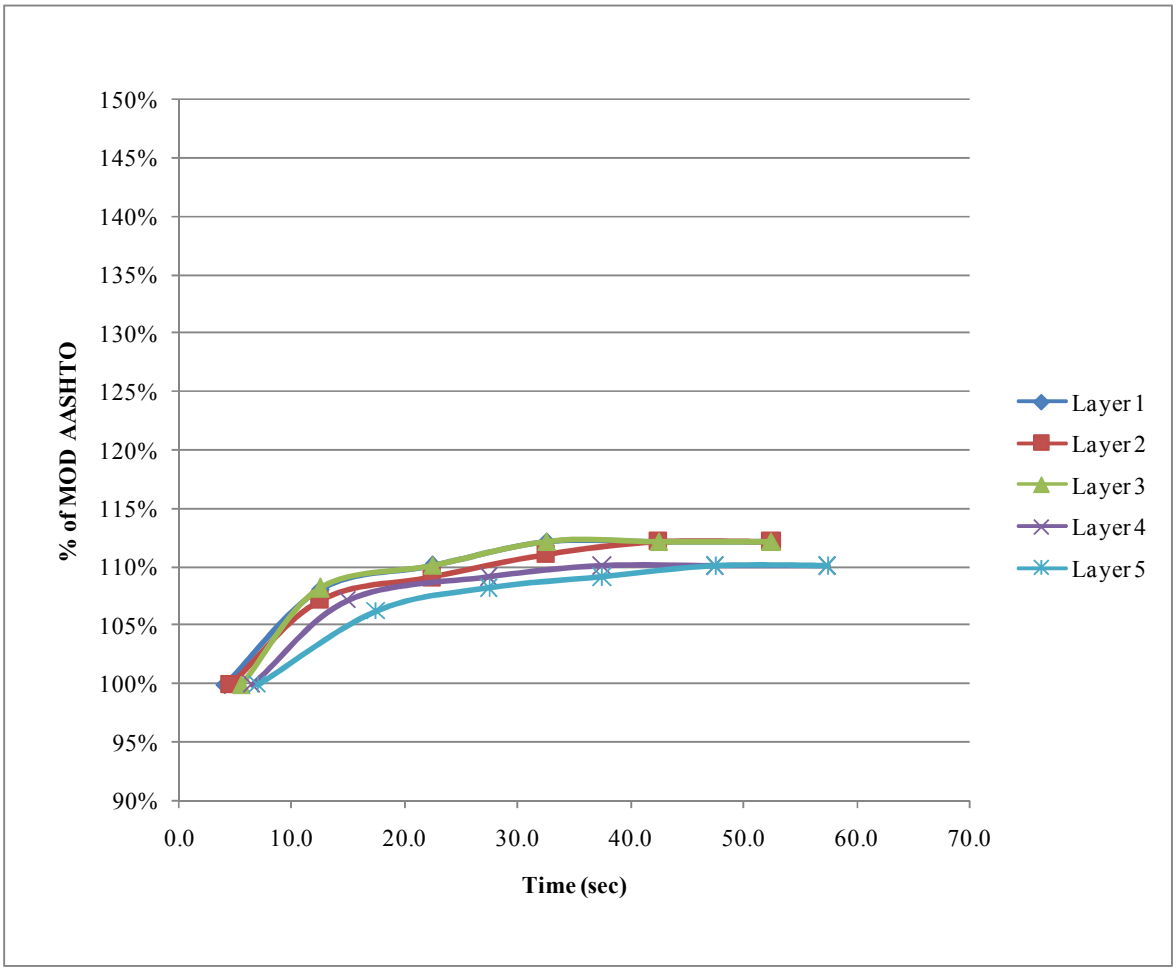

Figure B - 100: Compaction Profile for 4.6kg Tamper, 5kg Surcharge and 90% OMC – G4RFR

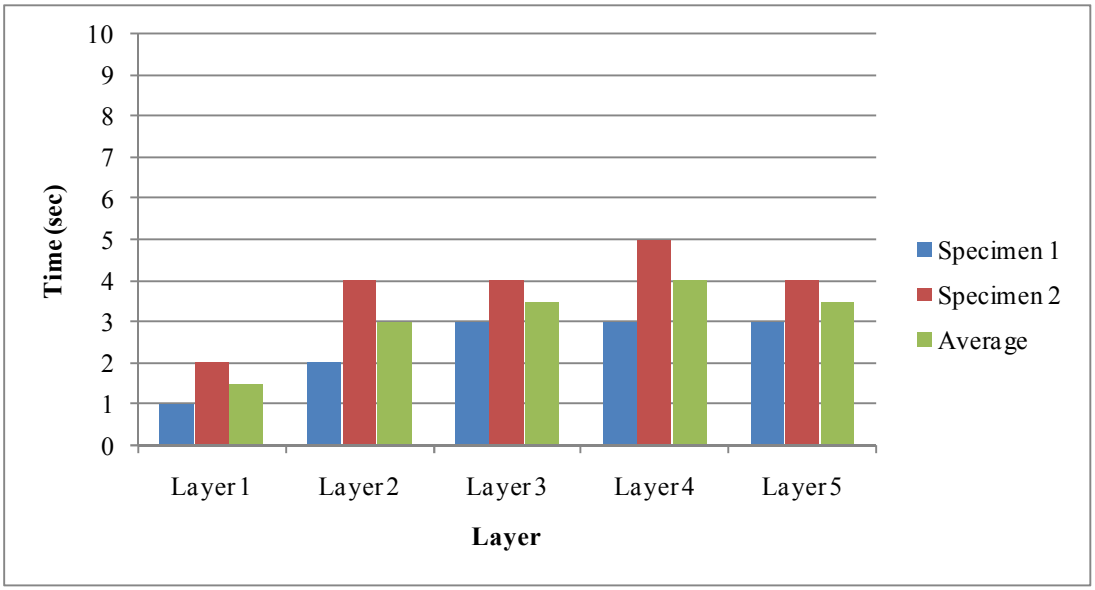

Figure B - 101: Compaction Time for 3kg Tamper, 15kg Surcharge and 90% OMC – G4RFR

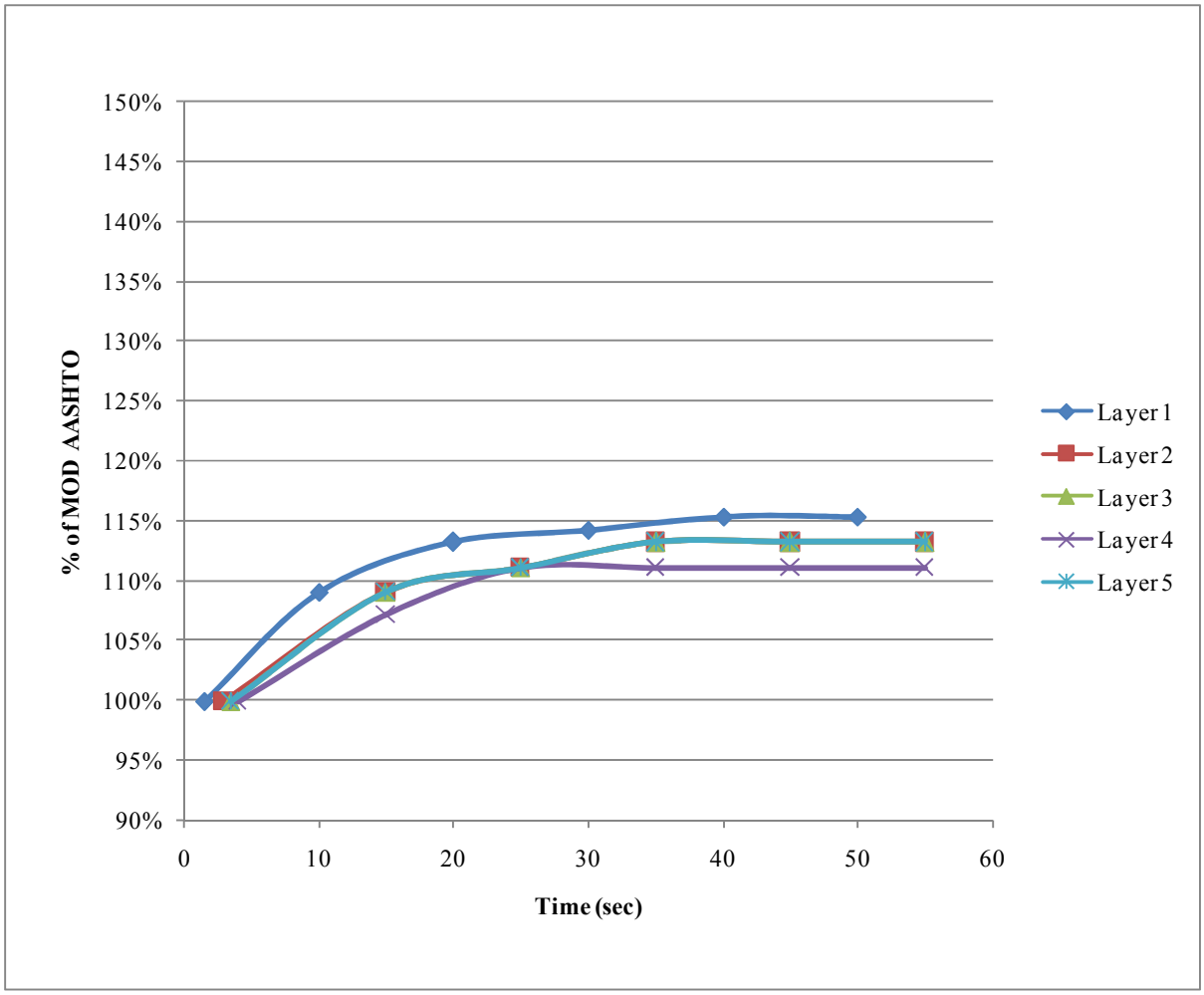

Figure B - 102: Compaction Profile for 3kg Tamper, 15kg Surcharge and 90% OMC – G4RFR

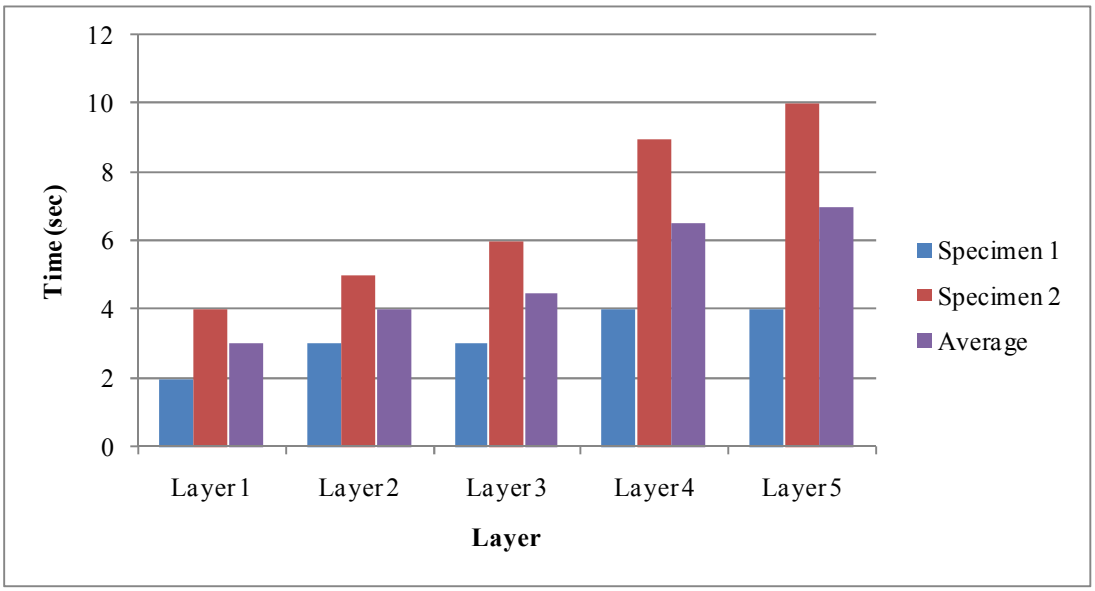

Figure B - 103: Compaction Time for 4.6kg Tamper, 15kg Surcharge and 90% OMC – G4RFR

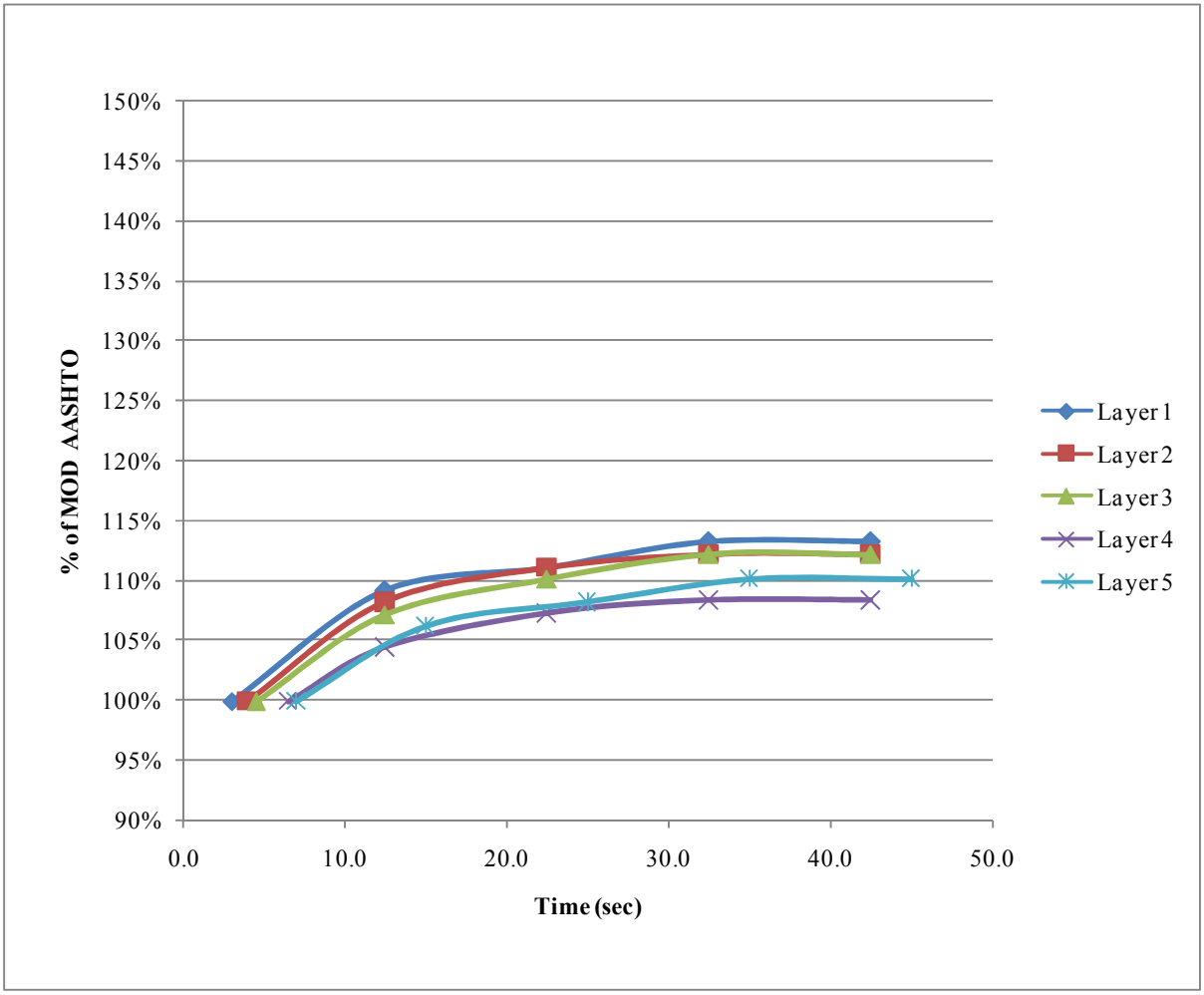

Figure B - 104: Compaction Profile for 4.6kg Tamper, 15kg Surcharge and 90% OMC – G4RFR

Effect of Moisture on Compaction Time – G4 (RFR)

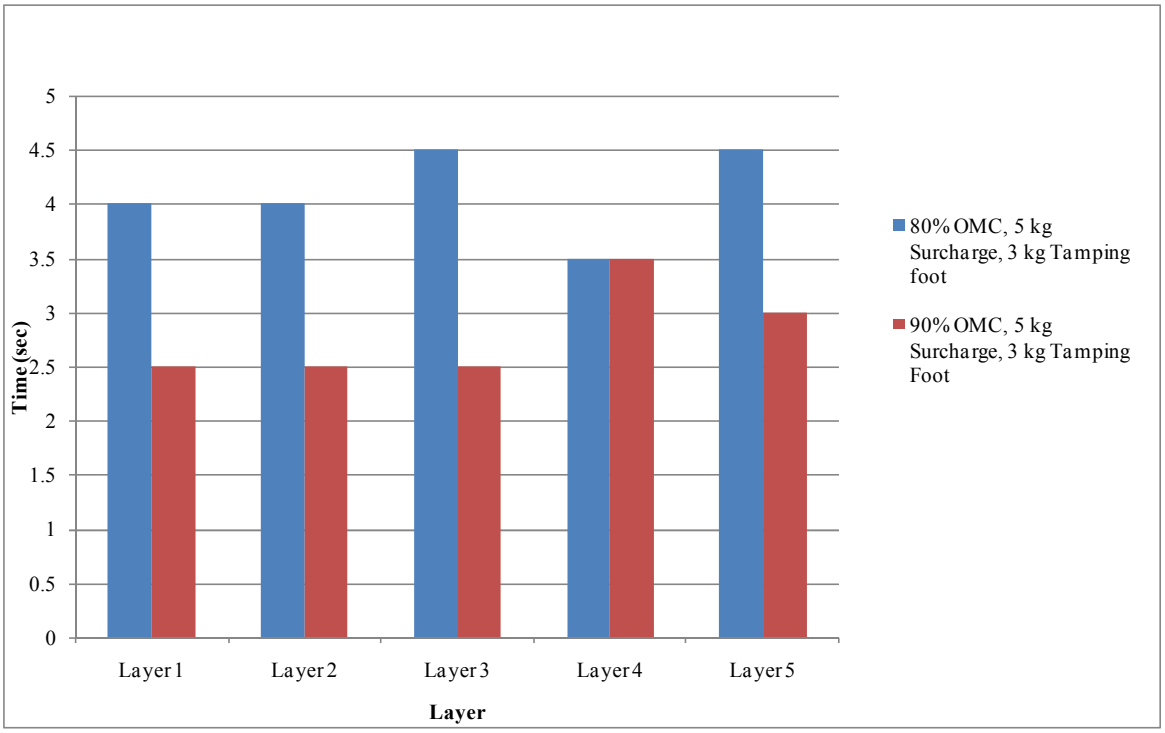

Figure B - 105: Effect of Moisture at 5kg Surcharge and 3kg Tamper – G4RFR

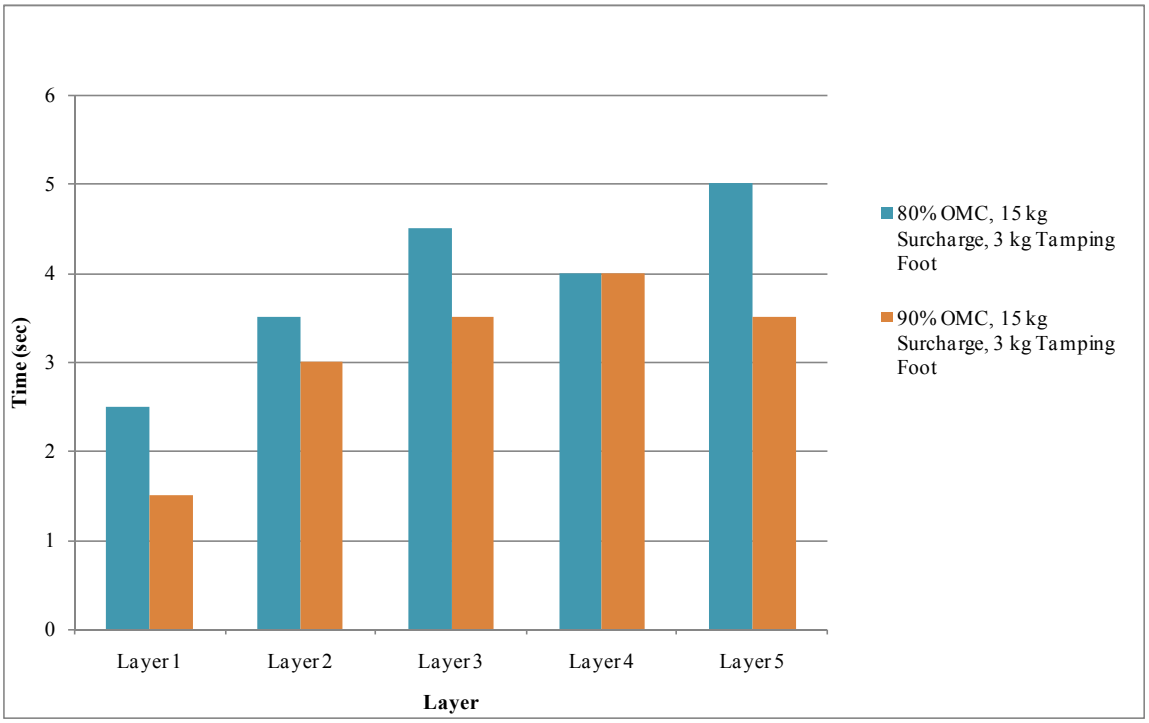

Figure B - 106: Effect of Moisture at 15kg Surcharge and 3kg Tamper – G4RFR

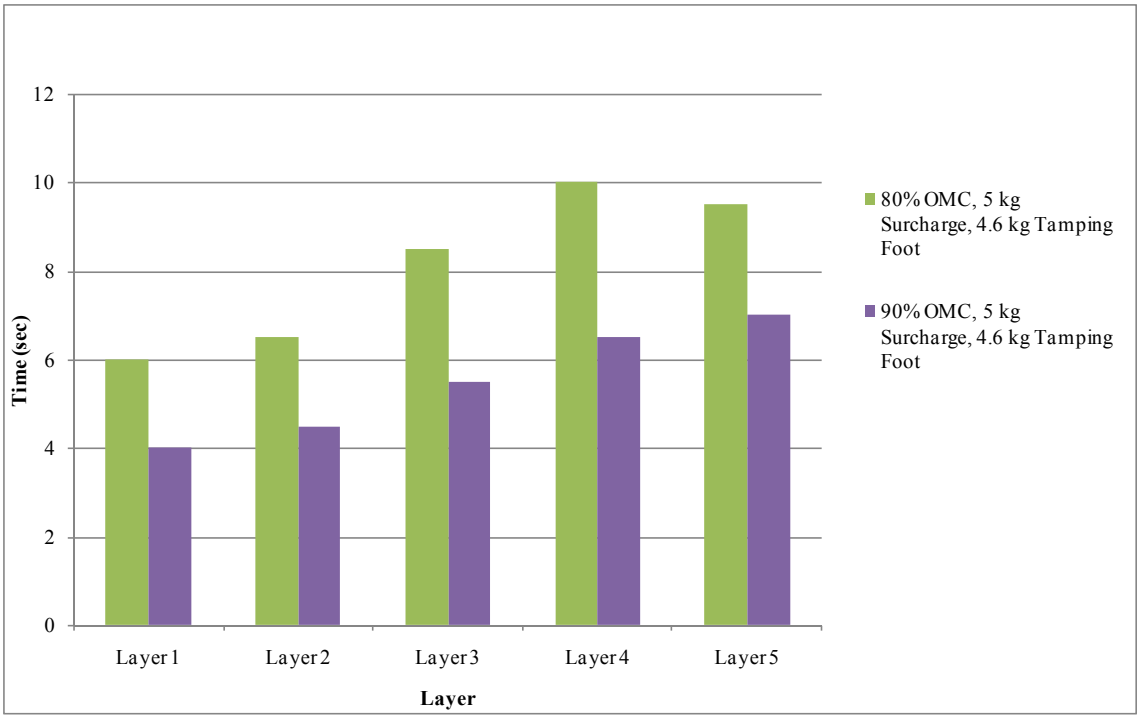

Figure B - 107: Effect of Moisture at 5kg Surcharge and 4.6kg Tamper – G4RFR

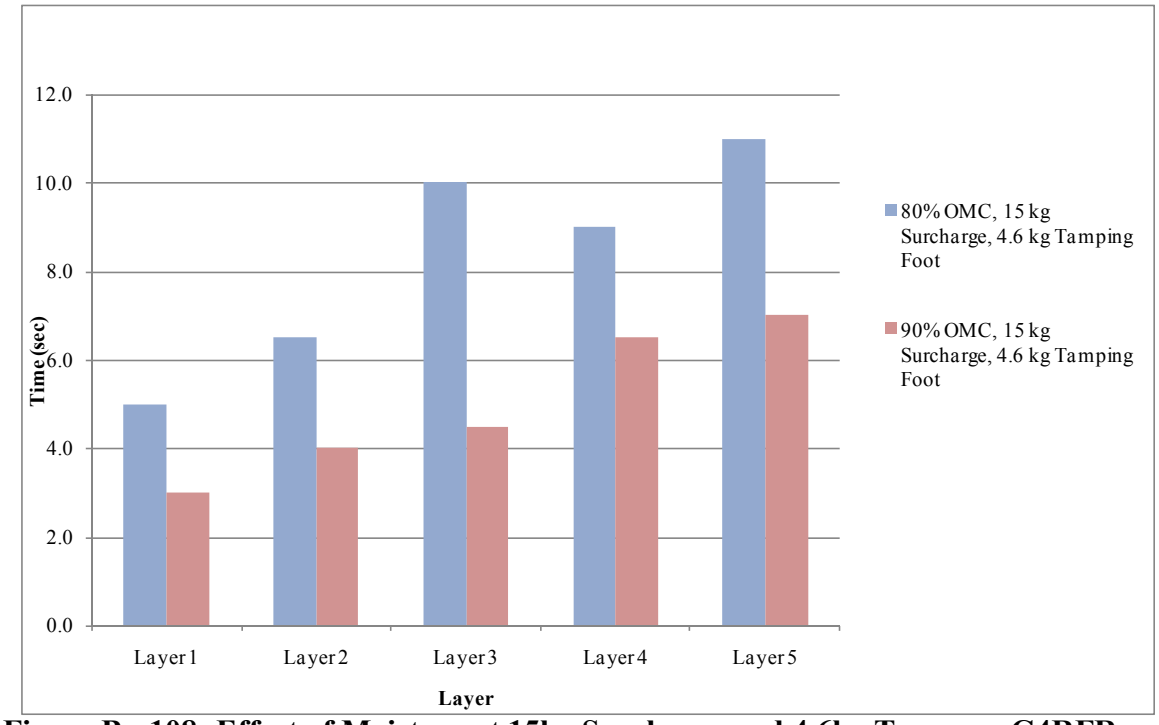

Figure B - 108: Effect of Moisture at 15kg Surcharge and 4.6kg Tamper - G4RFR

Effect of Tamping Foot on Compaction Time – G4 (RFR)

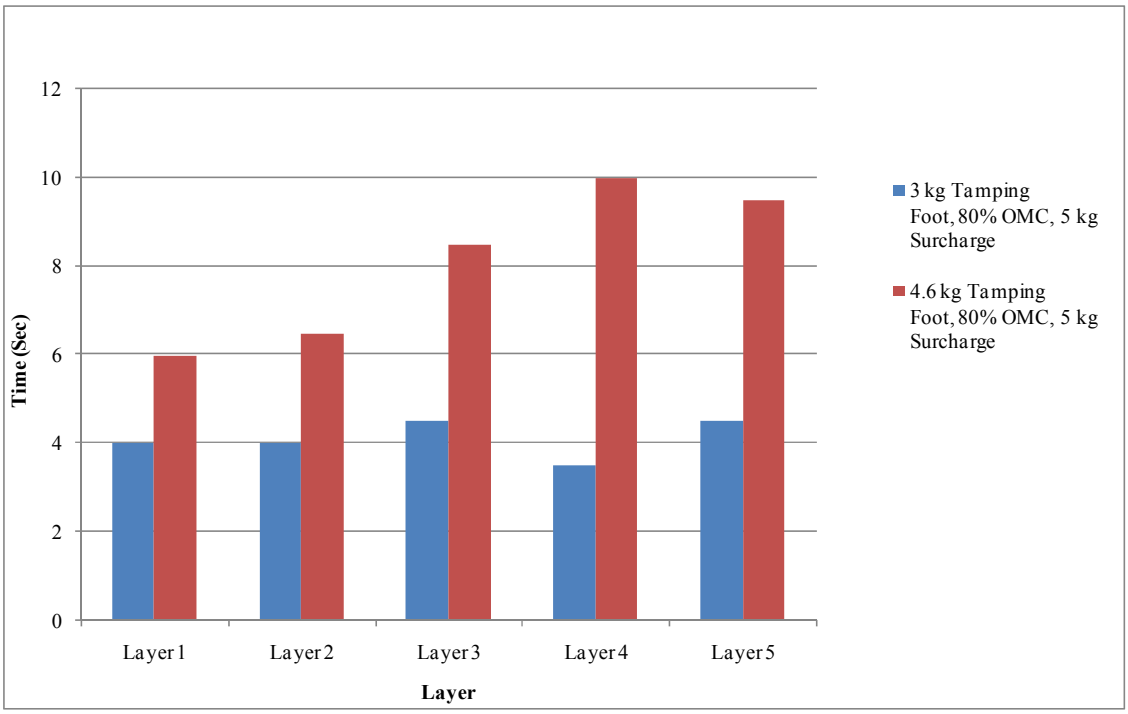

Figure B - 109: Effect of Tamper at 80% OMC and 5kg Surcharge – G4RFR

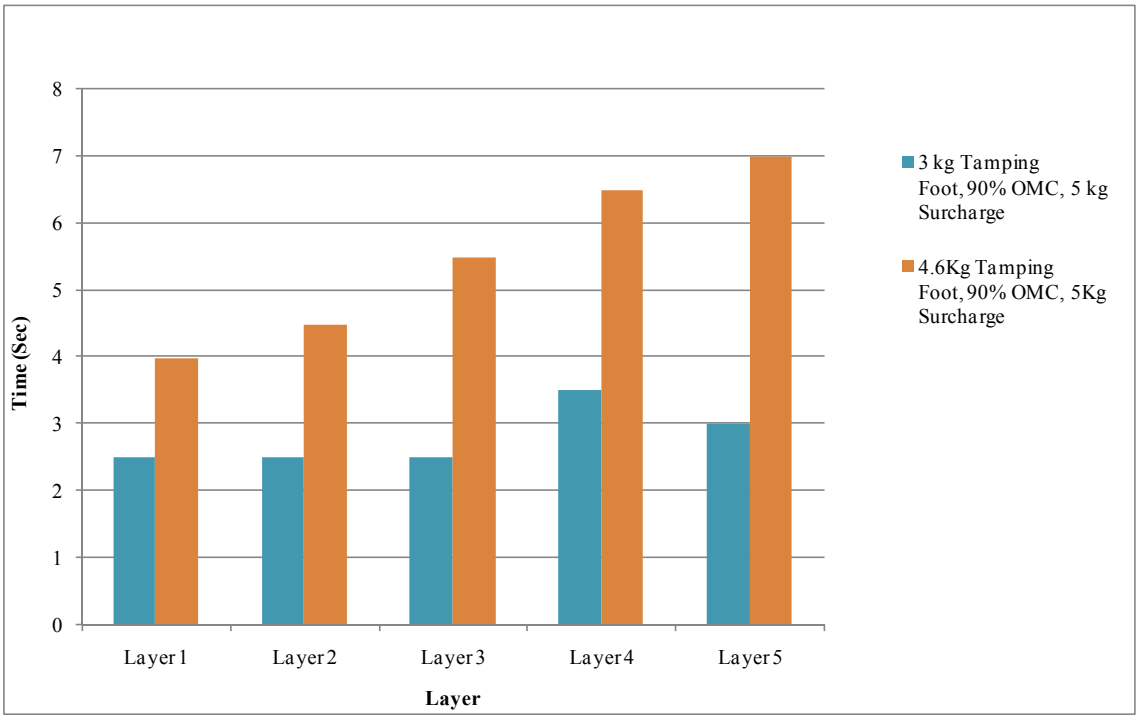

Figure B - 110: Effect of Tamper at 90% OMC and 5kg Surcharge – G4RFR

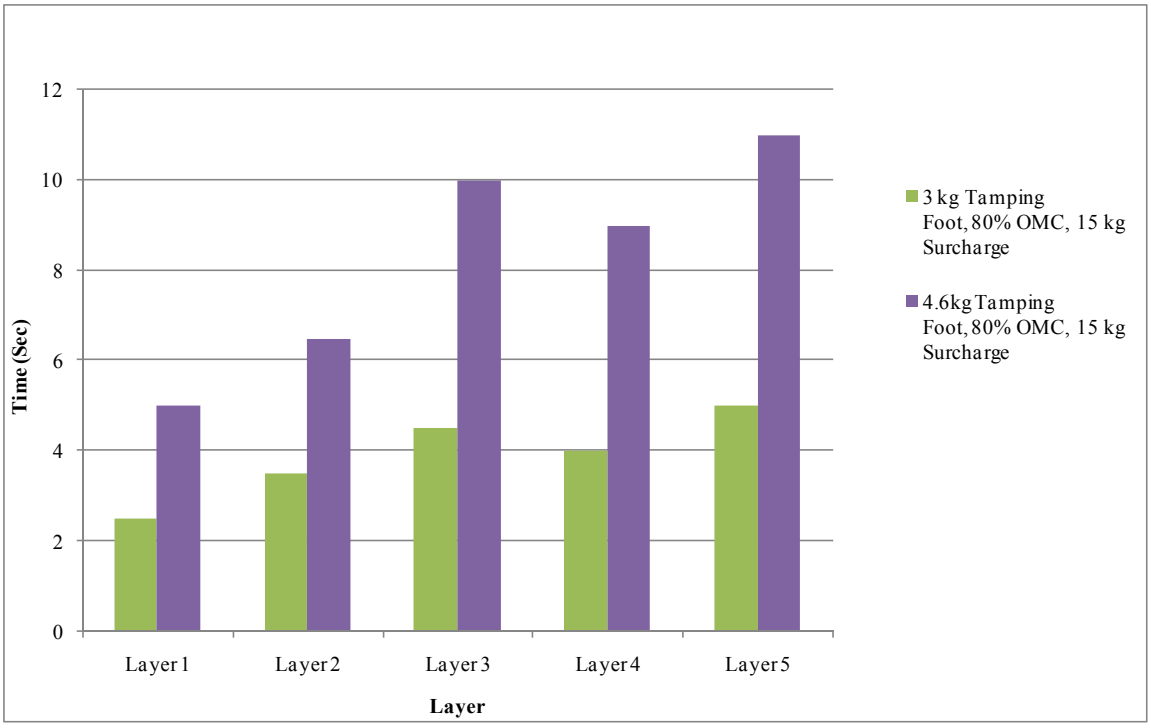

Figure B - 111: Effect of Tamper at 80% OMC and 15kg Surcharge – G4RFR

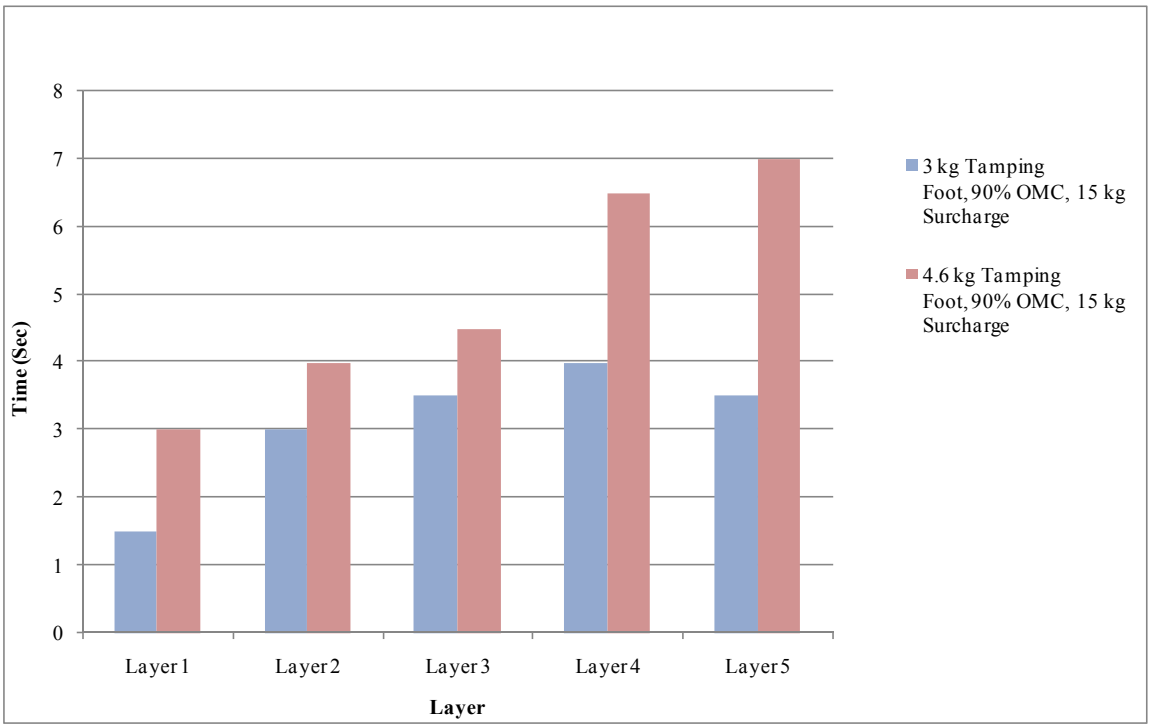

Figure B - 112: Effect of Tamper at 90% OMC and 15kg Surcharge – G4RFR

Effect of Surcharge Load on Compaction Time – G4 (Rigid Frame)

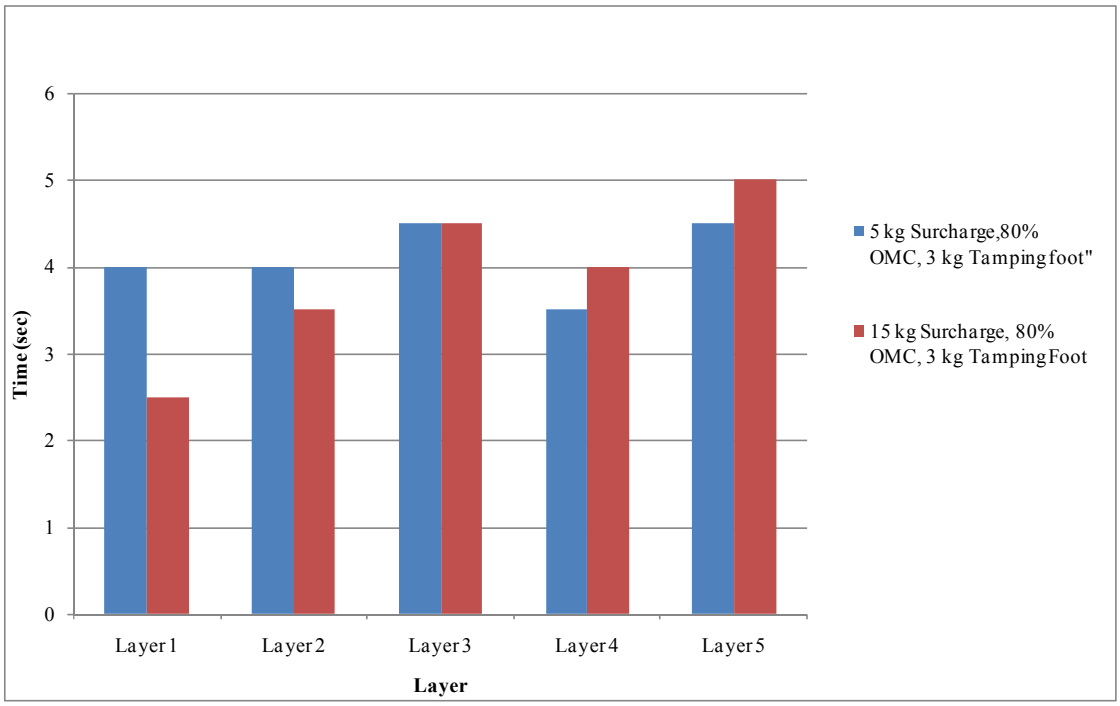

Figure B - 113: Effect of Surcharge at 80% OMC and 3kg Tamper – G4RFR

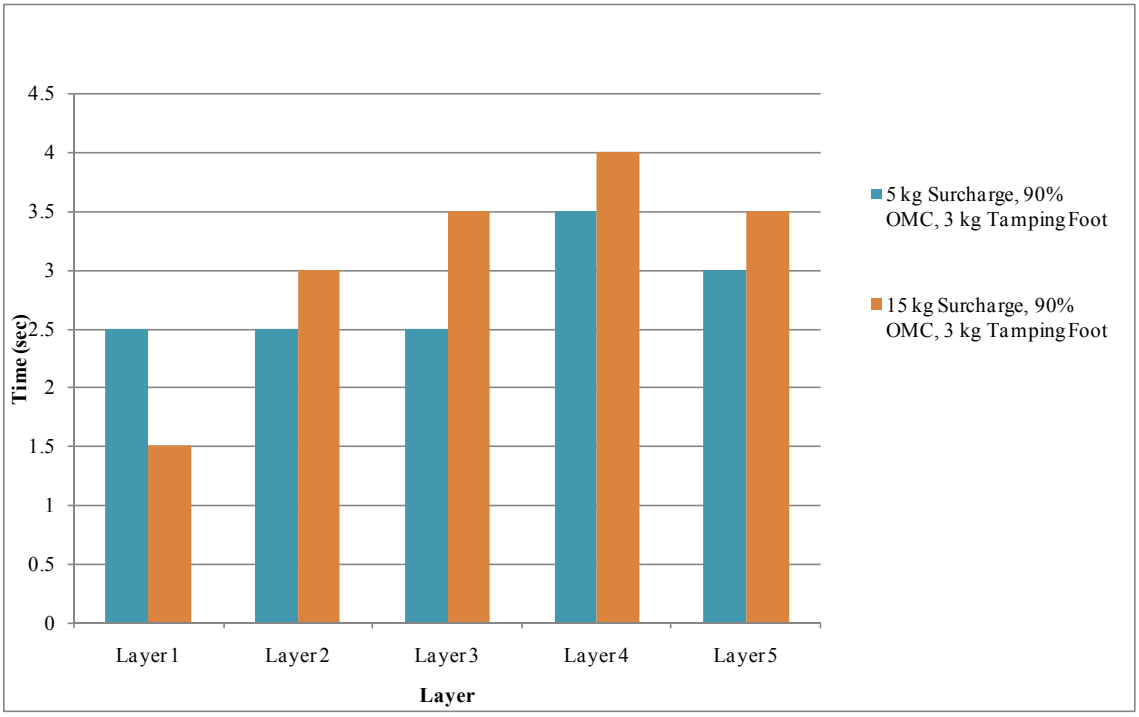

Figure B - 114: Effect of Surcharge at 90% OMC and 3kg Tamper – G4RFR

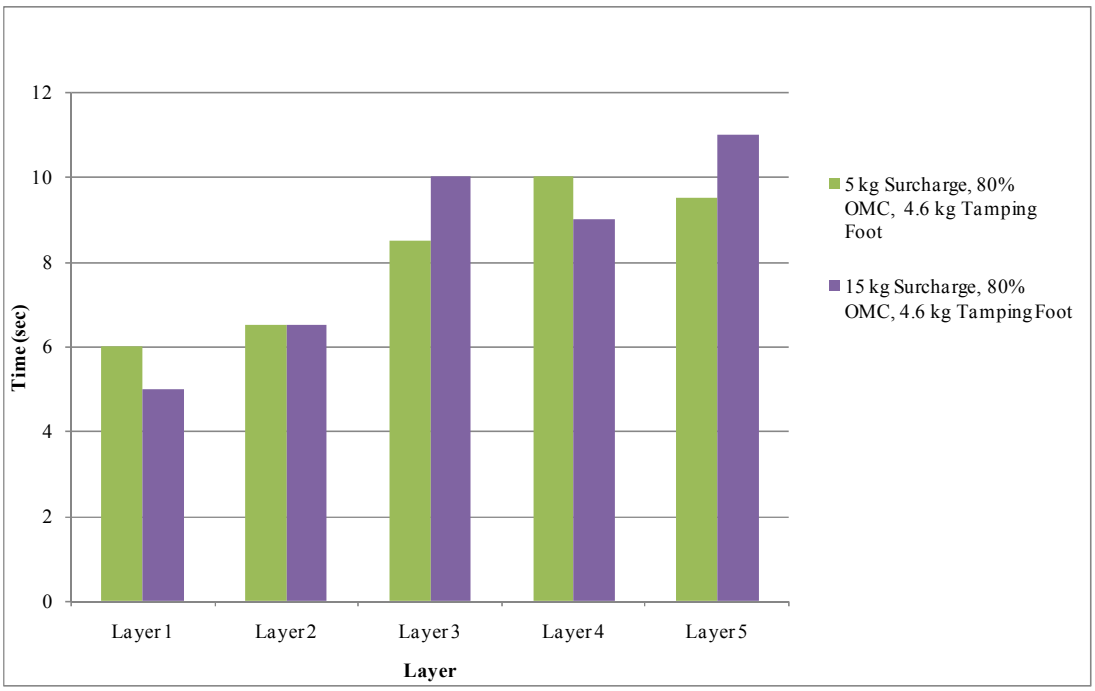

Figure B - 115: Effect of Surcharge Load at 80% OMC and 4.6kg Tamper – G4RFR

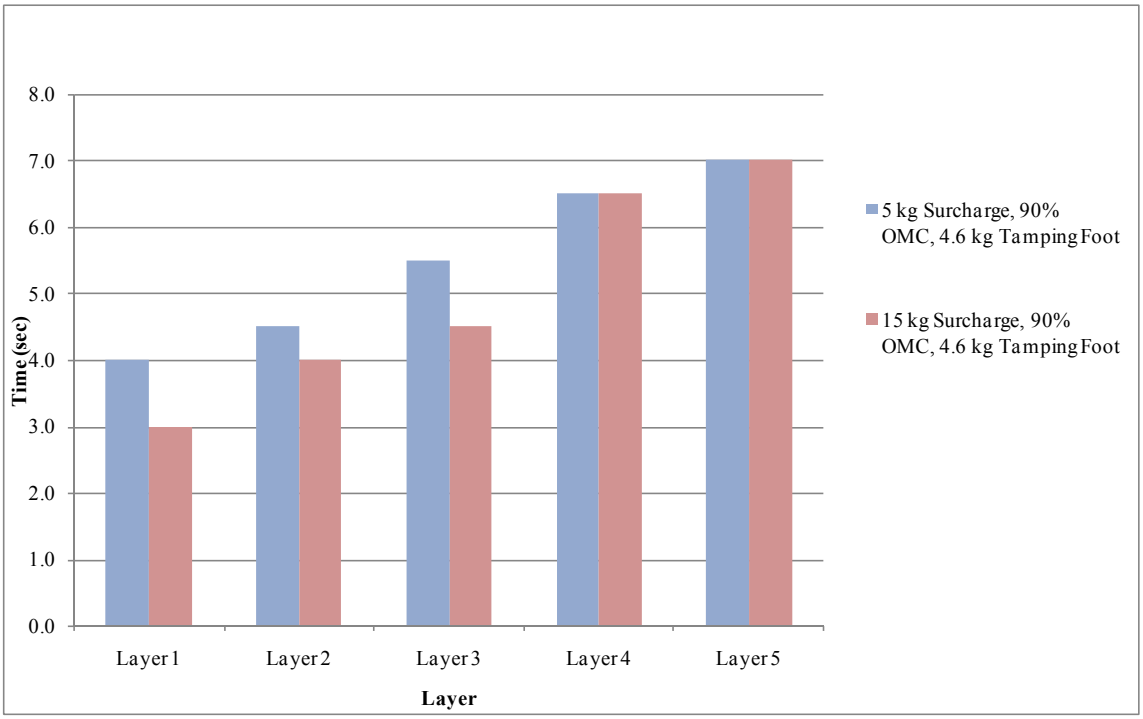

Figure B - 116: Effect of Surcharge Load at 90% OMC and 4.6kg Tamper – G4RFR

APPENDIX G: Test results for G7 material/ vibratory hammer compaction/soft frame

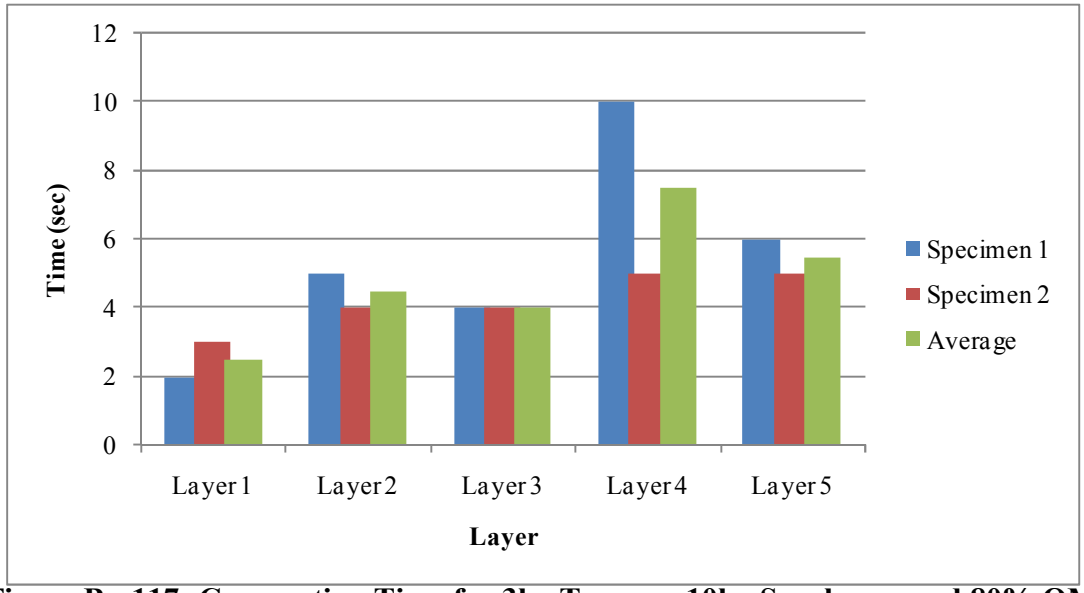

Figure B - 117: Compaction Time for 3kg Tamper, 10kg Surcharge and 80% OMC – G7SFR

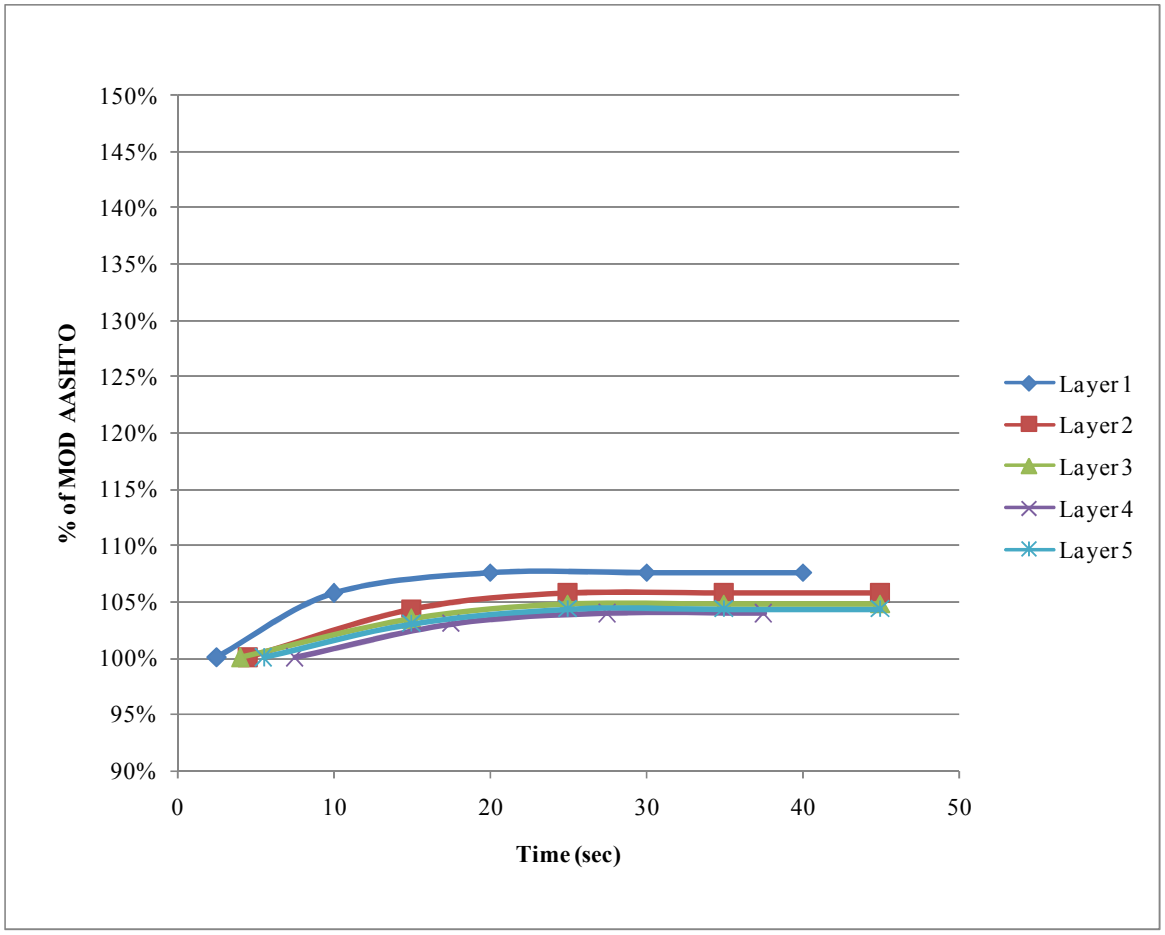

Figure B - 118: Compaction Profile for 3kg Tamper, 10kg Surcharge and 80% OMC – G7SFR

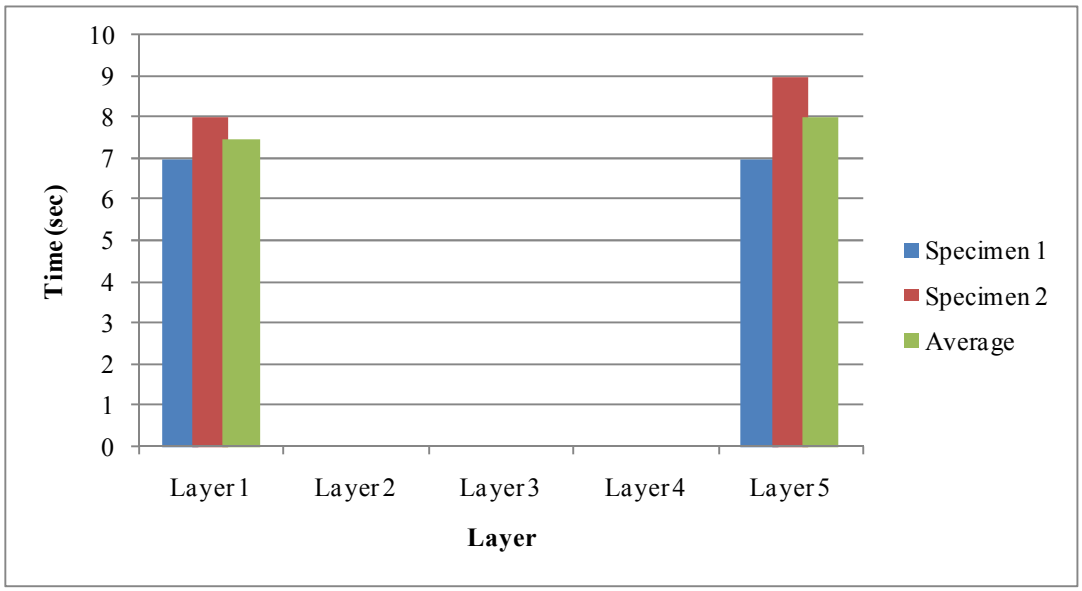

Figure B - 119: Compaction Time for 4.6kg Tamper, 10kg Surcharge and 80% OMC – G7SFR

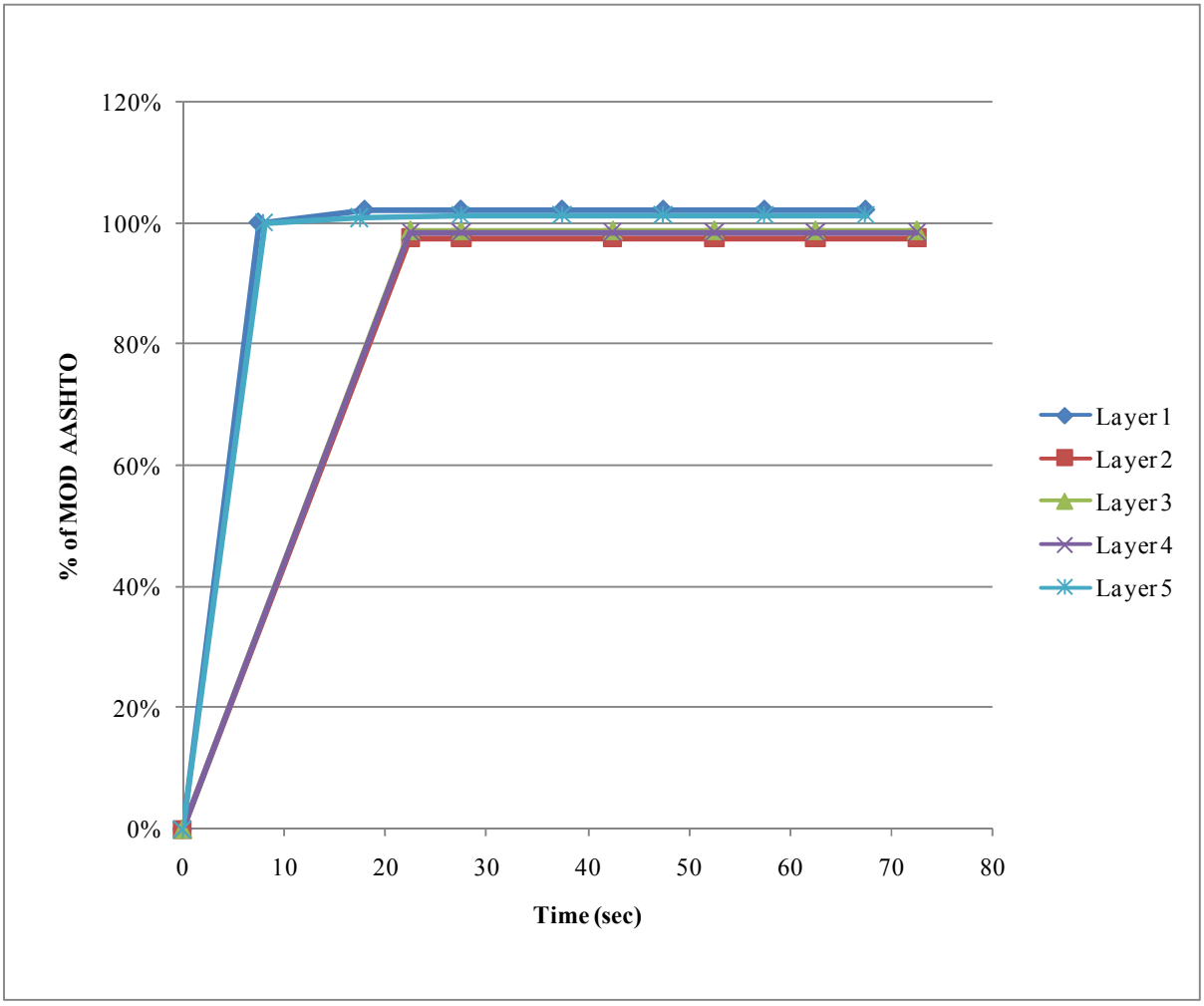

Figure B - 120: Compaction Profile for 4.6kg Tamper, 10kg Surcharge and 80% OMC – G7SFR

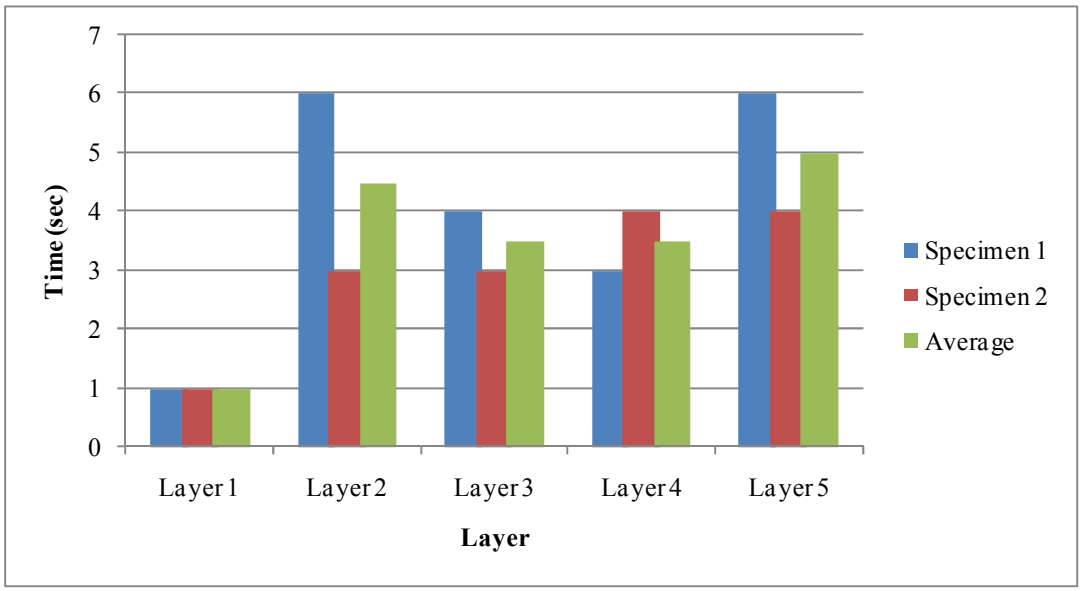

Figure B - 121: Compaction Time for 3kg Tamper, 20kg Surcharge and 80% OMC – G7SFR

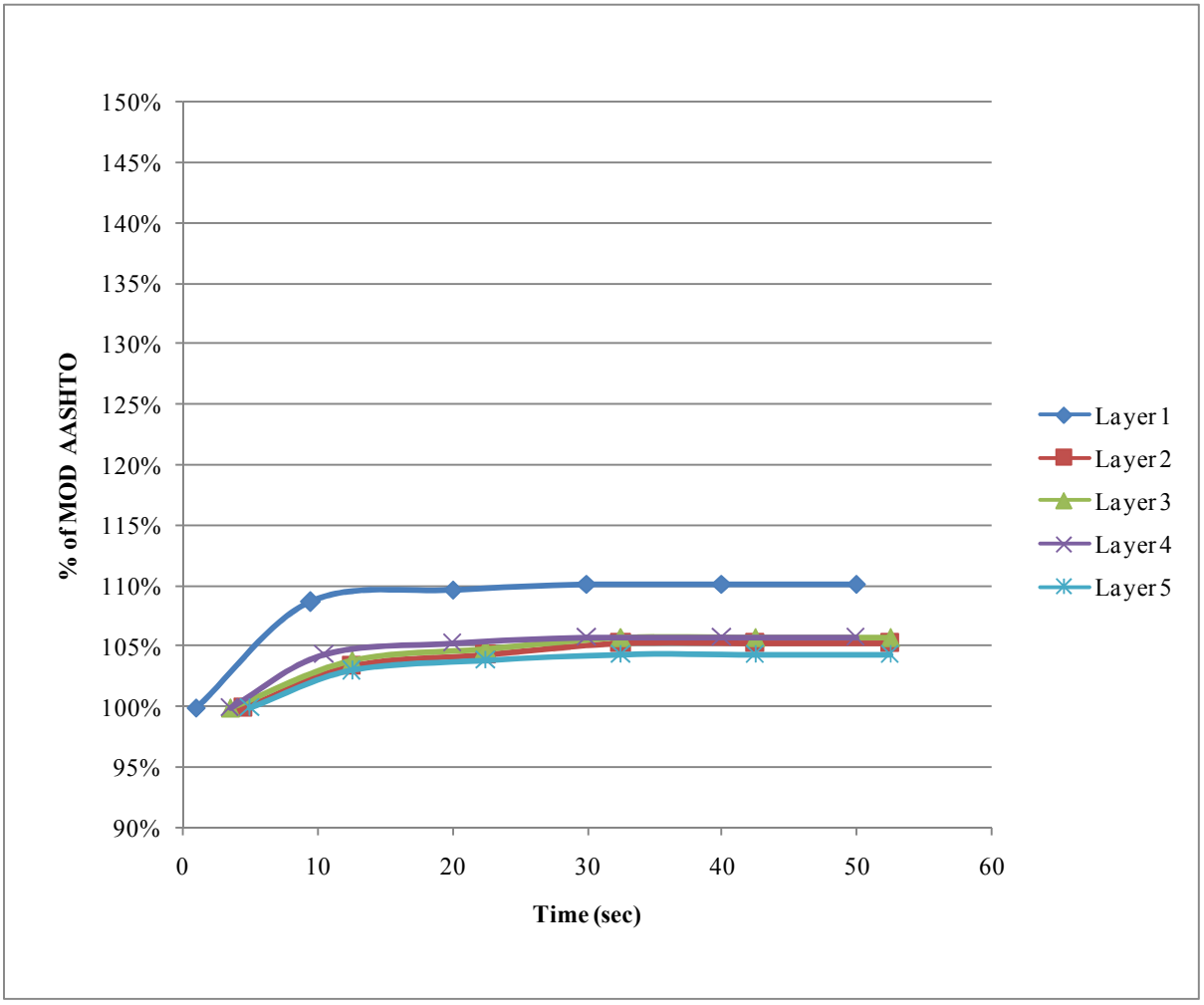

Figure B - 122: Compaction Profile for 3kg Tamper, 20kg Surcharge and 80% OMC – G7SFR

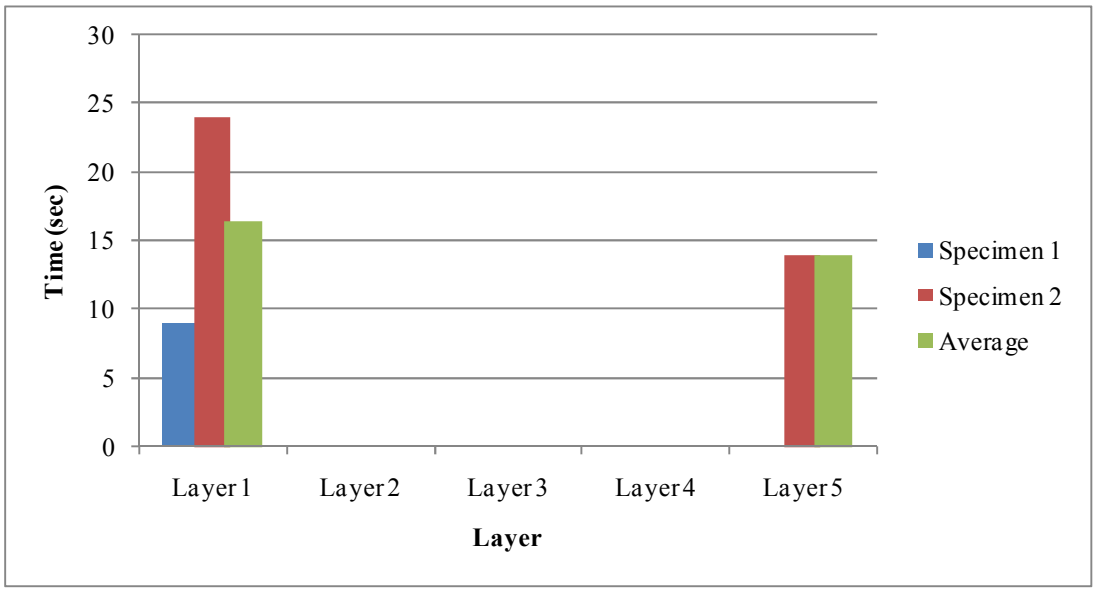

Figure B - 123: Compaction Time for 4.6kg Tamper, 20kg Surcharge and 80% OMC – G7RFR

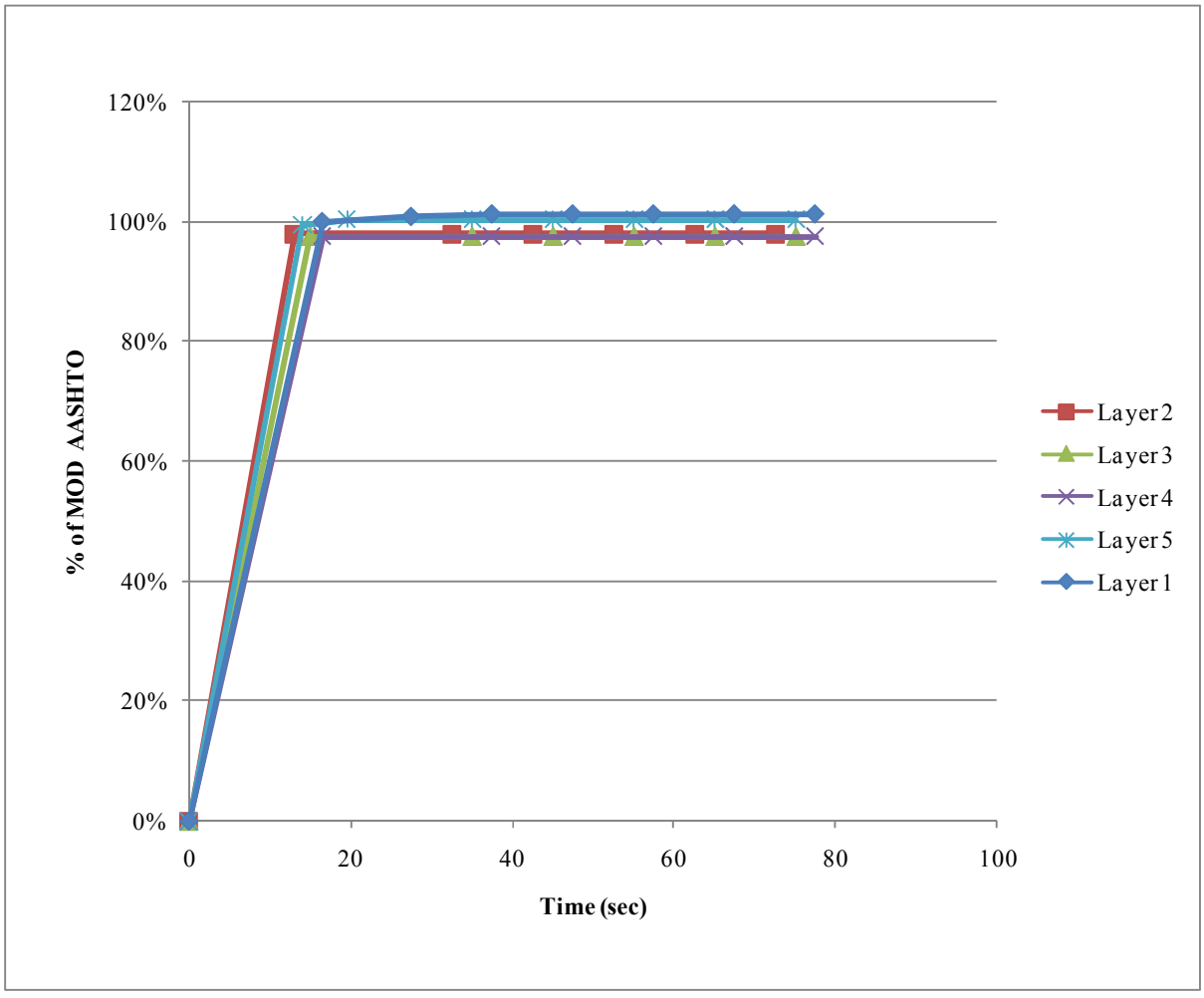

Figure B - 124: Compaction Profile for 4.6kg Tamper, 20kg Surcharge and 80% OMC – G7SFR

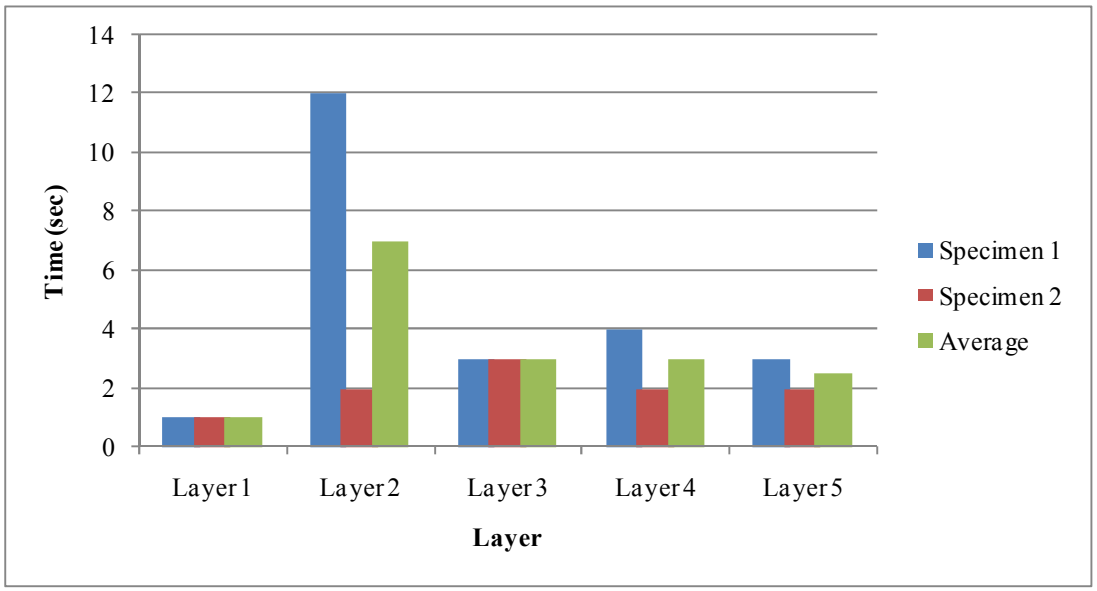

Figure B - 125: Compaction Time for 3kg Tamper, 10kg Surcharge and 90% OMC – G7SFR

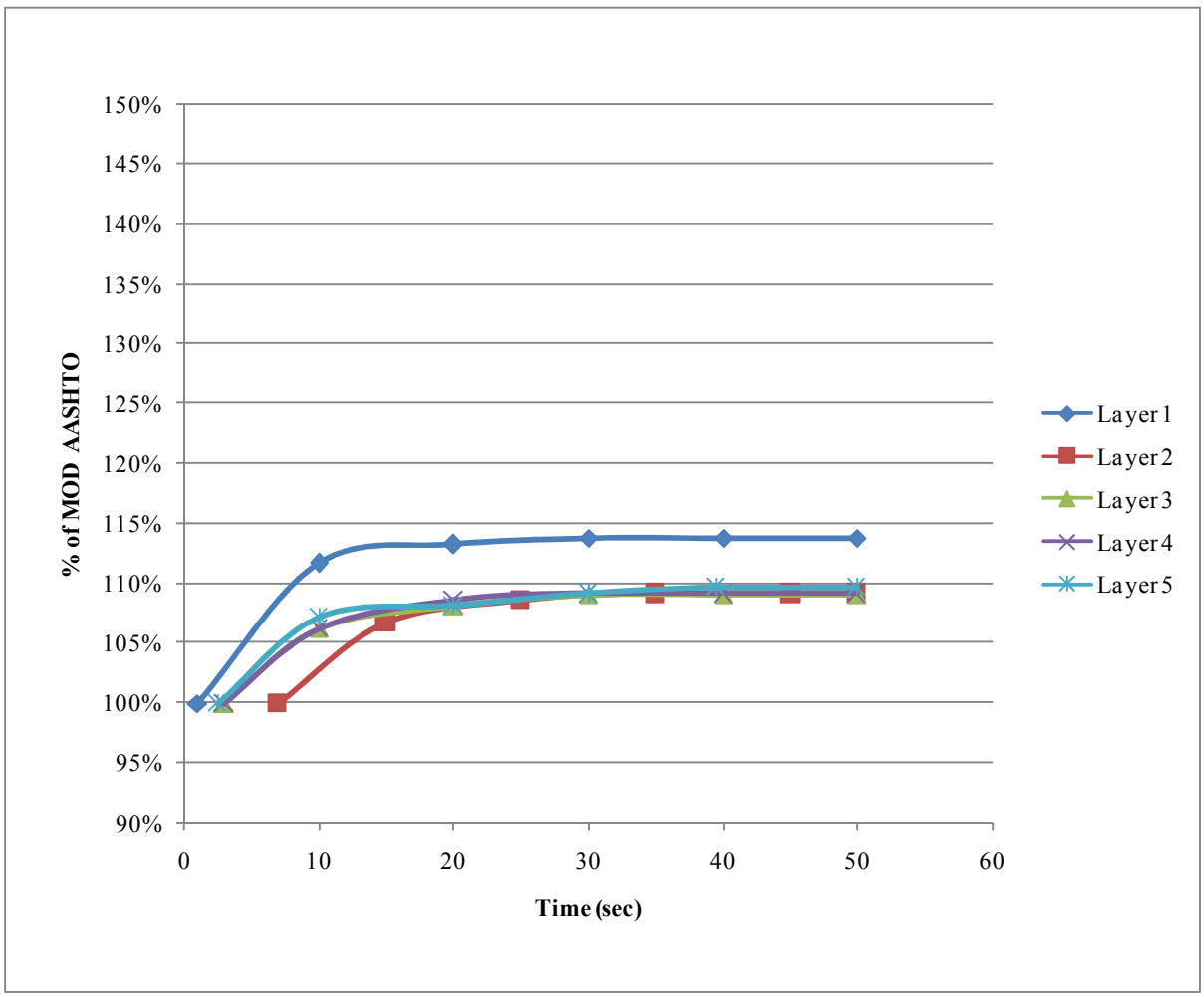

Figure B - 126: Compaction Profile for 3kg Tamper, 10kg Surcharge and 90% OMC – G7SFR

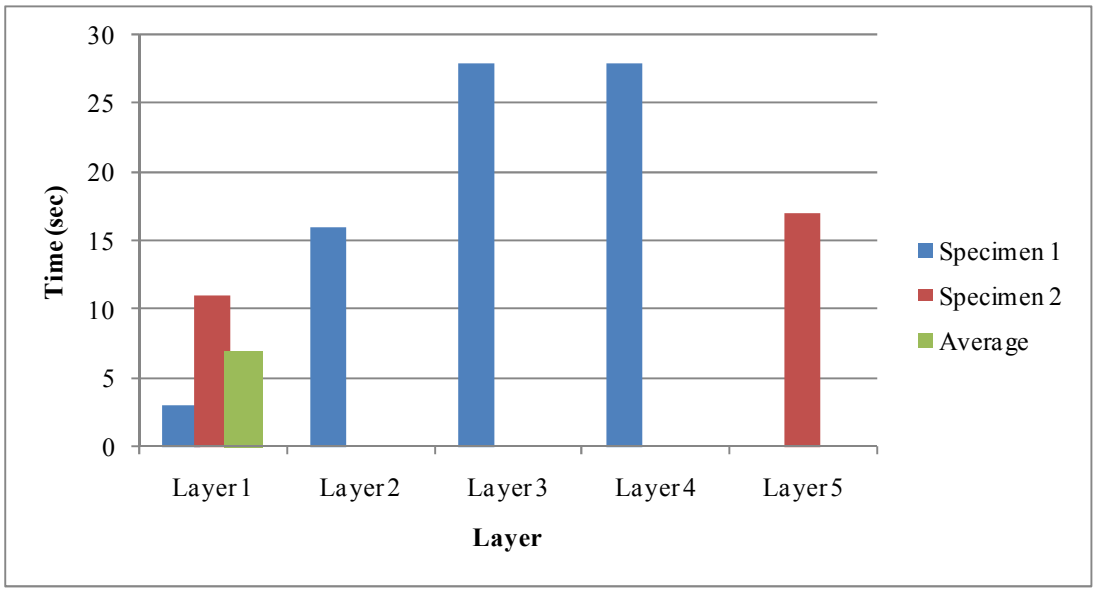

Figure B - 127: Compaction Time for 4.6kg Tamper, 10kg Surcharge and 90% OMC – G7SFR

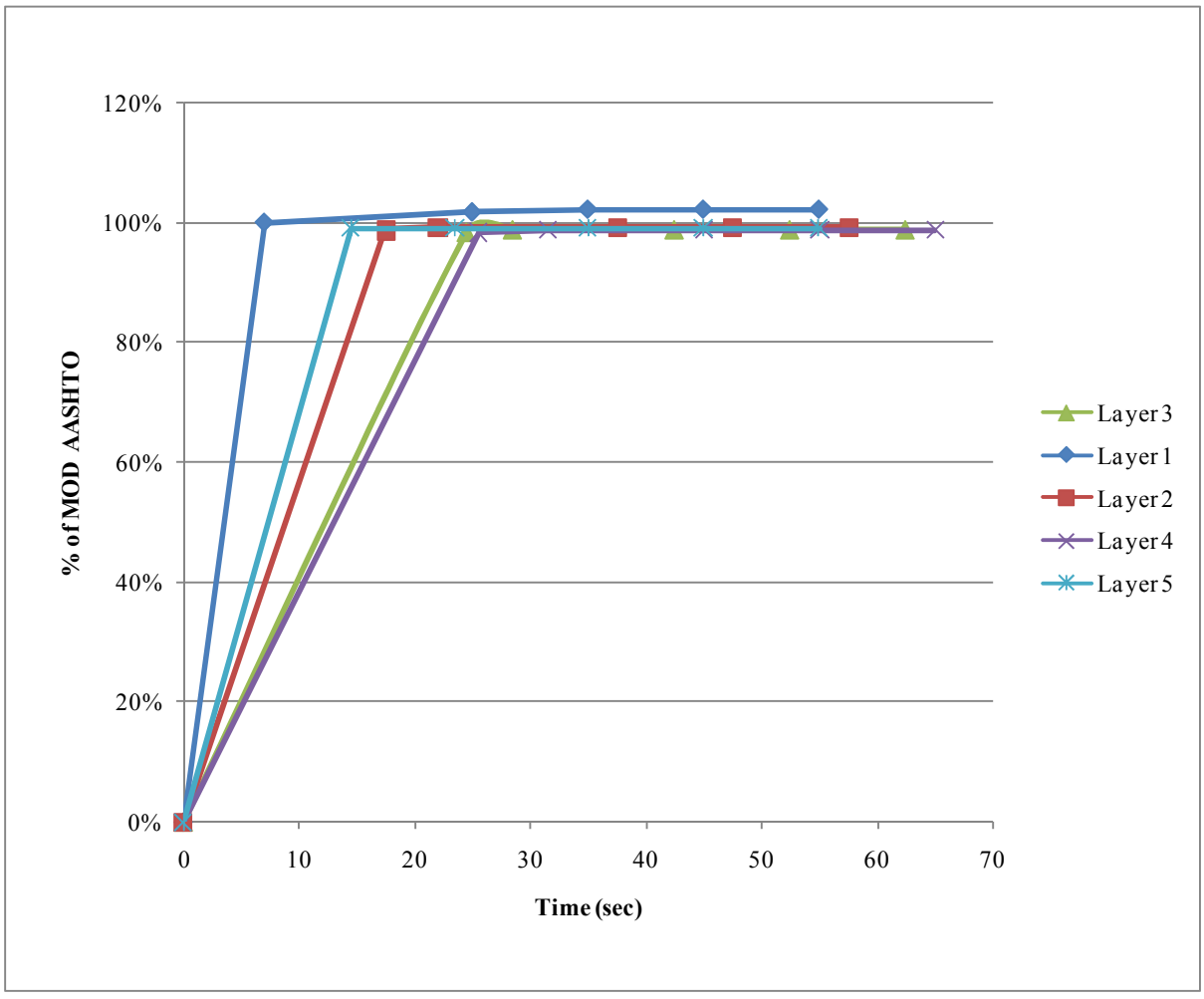

Figure B - 128: Compaction Profile for 4.6kg Tamper, 10kg Surcharge and 90% OMC – G7SFR

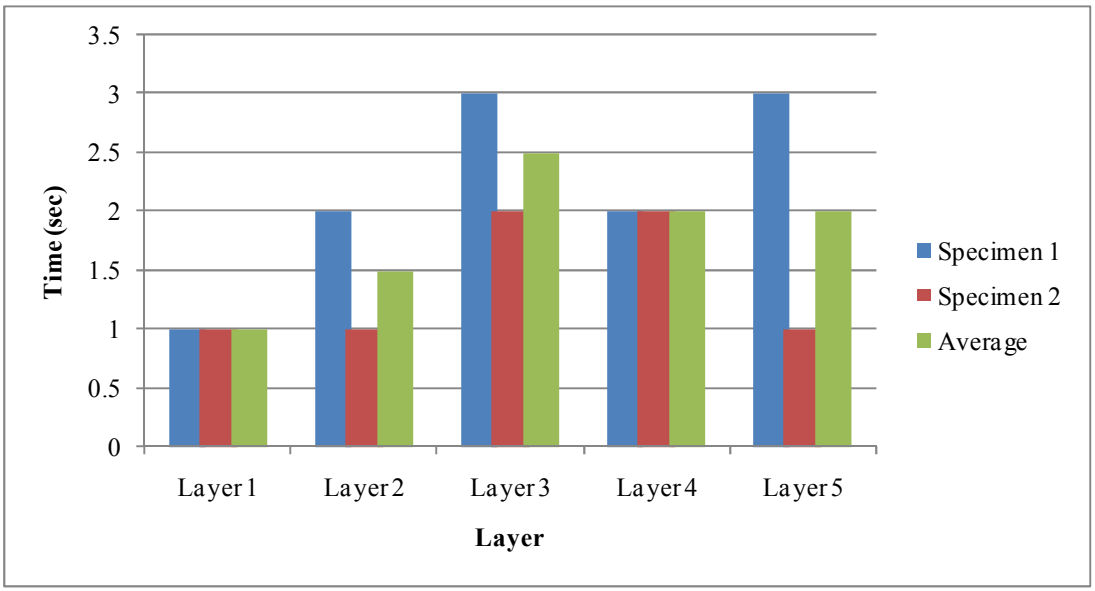

Figure B - 129: Compaction Time for 3kg Tamper, 20kg Surcharge and 90% OMC – G7SFR

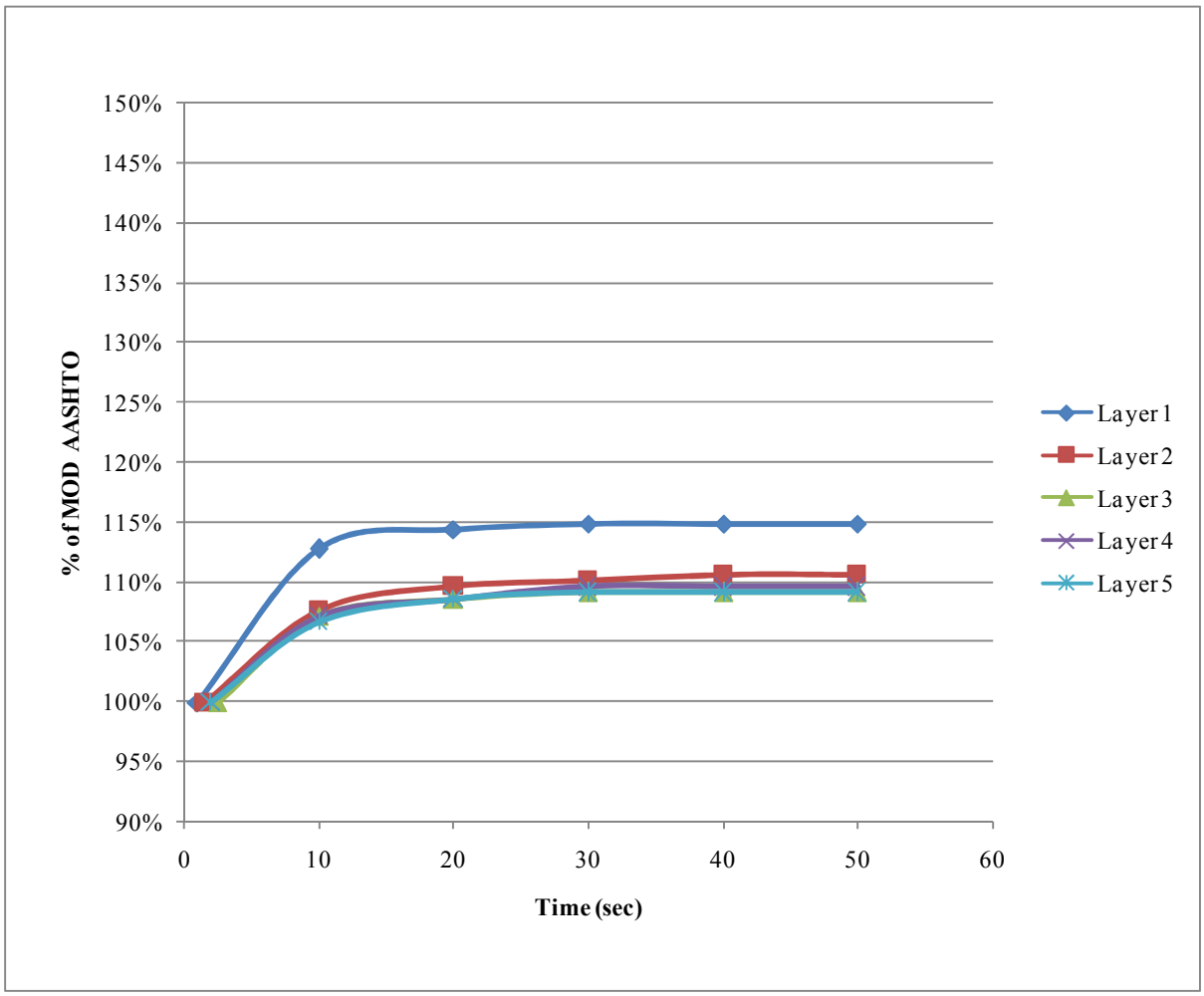

Figure B - 130: Compaction Profile for 3kg Tamper, 20kg Surcharge and 90% OMC – G7SFR

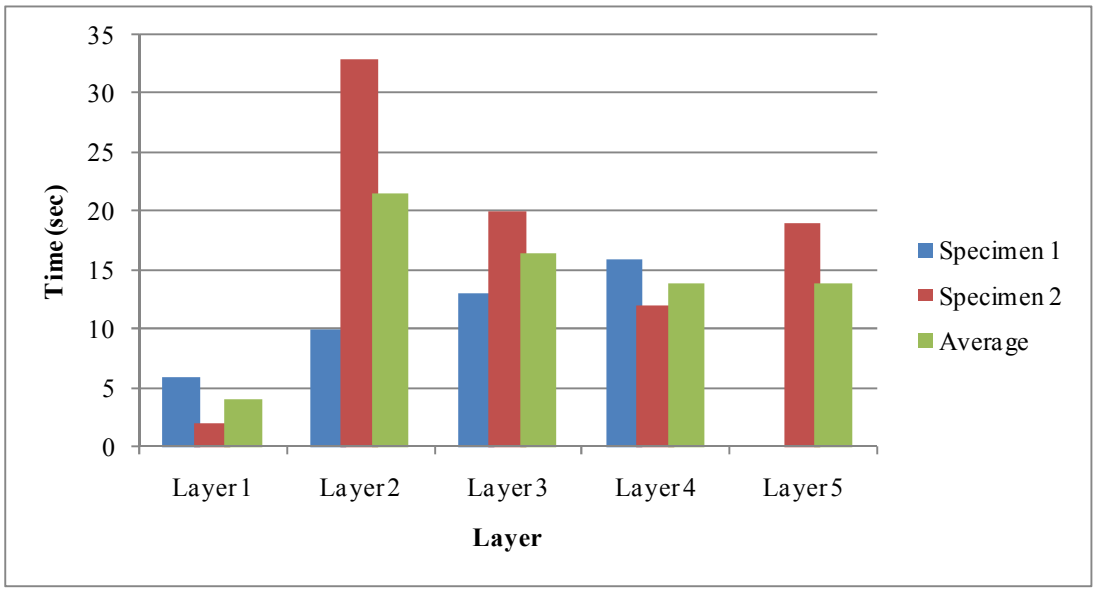

Figure B - 131: Compaction Time for 4.6kg Tamper, 20kg Surcharge and 90% OMC – G7SFR

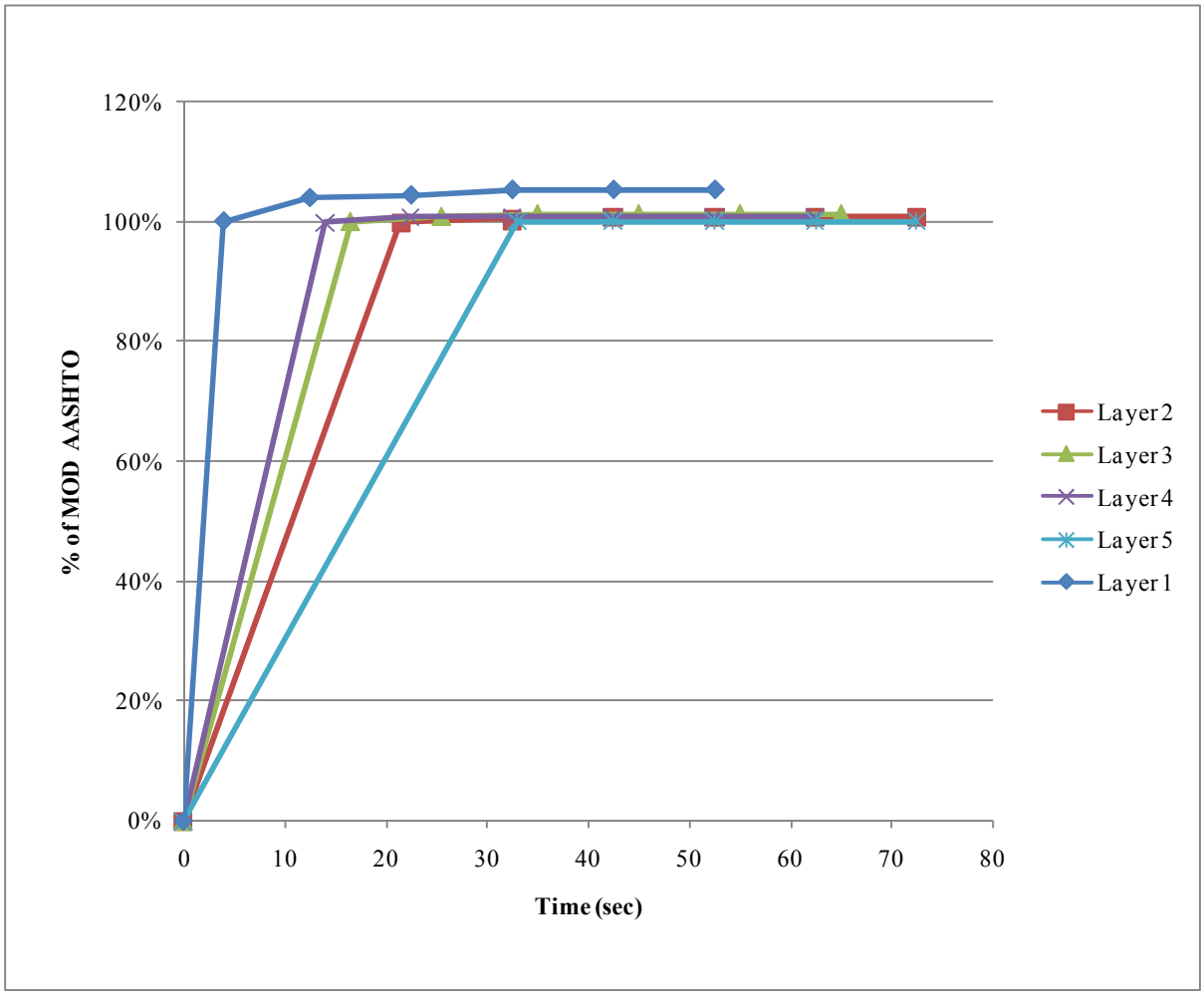

Figure B - 132: Compaction Profile for 4.6kg Tamper, 20kg Surcharge and 90% OMC – G7SFR

Effect of Moisture on Compaction Time – G7 (SFR)

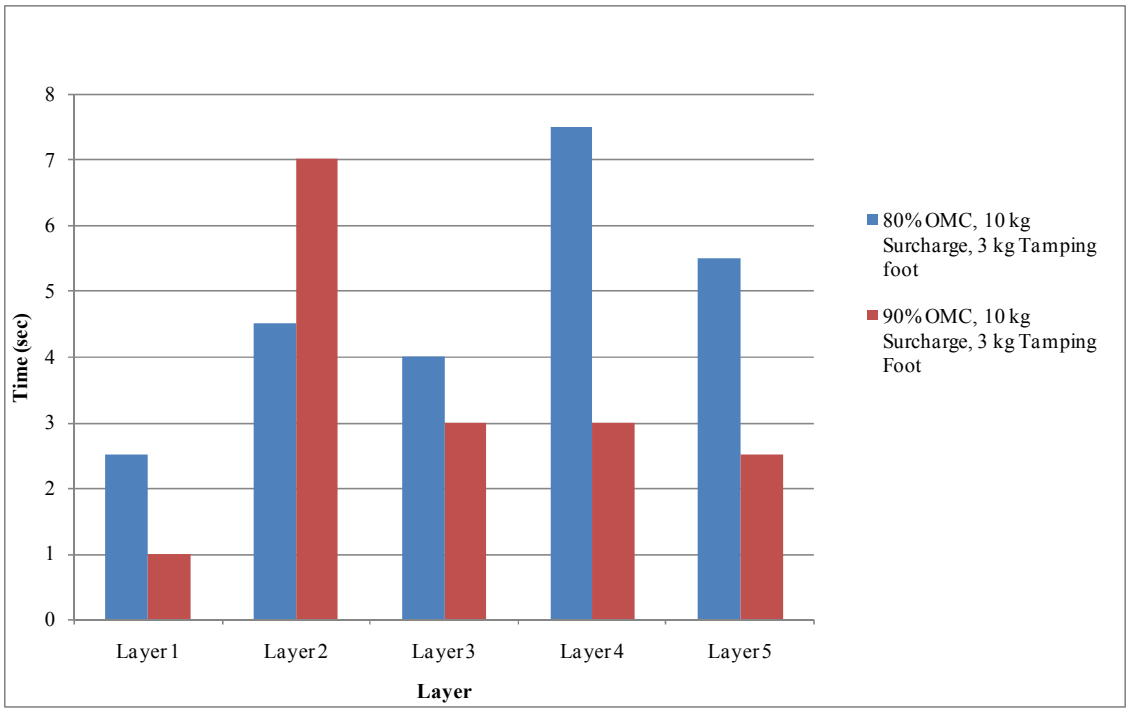

Figure B - 133: Effect of Moisture at 10kg Surcharge and 3kg Tamper – G7SFR

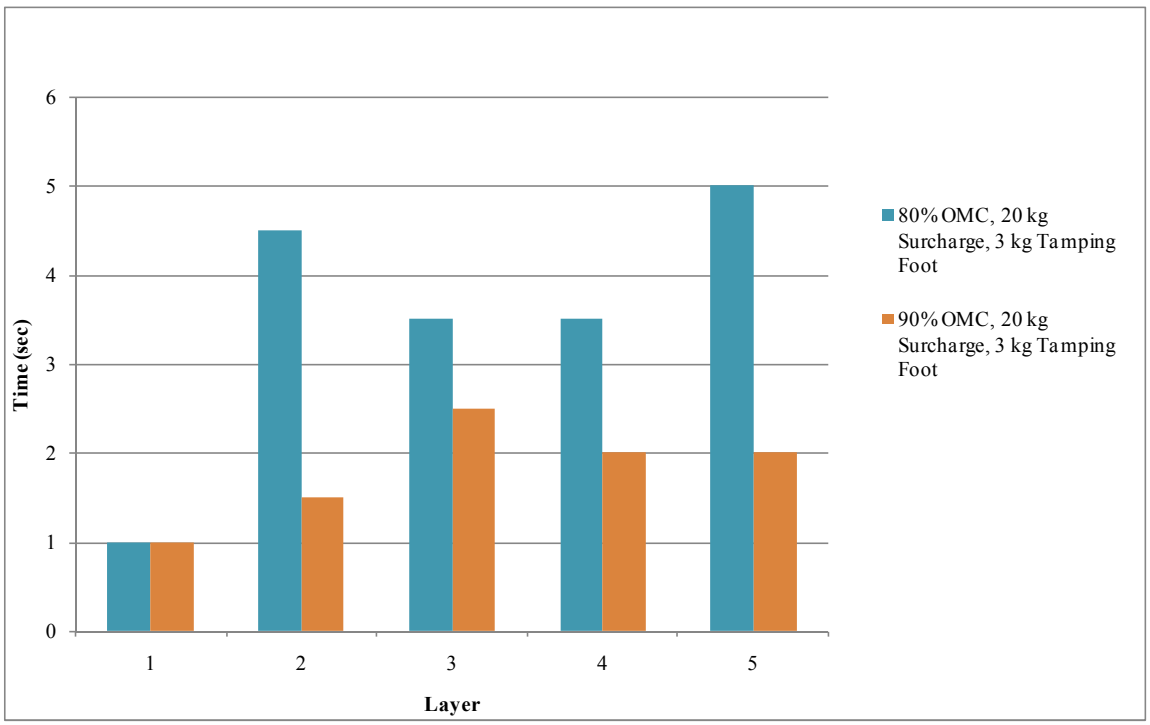

Figure B - 134: Effect of Moisture at 20kg Surcharge and 3kg Tamper – G7SFR

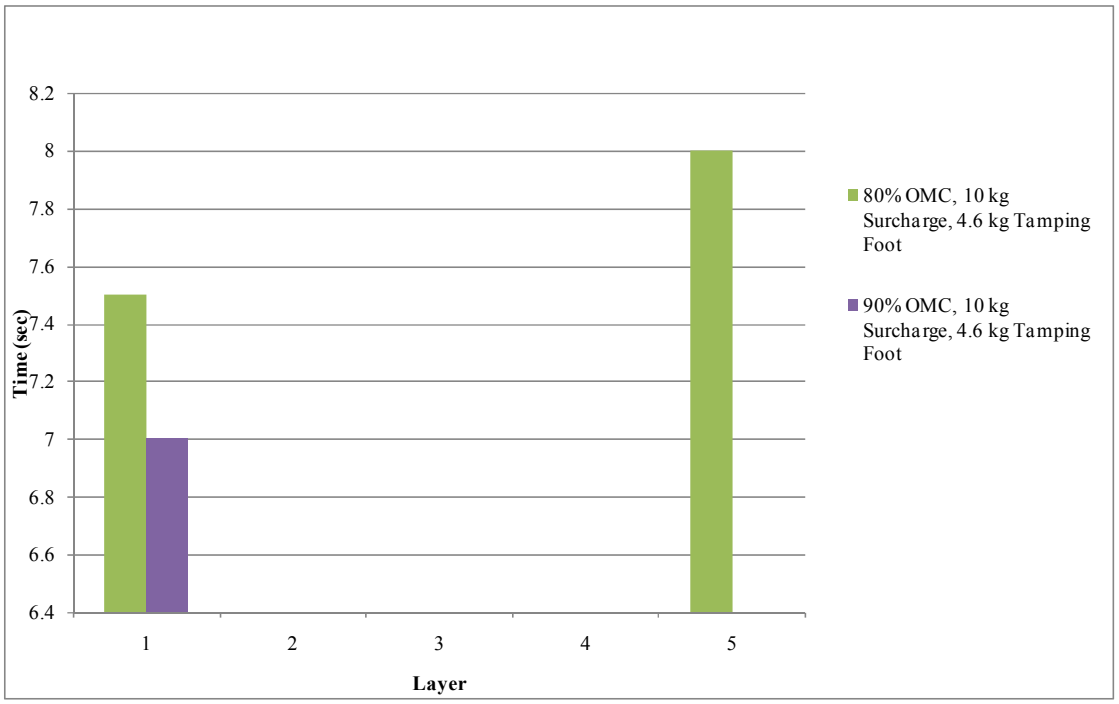

Figure B - 135: Effect of Moisture at 10kg Surcharge and 4.6kg Tamper – G7SFR

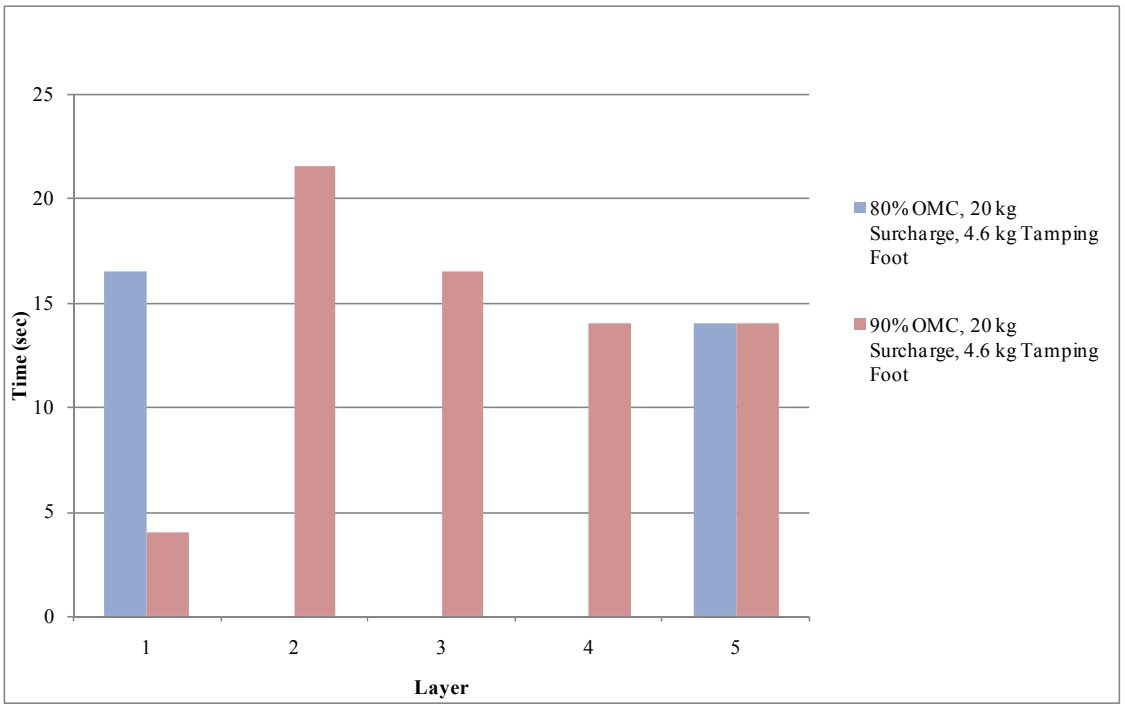

Figure B - 136: Effect of Moisture at 20kg Surcharge and 4.6kg Tamper – G7SFR

Effect of Tamping Foot on Compaction Time – G7 (SFR)

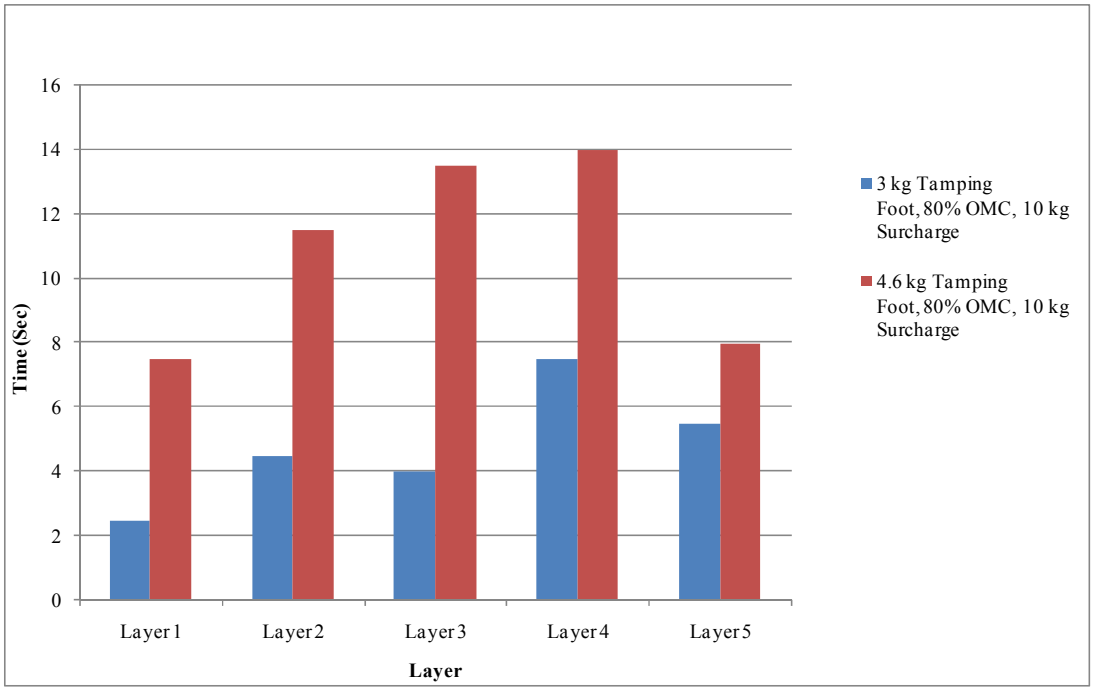

Figure B - 137: Effect of Tamper at 80% OMC and 10kg Surcharge – G7SFR

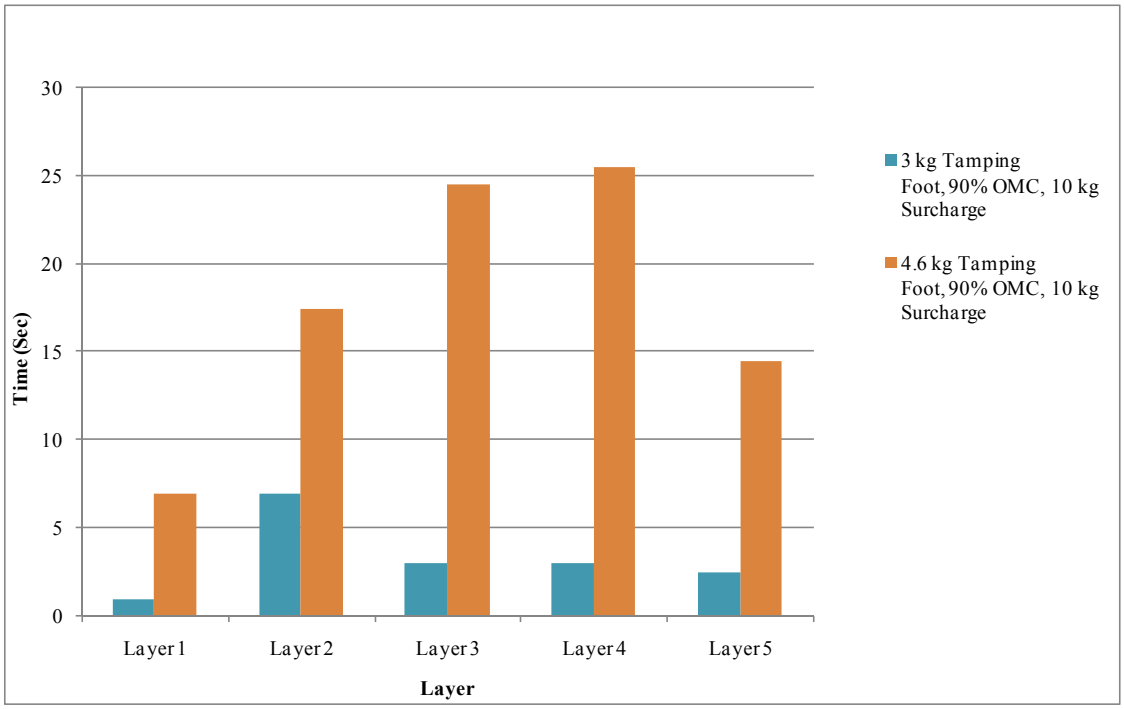

Figure B - 138: Effect of Tamper at 90% OMC and 10kg Surcharge – G7SFR

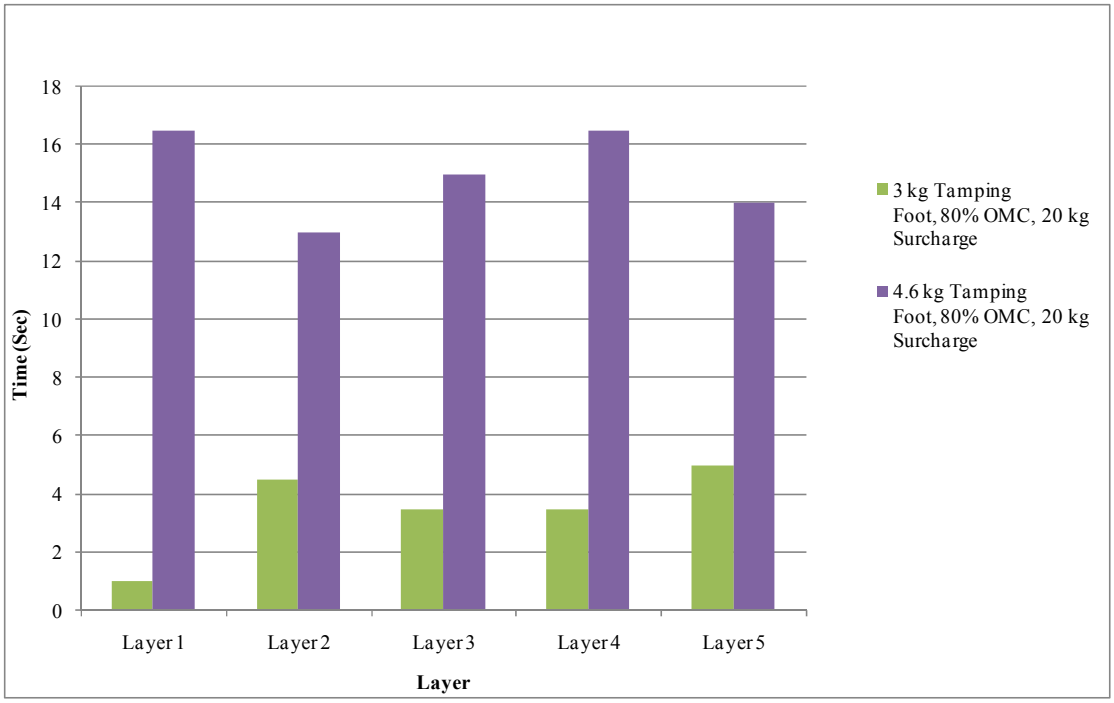

Figure B - 139: Effect of Tamper at 80% OMC and 20kg Surcharge – G7SFR

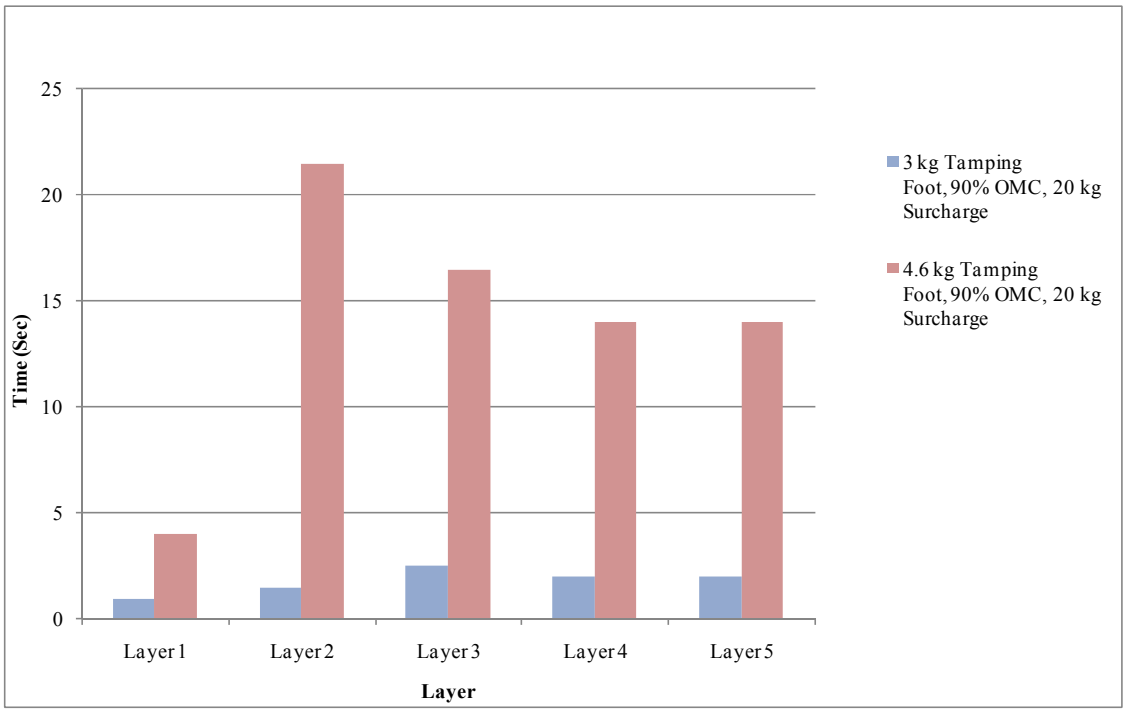

Figure B - 140: Effect of Tamper at 90% OMC and 20kg Surcharge – G7SFR

Effect of Surcharge Load on Compaction Time – G7 (SFR)

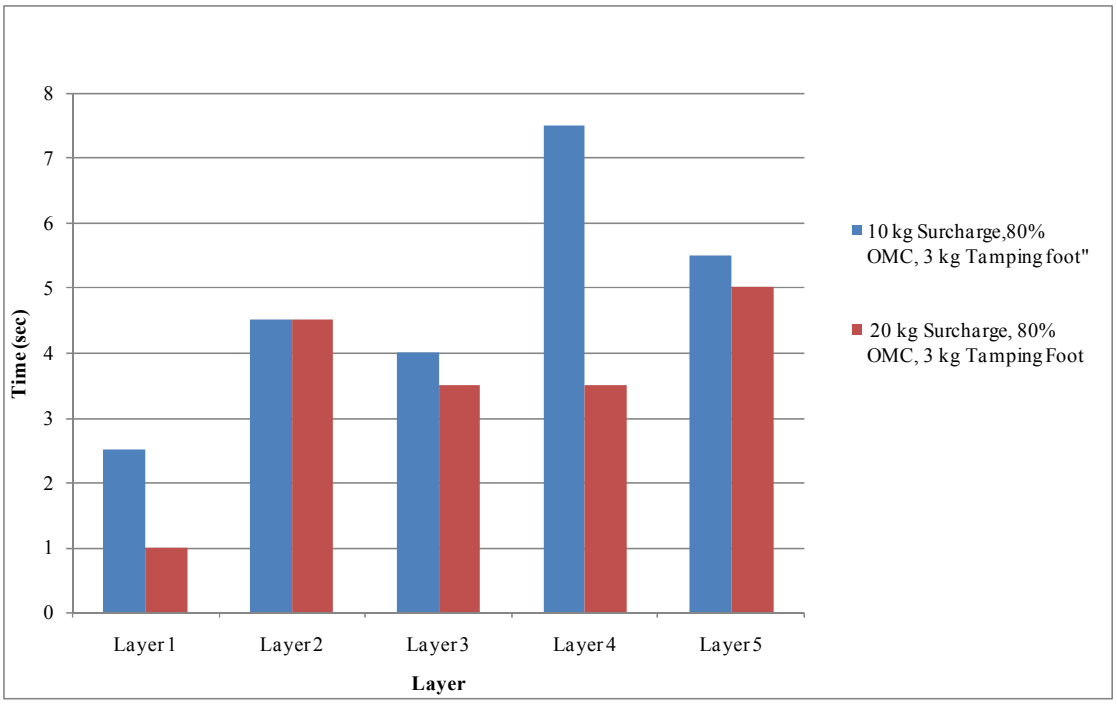

Figure B - 141: Effect of Surcharge Load at 80% OMC and 3kg Tamper – G7SFR

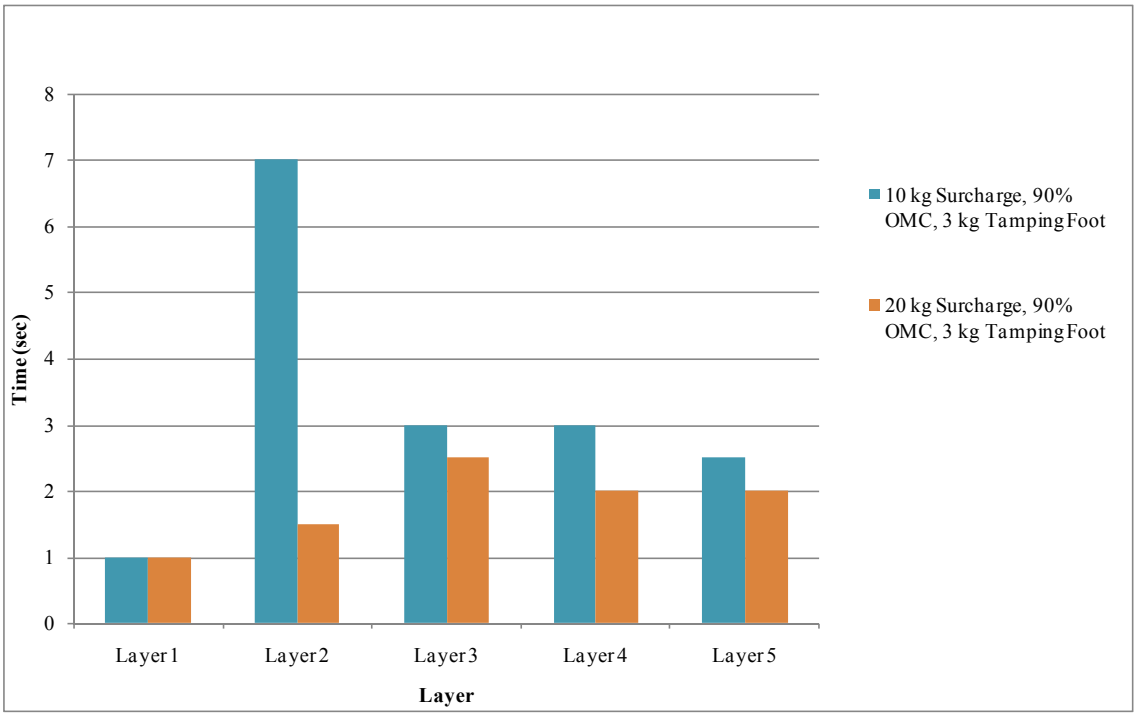

Figure B - 142: Effect of Surcharge Load at 90% OMC and 3kg Tamper – G7SFR

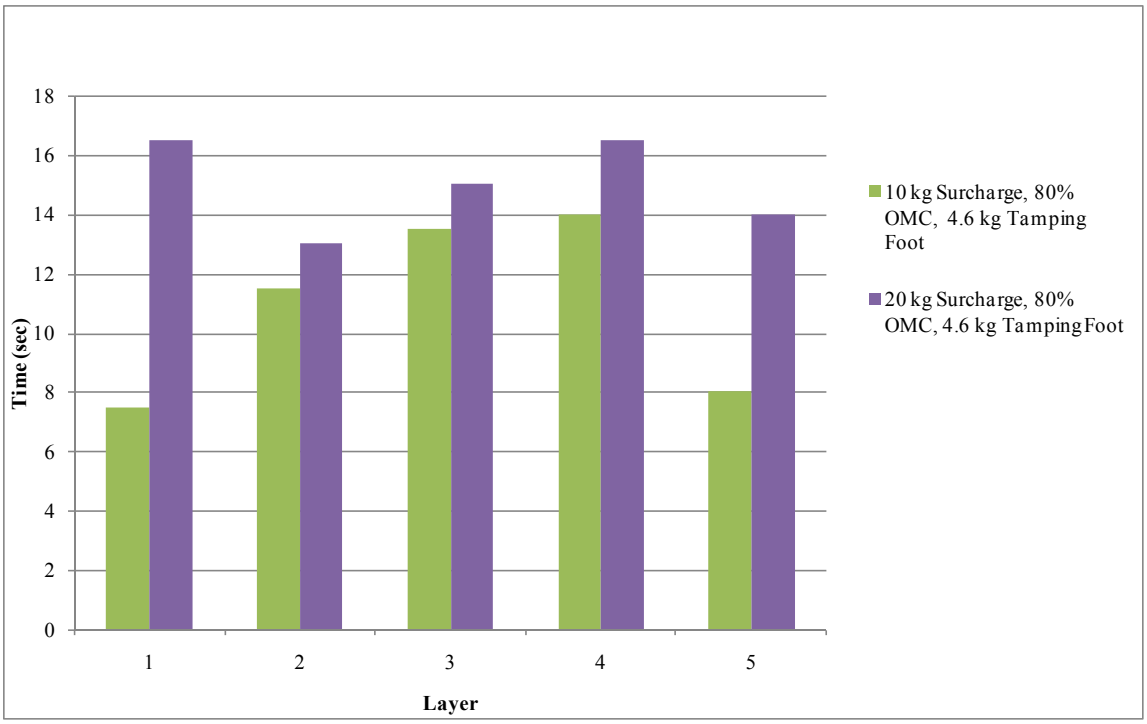

Figure B - 143: Effect of Surcharge Load at 80% OMC and 4.6kg Tamper – G7SFR

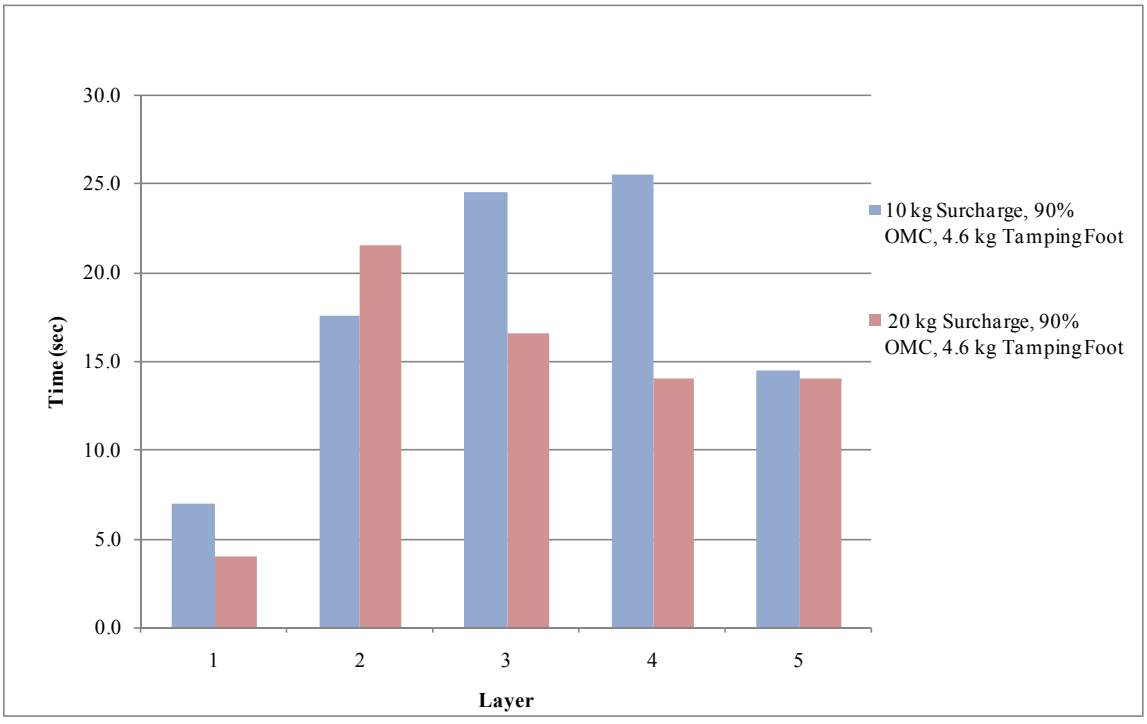

Figure B - 144: Effect of Surcharge Load at 90% OMC and 4.6kg Tamper – G7SFR

APPENDIX H: Test results for G7 material/ vibratory hammer compaction/rigid frame

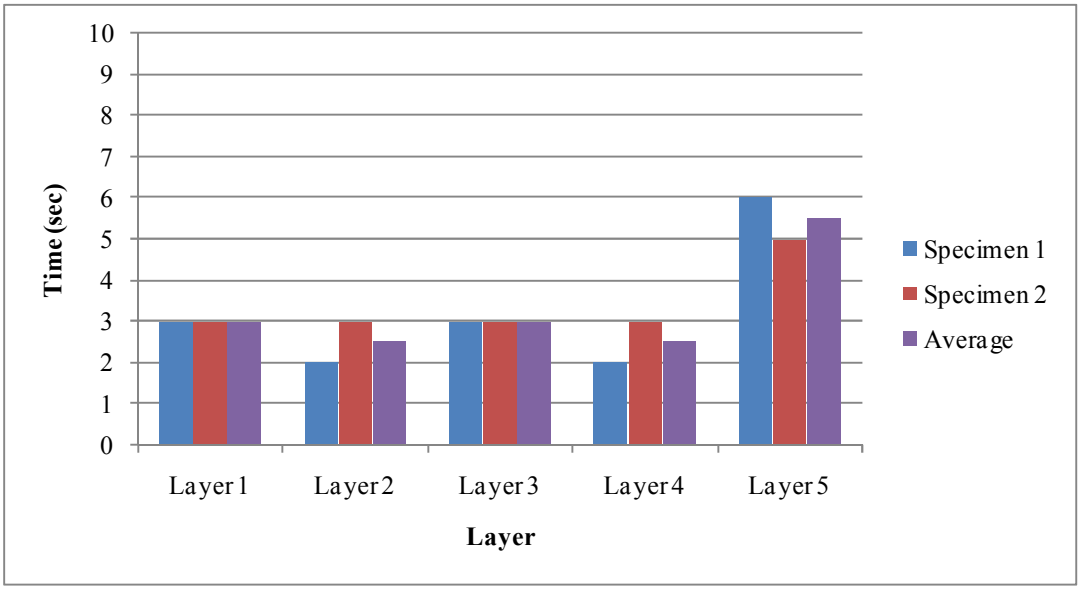

Figure B - 145: Compaction Time for 3kg Tamper, 5kg Surcharge and 80% OMC – G7RFR

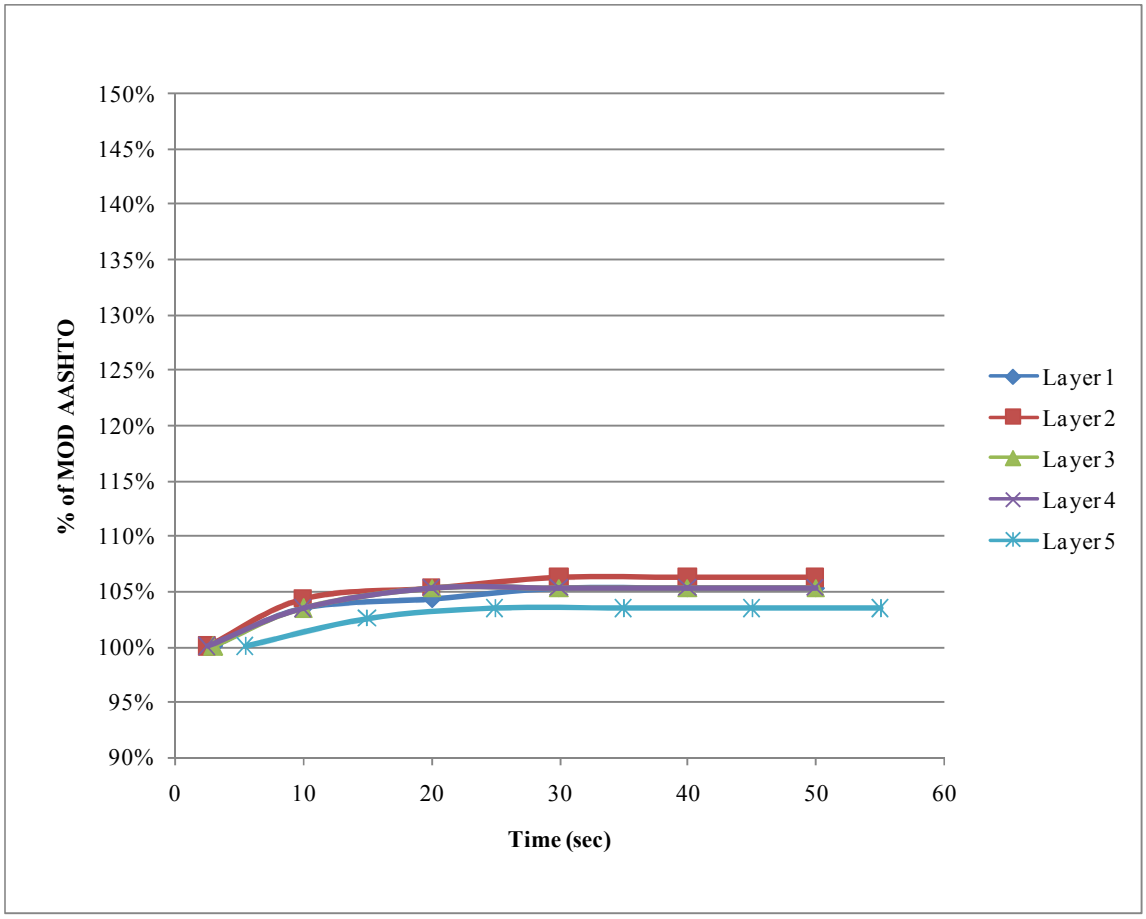

Figure B - 146: Compaction Profile for 3kg Tamper, 5kg Surcharge and 80% OMC – G7 RFR

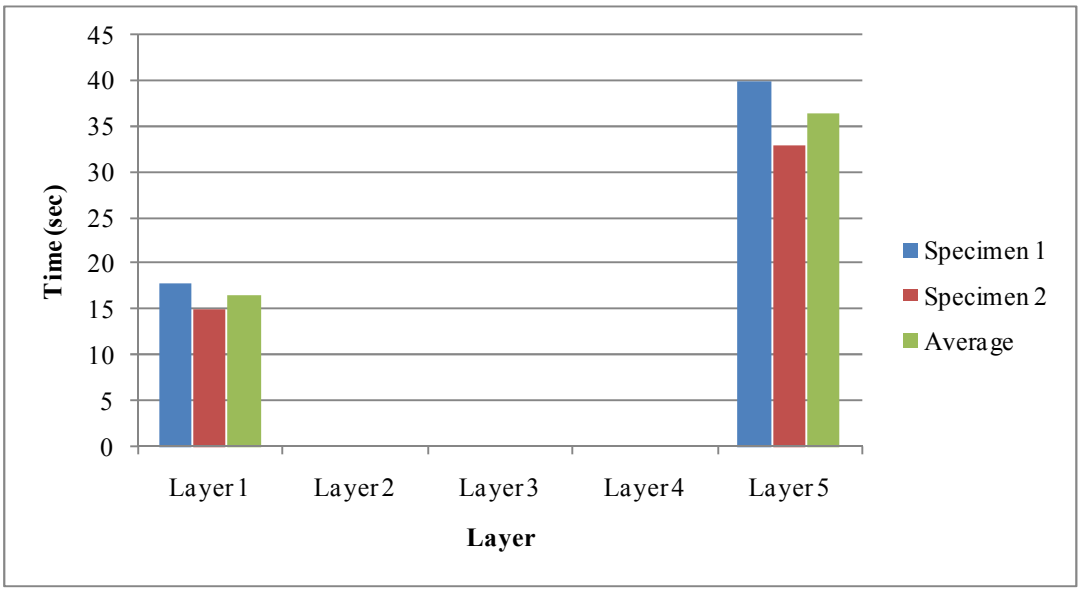

Figure B - 147: Compaction Time for 4.6kg Tamper, 5kg Surcharge and 80% OMC – G7RFR

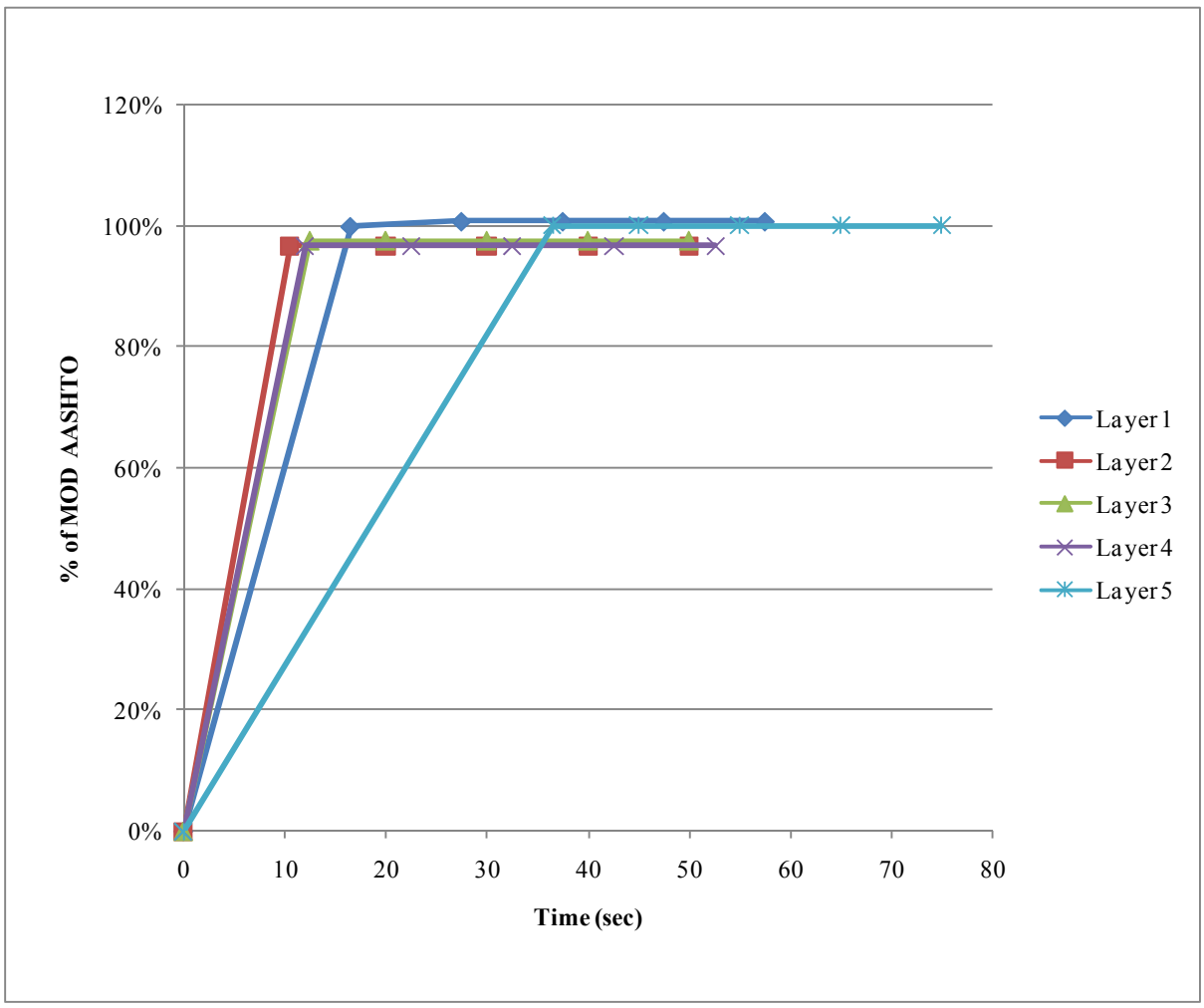

Figure B - 148: Compaction Profile for 4.6kg Tamper, 5kg Surcharge and 80% OMC – G7RFR

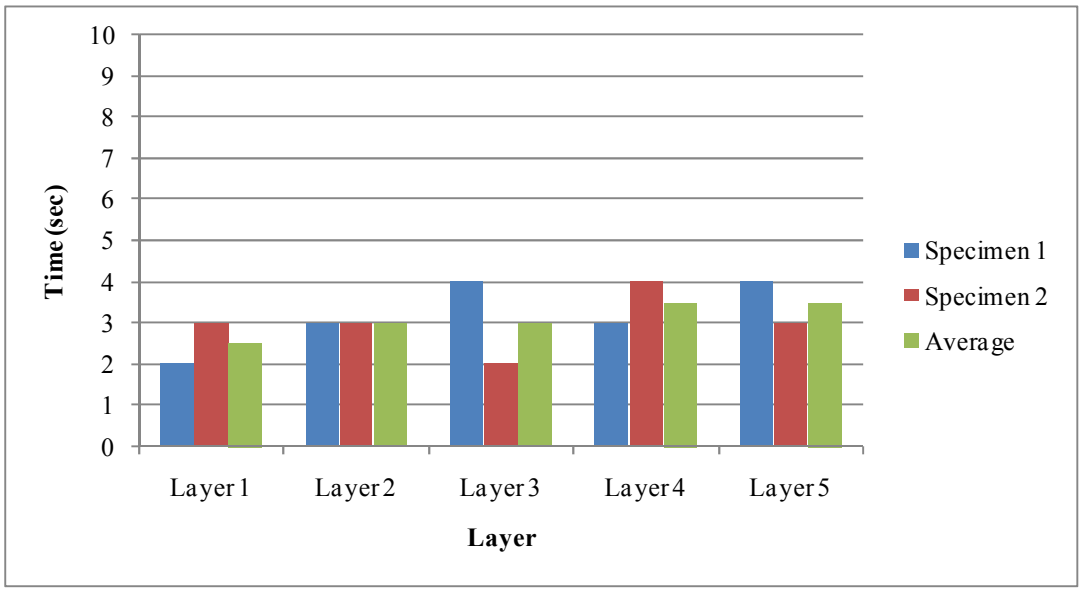

Figure B - 149: Compaction Time for 3kg Tamper, 15kg Surcharge and 80% OMC – G7RFR

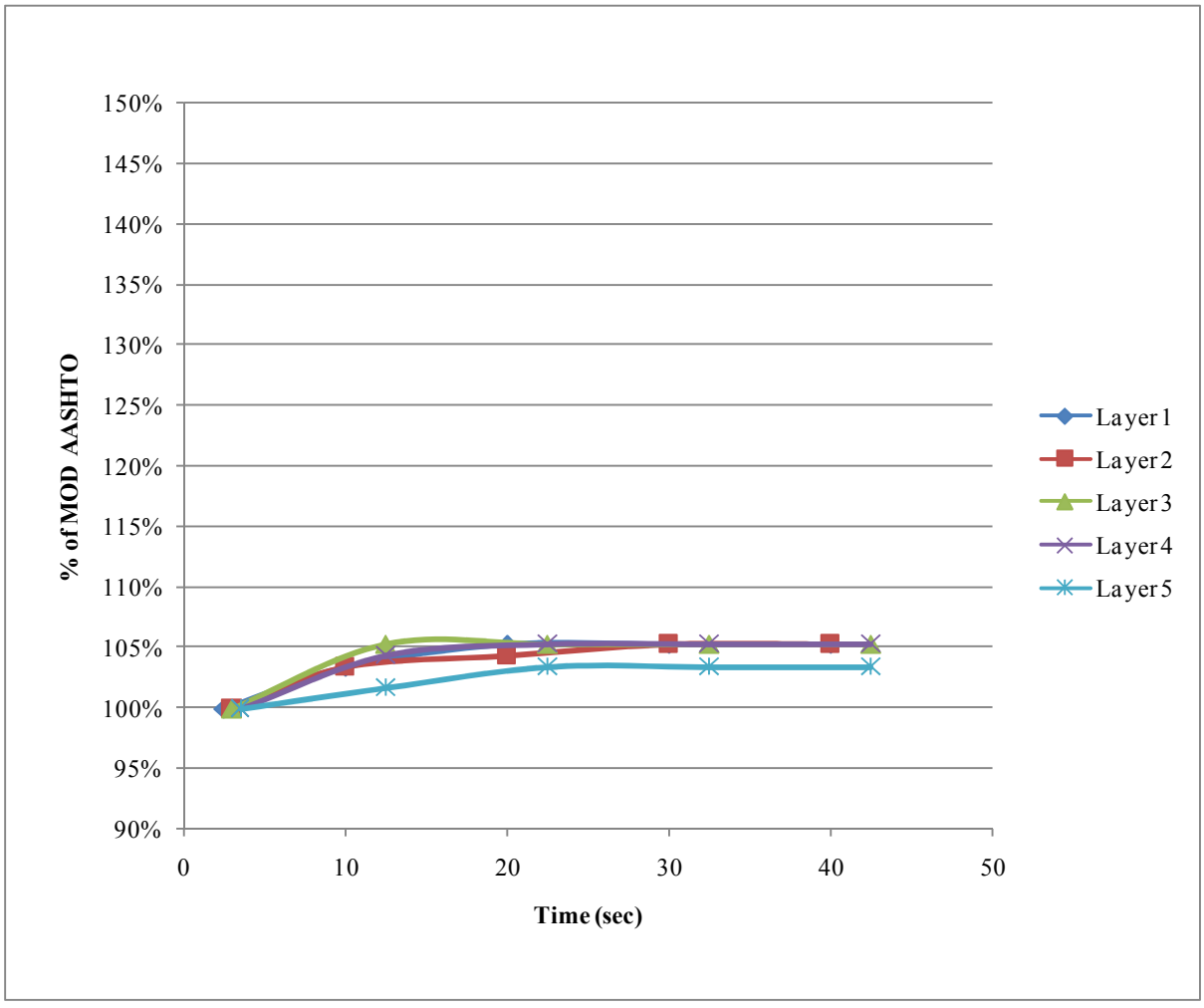

Figure B - 150: Compaction Profile for 3kg Tamper, 15kg Surcharge and 80% OMC – G7RFR

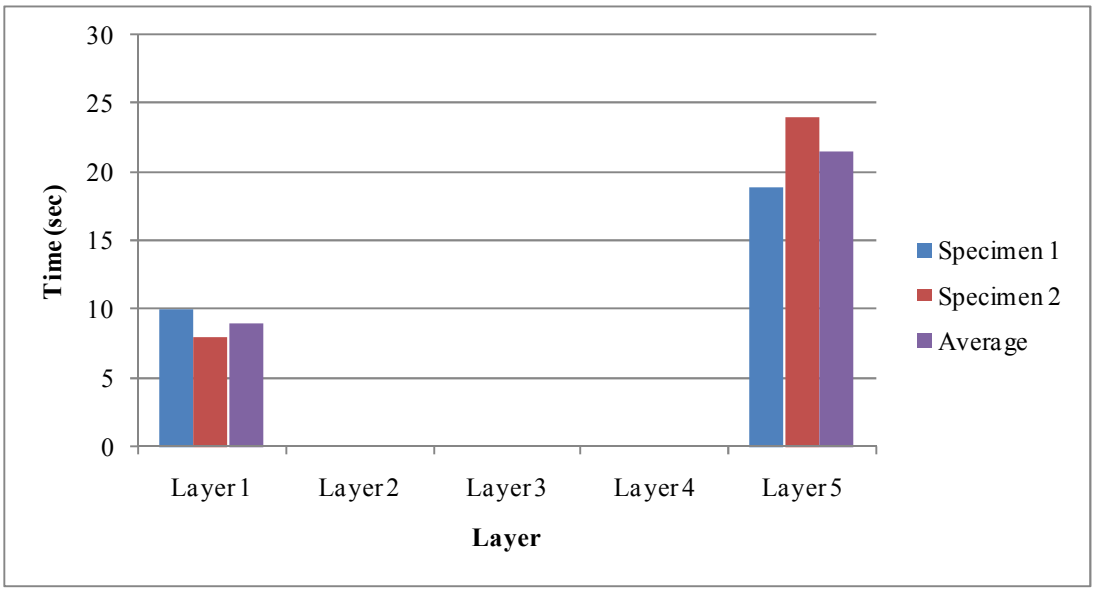

Figure B - 151: Compaction Time for 4.6kg Tamper, 15kg Surcharge and 80% OMC – G7RFR

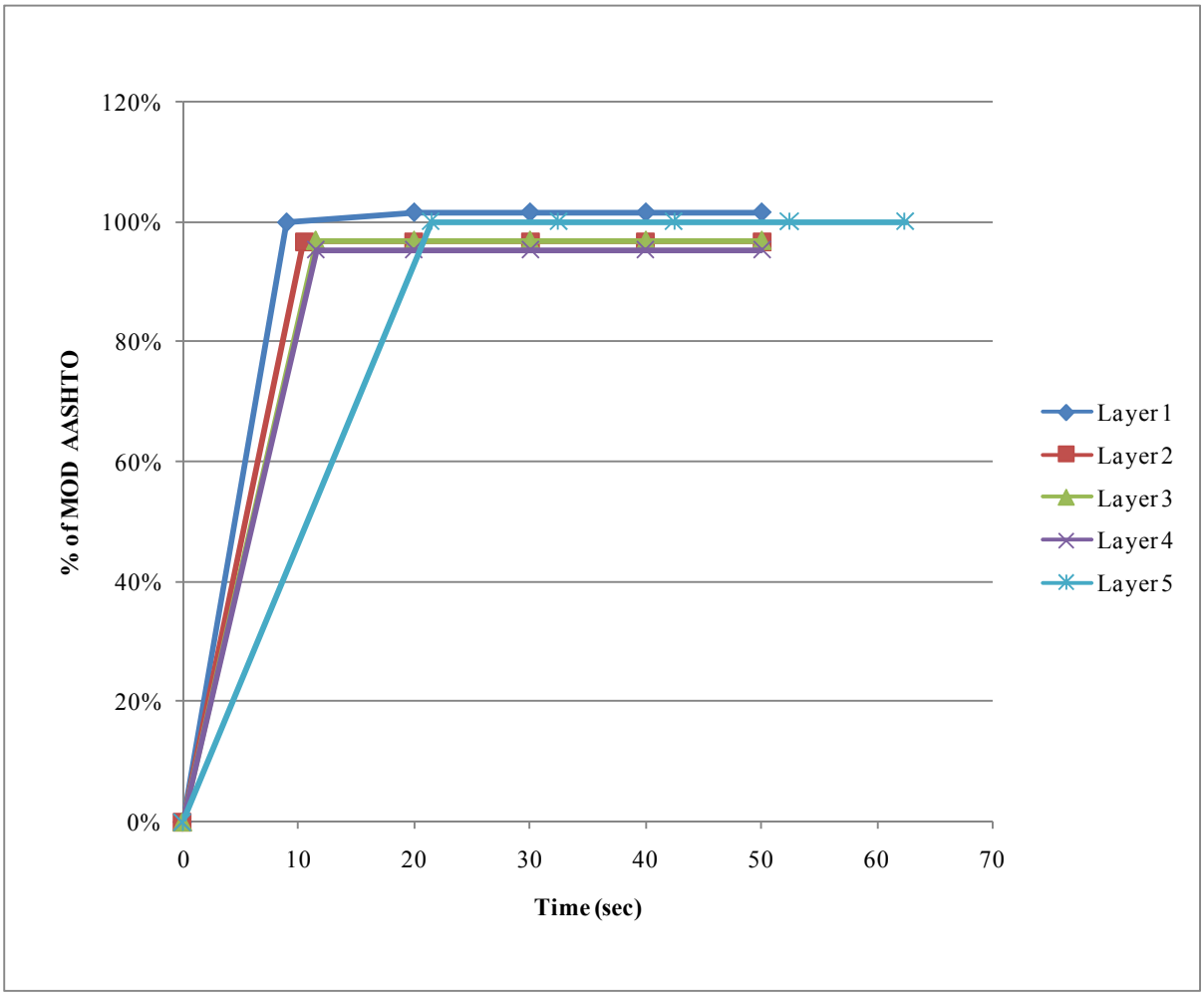

Figure B - 152: Compaction Profile for 4.6kg Tamper, 15kg Surcharge and 80% OMC – G7RFR

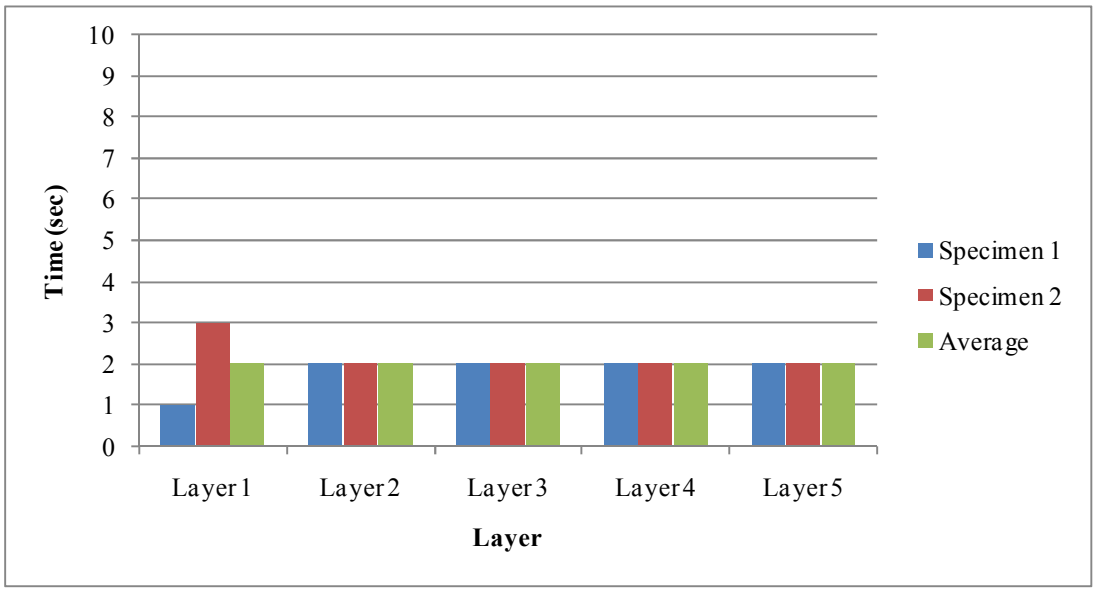

Figure B - 153: Compaction Time for 3kg Tamper, 5kg Surcharge and 90% OMC – G7RFR

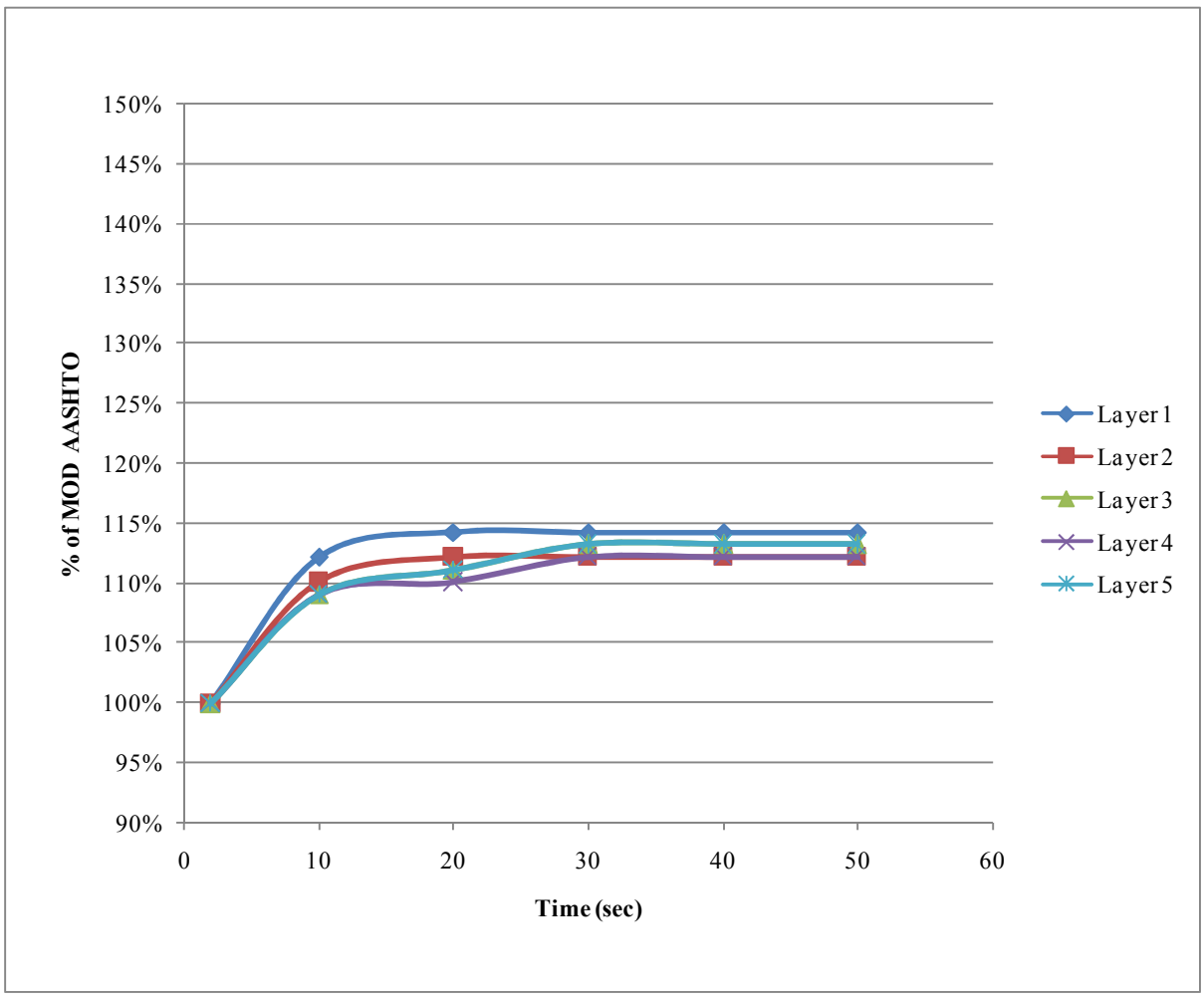

Figure B - 154: Compaction Profile for 3kg Tamper, 5kg Surcharge and 90% OMC – G7RFR

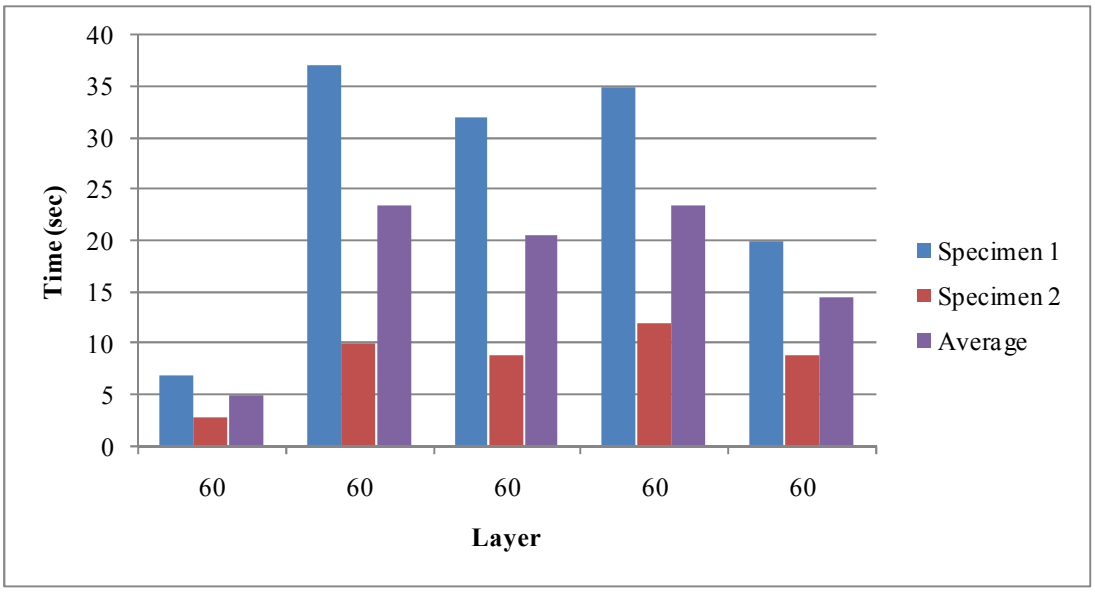

Figure B - 155: Compaction Time for 4.6kg Tamper, 5kg Surcharge and 90% OMC – G7RFR

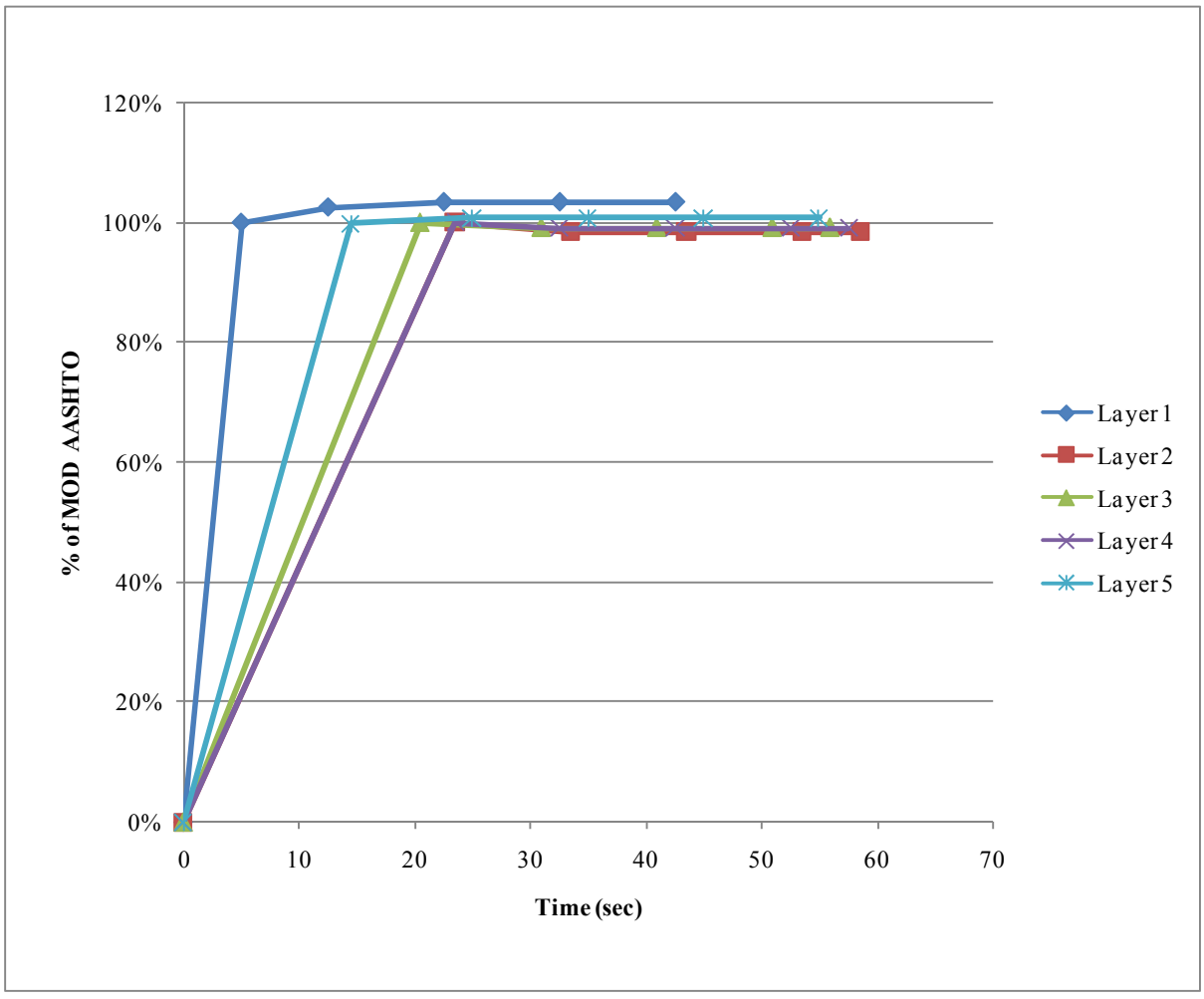

Figure B - 156: Compaction Profile for 4.6kg Tamper, 5kg Surcharge and 90% OMC – G7RFR

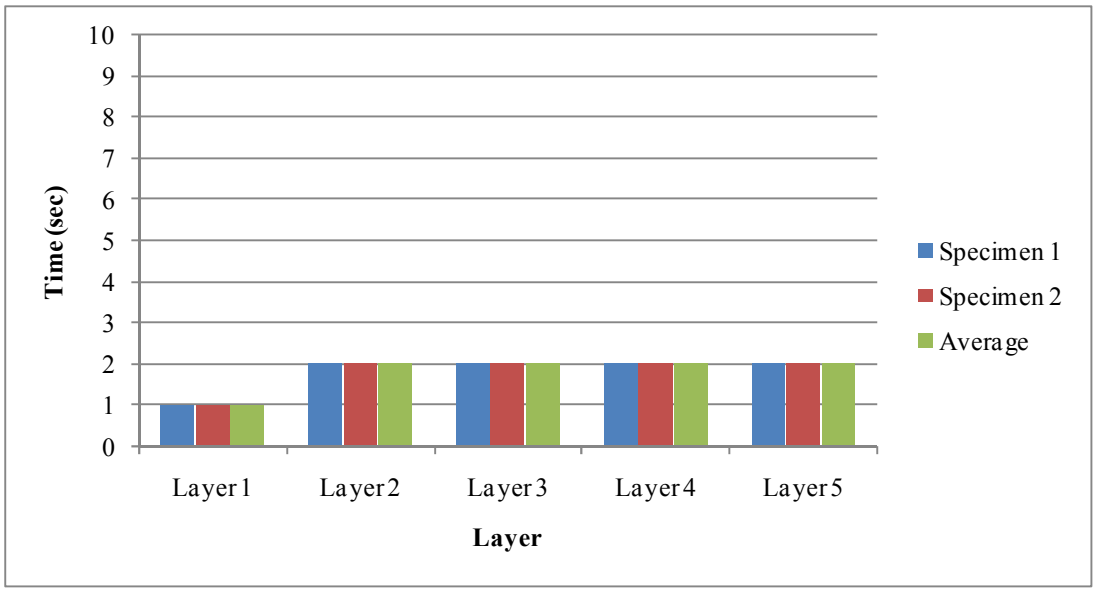

Figure B - 157: Compaction Time for 3kg Tamper, 15kg Surcharge and 90% OMC – G7RFR

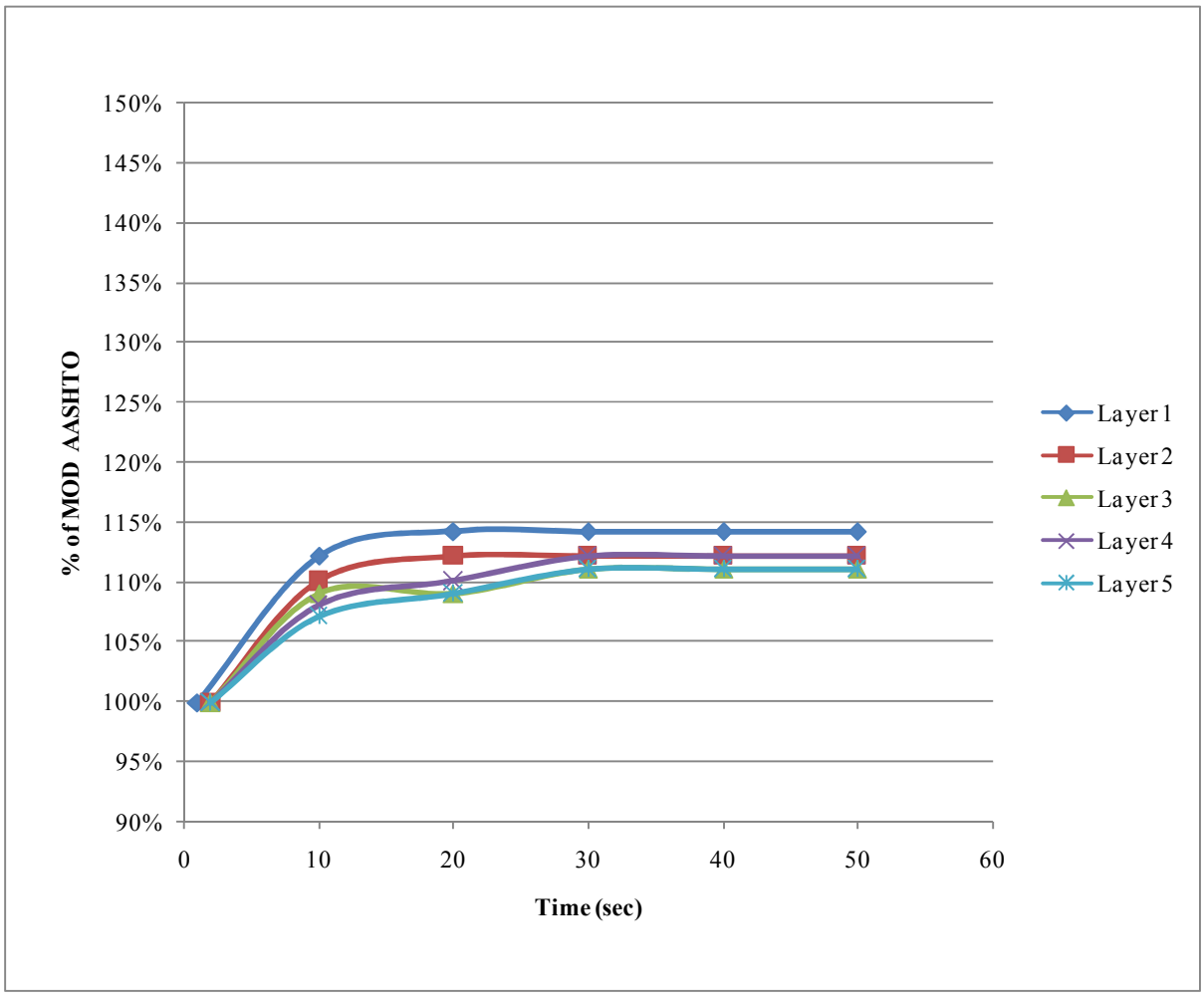

Figure B - 158: Compaction Profile for 3kg Tamper, 15kg Surcharge and 90% OMC – G7RFR

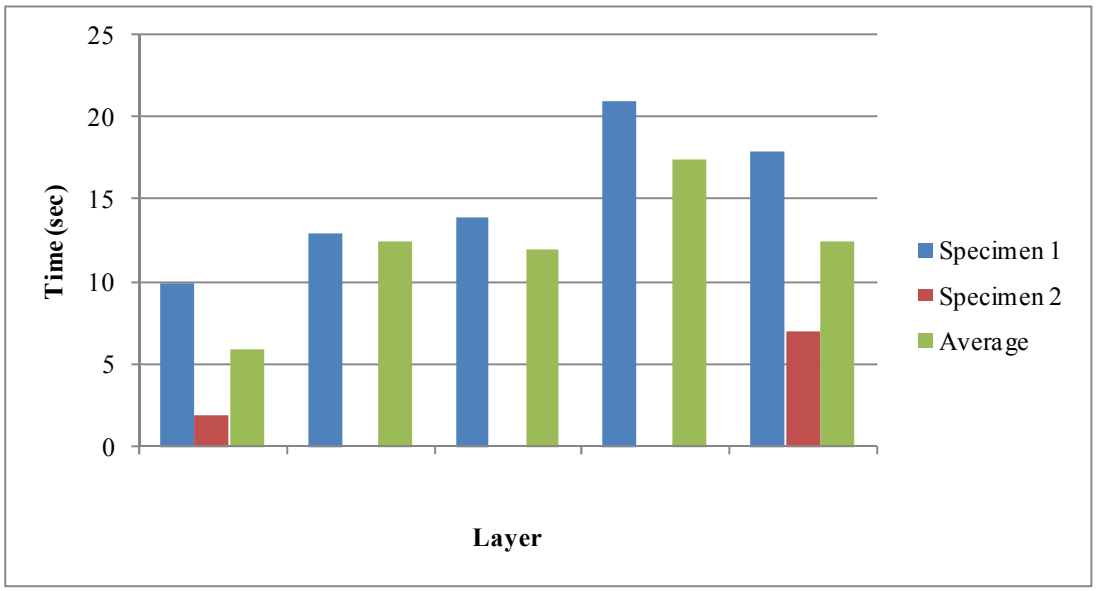

Figure B - 159: Compaction Time for 4.6kg Tamper, 15kg Surcharge and 90% OMC – G7RFR

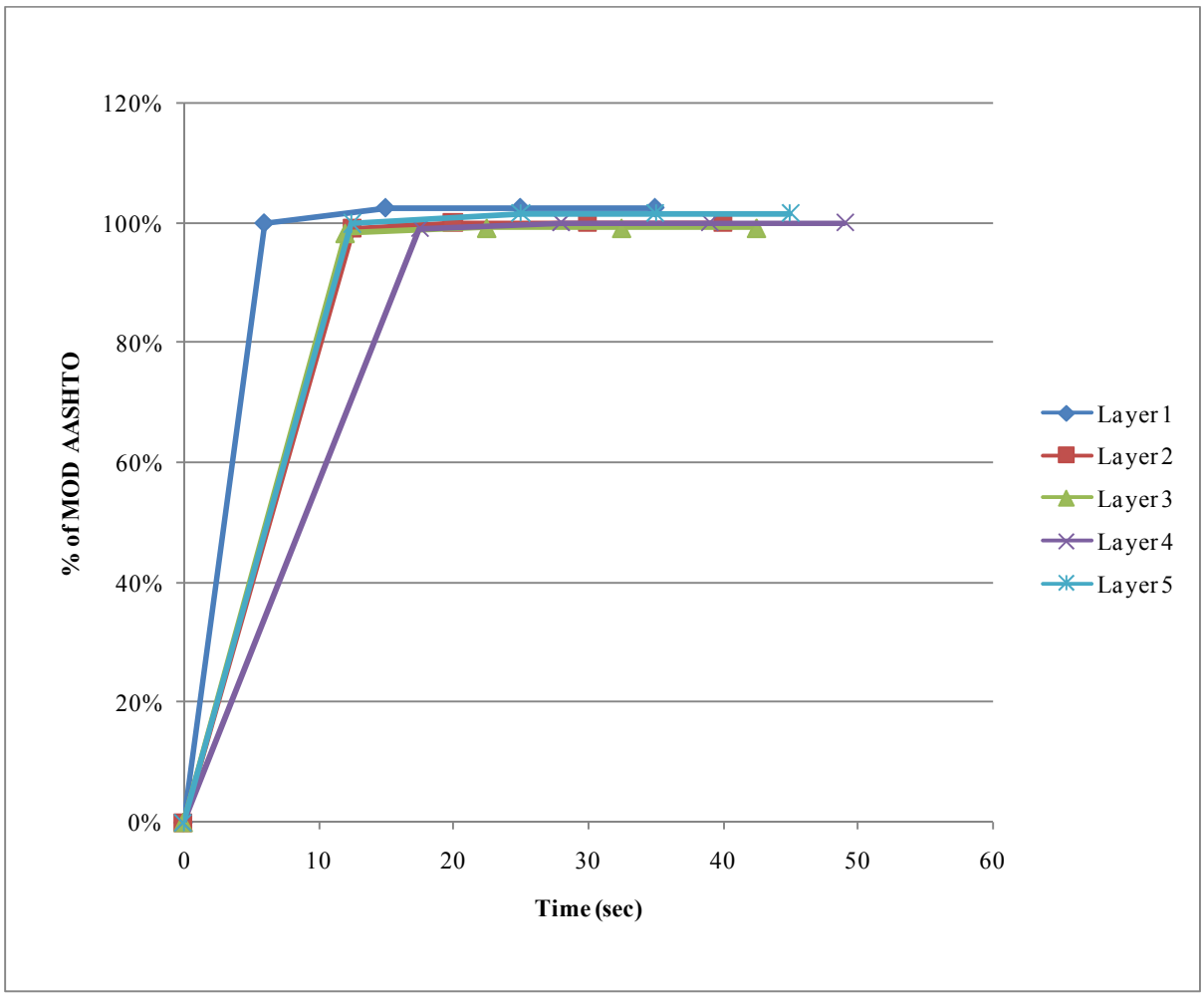

Figure B - 160: Compaction Profile for 4.6kg Tamper, 15kg Surcharge and 90% OMC – G7RFR

Frequency Tests – G7 (RFR)

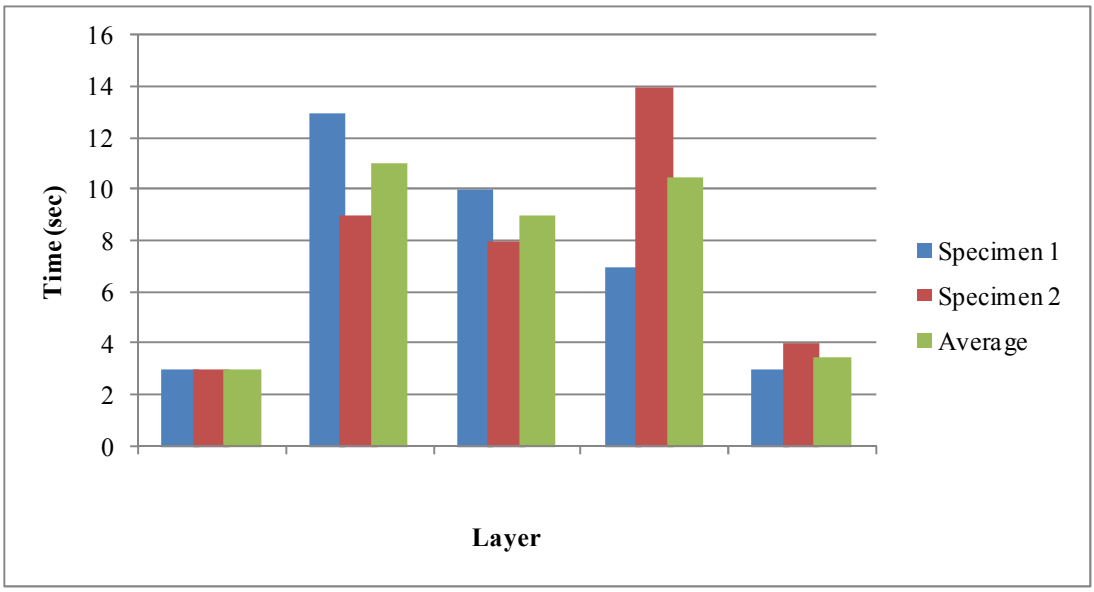

Figure B - 161: Frequency Test at 25.67Hz – Compaction Time (G7)

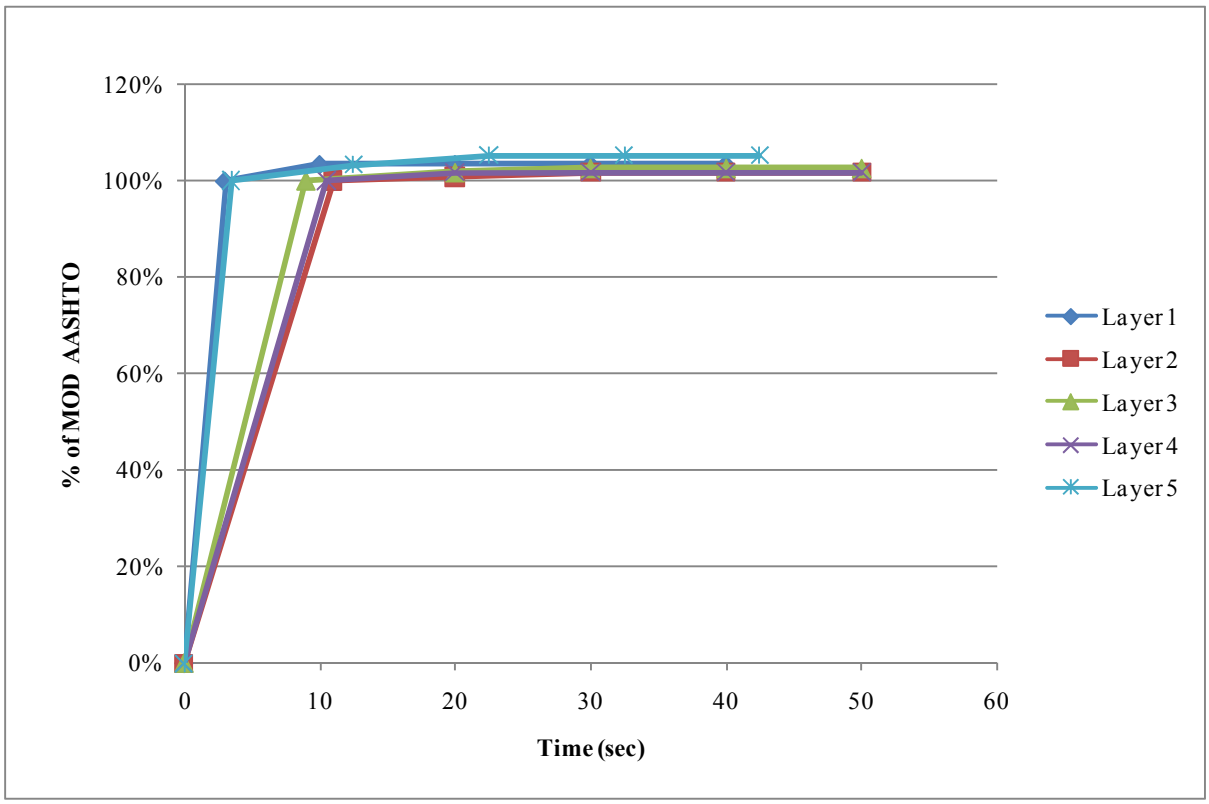

Figure B - 162: Frequency Test at 25.67Hz – Compaction Profile (G7)

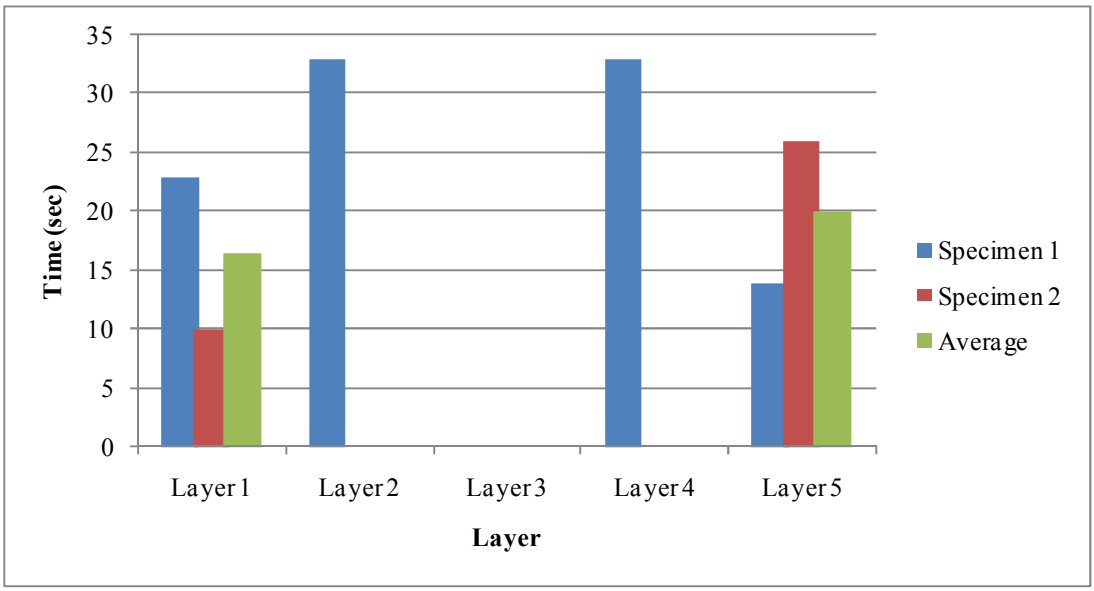

Figure B - 163: Frequency Test at 19.67Hz – Compaction Time (G7)

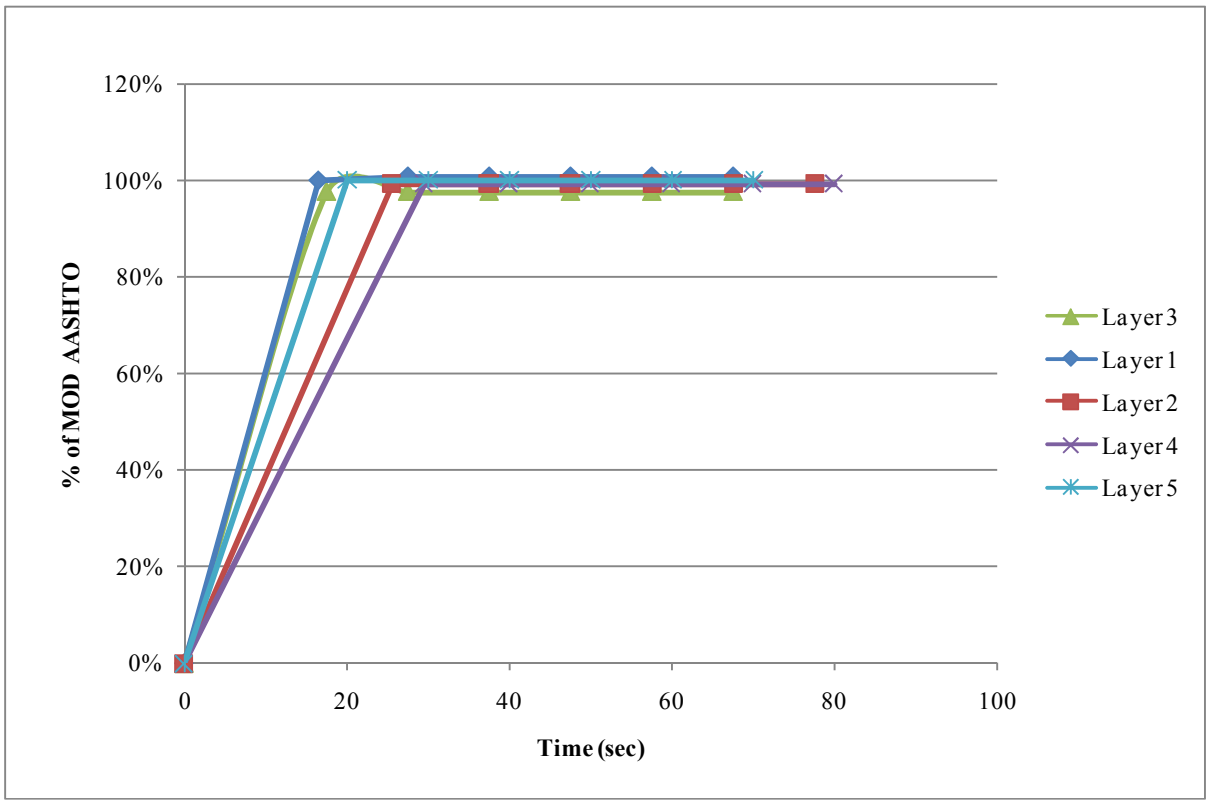

Figure B - 164: Frequency Test at 19.67Hz – Compaction Profile (G7)

Effect of Moisture on Compaction Time – G7 (RFR)

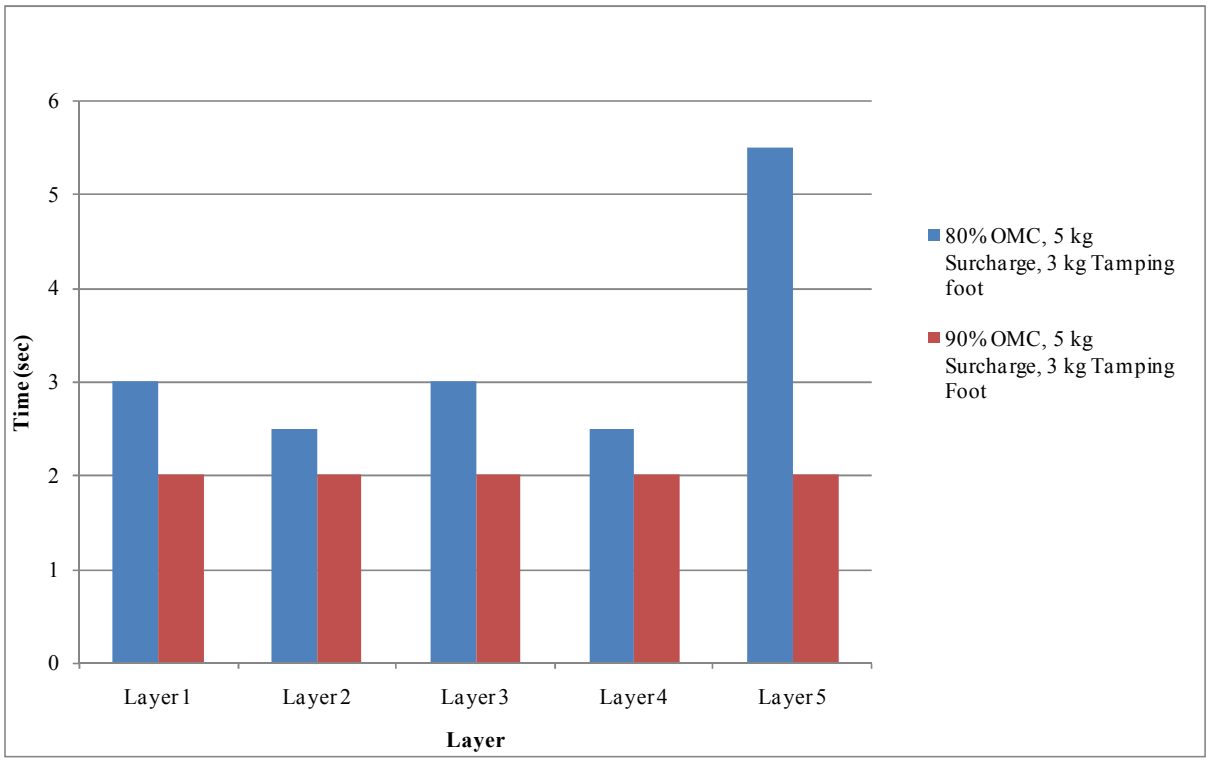

Figure B - 165: Effect of Moisture at 5kg Surcharge and 3kg Tamper – G7RFR

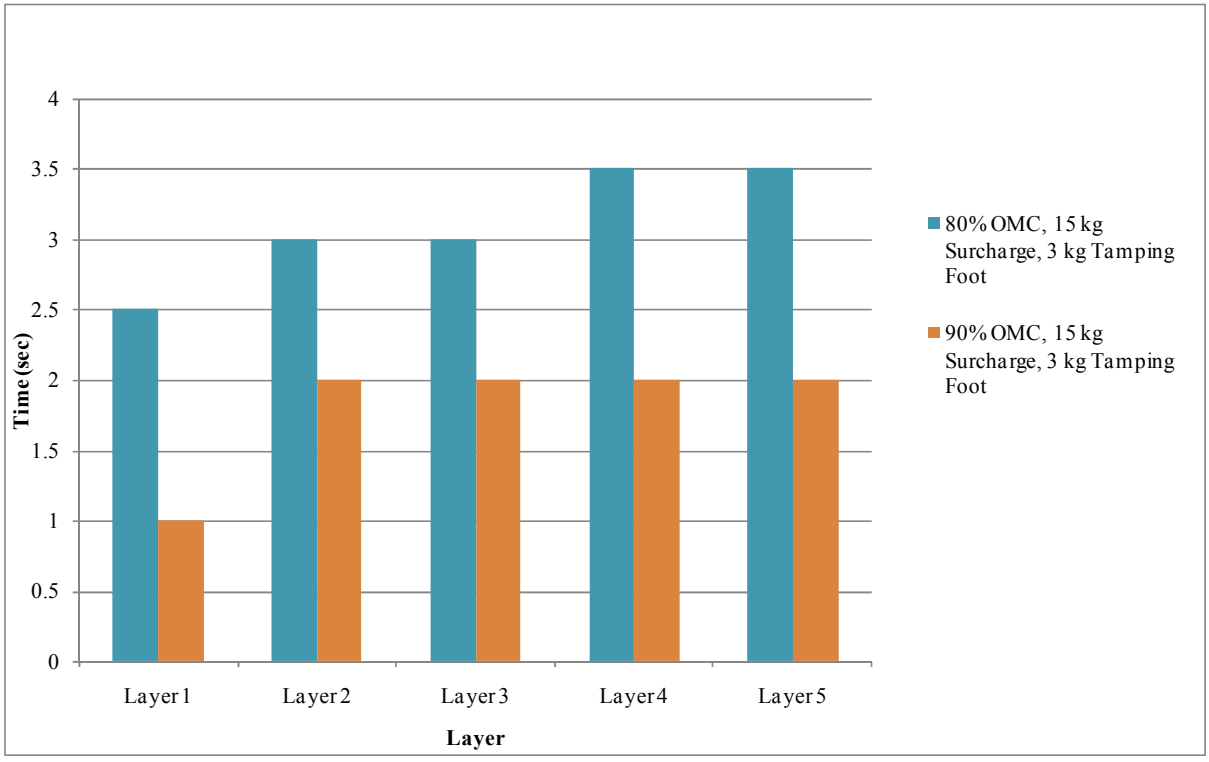

Figure B - 166: Effect of Moisture at 15kg Surcharge and 3kg Tamper – G7RFR

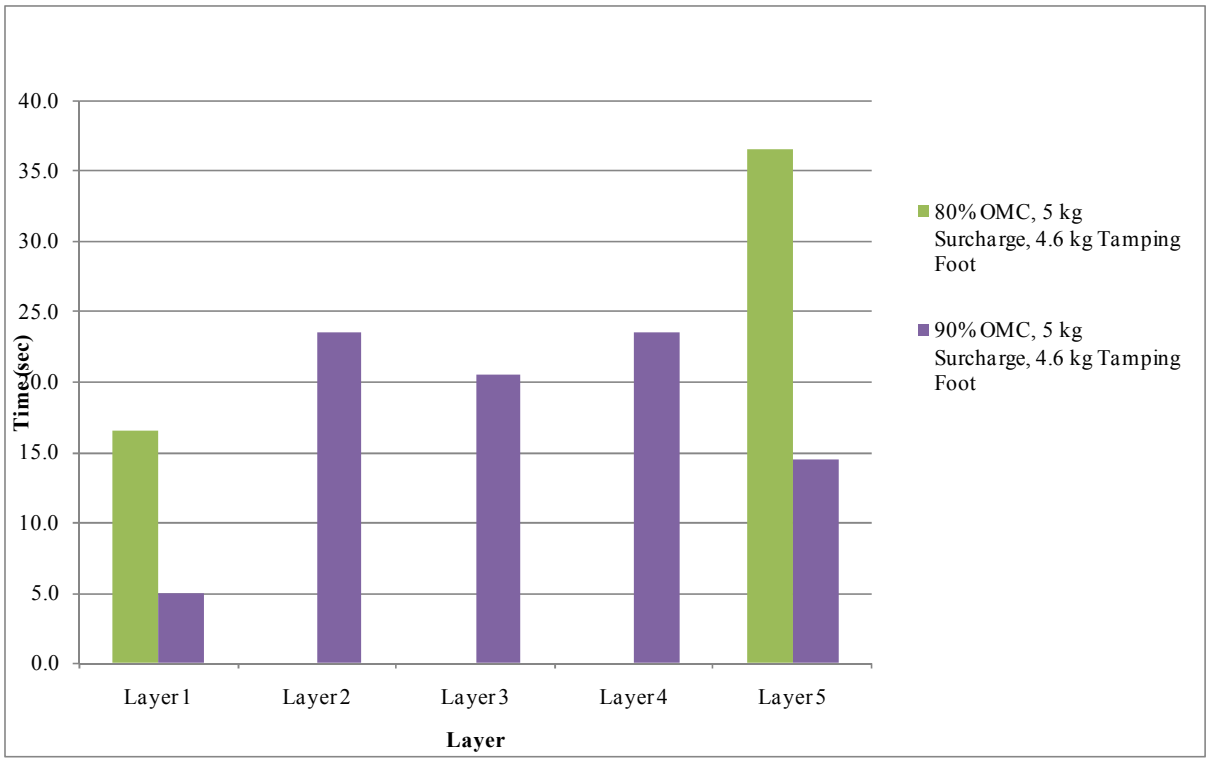

Figure B - 167: Effect of Moisture at 5kg Surcharge and 4.6kg Tamper – G7RFR

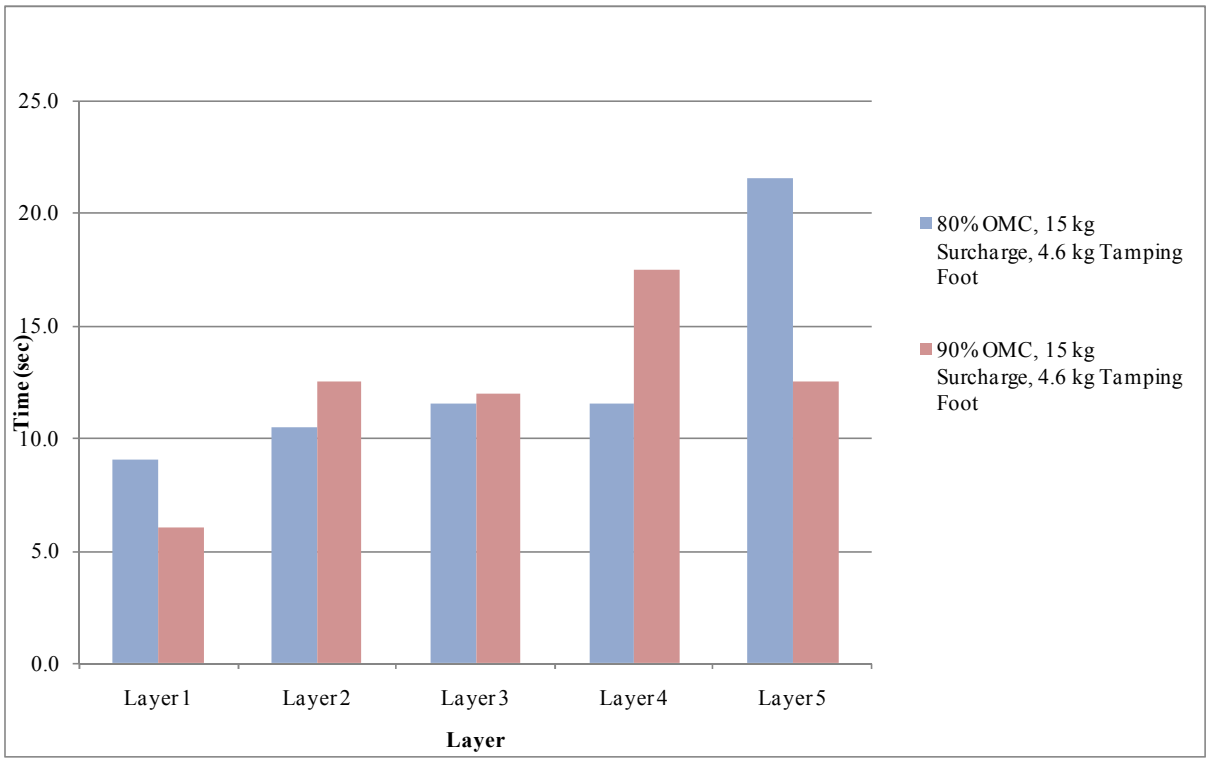

Figure B - 168: Effect of Moisture at 15kg Surcharge and 4.6kg Tamper – G7RFR

Effect of Tamping Foot on Compaction Time – G7 (RFR)

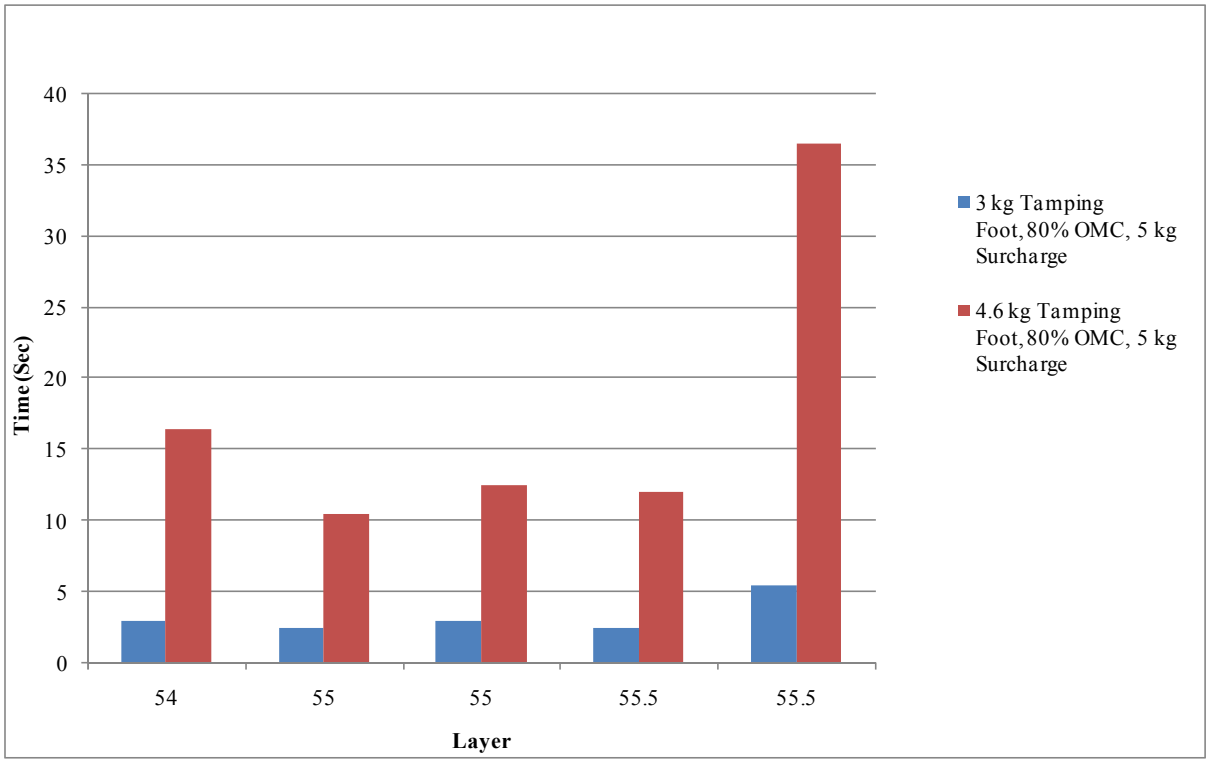

Figure B - 169: Effect of Tamper at 80% OMC and 5kg Surcharge – G7RFR

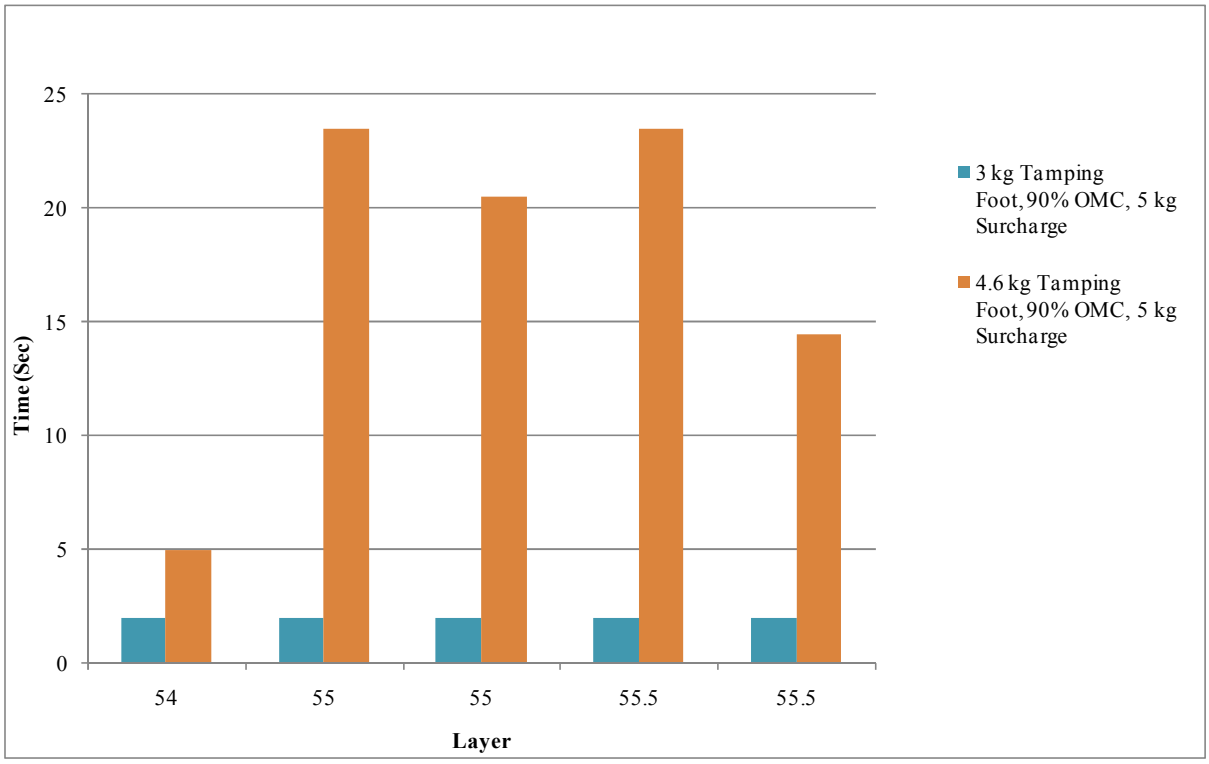

Figure B - 170: Effect of Tamper at 90% OMC and 5kg Surcharge – G7RFR

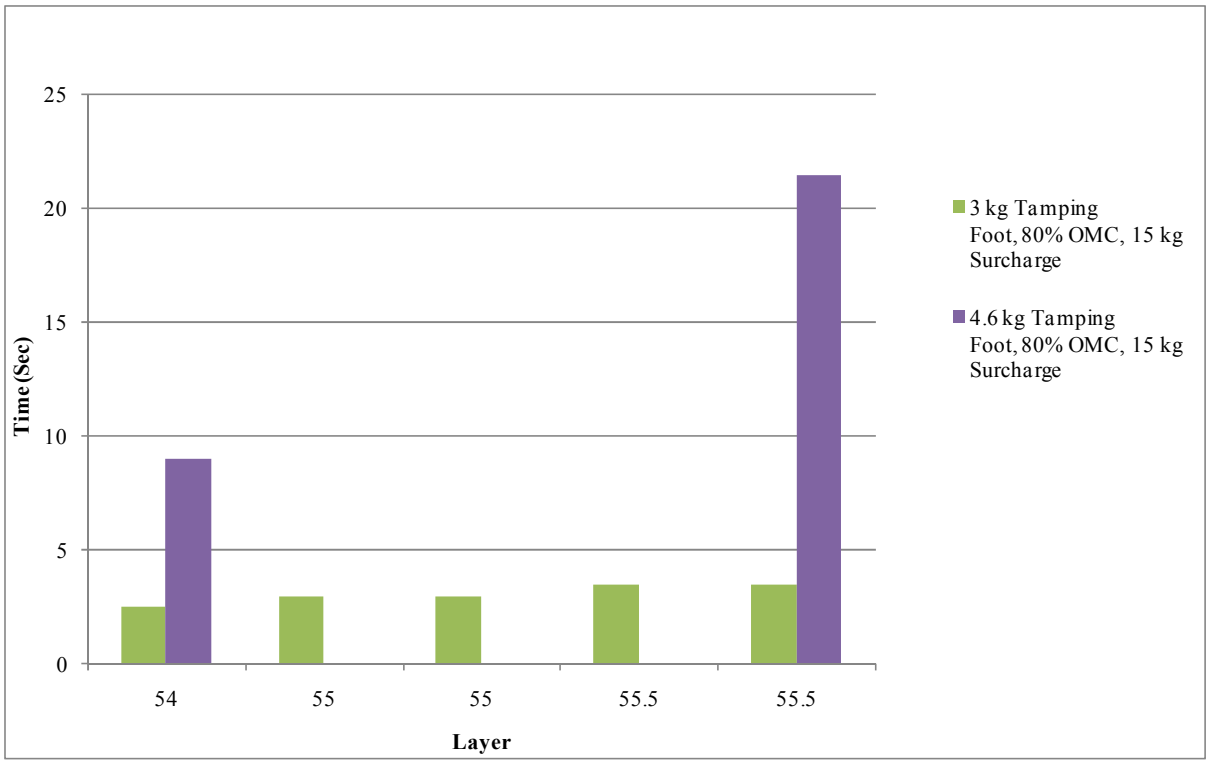

Figure B - 171: Effect of Tamper at 80% OMC and 15kg Surcharge – G7RFR

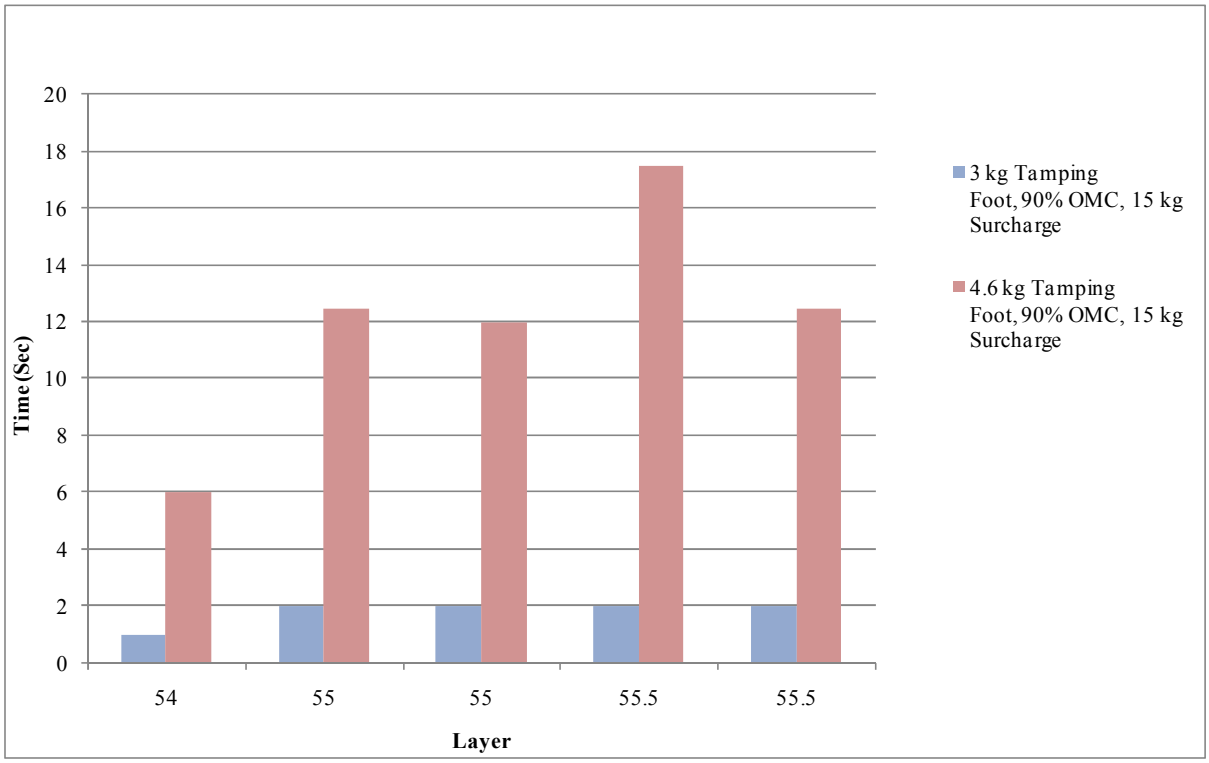

Figure B - 172: Effect of Tamper at 90% OMC and 15kg Surcharge – G7RFR

Effect of Surcharge Load on Compaction Time – G7 (RFR)

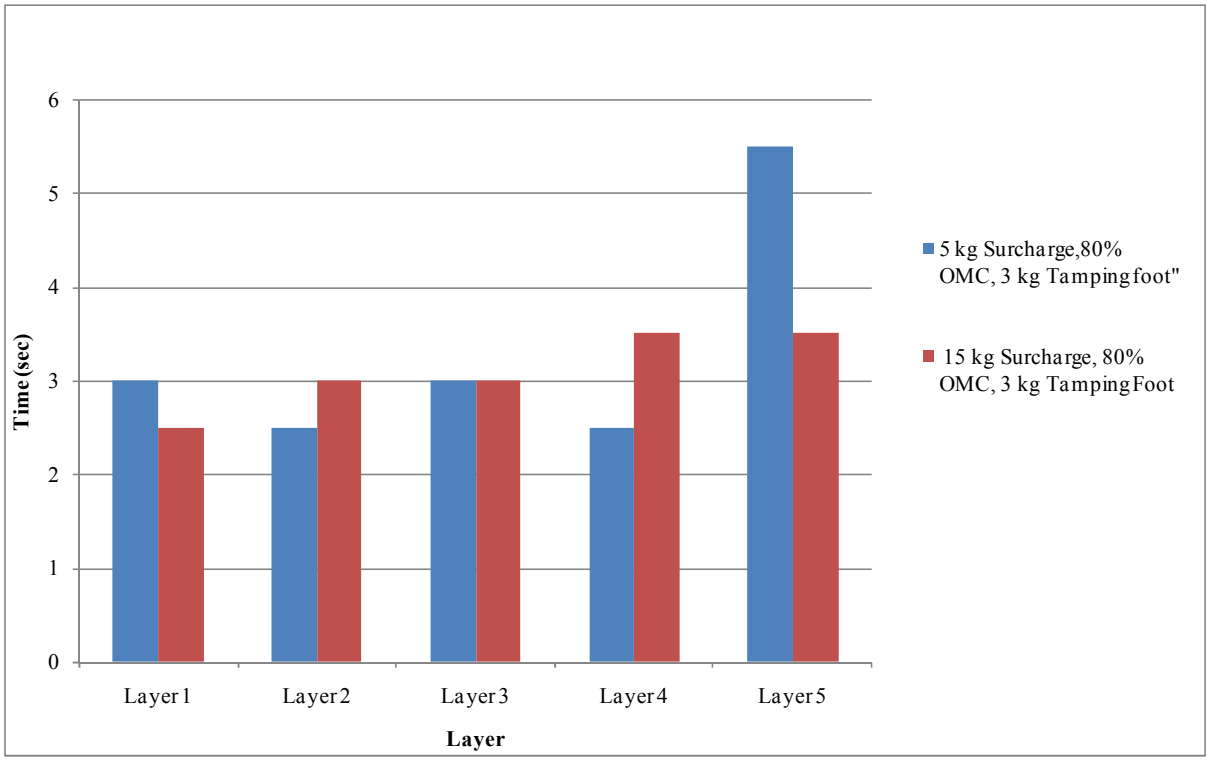

Figure B - 173: Effect of Surcharge Load at 80% OMC and 3kg Tamper – G7RFR

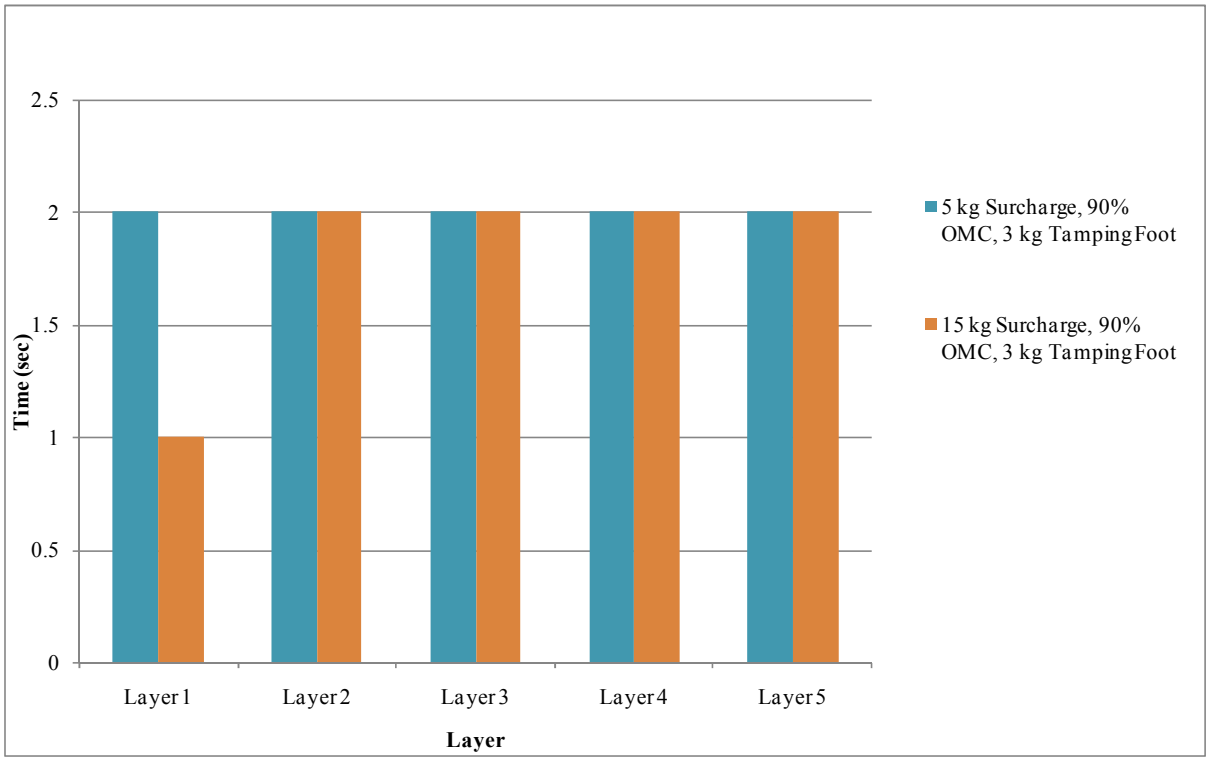

Figure B - 174: Effect of Surcharge Load at 90% OMC and 3kg Tamper – G7RFR

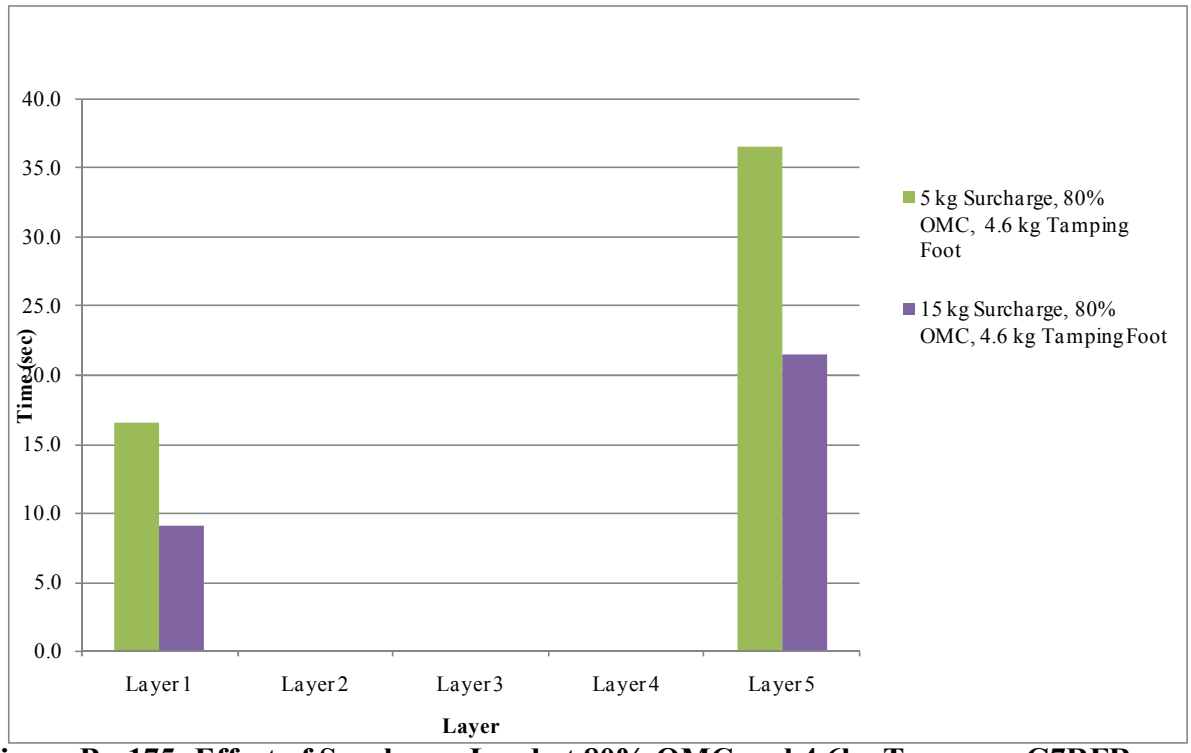

Figure B - 175: Effect of Surcharge Load at 80% OMC and 4.6kg Tamper – G7RFR

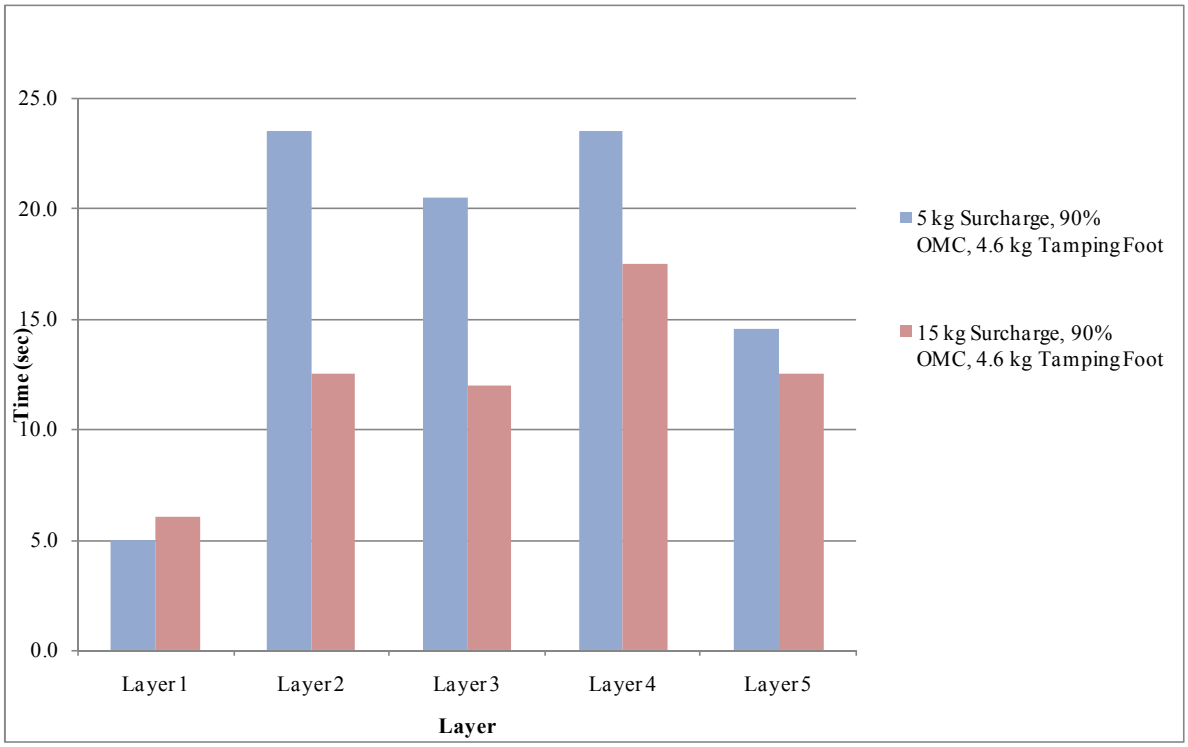

Figure B - 176: Effect of Surcharge Load at 90% OMC and 4.6kg Tamper – G7RFR

APPENDIX J: Test results for G3/G4/G7 materials/vibratory table compaction

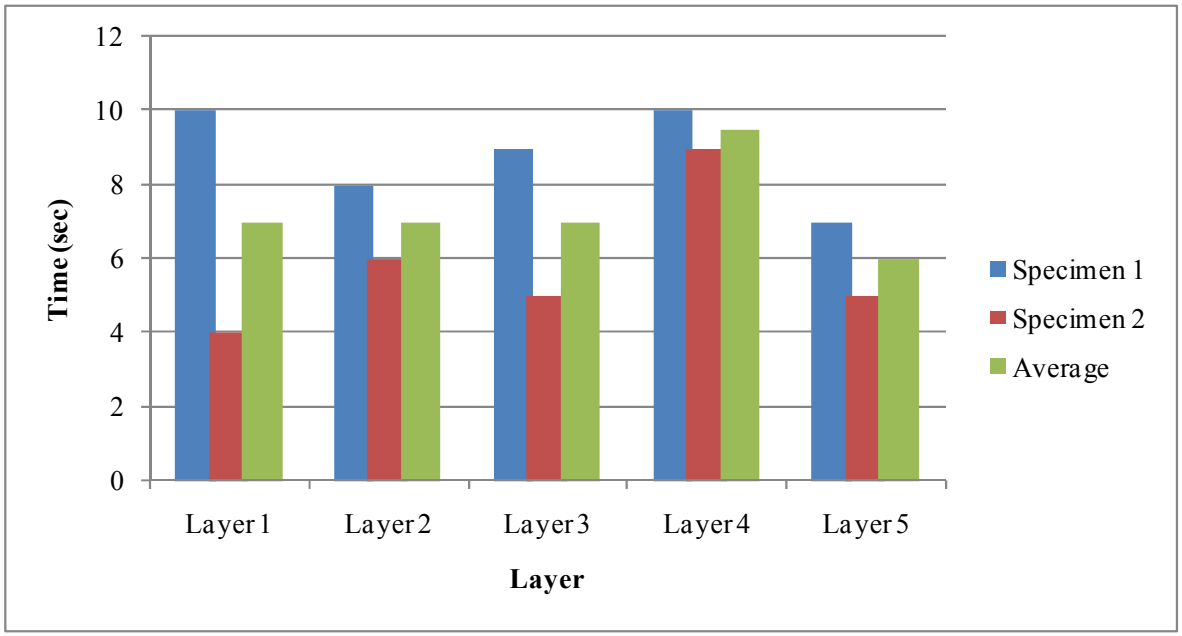

Figure B - 177: Vibratory Table tests – G3

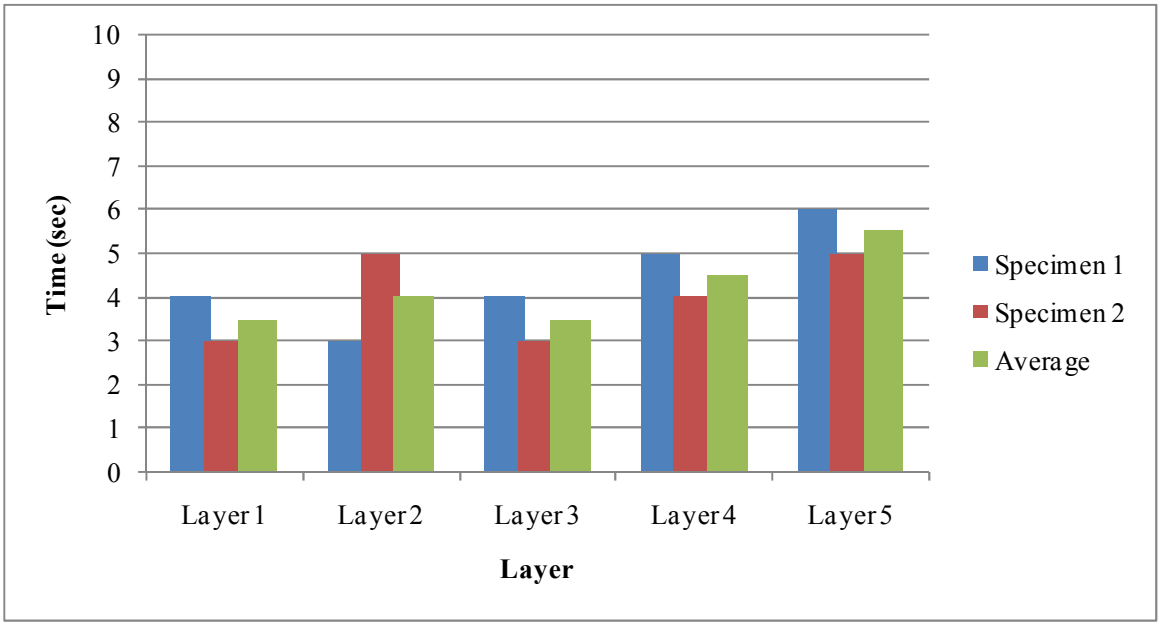

Figure B - 178: Vibratory Table tests – G4

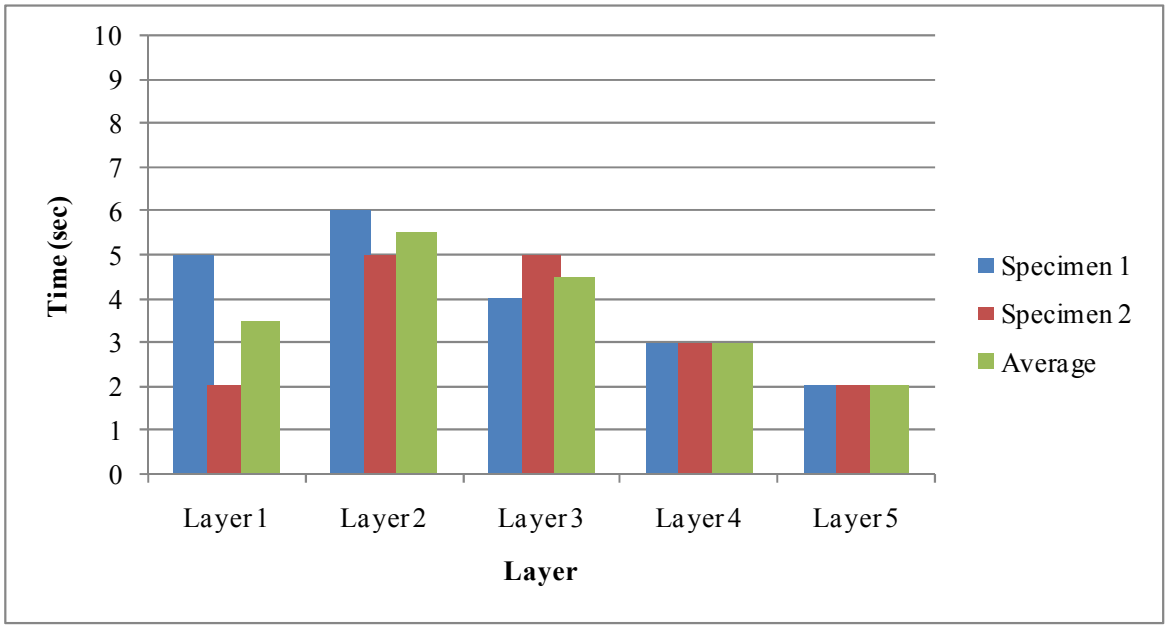

Figure B - 179: Vibratory Table tests – G7

APPENDIX K: Test results for RA material

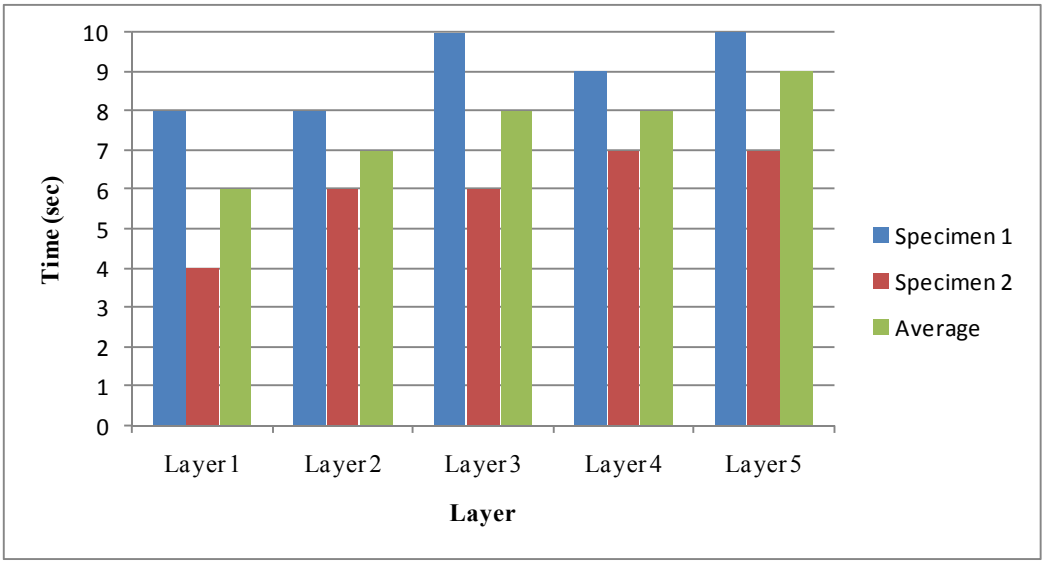

Figure B - 180: Compaction Time for 3kg Tamper, 5kg Surcharge and 90% OMC – RA

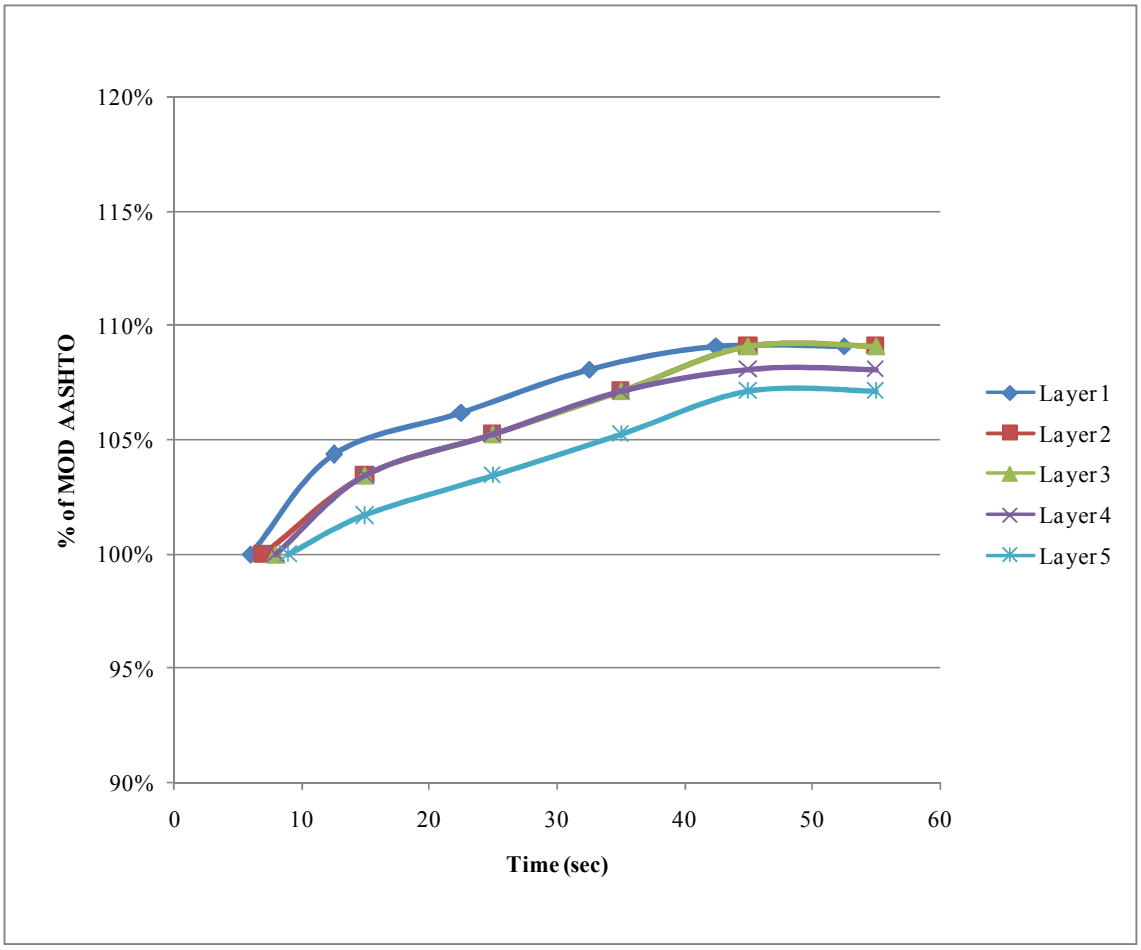

Figure B - 181: Compaction Profile for 3kg Tamper, 5kg Surcharge and 90% OMC – RA

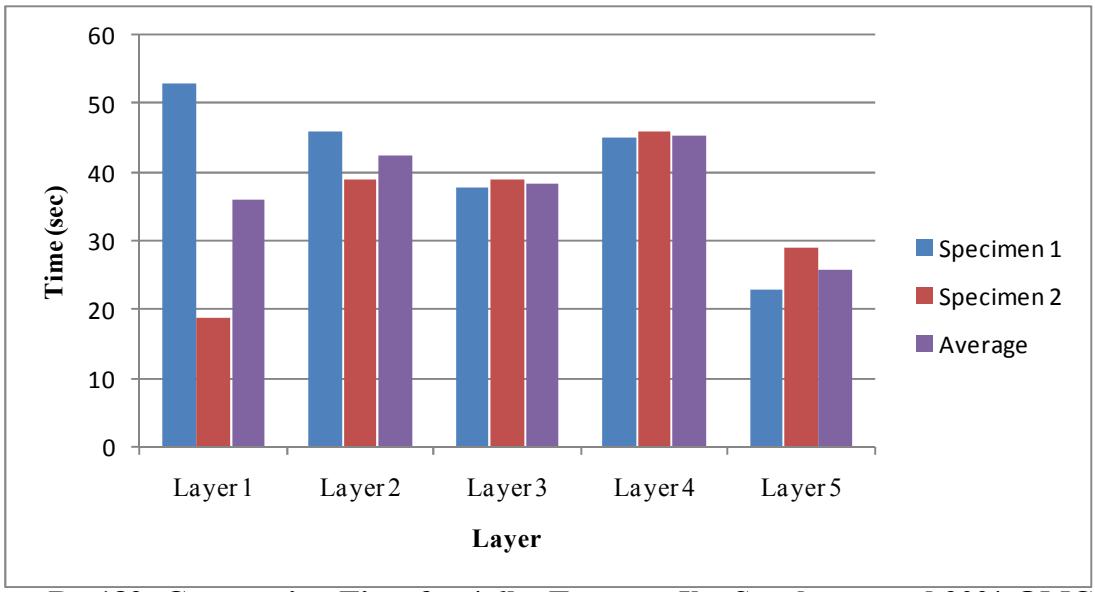

Figure B - 182: Compaction Time for 4.6kg Tamper, 5kg Surcharge and 90% OMC – RA

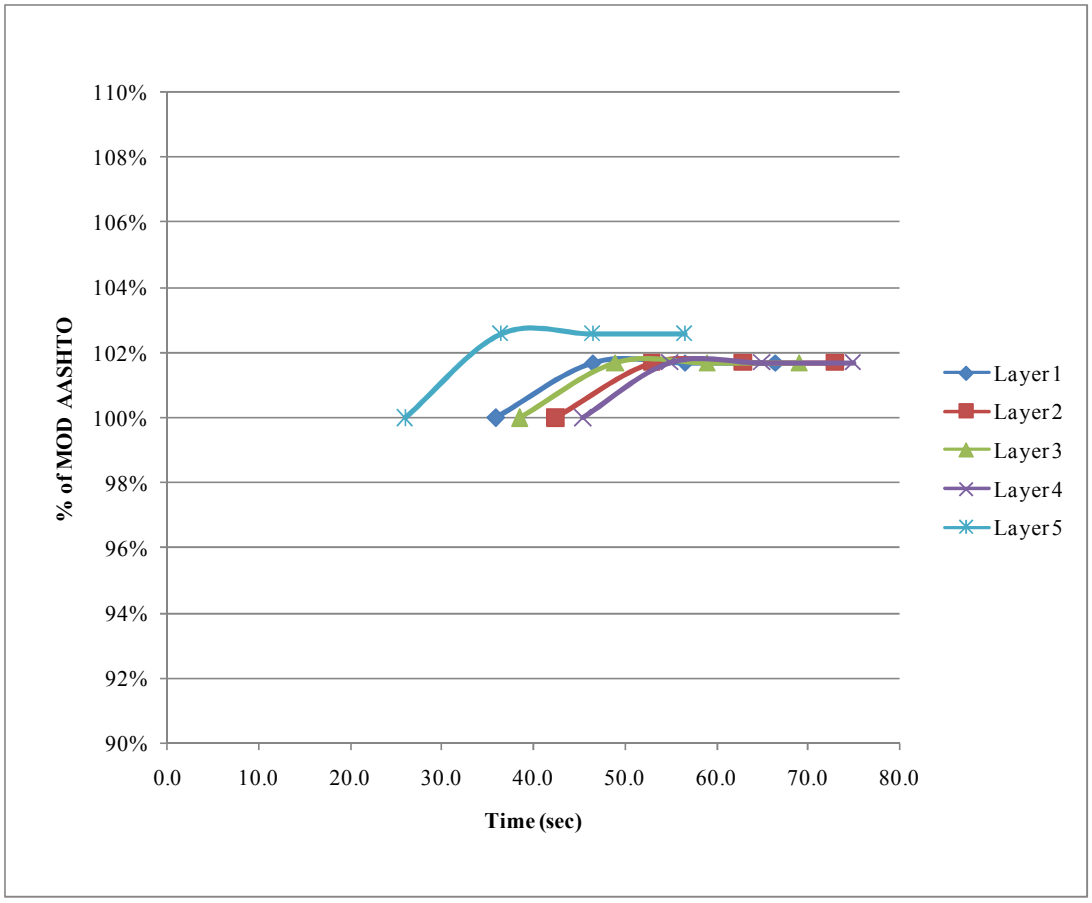

Figure B - 183: Compaction Profile for 4.6kg Tamper, 5kg Surcharge and 90% OMC – RA